Utilization of High Throughput Screening to Identify Therapeutic Targets for Defective MCPH1/BRIT1 Function-Induced Premature Chromosome Condensation in Breast and Ovarian Cancer.

By

Aeshah Ali Awaji

Submitted in accordance with the requirements for the degree of
Doctor of Philosophy

The University of Leeds
School of Medicine

March, 2016

The candidate confirms that the work submitted is her own and that appropriate credit has been given where reference has been made to the work of others.

This copy has been supplied on the understanding that it is copyright material and that no quotation from the thesis may be published without proper acknowledgement.

Acknowledgements

Abstract

Mutations in the *N*-terminal region of MCPH1/BRIT1 cause premature chromosome condensation (PCC), whereby cells enter mitosis before completing DNA replication. 792 chemical compounds (CC) were selected based on the crystal structure of the *N*-terminus of MCPH1/BRIT1 and assayed using high throughput-high content imaging to identify CC that induced PCC. Hit validation revealed 4 potential CC, 2 of which induced high PCC at low concentrations.

A screen using a human protein kinase (hPK) siRNA sub-library was performed to identify genes that induced PCC. Four hits were selected for validation, however PCC induction was not confirmed. A complementary hPK siRNA screen combined with *MCPH1*/*BRIT1* siRNA knockdown was performed. The cell number outputs from both hPK siRNA screens were analysed to identify synthetic lethal (SL) genes in MCPH1/BRIT1-deficient cells. *CDK1*/*CDC2*, *STK39*, *VRK1* and *TTK*/*MPS1* were subsequently validated as potential *MCPH1/BRIT1* SL genes.

The expression of MCPH1/BRIT1 was examined by immunostaining in breast cancer (BC) tissue pre and post neoadjuvant chemotherapy (NACT) to determine its effect on response and survival. *MCPH1*/*BRIT1* expression increased in response to NACT with high expression in 51.4% (36/70) of cases pre-NACT compared to 81.4% (57/70) post-NACT (p = 0.0002). Reduced MCPH1/BRIT1 expression correlated with longer overall survival (OS) pre- but not post-NACT (p = 0.017). Change in MCPH1/BRIT1 expression (from low-high) post-NACT was significantly correlated with better OS (p = 0.010). MCPH1/BRIT1 has previously been found to regulate p53 stability in BC cell lines. Notably, in this study a significant increase in MCPH1/BRIT1 staining was accompanied by a decrease in p53 staining in post-NACT samples (p < 0.0001).

In conclusion, these data support the idea that CC inhibitors targeting MCPH1/BRIT1 may sensitize BC cells to chemotherapy. Additionally, genes whose inhibition could promote cell death in MCPH1/BRIT1–deficient cells have been identified as potential therapeutic targets in tumours where MCPH1/BRIT1 expression or function has been compromised.

Table of Contents

List of Tables

List of Figures

Abbreviations

APAF-1	Apoptotic peptidase activating factor 1
AR	Androgen receptor
ATCC	American type culture collection
ATF	Activating transcription factor
ATM	Ataxia telangiectasia mutated kinase
ATR	Ataxia telangiectasia and Rad3-related
BAF	Barrier to autointegration factor
BAX	BCL2-associated X protein
BC	Breast cancer
BCOS	Breast cancer overall survival
53BP1	53 binding protein 1
BRCA1	Breast and ovarian cancer susceptibility protein 1
BRCA2	Breast and ovarian cancer susceptibility protein 2
BRCT	BRCA1 carboxyl-terminal
BRIT1	BRCT-repeat inhibitor of TERT expression
BRUCE	Baculoviral inhibitor of apoptosis repeat-containing Birc 6 Gene
BSA	Albumin bovine serum
BSTG	BioScreening Technology Group
CC	Chemical compounds
c-Jun	Jun Proto-Oncogene
Cal A	Calyculin A
cDNA	Complementary deoxyribonucleic acid
CGH	High-density array comparative genomic hybridization
CHK1	Checkpoint kinase 1
CI	Confidence interval
CPC	Chromosome passenger complex
CR	Complete response
CRISPR/CAS9	Clustered regularly interspaced short palindromic repeats/Cas9
Ct value	Cycle threshold value
DCIS	Ductal carcinoma in situ
ddH2O	Double distilled water
DM	Double minute
DMSO	Dimethyl sulfoxide
DNA	Deoxyribonucleic acid
DPBS	Dulbecco's phosphate buffered saline
DRAM	DNA damage regulated autophagy modulator
DSBs	DNA double-strand breaks
DSBs	DNA Double strands breaks
FASAY	Functional analysis of separated alleles in yeast
FCS	Fetal calf serum
FOXM1	Forkhead box M1
FT siRNA	Forward siRNA transfection
FUOS	Follow up overall survival
g	Gravitational
GGI	Genomic grade index
hPK	Human protein kinase
hUbq	Human ubiquitin
HEK293	Human embryonic kidney 293
HK 36B4 primer	Housekeeping gene 36B4 primer
HMECs	Human mammary epithelial cells
HR	Homologues recombination

hTERT	Human telomerase reverse transcriptase
4-OH-Cy	4-hydroxycyclophosphamide
HU	Hydroxyurea
IBC	Inflammatory breast cancer
ICE	Interleukin-1h converting enzyme
IDC	Invasive ductal carcinoma
IF	Immunofluorescence
IMCD3	Inner medullary collecting duct cell line
INCENP	Inner centromere protein
IRIF	Ionising radiation–induced foci formation
kDa	Kilodaltons
LNS	Lymph node status
LOF	Loss of function
LOH	Loss of heterozygosity
LVI	Lymphovascular invasion
MAD	Median absolute deviation
MAPT	Microtubule associated protein in tau
MDC1	Mediator Of DNA-damage checkpoint 1
MDM2	Murine double minute 2
MEFs	Mouse embryonic fibroblasts cells
miRNA	Micro RNA
Mol.Bio.H2O	Molecular biology grand water
MP	Master plate
MPF	M-phase promoting factor
MRI	Magnetic resonance imaging
mRNA	Messenger Ribonucleic acid
NACT	Neoadjuvant chemotherapy
NBS1	Nijmegen breakage syndrome Protein
NES	Nuclear export signal
Nibrin	NBS1Nibrin/Nijmegen Breakage Syndrome 1
NLS	Nuclear localisation signal
NT-siRNA	Non-targeting
NPI	Nottingham prognostic index
NR	No response
NTC	No template control
OA	Okadaic Acid
ORF	Open reading frame
OS	Overall survival
OSSC	Oral squamous cell carcinoma
OTE	Off target effect
OVCA	Ovarian cancer
PARP	Poly ADP ribose polymerase
PASK	Proline–alanine-rich Ste20-related kinase
PCNT	Pericentrin
pCR	Pathological complete response
PR	Partial response
pRB	Retinoblastoma protein
PVDF	Polyvinylidene difluoride membrane
qRT-PCR	Quantitative reverse transcription-polymerase chain reaction
RCF	Relative centrifugal force
RNase	Ribonuclease
RPM	Revolutions per minute
RS	Recurrences score
RT	Room temperature
RT siRNA	Reverse siRNA transfection
SAC	Spindle assembly checkpoint

siRNA	Small Interfering RNA (duplexes)
SMS	Small molecule screen
SSDB	Single-stranded DNA break
SSMD	Strictly standardised mean difference
STK39	STK39 serine threonine kinase 39
SWI/SNF	Switch/sucrose nonfermentable
3D	Three dimensional structure
TILs	Tumour-infiltrating lymphocytes
TMA	Tissue microarray
TopBP1	Topoisomerase (DNA) II binding protein 1
TS	Thymidylate synthase
TSG	Tumour suppressor gene
Tyr15	Tyrosine 15 phosphorylation
U	Unit
USP8	Ubiquitin-specific peptidase 8
USS	Ultrasound scan
UV	Ultra Violet
V	Volt
VRK1	Vaccinia-related kinases
WB	Western blotting
WSTF	Williams –Beuren syndrome transcription factor
3'-UTR	3'-untranlated region
WB	Western Blotting
WSTF	Williams –Beuren syndrome transcription factor)
3'-UTR	3'-untranlated region

Chapter 1 General introduction

1.1 MCPH1/BRIT1

Autozygosity mapping was Initially utilised to identify the first locus involved in primary microcephaly. This was *MCPH1/BRIT1*, which is positioned on chromosome 8p23 (Jackson *et al.*, 1998). Three years later, Jackson *et al.* (2002) reported that *MCPH1/BRIT1* was a causative inherited gene of primary microcephaly, encoding a protein called Microcephalin, which is involved in developing the cerebral cortex of human fetal brain.

1.1.1 Autosomal recessive primary microcephaly (MCPH)

Human MCPH is a neurodevelopmental disorder, clinically characterised by a remarkable reduction in brain size particularly affecting the cerebral cortex, which is at least 2 standard deviations below the mean for age and sex, and is associated with a mild to moderate mental retardation (Kaindl *et al.*, 2010) (Figure 1.1A). Twelve *MCPH* genes for microcephaly have been identified (Table 1.1).
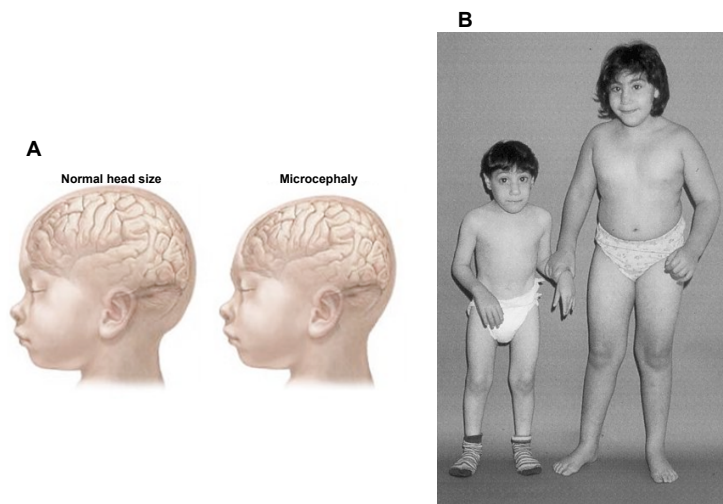
Figure 1.1. Phenotypic characterisation of primary microcephaly patients.
Image **(A)** shows the normal head size compared to reduced head size in microcephaly patient which is smaller than 2 SD below the mean. Image **(B)** shows two siblings at age 7 and 5 years old affected with premature chromosome condensation (PCC) syndrome, Source: Image A is adapted from http://www.nlm.nih.gov and Image B from (Neitzel *et al.*, 2002).

Table 1.1. Genetic heterogeneity causes (Loci, genes and protein) for autosomal recessive primary microcephaly disorder.

Source: adapted from (Kaindl, 2014; Barbelanne and Tsang, 2014; Faheem *et al.*, 2015).

Locus	Chromosomal location	Gene	Protein	Reference
MCPH1	8p23.1	*MCPH1/BRIT1*	Microcephalin	(Jackson *et al.*, 1998; Jackson *et al.*, 2002)
MCPH2	19q13.12	*WDR62*	WD repeat containing protein 62	(Roberts *et al.*, 1999)
MCPH3	9q33.2	*CDK5RAP2*	Cyclin dependent kinase 5 regulatory associated protein 2	(Moynihan *et al.*, 2000)
MCPH4	15q15.1	*CASC5*	Cancer susceptibility candidate 5	(Jamieson *et al.*, 1999)
MCPH5	1q31.3	*ASPM*	Abnormal spindle–like, microcephaly associated protein	(Pattison *et al.*, 2000)
MCPH6	13q12.12	*CENPJ*	Centromere protein J	(Bond *et al.*, 2005)
MCPH7	1p33	*STIL*	SCL/TAL1 interrupting locus	(Kumar *et al.*, 2009)
MCPH8	4q12	*CEP135*	Centrosomal protein 135	(Hussain *et al.*, 2012)
MCPH9	15q21.1	*CEP152*	Centrosomal protein 152	(Guernsey *et al.*, 2010)
MCPH10	20q13.12	*ZNF335*	Zinc finger protein 335	(Yang *et al.*, 2012)
MCPH11	12p13.31	*PHC1*	Polyhomeotic-like protein 1	(Awad *et al.*, 2013)
MCPH12	7q21.11	*CDK6*	Cyclin-dependent kinase 6	(Hussain *et al.*, 2013)

1.

2.

3.

MCPH1 +/+   MCPH1 +/+

MCPH1 -/-   MCPH1 -/-
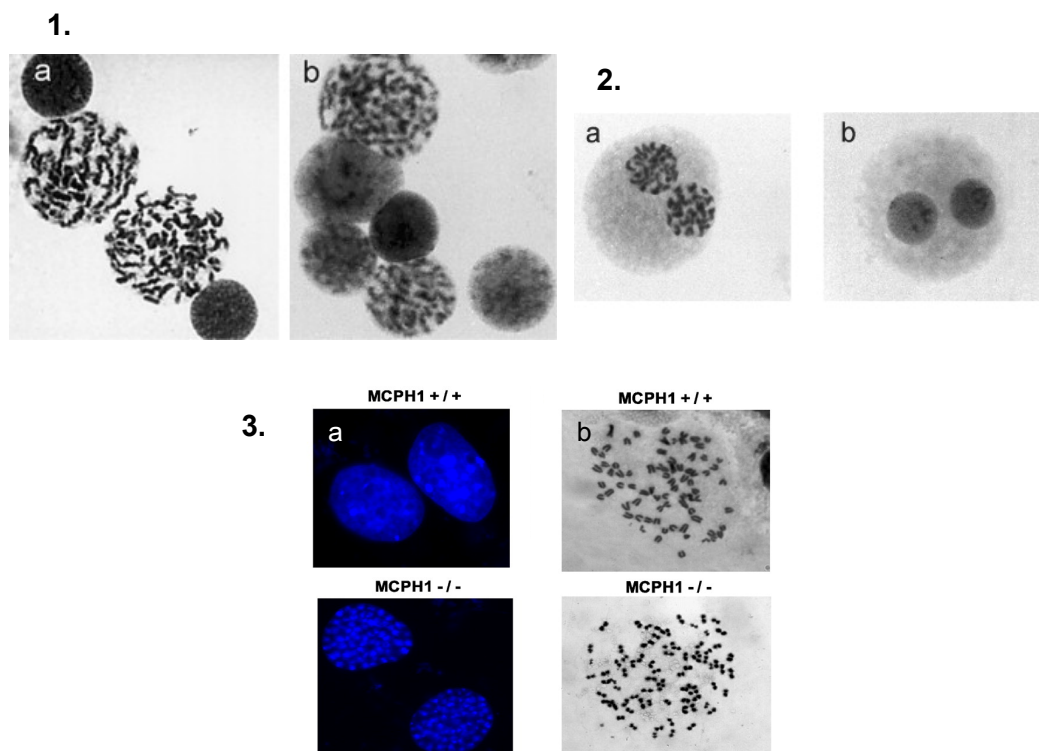
Figure 1.2. The morphology feature of premature chromosome condensation.
(Image 1) Peripheral blood lymphocyte samples from *MCPH1/BRIT1* primary microcephaly patients **(1a)** and PCC syndrome patients **(1b)** display prophase like cells with premature condensed chromosomes (PCC) in G2 phase. **(Image 2)** *MCPH1/BRIT1* mutated cells derived from these patients present a binucleated cells with a delay in chromosome decondensation in G1 phase as shown in **(2a)** compared to the control in **(2b)** showing the binucleated lymphoblastoid cell with decondensed chromosomes. **(Image 3)** PCC induced in a mouse embryonic fibroblast cells (MEFs) with *Mcph1/Brit1* knockout (*Mcph1/BRIT1$^{-/-}$*.) **(3a)** An example of DAPI staining of MEFs cells with the WT *Mcph1/Brit1$^{+/+}$* (Top) presenting normal prophase condensed DNA, with clusters of bright dots of heterochromatin regions whereas the *Mcph1/BRIT1$^{-/-}$* (Bottom) shows the PCC cells with a intense DAPI staining of abnormal dotted condensed chromosomes and unstained spaces in the nucleus. **(3b)** Shows the metaphase chromosome spreads in MEFs cells displaying the normal, long and thin chromosomal morphology in WT *Mcph1/Brit1$^{+/+}$* (Top) compared to the short, thick (dumpy) chromatids in *Mcph1/Brit1$^{-/-}$* (Bottom). Source: images 1 and 2 are adapted from (Trimborn *et al.*, 2004), image 3 is adapted from (Wood *et al.*, 2008).

The phenotypic features of *MCPH1/BRIT1* patients are thought to be related to uncontrolled cell division and high levels of apoptotic cells. Thus, a reduction in brain size may be a result of an abnormal cell cycle division and apoptosis. Mutation in *MCPH1/BRIT1* has also been found in patients with premature chromosome condensation (PCC) syndrome, which is characterized by microcephaly, short stature and premature chromosome condensation (Trimborn *et al.*, 2004) (Figure 1.1B). This finding demonstrates that both MCPH1/BRIT1 and PCC syndromes are allelic diseases. Cells derived from theses patients exhibited prophase like cells with misregulated chromosome condensation in G2 phase and delayed decondensation in G1 phase (Figure 1.2 /images 1a and 1b and

respectively), suggesting MCPH1/BRIT1 is involved in the regulation of chromosome condensation. The difference between the normal and/or abnormal chromosome condensations has been investigated by Wood *et al*. (2008) using a *Mcph1*/*Brit1* knockout mouse embryonic fibroblast (MEFs) model (Figure 1.2 images 3a and 3b).

Microcephalin plays an essential role to sustain cerebral cortex size via regulation of the division mode of neurogenic cells (Gruber *et al.*, 2011). *Mcph1*/*Brit1* knockout mice model revealed that MCPH11/BRIT1 deficiency abolishes the centrosome localization of CHK1, causing early activation of CDK1/CDC2 and premature entry into mitosis and apoptosis (Tibelius *et al.*, 2009). As a result, the abnormal orientation of mitotic spindles leads to a switch from neuroprogenitor (symmetrical) division mode, where division results in the production of two daughter neural progenitor cells (NPCs) to asymmetrical division where one NPC and one post mitotic neuron are created. This would lead to a decrease in the number of neurones. Experimentally, using U2OS cells, genetically silenced for CDC25B mediates the activation of CHK1 and CDK1/CDC2 to repress their uncontrolled functions and couple the centrosomal cycle with mitotic progression (Löffler *et al.*, 2006). Overall, MCPH1/BRIT1 has a critical role in mitotic spindle orientation and regulates neuroprogenitor proliferation through the CHK1- CDC25- CDK1/CDC2 pathway that leads to couple the mitosis with centrosome cycle and brain developmental.

1.1.2 *MCPH1*/*BRIT1* gene structure

The human *MCPH1*/*BRIT1 gene* contains 14 exons (90, 92, 119, 88, 115, 144, 90, 1155, 110, 38, 163, 78, 238 and 512bp in size) (Jackson *et al.*, 2002) (Figure 1.2a). It has genome size of 241,905 base pairs (bp) and an 8,032 bp open reading frame (Jackson *et al.*, 2002; Kaindl *et al.*, 2010). Four different transcripts of human *MCPH1*/*BRIT1* have been identified in 562T fibroblast cells (Gavvovidis *et al.*, 2012). These transcripts include the full length (FL) and the alternative isoforms Δe 9–14, Δe 1–3, and Δe 8 (Gavvovidis *et al.*, 2012).

1.1.3 MCPH1/BRIT1 protein domain structure

The human *MCPH1/BRIT1* gene encodes an 835 amino acid (aa) protein of 110 KDa molecular weight, called Microcephalin. Microcephalin consists of three BRCA1 carboxyl-terminal (BRCT) domains (Figure 1.3b).

a. Human *MCPH1/BRIT1* gene coding structure

b. Human MCPH1/BRIT1 protein domain structures
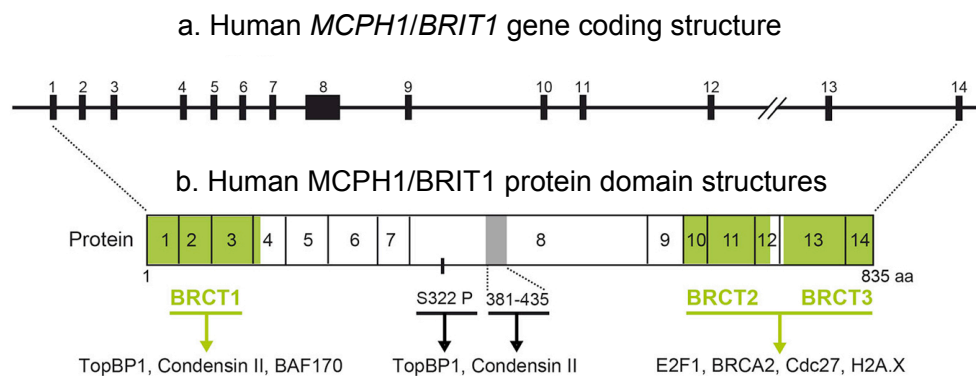
Figure 1.3. Gene coding and protein domain structure of human MCPH1/BRIT1.
(a) This represents the coding region (intron-exon structure) of *MCPH1/BRIT1* gene, which includes 14 exons displayed as bold black rectangles. **(b)** This shows the protein domain structures, containing three BRCT domains highlighted in green. Interactor proteins with the BRCT domains of MCPH1/BRIT1 are indicated below each domain. The middle IMPDH domain, including residues 381–435 (highlighted in grey), also interacts with condensin II. Also at the middle domain site, as shown, is essential for ATR phosphorylation of Ser322 (S322P) of MCPH1/BRIT1 for recruitment of topoisomerase (DNA) II binding protein 1 (TopBP1). Source: Image (a and b) is adapted from (Pulvers *et al.*, 2015).

The *N*-terminus BRCT1 domain extends from aa 7 to 83, the *C*-terminus BRCT 2 from aa 642 to 720 and the *C*-terminus BRCT 3 from aa 753 to 823 Jackson *et al.* (2002). BRCT domains, are phospho-peptide-binding amino acid tandem repeats found in BRCA proteins, such as BRCA1 and BRCA2, that are involved in cell cycle checkpoints and repair DNA damages (Huyton *et al.*, 2000; Gerloff *et al.*, 2012).

Microcephalin *N*-terminus domain is required for centrosomal localization in irradiated cells (Jeffers *et al.*, 2008). In addition, the *N*-terminal BRCT1 domain fragment (residues 1-195) has been found to interact with Condensin II to regulate DNA condensation (Figure 1.3b) (Yamashita *et al.*, 2011). Another fragment (residues 1-48) is essential for the recruitment of BAF170, a component of the ATP-dependent chromatin remodeling complex (switch/sucrose nonfermentable) (SWI/SNF). This promotes chromatin relaxation in DNA double strand breaks (DSBs) in an as yet poorly understood mechanism (Figure 1.3b) (Peng and Lin, 2009c; Peng *et al.*, 2009). The other two BRCT domains (BRCT 2 and 3) are localised at the *C*-terminal domain of Microcephalin protein (Figure 1.3b). The *C*-terminal BRCT 2/3 domains bind to several phosphorylated proteins, such as breast cancer susceptibility gene 1 (BRCA1) and the mediator of DNA damage checkpoint protein 1 (MDC1) (Bork *et al.*, 1997), mediating the interaction between MCPH1/BRIT1 and the γH2AX to induce foci formation in response to DNA damages (Wood *et al.*, 2007; Wood *et al.*, 2008; Jeffers *et al.*, 2008; Singh *et al.*,

2012a). The BRCT 2/3 domains of MCPH1/BRIT1 bind at the promoter of the transcription factor E2F1 to activate the transcription of *BRCA1* and *CHK1* (Yang *et al.*, 2008). Additionally, the interaction between the *C*-BRCT terminus domains of MCPH1/BRIT1 with the *N*-terminus of BRCA1 protein facilitates the localization of Rad51 at damage sites without influencing the formation of a BRCA2-Rad51 complex. However, this interaction activates the BRCA2-Rad51-dependent homologous recombination (HR) repair of DNA damage (Wu *et al.*, 2009). Moreover, the *C*-BRCT tandem domains interact with the cell division cycle protein 27 (Cdc27), a subunit of the anaphase- promoting complex (Singh *et al.*, 2012e). Individual downregulation of the endogenous MCPH1/BRIT1 FL and the transcript variant that lacks the two BCRT domains (Δe 9–14), using specific siRNA for each transcript, has no effect of chromosome condensation. Only the simultaneous depletion of these two transcripts has been found to induce PCC in HeLa cells, indicating their redundancy in preventing PCC (Gavvovidis *et al.*, 2012).

Microcephalin protein has one nuclear localization signal (NLS) motif and possesses a large middle IMPDH domain (Liang *et al.*, 2010g). A deletion in the NLS domain (residues 301-400 aa) of *MCPH1/BRIT1* in human embryonic kidney 293T cells (HEK293T) caused accumulation of MCPH1/BRIT1 in the cytoplasm and affected the localisation of the *C*-terminal domain to the nucleus, which prevents foci formation in response to DNA damage (Wood *et al.*, 2007). This is a canonical NLS sequence (RKRVSHGSH- SPPKEKCKRKR) spanning the region of the NLS domain from aa 355 to 375 which is thought to function as a regulator for MCPH1/BRIT1 localisation in the nucleus (Wood *et al.*, 2007).

Although the function of the IMPDH middle domain is not yet clarified, a fragment of the middle domain (aa 376–485) in exon 8 binds with condensin II (CAP-G2 subunit) as apart of the HR repair mechanism (Figure 1.3b) (Wood *et al.*, 2008; Yamashita *et al.*, 2011). The shape of metaphase chromosomes are thought to be regulated by binding of the *N*-terminal and middle domains of MCPH1/BRIT1 to CAP-D3 and CAP-G2 of condensin II, respectively (Yamashita *et al.*, 2011). Also ATR mediates the phosphorylation of Ser322 (S322P) in the middle domain of MCPH1/BRIT1 (Figure 1.3b) which is essential for recruitment of topoisomerase (DNA) II binding protein 1 (TopBP1) to maintain ATR signaling for DNA repair (Zhang *et al.*, 2014).

1.1.4 MCPH1/BRIT1 expression and cellular localisation

MCPH1/BRIT1 is mainly localised in the nucleus and is expressed at an elevated level in different human tissues such as the brain, liver, testes and pancreas (Liang *et al.*, 2010g; Lin *et al.*, 2010). MCPH1/BRIT1 transcripts are also expressed at high levels in fetal brain and kidney and at low levels in fetal heart and lungs (Jackson *et al.*, 2002).

A human breast cancer study in Dr. Sandra Bell's lab using immunohistochemistry (IHC) reported that detection of a high level of MCPH1/BRIT1 protein expression in placental tissue samples that were used as the control in a tissue microarray (TMA) slide. In the same lab, in normal breast tissue samples, MCPH1/BRIT1 expression was detected in the nucleus and nuclear foci and cytoplasm (Richardson *et al.*, 2011). Similarly, in primary cultures of normal ovarian samples, the localisation of MCPH1/BRIT1 expression has been detected in the nucleus and nuclear foci and in the cytoplasm (Bruning-Richardson *et al.*, 2011).

In their comparison of MCPH1/BRIT1 expression in human tissues, Venkatesh and Suresh (2014) summarised the localisation of MCPH1/BRIT1 in different cells lines. They reported for instance, that MCPH1/BRIT1 localises at the centrosomes in U2OS cell line (osteosarcoma) (Zhong *et al.*, 2006) and accumulates at DNA repair foci in U2OS cells (Rai *et al.*, 2006), HeLa cells (Wood *et al.*, 2007) and cells derived from *MCPH1/BRIT1* patients (Gavvovidis *et al.*, 2010).

1.1.5 PCC is a hallmark of MCPH1/BRIT1 mutation

1.1.5.1 PCC overview

Johnson and Rao (1970) were the first to describe the phenotype of PCC. Using ultra violet (UV) inactivated Sendai virus, they found that PCC occurs when two cells in different phases of the cell cycle fuse, when one of them was in mitosis. The morphology features of PCC during the cell cycle phases (G1, S, G2, and M) (Johnson and Rao, 1970) reveal the rate or level of chromosome condensation of PCC. For instance, the presence of early G1 phase increases chromatid condensation whilst all the late G1 cells show the significant extent of G1 PCC (Hittelman and Rao, 1978).

Hittelman *et al*. (1980) demonstrated that PCC is a useful tool for investigating cell division and chromosome structure in normal and cancerous cells during all phases of the cell cycle. In early G1 phase, the PCC chromosomes are long and single stranded. At G2, after DNA replication (S phase), they duplicate and become two identical chromatids that maintain their length when compared to prophase chromosomes. Experimentally, PCC phenotype is observed in the bone marrow cells (Hittelman and Rao, 1978).

Additionally, PCC has been identified in many types of human cancer such as breast and ovarian carcinoma (1.5-8.9% PCC) (Miles and Wolinska, 1973); leukemia (3.6% PCC) (Williams *et al.*, 1976); carcinoma of the bladder (Atkin, 1979); large bowel and colon cancer (6.6% - 6.9%) (Reichmann *et al.*, 1981; Reichmann and Levin, 1981). Human cervical carcinoma cells present PCC ranging from 1.5-8.9% and exhibit hyperdiploidy that may due to the induction of polyploidy. Thus, further analysis of patients with different stages of cancer with PCC may provide a clinical correlation with cytogenetic data (Sreekantaiah *et al.*, 1987).

PCC can be induced by the phosphatase inhibitors Okadaic Acid (OA) or Calyculin A (Cal A) (Kanda *et al.*, 1999; Alsbeih and Raaphorst, 1998), which can phosphorylate histone H3 at Ser10 in human leukemia-60 (HL-60) cells and in A599 cells (pulmonary carcinoma A). All these modifications are potentially related to the induction of the PCC phenotype.

1.1.5.2 Molecular feature of PCC during the cell cycle

Commencement of chromosome condensation relies on the completion of DNA replication and faithful repair of all genetic material errors that are produced during the S phase (Rybaczek and Kowalewicz-Kulbat, 2013). Thus, the normal cell cycle transition from S phase to G2 phase is controlled by the central kinases ATM (Ataxia telangiectasia mutated) and ATR (Ataxia telangiectasia and Rad3 related); these phosphorylate proteins to block cell progression in the event of an abnormal genetic structure or synthesis during or after DNA replication. They also maintain the activity of the M phase promoting factor (MPF), which is mainly based on the inactive state of the cycle dependent kinase (CDK1/CDC2) that is a principal factor in the mitotic initiation process.

In the normal cell cycle in the G2 phase, the active state of CDK1/CDC2 is induced by the phosphatase CDC25, which is necessary for commencement of chromosome condensation. The active state of CHK1 leads to phosphorylation of

the phosphatase CDC25 and subsequently its degradation, which is mediated by ubiquitin-dependent proteolysis, simplifying its removal from the nucleus. In addition, ATM and ATR can activate the WEE1 kinase, which is essential for preventing cell progression to G2 phase to facilitate DNA damage repair, suggesting the implication of WEE1 in the activation of CHK1 and CHK2. Therefore, the transition of incomplete DNA replication cells with aberration in the S phase checkpoint to G2 phase and with unrepaired post-replication errors could allow early initiation of mitosis, accompanied by a defect in the chromosome condensation process, leading to the generation of PCC cells. Thus, PCC cell chromosomes could be anticipated to show genetic aberrations and an abnormal morphology emerging in the form of deletions or breaks.

The response of cells to DNA damage leads to the activation of the ATR and ATM kinases by phosphorylation to CHK1 for single-stranded DNA (SSDB) and CHK2 for DNA double-strand breaks (DSBs), respectively. However, blocking the activity of ATR or/and ATM would diminish the ability of checkpoint kinases in both S and G2/M phases allowing premature mitosis. Indeed, treating cells with caffeine (CF) proved effective in inducing PCC. CF inactivates the ATR or/and ATM, preventing phosphorylation of their kinases' substrates (CHK1 and CHK2 respectively). As previously mentioned, this, in turn, causes a hyper-activation of phosphatase CDC25, triggering phosphorylation of CDK1/CDC2 to form a complex with Cyclin B and entering earlier into mitosis.

Progression into mitosis is required as a mechanism of chromosomal assembly and segregation which consists of precise chromosome condensation and the subsequent process of sister chromatids resolution. This allows for production of identical daughter cells with the same genetic materials (Nasmyth, 2002; Swedlow and Hirano, 2003). The principal molecules in these processes are Cohesion and condensin I and II proteins, Hirano *et al*. (2005) hypothesised that CDK1/CDC2-Cyclin A phosphorylates condensin II to initiate chromosome condensation within the prophase nucleus while CDK1/CDC2-Cyclin B activates condensin I, allowing its access into chromosomes after nuclear envelope breaks down. Phosphorylation of condensin II by CDK1/CDC2 is mediated by polo-like kinase 1 (PLK1) to initiate the DNA condensation and mitotic entry (Abe *et al*., 2011). The processes of chromosome assembly and segregation can be summarised as follows (Shintomi and Hirano, 2010; Nasmyth, 2002; Swedlow and Hirano, 2003): The replicated chromatids are linked together by Cohesion at the beginning of mitosis (prophase), Cohesion is released from the chromosome arms, allowing chromosome axis formation and the loading of the condensin into the

chromosome arms to induce condensation. This requires chromatin compaction to reduce the volume of DNA length by 10,000 - to 20,000-fold before chromosome segregation allows for the production of metaphase chromosomes. This mechanism is known as chromatin resolution. Finally, at the end of mitosis (early anaphase), the residual Cohesion that is already linked to the chromosome arms, is cleaved and removed, which allows for the separation of chromatids and subsequent chromosome segregation.

Phosphorylated histone H3 (pHH3) is another factor that is implicated in regulating chromosome condensation during mitosis (Hendzel *et al.*, 1997; Sauvé *et al.*, 1999). In mammalian cells, pHH3 at serine 10 (Ser10) is mediated by Aurora-B kinase and initiates at G2 phase in the pericentromeric heterochromatin regions; it then greatly increases and labels the entire length of the metaphase chromosome which then reduces in late anaphase and early telophase (Hendzel *et al.*, 1997). When interphase mammalian cells are fused with mitotic cells, PCC is induced and followed by an elevated level of pHH3 (Johnson and Rao, 1970; Hanks *et al.*, 1983). Van Hooser *et al.* (1998) found that pHH3 is essential for the initiation of chromosome condensation and for entry into mitosis, but may not be required for maintaining chromosome condensation. They reported that OA-induced PCC during S phase is associated with pHH3 but the metaphase chromosome morphology did not develop. This may mean that the protein kinase that phosphorylates histone H3 is required for regulation of chromatin structure modification throughout cell cycle progression but may not be required for the condensation (Van Hooser *et al.*, 1998).

1.1.5.3 MCPH1/BRIT1 plays a vital role in chromosome condensation regulation

As mentioned previously (Section 1.1.1) *MCPH1/BRIT1* and PCC patients exhibit some identical clinical symptoms alongside their distinctive cellular phenotype known as PCC (Jackson *et al.*, 1998; Jackson *et al.*, 2002; Neitzel *et al.*, 2002). Thus, this evidence suggests that MCPH1/BRIT1 mutations lead to the disruption of the functioning of the Microcephalin protein and hence PCC could be a surrogate marker for MCPH1/BRIT1 aberrations (Trimborn *et al.*, 2004).

The unique feature of MCPH1/BRIT1 deficient cells is that they exhibit a large number of prophase-like PCC cells (10-20%) compared to <1% in controls using peripheral blood cells of patients' samples during the routine cytogenetic

preparation (Neitzel *et al.*, 2002; Trimborn *et al.*, 2004). This is also the case for cell lines such as SV40-transformed fibroblast (LN9SV) and HeLa cells when transfected with siRNA against *MCPH1/BRIT1* (Trimborn *et al.*, 2004; Trimborn *et al.*, 2006). PCC is a consequence of early mitotic entry when cells begin mitosis before completing DNA replication (Trimborn *et al.*, 2004). When Trimborn *et al.* (2004) used a siRNA-mediated depletion of *MCPH1/BRIT1* to reproduce the PCC phenotype that also showed delayed decondensation in early G1 phase (post-mitosis) using cytochalasin-B block. This study provided strong support for the argument that MCPH1/BRIT1 plays an essential role in both neurodevelopment and chromosome condensation regulation.

Chromosome condensation is a fundamental step that ensures proper mitotic entry. MCPH1/BRIT1 is an essential protein that prevents PCC (Richards *et al.*, 2010). Depletion of condensin II*,* but not condensin I*,* using siRNA has been shown to reverse the abnormal PCC phenotype in *MCPH1/BRIT1* primary microcephaly patient cells (Trimborn *et al.*, 2006). Indeed, the MCPH1/BRIT1 *N*-terminus domain was found to be a key factor in inhibiting premature loading of condensin II onto the chromosome, preventing early entry into mitosis and confirming the principle role of condensin II in PCC induction in MCPH1/BRIT1 deficient cells (Trimborn *et al.*, 2006; Yamashita *et al.*, 2011).

The *N*-terminal BRCT domain of MCPH1/BRIT1 has a hydrophobic pocket that is structurally in a position equivalent to the phosphate peptide binding sites in BRCT proteins that play a vital role in protein-protein interactions. This may mean that this pocket is required for protein interactions, which are necessary for regulating normal chromosome condensation (Richards *et al.*, 2010). The same authors experimentally demonstrated that MEFs cells with *Mcph1/Brit1* knockout showed caused 30-40% PCC. This percentage was greatly reduced when full-length MCPH1/BRIT1 was expressed, but not in conditions with the mutant lacking the *N*-terminus domain, confirming the substantial role which this domain plays in rescuing normal chromosome condensation.

Mutations in the *N*-terminal pocket had no effect on the MCPH1/BRIT1 *C*-terminal BRCT domain's function in localization at γ-H2AX foci after IR, indicating that the *N*-terminal BRCT domain may not be involved in DNA repair (Wood *et al.*, 2007; Wood *et al.*, 2008; Leung *et al.*, 2011). However, the *N*-terminal BRCT domain may interact with undefined proteins to regulate chromosome condensation. As previously mentioned, there is an association between PCC induction and the misregulated function of condensin II in *MCPH1/BRIT1* patients

(Trimborn *et al.*, 2006). This observation has led to investigations of the association between MCPH1/BRIT1 and condensin II. Interestingly, the middle IMPDH region of MCPH1/BRIT1 that mediates the interaction with condensin II (CAP-D3 sub-unit) has been found not to regulate chromosome condensation or prevent PCC, but this interaction is required to regulate the HR repair efficiency although there is no obvious impact of condensin II on G2/M checkpoint control (Wood *et al.*, 2008).

However, Leung *et al*. (2011) have demonstrated that the SET oncogene protein binds directly to the *N*-terminal BRCT domain of MCPH1/BRIT1. Both MCPH1/BRIT1 and SET play a vital role as negative regulators of condensin II and in regulating chromosome condensation. Thus, a high percentage of abnormal metaphase chromosome condensation is observed with *SET* siRNA knockdown in human H1299 (human non-small cell lung carcinoma) cells. PCC phenotype in H1299 cells is partially alleviated when the sub-unit of condensin II, CAP-D3, was depleted by siRNA. A similar result is obtained in MCPH1/BRIT1 deficient MEFs cells.

Interestingly, *MCPH1*/*BRIT1* patients with a marked PCC phenotype, exhibit a normal G2/M checkpoint after IR, normal chromosomal breakage and sufficient localization of all DNA repair proteins induced foci formation that normally interact with MCPH1/BRIT1, preventing any progression of damaged cells into mitosis (Neitzel *et al.*, 2002; Gavvovidis *et al.*, 2010). This means that cells with *MCPH1*/*BRIT1* gene mutations differ significantly in their response to DNA damage compared to the response of cells with *MCPH/BRIT1* siRNA or mice *Mcph1/Brit1* depleted cells. These results are potentially related to the degree of chromatin condensation associated with different *MCPH1*/*BRIT1* mutations. Therefore, the type and location of mutation in *MCPH1/BRIT1* may reflect their sensitivity to DNA damage agents. The DNA damage response in *MCPH1*/*BRIT1* patients is not highly impaired, potentially explaining the absence of cancer development in these patients (Gavvovidis *et al.*, 2010). For example, it has been confirmed that a mutation in the *N*-terminal domain at Ser 25 (S25X) (Alderton *et al.*, 2006) has an alternative translation start site for MCPH1/BRIT1 transcript in *MCPH1*/*BRIT1* S25 X patient cells which allows the truncated MCPH1/BRIT1 protein to be made, despite the partial deletion of the *N*-terminal domain. It has been suggested that the truncated protein within this mutation functions in the DNA damage response (Leung *et al.*, 2011).

1.1.6 MCPH1/BRIT1 functions

Since the MCPH1/BRIT1 protein containing conserved BRCT domains has been found to be implicated in the regulation of different cellular processes such as chromatin condensation, cell cycle checkpoints, DNA damage response, DNA repair and apoptosis (Figure 1.4). Here, all these functions will be described briefly.
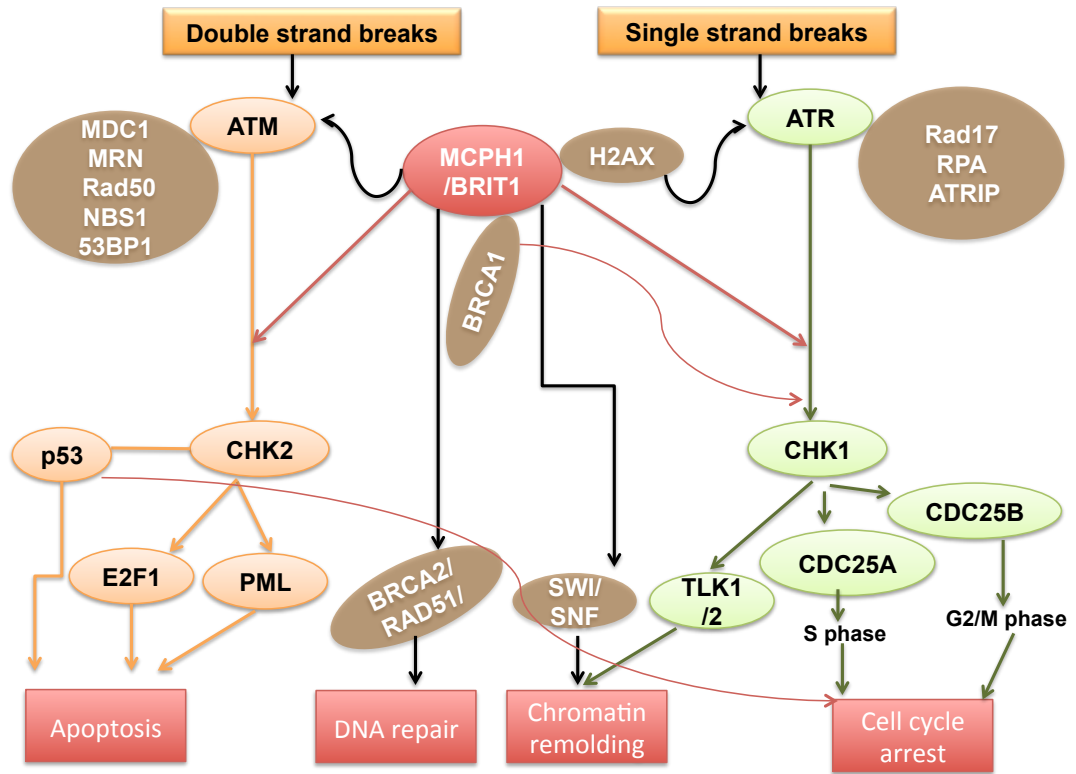
Figure 1.4. MCPH1/BRIT1 functions.
MCPH1/BRIT1 is involved in multiple cellular pathways **(A)** MCPH1/BRIT1 is involved in apoptosis by interacting with E2F1 leading to up-regulate activity of pro-apoptotic related genes. **(B)** MCPH1/BRIT1 plays a role in DNA damage response by interacting with H2AX to localise other DNA repair genes at damage sites to induce foci formation. **(C)** MCPH1/BRIT1 interacts with the SWI/SNF complex to facilitate chromatin relaxation and increasing the accessibility of DNA repair proteins. **(D)** It controls cell cycle checkpoints at G1/S and G2/M by regulating the expression of BRCA1 and CHK1 and stability of p53 expression.

1.1.6.1 MCPH1/BRIT1 and cell cycle checkpoint control

DNA damage requires sufficient time to repair, therefore the cell cycle checkpoints control systems delay cell cycle progression (Zhou and Elledge, 2000). MCPH1/BRIT1 plays a novel role in regulating the ATM/ATR signalling pathways and activating BRCA1 expression (Lin *et al.*, 2005; Xu *et al.*, 2004), leading to regulation of the intra-S phase checkpoint (Chaplet *et al.*, 2006).

Additionally, MCPH1/BRIT1 plays a vital and distinct role in controlling the G2/M checkpoint (mitotic entry), via the activation of ATM or ATR pathways and regulation of the expression of BRCA1 and CHK1 (Zhou and Elledge, 2000; Alderton *et al.*, 2006). Phosphorylation of BRCA1 via ATM is essential for mediating S phase checkpoint arrest after IR (Cortez *et al.*, 1999). Moreover, It has been found that the absence of MCPH1/BRIT1 leads to a reduced level of BRCA1 and CHK1 as well as little NBS1 (Nijmegen Breakage Syndrome 1 (Nibrin)) phosphorylation. As a result, defective checkpoint arrest of both intra S-phase and G2/M phase occurs (Lin *et al.*, 2005; Xu *et al.*, 2004). A high percentage of U2OS cells with *MCPH1/BRIT1* siRNA knockdown achieve mitotic entry after IR; these cells were not sensitive to ionizing radiation (IR) and preserve their DNA synthesis increasing the level of pHH3 Ser10, confirming a defective G2/M arrest (Lin *et al.*, 2005; Xu *et al.*, 2004). In addition, the cells derived from patients with chronic myeloid leukaemia (CML) display a defective G2/M arrest when exposed to hydroxyurea (HU) (Giallongo *et al.*, 2010). ATR is required to function in regulating CHK1 during G1/S phase undergoing DNA damage in U2OS cells; thus loss of p53 leads to ATR dysfunction and subsequent induction of PCC (Nghiem *et al.*, 2001). Therefore, MCPH1/BRIT1 functions downstream of CHK1 in the ATR pathway, controlling Cdc25A stabilization and regulation of the G2/M phase after DNA damage (Alderton *et al.*, 2006).

MCPH1/BRIT1 functions independently to activate phosphorylation of CDK1/CDC2-Cyclin B that is required for mitotic entry (Alderton *et al.*, 2006). Thus, the clinical characterisations of MCPH patients harbouring *MCPH1*/*BRIT1* gene mutation have not been linked to the deficiency in the transcription of CHK1 and BRCA1 that are regulated by MCPH1/BRIT1 since lymphoblastoid cells derived from these patients displayed intact ATR signalling and normal CHK1 activity. However, Alderton *et al.* (2006) have demonstrated that *MCPH1*/*BRIT1* mutant cells exhibit a low level of phosphorylated tyrosine 15 (Tyr15) of CDK1/CDC2 phosphorylation in S and G2 phases, leading to premature entry into mitosis and PCC. Experimentally, *MCPH1*/*BRIT1*-deficient primary microcephaly patient cells showed unchangeable levels of CDC25A companied with undiminished levels of chromatin-bound CDC45, (a protein which has a role in initiating DNA replication and is regulated by the activity of CDC25A in S phase), decreased levels of CDK1/CDC2–Cyclin B complex, leading to PCC (Donzelli and Draetta, 2003; Costanzo *et al.*, 2000; Bell and Dutta, 2002; Tercero *et al.*, 2000; Alderton *et al.*, 2006). Continual DNA synthesis was demonstrated in the absence of MCPH1/BRIT1 after cellular exposure to IR, confirming deficient intra-S checkpoint

control (Chaplet *et al.*, 2006). When cells are exposed to IR, ATM responds and triggers CHK2, resulting in DNA synthesis arrest. CHK2 phosphorylates CDC25A, leading to its proteasome-mediate degradation. Degradation of CDC25A prevents CDK11/CDC2-Cyclin B complex activity, leading to discontinued DNA synthesis throughout DNA repair (Abraham, 2001; Margolis and Kornbluth, 2004).

Overall, MCPH1/BRIT1 overlaps either dependently with the ATR-signalling pathway to control CDC25A, or it has an ATR–independent role to regulate the activity of the CDK1/CDC2-Cyclin B complex (Alderton *et al.*, 2006). Both CDC25A and CDK1/CDC2 contribute to the regulation of mitotic entry and the control of BRCA1 and CHK1 expression (Lin *et al.*, 2010). Finally, MCPH1/BRIT1 has a vital role in controlling the G2/M checkpoint (Alderton *et al.*, 2006); however, its function in mitotic entry is distinct from the down regulation of CHK1 and BRCA1 protein expression as their expression was not affected by MCPH1/BRIT1 mutation in MCPH1 patients' cells (Xu *et al.*, 2004; Lin *et al.*, 2005). Potentially, MCPH1/BRIT1 may function in the regulation of the gene expression of CHK1 and BRCA1 similarly to regulation the expression of genes implicated in cell checkpoints or DNA repair such as BRCA1 and MDC1 (mediator of DNA damage checkpoint protein 1). Thus, as previously mentioned (Section 1.1.3), in the response to DNA damage, the *C*-terminal of MCPH1/BRIT1 interacts with γH2AX for recruitment of BRCA1 and MDC1 at the DNA damage site, suggesting that MCPH1/BRIT1 is involved in the DDR mechanism (Xu *et al.*, 2004; Lin *et al.*, 2005; Wood *et al.*, 2007), which will be explained in more detail below (Section 1.1.6.3).

1.1.6.2 MCPH1/BRIT1 and centrosome stability

MCPH1/BRIT1 localises at the centrosome in interphase then co-localises with γ-tubulin during metaphase (from prophase to telophase) in U2OS and HeLa cells, suggesting the existence of MCPH1/BRIT1 centrosomal function (Zhong *et al.*, 2006). The *N*-terminal BRCT domain of MCPH1/BRIT1 accumulates at the centrosome.

Combining the two components MCPH1/BRIT1 and MDC1 and their localisation with γ-tubulin has been found to form integral components of centrosomes, which are required for regulation of centrosomal duplication during mitosis (Rai *et al.*, 2008); thus, defects in any one of these components can lead to centrosome aberrations. MCPH1/BRIT1 depleted U2OS cells present the mis-orientation of mitotic spindles leading to mitotic failure with lagging chromosomes. As a result, MCPH1/BRIT1 deficient cells exhibit defective cytokinesis and

production of a single polyploidy cell (Rai *et al.*, 2008). Depletion of MCD1 leads to centrosome amplification, aneuploidy, multipolar mitotic spindles, chromosome mis-segregation and generation of aneuploid cells (Rai *et al.*, 2008). Additionally, MCPH1/BRIT1 and pericentrin (PCNT) are required to prevent premature entry into mitosis by regulating the localisation of CHK1 at the centrosome for subsequent regulation of CDK1/CDC2-Cyclin B activity (Tibelius *et al.*, 2009). Thus, the centrosomal activity of CDK1/CDC2-Cyclin B complex is vital for timely regulation and for subsequent and proper controlling of cytoplasmic and nuclear mitotic events (Venkatesh and Suresh, 2014; Tibelius *et al.*, 2009). The absence of centrosome-associated CHK1 in MCPH1/BRIT1 patient cells leads to the failure to promote proteasomal degradation of CDC25B phosphatase. Inhibitory of CDC25B phosphatase causes early activation of CDK1/CDC2-Cyclin B complex and prevents inhibitory phosphorylation of Tyr15 on CDK1/CDC2 triggering PCC (Alderton *et al.*, 2006). Therefore, *MCPH1/BRIT1* mutant cells induced PCC cells, which display a low level of p-Tyr15-CDK1-CDC2 (Alderton *et al.*, 2006).

Overall, MCPH1/BRIT1 has a vital role to play in organizing centrosome integrity, spindle assembly, via its function in the CHK1-CDC25-CDK1/CDC2 pathway, which regulates proper mitotic entry with normal spindle formation and segregation (Alderton *et al.*, 2006; Tibelius *et al.*, 2009; Gruber *et al.*, 2011). The centrosomal function of MCPH1/BRIT1 also has been found to promote genomic stability and suppress malignant transformation (Rai *et al.*, 2008).

1.1.6.3 Role of MCPH1/BRIT1 in DNA repair in response to DNA damage

Various studies have reported that MCPH1/BRIT1 is a key regulator in the DDR pathways at multiple levels. MCPH1/BRIT1 has been considered to be an important factor in response to DNA damage by regulating the two kinases ATM and ATR (Rai *et al.*, 2006)..

Localization of MCPH1/BRIT1 at DNA damaged sites is dependent upon the *C*-terminal BRCT domains (Wood *et al.*, 2007), which when interacting with the BRCT domains of phosphorylated (γH2AX), (but not TP53BP1 or MDC1), forms nuclear foci at sites of DNA DSBs (Wood *et al.*, 2007; Jeffers *et al.*, 2008). Experimentally, Wood et al. (2007) have used MEFs that lacked a variety of DNA damage checkpoint proteins such as ATM, NBS1, 53PB1, MDC1, and H2AX. The study observed that phosphorylated H2AX plays an important role in the formation

of MCPH1/BRIT1 foci following IR (Lin *et al.*, 2005; Rai *et al.*, 2006; Wood *et al.*, 2007; Wood *et al.*, 2008). Tyrosine 142 (Tyr142) and serine 139 (Ser 139) of the *C*-terminal H2AX are phosphorylated by the transcription factor WSTF (Williams–Beuren syndrome transcription factor) and the kinases ATM and ATR, respectively in response to DSBs (Singh *et al.*, 2012a). Interestingly, MCPH1/BRIT1, an early DDR protein, has emerged as a versatile sensor that mediates these signal modifications of H2AX phosphorylation (Singh *et al.*, 2012a; Shao *et al.*, 2012). MCPH1/BRIT1 has been found to form ionizing radiation induced foci (IRIF) in chicken cells deficient in ATM, BRCA1, but not in H2AX deficient cells, confirming the essential interaction between the *C*-terminal BRCT domain of MCPH1/BRIT1 and γH2AX in cellular response to DNA damage (Jeffers *et al.*, 2008).

This interaction is essential for co-localisation of MCPH1/BRIT1 with other DNA damage proteins, such as MDC1, TP53BP1, NBS1, p-ATM, ATR, p-RAD17 (RAD17 homolog (*S. pombe*)) and RPA34 (DNA-directed RNA polymerase I sub-unit RPA34) (Rai *et al.*, 2006). All of these regulate cell cycle checkpoints (CHK1 and CHK2) (Wood *et al.*, 2007) and DNA repair (Seviour and Lin, 2010) by recruiting repair proteins to sites of damaged DNA to induce foci formation in U2OS cells. Thus, MCPH1/BRIT1 deficiency prevents IR induced phosphorylation of TP53BP1, MDC1, and NBS1. In addition, it abolishes the ATR phosphorylation of RPA34 and decreases the level of RAD17 phosphorylation (Rai *et al.*, 2006).

MCPH1/BRIT1 is involved in modulating chromatin structure during DNA repair. Chromatin structure limits the access of some specific enzymes during DNA development (Morrison *et al.*, 2004; Falbo and Shen, 2006). Thus, chromatin modification plays an essential role in regulating various processes during DNA repair, controlling the activation or inhibition of genes (Morrison *et al.*, 2004; Falbo and Shen, 2006). MCPH1/BRIT1 plays a fundamental role in regulating the ATP-dependent chromatin remoulding complex SWI/SNF (switch/sucrose non-fermentable) during DNA repair (Peng *et al.*, 2009; Peng and Lin, 2009a; Peng and Lin, 2009c). After DNA damage, high-level interactions occur between MCPH1/BRIT1 and the BAF170 and BAF155 sub-units of the SWI/ SNF complex, which are mediated via ATM/ATR dependent phosphorylation of BAF170 (Peng *et al.*, 2009). MCPH1/BRIT1 therefore functions as a tie that facilitates the recruitment of SWI/SNF to DNA DSB sites to regulate chromatin relaxation, allowing access of other essential proteins, such as RAD51, NBS1, MDC1, 53BP1, ATM, ATR, and RPA, to DNA damage sites during DNA repair (Peng *et al.*, 2009; Lin *et al.*, 2010). All the previous studies confirm the essential role of MCPH1/BRIT1 in maintaining genomic integrity by its interaction with γH2AX and subsequent recruitment to

DSBs, which is essential for chromatin relaxation during the DNA repair process. Experimentally, the mechanism of recruitment of MCPH1/BRIT1 at DNA damage sites has been investigated to reveal the involvement of BRUCE (the baculovirus inhibitor of apoptosis protein repeat (BIR)-containing ubiquitin-conjugating enzyme) and USP8 (ubiquitin-specific peptidase 8), in the regulation of MCPH1/BRIT1-SWI/SNF DSB–response pathway (Ge *et al.*, 2015). Ge *et al.* (2015) showed that, under un-stimulated conditions, MCPH1/BRIT1 is attached to and ubiquinated with K36-linked polyubiquitin chain, which often plays a role in signalling transduction (Pickart and Fushman, 2004). Thus, MCPH1/BRIT1 de-ubiquination requires BRUCE and USP8 activity that promotes its recruitment to the DNA damage site via γH2AX (Ge *et al.*, 2015).

Moreover, DNA DSB repair depends on two pathways: HR and NHEJ (Bassing and Alt, 2004). As previously mentioned that MCPH1/BRIT1 has been identified as functioning via HR, using condensin II (Wood *et al.*, 2008), and NHEJ pathways to repair DNA DSBs. MCPH1/BRIT1 plays an essential role in HR at DSB sites, regulating the localization of RAD51 to DNA lesion sites (Wu *et al.*, 2009; Peng and Lin, 2009a; Liang *et al.*, 2010a). Binding of MCPH1/BRIT1 to RAD51 is mainly dependent on the interaction of the *C*-terminal domain of MCPH1/BRIT1 with the *N*-terminal domain of BRCA2, and this interaction mediates the HR DNA repair activity of the BRCA2-RAD51 complex (Wu *et al.*, 2009). Peng *et al.* (2010) have generated a mouse *Mcph1/Brit1* knockout model which demonstrated that depletion of *Mcph1/Brit1* results in extreme sensitivity to IR, chromatid breaks and decreased RAD51 foci formation which indicated the specific function of MCPH1/BRIT1 in HR DNA repair (Liang *et al.*, 2010a). Moreover, productivity of NHEJ repair decreases with depletion of MCPH1/BRIT1, confirming the implication of MCPH1/BRIT1 in both HR and NHEJ mechanisms (Peng *et al.*, 2009).

Overall, the interaction between human MCPH1/BRIT1 and the BRCA2/RAD51 complex enables recruitment to DSBs sites (Wu *et al.*, 2009; Lin *et al.*, 2010). Mcph1/Brit1 deficient mice have shown a significant reduction in the recruitment of RAD51 and BRCA2 at damaged DNA sites while their protein levels remain unaltered (Liang *et al.*, 2010a). Consequently, MCPH1/BRIT1 regulates the presence of the RAD51/BRCA2 complex at DNA damage sites (Wu *et al.*, 2009; Liang *et al.*, 2010a), indicating the fundamental role of MCPH1/BRIT1 in maintaining genomic stability.

1.1.6.4 The role of MCPH1/BRIT1 in cancer progression

Since MCPH1/BRIT1 plays a fundamental role in DNA repair and cell cycle checkpoints, any cellular errors in one of these mechanisms may lead to genomic instability and cancer development (Rai *et al.*, 2006; Liang *et al.*, 2010a). The presence of *MCPH1/BRIT1* mutation in various types of human cancers suggests the involvement of MCPH1/BRIT1 deficiency in tumorigenesis. Indeed, MCPH1/BRIT1 is located at chromosome 8p32.1, a region which is frequently deleted in breast, ovarian, prostate (Rai *et al.*, 2006), liver (Lu *et al.*, 2007)*,* head and neck cancers (Bockmühl *et al.*, 2001) and coreloctal carcinoma (Fujiwara *et al.*, 1993).

Centrosome amplification and aberrant mitotic spindles are associated with genomic instability and tumour progression in breast and ovarian cancer (D'Assoro *et al.*, 2002; Hsu *et al.*, 2005). MCPH1/BRIT1 protein level was significantly decreased in 7/10 (70%) BC samples compared to normal breast tissue (Rai *et al.*, 2008). Rai *et al.* (2008) also reported that reduced MCPH1/BRIT1 in 12% of cells in BC samples was correlated with overexpression of PLK1 at the midbody in the absence of MCPH1/BRIT1 staining. MCPH1/BRIT1 has been found to be a negative regulator of Aurora A and PLK1, leading to the overriding of the activated spindle assembly checkpoint and therefore permitting mitotic entry (Rai *et al.*, 2008). This finding confirms the association between centrosome aberration, cancer progression and genomic instability (Lingle *et al.*, 2002; Nigg, 2002; Salisbury *et al.*, 2004; Fukasawa, 2005). BC samples with low level of MCPH1/BRIT1 protein develop metastases in a shorter time compared to those with normal or high MCPH1/BRIT1 expression (Rai *et al.*, 2006; Rai *et al.*, 2008). Collectively Rai *et al.* (2008) experimentally proved the link between centrosome/cytokinesis abnormalities and cancer progression and how MCPH1/BRIT1 expression is essential for restricting the development of cancer.

Recurrent heterozygous *MCPH1/BRIT1* mutation was significantly associated with increased BC susceptibility in familial (5/145; *p* = 0.003) and unselected (16/1150; *p* = 0.016) cases (Mantere *et al.*, 2016). Additionally, another study has been conducted, to evaluate the expression of DNA response proteins and investigate their contributions in familial and sporadic BC predisposition (Partipilo *et al.*, 2016). MCPH1/BRIT has been found in 125 sporadic cases (50 cases with negative and 75 cases with positive MCPH1/BRIT1 expression) and 72 familial (47 cases with negative and 25 cases with positive MCPH1/BRIT1 expression) BC. This suggests that PARP inhibitors may be preferable for tumours with

MCPH1/BRIT deficiency. However, Mantere *et al*. (2016) have demonstrated that MCPH1/BRIT1 depleted MCF7 BC and normal breast MCF10A cell lines showed a modest sensitivity to a PARP inhibitor, suggesting that the function of MCPH1/BRIT1 in DNA damage response may slightly different from those directly implicated in DSB repair via HR mechanism. Thus, addition of PARP inhibitors to the systemic chemotherapy regimen to sensitise sporadic or familial BC with defective function of MCPH1/BRIT1 may not significantly improve patient survival.

Additionally, utilising high-density array comparative genomic hybridization (CGH) reveals that a reduction in *MCPH1/BRIT1* DNA copy number has been detected in 37/52 breast cancer cell lines (72%) and 35/87 of advanced epithelia ovarian cancer cases (40%) (Rai *et al.*, 2006). The BC cell lines show a decrease in the mRNA and protein levels compared to normal breast epithelial cells such as human mammary epithelial cells (HMECs), MCF10A and MCF10F. Sequence analysis of the *MCPH1/BRIT1* coding region in 10 BC cases reveals a deletion in exon 10 in one patient. This resulted in a premature stop codon and consequently affects DDR as this mutation positions on the *C*-terminal domain of *MCPH1/BRIT1* (Jeffers *et al.*, 2008; Venkatesh and Suresh, 2014; di Masi *et al.*, 2011).

Abnormalities in cell proliferation and uncontrolled DDR are common characteristics in cancer development (Chaplet *et al.*, 2006). Normal somatic cell division is controlled by the very low activity of the catalytic sub-unit of the human telomerase reverse transcriptase gene (hTERT). MCPH1/BRIT1 is also known as BRCT-repeat inhibitor of TERT expression, which has been found to negatively regulate hTERT in somatic cells (Lin and Elledge, 2003). Shi *et al*. (2012) have identified the mechanism of MCPH1/BRIT1 repression of hTERT activity as directly binding to the hTERT proximal promoter, causing decreased expression levels of hTERT and telomerase activity in U2OS cells.

MCPH1/BRIT1 defects can be a useful pathological candidate for identifying the stages of cancer development. MCPH1 expression levels decreased in 19/30 (63%) of ovarian cancer cases. Conversely, an elevated expression level of MCPH1/BRIT1 in the nucleus is associated with low-grade tumours and was linked with better patient survival (Richardson *et al.*, 2011).

Reduced MCPH1/BRIT1 (mRNA/protein) expression and overall alteration (deletion/methylation) have been detected in 121/126 BC cases (96%) (Bhattacharya *et al.*, 2013). Alteration of MCPH1/BRIT1 was correlated with negative ER status (p = 0.004) and a similar result was observed in patients with MCPH1/BRIT1 methylation (p = 0.01). The co-alteration of MCPH1/BRIT1 with

ATM was significantly correlated with high tumour grade (p = 0.003-0.0.05). Patients with either alteration of MCPH1/BRIT1 alone or with co-alteration of MCPH1/BRIT1-ATM did not respond effectively to DNA-interacting drugs and/or radiation, showing a poor survival outcome (p = 0.01-0.05) (Bhattacharya *et al.*, 2013).

A study performed using oral squamous cell carcinoma (OSCC) showed that loss of heterozygosity (LOH) was observed in 14/71 (19.72%) cases (Venkatesh *et al.*, 2013). Additionally, a low level of MCPH1/BRIT1 promoter methylation was detected in 4/40 OSCC samples (10%). Studies performed on OSCC and renal cancer samples reveal that the three prime untranslated region (3'-UTR) of *MCPH1*/*BRIT1* accommodates two non-overlapping functional seeded regions for micro RNA (miRNA -27a), which is found to negatively regulate MCPH1/BRIT1 protein level (Venkatesh *et al.*, 2013; Wang *et al.*, 2014a). Overexpression of MCPH1/BRIT in human cervical cancer cell line (SiHa) inhibits the tumour cellular growth by activating the S phase arrest and stimulating different cell cycle-related proteins such as CDK2/CDC1-Cyclin A complex, CDK1/CDC2-Cyclin B and p53/p21(Mai *et al.*, 2014). Furthermore, the mitochondrial apoptosis pathway including proteins such as p53, Bcl-2, cytochrome *c*, and PARP-1, were activated in response to MCPH1/BRIT1 up regulation (Mai *et al.*, 2014). Activating these cellular pathways by MCPH1/BRIT1 leads to inhibited cell invasion and migration.

Overall, MCPH1/BRIT1 deficiency is related with tumorigenesis and genomic instability; thus its expression may be essential for improving the response to anti-cancer therapy and subsequently, the increase in the rate of patient survival.

1.2 Breast cancer (BC)

1.2.1 Female breast (mammary glands) anatomy

The healthy female breast (known in medicine as the mammary glands) consists of three fundamental parts, namely the adipose tissue (fat cells), the lobes, lobules and milk ducts (the areas where the BC usually starts to grow) (Figure 1.5). The third part is the lymph system (which is a part of the immune system and consists of a network of lymph vessels and nodes. The lymph vessels transport fluids and disease and/or fighting infection and protecting cells. Lymph nodes are located in areas throughout the lymph system, clustering principally in the armpits (axilla), neck and groin areas. They function as filters removing abnormal cells from

healthy tissue) (Figure 1.5). Detecting cancer cells in neighbouring lymph nodes is an indicator that cancer has spread outside the breast. (http://www.nationalbreastcancer.org/breast-anatomy) (Osborne, 1996; Jatoi and Kaufmann, 2010; Gabriel and Long, 2011).
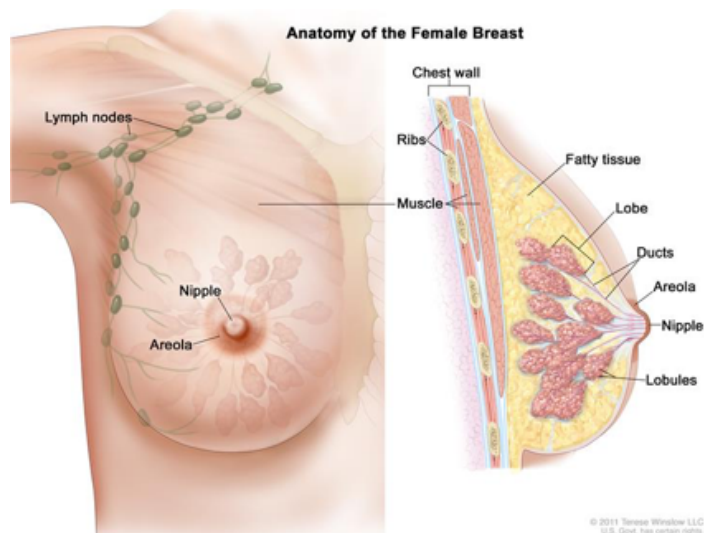
Figure 1.5. Anatomy of female breast (mammary glands).

Source: Image cited from: (http://www.cancer.gov/types/breast/patient/breast-treatment-pdq).

1.2.2 Prevalence of BC, risk factors and survival rates

Globally, BC is the most frequent type of cancer and the leading cause of cancer deaths in women (Jemal *et al.*, 2011; Bray *et al.*, 2013; Torre *et al.*, 2015).

In England, over 50,800 cases were diagnosed in 2012, with about quarter of these in individuals aged ≥75 (http://www.cancerresearchuk.org/health-professional/breast-cancer-statistics). In addition, more than 41,000 new cases of BC are diagnosed annually (http://www.ons.gov.uk/ons/rel/cancer-unit/breast-cancer-in-england/2010/sum-1.html) (Gathani *et al.*, 2014). There was an improvement in the five year estimate for BC survival from 54% between 1971 and 1975 (Coleman *et al.*, 1999) to approximately 84% between 2006 and 2011 (Office for National Statistics: http://www.ons.gov.uk/ons/rel/cancer-unit/cancer-survival/2006---2010--followed-up-to-2011/stb-cancer-survival.html) (Coleman *et al.*, 1999). This improvement reflects developments in the early detection of BC and Its treatment. However, in comparison to other types of cancer, the survival rate for BC is better in older patients in the age group 40–69 (89–90%) than in younger patients aged 15–39 (84%) (Office for National Statistics: http://www.ons.gov.uk/ons/rel/cancer-unit/cancer-survival/2006---2010--followed-up-to-2011/stb-cancer-survival.html). This association of lower survival rates for BC

with younger individuals may be attributed to their diagnosis with the most aggressiveness BC molecular subtype, known as triple negative (Dent *et al.*, 2007; Tischkowitz *et al.*, 2007). For patients diagnosed with this molecular subtype, the risk of recurrence within three years of diagnosis is increased while mortality rates show an increase some five years after diagnosis (Boyle, 2012).

Although the risk of BC may be modified by lifestyle and environmental factors, their exact correlation with BC risk has not been yet elucidated (Chen, 2013). However, some factors are associated with an increased or decreased risk of BC. Those factors that reduce the risk of BC include age at menarche (Chen, 2013; Gathani *et al.*, 2014), increased duration of breastfeeding (Gathani *et al.*, 2014), shorter stature (Green *et al.*, 2011) and lower body mass index (Reeves *et al.*, 2007). While the factors that increase the risk of BC such as alcohol consumption (Mukamal, 2010), menopausal hormone therapy and a family history of the disease (Weiderpass *et al.*, 2011).

1.2.3 Histological taxonomy of BC

When the cancer is detected in the breast, it can sometimes appear noticeably solid, thus a woman may feel it when carrying out her normal breast check. But if the cancer is not visible, mammographic screening can detect it. Next, a pathologist performs a microscopic examination of a core biopsy of the suspected tumour sample. In the laboratory, a histopathologist can identify any changes in the breast sample including the structural morphology of epithelial cell. In normal breast tissue, stromal cells gather around the large duct and terminal duct lobular units. In contrast, in BC, the epithelial cells of duct lobular units expand across of cell membrane, and cells appear with a condensed nuclei located in the centre of the cell. Therefore, BC has been histologically classified based on the morphological features and growth patterns of tumour tissues. Some cancer cells are histologically classified as non-invasive meaning that their growth has not spread out into the milk ducts. This type is known as ductal carcinoma in situ (DCIS). The National Comprehensive Cancer Network has only accepted the use of the status of the molecular pathology ER (estrogen receptor) but not other molecular markers PR (progesterone receptor), HER2 (human epidermal growth factor receptor 2) and p53, during the diagnostic examination of DCIS (Malhotra *et al.*, 2014). When cancer growth does not extend out into the lobules thus it referred to as lobular carcinoma in situ (LCIS).

Cancer that possesses invasive characteristics and grows outside the cell membrane of the ducts or lobules is classified as invasive ductal carcinoma (IDC) or invasive lobular carcinoma (ILC), respectively. The histological types of BC have been combined with the Nottingham Prognostic Index and the online adjuvant programme for determining the most effective chemotherapy (Mook *et al.*, 2009).

The commonest types of invasive BC are IDC which accounts for 50%-80% of invasive BC whereas ILC accounts for 5%-15% (Li *et al.*, 2005). In comparison to DCIS, the utility of molecular pathological markers (ER, PR and HER2) in the diagnosis of IDC is well accepted (Harris *et al.*, 2007).

Utilising these molecular markers in diagnosing invasive BC has not only helped in making effective clinical decisions but also in predicting the response to targeted therapies such as Trastuzumab or Lapatinib for patients with overexpression of HER2 or Tamoxifen or Aromatase inhibitors for patients with ER/PR receptors positive BC (Maughan *et al.*, 2010; Rakha *et al.*, 2010). A study by the International Breast Cancer Group was conducted on a large cohort of 9374 BC patients diagnosed with IDC or ILC and registered in 15 clinical trials with a median follow-up of 13 years. Tumours in the ILC cohort were correlated with older age, better differentiation and positive ER status. In addition, the ILC cohort showed remarkable early progress after six years compared to IDC with late progress after 10 years in disease-free survival and overall survival. However, ILC was correlated with increased occurrence of bone metastasis and a diminished incidence of lung metastases (Viale, 2012).

1.2.4 Molecular pathology classification of BC

BCs are classified based on the basis of their gene expression profile into molecular subtypes (Table 1.2). This mainly depends on the expression status of hormone receptors, namely ER or PR receptors in the cell nucleus and the gene amplification and/or the protein overexpression of HER2 receptor on the cell surface.

1.2.5 BC grades

The grade is the score that provides information about the microscopic morphology and growth pattern of BC biopsy cells compared to the normal breast cells or how rapidly the breast tissue sample is dividing. Grade has been correlated

with microarray-based genomic or transcriptomic signatures of BC (Weigelt *et al.*, 2010; Sotiriou *et al.*, 2006; Sotiriou and Pusztai, 2009). Identifying the cancer grade is one of the factors that assists patient prognosis, predicting whether cancer has spread to other parts of the body and informing clinicians if patients need additional treatment after surgery. The pathologist usually classifies the histological grade of BC on a scale from 1 to 3 as follows;

Grade 1 or low grade (known also as well differentiated): Grade 1 displays cancer cells, which slightly look different from normal cells, have a slow growth and well-organized patterns. Few cancer cells are dividing to produce new cancer cells.

Grade 2 or intermediate/moderate grade (moderately differentiated): Grade 2 displays cancer cells which are different to normal cells, cancer cells are growing and dividing a slightly faster than normal.

Grade 3 or high grade (poorly differentiated): Grade 3 displays cancer cells which appear extremely different from normal cells, growth is rapid and cells are dividing quickly in irregular and disorganized pattern.

(http://www.breastcancer.org/symptoms/diagnosis/cell_grade).

1.2.6 BC stages

The stage of the BC is usually defined by the tumour size and the pattern of cancer spread whether non-invasive cancer (with growth remaining within the breast) or invasive cancer (usually spreading outside the breast through the lymph node system to other parts of the body). Doctors can refer to BC stage as "local" meaning the tumour is limited to within the breast, "regional" in which the tumour is found in lymph nodes and "distant" in which the tumour has spread and is found in different parts of the body. The cancer stage helps to understand the prognosis and outcome of the disease and make decisions about treatment. Researchers usually use the TNM (Tumour size, lymph Node involvement, Metastasis) staging system to characterise the cancer behaviour (Table 1.3).

(https://cancerstaging.org/references-tools/Pages/What-Cancer-Staging.aspx and http://www.cancer.org/cancer/breastcancer/detailedguide/breast-cancer-staging).

Table 1.2. Breast cancer molecular subtypes. Table contents are adapted from (Allison, 2012; Cornejo *et al.*, 2014).

Molecular subtype	Receptor status	Surrogate IHC marker	Molecular pathways	Histological grade	Response to therapy	Targeted therapy	Reference
Luminal-A	ER+, PR+, HER2-	CK8+, CK18+, GATA3+, low Ki67	ER-responsive genes	Low	Low	Endocrine therapies	(Andre and Pusztai, 2006; Reis-Filho *et al.*, 2006; Parker *et al.*, 2009)
Luminal-B	ER+, PR+/-, HER2+/-	CK8+, CK18+, GATA3+, high Ki67	ER-responsive genes, TP53 mutations	Intermediate	Intermediate	Endocrine therapies	(Perou *et al.*, 2000; Sørlie *et al.*, 2003; Geyer *et al.*, 2009; Weigelt *et al.*, 2010)
HER2	ER-, PR-, HER2+		HER2 genes, TP53 mutations	High	High	Trastuzumab	(Rouzier *et al.*, 2005; Weigelt and Reis-Filho, 2009)
Basel like breast cancer	ER-, PR-, HER2-	CK5+, CK14+, CK17+, EGFR+, c-KIT+, CD44+, nestin+, caveolin1 +, caveolin2+, P-cadherin+	TP53 mutations, BRCA1 pathway	High	High	Under investigation	(Gusterson *et al.*, 2005; Turner *et al.*, 2007; Cheang *et al.*, 2008; Rakha *et al.*, 2008; Reis-Filho and Tutt, 2008; Turnbull and Rahman, 2008; Klingbeil *et al.*, 2010; Nielsen *et al.*, 2004)
Breast-like	ER+/-, PR+/-, HER2-			Low			(Correa and Johnson, 1978; Peppercorn *et al.*, 2008)

Table 1.3. Description of TNM staging system for characterisation of breast cancer behaviour.

TNM stages of BC	Category	Description
T stages (tumour size): This describes the primary tumour. The numbers from T0 to T4 refer to the tumour size and its growth extension into nearby breast tissue. A higher T number reflects a larger tumour size and/or may indicate that the tumour may have extended to the breast tissue or outside the breast	TX	Primary tumour is absent and can not be measured or evaluated
	T0	No evidence of the primary tumour
	Tis	Cancer is in situ (non-invasive) and has not invaded into the healthy breast tissue.
	T1 to T3	The extent the of tumour size
	T4	Growth of the primary tumour has spreads to the chest wall or outside the breast
N stages (lymph node involvement): This describes whether the tumour is found nearby the lymph nodes. The numbers from N0 to N3 refer to the number of lymph nodes involved and the amount of cancer is found in them. The higher the N number the greater the extent of lymph node involvement	NX	Cancer cells can not be found nearby the lymph nodes
	N0	Absence of cancer cells in the axillary lymph nodes
	N1	Cancer is involved in 1 to 3 axillary lymph nodes
	N2	Cancer is involved in 4 to 9 axillary lymph nodes
	N3	Cancer is involved in ≥10 axillary lymph nodes and has extended to the ipsilateral supraclavicular lymph nodes
M stages (Metastases): This describes whether the cancer has spread beyond the breast to other organs of the body	MX	Absence of metastases
	M0	No distant metastases
	M1	Distant metastases are present

Table contents are adapted from: American Joint Committee on Cancer (https://cancerstaging.org/references-tools/Pages/What-is-Cancer-Staging.aspx).

1.2.7 Genetic causes of BC

BC is genetically, biologically and clinically a heterogonous disease. Mutations in human genes, such as *BRCA1* and *BRAC2*, are significant in maintaining genomic integrity and loss of their functions increases susceptibility to breast and/or ovarian cancer. Inherited BRCA1 and BRAC2 mutations may not only be responsible for a predisposition to BC, but other rare genetic mutations have also been found in new genes including *TP53, PTEN, STK11, CHEK2, ATM, PALB2 and BRIP1* (Apostolou and Fostira, 2013) (http://www.breastcancer.org/risk/factors/genetics and Cancer Research UK: http://www.cancerresearchuk.org/about-cancer/type/breast-cancer/about/risks/breast-cancer-genes)

1.2.7.1 BRCA1 and BRCA2

Mutations in BC genes are associated with about 40% of sporadic BC and over 80% of inherited breast and ovarian cancer cases (Green and Lin, 2012). *BRCA1* and *BRCA2* mutations are responsible for about 20%-25% of hereditary (familial) BC cases (Easton, 1999) and 5%-10% of all BC cases (Campeau *et al.*, 2008). The estimated percentage of women who have inherited a BRCA1 mutation is 55-65% whereas 45% of women inherit a *BRCA2* mutation; and it is predicted that *BRCA1* and *BRCA2* mutations confer high risk of BC to carriers at the age of 70 (Antoniou *et al.*, 2003; Chen and Parmigiani, 2007).

BRAC1 and *BRCA2* genes are located in chromosomes 17q and 13q, respectively (Hall *et al.*, 1990; Miki *et al.*, 1994; Wooster *et al.*, 1994; Wooster *et al.*, 1995). Both *BRCA1* and *BRCA2* genes have been considered to act as tumour suppressor genes (TSG) due to the loss of the WT allele that has been detected in heterogeneous carries of tumours with BRAC1 or BRCA2 mutations (Banin Hirata *et al.*, 2014; Scully and Livingston, 2000). However, somatic mutations in *BRCA1 and BRCA2* are rarely detected in sporadic BC cases (Venkitaraman, 2002; Bertwistle and Ashworth, 1998) as the inactivation of BRAC1 or BRCA2 requires mutation or complete deletion of both copies of the gene (Kenemans *et al.*, 2004). Thus, suppressing the function of these genes, which lead to sporadic BC, can occur as a consequence of hyper-methylation of the BRCA1 promoter (Catteau *et al.*, 1999; Esteller *et al.*, 2000) or binding of BRCA2 by EMSY (Hughes-Davies *et al.*, 2003).

They are responsible for fundamental cellular functions including the control of cell cycle checkpoints, the regulation of HR and the DNA repair process, transcriptional regulation, cellular growth and differentiation (Welcsh *et al.*, 2000; Venkitaraman, 2002).

Loss of the cellular function of BRCA1 or BRCA2 leads to deficiency in the HR DNA repair mechanism (Green and Lin, 2012). Thus, when the abnormal cells with BRCA1 or BRCA2 mutations are unable to repair DNA damage by HR, cells may activate the NHEJ repair mechanism. Therefore, inhibition of PARP, that is involved in DNA repair mechanism and repairing single and double strand DNA breaks, may simplify the activation of the HR process to repair DNA damage in normal cells and terminate HR repair of DNA damage in cells with mutated BRCA1 or BRCA2 leading to subsequent cell death (Green and Lin, 2012). Thus, using a PARP inhibitor such as Olaparib, may be an effective treatment for increasing sensitivity to chemotherapy or radiation in breast and ovarian tumours harbouring inherited BRCA1 or BRCA2 mutations, patients with triple negative BCs (Annunziata and Bates, 2010), sporadic cancers with aberrations in BRCA genes (Turner *et al.*, 2004) and in the HR pathway (Farmer *et al.*, 2005).

1.2.7.2 p53

p53 (encoded by the *TP53* gene) has been widely studied in comparison to other genes or proteins for over 30 years ago and since its discovery it has remained the most popular gene or protein to study (Levine and Oren, 2009). Alteration of p53 function is detected in approximately 50% of cancers (Vogelstein *et al.*, 2000).

1.2.7.2.1 p53 protein structure

p53 protein was first described In 1979 (Lane and Crawford, 1979; Linzer and Levine, 1979; Kress *et al.*, 1979; Smith *et al.*, 1979; DeLeo *et al.*, 1979).
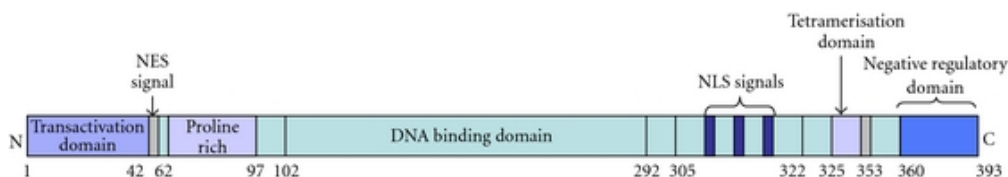
Figure 1.6. The protein structure of human p53.
Source: image is adapted from (Varna *et al.*, 2011).

As previously mentioned, p53 protein is encoded by the *TP53* gene, which is located in chromosome 17p31.1. p53 protein is composed of 393 amino acids (aa) including the *N*-terminal region (aa 1-42), which is rich in proline residues (aa 63-97) and, which serve to induce apoptosis (Hetts, 1998). This domain has also been found to be responsible for slowing-down the migration of the protein in SDS-polyacrylamide gel, causing it to present an overestimated molecular mass of p53 protein at 53kD although its actual size is 43.7kD as stated by Levin and Oren (2009). p53 protein also consists of a large middle domain, a tetramerisation domain (aa 323-356) and a *C*-terminal region (aa 363-393). The large middle domain (aa 102-292) which is important for DNA binding thus the majority of mutations detected in various types of human cancers have been detected in this domain (Soussi, 2000). The *C*-terminal domain of p53 binds to the *N*-terminal domain of MDM2 (Poyurovsky *et al.*, 2010). Fragments at the end of the *N*- and *C*-terminals, known as nuclear export signals (NES), are used for exporting to the cytoplasm whilst the fragment at the end of the *C*-terminal, known as the nuclear localisation signal (NLS), is for subcellular localisation of p53 (Lohrum *et al.*, 2001) (Figure 1.6).

1.2.7.2.2 p53 protein functions
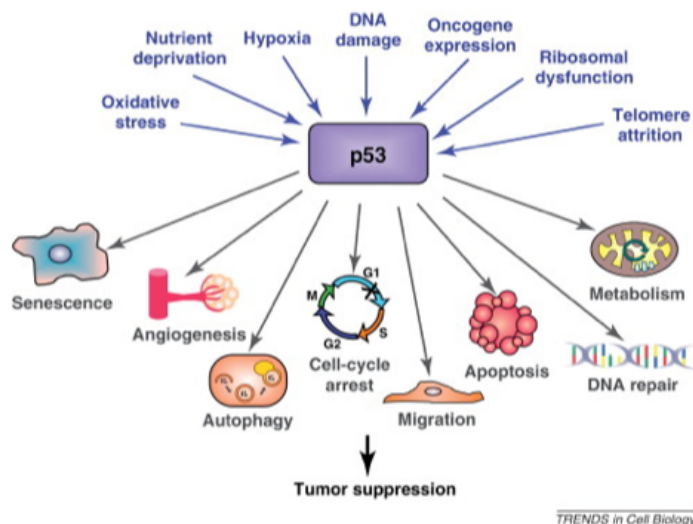
Figure 1.7. p53 response and activation in tumour cells.
In response to different stress signals (blue arrows), p53 is activated to regulate various cellular responses (black arrows) that may repress tumour progression. Source: Image is adapted from (Bieging and Attardi, 2012; Russo *et al.*, 2013).

Levine and Oren (2009) have summrised the intensive investigations and findings related to p53 during three decades of research. During the first decade of

studying p53, research, found that the simian virus 40 large T-antigen, a tumour virus that is responsible for inactivation of p53 in transformed cells (Lane and Crawford, 1979; Linzer and Levine, 1979; Kress *et al.*, 1979; Smith *et al.*, 1979).

Also, p53 DNA was successfully cloned in the 1980s (Chumakov *et al.*, 1981; Matlashewski *et al.*, 1984; Harlow *et al.*, 1985) and was determined that p53 is a TSG, which is the most frequently mutated gene in human cancers (Baker *et al.*, 1989; Baker *et al.*, 1990). Subsequent studies were performed to establish the role of p53 as a TSG. For example, over expression of the WT p53 in the murine tumour derived mutant p53 cells suppressed culture cell transformation by the oncogenic components MYC and H-RAS (Eliyahu *et al.*, 1989; Finlay *et al.*, 1989). Loss of the WT alleles of *TP53*, by mutation or deletion or a combination of both was identified in human colorectal cancer specimens (Baker *et al.*, 1989). Moreover, the *TP53* knockout mice model displayed cancer progression (Donehower *et al.*, 1992). All these observations led to the *TP53* gene being classified as a TSG.

In the second decade of p53 research, many findings described p53 as being negatively regulated by murine double minute 2 (MDM2) (Momand *et al.*, 1992). The negative feedback of p53 and MDM2 occurs when p53 stimulates the transcriptional activities of MDM2 and the latter inhibits p53 cellular activities by its ubiquitination and proteasomal degradation (Barak *et al.*, 1993; Wu *et al.*, 1993). The ubiquitination activity of MDM2 has been found to be essential for nuclear export and subcellular localisation of p53 to the cytoplasm (Toledo and Wahl, 2006).

Additionally, during this decade it was also discovered that the WT p53 plays putative roles in regulating multiple cellular events in response to different stress signals (Figure 1.7). Consequently, p53 activates diverse cellular processes including cell cycle arrest at G1 phase, which allows time to repair damaged DNA (Fan *et al.*, 1995). Thus, cells harbouring the mutant version of p53 may not be arrested in G1 phase and instead are accumulated in G2 (Green and Lin, 2012). If the DNA damage cannot be repaired, p53 can also induce apoptosis. It can directly initiate cell death by its localisation to the mitochondria activating mitochondria outer membrane permeabilisation mechanism that requires the formation of a complex with pro-apoptotic apoptosis regulator proteins such as BCL2 and BCL-XL by releasing cytochrome C (Mihara *et al.*, 2003; Rodier *et al.*, 2007).

In the third decade of research, p53 was shown to be required for other functions including inducing senescence (Serrano *et al.*, 1997). P53 seems to have a crucial role in regulating and maintaining cellular senescence that prevents the

cancer immortalisation phenotype, which could contribute to tumour suppression. Other proteins such as ATM/ATR and CHK1/CHK2 are activated to regulate p53 activity by phosphorylation during the activation of senescence in response to cellular stress (Wahl and Carr, 2001). Other cellular functions of p53 which were investigated, in the third decade, included the regulation of the metabolism (Jones *et al.*, 2005), angiogenesis (Faviana *et al.*, 2002) and mitotic catastrophe (Vakifahmetoglu *et al.*, 2008).

1.2.7.2.3 p53 accumulation and detection

Using immunohistochemistry (IHC) as a method for detecting nuclear p53 in cancer cells can be classified as an indirect way to demonstrate the potential existence of mutations in *TP53* (Elledge *et al.*, 1994). However, WT p53 can also be activated and stabilised in response to cellular stress (Blattner *et al.*, 1999; Tao and Levine, 1999). In addition, some tumour samples that carry specific *TP53* mutations (such as nonsense mutations or deletion/splices) could present negative p53 immunostaining despite the presence of the mutation (Geisler *et al.*, 2001). Thus, p53 positive immunostaining may not necessary be an accurate indicator of *TP53* mutation (Schmitt *et al.*, 1998). Therefore, along with detection of p53 by IHC, the status of p53 can be examined using different techniques such as functional analysis of separated alleles in yeast (FASAY), a method which is used for detecting mutations (germline and somatic) in the *TP53* gene in tumour samples (Flaman *et al.*, 1995).

The FASAY method is based on extracting human *p53* mRNA from normal and tumorous tissues followed by performing RT-PCR. The amplified PCR product (cDNA of the *p53*) is then transformed into yeast with a plasmid vector carrying the 5' and 3' ends of human p53 open reading frame. The yeast, in turn, contains an open reading frame (ORF) for adenine that is regulated by a promoter under the regulation of *p53*. The yeasts are plated in a specific medium that lacks leucine and contains adenine. Thus, if the WT *p53* is present in the sample, adenine is completely metaboised and consequently expressed then colonies of transfected yeast cells are displayed in white. If the *p53* is mutated, however, adenine is not wholly metabolised or expressed and thus yeast colonies appear to be red coloured (Flaman *et al.*, 1995). Other studies confirmed the status of the *p53* gene in tumour samples by using direct sequencing of the DNA coding sequence (Varna *et al.*, 2011).

1.2.7.2.4 *TP53* mutations in BC

The inactivation of p53 is associated with different mechanisms including mutations, which occur in the DNA binding domain or in the deletion of the *C*-terminal domain of the p53 protein (Soussi and Wiman, 2007). Most *TP53* mutations consist of missense mutations, which are positioned in the central region of the DNA binding domain in some 80%-90% of cancer cases (Soussi *et al.*, 2006; Petitjean *et al.*, 2007). The *TP53* mutation is responsible for about 25-30% of BC (Olivier *et al.*, 2006), a percentage which increases to 80% in basal-like BC and decreases to 15% or less in the luminal-A subtypes (Sørlie *et al.*, 2001). Additionally, the lack of p53 function is also associated with amplification of MDM2 gene or deletion of the p14^{ARF} gene in breast or lung cancers (Vogelstein *et al.*, 2000).

1.2.8 BC treatment

Oncologists usually decide the type of treatment in agreement with the patient and this is based on multiple elements relating to a woman's age, menopausal status and the tumour status (histological type, grade, size, status of hormone receptors [Her2^{+}, ER and PR], lymph node involvement and distant metastasis). The majority of patients' with tumours undergo loco regional therapies, which involves two forms: surgery and/or radiation therapy (RT). This type of treatment is usually combined with additional therapy for effective management of the cancer. This is known as systemic therapy and is usually provided to patients as a combination of two or three drugs either after surgery as adjuvant setting treatment or before surgery as neoadjuvant chemotherapy (NACT). Patients expose to adjuvant or NACT treatment may also be supplied with hormonal (endocrine) therapy depending on the positivity of their ER or PR receptors. A brief description of the types of BC treatments follows below.

1.2.8.1 Loco-regional therapy

Loco-regional treatments for BC can be divided into two types including surgical resection of the tumour mass and radiation therapy.

1.2.8.1.1 Surgery

Surgery is the main treatment used to remove BC in which the local tumour recurrence can be diminished. The majority of early operable BC is removed by

surgery. However, a number of factors are considered by surgeons before starting the procedure including the location and size of the tumour, the stage of the BC and the size of the breast. The majority of cases undergo either breast-conserving surgery or mastectomy. Breast surgery is sometimes combined with other procedures in the axilla such as an axillary node clearance or sentinel node biopsy dissection for patients with invasive BC. These additional procedures assess the pathological staging of the tumour and guide the post-operative treatment decisions.

1.2.8.1.2 Radiation therapy

Radiation therapy usually involves high-energy X-rays and is recommended for patients after breast-conserving surgery to eliminate any residual tumour cells in the breast, axilla and chest wall.

1.2.8.1.3 Chemotherapy

Chemotherapy drugs mainly aim to inhibit the cancer's ability to grow leading to a subsequent induction of apoptosis with a minimal effect on normal cells. Chemotherapy is recommended for patients whose tumour is expected to be metastasised (meaning that the tumour spreads to the axillary lymph node) or in cases of advanced and invasive BC (tumour size is increased and has expanded to distant areas of the body outside the breast) and for patients who are diagnosed with triple negative BC. Chemotherapy can be provided to patients by intravenous injection or orally so that it travels through the bloodstream to influence cancer growth in affected areas of the body. Chemotherapy treatment is usually given at specific period in the cycle. Patients usually have a recovery period after each period of chemotherapy treatment.

Medical oncologists recommend that post-operative patients obtain further adjuvant therapy since surgery alone may not be enough to eliminate any residual cancers, which have spread to other areas of the body and may not have been obvious during the BC surgery. NACT treatment has been used widely for treatment of larger primary, locally advancer BC patients and inflammatory disease. It offers an effective advantage by down-staging or shrinking the tumour growth allowing reduction the extent of BC surgery, increasing breast conserving therapy and identifying biomarkers as indicators for efficient response to NACT treatment (Thompson and Moulder-Thompson, 2012).

For both modes of chemotherapy treatment (adjuvant and NACT), in order to eliminate the majority of the BC, a combination of more than one drug can result in a better outcome. BC chemotherapy treatment can be classified as anthracyclines (for example: Adriamycine/Doxorubicine and Epirubicin) and the Taxanes (for example: Docetaxel/Taxotere and Paclitaxel/Taxol). These may be used in combination with certain other drugs, such as Cyclophosphamide (Cytoxan®) Fluorouracil (5-FU), Carboplatin or Cisplatin. The most common combination chemotherapy drugs (regimens) used for the management of BC is as follows;

- ❖ FEC: Fluorouracil, Epirubicin, Cyclophosphamide
- ❖ ECF: Epirubicin, Cisplatin, Fluorouracil
- ❖ EC - P (or EC - D): Epirubicine, Cyclophosphamide, which is combined by either Daclitaxane or Docetaxane
- ❖ TC: Docetaxane, Cyclophosphamide

1.2.8.1.4 Endocrine therapy

Endocrine therapy is a type of therapy that is provided for hormone receptor positive BC breast cancer patients. Patients receive endocrine therapy in an adjuvant or neoadjuvant setting to help reduce the risk of cancer recurrence after surgery. In women, ovaries are the main source of the hormone estrogen until the menopause. After menopause, a smaller amount of estrogen is still made in the fatty tissue of the female body by the adrenal gland Thus, endocrine therapy is used to lower the level of hormone receptors in female patients including ER or/and PR and block their activities of enhancing tumour growth and survival. It is suitable only for cancer cells with positive hormone receptors including ER-positive or/and PR positive tumours. BC patients who are pre-menopausal receive Tamoxifen to bind to ER receptor and blocks its transcriptional activations and those who are post-menopausal receive Aromatase inhibitor, which greatly diminishes ER concentration.

HER2 receptor is a member of the epidermal growth factor receptor family. Amplification or overexpression of HER2 is common in about 15–30% of BCs and acts as a prognostic and predictive biomarker in BC (Burstein, 2005). HER2 positive BC receive the targeted drugs including Trastuzumab (Herceptin) which is often supplemented with one of the Taxane agents such as Paclitaxel/Taxol or Docetaxel/Taxotere. HER2 positive cancers can also receive Pertuzumab (Perjeta), which is a monoclonal antibody targets HER2 positive cancers, and can be combined with Trastuzumab and Docetaxel.

1.3 Integrating high throughput siRNA and small molecule screens to enhance cancer drug discovery

1.3.1 Cell based high throughput screens

Cell-based high throughput screens (HTS) utilise a cell culturing system and can be employed for the large-scale examination of potential biological or genetic effectors directed against defined target of biological or cellular phenotype events (ARMSTRONG, 1999). A cell-based HTS relies on screening a particular RNAi library or screening a set of small molecules in which both are targeted to identify biological modulators of particular cellular event. For instance, siRNA screenings have been used widely for identifying of genes which stimulate the effect of PARP inhibitor on cell survival (Stec *et al.*, 2012), induce or modify premature chromosome condensation (Adams *et al.*, 2014), genes which are associated with survival and growth of pancreatic cancer cells (Henderson *et al.*, 2011), modulators of Cisplatin in ovarian cancer cells (Arora *et al.*, 2010) and genes that increase sensitivity to Paclitaxel/Taxol in BC cells (Bauer *et al.*, 2010).

1.3.2 RNAi screen

Rapid developments have been made in studying gene activity since the discovery of RNAi. Gene knockdown using the RNAi approach is a fundamental tool enabling genome scale screening to be performed on cultured *Drosophila melanogaster* and mammalian cells and paved the way for the identification of potential therapeutic targets (Kiger *et al.*, 2003; Nicke *et al.*, 2005).

1.3.2.1 Biology and mechanism of RNAi interference

There are different forms of RNAi silencing reagents which include synthetic small interfering RNA (siRNA), short hairpin RNA (shRNA) and double stranded RNA (dsRNA) (Iorns *et al.*, 2007). The two forms most frequently used experimentally for RNAi screenings are siRNA and shRNA. Long dsRNA consisting of a few hundred base pairs (bp) has been used experimentally to induce siRNA for gene expression silencing of various organisms such as plants, *Drosophila melanogaster* and *Caenorhabditis elegans* (Iorns *et al.*, 2007; Echeverri and Perrimon, 2006). However, the use of long dsRNA can induce an interferon response that causes non-specific silencing of the target mRNA transcript resulting

in global inhibition in protein synthesis (Iorns *et al.*, 2007). To remedy this problem, siRNA duplex with a length of 21-25 nucleotides and two nucleotides 3ʹ overhangs can be used to inhibit gene expression without inducing interferon response (Tuschl *et al.*, 1999)
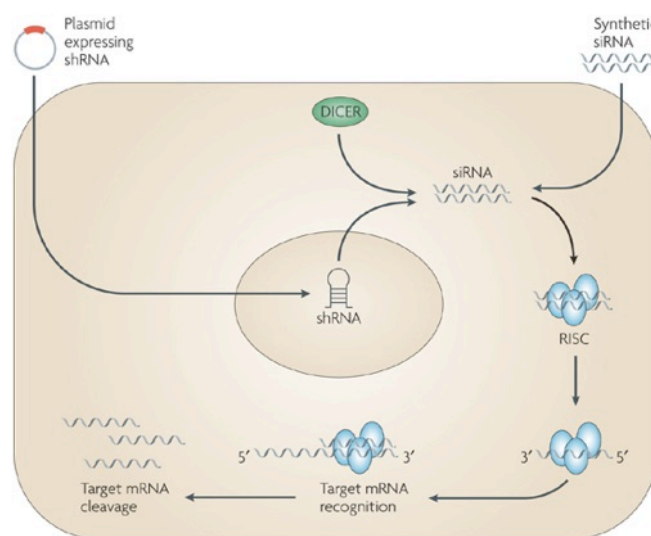
Figure 1.8. Mechanism of gene silencing by RNA interference (RNAi).
When the plasmid expressing short-hairpin RNAs (shRNAs) are introduced into the cells, the Dicer enzyme processes into small-interfering RNA (siRNA). Also, synthetic siRNAs can be synthesized chemically and directly transfected into the cell using transfection reagents. Then, siRNAs are integrated with the RNA-induced silencing complex (RISC). Consequently, duplex siRNA is unwounded allowing the binding of its antisense strand to its complementary mRNA sequence. The targeted mRNA is degraded by RISC, resulting in an inhibition of gene expression and a reduction on protein synthesis. Source: Image is adapted from (Iorns *et al.*, 2007; Mohr *et al.*, 2014).

The mechanism of siRNA can be summarised in the following steps (Figure 1.8). First, siRNA is induced endogenously in the cell, either by transfection reagent using synthetic siRNA or ectopically using plasmid-expressed shRNA. The shRNA is processed by the RNase III-like enzyme (Dicer) into siRNA, (Tuschl *et al.*, 1999). The siRNA is then loaded into the RNA-induced silencing complex (RISC). Helicase within the RISC unwinds the siRNA duplex, allowing the guide strand (antisense strand) to bind to the complementary mRNA transcript of the target. The bound mRNA is then cleaved by the RNase within the RISC, resulting in mRNA degradation, gene expression silencing and a reduction in protein synthesis (Meister and Tuschl, 2004).

1.3.2.2 RNAi library formats and screening strategies

In both academic and commercial laboratories, researchers have developed a number of RNAi libraries using mammalian cells. These libraries are divided into two formats, namely synthetic siRNA libraries and vector-based shRNA libraries.

siRNA can be chemically designed to mimic the endogenous pattern of duplex siRNA, that is 21-25 nucleotides in length with 2-base overhangs at both 3'ends (Elbashir *et al.*, 2001). The synthetic siRNA library only provides short-term gene silencing since the duplex siRNA does not replicate; thus its delivery to cells is gradually decreased as the cells divide. However, synthetic siRNA offers highly efficient gene silencing which can potentially minimise off-target effects (Iorns *et al.*, 2007; Kittler *et al.*, 2007b). shRNA libraries can be also be subdivided into different types based on the vector used in the designed library; for example non-viral (plasmid), adenoviral, retroviral and lentiviral (Root *et al.*, 2006; Iorns *et al.*, 2007; Hu and Luo, 2012; Cowley *et al.*, 2014). Vector-based shRNA libraries, in turn, can be used for long-term and stable gene silencing since the vector generates multiple copies during its integration into the host genomic DNA.

In order to conduct a wide-scale RNAi screen, a specific screen paradigm or strategy has to be chosen. There are two main approaches used in RNAi libraries, namely, arrayed and pooled library screens (Iorns *et al.*, 2007; Boettcher and Hoheisel, 2010; Campeau and Gobeil, 2011; Hu and Luo, 2012).

The arrayed format of RNAi library screen, known also as systemic screen, can be performed using synthetic siRNA or vector-based shRNA libraries. This arrayed screen strategy offers the possibility to work either on a selected RNAi sub-library or on the whole genome. This strategy usually relies on targeting each gene individually, thus enabling the measurement of the resulting phenotype of interest. The transfected cells in multi-well plates (96 or 384 wells) are assayed using an appropriate instrument ranging from the simple readout assay, such as luminescent cell viability, to more a complex readout, using fluorescent microscopy and imaging software Operetta (PerkinElmer) for high content screening (MacKeigan *et al.*, 2005; Iorns *et al.*, 2007; Mohr *et al.*, 2010; Campeau and Gobeil, 2011).

Moreover, RNAi cell microarray is another format, which can be used for arrayed, or systemic RNAi screening. This type of assay is based on using siRNA, shRNA expressing plasmid mixed with the transfection reagents, or shRNA expressing lentiviral supernatants. Any of these can be plated on the cell spot microarray slides, enabling transfection of multiple cell types on the arrayed spots followed by a fast, multi-parametric analysis and readout of high-content imaging

screening (Silva *et al.*, 2004; Bailey *et al.*, 2006; Neumann *et al.*, 2006; Rantala *et al.*, 2013).

The second screening strategy employs a pooled RNAi library utilising shRNA to target many genes simultaneously (Iorns *et al.*, 2007; Mullenders and Bernards, 2009; Boettcher and Hoheisel, 2010; Campeau and Gobeil, 2011; Hu and Luo, 2012). This strategy makes use of pools of shRNA expressing plasmid or expressing viruses, which are transfected or infected into the cells, respectively. Then, cells are treated with selective agents such as small molecule inhibitor to measure the resulting phenotype. Cells which are resistant to the small molecule inhibitor, that carried the shRNA expressing vector, are identified by performing PCR amplification and subsequent DNA sequencing. The alternative method that can be used to identify target hits involves barcoded pooled shRNA vector screening. Each shRNA vector encodes a single shRNA sequence, which also contains a unique DNA barcoding sequence. The cells are transfected with this barcoded shRNA vector and then divided into two populations; one is exposed to small molecule inhibitor whilst the other is used as a control population. The cells from both populations containing this unique barcode are amplified using PCR, and are then labelled with different fluorescence and hybridised for microarray analysis. The alternations in the colour ratios are used to determine if the potential shRNA vector has encoded the gene responsible for altering the phenotype of interest.

1.3.2.3 Type of siRNA screens

1.3.2.3.1 Loss of function (LOF) siRNA screens

LOF is one of the applications used to conduct siRNA screening and involves the use of siRNA to knockdown genes of interest. This approach is based on single gene knockdown that allows for the characterisation of cellular and morphological phenotypic changes and the identification of the gene's function. A LOF siRNA screen can also be used to identify whether genes increase their phenotypic changes in comparison to untreated cells or the positive control. For example, PCC is an abnormal cellular phenotype, mainly induced by LOF of *MCPH1/BRIT1* gene. Thus, in order to identify other genes which induce PCC and their correlation with MCPH1/BRIT1 in regulating DNA condensation, a large-scale human druggable genome LOF siRNA screens was conducted by the BioScreening technology group (BSTG) at the University of Leeds (Adams *et al.*, 2014).

LOF siRNA screen simplifies the knockdown of many types of genes that are difficult to inhibit in cells such as genes functioning as receptors in the cell surface, transaction factor and enzymes (Echeverri and Perrimon, 2006). However, it is important to note that knockdown by siRNA may not be an effective method for detecting LOF phenotype, particularly in the case of genes harbouring specific features such as highly active, long-protein half-life and high-endogenous expression genes (Echeverri and Perrimon, 2006). Thus, an alternative format or strategy of RNAi approach must be applied such as plasmid- or vector-based shRNAs (Root *et al.*, 2006).

1.3.2.3.2 Synthetic lethal siRNA screen

Effectively, this process involves identifying a therapeutic target which tolerates selective destructive of cancer cells without affecting normal ones. This can be achieved by conducting a synthetic lethal (SL) RNAi screen. This serves to determine the essential genetic interactions between two genes whereby mutation in one gene has no effect on cell viability but the presence of mutation in both genes leads to cell death. Thus, identifying one of these mutations in cancer cells but not normal cells can simplify killing cancer cells by inhibiting the effect of the secondary gene mutation using targeted drugs (Chan and Giaccia, 2011). The most useful application of SL siRNA screen lies in identifying SL targets in cancer cells harbouring specific genetic lesions such as LOF mutations in TSG (Iorns *et al.*, 2007). SL RNAi screens can be performed using a cell culturing system by initially enhancing the genetic mutations that are related to cancer initiation or progression. This allows the required RNAi-modified phenotype, namely, cell death to be identified (Echeverri and Perrimon, 2006). Identification of the correlation between the SL gene and TSG would prove more effective for the selective killing of tumour cells containing mutations in TSG (Iorns *et al.*, 2007). PARP inhibitor has been shown to be a useful SL target, killing cancer cells with specific defects in BRCA1 and BRCA2 without having any significant effect on normal cells (Farmer *et al.*, 2005). Since the SL siRNA screen is based on the knockdown of two genes, it, however, needs to be conducted in a highly proficient and efficient manner in order to ensure adequate cell death.

1.3.2.3.3 Modifier RNAi screen

The modifier RNAi screen provides powerful data that allow for identifying both the function of genes and their involvement in the cellular pathways. In the modifier screens, the silencing of RNAi results in inducing or repressing a given phenotype of interest. This phenotype can be initially generated by targeting

phenotypic-related gene through gene overexpressing or gene silencing. Then, the phenotypic effect will be the consequence of initial drug (chemical compound) treatment or siRNA treatment, alone or in combination with the drug (Echeverri and Perrimon, 2006).

Combining the drug with siRNA provides a comprehensive explanation of the mechanism of the drug and the drug-targeted molecular pathway. In addition, this screen can determine the cellular pathways related to the function of the gene in which its suppression or silencing is associated with distinctive abnormal cellular phenotype. In addition, these methods are not only useful for identifying a novel therapeutic target but also for identifying genes that when depleted enhance sensitivity to the anti-cancer drug (MacKeigan *et al.*, 2005; Bauer *et al.*, 2010). These methods, particularly the suppression of the RNAi to the drug's action, would recognise novel prediction biomarkers that show low-response to the compound or even confer resistance to a specific chemotherapy. This will help to improve the optimisation process and model design of clinical trials for subsequent novel drug validation. Some examples of siRNA screens will be detailed below in (Section 1.3.4) to illustrate the powerful of such screens for identifying new modifier targets that either increase drug sensitivity or confer resistance to specific chemotherapy.

1.3.2.4 Essential concepts for RNAi screens

1.3.2.4.1 Screening strategy and approach

There is no standard protocol for performing the chosen RNAi screen. However, since RNAi screening is complex and costly, there are some essential Infrastructural procedures that must be considered when performing any RNAi screen, as described by Iorns *et al*. (2007) and Sittampalam *et al*. (2013).

The most important step in performing a RNAi screen is to choose the most robust and reproducible assay system. The phenotype of interest which is to be examined and measured must present both biologically and clinically the specific events that characterise the disease in question. A large range of RNAi screens are available which target the genome of different species in the vertebrate kingdom including human, mice and rats. However, the majority of scientific and industrial laboratories use human cell lines due to the cost-effective RNAi transfection reagents for human cell base RNAi screens. As adherent cell lines with a monolayer growth pattern, HeLa (Echeverri and Perrimon, 2006) and U2OS (Martin *et al.*, 2014; Adams *et al.*, 2014) both provide easy, robust and efficient RNAi

transfection. However, adhesion problems have been experienced by some researchers using HeLa cells for high through screening experiments. Highly adherent monolayer cell lines are the most appropriate for high content microscopic imaging systems, offering the required readouts efficiently.

The other key consideration that must be taken into account is the RNAi strategy if the pooling system relies on the vector-based library since this is expensive, time consuming and requires a stable knockdown system that warrants long-term gene silencing. The non-vector siRNA library format is widely preferred since it offers a sufficient transfection with gene silencing that can be extended for seven days. Conducting a genome-wide RNAi screen is less cost-effective compared to choosing a subset of the genome that is based on identifying a pharmacologically specific target such as screening a protein kinase sub-library (Iorns *et al.*, 2007).

Moreover, an appropriate screening technique should be used particularly with pooling RNAi libraries, for example, the recommended specific format 96-well or 384-well plates combined with an automated reagent-handling system that maintains a high level of accuracy such as BRAVO from PerkinElmer. In addition, it is worth considering an automated microscopy system such as the Operetta, that offers multi-parametric readouts and fluorescent channel imaging for measuring different phenotypic features. Image analysis also requires suitable software such as Columbus or cellHTS2 package that can rapidly and accurately analyse the previously generated images and store a large set of data (Boutros *et al.*, 2004; Pelz *et al.*, 2010). Other analysis packages have now emerged, such as CellProfiler and Cellenger, but they require more computing power and a highly skilled specialist to achieve output that is sufficiently precise for high throughput screenings (Echeverri and Perrimon, 2006).

1.3.2.4.2 Selection of positive and negative controls

It is essential to choose the correct positive and negative controls, particularly in replicated RNAi screening, to show the anticipated changes in an assay and to improve the quality of screening data. The most commonly used negative control in RNAi screening is non-targeting siRNA (NT-siRNA). However, it needs to be borne in mind that although most commercial NT-siRNA has no effect on the phenotype being investigated, some can induce a high level of cell death, which then maximises the off-target effect. Thus, in order to ascertain the suitability of negative controls, it is advisable to compare between the effect of NT-siRNA and that of mock transfected cell on the phenotype of interest (Iorns *et al.*, 2007). Similarly, in

order for a positive control to offer a biological readout threshold for identifying hits from an RNAi screen, it must be verified as reliable to observe the required biological effect, which can then confirm that the screen is generating a valid biological data (Iorns *et al.*, 2007).

Thus, comparison between the negative and positive controls is warranted using some form of statistical analysis such as strictly standardised mean difference (SSMD) (Birmingham *et al.*, 2009; Goktug *et al.*, 2013) that can describe the quality of screening performance and controls, respectively (Figure 1.9). Checking statistically to improve the screening system and its quality is important as it helps to minimise false positives and negatives.

1.3.2.4.3 Statistical analysis for hits identification

Birmingham *et al.* (2009) described several statistical methods, which can be used for hits identification in siRNA screening, the most suitable being Z score and Robust Z score.

A
$$SSMD = \frac{mean(C_{pos}) + mean(C_{neg})}{\sqrt{std(C_{pos})^2 + std(C_{neg})^2}}$$

B $$Z\text{-score} = \frac{S_i - mean(S_{all})}{std(S_{all})}$$

C $$Robust\ Z\text{-score} = \frac{S_i - median(S_{all})}{MAD(S_{all})}$$

Figure 1.9. Statistical methods for analysis of high throughput RNAi screening data. **(A)** The strictly standardised mean difference (SSMD) is used to evaluate the quality of positive and negative controls in the RNAi screen; Terms C = control; pos = positive control; neg = negative control. **(B and C)** Z score and Robust Z score are used for hits identification. The Z score relies on mean and standard deviation (std), which are replaced in Robust Z score with median and median absolute deviation (MAD), respectively; Terms S_i = each value of the data set; mean or median S_{all} = mean or median of all values in the data set; std or MAD S_{all} = the standard deviation or the median absolute deviation of all values in the data set. Source: Equations are adapted from (Goktug *et al.*, 2013).

The Z score can be used to evaluate the difference in the value of siRNA compared to the mean and standard deviation (SD) of the selected control. But, because the Z score is sensitive to outliers, a variation know as the Robust Z score is considered to be preferable for analysing RNAi screens since this substitutes the outlier-insensitive median and median absolute deviation (MAD) for mean and SD in the selected control (Goktug *et al.*, 2013) (Figure 1.9).

1.3.3 Small molecules screen (SMS)

The main difference between RNAi and small molecule inhibitors is their biological action, which involves the inhibition of protein expression by siRNA and the inhibition of protein activity by small molecules. Small molecule inhibitors are useful for inhibiting protein function meaning that the subsequent biological changes can be studied and a potential novel therapy can be developed. (Weiss *et al.*, 2007) provided some recommendations that have to be considered during performing SMS, some of which will be detailed below.

In order to eliminate the off-target effect for small molecule screens, an appropriate functional readout control at the lowest concentration is sought (Weiss *et al.*, 2007). This should allow for inhibition of the target either *in vitro* or in systematic cell culturing which avoids non-specific protein binding. For instance, kinase inhibitors to block adenosine triphosphate (ATP) binding may potentially show an off-target effect in binding with proteins that have the same conformation. In this case, the off-target effect may exist among protein kinases compared to other classes of proteins.

In addition, another control is suggested for the alignment of functional screening readout, such as small molecule inhibitors that are structurally different but functionally block the same target, (Knight and Shokat, 2005). It is also recommended to use a concentration below 10µM, particularly when testing novel small molecules, in order to preserve the specificity of the compound's binding (Weiss *et al.*, 2007).

Moving to the validation stage of small molecule, RNAi can serve as a useful tool for confirming and validating the small molecule inhibitor results. Weiss *et al.* (2007) stated that when either a small molecule inhibitor or RNAi is used against the same target, the resulting phenotype, which is observed, should be consistent, increasing its potency and selectivity, both biologically and therapeutically. Currently, the use of siRNA in most cases to verify the results from the small molecule inhibitors under investigation shows an alignment between the phenotype observed in the inhibitor and the siRNA. However, Weiss *et al.* (2007) mentioned that other reviewers' opinion stated that the loss of alignment in the resulting phenotype could be attributed to the lack of specificity for small molecule inhibitors. Weiss *et al.* (2007) explained that the lack of congruency in the results reflects the biological differences between the small molecule inhibiters and siRNA. More specifically, these differences can be attributed to protein-protein interactions. Small molecules usually inhibit the target protein, but this protein may still be active,

functioning physically as a scaffold, which is biologically important for protein-to-protein interactions. Nevertheless, these interactions would be totally inhibited by using siRNA. However, utilising Aurora kinases as a case study for clarifying the lack of phenotypic alignment between RNAi and small molecule inhibition contributed to hypothesise that the dissimilarity in phenotypic results between Aurora B siRNA or using a small molecule inhibitor of Aurora B (ZM447439) in Nocodazole-treated cells can be attributed to the use of different experimental methods for blocking the activity of Aurora B (Keen and Taylor, 2004; Ditchfield *et al.*, 2003). For example, Aurora B contributes structurally with other molecules to the formation of chromosome passenger complex (CPC) at the centrosomes and substrate phosphorylation (Ruchaud *et al.*, 2007). Exposing the cells to the inhibitor ZM447439 leads to inhibition of Aurora B activity and prevents the substrate phosphorylation without affecting the structure or localisation of CPC.

These results show how the small molecule inhibitor can inactivate the enzymatic activity of the target without influencing its stoichiometry, which can be a useful means of investigating biological and physiological functions. Weiss *et al*. (2007) concluded that in the case of Aurora kinases, there is a biological difference between the functions of small molecule inhibitor and RNAi; thus the phenotypic results from both approaches would be correct and acceptable as long as the appropriate functional read out for both small molecule or RNAi systems is present to minimise the off-target effect. Thus, there is no standard scientific reason to assume that the phenotypes, which resulted from the two approaches, should always be aligned. (Eggert, 2013) stated that performing parallel siRNA and known small molecules screens of target the same pathway prevents the confounding variables and the phenotypic results from siRNA knockdown and small molecules inhibitors are not necessarily aligned since the inhibitor only blocks the enzyme activity while the siRNA inhibits the enzyme and its scaffold interactions (Weiss *et al.*, 2007).

Thus, identifying the specific targets of the small molecule inhibitors is the most difficult technical problem to be faced when using phenotypic screening in drug discovery. However, the availability of systematic RNAi sources offers the chance for conducting a parallel RNAi and small molecule inhibitor screening together with high-content automated image analysis. This can be used to identify and characterise the active small molecules, and the similarities and differences in the resulting phenotypes of these molecules with RNAi data set. For example, Eggert *et al*. (2004) managed to conduct parallel small molecule inhibitor and RNAi screens in *Drosophila* Kc cells in order to identify cytokinesis inhibitors. They

identified an inhibitor known as Binucleine 2 and a new protein in the Aurora B pathway (Borr) (borealin-related). This suggests that Binucleine 2 targets protein functions in the Aurora B pathway. Thus, comparison between parallel screens would help to identify the pathway in which small molecules function. It would also help clarify the biological mechanism of the resulting phenotype of interest and identify all the components involved in the pathway. Subsequently, this could lead to identifying a novel therapeutic target for cancer.

1.3.4 Synergies between siRNA screens and small molecules for subsequent drug discovery

Iorns *et al*. (2007) described the streamline process of drug discovery, dividing this into five stages as follows: (1) target identification; (2) target validation; (3) high throughput small molecule screening; (4) lead optimisation and (5) clinical trial. (Figure 1.10).

The most challenging of these stages in drug development is the first. Previously, target identification was based on recognising changes in protein or gene expression, or genetic variations in specific human diseases. However, the data from these approaches may not correlate precisely enough to determine the main causative factors of the disease. Since the main aim of target identification is to identify new targets that are the most likely to be responsible for tumour growth and survival but are not usually required in normal cell, thus when these targets are inhibited this leads to reversal of tumour progression. Thus, conducting high throughput RNAi screening could reveal multiple targets related to reverse cancer progression, enhanced drug sensitivity and identification of targets that confer resistance to chemotherapy.

For example, the combination of siRNA screening was coupled with automated microscopy, using wound-healing assay as a control measurement for cell migration in ovarian cancer cell line SKOV-3, which harbours the most complex characteristics of cancer. This screen identified that depletion of the kinase MAP4K4 (mitogen-activated protein kinase 4) can inhibit migration and invasion. The activity of MAP4K4 in cancer cells is mediated by the kinase JNK (c-Jun N-terminal kinase) thus the small molecule inhibitor of JNK proved to be effective at preventing cell migration and metastases (Collins *et al.*, 2006). This case study provides a good example of conducting an RNAi screen for target identification and a small molecule inhibitor screen for target validation.
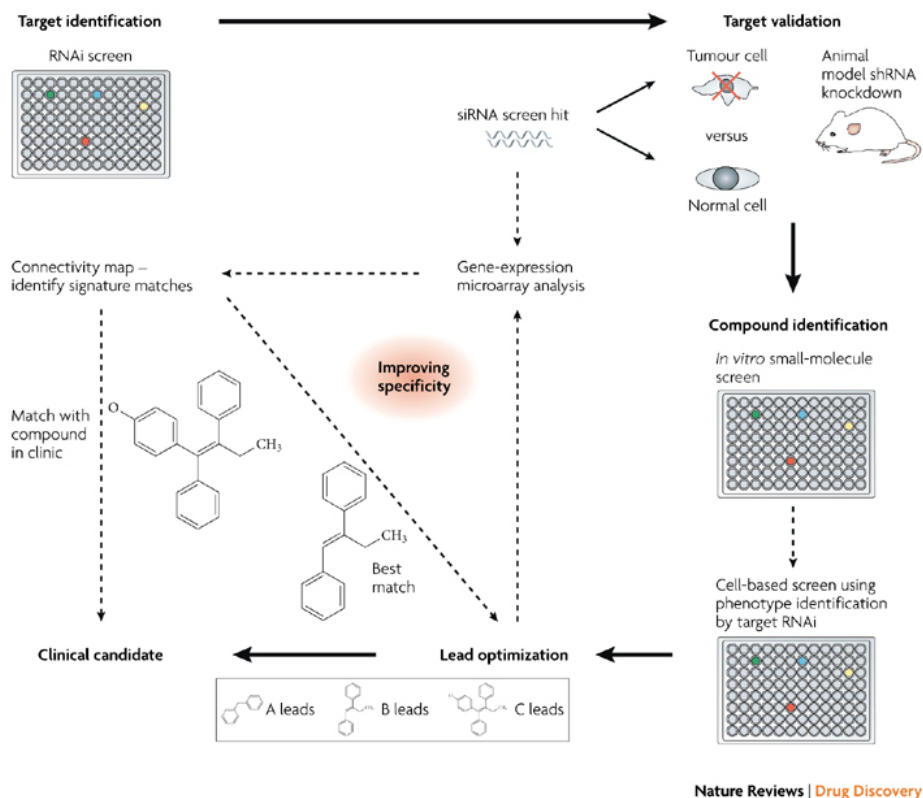
Figure 1.10. Summary of drug discovery process.
A number of stages are implemented in drug discovery. (A) Target identification: Novel targets can be identified utilising high-throughput RNAi screens. (B) Target validation stage can be performed using RNAi in *in vitro* (cell lines) and *in vivo* (mouse) models. (C) Selective identification of promising small molecule candidates by using *in vitro* small molecule screens that are designed based on specific cellular phenotypes that are associated with RNAi knockdown of a target molecule. This is followed by a secondary cell-based RNAi screen which is aimed at a selective identification of the target compound to determine which of the small molecule hits identified in the *in vitro* primary screens are the most potent candidates for development. (D and E) Lead optimization can be improved by comparing gene-expression database and cellular phenotypes that are produced by target RNAi screens to those produced by lead compounds and also by comparison to expression profiles within the Connectivity Map. The drug discovery stages used are represented by solid arrows and suggested applications are represented by broken line arrows. Source: image is adapted from (Iorns *et al.*, 2007).

RNAi screening is also very useful at identifying targets, because when they are inhibited in anti-cancer drug treated cells; they either enhance chemosensitivity or confer resistance. This may lead to the discovery of new mechanisms of drug sensitivity or resistance. In addition, these genes can be used as targets for combination chemotherapy (Kuiken and Beijersbergen, 2010). Several RNAi chemosensitiser screens were performed using different anti-cancer drugs such as Paclitaxel (Swanton *et al.*, 2007) and Cisplatin (Bartz *et al.*, 2006). In addition, conducting siRNA screening combined with a therapeutic target such as PARP inhibitor is another example of utilising a siRNA approach to identify other potential

chemosensitiser targets (Turner *et al.*, 2008). A kinase such as CDK5 is identified as a target because its depletion enhanced tumour sensitivity not only to PARP inhibitor but also to Camptothecin and Cisplatin, although the actual molecular mechanism of the correlation between the depletion of CDK5 and the increase in drug sensitivity remains to be explained (Kuiken and Beijersbergen, 2010).

In contrast, using RNAi screening simplifies the process of identifying targets that cause resistance to specific chemotherapy due to their depletion, clarifies the molecular mechanism behind the activation of resistance and predicts biomarkers for resistance to specific types of chemotherapy. This is clinically significance for patients' survival since it allows oncologists to decide on alternative anti-cancer treatments (Berns *et al.*, 2007). For example, a LOF RNAi screen has been conducted using a protein kinase sub-library to identify modulators of Tamoxifen sensitivity in the MCF7 breast cancer cell line that accommodate oestrogen receptor (ER) positive (Iorns *et al.*, 2008). They demonstrated that CDK10 depletion promotes the expression of c-RAF, which consequently activates the p42/p44 MAPK pathway that was previously found to be correlated with increasing expression of Cyclin D1 and inducing resistance to Tamoxifen.

The next stage of drug discovery is target validation, which addresses the clinical correlation between targets and their related cancer diseases. The selected targets should be present in an elevated number of cancer cells and function in a very critical pathway for cancer progression. Target validation can proceed using an RNAi strategy in animal models or a cell-culturing system (Neve *et al.*, 2006). In addition, comparing the phenotypic results of target knockdown by RNAi to those observed either from gene expression microarray or proteomic analysis could confirm if the targets are functional. Identification of any alterations in gene or protein expression as a consequence of target knockdown can be considered as a biomarker during the analysis of patient samples.

The third stage in processing drug discovery is small molecule screening for identifying compounds that would meet all the chemical and physical criteria of a drug-like compound. However, the challenge in such screening is to determine the authentic target for each active compound hit. Thus, performing parallel screens of small molecule inhibitor and RNAi aiming for the same phenotype would serve as means of selective and specific identification of the target compound that is determined in high throughput RNAi screening as previously mentioned (Section 1.3.3). Although the compound inhibitor screen conducted by Eggert *et al.* (2004) identified some compounds for cytokinesis inhibitors, the actual targets of these

compounds hits are underdetermined. In contrast, as the previous example in (Section 1.3.3) showed combining RNAi and compound inhibitor screens for the same phenotype revealed an inhibitor called Binucleine 2 that blocks Aurora B activity and affects cytokinesis, indicating the sufficient effect of RNAi screen in strength the target and compound identification. Thus, Iorns *et al.* (2007) suggested that the cellular phenotype associated with knockdown of a specific target can be used to perform a secondary cell-based screen for identification, specifically the most significant inhibitor hits that were recognised in the primary small molecule screen so the compound can be transferred to the last two stages of drug discovery, lead optimisation followed by transferring of the validated small molecule for clinical trial, which will be detailed below.

Identification of the most efficient and specific small molecules directed against the relevant target can be improved by comparing the phenotypes observed from the gene expression profile of the RNAi system to those observed by promising (or lead) small molecules, then comparing the gene expression microarray profile with the RNAi screen. This could lead to the identification of specific microarray signatures generated in combination with RNAi screen hits. These signatures can be compared with the reference signature in the Connectivity Map (Lamb *et al.*, 2006). The aim of this project is to create a comparison map using gene set enrichment analysis to identify the correlation between genes, chemical compounds (drugs) and diseases. It is based on determining the molecular or reference signatures for the resulting phenotype (produced by RNAi or a compound). These signatures are ranked in order according to the extent, which their expressions are different in comparison to the control (some are gene up- or gene down-regulated). Then, this expression profile is examined and compared to other references in the stored database. After the connectivity score is calculated to evaluate positive or negative matches, the positive match (targets) should show similar molecular signature to those observed in gene target knockdown. This method can successfully identify the compound intended to target similar pathways to the RNAi screen hits, which allows transfer the small molecule for clinical trial process and subsequent drug discovery.

1.4 Project aims

1. The main aim of this project is to use new technologies such as high throughput screening and small molecule and human partial genome siRNA libraries to identify molecules that cause premature chromosome condensation (PCC).

a) Perform a small molecule screen of compounds selected by computer analysis to cause PCC.

b) Analysis of human protein kinase (hPK) and ubiquitin (hUbq) siRNA sub-libraries for genes involved in the regulation of chromosome condensation.

c) Combine the cell number data from two complementary hPK siRNA screens with and with out MCPH1/BRIT1 siRNA knockdown to identify synthetically lethal siRNAs in MCPH1/BRIT1 deficient cells.

2. Investigate the role of MCPH1/BRIT1 in chemosensitivity by

a) IHC for MCPH1/BRIT1 and p53 in advanced BC samples of patients who had undergone treatment with NACT therapy.

i) Investigate the expression of MCPH1/BRIT1 and p53 pre- and post-NACT and their correlation to chemotherapy treatment data and patients survival.

ii) Investigate the correlation between MCPH1/BRIT1 and p53 expression pre- and post-NACT.

b) Chemotherapy drug assays on ovarian cancer cell lines treated with *MCPH1/BRIT1* siRNA or MCPH1/BRIT1 overexpression using a transfected HEK293 cell line with inducible stably overexpression of MCPH1/BRIT1.

Chapter 2 Materials and methods

2.1 Cell Culture

The experimental reagents used in this thesis were purchased from Invitrogen, Dharmacon, Abcam, Bio-rad and Sigma-Aldrich unless otherwise specified. All suppliers' addresses are listed in (Appendix 1). The cell culture was performed in a NuAire Labgard 437 ES Class II Biosafety Cabinet applying all required cell culture laboratory safety practices. Cells were incubated in a Sanyo MCO 20AIC incubator at 37°C with 5% CO_2.

2.1.1 Cell lines

Cell Lines used in this thesis are detailed in Table 2.1 below.

Table 2.1. Cell Lines utilized this PhD project including culture media and cell line suppliers.

Cell line	Cell histology type	Culture media	Source
1847	Human ovarian serous papillary adenocarcinoma	RPMI1640 + Glutamax™ 10% Fetal Calf Serum (FCS) and 1% PenStrep (P/S)	Cancer Research UK (CRUK)
SKOV-3	Human epithelial adenocarcinoma. ascites from a 64yr old Caucasian female.	McCoys 5a (Promocell) 15% FCS and 1% P/S	American Type Culture Collection (ATCC)
U2OS	Human bone osteosarcoma epithelial cells	DMEM + 4.5g/L D-glucose, 10% FCS and 1% P/S	ATCC
IND HEK293 (with MCPH1/BRIT1 construct)	Inducible stable cell line for MCPH1/BRIT1 over expression in human embryonic kidney 293 cells	DMEM + 4.5g/L D-glucose, 10% FCS, 1% P/S, 1:1000 of 100mg/ ml Hygromycin B (InvivoGen) and 1:2000 of 10mg/ml Blasticidin (InvivoGen)	Dualsystems Biotech AG
Inducible Flp-In T-REx system HEK293 cells (with wild type Parkin construct)	Inducible stable cell line for wild type Parkin over expression in human embryonic kidney 293 cells	DMEM + 4.5g/L D-glucose, 10% FCS, 1% P/S, 1:1000 of 100mg/ ml Hygromycin B (InvivoGen) and 1:2000 of 10mg/ml Blasticidin (InvivoGen)	Dualsystems Biotech AG

2.1.2 Cell sub-culture

All the cell types used in this thesis were adherent mammalian cells. Cells were grown in culture flasks ($25cm^2$ and $75cm^2$) containing the specific growth medium and incubated at 37°C in 5% CO_2 atmosphere. When the cells reached 80% confluence, they were sub-cultured. The media was discarded and cells washed with 3-5ml Dulbecco's phosphate buffered saline (DPBS) (PAA). Cells were detached from the flask with 0.5/2ml (for $25cm^2$/$75cm^2$ flasks) of 1:10 trypsin–EDTA (0.5g trypsin and 0.2g EDTA/L) in DPBS. The flask was incubated for 5mins at 37°C and then checked under a microscope (Olympus CKX41) to ensure all cells were fully detached and had formed a single cell suspension. The cell suspension was resuspended into 5ml specific growth medium depending on the cell type (Table 2.1), transferred to 15 ml falcon tube and cells pelleted by centrifugation at 200g for 5min (Eppendorf, 5810R). The cell pellet was resuspended in 10ml growth medium and the cell suspension was split into culture flasks containing media to a final volume of 5ml/15ml (for $25cm^2$/$75cm^2$ flasks) or counted to proceed to further experiments as detailed below.

2.1.3 Cell counting

An Invitrogen countess automated cell counter was used to obtain accurate cell counts. Ten microlitres of cell suspension were mixed with 10µl trypan blue in a sterile Eppendorf tube. Half of this mixture was loaded onto an Invitrogen Countess™ chamber slide. The slide was inserted into the slide port for imaging and analysis.

2.1.4 Cell freezing, storage and recovery

For cell stock preparation, the cell pellet was resuspended in 90% FCS and 10% Dimethyl sulfoxide (DMSO) and stored in 1ml aliquots in cryovials. The cryovials were slowly frozen overnight to -80°C in Nalgene® CryoBox™ containing isopropanol in a -80°C freezer (Innova U725 ultra low temperature freezer, New Brunswick Scientific). The cryovials were transferred for storage in liquid nitrogen. For cell recovery, cryovials containing frozen cells were removed from liquid nitrogen storage, defrosted in a water bath at 37°C. Then, a 15ml tube was prepared to add 9.5ml of growth medium (supplement with 10%FBS and P/S) with 1ml of defrosted stock cells. The tube was spun down for 5min at 200 RCF (relative

centrifugal force*)* to remove the freezing media. Then, cells was resuspended in 2ml of specific fresh growth medium depending on the cell type as detailed in (Table 2.1) and (Section 2.1.2). Cell suspension was added to culture flasks 25cm^2 containing 5ml culture growth medium and incubated overnight at 37°C in 5% CO_2 atmosphere. The culture growth medium was changed using the same flask and returned to incubator. When the cell culture were confluent 70-80%, a cell sub-culture was performed as previously described in (Section 2.1.2).

2.2 Small molecule screens to induce PCC

In the ovarian cancer cell 1847 a small molecule screen (SMS) was performed to identify inhibitors of MCPH1/BRIT1, which thus induce PCC. From a 33,000 small molecule library of chemical compounds (CC), 792 were selected as potential modifiers of MCPH1/BRIT1 based on the three dimensional structure (3D) of the *N*-terminus of Microcephalin identified and prepared by Dr. Richard Foster (Medicinal Chemistry Chemical Biology Technology Group, University of Leeds) (Richards *et al.*, 2010).

Initially, the SMS was optimized for cell density, CC concentrations and incubation period to define the optimal conditions in which the CC would efficiently induce PCC (Section 3.2.1.1). Eleven master "96–well" plates were supplied which contained 2µl of each of the 72 CC at a stock concentration of 10mM in 100% DMSO. The CC were plated in rows B-G and 100% DMSO vehicle control was plated in rows A and H. The preparation of the assay plates was as follows; screens were performed in duplicate in View Plates (PerkinElmer). Each assay plate contained 72 CC at a stock concentration 20µM in 0.2% DMSO, plated in rows B-G. Rows A and H contained the assay controls, which included negative/vehicle controls (0.2% DMSO), the positive control *MCPH1*/*BRIT1* siRNA and its corresponding NT-siRNA control, Doxorubicin was used as a positive control for the identification of CC hits which induced cell death) (stock 10mg/ml; Sigma) at a final concentration of 0.4µg/ml (Appendix 2.1) and Nocodozole was used as a positive control for induction of the mitotic cell phenotype /pHH3 Ser10/mitotic cells marker (stock 6.64mM; Sigma) at a final concentration of 1µM (Appendix 2.2). Doxorubicin and Nocodozole were only included in 4 plates in the first replicate and in all the 11 plates in the second replicate. The addition of controls or CC to the assay plates will be detailed below.

	1	2	3	4	5	6	7	8	9	10	11	12
A	0.2% DMSO	0.2% DMSO	0.2% DMSO	0.2% DMSO	*MCPH1* siRNA	*MCPH1* siRNA	NT-siRNA	NT-siRNA	1µM Nocodozole	1µM Nocodozole	0.4µg/ml Doxorubicin	0.4µg/ml Doxorubicin
B	CC	CC	CC	CC	CC	CC	CC	CC	CC	CC	CC	CC
C	CC	CC	CC	CC	CC	CC	CC	CC	CC	CC	CC	CC
D	CC	CC	CC	CC	CC	CC	CC	CC	CC	CC	CC	CC
E	CC	CC	CC	CC	CC	CC	CC	CC	CC	CC	CC	CC
F	CC	CC	CC	CC	CC	CC	CC	CC	CC	CC	CC	CC
G	CC	CC	CC	CC	CC	CC	CC	CC	CC	CC	CC	CC
H	0.2% DMSO	0.2% DMSO	0.2% DMSO	0.2% DMSO	*MCPH1* siRNA	*MCPH1* siRNA	NT-siRNA	NT-siRNA	1µM Nocodozole	1µM Nocodozole	0.4µg/ml Doxorubicin	0.4µg/ml Doxorubicin

Figure 2.1. An example of the 96 well plate layout for the small molecule screen.

2.2.1 SMS assay set up and *MCPH1/BRIT1* siRNA reverse transfection

The PCC positive control *MCPH1/BRIT1* siRNA reverse transfection, was previously optimized by Dr. Rawiah Alsiary in the ovarian cancer 1847 cell line at a final concentration of 75nM siRNA treatment for 48hr. All siRNAs used for the CC screen were purchased from Dharmacon or Invitrogen and siRNA sequences are recorded in (Appendix 3.1). Master mixes were prepared for control siRNAs, where, per well, 0.18µl *MCPH1/BRIT1* siRNA (stock 40µM) (Thermo Scientific™ Dharmacon) was diluted with 16.3µl Opti-MEM-1 (1×) low-serum media (Invitrogen) and 0.375µl of the Non-Targeting (NT)-siRNA control (stock 20µM) (Invitrogen) was diluted with 16.125µl Opti-MEM-1 (1×) in separate tubes. After preparing the two-transfection reagents, they were incubated at room temperature (RT) for 5mins. Then, 0.2µl Lipofectamine RNAiMAX/well (Invitrogen) was diluted with 3.3µl Opti-MEM-1 (1×) low-serum media/well and added to both tubes and mixed. The 20µl volume of *MCPH1*/BRIT1-siRNA-RNAiMAX and NT-siRNA-RNAiMAX was added individually to the test plate as denoted in (Figure 2.1) and incubated at RT for 20min.

The ovarian cancer 1847 cells were harvested and resuspended to a density of 7×10^4 cells/ml in (i) RPMI 1640 medium without antibiotics and containing 10% FCS for wells containing siRNA controls and (ii) RPMI 1640 media supplemented with 10% FCS and antibiotics (P/S) for the wells containing the CC. An 80µl volume of cell suspension was plated into each well and the plates incubated for 24hr at 37°C before the addition of the CC as described below (Section 2.2.2).

2.2.2 Chemical compound (CC) library preparation and addition of CC to assay plate

After optimisation of cell density, CC concentration and incubation time, the CC master plates were prepared as follows: Each plate contained 72 CC at a concentration of 10mM in 100% DMSO. 2µl of each of the 72 CC or 100% DMSO vehicle control was plated out and freshly diluted to 1:100 with 198µl RPMI 1640 + Glutamax™ media containing 10% FCS. 20µl (containing 0.2% DMSO) of this working stock of 100µM CC was added to the 80µl cell suspension already plated out into the SMS screen plate in rows B-G. This resulted in a final CC concentration of 20µM in 0.2% DMSO. Doxorubicin and Nocodazole controls were added to the desired wells in Rows A and H as shown in Figure 2.1. Transfer of cell suspension, CC dilution and CC transfer were carried out using a Bravo SRT G5409A automated liquid handling platform (PerkinElmer). One plate was then incubated for 24hr and the second for 48hr at 37°C. SMSs were performed in duplicate. Plates were fixed and immunofluorescently stained before evaluation by high-content imaging.

2.2.3 Cell fixation and Immunofluorescence (IF) optimization

The cell culture media was removed from each well of the CC plates after 24hr and 48hr respectively. Per well, the cells were washed 3 times with 100µl PBS, waiting 3-4 mins between each wash. The cells were fixed with 100µl of ice-cold methanol *(Sigma-Aldrich),* incubated at -20°C for exactly 5 mins. The cells were washed twice with 100µl PBS and blocked in 1% (w/v) non fat-milk/ PBS (usually 0.50g/50ml, spin for 10 min) for 15-30mins

Next, 60µl of the primary antibody pHH3 (Ser10) (Table 2.2) and initially active caspase-3 (Table 2.2) were both added to cells at a 1:6000 dilution in 1% non fat-milk in PBS to detect mitotic and apoptotic cells respectively and the plates incubated at RT for 1hr. The plates were washed 3x with PBS. A 1:1000 dilution of DAPI or secondary antibodies (Table 2.2) in 1% milk in PBS was prepared, and 60µl was added to each well using a FluidX cell dispenser (XRD-384). Plates were wrapped in foil, and incubated for 1hr at RT, then washed with PBS three times. The plates were imaged using the Operetta high content imaging system and analysed with the associated Columbus software (PerkinElmer).

Table 2.2. Antibodies ultlised for immunofluorescence assay.
Type, final concentration and company supplier of antibodies used to stain cells during Immunofluorescence processing.

Antibody	Type	Final concentration	Company supplier
Mouse ab to phospho-histone H3 (Ser10) 1mg/ml	Primary antibody	1:6000	Abcam, ab14955 Lot: GR115353-1
Rabbit ab to active caspase-3 0.9mg/ml	Primary antibody	1:6000	Abcam, ab13847 Lot: GR29703-1
Alex Fluor® 488 green goat anti mouse IgG (H+L) 2mg/ml highly cross adsorbed	Secondary antibody	1:1000	Life technologies A11029 Lot: 1306597
Alex Fluor® 594 red goat anti mouse IgG (H+L) 2mg/ml highly cross adsorbed	Secondary antibody	1:1000	Life technologies A11032 Lot: 51657A
DAPI (4',6-Diamidino-2-Phenylindole, Dihydrochloride) 10mg/ml	Secondary antibody	1:1000	Biotium Cat: 40011

2.2.4 High-content high-throughput imaging and software analysis systems

The phenotypic effects of these small molecule inhibitors were analysed using the Operetta high-throughput high content imaging system (PerkinElmer) as described below in Sections 2.2.4, 2.2.5 and 2.2.6. SMS assay set up and *MCPH1*/*BRIT1* siRNA reverse transfection

Plates were scanned and DAPI stained PCC and pHH3 Ser10/mitotic cells images were captured using the Operetta high content imaging system (PerkinElmer) and analysed using Columbus Data Manager Acapella software. Each plate was labelled with specific information barcodes and inserted into the workstation of a PerkinElmer Plate Handler II robotic arm, equipped with Plateworks software, which enables the barcoded plates to be scanned before insertion into the Operetta. Wells were imaged at 20x magnification with 15 fields of view for each well (510 X 675µm). The Acapella software (PerkinElmer) was used for image analysis as detailed below.

2.2.5 PCC and pHH3 Ser10/mitotic cells detection by Columbus software

In order to detect PCC cells, my colleague Dr. Victoria Cookson generated an image analysis algorithm (Adams *et al.*, 2014) using Acapella. Nuclei identification was based on whole nuclei stained with blue DAPI. Border objects were excluded to avoid analysing incomplete nuclei. A distinction between the phenotype of PCC cells (cells with compacted chromosomes) and normal nuclear morphology was identified. Acapella was instructed to identify the compacted chromosomes as spots in the nucleus and nuclei containing 14 or more spots were identified as PCC cells. The two main parameters used to generate data from the screen were the number of whole nuclei and percentage of nuclei with PCC.

In addition, an image analysis algorithm was designed using Acapella software to detect mitotic cells in cells stained with pHH3 Ser10 thus the latter was used as a surrogate marker for mitotic cells. A method for identifying mitotic cells, those cells with intensive nuclear pHH3 Ser10 intensity, was recommended by the screening's expert Dr. Heather Martian from BioScreening Technology Group (BSTG) at the University of Leeds (Martin *et al.*, 2014). A nuclear pHH3 Ser10 staining intensity cut–off unit for cells treated with 20µM of CC or 0.2% DMSO negative control was initially examined and optimised using a range of different pHH3 Ser10 intensity cut-offs units (For example; 600, 900, 1000 and 1200 units). The optimal cut-off staining intensity unit of pHH3 Ser10 in the nucleus was selected based upon the nuclear pHH3 Ser10 intensity for 0.2% DMSO negative controls cells, which was between 600-900 units. An increase in the number of pHH3 Ser10 expressing cells in the CC wells compared to the DMSO negative control wells constituted a CC hit for increasing mitotic cells.

SMSs were performed in duplicate. Plates in the first repeat were stained with the secondary antibody Alex Fluor® 549 Red and mitotic cells were identified with pHH3 Ser10 with an intensity cut-off of greater than 600 units. However, an intensity cut-off of pHH3 Ser10 at 900 units was used to analyse the second repeat plates that were stained with Alex Fluor® 488 Green. The percentage of pHH3 Ser10 was the key parameter used to define whether CC could induce a high-level of mitotic cells or increase cell proliferation.

2.2.6 Statistical analysis

The statistical analysis was executed for each plate individually using Z score and robust Z score calculation methods (Zhang, 2011; Goktug *et al.*, 2013). The Z score is the number of standard deviations (SD) away from the mean of negative control (DMSO). The robust Z score was used as an alternative hit identification method and this method statistically supported selected CC hits previously revealed using the Z score method. The Z score and robust Z score formulas are similar, only the mean and standard deviation (SD) in Z score are replaced with median and median absolute deviation (MAD) in robust Z score.

The formula of Z score = (%PCC (CC)– mean %PCC (DMSO))

(SD) %PCC (DMSO)

The formula of Robust Z score = (%PCC (CC)– median %PCC (DMSO))

MAD %PCC (DMSO)

The Z score or Robust Z score cut-off value for hits identification was as follows; ≥ 2 for CC that increased %PCC or increased %mitotic cells (pHH3 Ser10) whereas ≤ -2 for CC hits decreased cell number.

2.3 High- throughput partial genome siRNA screen for genes inducing PCC

The high-throughput human partial genome siRNA screen for genes that induced PCC in U2OS osteosarcoma cells, was developed and performed by BSTG, University of Leeds for the Microcephaly and Cancer Group. The siRNA screen contained 4 different human sub-libraries, Protein Kinase (hPK) (9 plates), Ubiquitin (hUbq) (9 plates), Protease (6 plates) and Drug Targets (60 plates)). Each siRNA library, consisted of Dharmacon siGenome SMARTpool siRNAs (4 siRNAs targeting a single gene per well), and was performed in duplicate in 96-well plate format.

siRNA resuspension

The hPK and hUbq siRNA sub-libraries were ultlised in this PhD study. According to BSTG's siRNA screen development protocol, theses two siRNA sub-libraries were individually performed as follows (Adams *et al.*, 2014); A Dharmacon siGenome SMARTpool siRNAs (Thermo Fisher Scientific, Pittsburgh, PA) were provided as a lyophilized pellet in a 96-well plate format. The plates were centrifuged for 1min to collect the pellet at the bottom of each well. The pellets were resuspended in 50µl 1x siRNA buffer (Thermo Fisher Scientific) to give a final working concentration of 2µM, then the siRNA solution was mixed on a plate shaker for 90mins at RT.

The siGenome pooled NT-siRNA controls and pooled *PLK1* siRNA (a positive transfection control which induces cell death) (Dharmacon) (Appendix 4) were reconstituted with 1x siRNA buffer to a final stock concentration 20µM according to Dharmacon™ recommended basic siRNA's protocol and then diluted to a 2µM working concentration. Human *MCPH1*/*BRIT1* siRNA (stock 40µM) was diluted to a working concentration of 2µM using 1x siRNA buffer and was used as a positive control for evaluating the level of PCC. The resuspended siRNA plates and controls were stored at -20 °C.

siRNA reverse transfection

Each negative or positive control was added to columns 1 and 12 and siRNA sub-libraries into Columns 2-11 in 96-well plates (View Plates; PerkinElmer) (plate map; Appendix 4). The reverse transfection of siRNA sub-libraries and controls was performed at a final concentration of 50nM.

Then, Fluid-X XRD-384 dispenser (at 300 rpm) was used to add the transfection reagent mixture containing 17.5µl Opti-MEM-1 (1x) low serum media (Invitrogen) that was mixed with 0.1µl Lipofectamine RNAiMAX (Invitrogen) per well. Plates were covered and transferred to the laboratory rotary shaker allowing the transfection solution to be mixed with siRNA at RT for 20min. Next, 80µl U2OS cell *suspension* at a density of 7.5×10^4 cells /ml in DMEM growth medium supplemented with10% FCS*,* that was maintained under constant magnetic stirring, was aliquoted into each well, using a Fluid-X XRD-384 dispenser at 300 rpm. To reduce the edge effects the plates were incubated at RT for 1hr in a laminar flow cell culture hood then transferred to a 37°C in 5% CO_2 incubator for 72hr. Post incubation, the cells were fixed with methanol, blocked with 1% non-fat milk and

stained with DAPI to detect the nuclei or pHH3 Ser10 as a marker of mitotic cell as previously described in (Section 2.2.3). The plate was scanned and imaged using Operetta and analysed using Columbus software as previously described in (Sections 2.2.4 and 2.2.5).

2.3.1 Image analysis siRNA screen controls

Images of the positive and negative controls in each plate were manually visualised and the previously described Acapella software PCC analysis protocol (Sections 2.2.4 and 2.2.5) used to assess the efficiency of *MCPH1/BRIT1* siRNA knockdown to induce a clear PCC phenotype. Plates were cleaned prior to imaging to ensure artefact effects from dust did not interfere with image acquisition or analysis. Fifteen fields of view per well were imaged and analysed.

2.3.2 Statistical analysis of PCC inducer hPK and hUbq siRNAs libraries for genes which induced PCC

The Z score calculation, with a cut off value of ≥ 2, was used on each plate of PCC inducer hPK or Ubq siRNA sub-libraries to identify potential genes which induced PCC. The flowchart (Figure 2.2), below, briefly describes the statistical methodology that was used to analysis the hPK siRNA library. As described in Section 2.3 and based on Adams *et al*., (2013), each siRNA library screen was performed in duplicate (hPK siRNA library contains 9 plates). The positive control (*MCPH1/BRIT1* siRNA) for each plate for both duplicates was visually inspected for the PCC phenotype cells using the Columbus software analysis system as previously described in (Sections 2.2.4 and 2.2.5).

Initially, the negative control (NT-siRNA) was used as a reference for calculating the Z score (%PCC) or (cell number) in duplicate plates. Hits were scored if a Z score (%PCC) of ≥ 2 was achieved in both replicates plates. The Z score (cell number) of ≤ -2 was used as cut-off for identifying of siRNAs that reduced cell number. For each siRNA hit, the average (Standard deviation (SD)) for Z score of %PCC from both replicates was calculated. Also, average (SD)) for Z score of cell number from both replicates was calculated so this could minimize the variations of Z score values between the two replicates. A large numbers of potential inducer hPK siRNAs hits were generated.

PCC phenotype is a distinguish marker of downregulation of the cellular function of MCPH1/BRIT1 (Trimborn *et al.*, 2004). In addition, the main aim of the existing siRNAs screens was to identify genes which induced PCC. To minimise identification of the false negative hits as a consequence of using negative controls for Z score analysis, we attempted to use more stringent control, which was the positive *MCPH1/BRIT1* siRNA control, for Z score analysis (%PCC) of each plate individually in the hPK siRNA screen in both replicates. Consequently, the Z score analysis unexpectedly revealed one potential siRNA hit.

Considerable plate-to-plate variation was observed for the %PCC and/or cell number in the positive control (*MCPH1/BRIT1* siRNA) on some replica plates. Therefore, calculation of the Z score based on the total average of %PCC of *MCPH1/BRIT1* siRNA in each batch of plates (known as Z score batch analysis) was performed. The following calculations for positive control were first executed to achieve the Z score batch analysis. For each individual batch of plates, where each plate contained two positive controls *MCPH1/BRIT1* siRNA, the average %PCC and cell number of positive controls per plate was calculated. Then, the total average of these individual values (average %PCC/ or cell number) in each plate were also calculated resulting in one value for batch 1 and another for batch 2. The batch analysis Z score using an average %PCC of the positive control *MCPH1/BRIT1* siRNA of each batch individually was used to identify hPK siRNAs hits that induced PCC. Again, the analysis identified a similar siRNA hits that was previously observed during the Z score analysis of hPK siRNA screen using positive control in each plate individually.

Next, the siRNA hit list, that was initially generated by using the Z score analysis (negative NT-siRNA control) method, to select the top siRNA hits that showed a significant Z score and higher %PCC for hits validation (Chapter 4; Section 4.2.1.4; Table 4.1). The PCC induced siRNAs hits generated from the hPK library based on Z score analysis (%PCC of negative control NT-siRNA), were evaluated using Columbus software analysis as described in the flowchart above (Figure 2.2; point 6). Further experimental siRNA hit validation was carried out as detailed below in (Section 2.3.3).

Similarly, the PCC inducer human Ubiquitin (Ubq) siRNA library was analysed for both %PCC and cell number using Z score based on the %PCC and cell number of the negative control NT-siRNA. A list of potential PCC inducer hUbq siRNAs hits was generated (Chapter 5; Section 5.2.1.3; Table 5.1).
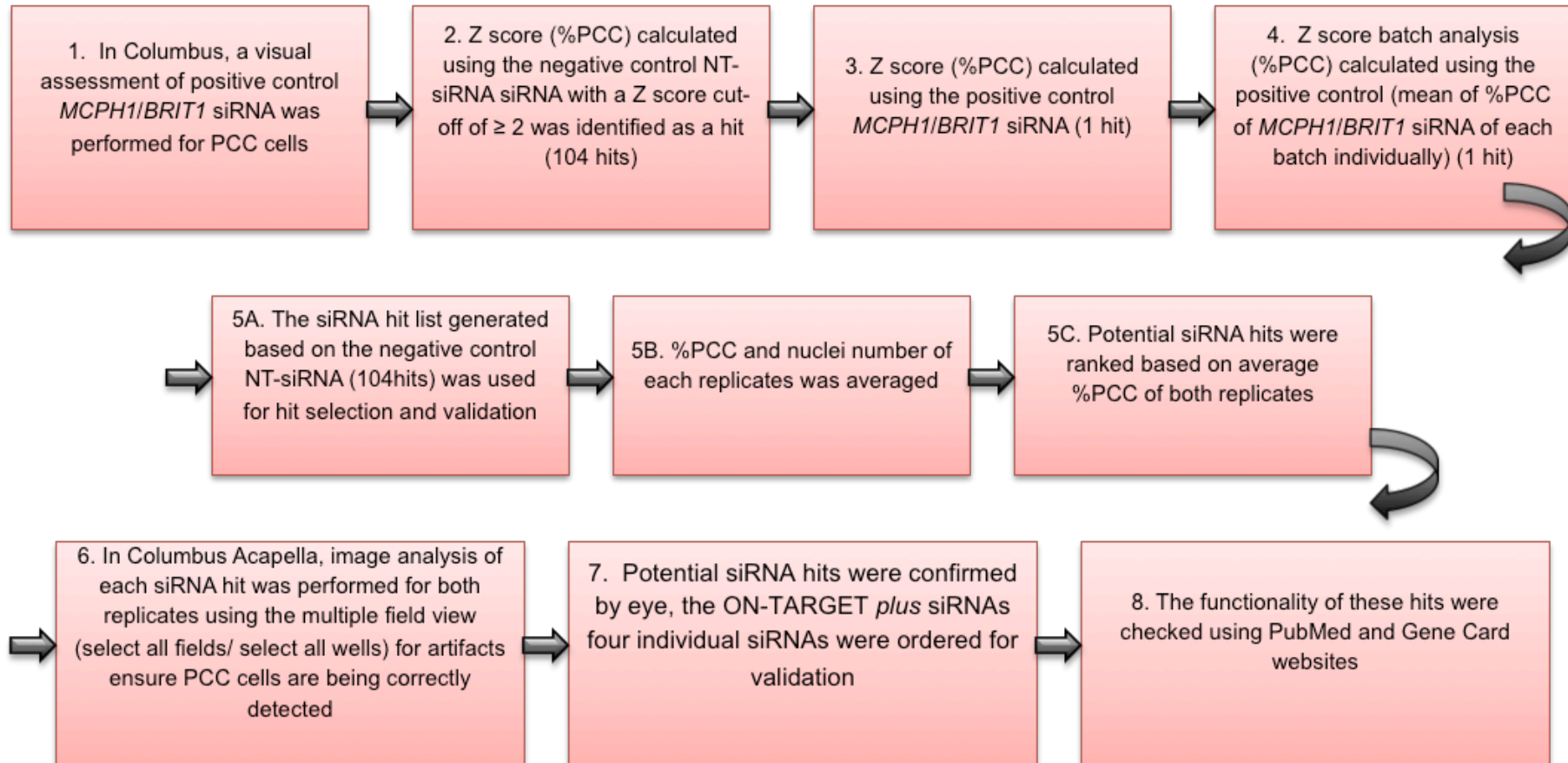
Figure 2.2. Flowchart describing the process of statistical analysis used to analyse the PCC inducer hPK siRNAs library for hits which induced PCC.

2.3.3 siRNA hits validation using four individual ON-TARGET plus siRNAs

The validation of the selected potential PCC inducer hPK siRNAs or hUbq siRNA hits was performed using Dharmacon ON-TARGET *plus* siRNAs (Appendix 3.1 and 3.2).

2.3.3.1 Dharmacon ON-TARGET *plus* siRNA resuspension

For small scale reverse transfection of candidate siRNAs, a Dharmacon ON-TARGET *plus* siRNA set comprising of a set of four individual siRNAs to target an individual gene, was provided as a lyophilized pellet in a 96-well plate format and was resuspended with 1x siRNA buffer to a working concentration of 2μM as previously described above in Section 2.3. Control siRNAs including Dharmacon ON-TARGET *plus* single NT-siRNA siGenome SMARTpool *PLK1, MCPH1/BRIT1* siRNA (stock 40μM) were reconstituted with 1x siRNA buffer to a concentration of 2μM as previously described above in Section 2.3.

The reverse transfection of hPK or Ubq siRNA hits and controls was performed at a final concentration of 50nM as previously described in Section 2.3; or 100nM, which will be explained below.

2.3.3.2 The reverse siRNA transfection procedures for siRNA hits validation

The four ON-TARGET *plus* siRNAs or controls (5μl) targeting each selected hit alongside the NT-siRNA controls were individually aliquoted into the desired well. Then, for each well, the transfection reagent mixture containing15μl Opti-MEM-1 (1x) low serum media (Invitrogen) was mixed with 0.1μl Lipofectamine RNAiMAX (Invitrogen), incubated at RT for 5min and the transfection reagent mix was added to the desired well. Next, the plate was covered and transferred to the laboratory rotary shaker allowing the transfection solution to be mixed with siRNA for 20min at RT. Then, 80μl U2OS cells, at a density of 7.5×10^4 cells /ml in DMEM growth medium supplemented with only 10% FCS, was aliquoted into each well. The plate was incubated at RT for 1hr in a laminar flow cell culture hood then transferred to a 37°C in 5% CO_2 incubator for 72hr.Then, cells fixation and DAPI or pHH3 Ser10 staining and imaging analysis were previously described in Sections 2.2.3, 2.2.4 and 2.2.5.

2.3.4 Conformation of hit siRNA and control siRNA knockdown by western blotting (WB)

For large scale reverse transfection of candidate siRNAs, the four ON-TARGET *plus* siRNA (5 nmol) (Dharmacon) and ON-TARGET *plus*™ control NT-siRNA (5 nmol) (Dharmacon) were diluted to the recommended final concentration of 20µM using 1X siRNA buffer following the Dharmacon™ recommended basic siRNA Resuspension's protocol. The reverse transfection candidate hit or control siRNA knockdown was performed in a 6 wells plate at a final concentration of 50nM siRNA. Each individual hit siRNA/or control siRNA (7.5µl) was aliquoted in triplicate. A transfection mixture of 3µl Lipofectamine RNAIMAX and 525µl Opti-MEM-1 (1x) low serum media was mixed and incubated at RT for 5 min. The transfection solution was then added to candidate hit siRNA or control siRNA and incubated at RT for 20 min. Then, 2.4ml U2OS cells, at a density of 7.5×10^4 cells /ml in DMEM growth medium supplemented with 10% FCS, were seeded into each well. The plates were incubated at RT for 1hr in a cell culture hood then transferred to a 37°C in 5% CO_2 incubator for 72hrs.

After the 72hr incubation, a set of 15ml falcon tubes were labelled based on the hit siRNA or control siRNA used in the experiment then they were placed in ice in preparation for cell lysate collection. The growth medium was removed from wells, and cells washed twice with 3ml fresh ice cold PBS, the first wash removed any residual growth medium while the attached cells were scraped off the well using a sterile cell-scraper into the second PBS solution which was then transferred to the corresponding flacon tube. The tubes were centrifuged at 450g for 10min at 4°C. The supernatant was removed and the flacon tubes within cell pellet were either stored in -80 °C freezers to be used later or were kept in ice prior to protein or RNA extraction.

2.3.4.1 Protein quantification by western blotting

Protein extraction reagents such as the Radio Immunoprecipitation Assay buffer (RIPA) (Appendix 6.1), Phenylmethanesulfonyl fluoride (PMSF/ 1mg/ml stock in isoproponal) and sodium orthanovanadate (1:100 of 100mM stock) were prepared by Dr. Victoria Cookson or Dr. Sandra Bell. 1ml of RIPA buffer was mixed with 10µl (100mM stock) sodium orthanovanadate,1:50 (20µl) protease inhibitors cocktail tablets (Roche Diagnostics GmbH) and 100µl PMSF. The cell pellet was resuspended in 50µl to 100µl RIPA lysis buffer and left on ice for 30min. Next, the

cell lysate samples were transferred to Eppendorf tubes and were centrifuged at 15000g for 10min at 4°C to pellet the cell debris. The supernatant was transferred to a new Eppendorf tube and the sample tubes were stored at -20°C and an aliquot removed for determination of protein quantification by a Bradford protein assay.

2.3.4.1.1 Bradford protein assay

To measure the protein concentration in the samples, a Bradford protein assay (DC™ protein assay, Bio-Rad) was performed. The extracted protein samples were diluted 1:10 in ddH$_2$O water. A standard BSA protein curve was prepared as follows. Firstly, 300ml RIPA buffer was diluted to a 10% concentration in 3ml ddH$_2$O. Secondly, 20mg/ml bovine serum albumin (BSA) buffer was prepared by dissolving 0.2 g BSA (SIGMA) in 1ml ddH$_2$O, then, the BSA solution was diluted at 1:10 in 10% RIPA buffer to final concentration 2mg/ml. Thirdly, a standard dilution series was prepared (0, 0.1, 0.25, 0.5, 0.8, 1, 1.5 to 2µg/µl) from the 2mg/ml BSA and 10% RIPA buffer solutions (Appendix 6.2).

In a 96 well plate, controls, BSA standards and protein sample were set up in triplicate. 5µl each of the 10% RIPA buffer blank control, each BSA standard curve dilution and extracted protein sample was added to the plate.

Next, 20µl Bio-Rad DC™ Protein assay Reagent S (Bio-Rad laboratories) was mixed with Bio-Rad D$_c$ Protein assay Reagent A and 25µl of mixture was added onto each well. A, 200µl Bio-Rad DC™ Protein assay Reagent B was added per well. The plate was then mixed on the laboratory rotary shaker at RT for 15min and loaded into the microplate reader Titertek$^{®}$ (Thermo ELECTRON COPERATION/ ORGINAL Multiskan EX/ Scientific Laboratory Supplier). The Ascent software was used to read the absorbance at 690nm.

Microsoft Excel was used to determine the total concentration of protein in each sample. Readings from the triplicate BSA standards for each protein concentration were averaged and a scatter chart plotted (concentration versus corresponding absorbance reading). Then, the trendline equation result (y=mx+c) was displayed on a chart. The triplicate absorbance readings of each sample were averaged and the total protein concentration (µg/µl) was calculated from the standard BSA curve and multiplied by 10 (as the protein sample dilution was 1:10).

Total Protein concentration (µg/µl) = Average reading of sample absorbance ÷ the resulting equation y value of BSA standard ×10.

2.3.4.1.2 Gel electrophoresis

Gel Electrophoresis and protein transfer were performed in an Invitrogen Surelock gel tank and associated blotting module. For sample preparation the selected protein sample concentration (typically 10-100µg) was diluted to a final volume of 37µl in ddH$_2$O and combined with 1.8µl 50mM DTT (1:20 from 1M stock) (Sigma) and 9µl NuPAGE$^®$ LDS sample buffer (4x) (Novex by Life Technologies). The sample was placed in a hot block at 95°C for 10mins to denature protein complexes and was centrifuged for 10 sec to collect the sample. The NuPAGE 4-12% Bis-Tris gel (Novex by Life Technologies) was placed in the gel tank after removing white tape at the bottom of the cassette. Then, 25ml of NuPAGE$^®$ MES running buffer (20x stock) (Novex by Life Technologies) (suitable to aid the separation of 3.5 to 160 KDa proteins in conjunction with the 4-12% gel) was diluted to a final volume of 500ml in dH$_2$O and was transferred to fill up the top of the middle compartment of the gel tank. The combs were gently removed from the gel and the wells washed with running buffer using 1ml pipette to ensure removal of residual gel at the top of the well and to simplify movement of the sample into the well. The samples were loaded into the well alongside each other with one protein molecular weight marker lane containing 7µl of Biorad precision Plus Protein™ Dual Colour standard. The gel was electrophoresised at 150 volts (V) at RT for 90min until the dye front moved toward the bottom of the gel.

For protein transfer onto PVDF membrane the Surelock Transfer module was set up as per manufacturers recommendation. 25ml (20x stock) of NuPAGE$^®$ transfer buffer (Invitrogen) containing 10% methanol (v/v) was made up to 500ml in dH$_2$O. Six sponges were washed with cold tap water to remove any bubbles then were soaked in the 1x transfer buffer. For membrane activation, the two PVDF membranes (Novex by Life Technologies) were first placed in methanol for 30sec then rinsed in dH$_2$O for 5min using a rotary rocker and finally soaked in 1x transfer buffer until ready to use. The two blotting papers (Novex by Life Technologies) were retained in the transfer buffer for later use when the gel is ready for assembling the blotting sandwich step.

The running buffer in the gel tank was poured away and the tank was rinsed with tap water. The gel was removed gently from the gel cassette placing the gel knife around the edge of the cassette allowing separation of both halves. Then, any excess and unwanted gel at the top and the bottom were removed. The gel was then placed into transfer buffer.

To assemble the blotting sandwich three wet sponges were placed into the cathode core. Then, the first blotting paper was added followed by the first PVDF membrane. The gel was gently placed on top of the blotting membrane. Next, the second PVDF membrane and the second blotting paper were respectively placed on top of the gel. The rest of the sponges were added. At each stage of the assembly, air bubbles were removed using a wet roller the sandwich to remove any air bubbles. The anode lid was carefully aligned onto the top of the sandwich and the blotting sandwich compressed together into the cathode core box and transferred to the gel tank. The blot module was filled with transfer buffer and iced water added to the gel tank surrounding the blotter to prevent overheating and hence protein degradation during the transfer process. The proteins transfer was performed for 1.5-2hrs at 30V.

The blotting sandwich was disassembled and complete transfer of the marker was checked as a reference for proper transfer. The membrane was blocked for 30min in 50ml of 10% (w/v) non-fat milk solution in TBST (Tris buffer saline (TBS/10x stock) (Alfa Aesar) in 0.1% (v/v) Tween-20 (G-Bioscience)). Then, the blotting membrane was incubated overnight at 4°C with primary antibody (Table 2.3) diluted in 5ml of 5% non-fat milk.

Table 2.3. Type, final concentration and company supplier of antibodies utilised to detect the target protein during western blot.

Antibody	Type	Final concentration	Company supplier
Anti -FBXO5/EMI1 purified rabbit antibody Immunogen affinity 0.6mg/ml	Primary	1:200	Novus Biologicals, NBP-84850, Lot: A89841
Monoclonal Anti-β-Actin, mouse antibody (clone AC-15 ascites fluid)	Primary	1:5000	SIGMA Life Science, A5441
Anti-MCPH1/BRIT1 rabbit Polyclonal antibody 100mg, 0.8mg/ml,	Primary	1:1000	Abcam, ab2612
The Parkin (Prk8); mouse monoclonal ab	Primary	1:1000	Cell Signalling Technology, 4211
Polyclonal Goat Anti-Rabbit immunoglobulins/HRP 0.30g/L	Secondary	1:5000	DAKO Cytomation
Polyclonal Rabbit Anti-mouse immunoglobulins/HRP 1.3g/L	Secondary	1:5000	DAKO

The blotting membrane was washed 3 times with TBST/Tween 20 each for 15mins. Next, the membrane was incubated for 1hr at RT in 1:5000 horseradish peroxidase HRP conjugated secondary antibody (DAKO, Glostrup, Denmark), diluted in 5% (w/v) non-fat milk in TBST/Tween 20 (Table 2.2). Again, the blotting membrane was rinsed into TBST 3 times each for 15mins. The SuperSignal® West Pico/Femto Chemiluminescent Substrate (Thermo Scientific) was then equally distributed across the membrane enabling protein detection and visualization on Chemiluminescence analyser (Biorad) using Quantity One® software (Bio-Rad).

2.3.4.2 mRNA determination using quantitative reverse transcription-polymerase chain reaction (qRT-PCR)

To perform RNA extraction or the complementary DNA (cDNA) synthesis, all the laboratory equipments used during qRT-PCR was sprayed with 70% (v/v) ethanol to reduce RNase contamination and chemical reagents were RNase free to prevent RNA degradation.

2.3.4.2.1 RNA extraction and quantification

After the large scale siRNA reverse transfection was performed (Section 2.3.4), cells were trypsinised and collected by centrifugation. Total RNA extraction from the cell pellets was perform using the RNeasy® Plus Mini Kit (QIAGEN, Valencia, CA) following the manufacturer's instructions.

The extracted RNA was quantified using a Nanodrop spectrophotometer instrument (Labtech International) to determine the RNA concentration per sample in ng/µl. The pure absorbance RNA was assessed using a ratio of absorbance 260/280 nm and ratio of about 2 was generally used as a reference for pure RNA.

2.3.4.2.2 cDNA synthesis

The hot block and water bath were heated to 65$^{\text{o}}$C and 50$^{\text{o}}$C, respectively. 9µl of the following mixture was prepared for each sample: 1µl random hexamers (50µM, 5nmole stock) (Roche Applied Biosystem); 1µl of 10mM stock deoxyribonucleotides (dNTPs), which were a set of 4 dNTPs, where 10µl of 100mM stock per nucleotide dC, dG, dA, dT (Smart Molecular Solutions, BIORON GmbH)

was mixed with 60µl molecular biology grade water (Mol.Bio.H_2O)); 7µl Mol.Bio.H_2O.

Then, 500ng-1µg RNA in 5µl of (Mol.Bio.H_2O) was prepared and added to the mixture. The sample was heated at 65^oC for 5mins, and then placed on ice for 2mins and quickly centrifuged using bench top centrifuge for 30sec. The hot block temperature was increased to 70^oC as a preparation step for later use. Next, 6µl of the following mixture was added to each sample: 4µl of 1st stand buffer (5x stock) (Invitrogen by Life Technologies); 1µl of dithiothreitol DTT (0.1M stock) (Invitrogen by Life Technologies); 1µl superscript$^{®}$ III Revise Transcriptase (200U/µl) (Invitrogen by Life Technologies). Then, the sample was incubated at RT for 5mins, heated first in the water bath for 50mins, then transferred to the hot block at 70^oC for 15mins and placed on ice for 2mins and finally centrifuged for 30sec before the cDNA sample was stored at -20^oC until further use.

2.3.4.2.3 Primer optimization for qRT-PCR performance of four on target *plus* siRNAs

All the reverse and forward primers used in this project are listed in Table 2.4, were designed by Dr. Victoria Cookson and purchased from SIGMA. They were individually diluted with Mol.Bio.H_2O to a 100µM final stock concentration and the diluted forward and reverse primers combined and diluted to 10µM as a working concentration by adding 10µl of each primer to 80µl Mol.Bio.H_2O, giving a final volume of 100µl.

Table 2.4. Showing the qRT-PCR primers sequences used in this project for assessment of siRNA hit knockdown.

Primer name	Sequence
FBOX5/*Emi1* Forward	5′- ACCAAGTTATCCAATCAAGGTGATC
FBOX5/*Emi1* Reverse	5′-TTGAGGCTTTCGTTCTTTTTCAAT
36B4 Forward	5′-ACATGCTCAACATCTCCC
36B4 Reverse	5′-TTCAAGGTTAGCTGGGG

Next, to evaluate the mRNA level of target gene, 10µM- working concentration of primer mixture was used to optimise the primer concentration for RT-PCR using a range of concentrations (50/50nM, 100/100nM and 300/300nM), which will be detailed below. The qRT-PCR workstation was prepared with all real time PCR requirements consumables (96-well plat, e-Eppendorf tubes, plate seal

and nuclease free water (QIAGEN) that which were decontaminated under UltraViolet light (UV) for 15mins.

In order to evaluate the mRNA level of the target gene, forward/reverse primer concentration for qRT-PCR were optimised using a range of concentrations (50/50nM, 100/100nM and 300/300nM). The volume of qRT-PCR components for each primer concentration are described in (Table 2.5). For each concentration of primer, 23µl of the PCR/primer mix was added to four wells. The cDNA from untreated cells was diluted to 1:10 in Mol.Bio.H_2O and 2µl cDNA was added to two wells while the rest remained without cDNA.

Table 2.5. Optimisation of a primer of target gene for RT-PCR.
Description for the composition of the qRT-PCR reaction per well including the SYBR Green PCR master mix with different primer concentrations.

Primer concentration/ master mix reagents	SYBR Green PCR Master Mix	Primers	Mol.Bio.H_2O
50/50nM (per well)	12.5µl	0.25µl	10.25µl
100/100nM	12.5µl	0.5µl	10µl
300/300nM	12.5µl	1.5µl	9µl
100/100 Housekeeping gene primer *36B4* (control)	12.5µl	0.5µl	10µl

Meanwhile, to identify the amplification efficiency of target gene target primers and to determine the difference in gene expression level, a standard curve for each target gene primer or primer control (36B4) at concentration of 100/100nM was prepared using the following serial dilution of cDNA from untreated cells ranging from neat, 1:5, 1:10, 1:20 to 1:40. Then, 23µl (100/100nM) of each individual master mix primer was added into a 96-well plate in duplicate and mixed with 2µl cDNA of each dilution separately. Two replica wells per primer containing 2µl nuclease free water were used as a no template control (NTC).

The plate was carefully sealed especially around the edge to prevent evaporation and centrifuged at 2000rpm for 1min, then it was loaded into a 7500-real time machine. 7500HT software was used to select the detector (primers) and the task (sample dilution (input value/ or unknown)) per well in the plate map. Using the instrument tab (Reps), the cycle number was increased to 50, the sample volume to 25µl, the tick on 9600 emulation box was removed, dissociation curve was added and finally the machine was run after the plate document was saved.

The cycle threshold (C_t) value of each sample was identified using the 7500HT software (Applied Biosystems®). All primer concentrations presented a precise C_t value (about 23-25) and 100/100nm was the optimal primer concentration that was selected for future experiments.

qRT-PCRs were performed in duplicate. To determine the transfection efficiency of individual ON-TARGET *plus* siRNAs targeting an individual gene, compared to the NT-siRNA or untransfected cells controls, qRT-PCRs were performed using the SYBR® Green Master Mix (Applied Biosystem by life Technologies) containing a 100/100nM primer concentration and 1:10 cDNA dilution. cDNA from each individual siRNA or control sample was added to four wells, two of which contained the reagents including the target gene primer while the other two contained the control primer HK *36B4*. The standard curve dilution was performed, as previously specified (Section 2.3.4.2.3) to assess the amplification efficacy of the primers. The fold change level of the gene among 4 siRNAs/controls was calculated. The analysis results were exported into Microsoft excel where the relative quantitation of a target gene expression in each sample (siRNAs/controls) were normalized versus the control HK *36B4* gene.

2.4 Combining two (hPK) siRNAs screens –a PCC inducer and PCC modifier screen- to identify synthetically lethal siRNAs

Two complementary human Protein Kinase library siRNA screens (PCC inducer and modifier) provided a powerful data set that allows identification of Synthetically Lethal (SL) siRNAs that cause cell death in combination with *MCPH1/BRIT1* knockdown. The *MCPH1/BRIT1* PCC inducer and PCC modifier siRNA screens were performed by BSTG for the Microcephaly and Cancer Group. The PCC inducer hPK siRNA screen is described in (Section 2.3). The PCC modifier hPK siRNA screen was performed as a double siRNA knockdown to identify genes that kill or modify the number of PCC cells in MCPH1/BRIT1 deficient cell populations. For this screen, the reverse transfection (RT) of 50nM hPK library siRNAs was followed 24hr later by a forward transfection (FT) of 100nm *MCPH1/BRIT1* siRNA. The plate was then incubated for a further 48hr at 37°C, 5% CO_2 (plate map; Appendix 5).

Combining the two different versions of hPK siRNA screens to enhance our understanding of the function of MCPH1/BRIT1 either in its presence (in this case PCC inducer screen) or in its absence (PCC modifier screen) would enrich our analysis and facilitate the determination of genes involved in the regulation of chromosome condensation, or that reduce PCC levels or inhibit apoptosis in MCPH1/BRIT1 deficient cells.

2.4.1 Control selection in modifier and inducer PCC screens for identification of SL siRNA hits

The hPK siRNA modifier and inducer PCC screens were utilized to identify the molecular components that could interact with MCPH1/BRIT1 to regulate different cellular phenotypes, such as chromosome condensation, mitotic entry and apoptosis.

The statistical analysis performed on PCC inducer and modifier hPK siRNAs screens was aimed at identifying the effect of each SMARTpool siRNA from hPK sub-library on the whole cell number. An SL siRNA hit has to show a reliable reduction on cell viability in the absence of MCPH1/BRIT1 in the PCC modifier hPK screen and has no lethal effect in the presence of functional MCPH1/BRIT1 in the PCC inducer hPK screen.

To identify SL siRNA hits in the absence of MCPH1/BRIT1, a negative control double transfection of NT-siRNA (RT) and *MCPH1/BRIT1* siRNA (FT) was used as a reference to measure the effect of hPKs siRNA in combination with *MCPH1/BRIT1* siRNA on cell viability. The control was prepared as follows: the RT of NT-siRNA (50nM) was followed 24hr later by a FT of *MCPH1/BRIT1* siRNA (100nM). Whereas the single knockdown for NT-siRNA (RT of 50nM) was used as a negative control to identify the effect of hPKs siRNA in the presence of functional MCPH1/BRIT1 on cell viability.

2.4.1.1 Statistical analysis of modifier and inducer PCC in hPK siRNA for SL siRNA hits
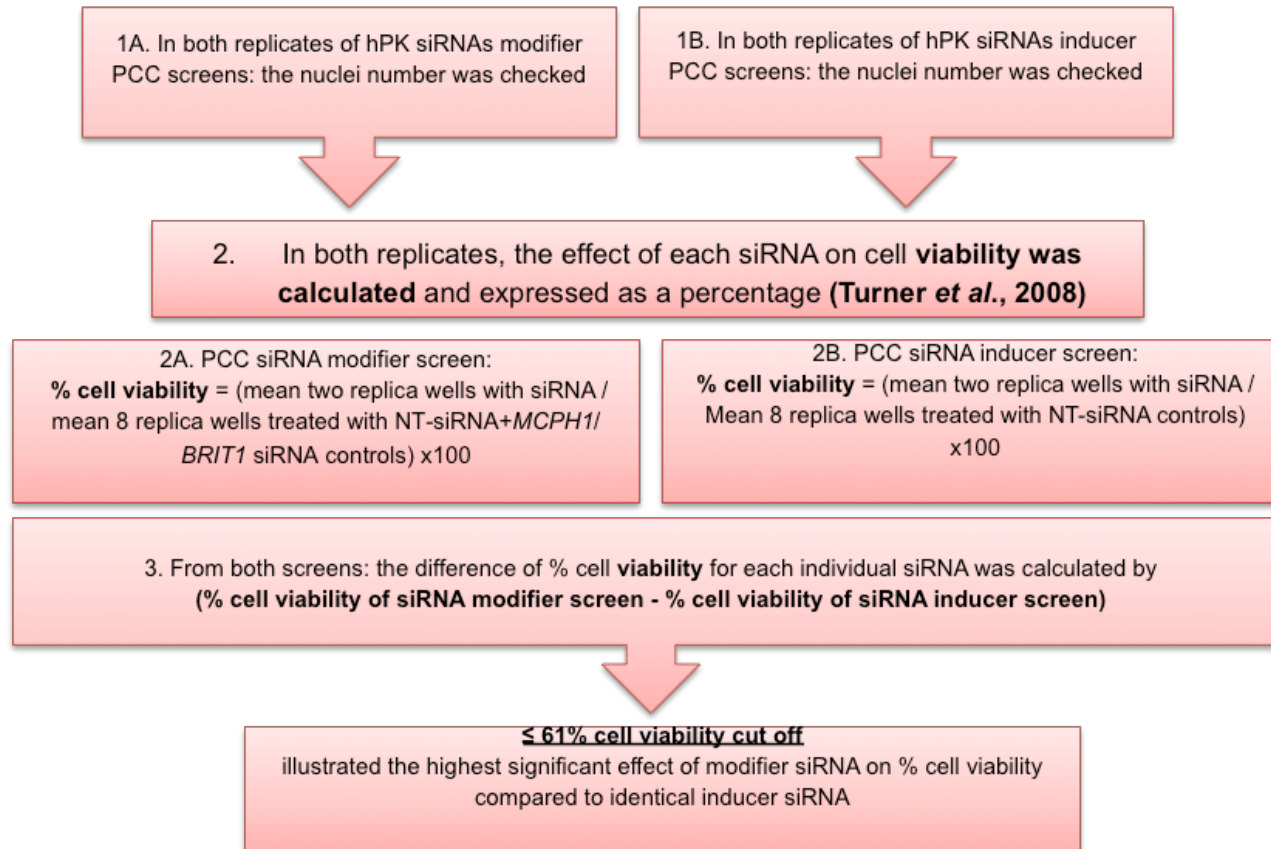
Figure 2.3. The flowchart presenting the statistical method utilized to analyse the two hPK siRNA screens (PCC inducer and PCC modifier) for identifying synthetic lethality genes in MCPH1/BRIT1 deficient cells.

Figure 2.3 describes the statistical methodology used to identify SL siRNA hits. Briefly, analysing PCC siRNAs inducer and modifier screens were dependent on the effect of each SMARTpool siRNA on the whole cell number. As previously described each hPK siRNA screen (PCC inducer/ or PCC modifier) was performed in replica and was analysed individually. For both replicates, the influence of each individual siRNA on cell viability was calculated as follows, the mean of two replica wells transfected with siRNA was divided by the mean of eight replica wells transfected with the control, either NT-siRNA+*MCPH1/BRIT1* siRNA (FT) that was used as a negative control in PCC modifier screens or NT-siRNA that was used as a negative control in PCC inducer screen. Then, the cell viability values of both replicates produced from this calculation were averaged and expressed as a percentage (Turner *et al.*, 2008). Next, the difference of % cell viability of each siRNA in PCC inducer and modifier screens was calculated by subtracting the % average cell viability of each siRNA in PCC modifier screen with the average % of cell viability of the identical siRNA in PCC inducer screen (Figure 2.3). The cut off percentage (approximately ≤ 61% was chosen as the significant effect of siRNA from PCC modifier screen on cell viability compared to the matched siRNA in PCC inducer screen. A list of SL siRNA hits was generated and 5 siRNA hits were validated as described below.

2.4.1.2 SL hPK siRNA hit validation using ON-TARGET *plus* four individual siRNAs

Briefly, the analysis of the hPK screen for SL was designed to assess the impact of each siRNA on cell number, compared to the double transfection with the *MCPH1/BRIT1* siRNA (RT siRNA hit followed by a FT of *MCPH1/BRIT1* siRNA) or with NT-siRNA (RT siRNA hit followed by a FT of NT-siRNA). To identify the SL siRNAs in which single RT siRNA has no significant effect on cell number, however, in combination with *MCPH1/BRIT1* siRNA (forward double transfection) induces a high level of apoptosis compared to forward transfection with NT-siRNA that showed no effect on cell number.

2.4.1.2.1 A brief description of principle components for validation of SL siRNA hits

First, the following controls were plated individually at two different final concentrations 25nM and 50nM into a 96-well plate. The RT transfection of h*PLK*1

siRNA was plated in duplicate and used as a positive control for siRNA transfection efficacy based on reduction in cell number.

The RT of negative control NT-siRNA was individually aliquoted into six wells for each concentration (25nM or 50nM). Two of which were selected for single knockdown (RT 25nM or 50nM) and used to identify the effect of hPKs siRNA in the presence of functional MCPH1/BRIT1 on cell viability. The other wells containing NT-siRNA (RT/ 25nM or 50nM) was followed 24hr later by a FT of *MCPH1/BRIT1* siRNA (100nM) (n = 2 wells) or a FT of NT-siRNA (25nM or 50nM) (n = 2 wells). The double siRNA transfection of the negative controls NT- *MCPH1/BRIT1* siRNA was used as a reference to measure the effect of hPKs siRNA on cell viability in *MCPH1/BRIT1* deficient cells. The PCC induced by the controls NT- *MCPH1/BRIT1* siRNA was used as readout of *MCPH1/BRIT1* siRNA transfection efficiency. Thus, the double siRNA transfection of the negative controls NT- NT siRNA was used to evaluate the transfection efficiency of the controls NT- *MCPH1/BRIT1* siRNA on cell viability and induction of PCC. Also, RT of *MCPH1/BRIT1 siRNA* (100nM) was used as a positive control to induce PCC (Figure 2.4).

Second, each selected SL siRNA hits were validated using four individual ON-TARGET *plus* siRNA using two final different concentrations 25nM and 50nM. The RT of SL siRNA hits or controls were performed in duplicate in a 96-well plate and the effect on cell number evaluated (Figure 2.4). Each SL siRNA hit (the four individual ON-TARGET *plus* siRNA) was plated in triplicate. Thus, a single RT for each SL siRNA hit (at 25nM or 50nM) was performed in three replicates. Then, after 24hr incubation, the first replicate of each SL siRNA hit (the four individual ON-TARGET *plus* siRNA) contained only the single RT (at 25nM or 50nM). The other two replicates containing a single RT (at 25nM or 50nM) followed by a double knockdown with either a FT of *MCPH1/BRIT1* siRNA (100nM) or ON-TARGET *plus* NT siRNA control (at 25nM or 50nM) (Figure 2.4).
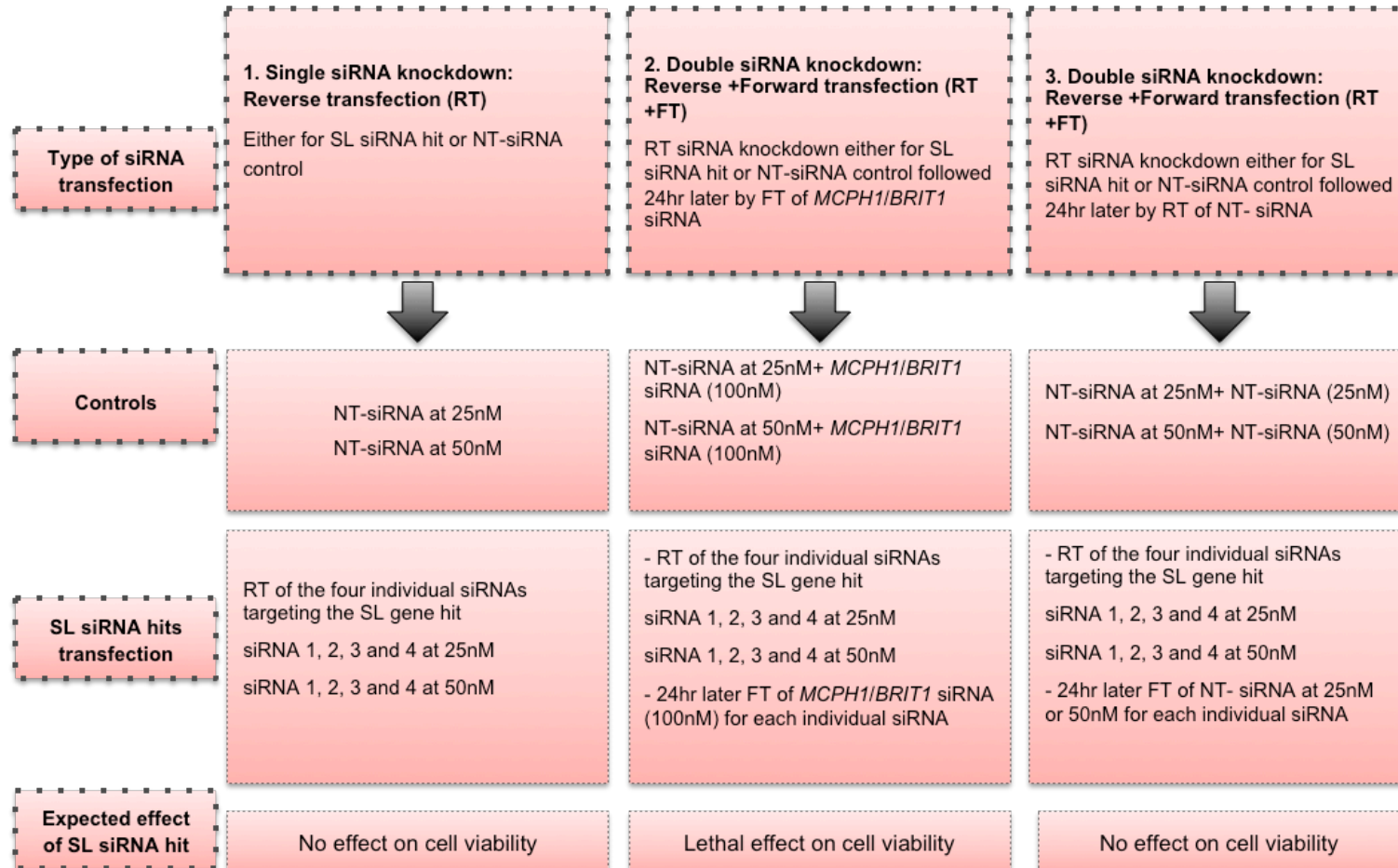
Figure 2.4. Flowchart describing the principal components for validation of SL siRNA hits.

2.4.1.2.2 Dharmacon ON-TARGET *plus* siRNA resuspension

The procedures used to resuspend the Dharmacon ON-TARGET *plus* either the set of four individual siRNA for targeting one gene (0.1nmol) or NT-siRNA controls (5nmol) at a final working concentration of 2µM, which were previously described in (Section 2.3.3.1).

2.4.1.2.3 RT and FT siRNA transfection procedures for validation of SL siRNA hits

The single RT for each SL siRNA hit (the four individual ON-TARGET *plus* siRNA) or NT-siRNA control was performed at two different final concentrations 25nM or 50nM. A, 1.25µl or 2.5µl of SL siRNA hit or NT-control siRNA was aliquoted into relative wells, respectively. Alongside this the transfection mixture, (0.1µl Lipofectamine RNAIMAX transfection reagent mixed with 18.75µl or 17.5µl Opti-MEM-1 (1x) low –serum media, was added to each well containing 25nM or 50nM SL siRNA hit or NT-siRNA control. Meaning that each well contains a total volume of 20µl siRNA solution complex including siRNA (SL siRNA hit or NT-siRNA control) and transfection mixture regent (Opti-MEM-1). The plate was incubated in the cell culture hood for 20min.

At the same time, RT of *PLK1* siRNA was performed at 25nM and 50nM each in duplicate. Also, RT of *MCPH1/BRIT1* siRNA solution was prepared to a final concentration of (100nM) using a previously described method in (Section 2.3.3.2) and 20µl was added in only 4 wells. Next, U2OS cells were resuspended at a density of 7.5×10^4 cells/ml in DMEM media supplemented with only 10%FCS then 80µl cells were seeded into each well. The plate was placed in a 37 $^{\circ}$C 5%CO$_2$ incubator.

After 24hr of incubation, the double knockdown was performed using FT of *MCPH1/BRIT1* siRNA at 100nM final concentration or FT of ON-TARGET *plus* NT-siRNA control at two different final concentrations of 25nM or 50nM.

First, for FT of *MCPH1/BRIT1* siRNA, two separate mixtures were prepared; whereby, per well, the siRNA mix consisting of 0.25µl *MCPH1/BRIT1* siRNA (40µM stock) mixed with 16.25µl Opti-MEM-1. The transfection reagent mix per well consisting of, 0.2µl Lipofectamine RNAIMAX transfection reagent mixed with 3.3µl Opti-MEM-1 and incubated for 5min at RT. Then, the siRNA solution was combined with a transfection reagent mix and incubated for 20min at RT. Then 20µl of the *MCPH1/BRIT1* siRNA/ Lipofectamine transfection mixture was added to the desired

wells (to the replicate 2 of the four individual ON-TARGET *plus* siRNA at 25nM or 50nM respectively) as described above in (Section 2.4.1.2.1).

Second, for FT of ON-TARGET *plus* NT-siRNA single control was prepared at a final concentration of 25nm and 50nm using 1.25μl or. 2.50μl siRNA in a final total volume of 18.75μl or 17.5μl Opti-MEM-1 respectively. The transfection reagent mixture was prepared per well: 0.1μl Lipofectamine RNAIMAX transfection reagent mixed with 18.75μl Opti-MEM-1 and incubated for 5min at RT. Then, Lipofectamine transfection complex was mixed with NT-siRNA incubated for 20mins at RT. Then added to the selected wells (to replicate 3 of the four individual ON-TARGET *plus* siRNA at 25nm and 50nm respectively) as described above in Section 2.4.1.2.1.

Finally, the plate was returned to 37°C 5% CO_2 incubator for a 48hr incubation. The cells were fixed as previously described in (Section 2.2.3) with methanol, blocked with 10% non-fat milk and stained with DAPI using a Fluid-X XRD-384 dispenser. Then, the plate was scanned and analysed utilising Operetta and Columbus software, respectively as detailed in (Sections 2.2.4 and 2.2.5). Microsoft Excel was used to distinguish the potential SL hPK siRNA hit induced significant reduction in cell number only in combination with *MCPH1/BRIT1* siRNA while the single siRNA transfection or siRNA transfection with NT-siRNA had no significant effect on cell number.

2.5 Evaluation of the role of MCPH1/BRIT1 expression in breast cancer chemosensitivity

2.5.1 Breast cancer patients' selection and ethical approval

A cohort of primary and invasive breast carcinoma (BC) patients including inflammatory and locally advanced breast tumour sufferers who had been treated with neoadjuvant chemotherapy (NACT) at Leeds Teaching Hospital NHS Trust were selected using the NHS trust databases. All the NACT BC treated patients underwent a clinical follow up for tumour response evaluation. Selection criteria involved patients with invasive breast carcinoma treated with NACT from 2004-2012 followed by breast surgery. Exclusion criteria were BC patients without NACT treatment and NACT treated BC patients without breast surgery operation or MRI follow up.

2.5.2 Chemotherapy regimens, clinical and pathological data

Invasive BC patients were treated with a variety of chemotherapies. FEC chemotherapy is a combination of Fluorouracil (5FU), Epirubicin and Cyclophosphamide, EC chemotherapy comprises of Epirubicin and Cyclophosphamide. EC or FEC combined with Taxotere (Docetaxel). ECF regimen consists of Epirubicin+Cisplatin+5-Fluorouracil. Combination of Taxotere (Docetaxel) and Carboplatin chemotherapies. The Neo-tAnGo trial has been given to patients as a combination of Epirubicin and Cyclophosphamide (EC) with Taxotere

All the clinical data including chemotherapy type and surgery type were available. The pathological data of matching pairs samples (pre- and post-chemotherapy) provided included age; tumour size; tumour grade; tumour type; lymph node status; Nottingham Prognostic Index, ER, PR and HER2 status for pre-chemotherapy treatment core biopsy; pathological response categorised as complete response CR), partial response (PR) and no response (NR).

Tumour cores from one hundred and thirty five pre and post chemotherapy BC cases were obtained from Dr. Abeer Shaaban (UK consultant specialist breast pathologist) at Leeds Teaching Hospital NHS Trust for immunohistochemical staining. After excluding unmatched pairs, core loss and un-scoreable cores, the MCPH1/BRIT1 cohort consisted of 96 cases, and the p53 study consisted of 92 cases. BC pre-chemotherapy treatment tissue was sectioned as core biopsy. While the corresponding residual invasive carcinoma matched pair (post-chemotherapy treatment/ pathological partial response) were constructed into tissue microarrays (TMA). Ethical approval for this part of the project was obtained from the Local Research Ethics Committee at the Leeds Teaching Hospital (06/Q1206/180 and amendment 4) (Appendix 7).

2.5.3 Optimization of anti-MCPH1/BRIT1 and anti-p53 antibodies

Immunohistochemical staining protocols of MCPH1/BRIT1 and p53 antibodies were optimized in collaboration with Dr. Filomena Esteves (Leeds Institute of Cancer and Clinical Pathology, University of Leeds). Different dilutions of primary antibody, incubation times and antigen-retrieval methods were used for each antibody. For batch–batch variation, a control TMA BC slide was routinely included in each MCPH1/ BRIT1 or p53 IHC staining batch.

2.5.4 Immunohistochemistry (IHC) staining

For MCPH1/BRIT1 IHC staining, the slides were deparaffinised in Xylene, then transferred through graded ethanol to water. To block endogenous peroxidase activity, slides were placed in 0.3% (v/v) Hydrogen peroxide (H_2O_2) in methanol for 20min. Antigen retrieval 10mM citric acid buffer (pH 6.0) (Appendix 6.3) was freshly prepared for each IHC run and heated in the microwave for 4min on high power. Slides were placed in this preheated solution and heated again in the microwave for 5min on high power then washed with tap water. 100μl of a 1:10 mixture 10x Casein solution (Vector Labs) in dH_2O was used to block non-specific staining. Both pre- and post -treatment BC slides and TMAs were incubated in three washes with 100ml TBS (10x stock) in 0.01% (v/v) Tween 20 each for 5min and incubated in antibody diluent solution (Invitrogen) with 1:100 MCPH1/BRIT1 primary antibody (100mg, 0.8mg/ml, ab2612) (Abcam) overnight at 4°C. Slides were washed three times with TBS. Two drops of secondary antibody labelled polymer HRP anti-Rabbit (Dako) were added and slides incubated for 30min at RT. Slides were washed with TBS. 100μl of DAKO detection buffer mixture (1ml DAKO Real™ substrate buffer mixed with 1 drop DAKO Real™ DAB+ Chromgen) was added to the slides and the slides placed in a dark humidifying chamber for 10min. Slides were washed with tap water, counterstained with copper sulphate for 1min, rinsed in water for 1min, stained in Haematoxylin for 30sec, incubated in Scott's tap water for 1min and running water for 1min. Sections were dehydrated in graded ethanol, then transferred to Xylene and mounted in DPX. The anti-MCPH1/BRIT1 antibody specificity had been validated previously for IHC and western blotting in different cancer tissues and cell lines (Xu *et al.*, 2004; Alsiary *et al.*, 2014). Our group, the Microcephaly and Cancer Group at the University of Leeds, confirmed the antibody specificity by *MCPH1/BRIT1* siRNA western blotting in ovarian cancer cell lines (Adams *et al.*, 2014).

For p53 IHC staining, pre-chemotherapy biopsy cores and post-chemotherapy TMAs of residual tumour were stained in collaboration with Mrs. Shivani Shukla at the University of Leeds. The procedures of dewaxing and rehydrating paraffin slides of p53 were performed as previously described above with MCPH1/ BRIT1 IHC staining. The following stages were altered. The H_2O_2 was diluted at 1:10 in dH_2O. p53 antigens were retrieved in a routinely prepared antigen retrieval solution, 10mM citric acid buffer (pH 6.0), by microwave heat at 900W for 20min. The heated antigen retrieval solution containing slides was transferred into ice for 20min. The 10x Casein solution was diluted 1:10 in antibody diluent solution. The primary

antibody p53 monoclonal mouse anti-human clone DO-7 (3.4g/L) (Leica Biosystem / Novocastra™) was used as recommended previously (Varna *et al.*, 2011; Axelrod *et al.*, 2012), for both pre- and post -treatment BC slides and TMAs, at 1:50 dilution and overnight incubation. The slides were incubated in post primary (Leica Biosystem / Novocastra™) and secondary antibody mouse Novolink™ polymer HRP for 30mins and 1hr, respectively.

2.5.5 IHC Scoring

The breast cancer section images captured using an Olympus BX41 microscope at 40X magnification and scored using CellP software (Olympus). TMAs slides were scanned using APERIO AT2 (Leica) and images were visualized using slides.virtualpathology.leeds.ac.uk (web or image scope) and scored at 20X magnification. MCPH1/BRIT1 IHC of pre and post treatment slides were scored by two observers (Dr. Sandra Bell (SMB)) and (Aeshah Awaji (AAW)). p53 IHC staining of pre-treatment cores were scored by SMB and (Shivani Shukla (SS)) while the post-treatment TMAs slides were scored by SS and AAW and the scoring results were reviewed by SMB. Nuclear staining was scored as a percentage of the positive cells in relation to the total number of tumour cells present. A number of slides showed a remarkable cytoplasmic background staining thus cytoplasm-scoring results were not included in this study. The scoring of representative samples was reviewed by Dr. Abeer Shaaban.

2.5.6 Statistical analysis

Continuous and categorical analyses were used to evaluate the status of MCPH1/BRIT1 expression in this cohort as previously described (Richardson *et al.*, 2011). To dichotomise MCPH1/BRIT1 IHC staining into high and low expression based on the percentage of nuclear MCPH1/BRIT1 staining, four different cut-off values (10%, 15%, 30% and 35%) were tested individually in relation to breast cancer overall survival (BCOS) using Kaplan-Meier analysis. The cut-off of 35% showed a significant result within the group of patients. All statistical analyses were performed using SPSS version 21.0 (IBM Corp. Armonk, NY: IBM Corp). The correlation between changes in expression and overall survival (OS) were evaluated by Pearson paired parametric t-test and Kaplan-Meier analysis, respectively. The continuous analysis (Pearson) was performed to identify the correlation between percentage of MCPH1/BRIT1 staining for both pre and post-

chemotherapy treatment and pathological variables. The Chi- square test or Spearman (non-parametric) was used for comparison among categorical variables of both pre and post- chemotherapy treatment. All statistical tests and comparisons were two sided and a *p* value of ≤ 0.05 was considered significant.

The cut off value of the percentage p53 IHC staining was 10%, allowing its dichotomisation into positive and negative among patients groups (Vojtěšek *et al.*, 1992; Bartley and Ross, 2002; Rohan *et al.*, 2006; Lara *et al.*, 2011; Yang *et al.*, 2013; Milicevic *et al.*, 2014). Similar statistical analyses were performed to evaluate nuclear p53 staining in this cohort unless otherwise stated in the result section. To identify the correlation between nuclear MCPH1/BRIT1 and p53 IHC staining pre and post chemotherapy treatment, the Chi-squared Fisher exact test was performed among categorical groups of patients.

2.6 Cell cytotoxicity assays

2.6.1 Anti-cancer chemotherapy drugs

Two anti-cancer drugs were utilised in this project to identify the effect of

MCPH1/BRIT1 siRNA knockdown or overexpression in chemosensitivity (Table 2.6).

Table 2.6. Anti-cancer chemotherapy drugs agents used in cell cytotoxicity assays.

Chemotherapy drug	Stock concentration	Company supplier	Mechanism of action
Carboplatin	10mg/ml	Sun Pharmaceutical Industries Europe BV	Interacts with the DNA to form intrastrand crosslinks and DNA adducts, interfering DNA replication and repair. Carboplatin is considered as a slow DNA binding activity causing less cytotoxicity profile and long lasting effects (Di Pasqua *et al.*, 2012)
Paclitaxel/Taxol	6mg/ml	Mayne Pharma Plc	A microtubule-stabilizing molecule activating the mitotic arrest in the cells preventing chromosome segregation and initiating apoptosis (Horwitz, 1993; Weaver, 2014)

2.6.2 MTS cell viability assay

An MTS assay was used to evaluate cell viability post drug treatment. Knockdown of *MCPH1*/*BRIT1* using siRNA with the corresponding NT-siRNA control was performed at a final concentration of 75nM for the induction of PCC. The *MCPH1*/*BRIT1* siRNA reverse transfection in 1847 or SKOV-3 cell lines ($5x10^4$ cells per well) was prepared at a final concentration of 75nM as previously described in (Section 2.2.1) and was plated on the same day as the cells were plated using a flat-bottomed 96- well cell culture plate (from column 1 to12).

After 24hr incubation; 1mM stock solution of chemotherapeutic drugs, Carboplatin or Paclitaxel/Taxol was prepared. To prepare 1mM of stock of (600mg/60mg (10mg/ml)) Carboplatin; 1ml of drug was diluted with 9mls of cell culture growth medium with 10% FCS and without addition of P/S solution individually for each cell line. To prepare 1mM of (6mg/ml) Paclitaxel/Taxol; 440µl of drug was diluted with 9.5ml of cell culture growth medium supplemented with15% FCS and without P/S solution individually for each cell line Then, 50µl of different drug concentrations, 0-600µM Carboplatin, or 0-10nM Paclitaxel was prepared and added to the cells in duplicate and the plate incubated for 72hr.

100µl of phenazine methosulfate (PMS) (0.92mg/ml stock) was diluted to 1:20 with (2mg/ml) stock of MTS **(**(3-(4,5-dimethylthiazol-2-yl)-5-(3-carboxymethoxyphenyl)-2-(4-sulfophenyl)-2H-tetrazolium). 10µl of PMS/MTS solution was added to drug treated cells, the plate was wrapped in foil to prevent light exposure, and was incubated at 37°C for 90 mins.

The absorbance was read at 490nm using a plate reader (Dynex technologies). Absorbance readings were analysed and the mean and standard deviation calculated using Microsoft Office Excel software. IC_{50} concentrations were identified using a programme designed by Sally Jackson (Laboratory of Children Cancer Research) as detailed below in (Section 2.6.5).

2.6.3 DAPI whole cell number assay

In order to validate the *MCPH1*/*BRIT1* knockdown the experiment was duplicated in a 96 well imaging plate (PerkinElmer) and analysed for cell number by DAPI counting nuclei. PCC, the hallmark of reduced MCPH1, and whole nuclei number were identified by DAPI staining using the Operetta for image capture and a Columbus analysis programme as previously described (Sections 2.2.4 and 2.2.5).

To evaluate the whole cell number after the combination of *MCPH1/BRIT1* siRNA and chemotherapy treatment, the mean and standard deviation were calculated using Microsoft Office Excel software. IC_{50} concentrations were identified using a programme designed by Sally Jackson (Laboratory of Children Cancer Research) as detailed below (Section 2.6.5).

2.6.4 Vi-CELL trypan blue dye cell viability assay

Inducible HEK293 for MCPH1/BRIT1 overexpression (IND HEK293) cell line and Inducible Flp-In T-REx system HEK293 for WT Parkin overexpression (used as a control) cell line were cultured in DMEM media as shown in Table 2.1 and incubated at 37°C, 5%CO_2 to reach 80% confluence. To determine the optimal cell density for accurate cell viability results, three different cell densities were tested ($2.5x10^5$, $1x10^5$ and $5x10^4$ cells /ml). After optimization, the cell density of $5x10^4$ cells/ml was selected for the Vi-CELL assay. Then, 400µl of each cell suspension was seeded separately in replicates using 24- wells plate. The four plates were incubated overnight at 37°C, 5%CO_2.

After a 24hr incubation, the growth medium was removed from all plates. A stock of tetracycline in ethanol at 2mg/ml was prepared by Dr. Katherine Roper (University of Leeds), which was diluted in a selected growth medium at 1:2000 (1µg/ml). Half of the 24 well plate for each cell line was treated with 200µl of the 1µg/ml tetracycline (to induce expression of MCPH1/BRIT1 or WT Parkin) followed by 200µl of selected growth medium while the rest of the wells were refreshed with 400µl standard growth medium without tetracycline addition. The plates were incubated again for 24hr at 37°C, 5%CO_2.

Post incubation the growth medium was removed from the plates. Half the wells were refreshed with a 200µl of fresh double concentrated tetracycline (2:2000 / 2µg/ml in a selected growth medium) while the second half of the plate was treated with 200µl of fresh standard growth medium without the addition of tetracycline. Simultaneously, 200µl of different drug concentrations ranging from 0-600µM Carboplatin or 0-10nM of Paclitaxel were added to plates in duplicate for each individual cell line (cells treated with/without tetracycline). The plates were incubated at 37°C, 5%CO_2 for 72hrs.

A group of 15ml falcon tubes were prepared based on the number of plates used in the experiment and labelled as follows (with/without tetracycline, drug type and drug concentration). Then, for each individual well in each plate, the media was

transferred to the corresponding 15 ml falcon tubes. Each well was washed twice with 1ml PBS and the mixture was transferred to the corresponding falcon tube. Then, 400µl of trypsin-EDTA was added to each well and plates were incubated for 5mins. The selected growth medium (400µl) was added to each well and the cell suspension was transferred to the matching falcon tube. The falcon tubes were centrifuged at 200g for 5mins. The supernatant was discarded and the pellets resuspended in 500µl of selected growth medium and transferred to Vi-CELL specific tubes. The Vi-CELL tubes were placed on the Vi-CELL machine (Beckman Coulter) for cell viability and counting analysis.

2.6.5 Statistical calculation of inhibitory cellular proliferation by 50% (IC_{50})

All the data generated using the previously described cell viability assays (MTS, DAPI and Vi-CELL) allowed the plotting of the dose response curve using Microsoft Excel software to identify IC50 values, which is the selection of the effective drug concentration that kills 50% of cancer cells. The 'calculating 50% inhibition concentrations' method, produced by Sally Jackson (Children's Cancer Research Laboratory), was used. The relative viable cell number results in each drug concentration were normalized to untreated cell number. Then, the normalized values for each drug concentration were multiplied by 100. The data was transferred to Microsoft Excel using an IC50 calculation specific template. The log data transformation and regression analysis were performed and IC50 was calculated using the following formula IC50 = Exp (- interep/_X variable) (For more details see Appendix 8).

Chapter 3 Induction of PCC by small molecule inhibitors in the ovarian cancer 1847 cell line

3.1 Introduction

The completion of DNA replication during S phase is necessary to allow the commencement of chromosome condensation. Mitotic chromosome assembly involves two elements. One of these is compaction of the chromatin of interphase cells into metaphase chromosomes, which is mainly regulated by condensin protein complexes (Swedlow and Hirano, 2003). The other prerequisite element is sister chromatid resolution that requires Cohesion release from chromatin at prophase; (Swedlow and Hirano, 2003; Losada *et al.*, 2002). Thus, chromosome condensation as a cellular process is crucial for proper entry into mitosis and subsequent correct chromosome segregation. Some additional molecules related to the regulation of chromosome condensation, such as topoisomerase II and histone H3, have been investigated (Hirano, 2000; Wei *et al.*, 1999; Prigent and Dimitrov, 2003), however, a comprehensive insight into their mechanism of action has yet to be gained.

A very distinctive cellular phenotype occurs when interphase cells initiate mitosis before completion of DNA replication, referred to as premature chromosome condensation (PCC) (Johnson and Rao, 1970). PCC has been demonstrated to be a useful tool in biological and cytogenetic analysis for studying chromosome condensation during interphase and metaphase (Schor *et al.*, 1975). Virus-mediated PCC was the first method employed to recognise PCC (Kato and Sandberg, 1967). This method used Sendai virus to cause the fusion of interphase cells with mitotic cells. However, this method was beset by technical problems. Thereafter, CC such as protein phosphatase inhibitors were used to induce PCC. Okadaic acid and Calyculin A, both of which are naturally occurring toxins isolated from different species of marine sponge, were used to induce PCC in somatic cells during all phases of the cell cycle (Gotoh *et al.*, 1995). The presence of double minutes (DMs) on interphase PCC, in addition, was used as a functional readout for gene amplification in cytogenetic studies using various human metastatic carcinoma tissues (Brüderlein *et al.*, 1986).

Peripheral lymphocyte cells derived from either primary microcephaly or PCC syndrome patients, with mutations in the *MCPH1/BRIT1* gene, display 15-20% prophase–like cells among metaphase cells (Trimborn *et al.*, 2004; Neitzel *et al.*, 2002). Also, the PCC phenotype has been detected previously in many types of

human carcinoma cells such as leukaemia, ovarian and colon cancers (Augustus *et al.*, 1985; Reichmann and Levin, 1981; Kovacs, 1985; Hittelman *et al.*, 1980).

Studies on PCC in relation specifically to MCPH1/BRIT1 have greatly increased, confirming its auxiliary implication in regulating chromosome condensation. The X-ray crystal structure of human *N*-terminal BRCT domain of MCPH1/BRIT1 has been determined and this pocket of *N*-terminal domain is required to prevent PCC (Richards *et al.*, 2010). Studies showed the essential role of N-terminal domain of MCPH1/BRIT1 in combination with SET in regulating chromosome condensation and shaping metaphase chromosomes by inhibiting the activity of the condensin II complex and allowing proper entry into mitosis (Leung *et al.*, 2011; Yamashita *et al.*, 2011).

To date, no study has investigated the potential implication of a defective *N*-terminal domain of MCPH1/BRIT1 in cancer. Thus, we hypothesised that identifying the small molecule inhibitors which target the *N*-terminal domain and induce PCC by preventing normal MCPH1/BRIT1 protein interactions would be a useful laboratory tool for studying the biology of cancer cells and could assist in verifying the function of MCPH1/BRIT1 in different cellular pathways. To this end, a small molecule inhibitors of a library of 792 CC selected from a library of 33,000 compounds, based on their predicted ability to fit into the 3D structure of the N-terminal of MCPH/BRIT1. The aim of this study was to utilise a high-throughput high-content imaging system (Operetta) and analysis software (Columbus Acapella) to perform a small molecule screen (SMS) to identify molecules that induce PCC in the ovarian cancer (OVCA) cell line 1847.

3.2 Results

3.2.1 Development of small molecule screen assay

In order to conduct large-scale assays using an SMS for CC that induce PCC, it was necessary to determine the optimal diluent type for the CC, cell density, incubation period, CC concentration, and positive (*MCPH1*/*BRIT1* siRNA) and negative controls (DMSO, vehicle control).

3.2.1.1 Selection of the optimal diluent type for CC dilution

A library of 792 CC was supplied as 2µl solutions at a10mM concentration in 100% DMSO, in a 96-well plate format. Previous exploration of the percentage of DMSO tolerated by the 1847 cell line had identified that a concentration of 0.2% DMSO was optimal (Data not shown). A two-step dilution protocol was decided upon where the CC would initially be diluted to a working stock of 100µM (1% final concentration of DMSO) prior to a 1:5 dilution in the cell suspension (0.2% final concentration of DMSO, 20µM CC concentration).

To identify the best working stock diluent which would ensure CC stability was maintained, both during storage and their use for SMS to avoid presenting high cytotoxicity,, two different diluents were tested, (i) RPMI media containing 10% FCS and 1% P/S (the recommended culture media for culturing the cell line 1847, (Chapter 2; Table 2.1)) and (ii) PBS. A 96-well test plate containing 2µl of 100% DMSO was supplied and one half of the plate diluted into 198µl PBS buffer per well and the other half of the plate diluted with RPMI 1640 complete growth media. The ovarian cancer 1847 cell line was plated into two 96 well plates where one plate contained 80µl cell suspension in RPMI 1640 culture medium at a low cell density of 1000 cells/well and the second plate contained 80µl cell suspension at a higher density of 6000 cells/well. Cell suspension transfer was performed using a multichannel pipette. Then, half of each cell plate was treated with 20µl of 0.2% diluted DMSO with PBS while the other half was treated with 0.2% diluted DMSO with RPMI 1640 medium to examine the effect of each diluent. All reagent transfers were performed with a multi channel pipette. The low cell density plate was incubated at 37°C 5% CO_2 for a week to test any potential contamination whereas the high cell density plate was incubated for just 24hr to test the effect of each diluent on cell number. After 24hr, the plate was fixed with ice-cold methanol and stained with DAPI and anti-active casepase-3 antibody (Chapter 2; Section 2.2.3; Table 2.2) for assessment of cell number and the percentage of apoptotic cells, respectively. The plate was imaged using the high throughput Operetta microscope and then analysed with Columbus software, as detailed below.

3.2.1.1.1   Image analysis to evaluate the cell number

The Columbus analysis software automatically turns all the captured images generated by Operetta into quantitative data. Image analysis protocols constructed by Dr. Victoria Cookson enabled Columbus to detect a nucleus stained with DAPI

or active caspase-3 which automatically assessed the number of nuclei or apoptotic cells respectively in each image generating a value for cell number and percentage of apoptotic cells (Chapter 2; Section 2.2.4) (Adams *et al.*, 2014).

Analysis of the test plate containing the cells treated with the 2 diluents showed a significant variation in cell number between each well of the plate (Data not shown). However average cell number per well when treated with 0.2% DMSO/RPMI media was 7500 cells, however upon treatment with 0.2% DMSO/PBS an average cell number of 5500 cells was registered. It was determined that the variation in cell number may have resulted from the use of a multichannel pipette, therefore for future experiments cell plating was performed using an automated FluidX reagent dispenser to improve assay reproducibility. The cells treated with 0.2% DMSO/PBS did not show a significant increase in the percentage of active caspase-3 positive cells (0.2% apoptotic cells) compared to those treated with 0.2% DMSO/RPMI media (0.1% apoptotic cells) (Data not shown). It is possible that dead cells may have become detached from the well and been washed away during the PBS washing and fixation stages, or that cells grew slower in the PBS/DMSO mixture. A low value for apoptotic cell number may also have been due to the high background staining caused by the anti-active caspase-3 antibody, as preventing the accurate identification of active caspase-3 positive cells by the Columbus analysis system. Thus, the analysis of whole cell number was used surrogate read out for nuclei number. Since evaluation of nuclei number in each image using Columbus protocol analysis that was previously optimised by BSTG during other high through put siRNA assays (Adams *et al.*, 2014), it was concluded that whole cell number would be the best parameter for determining the suitability of the diluent to minimize cell cytotoxicity (Figure 3.1).
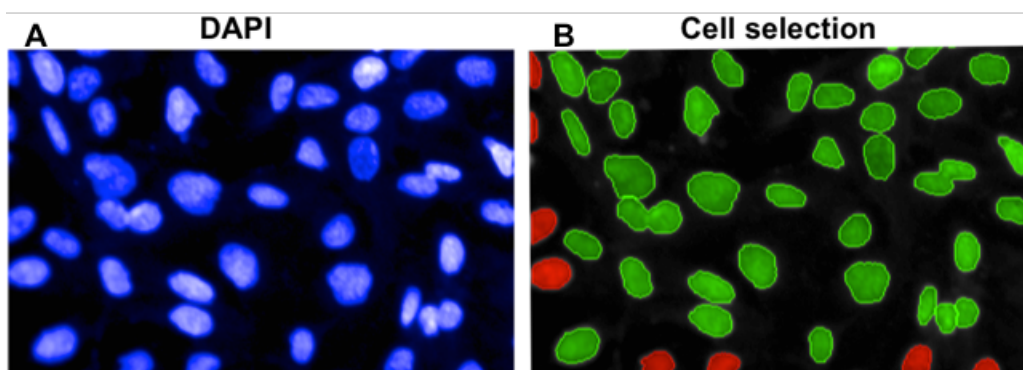
Figure 3.1. Evaluation of cell number using Columbus analysis software.
Ovarian cancer 1847 cell line treated with 0.2% DMSO diluted with RPMI media was stained with **(A)** DAPI (blue) and imaged using Operetta fluorescent microscope. **(B)** Columbus software determines the whole cell number by excluding the border objects (red) from the whole cells (green).

After incubation for one week the low cell density plate was examined under the high content Operetta microscope. Results revealed a contamination of 60% (58/96) of the wells across the plate and particularly on the side of the plate treated with 0.2% DMSO/PBS. Thus, potentially treating the cells with 0.2% DMSO/PBS buffer increased their sensitivity to bacterial infection and reduced their survival rate at either a long or short incubation time. It can be concluded that RPMI 1640, the selected growth medium of ovarian 1847 cancer line containing the antibiotic P/S, is a suitable diluent for the CC. In addition, increasing the cell density may minimise the variations in cell number that were observed.

3.2.1.2 Mitotic cells/pHH3 Ser10 immunofluorescence staining optimisation and analysis

Columbus software has the power to simultaneously analyse different channels where each channel shows a different antibody or stain. Initially the stronger green channel was used to detect active caspase-3 apoptotic cells using Alexa fluor 488 and the weaker red channel to detect mitotic cells expressing pHH3 Ser10 using Alexa fluor 594. Due to the high background staining caused by anti-active caspase-3 primary antibody it was not possible to accurately detect the apoptotic cells using Columbus. Columbus software was used to analyse whole cell number and % apoptosis visually estimated. This rendered the green channel available to detect mitotic cells/pHH3 Ser10.

A Columbus image analysis protocol that measured the staining intensity of pHH3 Ser10 positive cells and therefore identified the percentage of mitotic cells was created as previously detailed in (Chapter 2; Section 2.2.5). Initially optimisation of immunofluorescence staining for pHH3 Ser10 was performed using the ovarian cancer 1847 cell line treated with DMSO (0.2%) to detect mitotic cells utilizing either Alexa Fluor 594 (Red) (Figure 3.2 A and B) or Alexa Fluor 488 (Green) (Figure 3.2 C and D) secondary antibodies. However, Alexa fluor 594 (Red) was replaced by Alexa fluor 488 (Green) due to the increased intensity detected by the Operetta.

The detection of mitotic cells using pHH3 Ser10 positive cells was another parameter that could be useful for identifying any further cellular effects caused by CC on cells, such as reducing or increasing the number of cells in mitosis.
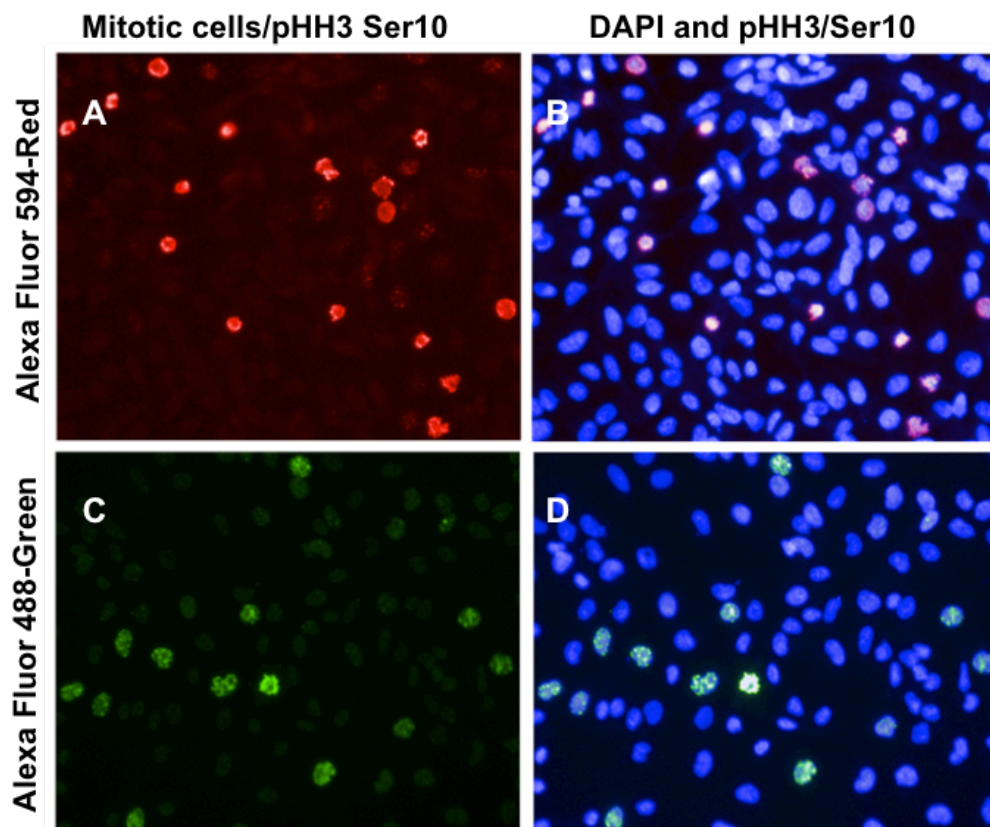
Figure 3.2. Optimisation of the immunofluorescence (IF) staining of phospho-Histone H3 (Ser10) to detect mitotic cells.
Representative Operetta images of the ovarian cancer cell line 1847 treated with 0.2% DMSO were acquired after staining with either (Alexa Fluor 594/red or 488/green) secondary antibodies to identify phospho-histone H3 positive cells. Image showing the pHH3 Ser10 positive cells/mitotic cell in red **(A)** and in green **(B)**. Merged images; **(C)** DAPI stained cells (blue) and pHH3 Ser10/red or **(D)** DAPI and pHH3 Ser10/green.

3.2.1.3 Optimisation of cell density, CC concentration and incubation time

Given that the previous results showed a striking variation in cell number when a cell density of 6000 cells/well was used, the cell density was increased to 8000 cells/well. This time *MCPH1/BRIT1* siRNA (75nM) was used as a positive control for PCC induction, NT-siRNA and untreated cells as negative controls and DMSO (0.2%) as vehicle control. All controls were introduced to the plate by manual pipetting.

Simultaneously, an initial trial plate containing a 2µl sample of 72 CC (10mM stock concentration) (master plate (MP)) code: 59-241) was diluted with 198µl RPMI medium (working concentration 100µM). The trial plate was run to test the optimization of the small molecule screen assay that was principally aimed at inducing and detecting PCC. The cells were treated with diluted CC at a final

concentration of 20μM containing 0.2% DMSO. After 24hr incubation, the plate was stained with DAPI and pHH3 to detect PCC and mitotic cells, respectively.

In order to identify the percentage of PCC, the Operetta system was once again utilised to take images from the trial plate and the Columbus image analysis protocol specifically devised for PCC detection was used to enable to automatically count the number of spots in each DAPI-stained nuclei, which was indicative of a prophase like cell (Figure 3.3A) PCC cells highlighted automatically by Columbus in red circle). Based on this analysis, the positive control *MCPH1/BRIT1* siRNA induced PCC in 14.47% of the cell population (n = 4 wells) which was significant to the siRNA NT control (75nM) 1.32% (n = 2 wells) or cells treated with the DMSO negative control 2.55% (n = 14 wells) or untransfected cells 2.14% (n = 2 wells) (p < 0.0001; Unpaired t-test) (Figure 3.3B). The mean cell number of the positive control reduced significantly to 3819 cells compared to DMSO negative controls (8522 cells) or untransfected cells (9492 cells) (p < 0.0001) (Figure 3.3C). However, cells treated with NT-siRNA unexpectedly revealed a reduction in cell number (3839 cells), which was similar to those observed within the positive control (Figure 3.3C). This may due to an error in the manual pipetting that was used to seed the cells into the wells. Also, the NT-siRNA (Invitrogen) occasionally presents low cell number in some cell lines and the same observation was seen previously by BSTG in other siRNA screens.

The trial plate showed an unanticipated high hit rate of PCC (3-4% of CC) after 24hr exposure to 72 CC compared to the estimated overall hit rate of small molecule screens (0.5-1%) (Figure 3.3D) (Personal communication Dr. Richard Foster). Visual examination of the plate revealed this was due to Columbus having identified clumps of two or three cells as single PCC cells (Figure 3.3E), causing an increase in % PCC and a low level false positive hit rate. Optimisation of the Columbus analysis protocol to reduce the permitted cell size (thus removing multiple cell clumps from the analysis) and to increase the number of spots detected (chromosomes) and reanalysis of the plate demonstrated no positive hit CC were identified that induced PCC after 24hr within this test plate.

In order to determine whether the failure to detect a high rate of PCC induction in the initial trial plate was a result of limiting levels of CC due to the use of a high cell density (8000 cells/well), we tried to improve the rate of PCC induction in cells and their detection by reducing cell density back to 6000 cells/well. The CC concentration, in addition, was increased to 50μM instead of 20μM; the DMSO concentration in the CC treated wells was therefore increased from 0.2% to 0.5%.

Furthermore, the incubation time was lengthened from 24hr to 48hr. However, considerable variation in cell number was still observed in the DMSO negative control at both 24hr and 48hr and the cell number in the PCC positive control decreased significantly (Data not shown).
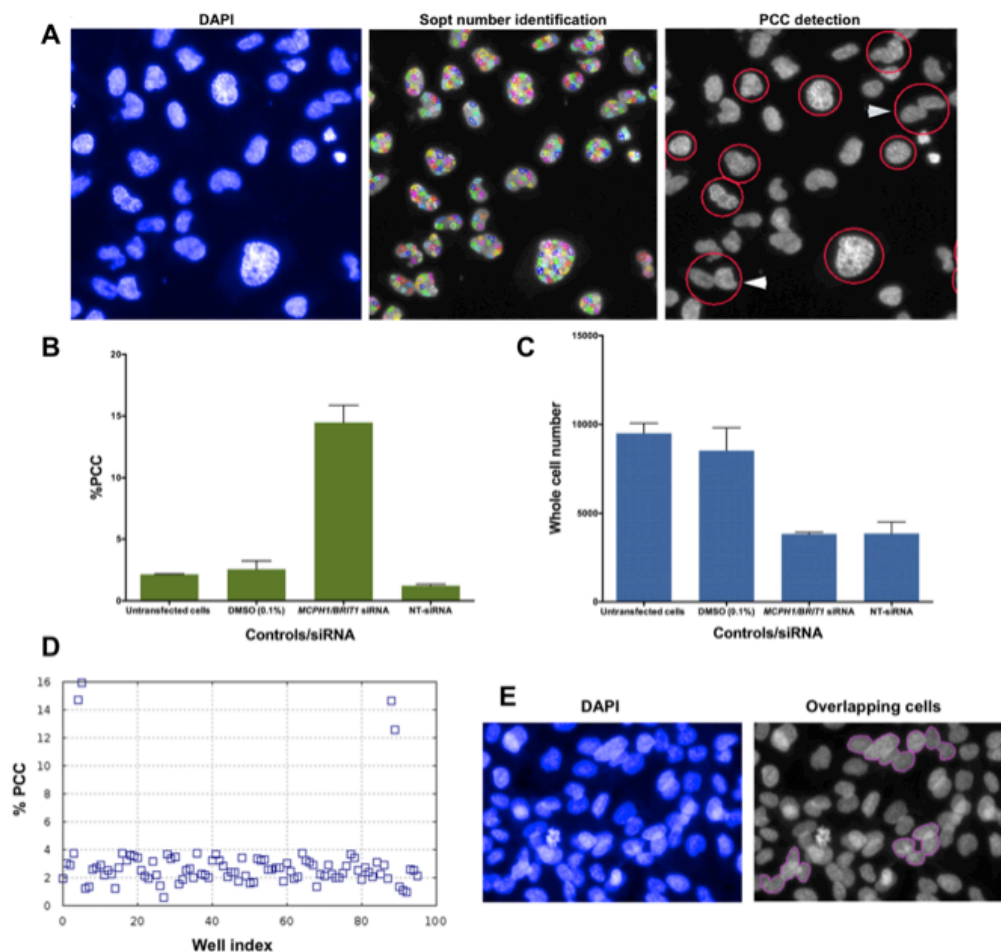
Figure 3.3. Optimization of small molecule screens using a trial plate containing 72 chemical compounds (CC) (master plate (MP) code:59-241).
A) The images were taken from Columbus demonstrating the detection of PCC in the ovarian cancer 1847 cell line transfected with the positive control *MCPH1/BRIT1* siRNA for 48hr. In each DAPI stained cell (blue), Columbus software protocol identifies PCC cells using an algorithm called 'find spot' (highlighted by coloured outlines). Cells with > 14 spots were designated as PCC (circled in red by Columbus), overlapping cells (indicated by an arrow) were occasionally detected as PCC cells. **(B)** Graph showing *MCPH1/BRIT1* siRNA induced an elevated level of %PCC compared with untransfected cells, negative/vehicle control DMSO (0.2%) treated cells or with NT-siRNA ($p < 0.0001$). **(C)** Graph showing the positive control reduced the cell number significantly to 42% compared with untransfected cells or negative control ($p < 0.0001$), but not significantly with cells transfected with NT-siRNA. **(D)** The scatter plot graph showing the %PCC from initial screening of the trail (MP:59-241) after 24hr exposure. Each blue solid square represents the %PCC induced either by CC or controls/siRNA. The four squares representing %PCC > 12% were the positive control *MCPH1/BRIT1* siRNA. The majority of CC showed unexpectedly high %PCC ranging from 3-4%. **(E)** Visual examination revealed that Columbus incorrectly identified the overlapping cells (highlighted in purple) as PCC cells.

To resolve these problems, an automated liquid dispenser was used to plate the cells at a density of 7000 cells/well. In addition, PCC detection was evaluated by treating the cells with a reverse transfection of *MCPH1*/*BRIT1* siRNA (75nM), which was exposed after 24hr to a three concentrations of DMSO (0.1%, 0.2%, and 0.5%). It was determined that of these 3 concentrations, 0.5% DMSO caused the highest cell death and lowest PCC induction (5.5%; n = 2 wells) whereas 0.1% DMSO induced (8.5%; n = 2 wells) PCC. The cells treated with 0.2% DMSO produced a high % PCC (14.2%; n = 2 wells) with a reasonable number of surviving cells (Data not shown). This finding indicated that at this specific cell density (7000 cells/well), 0.2% DMSO was not toxic. Thus, 20µM of a CC (containing 0.2% DMSO) could potentially induce PCC without the CC diluent DMSO non-specifically increasing cell death.

Therefore, for the SMS, a CC concentration of 20µM was used with a seeding density of 7000 cells/well and positive (*MCPH1*/*BRIT1* siRNA (75nM)) and negative controls (0.2% DMSO) added to each assay plate. The use of a dispenser gave more reproducible results compared to manual pipetting. Two incubation times for the CC were utilised, 24hr and 48hr, to identify and analyse the diverse and unknown biological and cellular effects of the CC's.

3.2.1.4 Screening of 792 CC

The biological activities of the CC used in this project have not been previously examined. Therefore, although these SMS were developed chiefly for the purpose of evaluating the phenotypic endpoint of %PCC cells, other assay endpoints were also investigated. These included changes in whole cell number and percentage of mitotic cells /pHH3 Ser10.

3.2.1.4.1 Assessment of screenings controls for induction of PCC, alterations in cell number and effects on mitosis

The stock concentration (10mM) of library of 792 CC was provided in 11 plates (96-well format), each of which included 24 wells (rows A and H) containing 100% DMSO and 72 CC (dispensed in row B to G). The screenings of these CC were performed in duplicate using a final CC concentration of 20µM in 0.2% DMSO and two incubation times: 24hr and 48hr. Each plate contained the negative control DMSO (0.2%), which was used as the main reference in assaying the alteration of the three phenotypic endpoints (%PCC, cell number and % mitotic cells) caused by

CC in these screens. The positive control *MCPH1/BRIT1* siRNA was used to assess PCC. The additional secondary controls included Doxorubicin (0.4µg/ml) for assessment of cytotoxic effects and Nocodazole (1µM) for assessment of pHH3 Ser10 positive cells/mitotic cells.

The controls in each plate for both replicates were assessed prior to the Operetta scanning stage by visual examination using a microscope and also after image capture using Columbus. The duplicate plates were run as two separate batches of the 11 CC plates and the results of the controls pooled for each batch of 11 plates.

The overall %PCC (mean ± SD) for the DMSO negative vehicle controls in 11 plates for the first batch was 0.75% ± 0.11 at 24hr and 1.09% ± 0.26 at 48hr time points respectively (total n = 128 wells), whereas for the *MCPH1/BRIT1* siRNA positive controls values of 8.84% ± 1.14 at 24hr and 19.30% ± 2.21 at 48hr (total n = 44 wells) (Figure 3.4A). This clearly demonstrated the significant difference in %PCC induced by positive and negative controls for the first batch at 24hr and 48hr (*p* < 0.0001; Unpaired t-test).
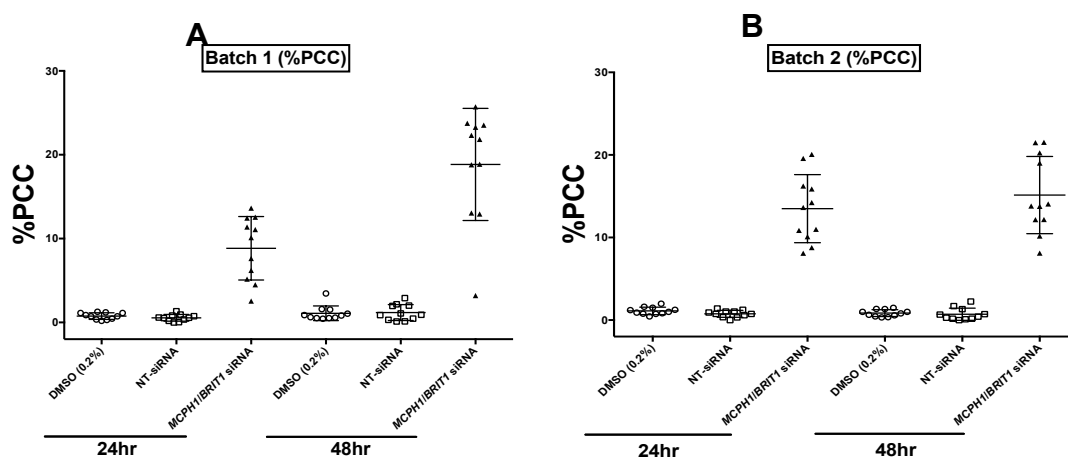
Figure 3.4. Assessment of % PCC observed in controls of small molecule screens (SMSs) negative control (0.2% DMSO) or positive control (*MCPH1/BRIT1* siRNA) at 24hr and 48hr for batches 1 and 2.

Plots showing mean %PCC of the screening controls; the negative control reduced the %PCC in batches 1 and 2 to 0.75% and 1.24% at 24hr and 1.09% and 0.84% at 48hr respectively. The positive control *MCPH1/BRIT1* siRNA increased the %PCC in batches 1 and 2 to 8.84% and 13.5% at 24hr and to 19.3% and 15.14% at 48hr, respectively. The NT-siRNA controls did not influence the %PCC in batches 1 and 2 giving 0.55% and 0.76% at 24hr and 1.17% and 0.70% at 48hr, respectively.

The second batch showed a similarly low frequency %PCC (mean ± SD) for DMSO negative controls in 11 plates giving 1.11% ± 1.24 at 24hr and 0.84% ±

0.12% at 48hr (total n = 88 wells) compared to the high frequency %PCC (mean ± SD) induced by the positive controls which was 13.5% ± 1.2% at 24hr and 15.14% ±1.4 at 48hr (total n = 44 wells) (Figure 3.4B). Again, a significant difference in the mean %PCC was identified between negative and positive controls in the second batch at 24hr and 48hr (*p* < 0.0001; Unpaired t-test).
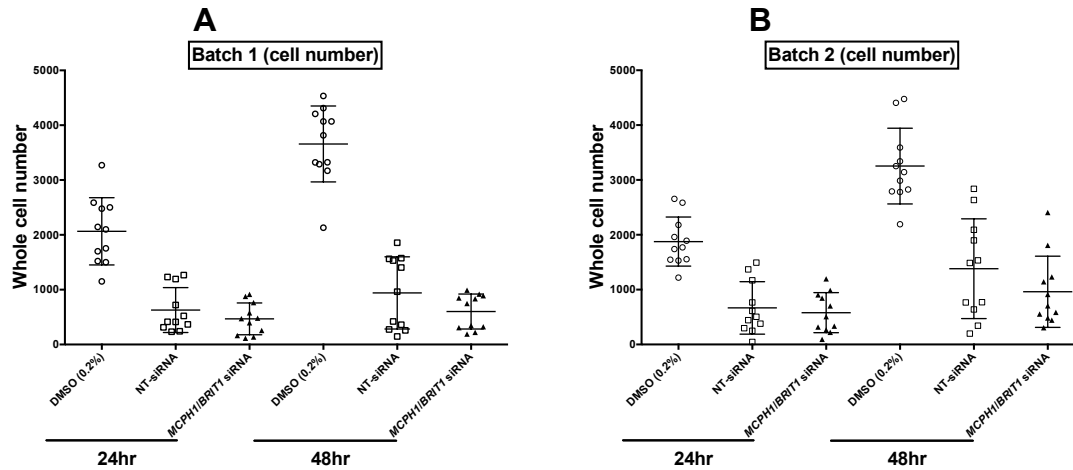
Figure 3.5. Evaluation of cell number of controls used in SMSs for batches 1 and 2 at 24hr and 48hr.
Plots showing mean cell number of the screening controls; the negative control (DMSO-0.2%) had no significant effect on cell number in batches 1 and 2 at 24hr (2065 cells and 1876 cells) compared to the significant reduction in cell number observed with the positive control *MCPH1/BRIT1* siRNA (468 and 576 cells respectively). After 48hr incubation, the mean cell number for the negative control increased in batches 1 and 2 to 3658 and 3253 cells, respectively. The positive control did not show any significant increase in mean cell number in either batch 1 or 2 after 48hr transfection (601 and 961 cells). The NT-siRNA controls showed a reduction on the mean cell number in batches 1 and 2 (629 and 666 at 24hr and 941 and 961 at 48hr, respectively).

The number of whole nuclei was used as a principal parameter to evaluate cell number using the modified Columbus software PCC analysis as previously described in this chapter (Section 3.2.1.1.1). In the SMS screen first batch at 24hr, the mean cell number for the DMSO negative control of 11 plates did not alter significantly (2065 cells) compared to the large reduction in cell number for the *MCPH1/BRIT1* siRNA positive control of 468 cells (*p* < 0.0001; Unpaired t-test) (Figure 3.5A). Likewise, after 48hr a comparison of the mean cell number for the DMSO negative control (3658 cells) with the *MCPH1/BRIT1* siRNA positive control showed that the cell number had significantly reduced by over 50% (601) (*p*< 0.0001; Unpaired t-test) (Figure 3.5A). Similar significant results were obtained in the second batch where the mean cell number for the DMSO negative and positive controls was 1876 and 579 at 24hr, respectively (*p* < 0.0001; Unpaired t-test) and 3253 and 961 at 48hr (*p* < 0.0001; Unpaired t-test) (Figure 3.5B).

As shown in (Figure 3.4 A and B) the NT-siRNA controls at 24hr and 48hr for both batches did not affect on %PCC compared to the positive controls *MCPH1/BRIT1* siRNA. The overall %PCC for the NT- siRNA controls in 11 plates for the first batch was 0.55% ± 0.12 at 24hr and 1.1% ± 0.28 at 48hr time points respectively (total n = 44 wells) (Figure 3.4A). The second batch showed a similarly low frequency %PCC giving 0.76% ± 0.12 at 24hr and 0.70% ± 0.22% at 48hr (total n = 44 wells) (Figure 3.4B). However, NT-siRNA controls at 24hr or 48hr displayed low mean cell number in both batches. This potentially may be due to the control siRNA and the procedure being slightly cytotoxic to the 1847 cell type (Figure 3.5). Another potential reason for the variation in cell number between each control well may be the way that the cells were dispensed- in some plates a FluidX cell dispenser (XRD-384) was used while in other plates the multichannel pipette was used instead. This was due to the unexpected technical problems with the machine. Therefore this may account for the reduced accuracy in cell number. The mean cell number for the NT-siRNA controls in the first batch was 629 at 24hr compared to 941 at 48hr (Figure 3.5A). Likewise, the second batch showed a low mean cell number of 666 at 24hr and 961 at 48hr (Figure 3.5B).

It is essential to point out that the visual assessment of the controls using Columbus showed comparative variations in %PCC and a significant reduction in cell number across the 11 replica plates at both 24hr and 48hr caused by the positive control *MCPH1/BRIT1* siRNA. Consequently, it was agreed that the more consistent negative control (DMSO/0.2%) would be used as the main reference for performing any statistical analysis instead of the positive control.

The percentage of mitotic cells /pHH3 Ser10 was evaluated by Columbus protocol analysis as previously described in this chapter (Section 3.2.1.2). In the first batch the overall mean ± SD of the %mitotic cells/ pHH3 Ser10 for the DMSO negative controls at both incubation times (9.4% ± 3.1 at 24hr and 6.2% ± 1.6 at 48hr) did not differ significantly from those of the positive controls (7.03% ± 2.1 at 24hr and 2.7% ± 0.6 at 48hr). The %mitotic cells/ pHH3 Ser10 for the NT-siRNA controls at both incubation times was (5.5% ± 1.6 at 24hr and 3.1% ± 0.7 at 48hr) (Figure 3.6A). However, the second batch showed a significant difference in the overall mean ± SD of the mitotic cells /pHH3 Ser10 between the DMSO negative and the positive controls at 24hr (13.82% ± 1.9 as opposed to 30.08% ± 3.77) ($p <$ 0.0010; Unpaired t- test) while at 48hr the overall mean ± SD of the %mitotic cells

/pHH3 Ser10 was 4.03% ± 0.3 for negative controls and 9.3% ± 1.4 for positive controls ($p < 0.0016$; Unpaired t-test).
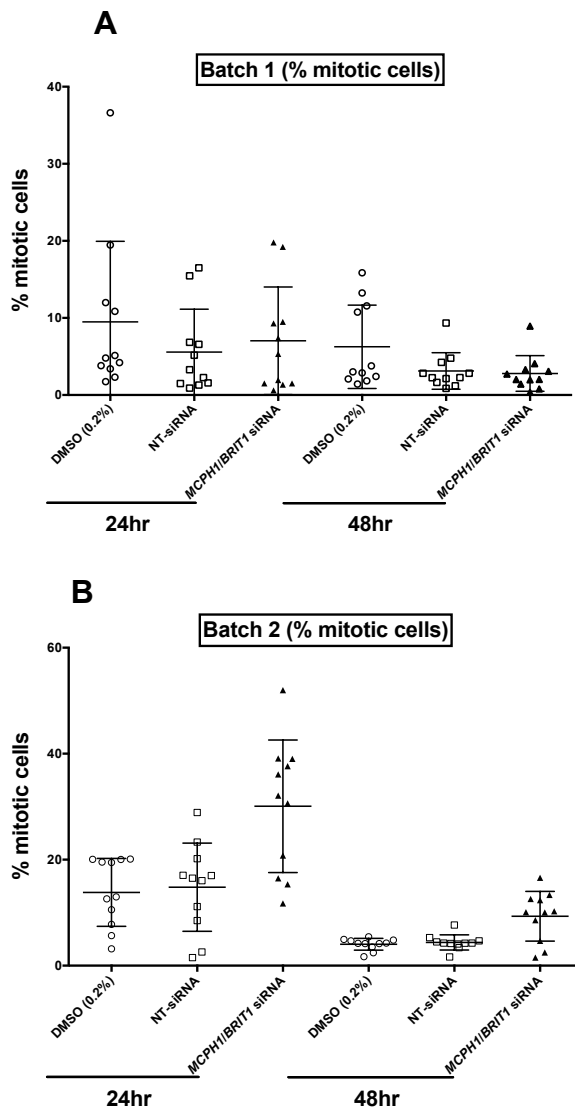
Figure 3.6. Evaluation of %mitotic cells observed by controls used in small molecule screens for batches 1 and 2 at 24hr and 48hr.
Plots showing mean %mitotic cells for the negative control (DMSO-0.2%) in batches 1 and 2 at 24hr (9.4% and 13.82%) whilst at 48hr it was 6.2% and 4.3%, respectively. The positive control *MCPH1/BRIT1* siRNA presented a mean %mitotic cell of 7.03% and 30% after 24hr whilst this was 2.7% and 9.3% after 48hr in batches 1 and 2, respectively. The NT-siRNA controls showed a mean %mitotic cell in batches 1 and 2 (5.57% and 14.79% at 24hr and 3.12% and 4.38% at 48hr, respectively).

The %mitotic cells/ pHH3 Ser10 for the NT-siRNA controls at both incubation times was (14.7% ± 2.5 at 24hr and 4.3% ± 0.4 at 48hr) (Figure 3.6B). This may indicate that the use of the Alexa Fluor® 594 conjugated secondary antibody to detect pHH3 Ser10 was not compatible with the filter set used on the Operetta and therefore resulted in non-specific measurement of %pHH3 Ser10 for both controls and exposure times (24hr and 48hr). The Alexa Fluor® 488 secondary gave a

strong signal when was used to detect active caspase-3 positive cells in the first batch. It was decided that the anti-pHH3 Ser10 antibody with a Alexa Fluor® 488 secondary antibody should be substituted for the anti active caspase-3 staining in the second screen batch to give a clearer and more consistent pHH3 Sert10 staining pattern.

3.2.1.4.2 Assessment of the reproducibility of small molecules screens

To analyse the overall screening reproducibility of %PCC between the two sets of replicates and at the two time points (24hr and 48hr), a Pearson's correlation was performed, showing a weak positive correlation between the two replicates of r = 0.3017; p < 0.0001; n = 792 CC at 24hr (Figure 3.7A). This may due to the difference in %PCC caused by some CCs in the first and second replicate at 24hr which may to decline the linear relationship between the replicates. However, this correlation increased significantly at 48hr to r = 0.7654; p < 0.0001; n = 792 (Figure 3.7B), suggesting a very strong relationship between the replicate 1 and 2 to identify CC inducing PCC.
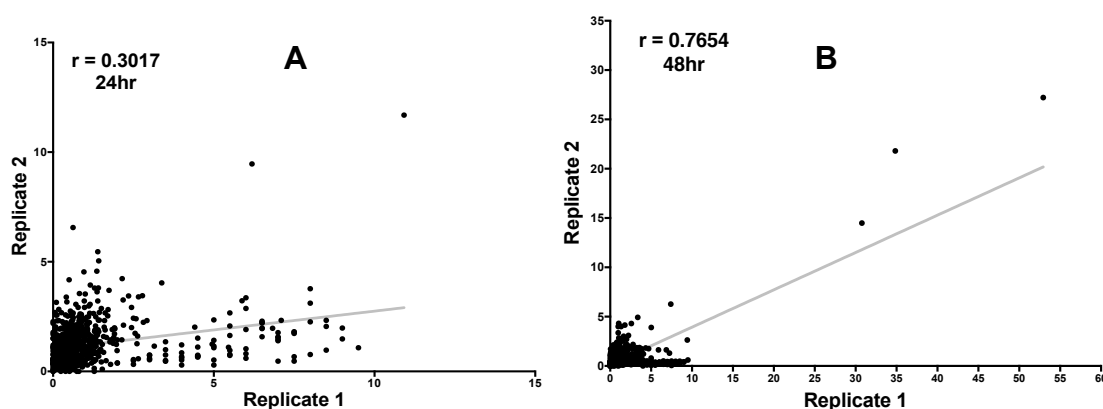
Figure 3.7. Comparison of small molecule screening reproducibility after 24hr and 48hr.
Graphs for 24 or 48hr showing the comparison of the %PCC induced by 792 CC between replicates 1 and 2. Pearson's correlation test demonstrated a weak positive correlation between the two replicates at 24hr **(A)** (r = 0.3017; p < 0.0001) and strong positive correlation at 48hr **(B)** (r = 0.7654; p < 0.0001).

3.2.1.4.3 Statistical analysis for hits identification

Statistical analysis was performed per plate for both replicates using Z score and Robust Z score as recommended for normalization and calculation methods, employing the plate negative DMSO controls versus samples (Birmingham *et al.*, 2009; Zhang, 2011; Goktug *et al.*, 2013). As expected, DMSO-treated wells

generated reliable results which constantly produced low %PCC without any significant effect on cell number, demonstrating its suitability and efficiency as the main reference for performing statistical analysis of CC-induced PCC, reduced cell number or increased percentage of mitotic cells (expressing pHH3 Ser10) at 24hr and 48hr. Candidate hits were identified for the induction of PCC (Z score or Robust Z score ≥ 2 for %PCC), increase in mitotic cell/pHH3 Ser10 (Z score or Robust Z score ≥ 2 for %mitotic cells) or an increase in apoptosis/decrease in cell division (Z score or Robust Z score of ≤ -2 for cell number. The overall screen of 792 CC were depicted as scatter plots representing the average Z score and Robust Z score for the average of both replicates for 3 phenotypic endpoints: %PCC cell number and %mitotic cells at both 24hr and 48hr exposure times. The initial statistical analyses for identifying CC that potentially induce PCC revealed 17 CC hits at 24hr and a further 27 CC hits at 48hr that showed statistically significant Z score or Robust Z score of ≥ +2 (Figure 3.8 A and B). Additional statistical analyses were performed to identify potential CC hits for cellular cytotoxicity/reduction in proliferation and irrelevant of PCC induction. These analyses displayed 150 CC hits at 24hr and 119 CC hits at 48hr that showed statistically significant Z score or Robust Z score of ≤ -2. (Figure 3.8 C and D) (Appendix 9 A and B). Further statistical analyses were conducted to identify potential CC hits inducing an increased number of mitotic cells/expressing pHH3 Ser10 and irrelevant of PCC induction. Consequently, 16 CC hits and another 4 CC hits were identified and showed statistically significant Z score or Robust Z score of ≥ +2 at 24hr and 48hr, respectively (Figure 3.8 E and F) (Appendix 10 A and B). The potential CC that induced PCC underwent further primary and secondary validation, which will be described in Sections 3.2.1.8 and 3.2.1.9. Further statistical hit filtration was carried out to identify the most potent CC hits, that initially showed cytotoxicity phenotype or increased mitotic index, using the positive controls Doxorubicin or Nocodazole, which will be described in Section 3.2.1.6 and 3.2.1.7, respectively.
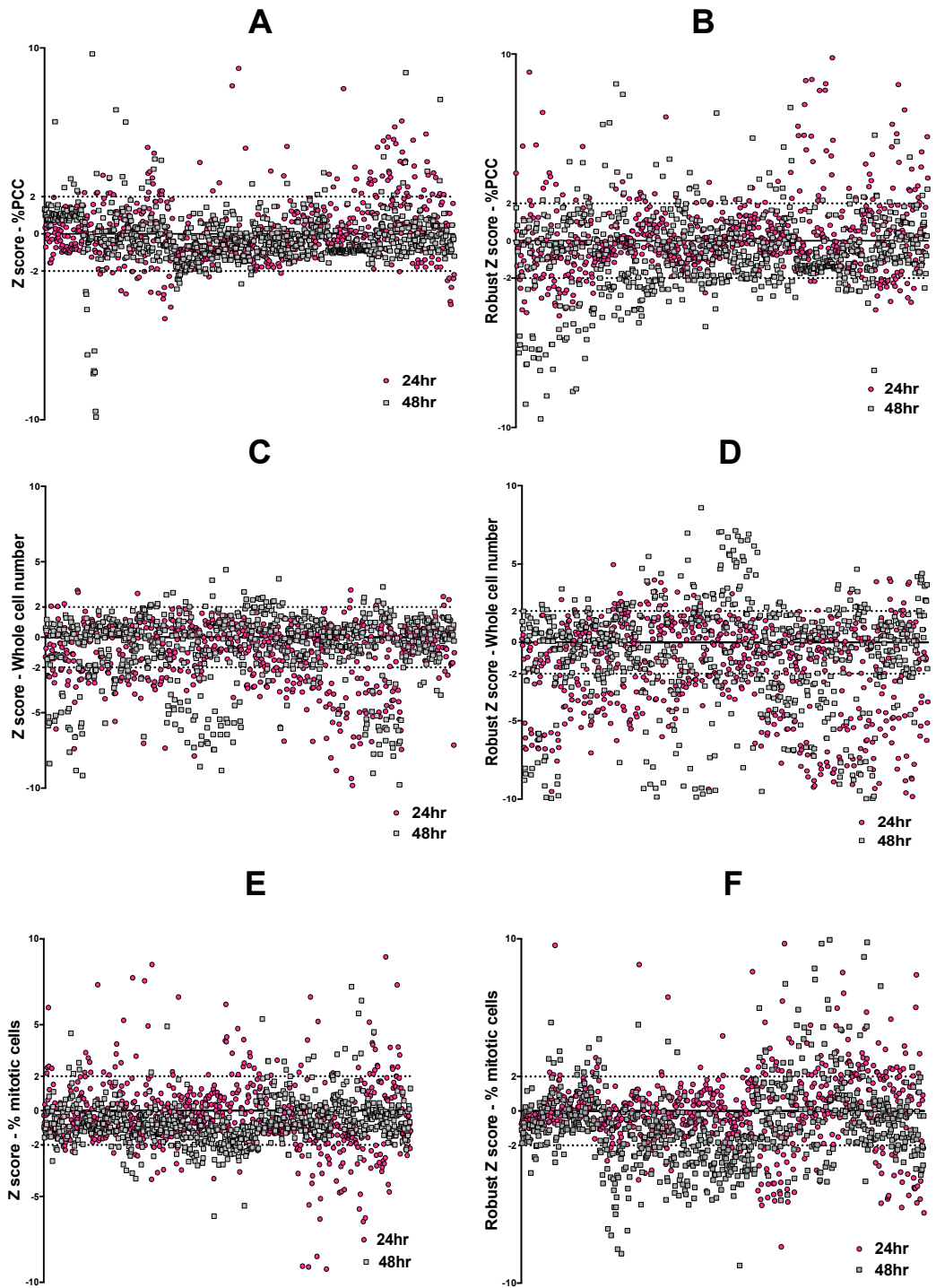
Figure 3.8. Screening of 792 CC for assessment of three phenotypic endpoints: %PCC, cell number and % mitotic cells.

The Z score or Robust Z score were calculated based on negative control DMSO (0.2%). (**A** and **B**) Scatter plots represent %PCC induced after 24hr (pink circles) or 48hr (solid grey squares) exposure to 792 CC. The CC displaying a Z score **(A)** or robust Z score **(B)** value with a cut-off of ≥ 2 was designated as candidate hits. (**C** and **D**) Scatter plots showing the effect of these CC on cell number after exposure of 24hr or 48hr. The dotted lines at ≤ -2 represent the cut-off points for Z score **(C)** or Robust Z score **(D)** selection hits with reduced cell number. (**E** and **F**) Scatter plots presenting the %mitotic cells induced after exposure of 24hr or 48hr to these CC. The Z score **(E)** or Robust Z score **(F)** cut-off point at ≥ 2 was used to identify hits, which altered %mitotic index.

3.2.1.5 Identification of CC hits inducing PCC, using Z score and Robust Z score

Based on statistical analysis using %PCC Z scores or %PCC Robust Z scores, replicate screens revealed 17 CC inducing PCC in both replicate screens at 24hr out of the original 792 (2.1% hit rate) (Table 3.1A) and an additional 27 CC candidate duplicate hits (3.4%) at 48hr (Table 3.1B). A visual examination of cell images related to these candidate hits was carried out to identify any technical or systemic errors that might have occurred within the replica plates during the processing of the screens.

The hit list at 24hr demonstrated that two CC, MP59-241/well F5 and MP64-65/well B2 had induced a %PCC ≥ 5% in both replicates in comparison to the remaining CC hits within the list (Table 3.1A). Interestingly, the list of CC hits generated after 48hr incubation showed an increase in %PCC induced by these two CC hits. The CC MP59-241/ well F5 induced an average %PCC of 7.8% at 24hr and 22.5% at 48hr while the CC MP64-65/well B2 caused 11.3% at 24hr and 28.3% at 48hr (Tables 3.1A (24hr CC hit list) and 3.1B (48hr CC hit list)).

Furthermore, the list of CC hits at 48hr showed a further 3 potential CC hits that had also caused a greatly elevated level of %PCC in comparison to the other CC hits, namely MP59-241/well C8, MP64-65/well F7, and MP66-67/well C1 (Table 3.1B). In contrast, the CC B11 and G11 in MP74-75 at 48hr showed a %PCC < 5% but their Z and Robust Z scores were highly significant (Table 3.1B).

Table 3.1. Identification of potential CC hits which induced the PCC phenotype.
Representative tables showing the plate code and well number of CC hits that were screened using a 96-well plate. **(A and B)** Tables presenting the statistical data for 17 and other 27 potential CC hits identified after 24hr and 48hr, respectively with a significant Z score or Robust Z score (%PCC) of ≥ 2. The blue highlighted wells indicate CC that induced ≥ 5% PCC at both replicates with a significant Z score or Robust Z score at either 24hr or 48hr. The average %PCC for the negative control (DMSO) in batches 1 and 2 was 0.75% and 1.24% at 24hr and 1.09% and 0.84% at 48hr, respectively.

A. Master plate name (24hr)	Well name	% PCC Replicate 1	% PCC Replicate 2	Z score (%PCC) Replicate 1	Z score (%PCC) Replicate 2	Robust Z score (%PCC) Replicate 1	Robust Z score (%PCC) Replicate 2
MP59-MP241	F5	6.19	9.46	11.14	12.22	12.61	17.24
	G3	1.74	3.7	2.07	2.81	2.37	4.05
MP60-MP61	E1	1.42	5.04	4.52	4.03	9.27	8.36
MP62-MP63	F1	1.1	2.49	2.34	2.21	5.21	4.11
MP64-MP65	B2	10.92	11.69	15.8	25.57	32.52	35.02
	F7	5.88	3.22	7.68	5.49	16.01	7.78
MP66-MP67	G1	6.83	1.97	3.57	2.54	19.33	3.72
MP68-MP69	E1	2.78	3.45	3.53	1.85	3.23	2.54
	G7	3.38	4.04	4.88	2.41	4.52	3.26
MP70-MP71	E1	1.59	2.02	1.51	0.69	2.32	2.14
MP72-MP73	F6	0.33	2.2	0.58	8.33	2.08	7.79
MP74-MP75	E1	2.44	2.92	3.46	2.14	5.86	2.48
	G8	1.5	2.87	1.38	2.06	2.4	2.39
MP76-MP77	E3	1.3	1.88	2.42	3.54	5.35	7.92
	G3	0.91	1.34	1.3	1.8	3.04	3.55
	G1	0.88	1.35	2.88	1.85	4.62	3.66
	E7	0.82	1.61	1.04	-1.12	2.51	2.67

B. Master plate name (48hr)	Well name	% PCC Replicate 1	% PCC Replicate 2	Z score (%PCC) Replicate 1	Z score (%PCC) Replicate 2	Robust Z score (%PCC) Replicate 1	Robust Z score (%PCC) Replicate 2
MP59-MP241	C8	9.43	2.63	14.54	2.76	17.79	8.59
	F5	30.77	14.49	51.59	22.7	63.04	65.07
	F7	2.23	3.1	2.06	3.55	2.53	10.83
MP60-MP61	E1	2.59	4.31	5.35	7.11	5.86	7.99
	D1	1.46	2.72	2.34	3.3	2.5	3.69
MP62-MP63	C1	1.91	1.68	2.81	2.11	7.58	4.87
	D1	1.54	2.52	1.81	3.79	4.48	8.17
	E1	1.33	4	1.25	6.79	2.76	14.03
	E3	1.53	1.2	1.78	1.13	4.4	2.95
	G1	1.42	1.32	1.48	1.38	3.48	3.43
MP64-MP65	F7	52.94	27.21	35.29	73.07	95.38	101.49
	B2	34.85	21.81	22.39	57.73	61	80.25
MP66-MP67	C1	7.4	6.27	11.85	8.3	23.46	16.5
MP68-MP69	G7	1.8	1.8	3.35	2.06	4.48	6.51
MP70-MP71	G5	1.93	0.48	3.85	0.89	6.57	2.01
	G3	1.19	1.02	1.83	4.76	3.26	11.02
MP72-MP73	D1	0.26	1.33	0.4	1.43	4	3.99
MP74-MP75	G1	3.81	1.04	13.34	3.11	24.76	6.42
	B11	3.37	4.93	11.6	23.25	21.59	48.23
	G11	1.05	2.84	2.41	12.41	4.94	25.72
	F1	0.78	0.66	1.35	1.14	3.03	2.33
MP76-MP77	E3	2.79	2.18	4.92	1.82	7.98	2.65
	G3	5.02	3.9	10.02	4.44	15.87	6.31
	G2	2	2.7	3.12	2.61	5.2	3.76
	B2	1.14	2.21	1.16	1.86	2.17	2.71
MP78-MP79	D1	4.08	0.87	2.45	1.67	5.43	9.46
	G1	3.31	0.57	1.69	0.74	3.87	5.28

3.2.1.5.1 Correlation of PCC hits with cell number reduction (cytotoxicity)

The biological activities of CC used in this project are as yet unknown. Thus, we sought to investigate any further cellular effects (phenotypic endpoints) that correlated with the induction of the PCC phenotype, such as cytotoxicity. This can be described as CC causes cells to either undergo, necrosis, slowdown mitosis, mitotic arrest with a subsequent cell death or induction of apoptosis.

The CC induced PCC hits that were initially identified at the two different time points (24hr and 48hr, Tables 3.1 A and B) also displayed additional phenotypes, including reduced cell number/cytotoxicity. For example, the cell number was reduced in MP59-241/well F5 (117 cells at 24hr and 141 at 48hr), MP64-65/well B2 (472 cells at 24hr and 184 at 48hr) and in MP 64-65/well F7 (385 cells at 24hr and 138 cells at 48hr) (Tables 3.2 A and B). Furthermore, CC hits on the SMS 24hr incubation candidate hit list such as MP72-73/F6 and MP 74-75/G8 showed a Z score or Robust Z score ≤ -2 indicating a reduction in cell number (Table 3.2A) although a low %PCC had been identified.

Similarly, the CC in well C8 (MP59-241) and well C1 (MP66-67) slightly increased the %PCC to an average of 6.03 and 6.83, respectively and reduced cell number to an average of 421 (C8) and 1469 (C1) respectively but only after 48hr exposure time (Table 3.2B). Other CC hits which produced reduction in cell number after 48hr incubation only induced a slight increase in %PCC (≤ 5%) such as in plates MP59-241/well F7, MP60-61/well E1, MP68-MP69/well G7, MP70-MP71/well G5 and MP74-75/wells B11 and G11 (Table 3.2B).

In contrast, few CC hits showed a Z score or Robust Z score (%PCC) ≥ 2 (Table 3.1 A and B) combined with an increase in cell number in both replicates. These CC at 24hr were distributed in the following plates: MP62-63 (well F1) and MP74-75 (well E1) (Table 3.2A). The CC F1 at 24hr displayed a weak %PCC with a mean Z score of 2.27 or a Robust Z score of 4.66 (Table 3.1A), which was combined with no massive variation on cell number at both replicates (1486 cells in batch 1 and 1751 cells in batch 2) (Table 3.2A). Similar lower %PCC results were emerged with the CC E1 at 24hr with a mean Z score of 2.8 or a Robust Z score (%PCC) of 4.17 (Table 3.1A) although the cell number was higher compared to CC F1. The CC in MP74-75 (well E1) displayed a cell number of 2926 in batch 1 and 2027 in batch 2 (Table 3.2A).

 Additionally, the CC with increased cell number at 48hr were located in the following plates: MP60-61 (well D1), MP62-63 (wells E1 and E3) and MP74-75 (well F1) (Table 3.2B). These CC showed a weak to moderate %PCC (Table 3.1B). For

instance, the mean Z or Robust scores (%PCC) for the CC D1 was 2.82 or 3.09 and the cell number for batch 1 was 4034 and 3334 for batch 2 (Table 3.2B). Also, the CC E1 showed a moderate mean Z score or Robust Z score (%PCC) (4.02 or 8.39 respectively) (Table 3.1B) while the cell number for batch 1 was 3150 and 3070 for batch 2 (Table 3.2B). The CC E3 presented a weak Z score or slightly significant Robust Z score (%PCC) (1.45 or 3.67 respectively) (Table 3.1B) while the cell number for batch 1 was 3622 and 3335 for batch 2 (Table 3.2B). The F1 showed no significant mean Z score and slightly significant Robust Z score (%PCC) (1.24 or 2.68 respectively) (Table 3.1B) while the cell number for batch1 was 4476 and 3694 for batch2 (Table 3.2B).

Overall, the cellular effects of the CC hits varied. Thus, some of the CC hits that potentially induced PCC were found to have toxic effects, inducing cell death whereas the CC that induced weak %PCC showed no effect on cell number.

Table 3.2. Correlation between the potential CC hits which induced the PCC phenotype with reduction of cell number after 24hr and 48hr.

(Tables A and B) show the significant alteration of whole cell number (Z score or Robust Z score) observed within 17 and other 27 potential PCC CC hits for both replicates after 24hr and 48hr, respectively. The pink highlighted wells show the CC hits with a Z score or Robust Z score ≤ -2, indicating the significant reduction in cell number caused by these specific CC. Some of these highlighted CCs identified as hits that greatly induced PCC. For example, in **(Table A)** at 24hr MP59-41/ well F5, MP64-65/ wells B2 and F7 induced PCC (≥ 5%) while in **(Table B)** at 48hr MP59-41/ wells C8 and F5, MP64-65/ wells B2 and F7 and MPMP66-67/ well C1 induced ≥ 5% PCC. The average cell number for the negative control (DMSO) in batches 1 and 2 was 2065 cells and 1876 cells at 24hr and to 3658 and 3253 cells at 48hr, respectively.

A. Master plate name (24hr)	Well name	Cell number Replicate 1	Cell number Replicate 2	Z score Replicate 1	Z score Replicate 2	Robust Z score Replicate 1	Robust Z score Replicate 2
MP59-MP241	F5	119	116	-5.65	-10.95	-9.13	-13.57
	G3	1109	1243	-2.11	-2.32	-3.55	-2.79
MP60-MP61	E1	886	1170	-6.58	-1.58	-6.86	-4.01
MP62-MP63	F1	1486	1751	-0.31	1.52	-0.81	1.7
MP64-MP65	B2	473	471	-5.43	-9.28	-10.19	-15.54
	F7	171	600	-9.49	-1.67	-9.89	-4.22
MP66-MP67	G1	592	2841	-0.77	1.71	-0.75	4.01
MP68-MP69	E1	3463	1566	1.08	0.67	1.33	1.67
	G7	1202	1021	-11.5	-0.39	-12.46	-0.41
MP70-MP71	E1	1849	2322	-4.93	0.79	-7.53	0.7
MP72-MP73	F6	1322	1163	-4.89	-7.03	-14.75	-8.25
MP74-MP75	E1	2926	2027	0.16	0.55	0.19	0.9
	G8	1728	1027	-6.43	-3.49	-9.77	-5.05
MP76-MP77	E3	1831	1388	-0.3	-1.53	-13.99	-2.19
	G3	1364	1503	-0.81	-1.22	-24.14	-1.75
	G1	2687	2764	0.65	2.14	4.62	3.05
	E7	2329	1541	0.25	-1.12	-3.16	-1.61

B. Master plate name (48hr)	Well name	Cell number Replicate 1	Cell number Replicate 2	Z score Replicate 1	Z score Replicate 2	Robust Z score Replicate 1	Robust Z score Replicate 2
MP59-MP241	C8	563	280	-23.87	-18.33	-31.34	-30.99
	F5	186	96	-26.44	-19.51	-34.76	-33
	F7	226	501	-26.17	-16.92	-34.39	-28.57
MP60-MP61	E1	1236	955	-2.11	-9.29	-9.5	-21.71
	D1	4034	3334	0.8	2.52	1.2	5.95
MP62-MP63	C1	2306	3065	-4.07	0.69	-4.77	0.82
	D1	3501	2783	0.88	-0.02	0.95	-0.01
	E1	3150	3070	-0.58	0.7	-0.73	0.83
	E3	3622	3335	1.38	1.36	1.53	1.61
	G1	3371	2408	0.34	-0.96	0.33	-1.11
MP64-MP65	F7	60	216	-22.75	-28.99	-58.86	-33.85
	B2	78	290	-22.62	-28.49	-58.54	-33.26
MP66-MP67	C1	1091	1848	-23.01	-10.01	-42.11	-15.02
MP68-MP69	G7	1486	1605	-6.7	-5.35	-8.63	-13.55
MP70-MP71	G5	1520	2625	-3.25	-2.09	-9.7	-4.02
	G3	4179	2488	0.51	-2.55	0.34	-4.82
MP72-MP73	D1	4578	2046	-0.07	-1.2	-1.53	-1.69
MP74-MP75	G1	3219	2839	-10.61	-8.52	-11.76	-12.43
	B11	121	260	-13.61	-37.75	-15.08	-55.42
	G11	305	148	-13	-39.01	-14.4	-57.28
	F1	4476	3694	0.9	0.32	0.93	0.57
MP76-MP77	E3	2307	1955	-5.76	-0.21	-7.68	-0.35
	G3	2339	644	-5.66	-1.4	-7.54	-1.65
	G2	3523	561	-1.79	-1.47	-2.57	-1.74
	B2	3172	986	-2.93	-1.09	-4.04	-1.32
MP78-MP79	D1	2228.5	2489	0.1	-1.52	0.5	-2.09
	G1	2081	4084	-0.05	1.33	-0.12	1.51

3.2.1.5.2 Correlation of PCC hits with increased mitotic index (increased pHH3 Ser10 expression)

The use of the molecular probe pHH3 Ser10 combined with a high-content imaging and analysis system provided additional information on cellular phenotypic changes caused by the CC alongside PCC induction. As described previously (Section 3.2.1.2) the % of mitotic cells/expressing pHH3 Ser10 was identified by a Columbus Acapella image analysis protocol in which the immunostaining intensity of pHH3 Ser10/ mitotic cells was measured. Thus, the assessment of additional phenotypic endpoints such as %mitotic cells/pHH3 Ser10 was performed. Cells stained with Alex Fluor® 594 Red in the first batch and with Alex Fluor® 488 Green in the second batch. Thus, cells displayed pHH3 Ser10 at intensity cut-off of greater than 600 units in the first batch or 900 units in the second batch were classed as mitotic cells (See Chapter 2; Section 2.2.5).

The two lists of CC hits at 24hr and 48hr that had previously been identified as inducing PCC in (Table 3.1 A and B) were supported by additional statistical data for %mitotic cells (Table 3.3 A and B). The results indicated that the CC hits in wells B2 and F7 (MP64-65) that had previously been identified statistically as inducers of PCC and cell death also significantly increased %mitotic cells by an average of 42% and 37% respectively at 24hr (Table 3.3A). However, the %mitotic cells for these two CC decreased by an average of 4% and 7% respectively at 48hr (Table 3.3B). This suggests that the rapid increase in the pHH3 Ser10 caused by the two CC may correlate to an increase in abnormal chromosome condensation after 24hr as previously shown in (Table 3.1A). The remaining CC hits did not present a significant Z score or Robust Z score for % mitotic cells (≥ 2), which may be due to the variations in %mitotic cells between the two replicates. This variation might be due to the use of the weaker red channel (Alexa Fluor® 594 secondary antibody) in the Operetta to detect mitotic cells expressing pHH3 Ser10 which was not suitable for the purposes of measuring the pHH3 Ser10 staining intensity accurately in the first batch compared to the strong green channel (Alexa Fluor® 488) which gave a better reliability and more consistent staining pattern in the second batch.

In comparison, the CC in well F5 (MP59-241) that initially correlated with the induction of PCC and cell death was associated with an increase in %mitotic cells. Interestingly, this CC did not present a marked reduction in the level of mitotic cells after 48hr, showing an average increase of 15% at 24hr exposure and 14% at 48hr. This CC caused different cellular phenotypic changes (potential induction of PCC,

reduction in cell number and increase in mitotic index) meaning it was considered to be a strong hit.

Furthermore, the other two CC in MP74-MP75/wells B11 and G11, gave a significant Z score or Robust Z score for %mitotic cells after 48hr (Table 3.3B). Although these CC hits initially did not induce high %PCC (< 5%) at 48hr, their Z score and Robust Z score values for % PCC were significant (Table 3.1B) and correlated significantly with a reduction in cell number (Table 3.2B).

In summary, the results of the SMS identified 17 CC hits at 24hr and 27 CC hits at 48hr that were found predominantly to induce PCC. Other cellular effects (phenotypic endpoints) caused by these CC hits were characterized as induction of cell death and mitotic cells expressing pHH3 Ser10. Some of the CC hits that potentially induced PCC caused mitotic arrest and/or cell death while the others did not, indicating that the CC caused various types of cellular alterations, which may be related to the chemical structures of these CC. The CC in MP59-241/ well F5 was considered to be a potentially strong hit, presenting a significant effect in all 3 cellular phenotypic endpoints: % PCC, reduction in cell number and increase in %mitotic cells.

Table 3.3. Correlation between the potential CC hits which induced the PCC phenotype with increased %mitotic cells after 24hr and 48hr.
(**Tables and B)** shows the %mitotic cells (Z score or Robust Z score) observed in 17 and other 27 potential CC PCC hits for both screen replicates after 24hr and 48hr, respectively. The green highlighted wells in both tables at 24hr or 48hr show the CC hits, which showed an increase in %mitotic cells with Z score or Robust Z score of ≥ 2. Three highlighted CC hits correlated with a significant increase in %PCC at both exposure times, 24hr or 48hr. For instance, in **(**Tables **A** and **B)** (MP59-241/ well F5) and (MP64-65/ wells B2 and F7). The CC in (MP74-75/ wells B11 and G11) at 48hr showed a lower %PCC (< 5%) with a significant Z or Robust Z scores of ≥ 2 for %PCC and significantly correlated with an increase in %mitotic cells. The %mitotic cells for the negative control (DMSO) in batches 1 and 2 at 24hr was 9.4% and 13.82% whilst at 48hr it was 6.2% and 4.3%.

A. Master plate name (24hr)	Well name	% Mitotic cells Replicate 1	% Mitotic cells Replicate 2	Z score Replicate 1	Z score Replicate 2	Robust Z score Replicate 1	Robust Z score Replicate 2
MP59-MP241	F5	6.57	24.12	0.7	1.79	2.14	2.7
	G3	1.49	62.95	-1.18	8.04	-2.6	11.21
MP60-MP61	E1	12.43	6.5	5.93	-0.46	8.74	-0.35
MP62-MP63	F1	3.18	11.57	-0.52	0.31	-0.33	0.25
MP64-MP65	B2	42.18	42.18	6.23	6.23	10.78	10.78
	F7	37.22	37.22	4.87	4.87	8.35	8.35
MP66-MP67	G1	56.95	15.14	0.81	1.3	1.1	1.46
MP86-MP69	E1	2.32	3.51	0.04	0.38	0.29	0.9
	G7	8.07	7.55	17.26	4.88	22.87	11.31
MP70-MP71	E1	18.02	21.08	3.01	0.5	2.85	1.09
MP72-MP73	F6	11.94	16.58	0.5	-1.88	1.15	-1.9
MP74-MP75	E1	10.31	5.68	-0.99	0	-2.21	0.45
	G8	8.53	2.87	-1.66	0.69	-4.1	1.76
MP76-MP77	E3	0.69	21.61	-1.47	0.73	-4.03	1.57
	G3	4.17	18.45	4.11	-0.75	10.53	-1.18
	G1	2.33	19.88	1.17	-0.08	2.85	0.07
	E7	1.87	15.89	0.42	-1.94	0.91	-3.42

B. Master plate name (48hr)	Well name	% Mitotic cells Replicate 1	% Mitotic cells Replicate 2	Z score Replicate 1	Z score Replicate 2	Robust Z score Replicate 1	Robust Z score Replicate 2
	C8	8.45	5.85	-1.39	3.56	-1.62	4.26
MP59-MP241	F5	15.38	14.49	1.71	35.57	2.68	42.81
	F7	1.63	10.21	-4.43	13.42	-5.86	16.14
MP60-MP61	E1	7.6	5.04	-1.8	1.03	-2.27	2.12
	D1	10.61	4.12	-0.08	-0.03	-0.31	0.01
MP62-MP63	C1	10.78	5.24	-2.03	0.31	-4.31	0.91
	D1	11.17	3.74	-1.71	-1.25	-3.55	-1.4
	E1	11.16	4.22	-1.72	-0.75	-3.57	-0.65
	E3	10.64	4.63	-2.14	-0.33	-4.59	-0.04
	G1	11.09	5.24	-1.77	0.31	-3.71	0.91
MP64-MP65	F7	4.2	10.53	1.81	7.42	4.03	11.65
	B2	2.18	6.96	-1.25	3.25	-2.46	5.16
MP66-MP67	C1	4.43	4	0.92	-0.39	2.38	-0.65
MP68-MP69	G7	1.32	2.02	-2.33	0.81	-4.03	0.98
MP70-MP71	G5	22.12	3.57	1.77	0.11	5.5	0.14
	G3	10.81	5.41	-0.66	4.66	-2.07	5.81
MP72-MP73	D1	2.88	4.37	1.99	-0.57	84.73	-1.02
MP74-MP75	G1	3.19	5.29	1.65	5.01	2.52	7.3
	B11	6.17	10.14	7.34	13.5	11.55	19.19
	G11	1.5	15.89	-1.58	23.56	-2.61	33.28
	F1	2.28	6	-0.09	6.25	-0.24	9.04
MP76-MP77	E3	2.79	5.91	-1.57	0.67	-2.52	1.09
	G3	1.29	7.63	-1.19	1.61	-1.92	2.4
	G2	2.12	8.54	0.17	2.11	0.23	3.1
	B2	1.76	7.2	-0.42	1.38	-0.7	2.07
MP78-MP79	D1	3.94	1.72	0.05	0.03	0.83	0.15
	G1	2.78	1.18	-1.88	-1.65	-3.54	-2.45

3.2.1.6 Identification of CC hits that reduce cell number

Visual assessment suggested that CC caused different cellular changes and, in particular, a reduction in cell number may indicate the potential involvement of these CC in cytotoxicity or decreasing cell proliferation, which may indicate useful CC to follow up for cancer treatment. The aim was to identify CC hits that reduce cell number.

As previously described in Section 3.2.1.2, cell number was evaluated using a Columbus Acapella imaging protocol analysis. The initial statistical analyses (Z score and Robust Z scores) for cell number were performed based on the 0.2% DMSO negative controls. Then, the cell number Z score or Robust Z score values for each of the 792 CC were ranked in ascending order for both replicates and also individually for the 2 different exposures: 24hr and 48hr. CC showing Z score or Robust Z scores of ≤ -2 were considered to be potential hits for cellular cytotoxicity/reduction in proliferation. To reduce variations between the replicates, the averages for cell number Z score and Robust Z score values for the duplicate screens were calculated. These analyses, as previously described (Section 3.2.1.4.3; Scatter plots C and D in Figure 3.8) displayed 150 CC hits at 24hr and 119 CC hits at 48hr that showed statistically significant Z score or Robust Z score of ≤ -2 (Appendix 9 A and B)

Next, to identify the most potent CC hits that reduce cell number, further statistical hit filtration was performed using Doxorubicin (0.4µg/ml), which was included on the screen plates as a positive control for inducing cell death. The average cell number for this secondary reference was 1059 cells at 24hr and 894 at 48hr (n = 16 wells) for the first batch (Figure 3.9A) and 844 cells at 24hr and 562 at 48hr (n = 44 wells) for the second batch (Figure 3.9B), compared to the average cell number in the negative 0.2% DMSO vehicle control, which showed 2065 cells at 24hr and 3658 at 48hr for the first batch and 1876 cells at 24hr and 3253 at 48hr for the second batch (Section 3.2.1.4.1; Figure 3.5). Additionally, the Z score and Robust Z score for the cell number in the positive control Doxorubicin were calculated based on the negative 0.2% DMSO vehicle control. Consequently, the average Z scores of -5 and -13 and the average Robust Z scores of -7 and -24 were identified at 24hr and 48hr, respectively, indicating that the assay can correctly identify a chemical inducing cell death. As the Robust Z score is a strong statistical method compared to Z score, the cut-off values used for identifying the final cytotoxic CC hits list were based on the average Robust Z scores for cell number of the positive control Doxorubicin at 24hr and 48hr.
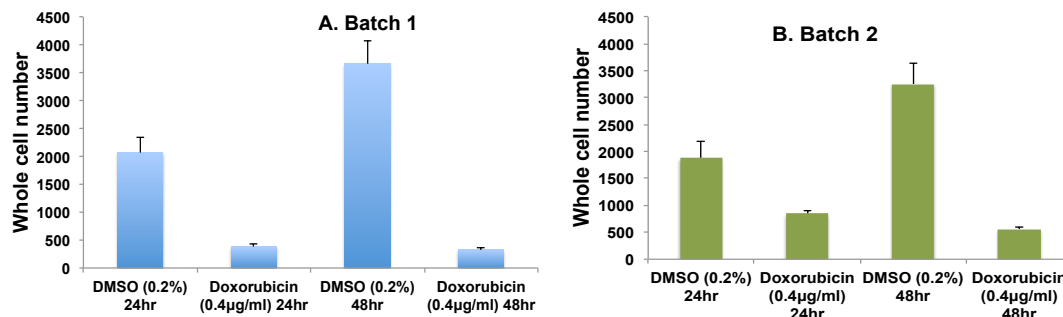
Figure 3.9. The whole cell number for the secondary control Doxorubicin in comparison to the negative control DMSO (0.2%).

Doxorubicin was included in the screening plates used for final assessment and identification of potential cytotoxic CC hits. The mean cell number for batches 1 **(A)** and 2 **(B)** at 24hr was 1059 and 894 cells whilst at 48hr numbers reduced to 844 and 562 cells, respectively. The average cell number for the negative control in batches 1 and 2 was 2065 cells and 1876 cells at 24hr and to 3658 and 3253 cells at 48hr, respectively.

A list of CC hits that were potentially linked to cell number reduction, irrelevant of PCC induction, was identified, consisting of 49/792 CC (6%) at 24hr and a further 12/792 (1.5%) at 48hr (Table 3.4 A and B).

Interestingly, the 24hr hit list included 3 CC that had initially been identified as potential CC hits which induced PCC, and were located in MP59-241/well F5 and MP64-65/wells F7 and B2 (Table 3.4). Furthermore, after 48hr, 7 CC that were designated as promising hits for decreasing cell number had previously been associated with PCC phenotype induction. These CC were located as follows: MP59-241/wells C8, F5 and F7; MP64-65/wells B2 and F7, and MP74-75/wells B11 and G11 (Table 3.4).

Although the CC were evaluated for cytotoxic activity, assessment of the effect on cell number was not the principal aim of this study nor was it used as an independent parameter in test screening. It was chiefly carried out to provide further biological characterisation of compounds identified as potential hits for inducing PCC. However, it did show that of this targeted library, cytotoxicity was not always accompanied by PCC induction. It also provided useful data about the CC used in this screen to the library supplier.

Table 3.4. Identification of CC hits that reduce cell number (cytotoxicity).
The Z score or Robust Z score for the cell number were initially calculated for 792 CC based on the negative 0.2% DMSO vehicle control. Doxorubicin was used in the screen plates as positive control for inducing cell death. The average Robust Z scores of -7 at 24hr and -24 at 48hr for the cells number in Doxorubicin controls were identified and used as cut-off values to identify statistically the most potent CC hits that reduce cell number. **(A)** A list of 49/792 CC (6%) hits at 24hr and **(B)** a further 12/792 (1.5%) at 48hr were identified. The highlighted pink rows included the validation of CC hits associated with PCC induction and cytotoxicity at **(A)** 24hr and **(B)** 48hr.

A. Cytotoxic CC hits (24hr)	Well Name	Batch 1			Batch 2			Average		
Master Plate Name	Well Name	Whole Cells Number	Z score	Robust z score	Whole Cells Number	Z score	Robust Z score	Whole Cells Number	Z score	Robust Z score
MP72-MP73	D11	42	-10.20	-30.08	56	-14.69	-17.48	49	-12.44	-23.78
MP72-MP73	D4	89	-10.00	-29.51	7	-15.03	-17.88	48	-12.52	-23.70
MP74-MP75	B11	220	-17.71	-26.81	243	-6.65	-9.72	232	-12.18	-18.26
MP76-MP77	E8	1136	-1.06	-29.10	1155	-2.15	-3.08	1146	-1.60	-16.09
MP64-MP65	**F7**	**171**	**-7.02**	**-13.21**	**600**	**-8.72**	**-14.55**	**386**	**-7.87**	**-13.88**
MP64-MP65	**B2**	**473**	**-5.43**	**-10.19**	**471**	**-9.28**	**-15.54**	**472**	**-7.35**	**-12.87**
MP72-MP73	F6	1322	-4.89	-14.75	1163	-7.03	-8.25	1243	-5.96	-11.50
MP59-MP241	**F5**	**119**	**-5.65**	**-9.13**	**116**	**-10.95**	**-13.57**	**118**	**-8.30**	**-11.35**
MP74-MP75	G11	1269	-9.86	-14.95	649	-5.01	-7.30	959	-7.44	-11.13
MP62-MP63	D11	514	-8.46	-15.54	828	-5.61	-6.70	671	-7.03	-11.12
MP70-MP71	F6	982	-11.71	-17.73	301	-2.10	-4.21	642	-6.90	-10.97
MP59-MP241	C8	403	-4.64	-7.53	145	-10.73	-13.30	274	-7.68	-10.41
MP74-MP75	C5	1119	-10.99	-16.65	1183	-2.86	-4.13	1151	-6.92	-10.39
MP76-MP77	G7	1913	-0.21	-12.21	4	-5.22	-7.46	959	-2.71	-9.83
MP72-MP73	G8	1664	-3.47	-10.65	1105	-7.43	-8.73	1385	-5.45	-9.69
MP72-MP73	D8	1768	-3.04	-9.41	967	-8.39	-9.88	1368	-5.71	-9.65
MP72-MP73	G6	1717	-3.25	-10.02	1071	-7.67	-9.02	1394	-5.46	-9.52
MP72-MP73	D6	1825	-2.80	-8.72	954	-8.48	-9.99	1390	-5.64	-9.36
MP72-MP73	B7	1709	-3.29	-10.11	1128	-7.27	-8.54	1419	-5.28	-9.33
MP59-MP241	F7	296	-5.02	-8.13	435	-8.51	-10.52	366	-6.76	-9.33
MP72-MP73	F8	1720	-3.24	-9.98	1127	-7.28	-8.55	1424	-5.26	-9.27
MP72-MP73	F7	1643	-3.56	-10.90	1248	-6.44	-7.54	1446	-5.00	-9.22
MP74-MP75	D5	1376	-9.06	-13.75	1138	-3.04	-4.39	1257	-6.05	-9.07
MP76-MP77	F6	1765	-0.37	-15.42	1378	-1.55	-2.23	1572	-0.96	-8.83
MP72-MP73	C6	1840	-2.74	-8.54	1090	-7.54	-8.86	1465	-5.14	-8.70
MP76-MP77	G5	1883	-0.24	-12.86	796	-3.10	-4.45	1340	-1.67	-8.65
MP72-MP73	E7	1877	-2.59	-8.10	1060	-7.75	-9.11	1469	-5.17	-8.61
MP72-MP73	G7	1924	-2.39	-7.54	998	-8.17	-9.63	1461	-5.28	-8.58
MP72-MP73	D7	1924	-2.39	-7.54	1008	-8.11	-9.54	1466	-5.25	-8.54
MP72-MP73	E8	1915	-2.43	-7.65	1106	-7.43	-8.73	1511	-4.93	-8.19
MP74-MP75	G7	1678	-6.80	-10.33	883	-4.07	-5.91	1281	-5.44	-8.12
MP76-MP77	E3	1831	-0.30	-13.99	1388	-1.53	-2.19	1610	-0.91	-8.09
MP74-MP75	D8	1688	-6.73	-10.22	948	-3.81	-5.52	1318	-5.27	-7.87
MP74-MP75	C7	1668	-6.88	-10.45	988	-3.65	-5.29	1328	-5.26	-7.87
MP70-MP71	E7	1410	-8.36	-12.69	910	-1.23	-2.73	1160	-4.80	-7.71
MP74-MP75	B7	1717	-6.51	-9.89	1009	-3.56	-5.16	1363	-5.04	-7.53
MP72-MP73	D5	1947	-2.30	-7.26	1227	-6.59	-7.72	1587	-4.44	-7.49
MP72-MP73	C7	1951	-2.28	-7.22	1223	-6.62	-7.75	1587	-4.45	-7.48
MP74-MP75	D6	1671	-6.85	-10.41	1126	-3.09	-4.46	1399	-4.97	-7.44
MP74-MP75	G8	1728	-6.43	-9.77	1027	-3.49	-5.05	1378	-4.96	-7.41
MP74-MP75	E6	1649	-7.02	-10.66	1196	-2.81	-4.05	1423	-4.91	-7.35
MP78-MP79	C10	907.5	-5.60	-8.71	761	-4.34	-5.94	834	-4.97	-7.32
MP74-MP75	B5	1685	-6.75	-10.25	1143	-3.02	-4.36	1414	-4.88	-7.31
MP72-MP73	B6	1967	-2.22	-7.02	1302	-6.07	-7.09	1635	-4.14	-7.06
MP60-MP61	F7	502	-9.49	-9.89	1150	-1.67	-4.22	826	-5.58	-7.05
MP70-MP71	G6	1678	-6.26	-9.54	254	-2.17	-4.33	966	-4.22	-7
MP74-MP75	F5	1735	-6.38	-9.69	1182	-2.86	-4.13	1459	-4.62	-7
MP74-MP75	E8	1808	-5.83	-8.86	1090	-3.23	-4.68	1449	-4.53	-7
MP70-MP71	B6	1708	-6.03	-9.19	367	-2.01	-4.05	1038	-4.02	-7

Continued Table 3.4.

B. Cytotoxic CC hits (48hr)		Batch 1			Batch 2			Average		
Master Plate Name	Well Name	Whole Cells Number	Z score	Robust Z score	Whole Cells Number	Z score	Robust Z score	Whole Cells Number	Z score	Robust Z score
MP64-MP65	**F7**	**60**	**-22.75**	**-58.86**	**216**	**-28.99**	**-33.85**	**138**	**-25.87**	**-46.35**
MP64-MP65	**B2**	**78**	**-22.62**	**-58.54**	**290**	**-28.49**	**-33.26**	**184**	**-25.56**	**-45.90**
MP66-MP67	F6	7	-34.19	-62.95	6	-17.21	-25.79	7	-25.70	-44.37
MP74-MP75	**G11**	**305**	**-13.00**	**-14.40**	**148**	**-39.01**	**-57.28**	**227**	**-26.01**	**-35.84**
MP74-MP75	**B11**	**121**	**-13.61**	**-15.08**	**260**	**-37.75**	**-55.42**	**191**	**-25.68**	**-35.25**
MP59-MP241	**F5**	**186**	**-26.44**	**-34.76**	**96**	**-19.51**	**-33.00**	**141**	**-22.98**	**-33.88**
MP59-MP241	**F7**	**226**	**-26.17**	**-34.39**	**501**	**-16.92**	**-28.57**	**364**	**-21.54**	**-31.48**
MP59-MP241	**C8**	**563**	**-23.87**	**-31.34**	**280**	**-18.33**	**-30.99**	**422**	**-21.10**	**-31.17**
MP66-MP67	C1	1091	-23.01	-42.11	1848	-10.01	-15.02	1470	-16.51	-28.56
MP64-MP65	B6	1949	-9.58	-25.13	458	-27.35	-31.92	1204	-18.46	-28.52
MP74-MP75	F11	432	-12.58	-13.94	1407	-24.75	-36.30	920	-18.66	-25.12
MP66-MP67	E8	961	-24.35	-44.61	3590	-3.19	-4.83	2276	-13.77	-24.72

3.2.1.7 Identification of CC hits inducing increased numbers of mitotic cells

The ability of the 792 CC screened here to increase the number of mitotic cells was investigated. As DMSO (0.2%) was used as a negative control in replicate plates, the initial statistical analyses (Z score and Robust Z scores) for %mitotic cells were performed based on DMSO negative controls. Then, the %mitotic cells Z score or Robust Z score values for each of the 792 CC were ranked in descending order for both replicates and also individually for the 2 different exposures: 24hr and 48hr. CC showing scores ≥ 2 Z score or Robust Z score for both replicates were considered to be potential hits for increase in %mitotic cells. To reduce variations between the replicates, the averages for %mitotic cells Z score and Robust Z score values for the duplicate screens were calculated. These analyses, as previously described (Section 3.2.1.4.3; Scatter plots E and F in Figure 3.8) displayed 16 CC hits at 24hr and 4 CC hits at 48hr that showed statistically significant Z score or Robust Z score of ≥ +2 (Appendix 10 A and B).

Next, to identify the most potent CC hits that increase %mitotic cell, further statistical hit filtration was performed using Nocodazole (1µM) as a positive visual assay control for induction of the mitotic cell phenotype. The average %mitotic cell number for this secondary reference was 7.12% at 24hr and 6.7% at 48hr (n = 32 wells) for the first batch (Figure 3.10A) and 17.08% at 24hr and 7.8% at 48hr (n = 44 wells) for the second batch (Figure 3.10B) compared to the average %mitotic cell in the negative 0.2% DMSO vehicle control, which showed 9.4% at 24hr and 6.2% at 48hr for the first batch and 13.82% at 24hr and 4.3% at 48hr for the second batch (See Section 3.2.1.4.1; Figure 3.6).
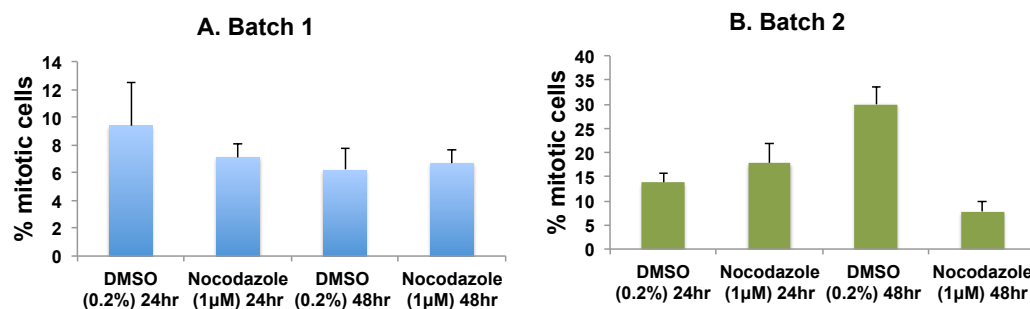
Figure 3.10. The %mitotic cells in batches 1 and 2 after exposure to Nocodazole in comparison to the negative control DMSO (0.2%).

Nocodazole was included in the screening plates and used for final evaluation and identification of potential CC hits which induced increased %mitotic cells. The mean %mitotic cells for batches 1 **(A)** and 2 **(B)** at 24hr was 7.12% and 17.08% while %mitotic cells at 48hr reduced to 6.7% and 7.8%, respectively. The %mitotic cells for the negative control in batches 1 and 2 at 24hr was 9.4% and 13.82% whilst at 48hr it was 6.2% and 4.3%.

Additionally, the Z score and Robust Z score for the %mitotic cell in the positive control Nocodazole were calculated based on the negative 0.2% DMSO vehicle control. Consequently, the average Z scores of 1.03 and 4 and the average Robust Z scores of 3.2 and 7.2 were identified at 24hr and 48hr, respectively, indicating that the assay can identify a chemical inducing increased number of mitotic cells. Since the Robust Z score values for %mitotic cells in the positive control Nocodazole at both 24hr and 48hr were ≥ 2 compared to those values observed with Z scores, theses values were used as cut-off for final identification of the potential CC hits inducing increased in mitotic cell number at 24hr and 48hr. Consequently, a list of CC hits, that were potentially associated with inducing increased mitotic cells number, irrelevant of PCC induction, was identified, consisting of 11/792 CC (1.1%) at 24hr and a further 3/792 (0.4%) at 48hr.

Interestingly, the hit lists containing CC inducing increased mitotic cells at 24hr and 48hr included some of the potential CC that had initially been identified as hits induced PCC in Section 3.2.1.5; Table 3.1 A and B. Two CC hits, MP64-65/wells B2 and F7 (Table 3.5A), which were found to increase %mitotic cell number at 24hr were also initially included in the list of CC hits inducing PCC alongside reduced cell number, suggesting that these specific CC had the possible propensity to increase %mitotic cells and early mitotic entry (PCC) that is associated with cytotoxicity. A further 3 CC which induced increased %mitotic cells at 48hr possibly correlated with PCC induction and were associated with decreased cell number which were distributed as follows: in MP59-241/well F5, MP64-65/well F7 and MP74-75/well B11 (Table 3.5B).

Although the assessment of the increase of the mitotic cells/ expressing pHH3 Ser10 induced by CC was an additional rather than a principal parameter, some of the CC hits that were identified for inducing PCC predominantly also increased %mitotic cells, indicating a possible correlation between induction of PCC and increased %mitotic cells.

Table 3.5. Identification of CC hits increase mitotic cell number.
The Z score or Robust Z score for %mitotic cells were initially calculated for 792 CC based on the negative 0.2% DMSO vehicle control. Nocodozole was used in the screen plates as positive control for a chemical inducing increased number of mitotic cells. The average Robust Z scores of 3.2 at 24hr and 7.2 at 48hr for the cells number in Nocodozole controls were identified and used as cut-off values to identify statistically the most potent CC hits that increase mitotic cell number. **(A)** A list of 11/792 CC (1.1%) hits at 24hr and **(B)** a further 3/792 (0.4%) at 48hr were identified. The highlighted green rows included the validation of CC hits associated with PCC induction and increased mitotic cell number at **(A)** 24hr and **(B)** at 48hr.

CC hits increase %mitotic cells (24hr)		Batch 1				Batch 2				Average			
Master Plate Name	Well Name	Whole Cells Number	%mitotic cells	Z score	Robust Z score	Whole Cells Number	%mitotic cells	Z score	Robust Z score	Whole Cells Number	%mitotic cells	Z score	Robust Z score
MP74-MP75	B11	220	38.84	9.78	27.98	243	32.50	22.60	43.46	232	35.67	16.19	35.72
MP64-MP65	**B2**	**473**	**42.18**	**6.23**	**10.78**	**471**	**42.18**	**6.23**	**10.78**	**472**	**42.18**	**6.23**	**10.78**
MP76-MP77	C3	2536	2.38	1.24	3.03	961	37.52	8.18	15.48	1749	19.95	4.71	9.26
MP64-MP65	**F7**	**171**	**37.22**	**4.87**	**8.35**	**600**	**37.22**	**4.87**	**8.35**	**386**	**37.22**	**4.87**	**8.35**
MP72-MP73	D8	1768	28.04	4.62	8.61	967	23.43	1.84	2.33	1368	25.74	3.23	5.47
MP74-MP75	G2	2667	15.02	0.79	2.77	1597	10.19	3.80	7.68	2132	12.60	2.29	5.23
MP74-MP75	B6	1927	15.58	1.00	3.37	1284	9.54	3.26	6.65	1606	12.56	2.13	5.01
MP72-MP73	D2	2562	25.63	2.94	5.28	2191	23.50	1.88	2.37	2377	24.56	2.41	3.82
MP78-MP79	C10	6.5	8.25	5.19	5.49	761	21.18	0.82	1.01	384	14.72	3.01	3.25
MP64-MP65	E7	1319	25.81	1.74	2.78	2337	25.81	1.74	2.78	1828	25.81	1.74	3
MP64-MP65	E8	1114	25.33	1.61	2.54	2017	25.33	1.61	2.54	1566	25.33	1.61	3

B. CC hits increase %mitotic cells (48hr)		Batch 1				Batch 2				Average			
Master Plate Name	Well Name	Whole Cells Number	%mitotic cells	Z score	Robust Z score	Whole Cells Number	%mitotic cells	Z score	Robust Z score	Whole Cells Number	%mitotic cells	Z score	Robust Z score
MP59-MP241	F5	186	15.38	1.71	2.68	96	20.00	35.57	42.81	141	17.69	18.64	22.75
MP74-MP75	B11	121	6.17	7.34	11.55	260	10.14	13.50	19.19	191	8.15	10.42	15.37
MP64-MP65	F7	60	4.20	1.81	4.03	216	10.53	7.42	11.65	138	7.36	4.61	7.84

3.2.1.8 Primary validation of CC hits that induce PCC at 24hr and 48hr

All CC hits validations were re- evaluated using a dose-response curve of 0, 2.5, 5,10, 20 and 40μM to minimize off-target effects. The ovarian cancer cell line 1847 was used for CC hit validation. The top and bottom rows of a 96-well plate comprised the negative controls DMSO (0.2%) (n = 8 wells), positive controls *MCPH1/BRIT1* siRNA (n = 4), and secondary controls Doxorubicin (n = 4) and Nocodazole (n = 4).

It was planned to re-test all CC hits which induced PCC, a total of 17 hits at 24hr and 27 hits at 48hr. However, in the first phase of primary validation, an

attempt was made to select CC hits that had shown a significant Z score or Robust Z score (%PCC) at both 24hr and 48hr, which can be examined for validation purposes using the dose response curve method. Consequently, 7 CC which potentially induced PCC at both 24hr and 48hr, were selected, which were as follows; MP59-241/well F5, MP60-61/well E1, MP64-65/well B2 and F7, MP68-69/well G7 and MP76-77/well E3 and G3 (Table 3.1 A and B). The results indicated that only two of these CC were validated showing a dose-related response for increased %PCC. These CC which were, MP64-65/well B2, that induced %PCC at both 24hr and 48hr whereas for MP59-241/well F5 increased PCC was only induced at 48hr. The remaining CC hits did not present an effective response curve pattern at either 24hr or 48hr (Data not shown).

Obviously, validation findings of the CC hits after 24hr showed only one CC which potential induced PCC. However, based on the fact that *MCPH1/BRIT1* siRNA induces elevated level of PCC after 48hr thus it may be more logical validation the CC that potentially induce PCC after 48hr. Thus, the second phase of primary validation focused on validating all the CC hits identified after 48hr CC exposure including the CC that were tested in the first phase, meaning the potential 27 CC hits. Consequently, the second phase primary validation results revealed that 10 of the total 27 CC hits displayed a dose dependent response after 48hr exposure (Figure 3.11A). These CC were MP59-241/wells C8, F5 and F7; MP64-65/wells B2 and F7; MP66-67/well C1; MP74-75/wells B11 and G11; and MP76-77 wells E3 and G3 (Figure 3.11A). Interestingly, the majority of these 10 potential CC hits that had shown a gradual increase in %PCC had also shown cell number reduction (Figure 3.11B). The image from Columbus representing the cells treated with a variety of concentrations of the selected CC hits (MP74-75/wells B11) showed that induction of the PCC phenotype (highlighted in red by Columbus) correlated with 2 other phenotypic endpoints, namely, pHH3 positive staining (mitotic cell) and reduction in cell number (Figure 3.12).

The validation results were reported to the library supplier (Dr. Richard Foster) to determine the structural characteristics of the10 selected CC before performing the secondary validation. Consequently, 2 CC were excluded, as their structures indicated poor solubility. These were the CC in MP59/241/well C8 and MP64-65/well B2.
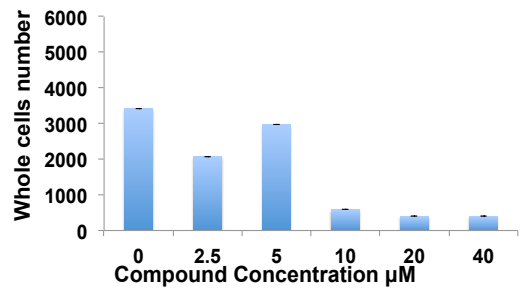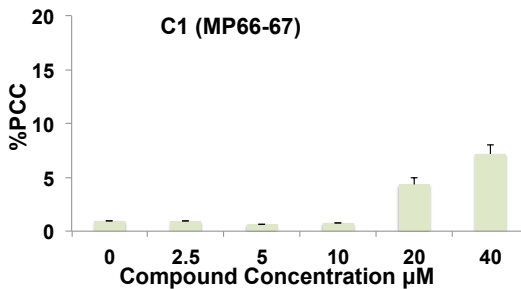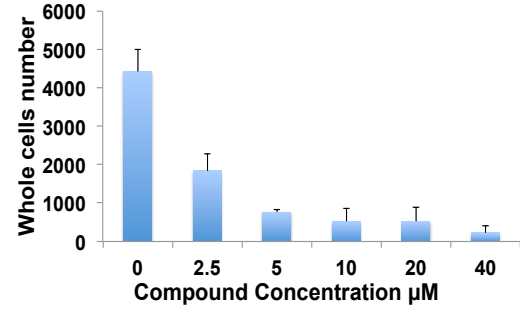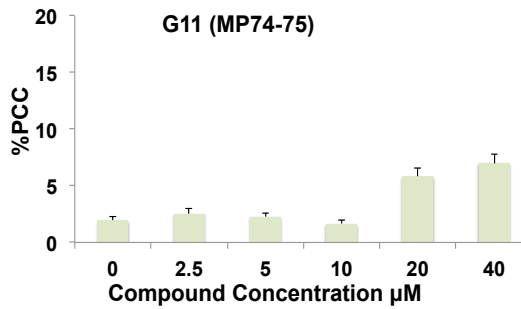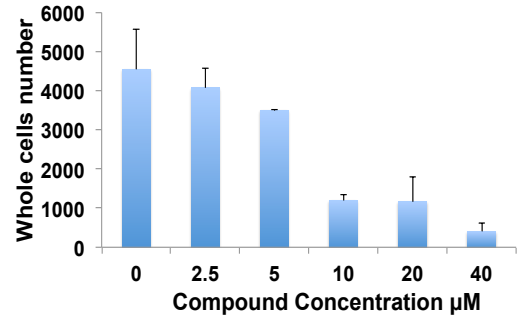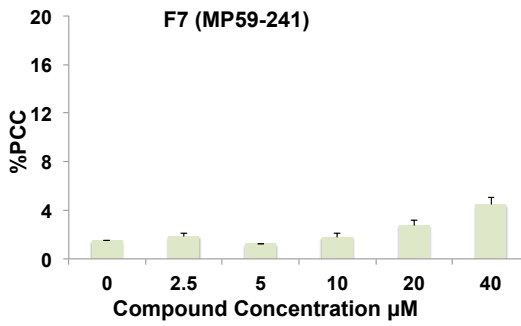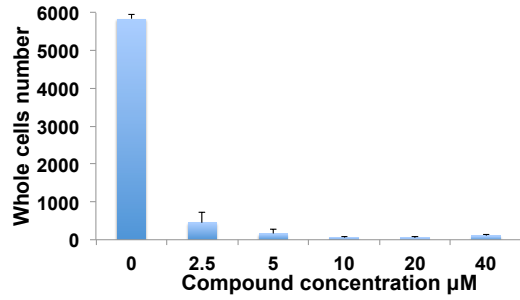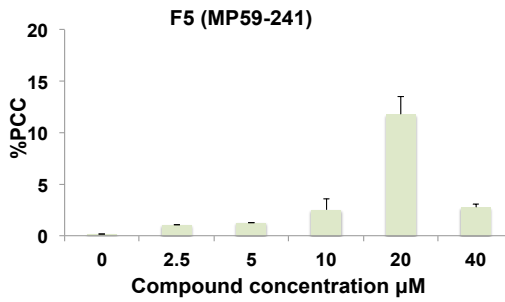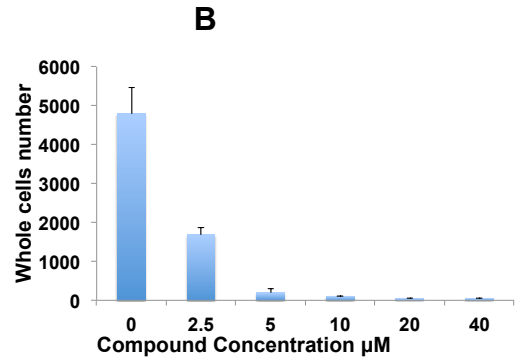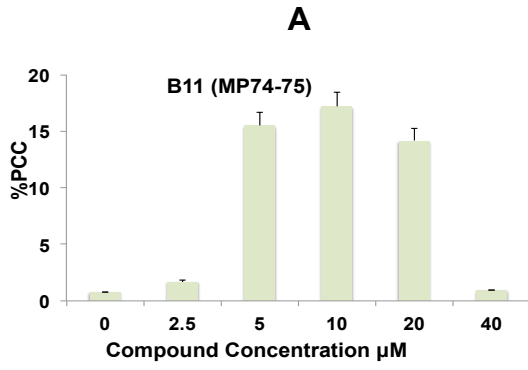
Continued   **A**   **B**
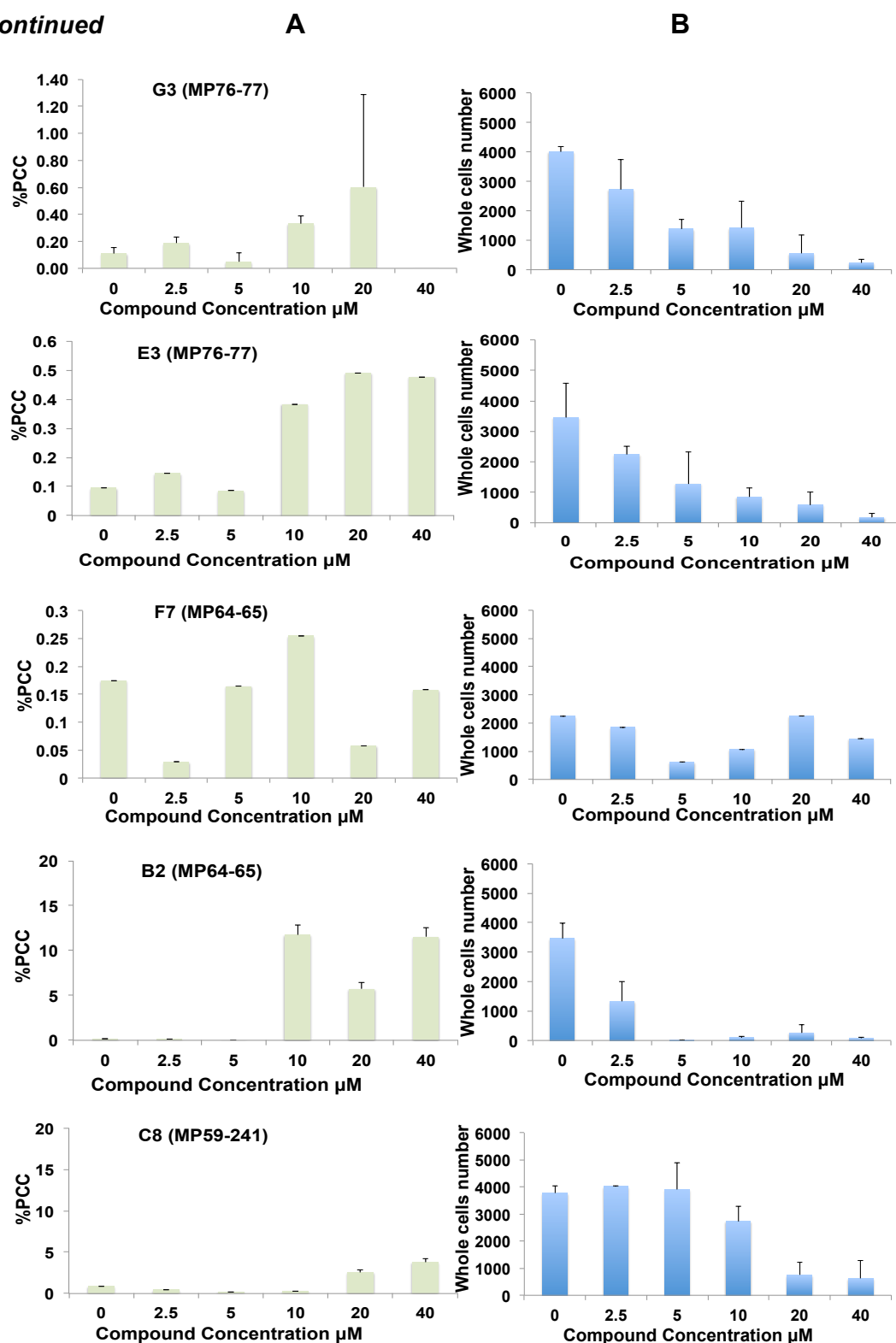
Figure 3.11. Validation of SMS hits which induced PCC after 48hr.

The validation results revealed 10 of the 27 CC that potentially induced PCC after 48hr were validated. The graphs of 10 potential CC hits presenting dose responses for both **(A)** increased %PCC and **(B)** reduction in cell number are shown. The top 8 CC were validated for increase in %PCC and cytotoxicity parameters. The remaining 2 CC, that are located at the end of this figure, were excluded as their structures indicated poor solubility.
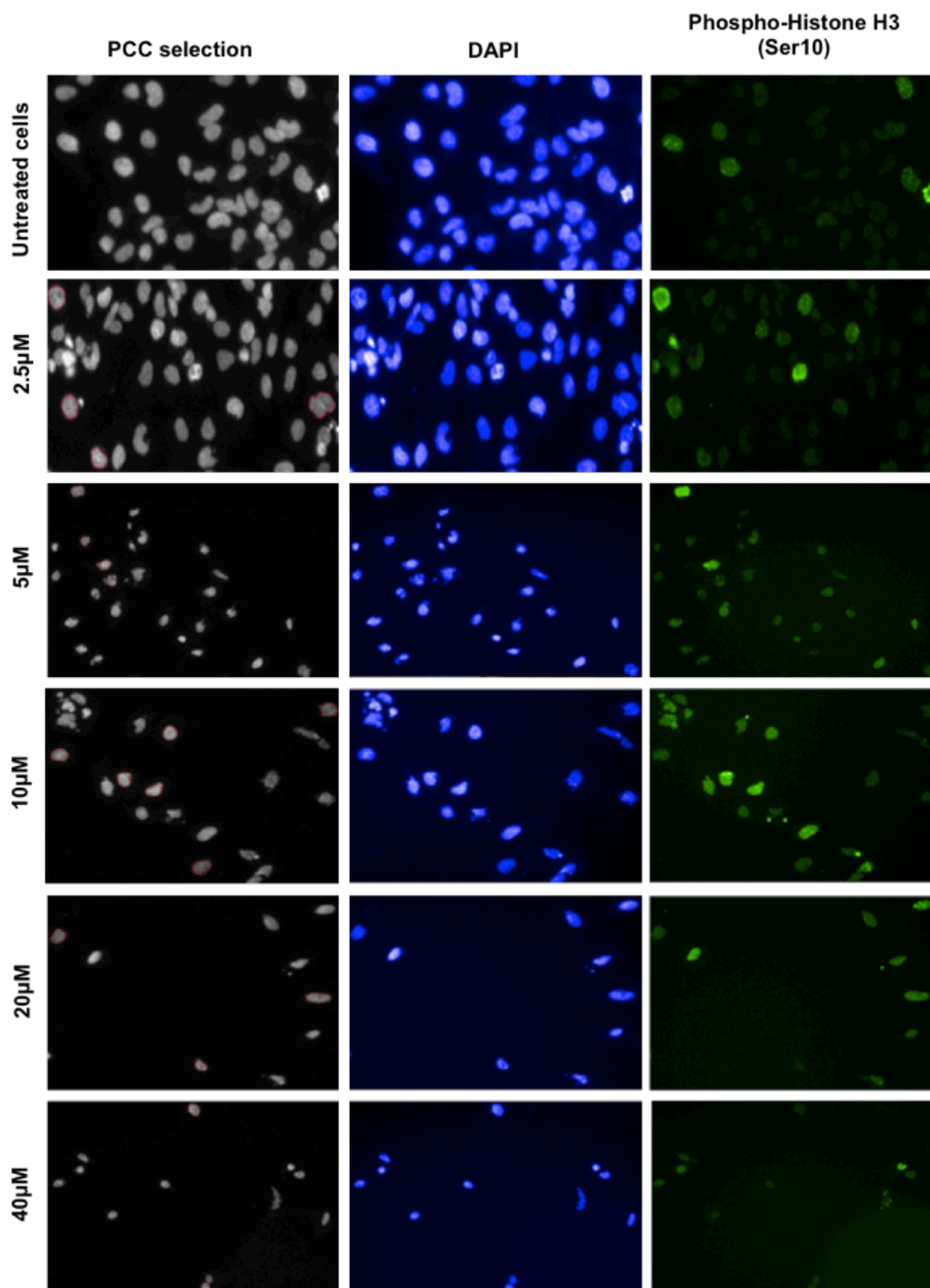
Figure 3.12. Cellular effects induced by the CC MP74-75/well B11 after 48hr.
Representative images from Columbus software (Acapella) of the ovarian cell line 1847 treated with a range of concentrations of the compound B11. The compound induced phenotypic changes in a dose responsive manner for the 3 phenotypic endpoints: induction of PCC (detected by Columbus and outlined in red), reduction of cell number (DAPI-stained cells in blue) and Increase in mitotic cell number (pHH3 Ser10-stained cells in green).

3.2.1.9 Secondary validation of PCC hits using individual dose response curve for each compound

The 8 remaining CC were supplied as a powder and diluted in 100% DMSO to a final stock concentration of 10mM. Additional validations for these 8 potential CC hits were executed using dose-responses with similar concentrations to those previously described at the first paragraph in the previous Section 3.2.1.8. However initial results showed that the previous dilution response curves for these CC was not effective enough to define or confirm the possibility of CC hits for increasing PCC. Therefore, to improve the effectiveness of the experiment, the specific range of concentrations for each individual CC hit was optimized before performing the secondary validation (Data not shown).

Next, the secondary validation for the remaining 8 CC was performed in duplicate using the optimal range of concentrations for each individual CC. The results indicated that 4 CC hits were confirmed, two of which clearly induced the highest %PCC. These were B11 (MP74-75; Leeds University code: LDS-016186) (20.64%) and F5 (MP59-241; Leeds University code: LDS-015654) (12.14%) at 5µM and 2.5µM, respectively (Figure 3.13 A and B). Two other CC, F7 (MP59-241; Leeds University code: LDS-015656) and G11 (MP74-75; Leeds University code: LDS-016246), induced a lower increase in %PCC (7.70%) and (3.63%) at 40µM and 10µM, respectively, and were considered to be weaker hits (Figure 3.13 C and D).

A

confidential

B11, LDS-016186

B

confidential

F5, LDS-015654
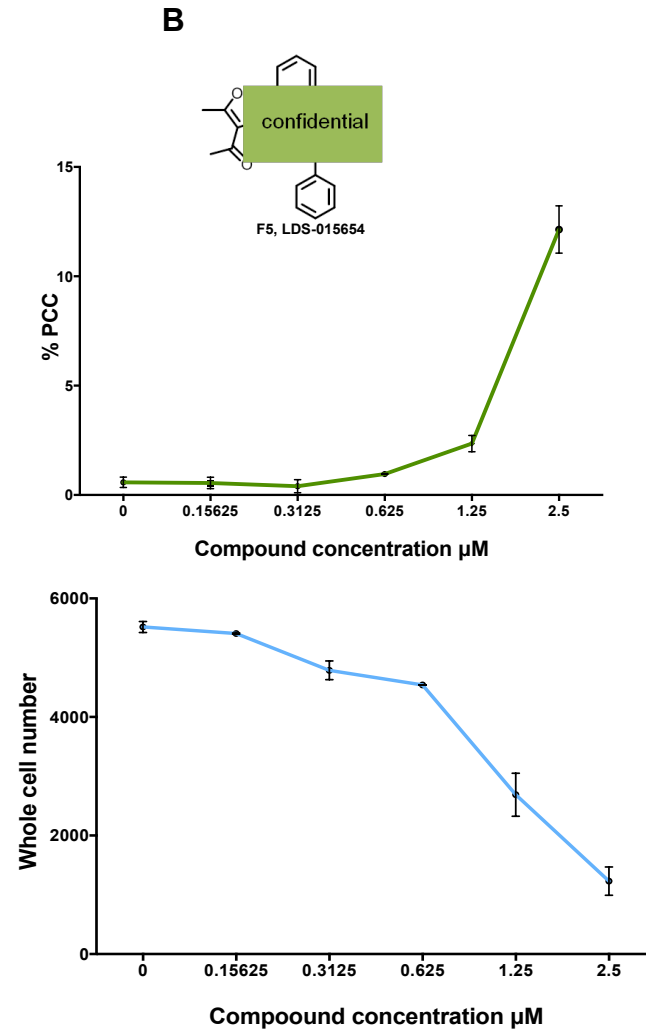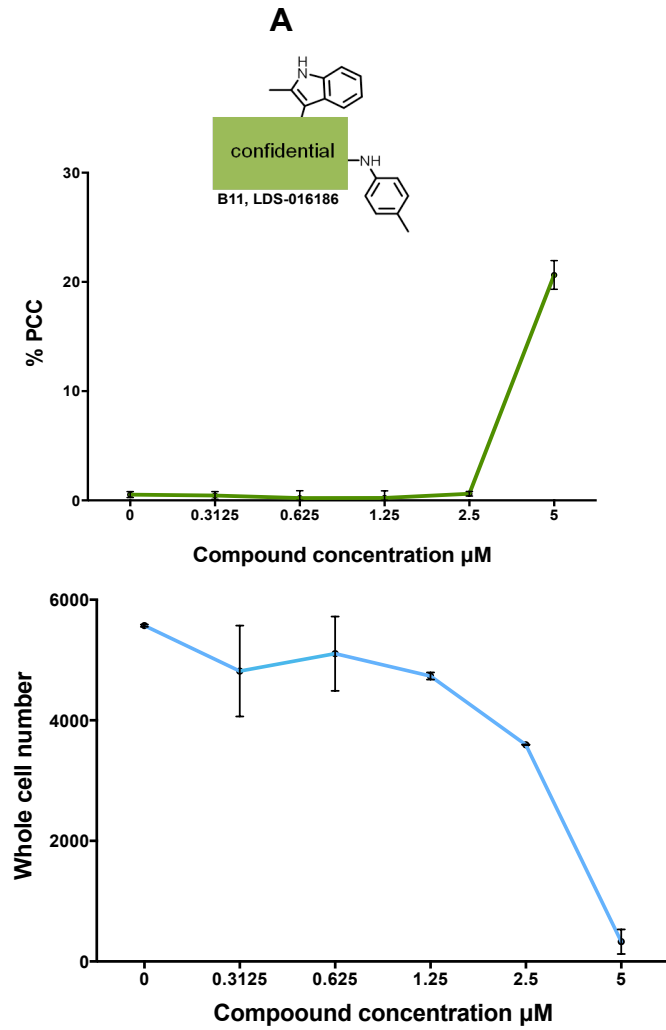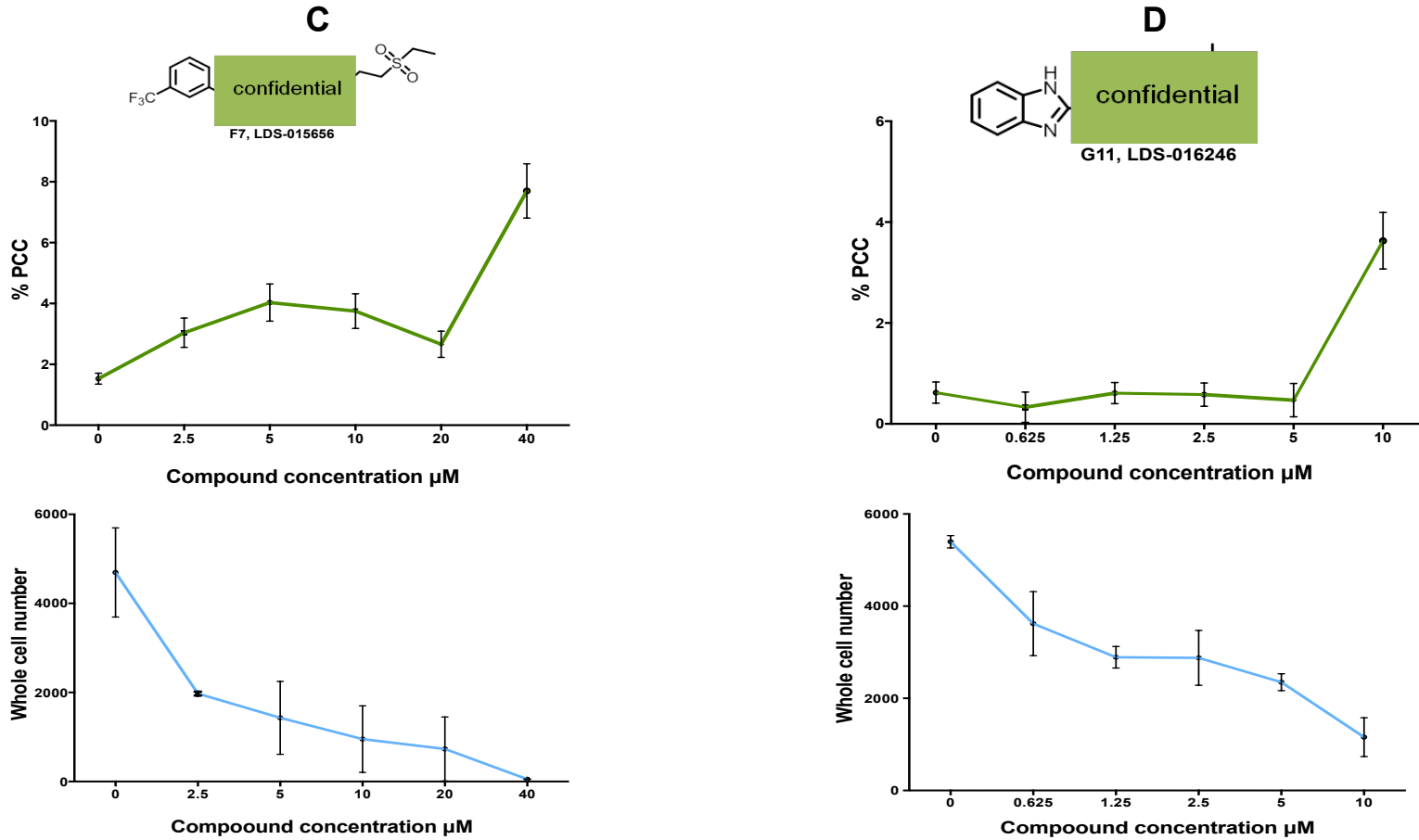
Figure 3.13. Secondary validating of the CC hits which induced PCC after 48hr.
Four of the 8 potential hits were confirmed by secondary validation for response of induction PCC and reduction in cell number. Two CCs, **(A)** B11 and **(B)** F5, induced elevated %PCC (20.64% and 12.14% at 5μM and 2.5μM, respectively) and were considered strong hits. Another 2 CCs, **(C)** F7 and **(D)** G11, induced lower increase in %PCC rate (7.70% and 3.63% at 40μM and 10μM, respectively) and were thus considered to be weaker hits.

3.3 Discussion

MCPH1/BRIT1 plays a vital role in regulating chromosome condensation. Specifically the *N*-terminal domain of hMCPH1/BRIT1 has been found to inhibit the action of condensin II by competing for its chromosomal binding sites *in vitro* (Yamashita *et al.*, 2011). However, MCPH1/BRIT1 deficiency, particularly in the pocket of the *N*-terminal BRCT domain, has been correlated with induction of the PCC phenotype, suggesting that this domain may be an essential part of protein-protein interaction, which regulates chromosome condensation (Richards *et al.*, 2010).

The aim of this study was the identification of CC that potentially target, or bind to the *N* -terminal pocket of MCPH1/BRIT1 and subsequently inhibit *N*-terminal activity thus inducing PCC. These would be ideal molecular tools for further cellular investigations of biological implications of MCPH1/BRIT1 in regulation of chromosome condensation in normal and cancerous cells. Also, the CC can be used as an inhibitor for confirming any novel cellular interactions with MCPH1/BRIT1. Thus, a library of 792 CC were selected from an original library of 33,000 compounds which, based on the 3D crystal structure of the *N*-terminal of MCPH1/BRIT1, were predicted to fit within the *N*-terminal pocket of MCPH1/BRIT1. The aim of this study was to test the selected 792 CC by performing SMS to identify CC inducing PCC using an automated high-content microscopy imaging system, Operetta, provides multi-channel imaging tools for imaging and measuring the desired phenotypic changes that could have been caused by the CC whilst the software Columbus offers a sophisticated phenotypic images and visualization of the whole 96 well-plate which simplifies the exclusion of plates with artefacts and analyses the images to convert them into quantitative data.

Indeed, using the Operetta system helped to assess three different parameters: detecting PCC, counting cell viability (cytotoxicity) and counting mitotic cells using the known mitotic marker pHH3 Ser10. However, the further evaluations of the 792 CC for the cytotoxic activity and increased mitotic cell number were not the principal aims of this study nor were they used as independent parameters in test screening. They were performed to provide further biological characterisation of compounds identified as potential hits for inducing PCC. Also, they also provided useful data about the cellular effects of these CC used in this screen to the library supplier.

The SMS was developed using an OVCA cell line 1847. This adherent cell line, which grows as a monolayer, has demonstrated from previous studies in our lab an efficient siRNA transfection at 75nM for targeting of *MCPH1/BRIT1* to induce the PCC phenotype, which was easily detected during image processing using the Operetta. A CC concentration of 20µM (containing 0.2% DMSO) was judged to be the appropriate strength for use in the primary small molecule inhibitor screen to induce PCC with low cell cytotoxicity in the selected OVCA 1847 cell line. Similar concentration 20µM (containing 0.2% DMSO) has been used in a HTS performed using U2OS cell line for identification of cytotoxic compounds (Martin *et al.*, 2014). Additionally, the CC incubation period was set at 24hr and 48hr since the cellular and biological effects of these new CC were unknown and this allowed for a comprehensive characterisation of all changes to phenotypes for each of the CC being tested at two different time points. Additionally, incubating the CC at 48hr was essential since *MCPH1/BRIT1* siRNA experimentally needs 24 to 48 hours to trigger (10%-20%) PCC in 1847 or U2OS cell lines.

In contrast, other studies have used drug-inducing PCC phenotypes such as Okadaic acid (OA) and Calyculin A (Cal A) inhibitors (Gotoh *et al.*, 1995). Cal A, in particular, at 50nM concentration and 3hr incubation in somatic cells are required to induce 20% PCC. In addition, PCC can be induced by 0.5µM of OA in less than 3hr using myeloid leukaemia cell lines HL-60 and U937 (Ishida *et al.*, 1992). However, the CC in the present study are structurally different since they were selected for their predicted ability to fit into the *N*-terminal pocket of MCPH1/BRIT1 (which is required for normal chromosome condensation) and therefore 20µM of CC concentration and 24hr to 48hr incubation would be appropriate and sufficient to induce PCC.

The reliability of the positive control *MCPH1/BRIT1* siRNA for inducing PCC compared to NT-siRNA was previously confirmed in HeLa and U2OS cell lines (Trimborn *et al.*, 2004; Trimborn *et al.*, 2006; Adams *et al.*, 2014). Although the positive control significantly induced an elevated level of PCC (from 8%-15%) compared to DMSO (≤ 1%) for both replicates and at the two exposure times, it significantly decreased the cell number to between 400-961 cells, in comparison to DMSO (between 1800-3650 cells) for both time points. This reduction in cell number can be explained as MCPH1/BRIT1 functions in cell apoptosis by interaction with E2F1. This interaction is responsible for activation genes involved in DNA damage response and apoptosis including BRCA1, CHK1, p73, TP53, caspases 3 and 7. Inhibition of MCPH1/BRIT1 has showed to reduce the activity of p73 in DNA repair or E2F1-dependent apoptosis (Yang *et al.*, 2008; Venkatesh *et*

al., 2013). This might contribute in decreasing genomic integrity thus other pro-apoptotic regulator proteins, such as BAX or BAK, may be activated which lead to reduce cell viability.

Since the positive control wells reflected variation in %PCC and cell number across all tested plates at both batches and different time points, this would significantly impact on identification of the most efficient on-target effect and maximise off-target effect. Thus, in this study the negative control 0.2% DMSO was used as a reference for Z or Robust Z scores to statistically evaluate the diverse cellular effects of CC. Since this screen used a reasonably low concentration of CCs (20µM) it is acceptable to use the cut-off scores of +2 for identifying CC hits that increase PCC /or mitotic index/pHH3 Ser10 expression and ≤ -2 for CC hits that reduce cell number (cytotoxicity) as these cut-off scores produced statistically significant *p* values at 0.0455 (Martin *et al.*, 2014).

The Z or Robust Z scores calculations for CC inducing PCC revealed there were potentially 17 and 27 hits after 24 and 48hrs, respectively. It was noted that the effect of the CC potentially inducing PCC differed for the two time points (Table 3.1 A and B). Interesting induction of PCC by some CC was correlated with reduced cell number (Table 3.2 A and B) or increased %mitotic cells/pHH3 Ser10 expression (Table 3.3 A and B), indicating that the CC were inducing similar cellular effects to those seen with the positive control *MCPH1/BRIT1* siRNA. Other CC hits, included in the hit lists at 24hr and 48hr, and identified to potentially induce PCC, did not show significant effect on cell number or mitotic index. This suggested that the diversity in the structure of these CC hits, which might influence their cellular and biological reactions. The reduction in cell number or increased mitotic cells expressing pHH3 Ser10, which accompanied PCC induction by some CC might be similar to the effects of the known PCC inducer compounds such as Cal A or OA in fibroblast and tumour cell lines. (Kanda *et al.*, 1999; Ishida *et al.*, 1992; Alsbeih and Raaphorst, 1998; Huang *et al.*, 2006). Expression of pHH3 Ser10 is considered to be a significant marker for chromatin condensation in mitosis and may be a causative factor for PCC induction (Huang *et al.*, 2006; Hendzel *et al.*, 1997; Sauvé *et al.*, 1999).

The primary validation for CC inducing PCC was conducted using the dose response curve method as previously mentioned in sections 3.2.1.8 and 3.2.1.9. Consequently, 8 CC were validated at 48hr including MP59-241/wells F5 and F7; MP64-65/well F7; MP66-67/well C1; MP74-75/wells B11 and G11; and MP76-77 wells E3 and G3 (Figure 3.11). Thus, this finding, in turn, may possibly confirm the

alignment in inducing PCC phenotype after approximately 48hr between the CC hits that were validated after 48hr and *MCPH1/BRIT1* siRNA.

The differences in the cellular morphology of PCC phenotype between the *MCPH1/BRIT1* siRNA positive control and the potential CC hits were expected. However, in this study, it was not possible to perform additional analysis to investigate these differences. Therefore, the visual inspection was carried out using Columbus with the support from Dr. Sandra Bell to ensure PCC cells that were detected by Columbus are real. The phenotypic differences of siRNA and CC may occur due the fact that small molecule inhibitor targets protein that may be continuously active as a scaffold, however, the siRNA would disrupt this whole protein-protein interaction. For instance, if the physical enzymatic activity of the scaffold is important for the biological function of the target protein, then siRNA can inhibit both functions while the small molecule inhibitor inhibits only the target protein (Weiss *et al.*, 2007). Moreover, since the primary screen was set with robust negative and positive controls for the compound or for siRNA in which the off-target effect can be assessed, the resulting biological phenotypes of both siRNA and the small molecule inhibitor are independently acceptable and they are not due to off-target effect (Weiss *et al.*, 2007).

In the secondary validation four CC hits displayed PCC at 48hr. The two strongest CC that induced the highest %PCC at lower concentrations are F5 (12.14%) (MP59-MP241) and B11 (20.64%) (MP74-MP75). Whereas G11 (MP74-MP75) and F7 (MP59-MP241) induced lower levels of PCC at very high concentration, leading these hits to be considered as weak CC hits. Obviously, the validated four CC hits induced higher or lower levels of PCC at different concentrations, which indicated that their chemical structures are not similar thus their biological reactions in inducing PCC were expected to be dissimilar.

Overall, a high throughput assay was developed and performed in duplicate to identify small molecules which induce PCC using the 1847 cell line. A secondary validation screen using dose response curves has revealed four potential CCs. Further experiments are warranted to confirm the fit of these validated CC hits in the *N*-terminal pocket of MCPH1/BRIT1. Additional analyses are required to confirm the cytotoxicity effect of these CC which could eventually allow for development of small molecule sensitizer that could promote the effect of existence chemotherapy for breast and ovarian cancer patients with deficiency in MCPH1/BRIT1 function.

Chapter 4 Analysis of human protein kinase and ubiquitin siRNA sub-libraries for genes inducing PCC

4.1 Introduction

Research has investigated the function of MCPH1/BRIT1 in different cellular pathways (See Chapter 1: Section 1.1.6). Depletion of MCPH1/BRIT1 using siRNA leads to the production of cells with a phenotype called premature chromosome condensation (PCC) in G2 phase, which is a consequence of premature entry into mitosis before completing DNA replication. However, the mechanism underlining MCPH1/BRIT1 function in regulating chromosome condensation during the cell cycle has yet to be fully elucidated. Thus, we hypothesised that since MCPH1/BRIT1 depletion is associated with the cellular phenotype PCC this can be utilised in a high throughput imaging system combined with siRNA library knockdown to identify genes that exhibit a similar phenotype to PCC. The BioScreening Technology Group (BSTG) at the University of Leeds performed a Dharmacon siGENOME SMARTpool siRNA screens that targets the human protein kinase (hPK) and ubiquitin (Ubq) sub-libraries using induction of PCC as a phenotypic read out, using a high throughput/high content imaging system (Operetta and Columbus software analysis system).

Utilising the siRNA libraries that target subsets of genes is a powerful application, providing a direct and clearer understanding of the gene expression function for subsequent drug discoveries and novel target validation, especially in cancer. The involvement of MCPH1/BRIT1 deficiency in cancer progression indicates there is an urgent need to clearly identify the role of MCPH1/BRIT1 in different cellular pathways. Therefore, given the natural function of RNAi in suppressing gene expression and inhibiting protein synthesis, this is an effective tool for identifying the molecular and cellular changes involved in cancer initiation and progression may pave the way to developing more effective targeted cancer therapies that interfere with these molecular targets, killing cancer cells effectively and sparing normal cells.

This PhD thesis aimed to analyse the hPK and hUbq siRNA sub-libraries using visual and Z score statistical analysis to identify genes that induce PCC in cells with intact MCPH1/BRIT1 function. Identification of genes where knockdown of which causes PCC could facilitate the identification of novel pathways involved in the regulation of chromosomal condensation.

4.2 Results

4.2.1 Statistical analysis of hPK and hUbq siRNAs for hits inducing PCC

The hPK and hUbq siRNA sub-libraries were selected to identify any further gene regulator of DNA condensation together with MCPH1/BRIT1 in the cell cycle or DNA damage pathways.

4.2.1.1 High throughput screening assay development performed by the BSTG

The hPK or hUbq siRNA screens were individually performed in duplicate by the BSTG with the aim of identifying genes that induce PCC in U2OS cells in the presence of functional MCPH1/BRIT. In both screens, a U2OS osteosarcoma cell line was used due to its monolayer growth with a large cytoplasmic area facilitating detection of nuclei at high resolution (Martin *et al.*, 2014; Adams *et al.*, 2014; Ghosh *et al.*, 2005). U2OS cells of the appropriate density (6000 cells/well) were incubated with 720 siRNA pools, which were distributed in 9 plates (96 wells format), at a final concentration of 50nM. Each individual siRNA sub-library (hPK or hUbq) were transfected using a single reverse transfection (RT) for 72hr. These cells were then fixed with ice-cold methanol followed by DAPI nuclear staining. The images were then automatically captured using the PerkinElmer Operetta high-content imaging system. The images for the 96 wells were acquired using an appropriate single focal plane that was set at a suitable angle for displaying a large area of complete nuclei. By using a 20× objective lens, fifteen fields were selected for each well, it was expected that detection of about 500-600 complete nuclei per field would be sufficient to generate a reproducible PCC inducer assay.

BSTG developed an analysis protocol to detect both nuclei number and PCC cells and confirmed the transfection efficiency of high through hPK and hUbq siRNA screens, which will be detailed below.

4.2.1.1.1 Detection of DAPI stained nuclei

Nuclei numbers were identified as separate objects (Figure 4.1A). Cell number was calculated using the Columbus software system and a specific analysis protocol that automatically recognised the nucleus and counted the number of

nuclei in each field for each well in the plate. Thus, any incomplete nuclei located at the edge of the image were excluded from the analysis (highlighted in red; Figure 4.1A). Whole DAPI stained nuclei with a size greater than 100µm^2 were selected as objects (highlighted in green; Figure.4.1A). Nuclear number analysis protocol also included irregular bright DAPI nuclei. For example, cells undergoing mitosis or apoptosis (arrowhead; Figure 4.1A) but excluded cell debris.

Also, during image analysis, irregular overlapping nuclei were seen and detected as one object (examples highlighted with arrows; Figure 4.1A). Though, this was only seen in a few cells per field of view and more specifically in wells with untransfected cells that had an increased density. Consequently, this low detection rate of overlapping nuclei was considered acceptable for a high-throughput screen. Overall, the automated nuclear number analysis protocol was used as a surrogate for assessment of cell number in hPK and Ubq siRNA screens.

4.2.1.1.2 Determining transfection efficiency of high throughput siRNA screen

In order to confirm a high level of siRNA transfection in U2OS cells, a number of siRNA transfection efficiency controls were silenced in U2OS cells by RT. *PLK1* has an important role in cell proliferation (Elmehdawi *et al*., 2013) thus, using RT siRNA to suppress this significantly and consistently reduces cell number. It was therefore considered to be a reliable readout for transfection efficacy. Moreover, the BSTG also examined knockdown of inner centromere protein (*INCENP*) and Kinesin family member 11 (*KIF11*). Silencing these genes showed a similar phenotype to that seen with *PLK1* siRNA, with a significant decrease in cell number observed compared with a non-targeting siRNA (Figure 4.1B).

Furthermore, another siRNA control targeting *Cyclophilin B* was transfected into U2OS cells. This control was recommended by Dharmacon for more than 20 different cell lines (www.thermoscientificbio.com/resource-library). Following transfection alongside NT-siRNA, RNA was extracted to perform qRT-PCR. A 94% knockdown of *cyclophilin B* expression was detected compared to NT-siRNA, indication the suitability of U2OS cell line for obtaining sufficient siRNA transfection (Figure 4.1C).

Overall, siRNA knockdown of *PLK1*, *INCENP, KIF11* or *Cyclophilin B* provided a functional and visual assessment of cell number reduction or a quantitative assessment of siRNA transfection efficiency in U2OS cell line.
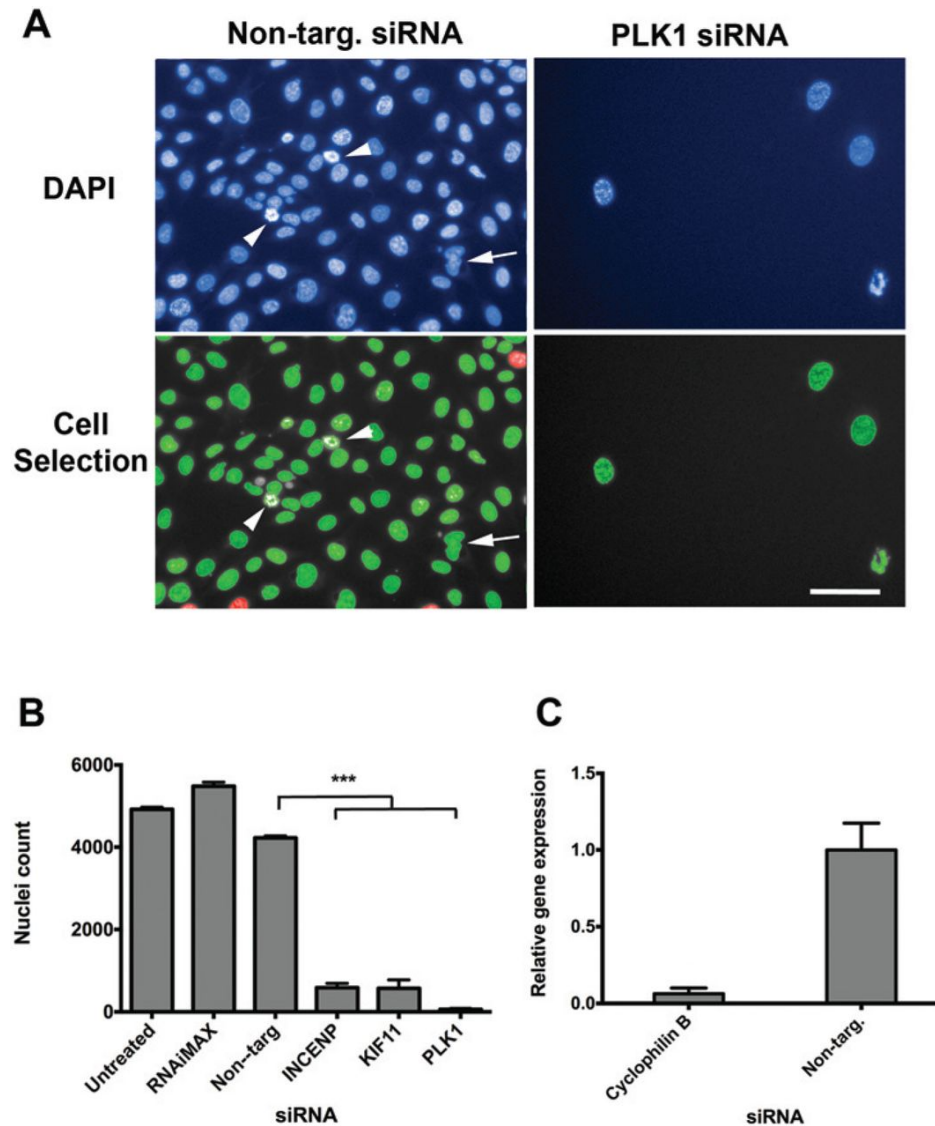
Figure 4.1. Detection of nuclei using Columbus and assessment of siRNA transfection efficiency.
(A) U2OS cells stained with DAPI (blue) were imaged using the fluorescence microscopy imaging system Operetta. Columbus software selected whole cells, which were highlighted in green compared to the border objects (incomplete cells) that were highlighted in red. *PLK1* siRNA caused a significant reduction in nuclei number compared with non-targeting siRNA. Arrow shows overlapping nuclei while arrowheads displays mitotic/apoptotic cells. **(B)** Graph presenting the siRNA RT of *PLK1, INCENP and KIF11*, which caused a significant reduction in cell number, compared with NT-siRNA (p < 0.01). **(C)** Graph showing the reverse siRNA transfection of *Cyclophilin B*, which caused a 94% reduction in mRNA level compared with non-targeting siRNA, demonstrating a quantitative evaluation of transfection efficiency. Source: Image is adapted from (Adams *et al.*, 2014).

4.2.1.1.3 Detection of DAPI stained PCC cells

MCPH1/BRIT1 siRNA was selected as an appropriate positive control since detection of PCC cells has previously been shown to provide a reliable readout of defective MCPH1/BRIT1 function in HeLa and U2OS cells (Adams *et al.*, 2014;

Trimborn *et al.*, 2004). Additionally, a quantitative analysis protocol had been optimized to detect the number of spots per DAPI stained nucleus in the U2OS cell line using Columbus software; thus, any nucleus with more than 14 spots was designated a PCC cell (Figure 4.2A; PCC cells highlighted in green) compared to the normal cell population (Figure 4.2A; highlighted in red).
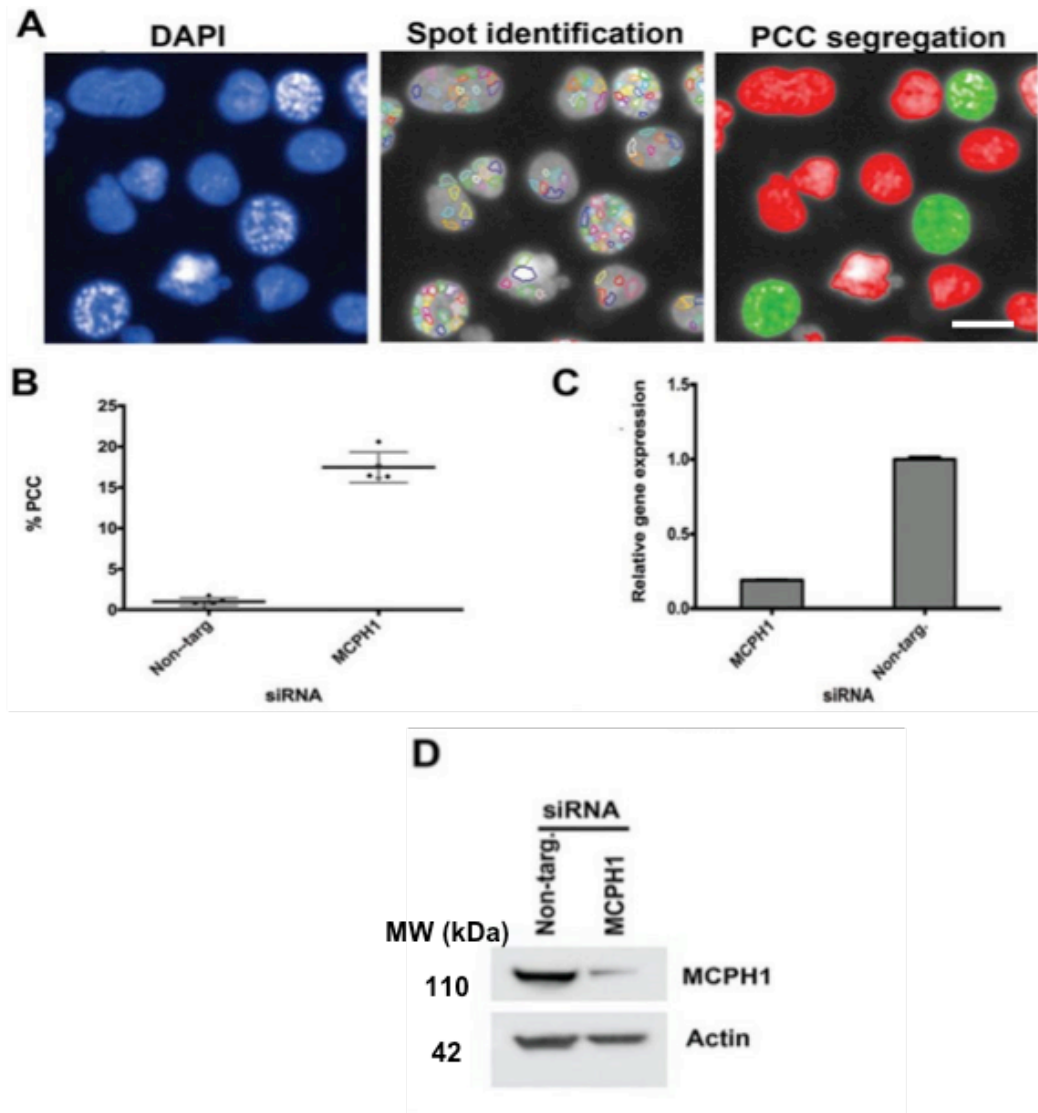
Figure 4.2. Detection of PCC and MCPH1/BRIT1 control validation.
(A) Images were taken from Columbus software. DAPI stained cells (blue): U2OS cells treated with *MCPH1/BRIT1* siRNA. Spot identification: the number of spots (highlighted by coloured outlines), for each DAPI stained cell, was identified by using modified "find spots" algorithm. PCC segregation: cells with greater than 14 spots were selected as PCC cells (green) compared to the normal cell population (red). **(B)** Graph to show that using different U2OS cell passage number did not reveal any significant difference in inducing % PCC by *MCPH1/BRIT1* siRNA ($p < 0.001$). **(C)** Confirming transfection efficiency of *MCPH1/BRIT1* siRNA at the mRNA level after 48hr in which *MCPH1/BRIT1* gene expression reduced to an 81% in compared with the non-targeting control. **(D)** Western blot image showing that *MCPH1/BRIT1* siRNA-treated U2OS cells reduced the protein expression of MCPH1/BRIT1 after a 72hr transfection. Source: Image is adapted from (Adams *et al.*, 2014).

Inducing PCC using siRNA knockdown of *MCPH1/BRIT1* has been repeated on 5 additional passages through a number of weeks examining different batches of each reagent. *MCPH1/BRIT1* siRNA induced PCC at a level of 15% to 20% of the total cell population. NT-siRNA showed a consistent level of PCC < 1%. The mean %PCC values of each passage are illustrated in (Figure 4.2B) ($p < 0.001$, Student t-test; n = 5). Different passage numbers did not reveal a significant difference in induced levels of PCC. Also, using different batches of reagent had no significant effect on induced levels of PCC. Thus, PCC cells were used as a functional readout for confirming MCPH1/BRIT1 knockdown in the hPK and hUbq siRNA screens. The transfection efficiency of *MCPH1/BRIT1* siRNA in U2OS cells was validated by the BSTG at both the mRNA and protein levels (Figure 4.2 C and D).

4.2.1.2 Image analysis to ensure fidelity of hPK and hUbq siRNA screening controls

Initially to identify PCC inducers from the hPK or hUbq siRNA screens, the reproducibility of the positive control (*MCPH1/BRIT1* siRNA) (n = 18 wells), negative control (NT-siRNA) (n = 36 wells) and transfection control (*PLK1* siRNA) (n =18 wells) in both replicates was assessed. An overall visual inspection was conducted across the screen replica plates of wells treated with controls or with a pool siRNA, to detect any artefact existing in any plate so that potential solutions for minimising such effects could be used, such as re-staining the plate with DAPI or re-scanning it using the Operetta. The efficiency of Columbus in correctly detecting cells with PCC was also evaluated.

Thereafter, the mean %PCC and cell number for each individual control were statistically assessed in both replicates for both siRNA sub-libraries. Since the function of MCPH1/BRIT1 is to regulate cell growth and apoptosis (Yang *et al.*, 2008; Mai *et al.*, 2014). The analysis conducted on the positive control in both replicates revealed that a RT of *MCPH1/BRIT1* (50nM) by siRNA caused a reasonable increase in %PCC accompanied by an expected reduction in cell number compared to the NT-siRNA in both batches as they illustrated in Figures 4.3 and 4.4 for both siRNA sub-libraries (hPK or Ubq) A and B or C and D, respectively. The mean cell number for the transfection control *PLK1* siRNA was also significantly lower at 92.89 and 114.1 in hPK siRNA screen while for the hUbq siRNA screen, it was 29.4 in the first batch and 52 in the second batch compared to the cell number for NT-siRNA, confirming successful siRNA transfection for the

entire screen in the first and the second batches for both siRNA sub-libraries ($p <$ 0.0001; Unpaired t test) (Figure 4.4).

Figure 4.3. Evaluation of the %PCC induced by controls used in hPK and hUbq siRNA screens in batch 1 and batch 2.
For the hPK siRNA screen, the %PCC induced by *MCPH1/BRIT1* siRNA was significant in both batches 1 and 2 (13%) and (15%) **(A and B),** respectively as opposed to NT-siRNA (p < 0.0001; Unpaired t-test). For the hUbq siRNA screen, the positive control was *MCPH1/BRIT1* siRNA (n = 18 wells), which induced a significant mean %PCC in batch 1 **(C)** and batch 2 **(D)** of (11%) and (14%), respectively, compared to the negative control NT-siRNA that had no effect on %PCC for either batches (n = 36 wells) (p < 0.0001; Unpaired t-test).

(hPK siRNA screen) A

B
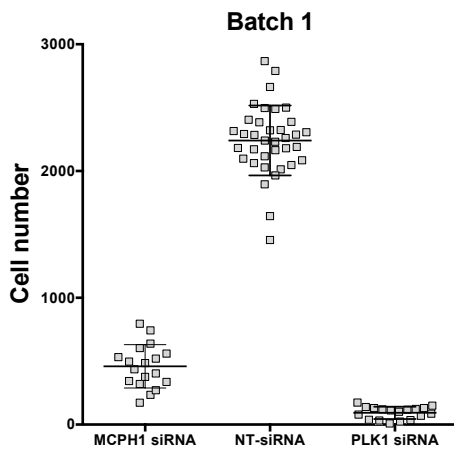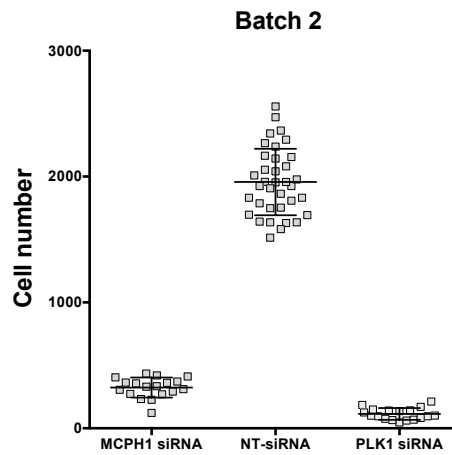
(hUbq siRNA screen) C
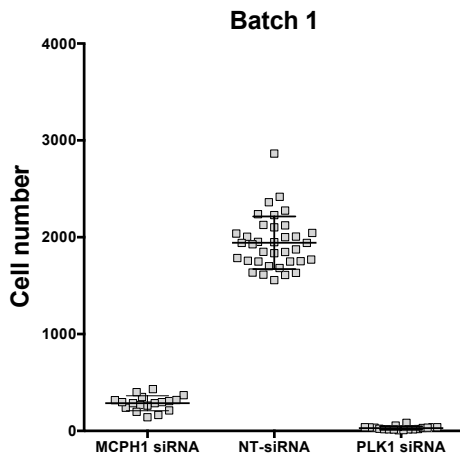
D
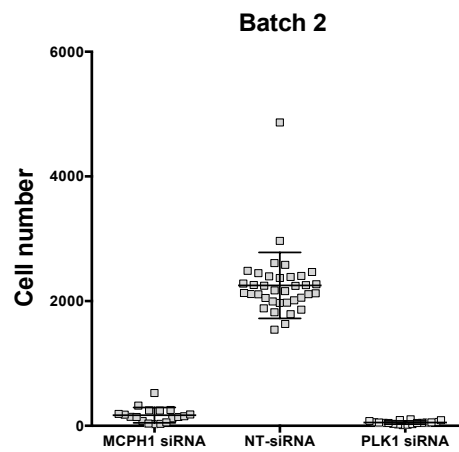
Figure 4.4. Evaluation of the cell number for the controls used in the hPK and hUbq siRNA screens in batches 1 and 2.

The positive control (*MCPH1/BRIT1* siRNA), in batches 1 and 2, significantly reduced the mean cell number to (459) **(A)** and (323) **(B)** compared to the negative control NT-siRNA (2241) **(A)** and (1957) **(B)**, respectively ($p < 0.0001$). *MCPH1/BRIT1* siRNA reduced significantly cell number in batches 1 **(C)** and 2 **(D)** (285.9) and (170.8), respectively, compared to the NT-siRNA at 1943 **(C)** and 2252 **(D)**. The transfection control *PLK1* siRNA in hPK and hUbq siRNA screens also displayed a significant reduction in cell number in both batches compared to NT-siRNA ($p < 0.0001$), confirming the siRNA transfection efficiency of the entire screens in both batches.

4.2.1.3 Validation of hPK siRNA screen reproducibility

As previously described, monitoring cell number by using the positive transfection control *PLK1* siRNA initially confirmed the high transfection efficiency using the screening procedures. However, the objective of the screen was to identify genes whose knockdown caused PCC. Thus, in order to assess the reproducibility of %PCC induced by hPK or hUbq siRNA screens in both replicates, a linear regression analysis was performed to determine if there was a significant positive

correlation between replicates 1 and 2 of the hPK or hUbq siRNA screens (r = 0.8391 (A)) or (r = 0.7986 (B)); *p* < 0.0001; n = 720) (Figure 4.5 A and B).
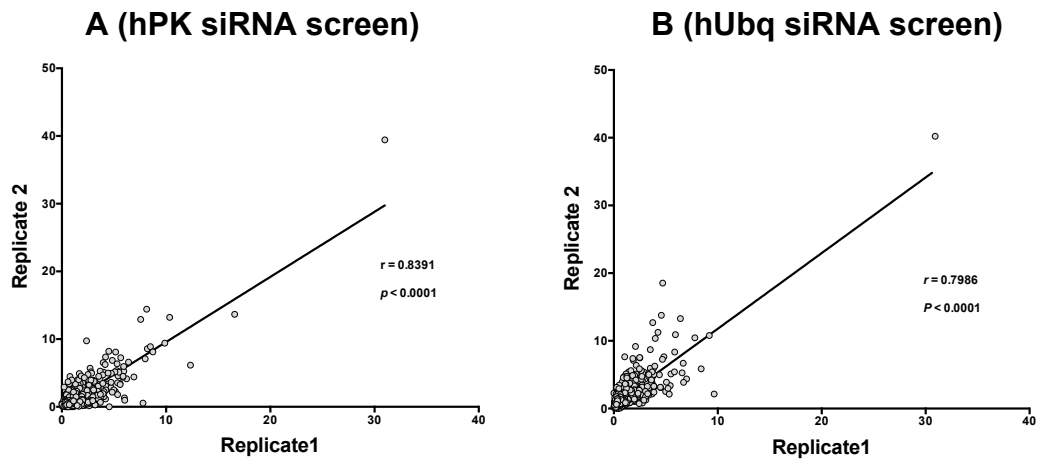
Figure 4.5. Linear regression plots representing the comparison of %PCC for the respective 720 siRNAs from the replica hPK and hUbq sub-libraries.
A strong significant correlation was identified between the two replicates of hPK **(A)** and hUbq **(B)** siRNA sub-libraries.

4.2.1.4 Analysis of hPK and hUbq siRNA screens for PCC hits identification

Different statistical methods were tested before performing the final analysis of the hPK siRNA screen in order to identify the most appropriate statistical protocol for identification of hits. Initially, the Z score analysis for hPK siRNA screen was performed using a comparison with the negative control NT-siRNA. This resulted in extremely high number of potential siRNA hits (104) that showed a Z score of ≥ 2 in both replicates. The scatter blots in (Figure 4.5 A and B) representing the Z scores - %PCC for 720 siRNAs from either the hPK or hUbq screens respectively in both replicates.

Thus, an attempt was made to use a more stringent control, which was the positive *MCPH1*/*BRIT1* siRNA control for Z score analysis of each plate individually in the hPK siRNA screen. The use of the positive control to calculate Z score for hPK siRNA screen showed only one siRNA hit which was *PLK1* and this gene may be considered as a false positive hit based on visual examination during imaging analysis that showed PLK1 depleted cells with fragmented nuclei, which are different to the morphology of PCC cells. Thus, the elevated %PCC observed in PLK1 depleted cells might be due to the experimental errors in the detection algorithm used which caused the false increased PCC.

A (hPK siRNA screen)
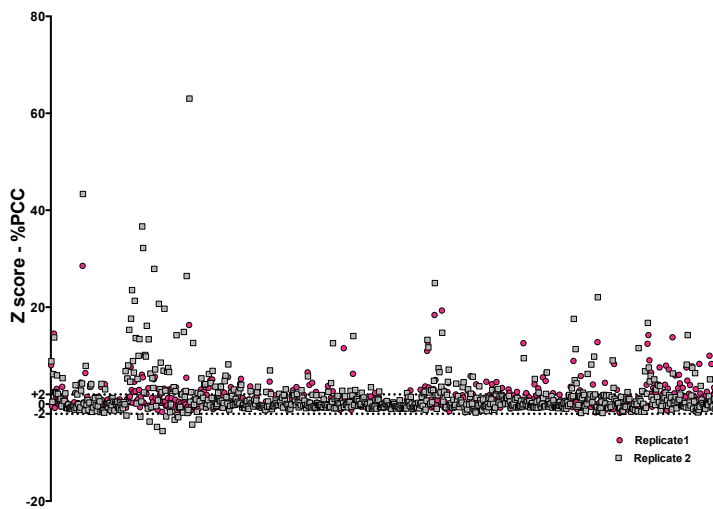
B (hUbq siRNA screen)
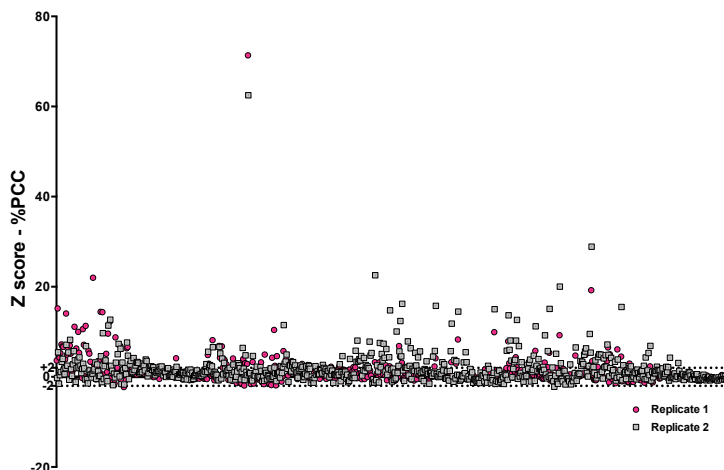
Figure 4.6. Scatter plots showing the distribution of Z scores -%PCC for 720 siRNAs from the hPK or hUbq screens.
The Z scores for each siRNA are shown as red circles in replicate 1 and grey squares in replicate 2. The Z score was calculated based on the negative controls NT-siRNA (mean %PCC) in each plate individually. Thus, siRNAs from both replicates showing an average Z score ≥ 2 are designated as hits.

Next, since the %PCC induced by the positive controls *MCPH1/BRIT1* knockdown revealed variation in %PCC between plates in both batches potentially causing an inaccurate Z score analysis, the mean %PCC (SD) produced by the positive controls was instead calculated individually for each batch (n = 18 wells/batch). The mean %PCC (SD) of each batch was then used as a main reference when calculating the %PCC Z score to ensure the correct identification of siRNA hits. However, the Z score batch analysis using the positive control did not demonstrate a significant improvement in the identification of siRNA hits, again only identifying one siRNA hit *PLK1*.

Lastly, a decision was made to select a small number of potential hPK siRNA hits for validation by using the hPK siRNA hit list, (CDK1/CDC2; TTK/MPS1; CAMK2N1 and WEE1), which was generated based on the negative NT-siRNA control alongside %PCC values of these potential siRNA hits. Utilising %PCC for hits selection was required to distinguish between siRNA hits with lower or higher %PCC (See below Table 4.1).

Similarly, the Z score statistical analysis for %PCC and cell number of the hUbq siRNA screen were performed for each plate individually in batch 1 and batch 2 using the negative control NT-siRNA. Consequently, only 33 siRNAs showed a Z score %PCC ≥ 2 and these were identified as hits that might potentially induce PCC. The siRNA hit FBXO5/EMI1 was selected from hUbq sub-library for further validation (See below Table 4.2).

In addition, since *MCPH1*/*BRIT1* siRNA greatly decreased the cell number, it proved to be of little practical use as a control for calculating the Z score-cell number in attempting to identify siRNAs with a significant reduction in cell number in hPK or hUbq siRNA screen. Therefore, the mean cell number of wells treated with NT-siRNA was used as a control in each plate individually to calculate the Z score-cell number, since these had no effect on cell number. Consequently, any siRNA hits producing a Z score cut-off ≤ -2 and causing noticeable cell death in both replicates were highlighted during the hit analysis procedure. In addition to reducing the identification of false negative hits, this method also provides further annotation for the phenotypic effect of the potential PCC inducer siRNA hits. For instance, an increase in the %PCC for some siRNA hits was accompanied by a reduction in cell number, while other siRNAs had no effect on cell number (See below Tables 4.1 and 4.2).

4.2.1.5 Validation of selected hPK siRNA hits using four deconvoluted ON-TARGET *plus* siRNAs

As previously mentioned that only 4 siRNAs from the hPK sub-library (CDK1/CDC2; TTK/MPS1; CAMK2N1 and WEE1) were selected for validation as potential PCC inducer hits, based on their %PCC (≥ 8%) and Z scores (≥ 2) (Table 4.1).

Table 4.1. A list of 104 siRNA hits generated from hPK siRNA screen in batches 1 and 2 based on the negative control NT- siRNA.

Potential siRNA hits showed a Z score of ≥ 2 in both replicates. Average %PCC of potential siRNA hits was ranked in descending order. The highlighted siRNA hits were selected for validation.

Human protein kinase siRNA screen name	Well name	Batch1				Batch2				Average				Gene symbol
		Cell number	%PCC	Z score-cell number	Z score-%PCC	Cell number	%PCC	Z score-cell number	Z score-%PCC	Cell number	Z score-cell number	%PCC	Z score-%PCC	
PK1	C6	95	31.0	-5.8	28.5	115	39.4	-7.9	43.4	105	-6.9	35.2	35.9	PLK1
PK1	D2	549	16.6	-4.6	14.5	749	13.7	-5.2	13.8	649	-4.9	15.1	14.2	CDC2
PK2	F10	1093	10.3	-1.6	16.3	1429	13.2	-1.7	63.0	1261	-1.6	11.8	39.7	CAMK2N
PK6	G3	1122	8.1	-3.6	18.4	814	14.4	-3.4	25.0	968	-3.5	11.3	21.7	CDK5R1
PK5	G2	766	7.6	-6.8	6.3	702	12.9	-10.4	14.1	734	-8.6	10.2	10.2	PRKY
PK1	A2	1121	9.9	-3.1	8.0	999	9.4	-4.1	8.9	1060	-3.6	9.6	8.4	TTK
PK7	G5	1017	12.3	-2.7	12.6	942	6.2	-6.0	9.5	980	-4.3	9.3	11.0	PFKL
PK6	G4	226	8.5	-5.8	19.3	55	8.9	-5.9	14.7	141	-5.8	8.7	17.0	WEE1
PK8	G5	1292	8.7	-3.6	12.8	838	8.1	-4.2	22.1	1065	-3.9	8.4	17.4	PCTK2
PK1	F6	2007	8.2	-0.7	6.4	1941	8.6	0.0	7.9	1974	-0.4	8.4	7.2	PHKG2
PK1	C2	1708	8.0	-1.5	6.2	1894	7.1	-0.2	6.2	1801	-0.9	7.5	6.2	ALS2CR2
PK7	H8	1062	6.9	-2.5	6.5	1062	6.9	-2.5	6.5	1062	-2.5	6.9	6.5	SRMS
PK6	G2	1596	5.2	-2.4	11.0	1003	8.1	-2.8	13.3	1300	-2.6	6.6	12.1	MAST2
PK8	E2	2113	6.4	-0.8	8.9	1548	6.6	-1.5	17.6	1831	-1.2	6.5	13.2	PTK9L
PK6	H2	1046	5.6	-3.8	12.2	755	7.3	-3.6	11.7	901	-3.7	6.5	12.0	TNK1
PK2	C4	946	4.5	-1.8	6.1	1117	8.2	-2.4	36.7	1032	-2.1	6.4	21.4	PFTK1
PK4	A10	888	2.4	-7.9	2.7	828	9.8	-4.9	12.6	858	-6.4	6.1	7.6	JAK2
PK3	H5	782	5.9	-8.1	5.6	720	6.0	-6.3	8.2	751	-7.2	5.9	6.9	PLK4
PK1	G2	1498	4.8	-2.1	3.2	1602	6.9	-1.5	5.9	1550	-1.8	5.9	4.5	ATM
PK1	E3	1526	5.3	-2.0	3.6	1395	6.4	-2.4	5.4	1461	-2.2	5.8	4.5	GRK5
PK2	D4	558	4.2	-2.5	5.5	520	7.4	-3.8	32.2	539	-3.2	5.8	18.9	MYLK2
PK1	B6	2057	5.8	-0.6	4.1	1244	5.4	-3.0	4.3	1651	-1.8	5.6	4.2	MASTL
PK1	D7	1877	5.9	-1.1	4.2	1705	5.3	-1.0	4.1	1791	-1.1	5.6	4.2	CRIM1
PK1	G8	1093	5.3	-3.2	3.6	1359	5.3	-2.5	4.2	1226	-2.8	5.3	3.9	MIDORI
PK3	G3	1292	5.5	-5.5	5.1	882	5.1	-5.6	6.9	1087	-5.5	5.3	6.0	STK22C
PK2	H5	477	4.0	-2.7	5.1	235	6.5	-4.5	27.9	356	-3.6	5.3	16.5	ADP-GK
PK2	C10	2396	4.2	0.7	5.5	1703	6.3	-1.0	26.4	2050	-0.1	5.2	16.0	AKT1
PK3	E5	2077	5.9	-1.6	5.5	1996	4.5	-0.2	5.9	2037	-0.9	5.2	5.7	FASTK
PK1	A6	930	6.2	-3.6	4.5	592	4.1	-5.9	2.8	761	-4.7	5.2	3.6	COASY
PK3	E11	1081	5.1	-6.6	4.7	669	5.2	-6.6	7.0	875	-6.6	5.1	5.8	PRKCL2
PK1	C9	1905	5.9	-1.0	4.1	2347	4.4	1.7	3.1	2126	0.4	5.1	3.6	MAP3K14
PK1	C7	1337	5.3	-2.5	3.6	1564	4.9	-1.6	3.7	1451	-2.1	5.1	3.6	MINK
PK2	G2	2271	5.4	0.5	7.6	1991	4.6	-0.3	17.6	2131	0.1	5.0	12.6	PRKCL1
PK4	F6	2416	4.8	1.5	6.6	2964	5.0	2.4	5.7	2690	1.9	4.9	6.2	DUSTYP
PK9	E2	1720	4.4	-3.3	12.5	1514	5.0	-3.9	16.8	1617	-3.6	4.7	14.6	AMHR2
PK1	C5	2499	4.0	0.6	2.4	2041	5.1	0.4	3.9	2270	0.5	4.6	3.1	ABL2
PK1	E5	1743	5.6	-1.4	3.9	1675	3.4	-1.2	2.0	1709	-1.3	4.5	2.9	UMPK
PK2	C3	1991	3.7	0.0	4.6	1748	5.3	-0.9	21.3	1870	-0.4	4.5	13.0	RPS6KB2
PK3	F7	1921	5.6	-2.3	5.2	2107	3.3	0.3	4.0	2014	-1.0	4.5	4.6	MKNK1
PK3	E3	1822	5.3	-2.8	4.9	1637	3.5	-2.0	4.4	1730	-2.4	4.4	4.7	PIP5K2A
PK3	C3	1783	3.9	-3.0	3.3	1667	4.7	-1.8	6.2	1725	-2.4	4.3	4.8	RELA
PK2	H2	1391	2.7	-1.0	2.9	1470	5.7	-1.6	23.5	1431	-1.3	4.2	13.2	TRIO
PK7	C7	2365	4.7	0.4	4.1	1766	3.6	-0.7	5.2	2066	-0.1	4.2	4.6	STK38
PK6	D4	2469	3.5	-0.3	6.9	2073	4.5	0.7	6.6	2271	0.2	4.0	6.8	RBKS
PK2	E6	1886	2.8	-0.2	3.1	1659	5.2	-1.1	20.7	1773	-0.6	4.0	11.9	EPHA10
PK3	G2	2065	4.5	-1.6	3.9	1781	3.4	-1.3	4.1	1923	-1.4	3.9	4.0	MAP3K12
PK2	C7	2199	2.9	0.4	3.2	2045	5.0	-0.2	19.7	2122	0.1	3.9	11.4	NEK4
PK3	C2	1049	3.7	-6.8	3.0	733	4.1	-6.3	5.3	891	-6.5	3.9	4.2	CSNK1E
PK3	E7	1756	4.7	-3.2	4.2	1781	2.9	-1.3	3.3	1769	-2.2	3.8	3.8	MPP1
PK9	F2	2217	5.0	-1.1	14.3	1777	2.5	-2.7	7.6	1997	-1.9	3.7	10.9	PASK
PK5	A3	1104	3.9	-5.1	2.7	1289	3.5	-5.7	2.9	1197	-5.4	3.7	2.8	AURKB
PK7	B2	1990	5.13	-0.46	4.56	1900	2.25	0.22	2.86	1945	-0.12	3.69	3.71	CDC2L5
PK3	H4	885	4.24	-7.59	3.68	546	3.06	-7.17	3.56	716	-7.38	3.65	3.64	KIAA0999
PK6	F5	2123	2.5	-1.1	4.33	1760	4.77	-0.33	7.12	1942	-0.72	3.64	5.73	PYCS
PK7	G8	1250	5.35	-2.12	4.79	1721	1.81	-0.94	2.12	1486	-1.53	3.58	3.46	FGFR4
PK9	H5	2429	4.83	-0.08	13.78	1866	2.17	-2.22	6.33	2148	-1.15	3.5	10.06	STK19
PK2	H8	2068	3.01	0.16	3.46	1723	3.93	-0.96	14.23	1896	-0.4	3.47	8.84	IRAK4
PK3	D5	2488	3.1	0.54	2.38	686	3.77	-6.5	4.73	1587	-2.98	3.43	3.56	PNKP
PK2	A6	1066	4.26	-1.62	5.64	1110	2.59	-2.41	7.16	1088	-2.02	3.42	6.4	EEF2K
PK2	D2	1935	4.02	-0.08	5.23	2074	2.75	-0.13	7.98	2005	-0.1	3.38	6.61	KIAA1811
PK3	H8	928	4.22	-7.38	3.66	767	2.48	-6.11	2.68	848	-6.74	3.35	3.17	MAPK3
PK2	B5	2260	2.91	0.5	3.29	1426	3.77	-1.66	13.37	1843	-0.58	3.34	8.33	MLCK
PK6	C4	2801	1.68	0.57	2.27	2064	4.92	0.66	7.39	2433	0.62	3.3	4.83	MAPKAP
PK2	H9	1171	2.5	-1.43	2.57	1000	4.06	-2.67	14.89	1086	-2.05	3.28	8.73	PCTK3
PK3	F2	3055	3.25	3.42	2.55	2694	3.31	3.11	4	2875	3.26	3.28	3.28	RPS6KA3
PK2	H4	1178	2.25	-1.42	2.12	604	4.3	-3.61	16.17	891	-2.51	3.28	9.15	ERK8
PK3	H9	1987	3.48	-2	2.81	1625	3.04	-2.01	3.58	1806	-2	3.26	3.2	YES1

Continued Table 4.1.

Human protein kinase siRNA screen name	Well name	Batch1				Batch2				Average				Gene symbol
		Cell number	%PCC	Z score-cell number	Z score-%PCC	Cell number	%PCC	Z score-cell number	Z score-%PCC	Cell number	Z score-cell number	%PCC	Z score-%PCC	
PK2	H3	2470	2.72	0.88	2.95	2308	3.78	0.42	13.43	2389	0.65	3.25	8.19	ETNK1
PK9	H7	1055	2.16	-6.38	4.86	1017	4.31	-6.33	14.25	1036	-6.35	3.23	9.56	GALK1
PK3	C6	2344	4.1	-0.19	3.53	1605	2.27	-2.1	2.35	1975	-1.15	3.19	2.94	TNK2
PK2	D3	1668	2.55	-0.55	2.66	1759	3.82	-0.88	13.64	1714	-0.71	3.19	8.15	PDK2
PK7	G7	1376	3.96	-1.84	3.25	1475	1.96	-2.54	2.37	1426	-2.19	2.96	2.81	CDK9
PK4	D9	514	3.01	-10.2	3.72	881	2.74	-4.74	2.55	698	-7.47	2.88	3.14	AURKA
PK9	G7	1384	2.97	-4.87	7.58	1003	2.66	-6.4	8.14	1194	-5.63	2.81	7.86	MYLK
PK6	H8	1409	1.62	-2.87	2.12	1293	3.99	-1.85	5.67	1351	-2.36	2.81	3.9	GCK
PK9	E8	932	3.04	-6.94	7.81	985	2.49	-6.48	7.51	959	-6.71	2.77	7.66	GALK2
PK9	H10	1803	3.69	-2.95	9.98	1771	1.84	-2.68	5.1	1787	-2.82	2.77	7.54	PRKACG
PK6	F3	2733	2	0.41	3.09	2331	1.53	1.53	4.81	2532	0.97	2.77	3.95	PANK2
PK2	F4	2480	2.3	0.89	2.21	2268	3.16	0.33	10.16	2374	0.61	2.73	6.19	CAMK2G
PK2	G4	2037	2.34	0.11	2.29	1505	3.1	-1.48	9.84	1771	-0.69	2.72	6.06	CKMT1B
PK3	F11	1857	3.24	-2.66	2.54	1641	2.11	-1.93	2.09	1749	-2.3	2.67	2.32	DGKQ
PK4	B5	1465	2.88	-4.35	3.51	1390	2.43	-3	2.11	1428	-3.68	2.65	2.81	CIB2
PK2	H7	1154	2.76	-1.46	3.01	967	2.49	-2.75	6.64	1061	-2.11	2.62	4.82	FGFR3
PK6	E5	1760	1.76	-2	2.48	1219	3.42	-2.09	4.61	1490	-2.05	2.59	3.54	STK22B
PK6	F8	2443	3.09	-0.31	5.81	2372	2.08	1.67	2.14	2408	0.68	2.59	3.97	TEC
PK9	G2	1395	3.41	-4.82	9.04	1422	1.72	-4.37	4.67	1409	-4.6	2.57	6.85	EPHA4
PK2	G6	2670	2.2	1.23	2.04	2375	2.86	0.58	8.56	2523	0.91	2.53	5.3	TNNI3K
PK4	F4	2208	2.48	0.22	2.86	2611	2.49	1.16	2.2	2410	0.69	2.49	2.53	LOC91461
PK2	B3	1820	2.44	-0.28	2.45	1913	2.47	-0.51	6.51	1867	-0.4	2.45	4.48	ITPKC
PK6	E11	1744	2.42	-2.04	4.11	1387	2.48	-1.55	2.87	1566	-1.79	2.45	3.49	CDK10
PK6	F4	1657	2.01	-2.25	3.11	1624	2.87	-0.77	3.6	1641	-1.51	2.44	3.35	EPHA3
PK7	A2	1407	3.11	-1.77	2.31	1150	1.76	-4.64	2.03	1279	-3.21	2.43	2.17	RET
PK6	C8	2380	1.89	-0.47	2.79	1723	2.58	-0.45	3.05	2052	-0.46	2.23	2.92	SBK1
PK9	B4	1208	2.97	-5.68	7.57	1415	1.48	-4.4	3.76	1312	-5.04	2.22	5.67	FES
PK6	A3	1995	2.14	-1.42	3.43	2084	2.23	0.73	2.41	2040	-0.35	2.19	2.92	FLJ13052
PK6	A5	1640	1.91	-2.29	2.84	1464	2.32	-1.3	2.57	1552	-1.8	2.11	2.7	TJP2
PK9	D3	1885	2.01	-2.57	4.38	1885	2.01	-2.57	4.38	1885	-2.57	2.01	4.38	EFNB3
PK9	B2	1928	1.44	-2.38	2.45	1497	2.29	-4.01	6.79	1713	-3.19	1.86	4.62	PRKCA
PK9	H3	2830	1.91	1.76	4.04	2256	1.52	-0.34	3.93	2543	0.71	1.72	3.98	PRKWNK1
PK9	H2	1341	1.34	-5.07	2.12	2040	2.04	-1.38	5.84	1691	-3.22	1.69	3.98	NEK7
PK9	H4	1027	1.9	-6.51	4.01	1928	1.1	-1.92	2.36	1478	-4.22	1.5	3.18	TSKS
PK9	D2	1340	1.9	-5.07	4	1622	1.03	-3.4	2.13	1481	-4.24	1.47	3.07	PLK3
PK9	F9	1786	1.36	-3.03	2.21	1339	1.47	-4.77	3.76	1563	-3.9	1.42	2.99	CDK3
PK9	F3	2033	1.42	-1.89	2.4	2245	1.28	-0.39	3.06	2139	-1.14	1.35	2.73	HUS1

To reduce the off-target effect of the SMARTpool siRNA used in the primary screen targeting CDK1/CDC2, TTK1/MPS, CAMK2N1 and WEE1 individually, four deconvoluted duplex siRNAs were used for validating each siRNA hit. As usual, the positive control was *MCPH1/BRIT1* siRNA, with its corresponding NT-siRNA and *PLK1* siRNA used as controls.

Initially, U2OS cells treated with a RT of 50nM of either a control or the four deconvoluted duplex siRNAs targeting each siRNA hit. After 72hr the plate was fixed and developed for imaging using Operetta and analysed for visual and quantitate evaluation of PCC cell induction using Columbus. In this validation plate the positive control showed an average %PCC (SD) of 8.2% (3.5%) (n = 4 wells) compared to NT-siRNA 0.42% (0.18%) (n = 4 wells) (Figure 4.7A). The anticipated decrease in cell number was seen in cells treated with positive control (174) as opposed to the negative control (3045) (Figure 4.7B).

Then, the %PCC output of siRNA hits was assessed in comparison with the negative and positive controls. CDK1/CDC2, TTK/MPS1, CAMK2N1 and WEE1 did not show any increase in the PCC level at 50nM (Figure 4.7A). Thus, in order to maximise the %PCC induced by the siRNA hits, the validation was repeated for a

second time using a higher concentrations of siRNA 100nM (Figure 4.7A). Although again induction of an elevated level of PCC by these four selected siRNAs hits was not confirmed compared to the NT-siRNA, the positive control, which was used as a functional readout for PCC induction work effectively (Figure 4.7A). Similarly *PLK1* siRNA concentrations of both 50nM and 100nM significantly reduced the cell number to 25 and 87, respectively, confirming the efficiency of the siRNA transfection (Figure 4.7B).
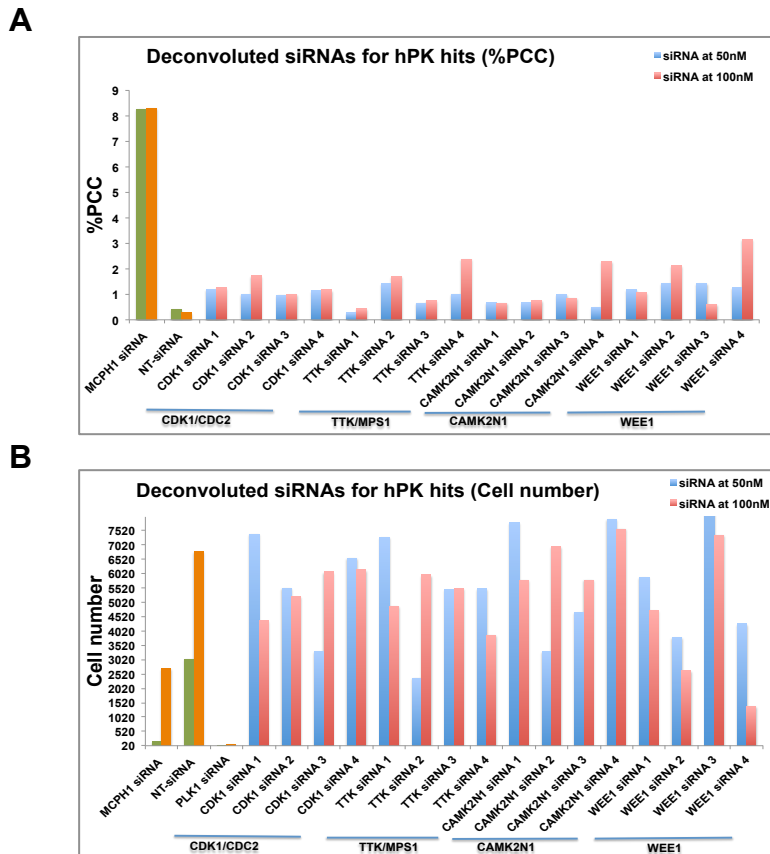
Figure 4.7. Validation test for four selected hits as potential PCC inducers from the hPK siRNA screen using four deconvoluted siRNAs.

For validation of siRNA hits, namely *CDK1/CDC2*; *TTK/MPS1*, *CAMK2N1* and *WEE,* U2OS cells were treated with controls; positive control *MCPH1/BRIT1* siRNA; negative control /NT-siRNA and *PLK1* siRNA (siRNA transfection control for reduced cell number). siRNA controls at 50nM illustrated with green bar and at 100nM with orange bar. Four deconvoluted duplex siRNA was used to target each hit at 50nM (Blue bar) and 100nM (Red bar). **(A)** Graph showing the low level of PCC induced by controls or the four individual siRNA for each hit; presenting no significant increase in the level of PCC compared to the negative or positive control for both siRNA concentrations and **(B)** no significant effect on cell number was caused by these four siRNA hits compared to the positive or negative controls**. (B)** *PLK1* siRNA significantly decreased cell number to 25 at 50nM and 87 at 100nM, indicating its suitability as indicator of the siRNA transfection efficiency.

It can be concluded that a single knockdown using low or high concentration of siRNAs targeting *CDK1/CDC2*; *TTK1/MPS1*, *CAMK2N1* and *WEE1* siRNA did not show an increase in PCC levels in U2OS cells.

4.2.1.6 Validation of selected hUbq siRNA hit using ON-TARGET *plus* deconvoluted siRNAs

Since *FBXO5/EMI1* siRNA was at the top of the hit list from the hUbq siRNA screen (Table 4.2), it was selected for validation as a potential PCC inducing gene.

Table 4.2. A list of 33 siRNA hits generated from Ubq siRNA screen in batches 1 and 2 based on the negative control NT- siRNA.

Potential siRNA hits showed a Z score of ≥ 2 in both replicates. Average %PCC of potential siRNA hits was ranked in descending order. The highlighted siRNA hit was selected for validation.

Human ubiquitin	Well name	Batch1 Cell number	%PCC	Z score-cell number	Z score-%PCC	Batch2 Cell number	%PCC	Z score-cell number	Z score-%PCC	Average Cell number	Z score-cell number	%PCC	Z score-%PCC	Gene symbol
2-1	F7	401	30.9	-5.2	71.3	383	40.2	-2.9	62.5	392	-4.1	35.6	66.9	FBXO5
3-1	F4	1169	4.7	-3.2	3.3	1371	18.5	-3.8	22.5	1270	-3.5	11.6	12.9	LOC644006
3-2	F10	1220	9.2	-2.3	9.9	1456	10.8	-1.6	15.0	1338	-2.0	10.0	12.5	TRIP
3-4	F3	1469	6.4	-2.5	19.2	1657	13.3	-1.6	28.9	1563	-2.0	9.8	24.1	DTX1
3-1	C8	2099	4.6	-0.3	3.1	2032	13.8	-1.5	16.2	2066	-0.9	9.2	9.7	RSPRY1
3-2	G5	796	7.8	-3.6	8.3	843	10.4	-2.8	14.5	820	-3.2	9.1	11.4	RNF44
3-1	A8	843	5.9	-4.3	4.5	1044	10.9	-4.9	12.4	944	-4.6	8.4	8.4	RNF32
3-2	G2	1132	4.2	-2.6	4.1	1261	11.3	-2.0	15.8	1197	-2.3	7.8	9.9	LMO6
2-2	D2	1706	4.0	-1.1	5.7	2616	10.4	0.2	11.5	2161	-0.4	7.2	8.6	LOC440456
3-1	H7	1869	8.4	-1.0	6.8	2082	5.9	-1.4	5.7	1976	-1.2	7.1	6.3	TRIM3
1-1	B9	989	5.9	-2.3	12.3	995	8.3	-2.0	12.7	992	-2.2	7.1	12.5	UBE2L3
1-1	B8	1752	6.7	-0.5	14.4	1566	6.7	-1.2	9.7	1659	-0.9	6.7	12.0	UBE2Z
1-1	H8	1224	4.8	-1.7	9.6	1453	7.6	-1.4	11.4	1339	-1.6	6.2	10.5	CUL4B
3-2	H4	1509	3.5	-1.5	3.3	1885	8.7	-0.7	11.8	1697	-1.1	6.1	7.5	TRIM55
3-1	C5	2415	4.7	0.7	3.2	3743	7.3	4.2	7.5	3079	2.5	6.0	5.4	PHF20L1
1-1	C3	1980	6.6	0.0	14.1	1970	5.3	-0.6	7.1	1975	-0.3	5.9	10.6	BIRC6
1-1	B2	1685	7.0	-0.7	15.2	1786	4.4	-0.9	5.5	1736	-0.8	5.7	10.3	HERC3
3-3	D9	549	5.5	-3.5	9.2	1052	5.4	-3.7	20.0	801	-3.6	5.6	14.6	RFWD3
1-1	H5	1858	5.5	-0.3	11.3	2030	5.1	-0.5	6.8	1944	-0.4	5.3	9.1	KIAA0317
1-1	H7	924	6.7	-2.4	14.4	1931	3.9	-0.7	4.6	1428	-1.5	5.3	9.5	DCUN1D4
1-1	G3	1422	3.8	-1.3	7.0	1477	5.9	-1.3	8.2	1450	-1.3	4.8	7.6	UBE2E3
2-1	H2	707	4.4	-4.4	8.2	904	5.0	-2.2	6.6	806	-3.3	4.7	7.4	FBXL16
3-4	F7	327	1.8	-6.7	4.5	284	7.4	-4.1	15.5	306	-5.4	4.6	10.0	RNF121
3-3	E2	1619	5.1	-1.1	7.9	1724	3.9	-2.1	13.7	1672	-1.6	4.5	10.8	WDR59
2-1	G3	2002	3.9	-0.8	6.9	2165	5.0	-0.6	6.7	2084	-0.7	4.4	6.8	FBXL20
2-2	G2	2067	2.9	-0.1	3.9	2530	5.4	0.1	4.9	2299	0.0	4.4	4.4	ASB18
1-1	E5	1786	5.2	-0.5	10.6	2322	3.0	-0.1	2.9	2054	-0.3	4.1	6.8	UBE2A
1-2	A8	2389	4.5	1.2	4.1	2479	3.2	-0.2	2.2	2434	0.5	3.8	3.2	WWP2
1-1	H9	1802	4.5	-0.4	8.8	2094	3.1	-0.4	3.2	1948	-0.4	3.8	6.0	UBE2L6
1-1	H4	2410	5.0	1.0	10.0	3245	2.5	1.3	2.1	2828	1.1	3.8	6.1	TIP120A
2-1	B11	1444	5.3	-2.3	10.4	2298	2.1	-0.5	2.1	1871	-1.4	3.7	6.2	CCNF
3-2	F2	1406	2.7	-1.8	2.3	1218	4.8	-2.1	5.8	1312	-1.9	3.7	4.0	LOC399937
2-1	H6	1993	2.4	-0.8	3.3	1800	4.9	-1.1	6.4	1897	-1.0	3.6	4.9	RAB40C

Based on the data from the hUbq siRNA screen that was originally performed by the BSTG, the *FBXO5/EMI1* siRNA showed the highest %PCC for all the siRNAs on the hit list. As shown in Table 4.2, %PCC for *FBXO5/EMI1* siRNA in the first batch was 30.92% with a Z score of 71.34 and 40.21% with a Z score of 62.92 in the second batch, presenting an average significant Z score of 66.92 for both batches.

Also, *FBXO5/EMI1* siRNA showed a low cell number for both batches, with 401 in the first and 383 in the second, with an average Z score of -4.06 for both batches.

To eliminate any off-target effect of the pooled siRNAs that were used in the original screen, 4 individual ON-TARGET *plus* deconvoluted siRNAs targeting *FBXO5*/*EMI1* were transfected into U2OS cells. The validation was initially performed individually at 2 different concentrations of 50nM and100nM. Similar positive and negative controls to those used in the primary hUbq siRNA screens were also included in the validation plate. Consequently, the validation experiments identified 2 individual *FBXO5*/*EMI1* siRNAs (2 and 4) showing a noticeable increase in %PCC compared to the remaining siRNAs and the NT-siRNA. The graphs in Figure 4.8 A and B show the %PCC and cell number for all 4 siRNAs targeting *FBXO5*/*EMI1* and for the controls in the validation plates at 50nM (Blue bar) and 100nM (Red bar).

For the plate at 50nM, the mean %PCC (SD) for the positive control *MCPH1*/*BRIT1* siRNA (50nM) was 8.27% (3.55%) (n = 4 wells) compared to the negative control NT-siRNA 0.42% (0.18%) (n = 4 wells). The %PCC induced by *FBXO5*/*EMI1* siRNAs 2 and 4 was 35.64% and 53.76%, respectively. In addition, these 2 siRNAs showed the lowest cell number values both in comparison with the remaining individual siRNAs (whether 1 or 3) and the negative NT-siRNA control. The mean cell number for the positive control was 174 compared to 3045 for its negative counterpart. The 2 selected *FBXO5*/*EMI1* siRNAs reduced cell number to 463 for *FBXO5*/*EMI1* siRNA 2 and 372 for *FBXO5/EMI1* siRNA 4.

For the plate at 100nM, the RT for all controls and the 4 individual duplex siRNAs was performed at 100nM. Subsequently, the RT siRNA for the positive control showed a reasonable mean %PCC (SD) 8.29% (4.34%) and a mean cell number of 2718 compared to %PCC of 0.27 (0.10%) and cell number of 6800 for the negative control (n = 4 wells). *PLK1* siRNA induced a sufficiently high cell death (mean cell number was 87 n = 2 wells), indicating an appropriate level of siRNA transfection. Similar to the results reported above for the plate at a siRNA concentration of 50nM *FBXO5*/*EMI1* siRNAs 2 and 4 displayed the highest %PCC at 100nM in comparison to the remaining siRNAs or controls. The %PCC induced by *FBXO5*/*EMI1* siRNAs 2 and 4 was 30.71% and 39.06%, respectively whilst the cell number value for *FBXO5*/*EMI1* siRNA 2 was 954 and 722 for *FBXO5*/*EMI1* siRNA 4.

A

Deconvoluted *FBXO5*/*EMI1* siRNAs (%PCC)

B

Deconvoluted *FBXO5*/*EMI1* siRNAs (Cell number)
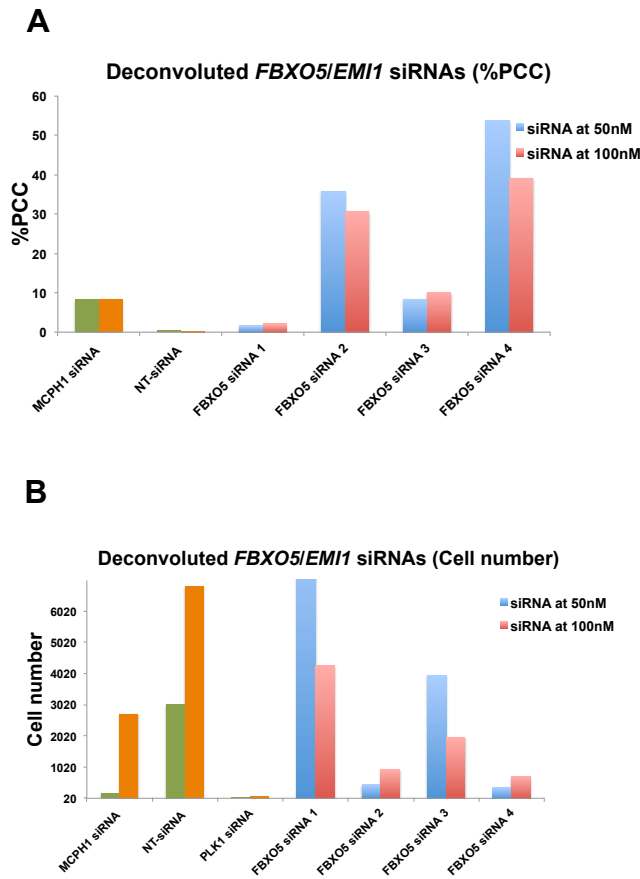
Figure 4.8. Validation of *FBXO5*/*EMI1* as a potential PCC inducing hit from the hUbq siRNA screen using four deconvoluted individual siRNA.
U2OS cells were treated with four individual *FBXO5*/*EMI1* siRNAs at 50nM (Blur bar) and 100nM (Red bar). *FBXO5*/*EMI1* siRNAs 2 and 4 displayed high %PCC **(A)** and reduced cell number **(B)** at both siRNA concentrations compared to the positive control *MCPH1/BRIT1* siRNA. The controls (*MCPH1/BRIT1*, NT and *PLK1* siRNAs) are exemplified at 50nm by a green bar and 100nm by an orange bar).

Image analysis of the two validation plates was performed using Columbus software. The analyses revealed that single siRNA knockdown of *FBXO5*/*EMI1* in cells with intact function of MCPH1/BRIT1 induced a specific cell phenotype with a large nucleus with condensed chromosomes which was slightly different to the one induced by *MCPH1/BRIT1* siRNA (PCC phenotype) (Figure 4.9). This lead to the investigation of whether *FBXO5*/*EMI1* siRNA induced the same large cell phenotype or had a different effect in the absence of *MCPH1/BRIT1*, which will be detailed below in Section 4.2.1.7.
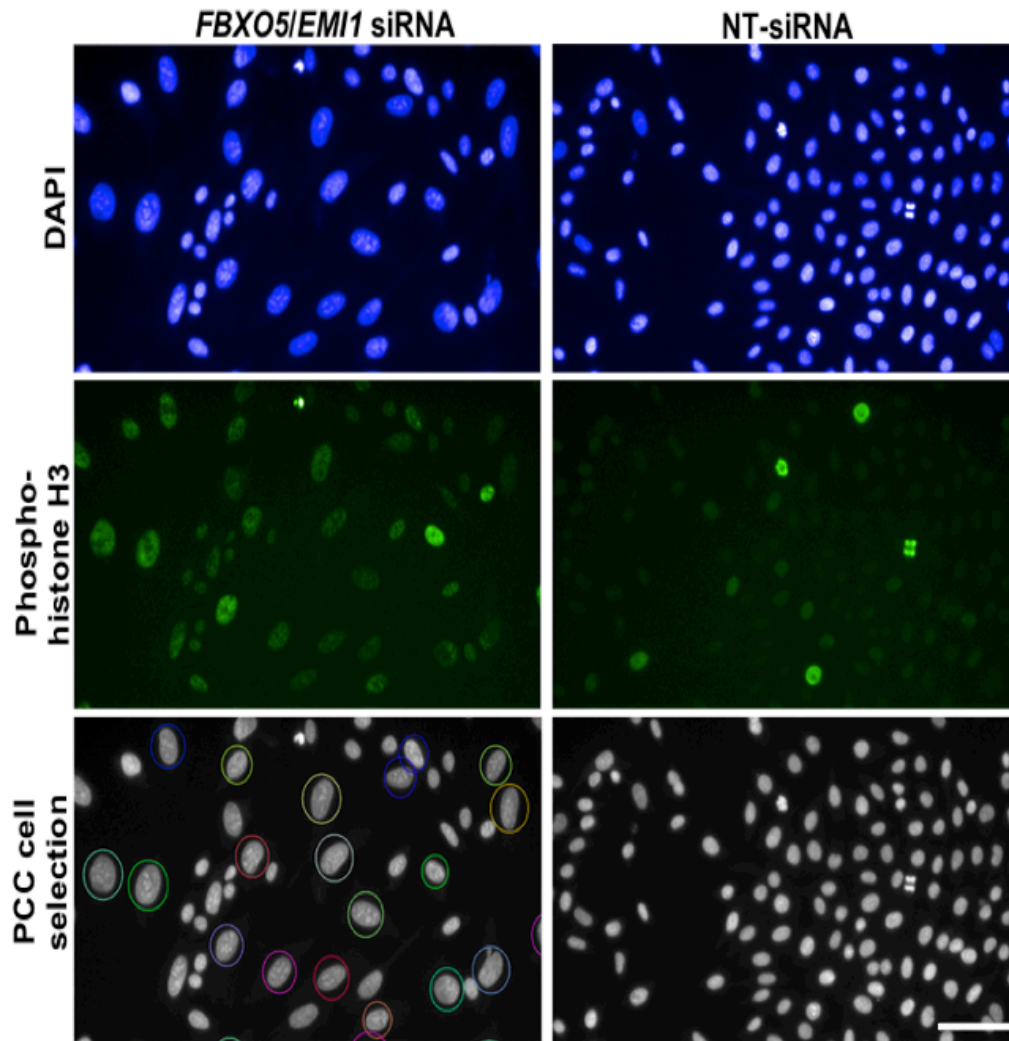
Figure 4.9. *FBXO5/EMI1* **siRNA induced a phenotype with large nuclei and condensed chromosomes that was slightly different to the MCPH1/BRIT1 knockdown PCC phenotype**.
U2OS cells treated with 50nM SMARTpool siRNA targeting *FBXO5/EMI1*, cells stained with DAPI (blue) and phospho-histone H3 cells (green). Cells were imaged using Operetta and analysed for PCC selection using Columbus software.

4.2.1.7 The effect of double siRNA knockdown of *FBXO5/EMI1* and *MCPH1/BRIT1* in inducing PCC phenotype

Dr Sandra Bell's group and the BSTG performed another Ubq siRNA screen aimed at identifying MCPH1/BRIT1 modifiers, genes that reduce or increase PCC in cells treated with *MCPH1/BRIT1* siRNA. Data from this PCC modifier Ubq siRNA screen was available. *FBXO5/EMI1* siRNA in combination with *MCPH1/BRIT1* siRNA showed a noticeable increase in %PCC compared to those observed in single knockdown in cells with functional MCPH1/BRIT1 (in the original PCC inducer Ubq siRNA screen; Table 4.2). The %PCC induced by double siRNA

knockdown of *FBXO5*/*EMI1* combined with *MCPH1*/*BRIT1* siRNA was similar in the first and the second replicate, thus mean of %PCC (SD) was 54.65% (0.35%) compared to the controls NT-*MCPH1*/*BRIT1* siRNA 11.5% (0.48) (n = 8 wells) or the aforementioned mean %PCC of single siRNA knockdown in (Table 4.2) which was 35.5% (6.5%).

A visual inspection for the wells containing *FBXO5/EMI1* siRNA was performed in the two replicates in the original PCC modifier Ubq siRNA screen using Columbus. This was to investigate the effect of *FBXO5/EMI1* siRNA in MCPH1/BRIT1 deficient cells on cell phenotype. In comparison to the cell phenotype characterised by cells with large nuclei that was induced by single siRNA knockdown of *FBXO5*/*EMI1* (as shown previously in Figure 4.9), double siRNA knockdown of *FBXO5*/*EMI1* and *MCPH1*/*BRIT1* induced a similar phenotype of large nuclear size with condensed chromosomes (Figure 4.10).
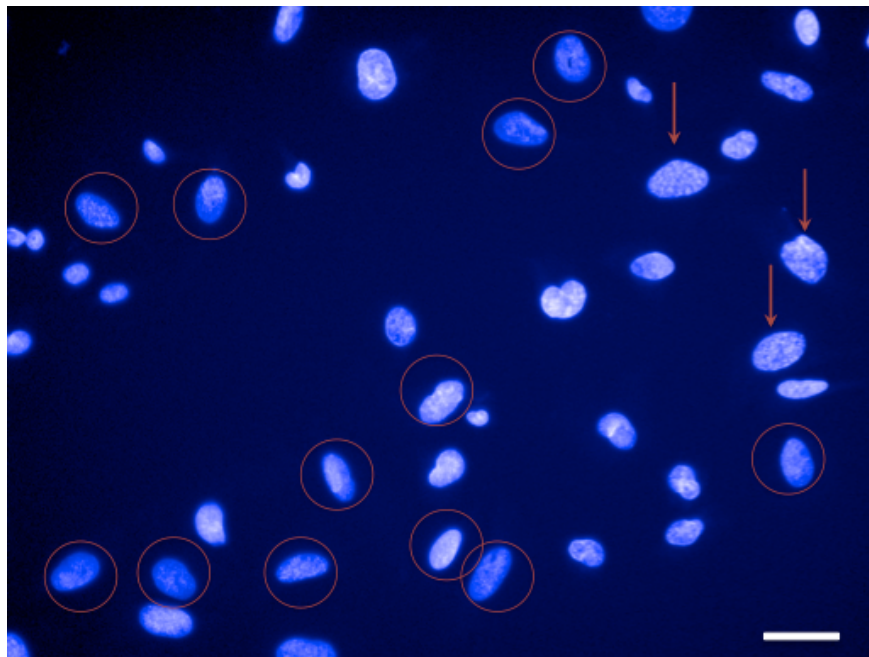
Figure 4.10. *FBXO5/EMI1* siRNA in combination with *MCPH1*/*BRIT1* siRNA induced a similar phenotype of large nuclei with condensed chromosomes to that observed in *FBXO5/EMI1* siRNA alone (as shown in Figure 4.9).
U2OS cells treated with 50nM SMARTpool siRNA targeting *FBXO5*/*EMI1* followed 24hr later by reverse transfection of 100nM *MCPH1*/*BRIT1* siRNA for 48hr. Cells were stained with DAPI (blue) and imaged using Operetta and analysed for PCC selection using Columbus software. Cell highlighted by red circle were the typical phenotype (cells with large nuclei) induced by *FBXO5*/*EMI1 in MCPH1*/*BRIT1* deficient cells whereas arrows indicate the known PCC phenotype with condensed chromosomes (white dots) induced by *MCPH1*/*BRIT1* siRNA, spread among other large nuclei cells.

Additionally, the double siRNA knockdown showed a noticeable reduction in overall cell number and specifically in the number of PCC cells (with clearly

condensed chromosomes) that were observed in cells with *MCPH1*/*BRIT1* siRNA alone. The mean cell number for *FBXO5*/*EMI1* in combination with *MCPH1*/*BRIT1* siRNA was 446.5 (262) (cell number was 635 in the first replicate and 261 in the second replicate) compared to mean cell number 2753 (828) for the controls NT-*MCPH1*/*BRIT1* siRNA (cell number was 3339 (579) in the first replicate and 2168 (175) in the second replicate (n = 4 wells/replicate). This reduction in cell number was similar to that observed in *FBXO5*/*EMI1* siRNA alone in the original screen (as shown above in Table 4.2) showing a mean cell number of 392 (12.7).

4.2.1.8 Identification of *FBXO5*/*EMI1* siRNA transfection efficacy

In order to assess the effectiveness of the 4 deconvoluted siRNAs targeting *FBXO5*/*EMI1* at the mRNA level*,* qRT-PCR was performed and the results suggested that all 4 of the individual siRNAs that had mediated the inactivation of *FBXO5*/*EMI1* induced depleted levels of the corresponding mRNA transcript compared to NT-siRNA or untransfected U2OS cells (Figure 5.9A).

Before we examined the effect of the 4 deconvoluted siRNAs targeting *FBXO5*/*EMI1* on its protein level using western blotting (WB), optimization of an anti-FBXO5/EMI1 antibody was performed. A sample of untransfected U2OS cells was blotted using 2 different quantities of protein (40µg/µl and 80µg/µl) with an antibody dilution of 1:100. Bands at about 50kD, the expected size of the FBXO5/EMI1 protein, were seen at both protein concentrations. However, a stronger signal was observed for sample 1 (80µg/µl) (Figure 4.11B1) in comparison to that for sample 2 (40µg/µl) (Figure 4.11B2). As a result the decision was made to reduce the FBXO5/EMI1 antibody concentration to a 1:200 dilution in any further western blotting experiments.

Following this, western blot (Figure 4.11C) was performed to define the extent to which the 4 individual siRNA duplexes reduced the protein levels of FBXO5/EMI1. As anticipated, the effects of these 4 *FBXO5/EMI1* siRNA duplexes varied. The initial statistical analysis of the siRNA duplexes targeting *FBXO5*/*EMI1* showed a potential increase in %PCC and reduced cell number using duplexes 2 and 4 (See above Figure 4.8A). Here, the *FBXO5*/*EMI1* siRNAs (2, 3 and 4) were found to affect FBXO5/EMI1 protein levels as compared to *FBXO5*/*EMI1* siRNA 1 or the controls (as illustrated in (Figure 4.11C). However, based on the results of the qRT-PCR and western blot data, *FBXO5*/*EMI1* siRNAs 2 and 3 showed the most appreciable effect on levels of both mRNA transcript and protein.

A

B   **C**

Untransfected U2OS lysate
1. (80 µg/µl);
2. (40 µg/µl)

U2OS lysate treated with four individual siRNAs;
1. FBXO5 siRNA 1
2. FBXO5 siRNA 2
3. FBXO5 siRNA 3
4. FBXO5 siRNA 4
5. NT-siRNA
6. Untransfected cells
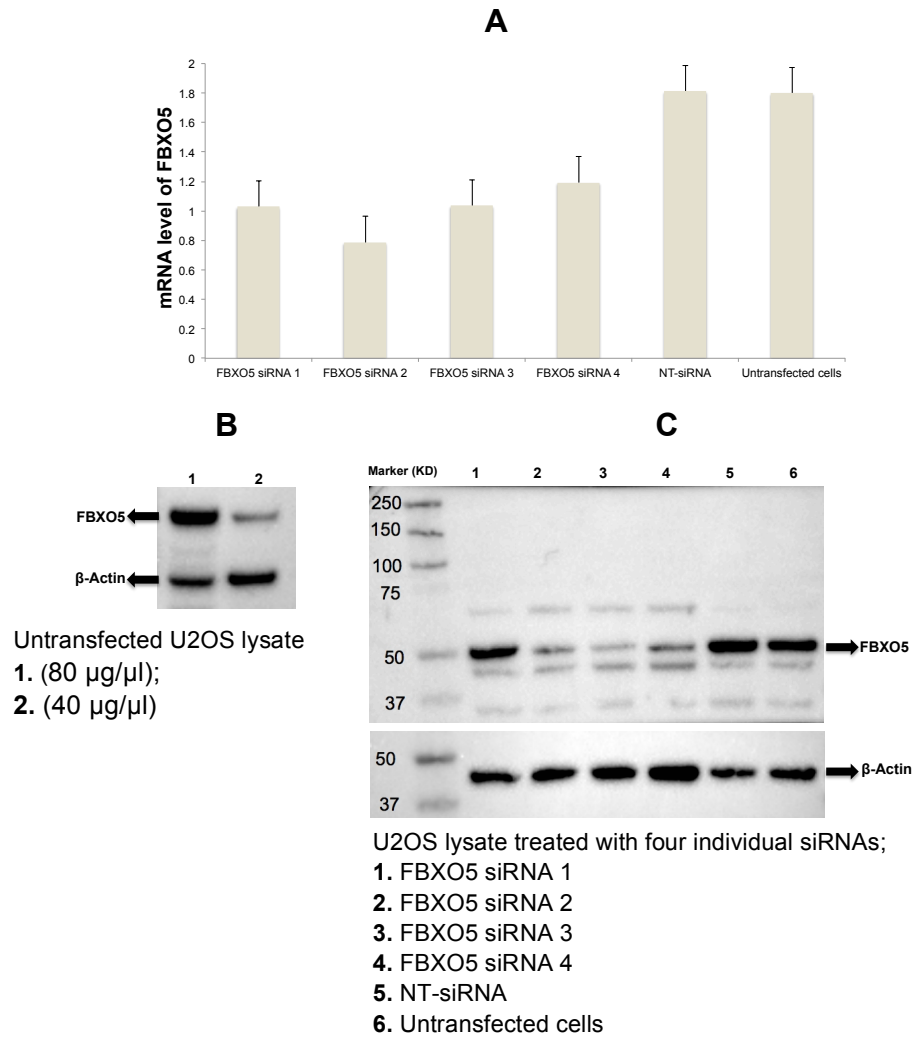
Figure 4.11. Confirmation of the efficacy of the 4 individual *FBXO5/EMI1* siRNAs using qRT-PCR and western blot (WB).
(A) Graph representing the effect of the 4 individual siRNAs on the mRNA level of FBXO5/EMI1. **(B)** WB optimization of the concentration of anti- FBXO5/EMI1 antibody at a dilution of 1:100 using untreated U2OS lysate with protein concentrations of 80µg/µl in **(B1)** and 40µg/µl in (**B2**). **(C)** WB evaluation of lysates from U2OS cells treated with a 50nM of 4 different siRNA duplexes targeting *FBXO5/EMI1* (samples from 1 to 4 in **(C)**), using NT-siRNA as a control (**C5**) and untransfected cells **(C6)**. Samples in **(C)** were probed with the anti-FBXO5/EMI1 antibody at a dilution of 1:200. Samples in **(B)** and **(C)** were counter-probed with a with the anti- β-Actin antibody (1:5000) as a loading control.

4.3 Discussion

Gene knockdown using siRNA enables functional screens to be conducted for the whole or part of the human genome in cultured cells. Defective MCPH1/BRIT1 is associated with abnormal phenotype known as PCC. The exact molecular and cellular mechanisms of MCPH1/BRIT1 function in regulation chromosome condensation in normal and cancer cells are poorly understood. Therefore, in this

study, 2 high throughput phenotypic-based hPK and hUbq siRNA screens were performed using Dharmacon siGENOME SMARTpool siRNAs by BSTG in order to identify genes inducing PCC; thus these screens are known as "PCC inducer screens". These 2 siRNA sub-libraries were examined and analysed using the Operetta fluorescence microscopy imaging system to detect the presence of PCC in U2OS cells with functional MCPH1/BRIT1. Columbus software was employed to convert the image data into numerical values to enable hit identification and subsequently to allow siRNA screen data to be shared between investigators working on similar projects.

One of the important factors in conducting a high throughput siRNA screen (HTS) is the accuracy and precision of the assay design and development (Goktug *et al.*, 2013). The BSTG performed the PCC inducer hPK and hUbq siRNA screens used in this study in a manner and using strategies that guarantee the production of high quality screening data. An evaluation of control quality and screen reproducibility merits further discussion.

First, the U2OS osteosarcoma cell line has previously been used in various siRNA screens (Adams *et al.*, 2014; Adamson *et al.*, 2012; Frankum *et al.*, 2015). Cells which grow at a sufficiently fast rate and display a consistent monolayer morphology during siRNA transfection are needed for an imaging system to detect nuclei at the necessary high resolution (Echeverri and Perrimon, 2006). Additionally, U2OS cells were also used to minimise financial costs and effort as 2 complementary siRNA screens were performed in tandem by the BSTG; the PCC inducer screen and a screen to identify genes that modified the PCC phenotype. Cell number data from both screens was combined to identify MCPH1/BRIT1 synthetic lethal genes (see Chapter 5).

Second, assessment of the quality of the assay controls, using strictly standardized mean difference (SSMD), is another parameter that is essential to ensure that a HTS is sufficiently robust, to minimise any batch specific or off-target effects and for adequate hit identification (Zhang, 2007; Birmingham *et al.*, 2009; Zhang, 2011). The main references in the PCC inducer hPK and hUbq siRNA screens were *MCPH1/BRIT1* siRNA (PCC positive control) (Leung *et al.*, 2011; Yamashita *et al.*, 2011; Frankum *et al.*, 2015; Trimborn *et al.*, 2004; Trimborn *et al.*, 2006; Adams *et al.*, 2014), which induced an elevated %PCC across the majority of plates in both batches compared to the NT-siRNA (PCC negative control) as previously illustrated in Section 4.2.1.2. The SSMD of the positive controls for %PCC in the first and the second batches was 3.85 4.33 for the hPK siRNA screen

and it was 3.6 and 4.9 for hUbq siRNA screen, respectively. These values indicate that the induction and increase in %PCC identified by the positive control wells was "very strong" compared with that for the negative control NT-siRNA wells, thus demonstrating the suitability of *MCPH1*/*BRIT1* siRNA as a positive control for increased PCC. Additionally, *PLK1* siRNA was used in these screens as a positive control for confirming siRNA transfection efficiency in each batch. The SSMD for the first and the second batches of *PLK1* siRNA was 7.69 and 6.87 for the hPK siRNA screen and it was 7.06 and 4.14 for the hUbq siRNA screen, respectively. Thus, based on the findings of the study by Zhang *et al*. (2007 and 2011) the SSMD values for *PLK1* have been classified as having an "extremely strong effect", meaning that *PLK1* siRNA can be considered to be a valid positive control for effects on cell number compared to control NT-siRNA.

Third, the significant positive correlation of the %PCC values produced by the siRNA samples (either from hPK or hUbq siRNA screens) between replicates 1 and 2, confirmed the assay reproducibility and the robustness of screens procedures (Section 4.2.1.3).

In this study, as the PCC inducer hPK and hUbq siRNA screens were performed in duplicate, the Z score calculation method for data normalisation and hit selection was used which mainly relies on using the negative control (NT-siRNA) and the cut-off Z score (%PCC) of ≥ 2 (Zhang, 1999; Douglas Zhang *et al.*, 2006; Birmingham *et al.*, 2009; Zhang, 2011; Goktug *et al.*, 2013). This method displayed (104) and (33) of potential siRNA hits from hPK and hUbq screens, respectively. For hPK siRNA screen, the overall false-negative rate was 5.5% (n = 36) and the overall false-positive rate was 0% (n = 72). For the hUbq siRNA screen, the overall false-negative and/or false-positive rates were 0.00%.

Initially 4 potential hPK siRNA hits were selected that displayed a %PCC ≥ 8% and a statistically significant Z scores (%PCC) of ≥ 2, namely *CDK1*/*CDC2*; *TTK*/*MPS1*, *CAMK2N1* and *WEE1*. We selected *CAMK2N1, TTK*/*MPS1* and *CDK1*/*CDC2* siRNAs for validation as they displayed a reasonable average cell number of 1261, 968 and 646, respectively in the original screen (Table 4.1). *CAMK2N1* and *TTK*/*MPS1* were located in the top 10 of the siRNA hit list displaying an average %PCC of 11.77% and 9.64%, respectively (Table 4.1). Also, *WEE1* showed an average low cell number of 141 (Table 4.1). The average %PCC caused by these siRNA hits was relatively high and possibly similar to the %PCC identified in ovarian cancer tissue at about 9% (Sreekantaiah *et al.*, 1987). Moreover, this rate of PCC also similar to the %PCC that has been detected in

cancer cells treated with *MCPH1/BRIT1* siRNA including HeLa or U2OS cells (15-20%) (Adams *et al.*, 2014; Trimborn *et al.*, 2006). Additionally, CDK1/CDC2 was selected as it expected to be a potentially strong hit since MCPH1/BRIT1 independently regulates and maintains inhibitory phosphorylation of Tyr15-CDK1/CDC2 for proper mitotic entry (Alderton *et al.*, 2006). In addition, the network of cellular regulation between CDK1/CDC2 and WEE1 during cell division (McGowan and Russell, 1993; Harvey *et al.*, 2005; Do *et al.*, 2013) may potentially suggest the contribution of these siRNAs to PCC induction.

However, none of these 4 potential hPK siRNA hits validated during the confirmatory siRNA screen stage that was employed using 4 deconvoluted ON-TARGET*plus* siRNAs. The failure of the siRNA hit validation in this study may due to number of factors. First, only 4 potential siRNA hits were selected from hPK siRNA hit list containing 104 siRNAs. Consequently, the initial selection of such a small number of siRNA hits may have contributed to the unsuccessful validation. Second, inhibition of the hits tested here may only be required for initiating depletion of the cellular pathway that regulates chromosome condensation. Thus, their effect may not be sufficiently strong to induce PCC in cells with an intact function of MCPH1/BRIT1 that regulates cell cycle checkpoints in response to abnormal cell cycle activity. Third, these hits may interact with MCPH1/BRIT1 in causing PCC but equally they could be in a different or unknown pathway. Thus, depletion of these hits may involve activation or/and inhibition of other unknown molecules, all of which contribute to PCC induction. Last, MCPH1/BRIT1 may be a critical component in regulating DNA condensation during the cell cycle. Consequently only a minority of other genes may cause a similar PCC phenotype.

Additionally, the sequence-dependent off-target effect (OTE) can hamper the validation of RNAi experiments. Sequence-specific siRNA is usually designed to target a complete cleavage of the desired complementary mRNA. However, it may affect and inhibit other unspecific mRNA transcripts due to partial complementarity between the siRNA and the mRNA, causing OTE (Boutros *et al.*, 2006; Birmingham *et al.*, 2006; Sledz *et al.*, 2003). OTE can also occur when the siRNA functions as micro RNA (miRNA) inducing a partial inhibition of mRNA translation. This is mainly due to the exact complementarity between the siRNA seed region (position 2-8 of the anti-sense strand) and the 3'-untranslated region (3'-UTR) of the non-targeted genes (Jackson *et al.*, 2003). Additionally, sequence-specific motifs induce the interferon response pathway (Sledz *et al.*, 2003). Thus, sequence-specific OTEs in RNAi experiments can increase the identification of false positive hits and complicate the interpretation of siRNA results.

One study developed a bioinformatics method called Genome–wide Enrichment of Seed Sequence matches (GESS) to identify novel off-targeted transcripts in several RNAi screens using the genome-wide database either of the full-length mRNA or of sub-regions such as 3'-UTR, 5'-UTR and coding sequence (Sigoillot *et al.*, 2012). Although we did not utilise any method to minimise the existence of sequence-dependent OTEs, focusing on the siRNA seed region using GESS (http://www.flyrnai.org/gess) (Schmidt *et al.*, 2013; Yilmazel *et al.*, 2014), common seed analysis (CSA) (Marine *et al.*, 2012) or Haystack (http://rnai.nih.gov/haystack/) (Buehler *et al.*, 2012b) are useful for identifying siRNAs sensitive to OTEs, which could subsequently improve the validation of siRNA hits.

A second siRNA screen was carried out was hUbq sub-library. The Z score batch analysis of PCC inducer hUbq siRNA screen revealed *FBXO5*/*EMI1* to be one of the top siRNA hits with an elevated level of %PCC and a significant Z score ≥ 2. The validation experiment revealed that the individual siRNA 2 and 4 targeting *FBXO5*/*EMI1* displayed elevated %PCC and reduced cell viability. The efficiency of the knockdown of these individual siRNAs was confirmed at the RNA and protein level.

FBXO5/EMI1 performs a number of functions. It regulates S-phase entry, inhibits proliferation, delays M phase progression and prevents cells from completing DNA replication that is normally controlled by the geminin protein. FBXO5/EMI1 has been implicated in various types of cancer, suggesting a possible role as an oncogene (Lee *et al.*, 2006; Lehman *et al.*, 2007; Gütgemann *et al.*, 2008; Wang *et al.*, 2014e). For instance, overexpression of FBXO5/EMI1 caused multi-cellular deficiencies such as hyper-proliferation, tetraploidy and increased genomic instability, particularly in p53 deficient cells. In addition, its depletion in cancer cells causes polyploidy and large nuclei (Machida and Dutta, 2007; Di Fiore and Pines, 2007; Shimizu *et al.*, 2013). The morphological changes resulting from FBXO5/EMI1 inhibition suggest that FBXO5/EMI1-depleted cells remain in S phase, leading to abnormal re-replication. Therefore, in our study it was decided not to pursue at this time the experimental investigation of the potential Ubq siRNA hit FBXO5/EMI1 although co-depletion of FBXO5/EMI1 with MCPH1/BRIT1 increased %PCC compared to a single siRNA knockdown of FBXO5/EMI1. However, *FBXO5*/*EMI1* siRNA in presence or absence of MCPH1/BRIT1 displayed the same phenotype of cells with large nuclei and condensed chromosomes, that is different to the PCC phenotype with condensed chromosomes induced by *MCPH1*/*BRIT1* siRNA.

The loss of FBXO5/EMI1 has been found to encourage DNA damage responses and induce apoptosis, particularly when *FBXO5/EMI1* siRNA is combined with the anti-cancer agent Doxorubicin as this enhances chemosensitivity (Verschuren *et al.*, 2007; Shimizu *et al.*, 2013), indicating its potential therapeutic interventions for cancer. However, the potential oncogenic role of FBXO5/EMI1 remains unknown. Indeed, depletion of FBXO5/EMI1, in this study, showed an overall reduction in cell number in the presence or absence of MCPH1/BRIT1 and a noticeable decrease in typical PCC cells with clear condensed chromosomes that are usually induced as consequence of *MCPH1/BRIT1* siRNA. Reduction of PCC cells may be associated with the loss of function of FBXO5/EMI1 that may contribute to killing these cells by the induction of apoptosis.

Furthermore, CDC27, a sub-unit of the APC/C, has been found to bind to the *C*-terminal domain of MCPH1/BRIT1 in a phosphorylation-dependent manner and depletion of CDC27 showed a similar mitotic defect phenotype to PCC (Singh *et al.*, 2012e). These authors referred to MitoCheck software which has been used with other available human protein complex resources (Hutchins *et al.*, 2010) to assess the defective phenotypes associated with the loss of MCPH1/BRIT1 and CDC27. MitoCheck analysis revealed that depletion of CDC27 displayed similar mitotic aberration phenotypes to those reported with depletion of MCPH1/BRIT1 such as the clustering of nuclei, unusual nuclear shape, segregation problems, metaphase and pro-metaphase delay and metaphase alignment defects. The PCC phenotype was not covered by MitoCheck analysis (Hutchins *et al.*, 2010) or examined by CDC27's investigators (Singh *et al.*, 2012e). Thus, it is still unknown whether CDC27 knockdown causes PCC despite the existence of an interaction between MCPH1/BRIT1 and CDC27.

As previously mentioned that the interaction of MCPH1/BRIT1 with CDC27 takes place at the *C*-terminal BRCT domains of MCPH1/BRIT1 that are not responsible for regulation of chromosome condensation, which involves the *N*-terminal BRCT domain (Richards *et al.*, 2010; Singh *et al.*, 2012e). Therefore, a similar scenario may exist with FBXO5/EMI1 and MCPH1/BRIT1 in which a potential interaction may occur between the two proteins but it may not necessarily be associated with regulation of chromosome condensation. Indeed, depletion of FBXO5/EMI1 in the presence or absence of MCPH1/BRIT1 consistently displays a cell phenotype with large nuclei; with condensed chromosomes, which is slightly different to PCC phenotype induced by *MCPH1/BRIT1* siRNA. This suggested that FBXO5/EMI1 might function in an independent pathway involved in the regulation of DNA condensation. However, the phenotype induced by depletion of

FBXO5/EMI1 may not be associated with PCC since other studies have showed that FBXO5/EMI1 deficient cells terminate in S phase causing abnormal DNA re-replication (Machida and Dutta, 2007; Di Fiore and Pines, 2007; Shimizu *et al.*, 2013). Consequently, cells may be appeared with larger nuclear size, meaning that cells may not entre into mitosis and participate in DNA condensation process but instead they may undergo cell death. This may explain the noticeable reduction in cell number observed in FBXO5/EMI1 depleted cells.

Alternatively, FBXO5/EMI1 functions as a regulator of the APC/C complex (Peters, 2003; Reimann *et al.*, 2001a; Reimann *et al.*, 2001c). CDC27 is a subunit of this complex that has been speculated to mediate the interaction between MCPH1/BRIT1 and APC/C, which may be responsible for proteosome-dependent degradation of MCPH1/BRIT1 (Singh *et al.*, 2012e). Thus, defective FBXO5/EMI1 function may cause an unknown ubiquitination mechanism leading to the inactivation of MCPH1/BRIT1. Thus, potentially suppression of FBXO5/EMI1 may be considered as a therapeutic intervention in PCC cancer cells with defective MCPH1/BRIT1 function. Further investigations are warranted to confirm the potential involvement of FBXO5/EMI1 in regulation of DNA condensation and in inducing lethality in MCPH1/BRIT1 deficient cells.

In summary, both hPK and hUbq siRNA screens were analysed for genes, whose suppression induced PCC. Hits validation was performed on only 4 genes from hPK sub-libraray (CDK1/CDC2; TTK/MPS1, CAMK2N1 and WEE1), none of which displayed PCC. Identifying further hPK siRNA hits that potentially induced PCC for validation may be required. Similarly PCC inducer hits may be identified in other siRNA sub-libraries such as the druggable genome screened for PCC by the BSTG.

The siRNA hit from hUbq sub-libraray namely *FBXO5*/*EMI1* was selected for validation. *FBXO5*/*EMI1* siRNA induced a cell phenotype of enlarged nuclei with condensed chromosomes in cells with or without *MCPH1*/*BRIT1* siRNA, which is slightly different to the PCC phenotype induced by *MCPH1*/*BRIT1* siRNA. Function of FBXO5/EMI1 in the cell cycle may be independent of MCPH1/BRIT1 function that is associated in regulation of DNA condensation. Lack of function of FBXO5/EMI1 may contribute to a reduction in PCC cells in MCPH1/BRIT1 deficient cells. Utilising–time-lapse microscopy to profile the data of cell division genes (Neumann *et al.*, 2010) would be a useful means of clarifying if there is any potential similarity in mitotic phenotypes between FBXO5/EMI1 and MCPH1/BRIT1 when they are depleted.

Chapter 5 A high throughput PK siRNA sub- library synthetic lethality screen in MCPH1/BRIT1 deficient cells

5.1 Introduction

High throughput screening using RNAi libraries is a useful means to identify molecular targets that induce synthetic lethality (SL). SL genes are two genes in which mutation in one gene alone has no effect on cell viability, however, mutation in both genes at the same time leads to cell death (Kaelin Jr, 2009; Kaelin, 2005). Thus, targeting a SL gene in a cancer with a specific mutation should kill cancer cells but not normal cells. SL offers the ability to target cancer cells that are harbouring a loss of function mutation, for example, a mutation in a TSG. Since the principal role of the majority of chemotherapeutic agents is to inhibit rather than activate the protein function thus it is essential to identify a SL target that is functionally associated with TSG to ensure subsequent induction of apoptosis in cancer cells (Iorns *et al.*, 2007). The SL approach has been utilised to kill BC cells with a defect in the BC genes *BRCA1* and *BRCA2*, which both play vital role in DNA repair mechanism, without affecting the normal cells, by using poly (ADP ribose) polymerase (PARP) inhibitor (Farmer *et al.*, 2005). So, the integration of loss of function of BRCA genes with PARP inhibitor presents an excellent example of identification of SL targets (Iorns *et al.*, 2007).

A number of lines have implicated *MCPH1/BRIT1* expression in cancer progression (Richardson *et al.*, 2011; Bruning-Richardson *et al.*, 2011; Rai *et al.*, 2006; Venkatesh *et al.*, 2013). This is described in detail in the main introduction (Chapter 1; Section 1.1.6.4). Since *MCPH1/BRIT1* is a cancer related gene, identifying its synthetic interactors would theoretically target only cancer cells with MCPH1/BRIT1 deficiency and preserve the life of normal cells that carry a functional copy of the *MCPH1/BRIT1* gene. Potentially these MCPH1/BRIT1 SL genes could lead to the identification of more effective and less harmful anti cancer drugs for patients with MCPH1/BRIT1 deficient cancers.

This study used two complementary screens of the hPK siRNA library that were performed by the BSTG. In one, a single knockdown using the hPK siRNA library was used in U2OS cells expressing MCPH1/BRIT1, its aim being to identify genes that induce a PCC phenotype (PCC inducer screen). The other screen was performed with a double knockdown whereby a reverse siRNA transfection using the hPK library was performed and then followed 24hr later by *MCPH1/BRIT1*

knockdown using a forward siRNA transfection. This screen, known as the PCC modifier screen, aimed to identify those genes that reduce or kill cancer cells with a PCC phenotype. The BSTG utilised the high throughput Operetta imaging system and Columbus analysis software to perform both screens.

Thus, in this study, we aimed to combine the cell number data from two complementary hPK siRNA screens with and with out *MCPH1/BRIT1* siRNA knockdown to identify SL siRNAs in MCPH1/BRIT1 deficient cells. Thus, the potential SL siRNA is expected to show a significant reduction in cell number in the absence of MCPH1/BRIT1 in the PCC modifier hPK siRNA screen but not in the presence of MCPH1/BRIT1 in the PCC inducer hPK siRNA screen.

Since loss of the function of MCPH1/BRIT1 facilitates cancer progression, identifying its SL partners would selectively kill cancer cells and aid breast and ovarian cancer sufferers whose tumours express low levels of MCPH1/BRIT1 and are resistant to current chemotherapy treatments.

5.2 Results

The BSTG developed and performed two hPK siRNA screens in order to identify genes which either induced PCC or modified PCC caused by *MCPH1/BRIT1* knockdown. Here, both versions of the hPK screens (PCC inducer and modifier screens) were utilised, to identify a significant decrease in cell number in the MCPH1/BRIT1 deficient hPK PCC modifier screen compared to the complementary PCC inducer screen that had functional MCPH1/BRIT1. This approach was expected to lead to the identification of MCPH1/BRIT1 SL siRNA hits.

5.2.1 Evaluation of the cell number in PCC inducer hPK siRNA screen and MCPH1/BRIT1 modifier hPK siRNA screen

Before performing SL analyses, appropriate controls were selected for both versions of the hPK siRNA screens, PCC inducer and modifier.

5.2.1.1 Controls' assessment in PCC inducer and modifier hPK siRNA screens

Since experimentally the negative control NT-siRNA had shown no effect on the cell number it was selected as a reference for analysing the cell number in PCC inducer hPK siRNA screen for identification of SL siRNA hits.

The hPK siRNA PCC inducer screen consisted of 9 plates and the screen was performed in duplicate. Each plate contained 4 wells treated with a single knockdown of a reverse transfection for the negative control NT-siRNA. Analysis of the replica PCC inducer hPK siRNA plates showed almost equal values of mean cell number in the negative control NT-siRNA across all the 9 plates in the two batches (n = 8 wells) (Figure 5.1A). The mean cell number (SD) for the negative control NT-siRNA for each replica plate was in plate 1, 2, 3, 4, 5, 7, 8 and 9 as follows; 2073 (337), 2104 (294), 2147 (281), 2243 (222), 2010 (141), 2026 (443), 1948 (381), 2071(375) and 2268 (136), respectively.

A. Single NT-siRNA conrtols PCC inducer hPK siRNA screen
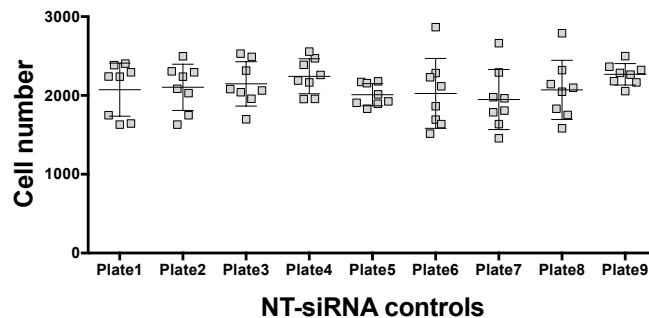
B. Single NT-siRNA controls PCC modifier hPK siRNA screen
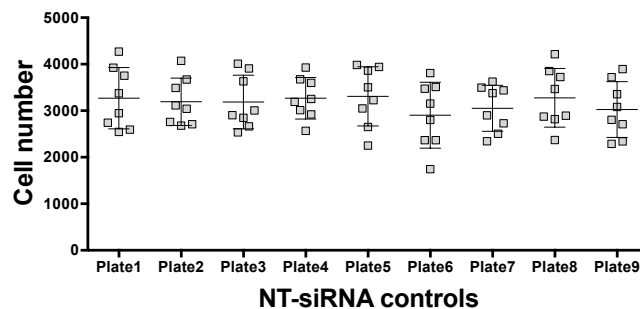
Figure 5.1. Negative controls assessment in the 9-replica plates in the hPK siRNA PCC inducer and modifier screens. Graphs showing the cell numbers for the NT-*MCPH1/BRIT1* siRNA treated in 8 wells in each replica plate in hPK siRNA PCC inducer (**A**) and PCC modifier (**B**) screens.

In contrast, the PCC modifier hPK siRNA screen involved a double transfection, first a reverse siRNA transfection of the hPK sub-library followed by a forward siRNA transfection of *MCPH1*/*BRIT1*. Thus, it was essential to select a control that would mimic the pattern of this screen without showing a significant effect on cell number, providing a statistical significance for identifying the SL siRNA hits. Consequently, the reverse transfection of NT-siRNA was followed 24hr later by a forward transfection of *MCPH1*/*BRIT1* siRNA which was used as a negative control to analyse the hPK siRNA PCC modifier screen for the selection of SL siRNA hits. Similar to the hPK siRNA PCC inducer screen, there were 4 wells were treated with the negative control (double knockdown) NT-*MCPH1/BRIT1* siRNAs for each plate in the hPK siRNA PCC modifier screen. The double siRNA transfection for the negative control did not show any side effects on cell number caused by the forward transfection MCPH1/BRIT1, indicating the efficiency of NT-MCPH1/BRIT1 siRNAs for use as a negative control to analyse the PCC modifier screen for hits with synthetic lethality effect. The mean cell number (SD) for the negative control NT-*MCPH1/BRIT1* siRNA for each replica plate (n = 8 wells) was in plates 1, 2, 3, 4, 5, 7, 8 and 9 as follows; 3268 (594), 3192 (443), 3188 (653), 3268 (434), 3309 (664), 2903 (688), 3052 (544), 3276 (532) and 3024 (580), respectively (Figure 5.1B).

5.2.1.2 Assessment of the transfection efficiency of PCC inducer and modifier hPK siRNA screens using the control *PLK1* siRNA

The two screens were performed by the BSTG utilising established controls to ensure successful transfection of the hPK siRNA sub library and without observing high cell death in the PCC modifier screen, which was performed as a double knockdown. Thus a RT of *PLK1* siRNA was used as a functional readout and a marker for the transfection efficiency as it was previously described in (Chapter 4; Section 4.2.1.2) Also, it also has been reported that *Plk1* siRNA presented a notable reduction in cell viability when used as a control in a screen employed a mouse IMCD3 cell line (inner medullary collecting duct) to select genes implicate in cell proliferation (Elmehdawi *et al*, 2013; Adams *et al*, 2014).

Similarly, a significant loss in cell viability was also was seen after silencing *PLK*1 siRNA using U2OS cell line compared to the aforementioned NT-*MCPH1/BRIT1* siRNA in PCC modifier hPK1 siRNA screen *PLK1* siRNA showed an average of cell number (SD) at 89 (67) in the first batch and at 105 (49) in the second batch (n = 18 wells/batch) while the average cell number for NT-

MCPH1/BRIT1 siRNA was 2708 (323) in the first batch and 3620 (359) in the second batch ($p < 0.0001$; n = 36 wells/ batch) (Figure 5.2 A and B). In addition, another control inner centromere protein (*INCENP)* siRNA was included in the PCC modifier screen and used as marker for the impact on cell number. It also displayed a significant decrease in cell number opposite to NT-*MCPH1/BRIT1* siRNA ($p < 0.0001$) (Figure 5.2 A and B). The mean cell number for *INCENP* siRNA was 637 (265) in the first batch and 908 (249) in the second batch (n = 18 wells/ batch).

Therefore, using the two controls *PLK1* and *INCENP* provided a quantitative and visual evaluation of the transfection efficiency in the PCC modifier screen. Not only this, but also the reduced gene expression of *Cyclophilin B* (Chapter 4; Section 4.2.1.1.2; Figure 4.1) supported a high level of transfection efficacy can be obtained in the U2OS cell line, demonstrating the logical, practical, and robust procedures used to perform the PCC modifier hPK siRNA screen.
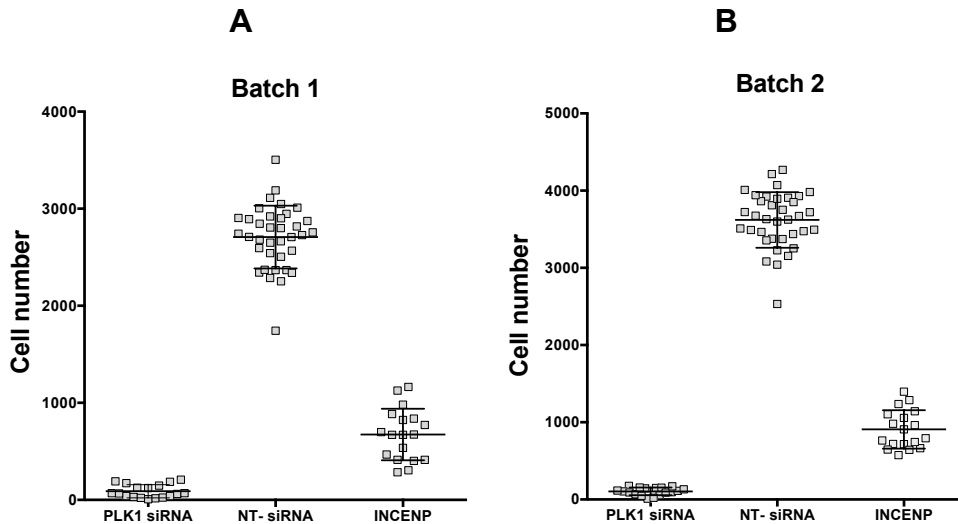
Figure 5.2. The controls *PLK1* and inner centromere protein (*INCENP*) siRNAs confirms the high transfection efficiency in U2OS cells in PCC modifier hPK siRNA screen.
PLK1 and *INCENP* siRNA decreased the cell number significantly compared to NT-siRNA in batch 1 **(A)** and batch 2 **(B),** providing a quantitative evaluation of transfection efficacy ($p < 0.0001$).

5.2.1.3 Evaluating the cell number in batches 1 and 2 in hPK siRNA of PCC inducer and modifier screens

In preparation for SL siRNA analysis, the cell number output from the two replicates in hPK siRNA PCC inducer screen was assessed.

In hPK siRNA PCC inducer screen, a comparison between the cell number output in replicates 1 and 2 was performed. Consequently, Pearson's correlation

analysis revealed a strong positive association between the two replicates (r = 0.6263; *p* < 0.0001; n = 720) (Figure 5.3A). In addition, the mean cell number output from the siRNA screen of both replicates was calculated to minimize the existence of variation in cell number between the replicates. The scatter plot in (Figure 5.3B) illustrates the distribution of average cell number of 720 siRNAs in the hPK PCC inducer screen.

Similarly, in the hPK siRNA PCC modifier screen, a strong positive correlation was identified between the cell number in replicates 1 and 2 of the siRNA screen (r = 0.5609; *p* < 0.0001; n = 720) (Figure 5.3C), demonstrating the robustness of the experimental process used during the performance of the two replicates and allowing a further sufficient analysis for identifying SL siRNA hits. Moreover, as preparation for SL siRNA analysis, the average of cell number produced from the hPK siRNA PCC inducer screen was calculated and presented as a scatter plot (Figure 5.3D).

5.2.2 Statistical analysis for identification of hPK-synthetic lethal siRNA hits based on percentage cell viability

The statistical analysis used to identify the SL siRNA was previously described in (Chapter 2; Section 2.4.1.1). Briefly, the statistical analysis process performed by (Turner *et al.*, 2008) was utilised. For each screen, whether PCC inducer or modifier, the method relies on calculating the effect of each individual siRNA on cell viability in relation to the control and expressing this effect as a percentage. Then, the differences between the screens in % cell viability for each individual siRNA were calculated.

The top 20 siRNA hits, that showed the largest reduction in cell viability in the PCC modifier screen compared to the identical siRNA in the PCC inducer screen, were selected. These were considered to be SL siRNA hits (Table 5.1). The % cell viability produced from each siRNA hit also allowed cell death rate to be defined by subtracting 100 from the value of cell viability of each siRNA in either the PCC modifier or inducer screen as shown in (Table 5.1). Thus, the largest decrease in cell viability in the PCC modifier screen was caused by the potential SL hit (*PLK1* siRNA) with a cell viability of 4% in the absence of MCPH1/BRIT1 (PCC modifier screen/ the pink highlighted column) opposite to the cell viability of 58% in the presence of MCPH1/BRIT1 (PCC inducer screen/ the pink highlighted column) this hit is shown at the top of (Table 5.1).
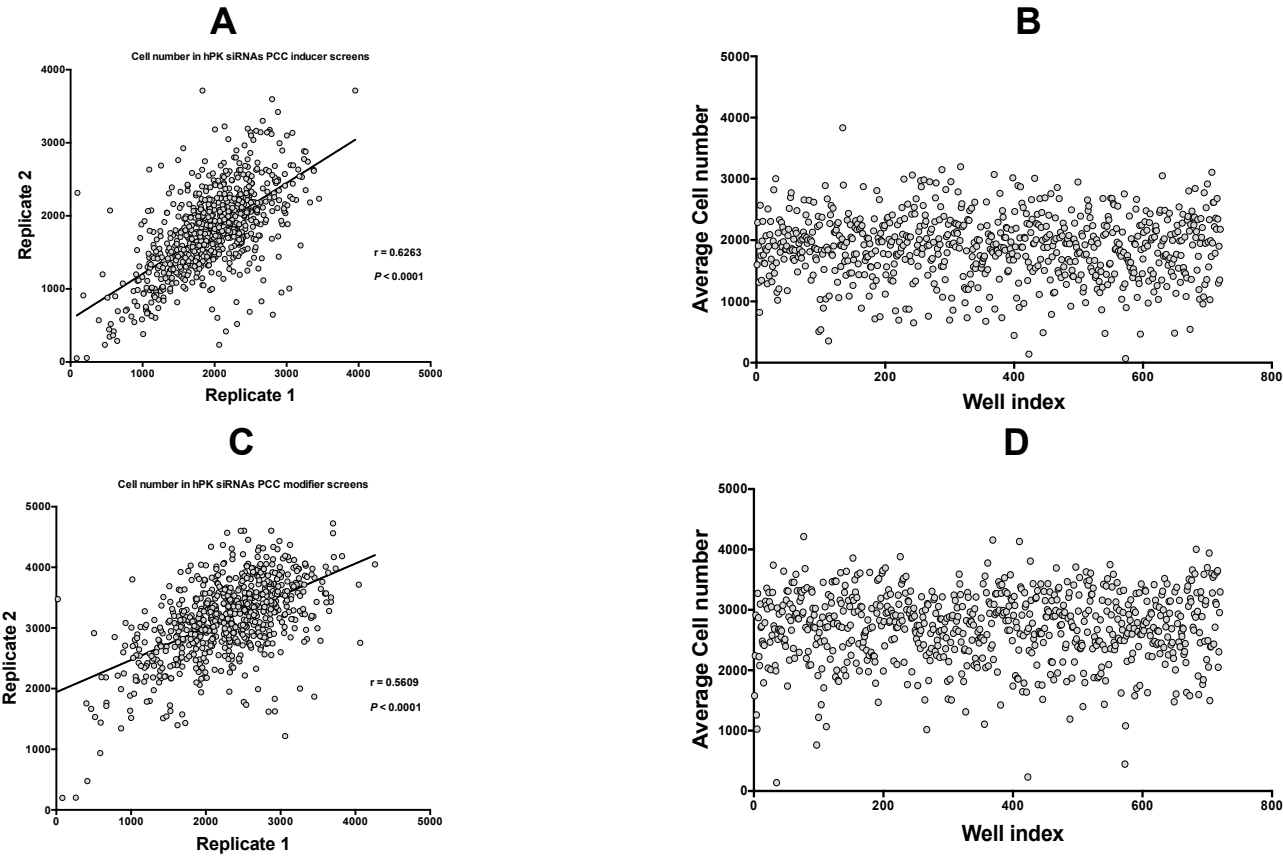
Figure 5.3. Assessment of the cell number output from the PCC inducer and modifier hPK siRNA screens.
(**A and C**) Graphs represent a comparison of cell number output between replicates 1 and replicate 2 in hPK siRNA in PCC inducer (r = 0.6263; *p* < 0.0001; n = 720) **(A)** and in PCC modifier screen (r = 0.5609; *p* < 0.0001; n = 720) **(C)**. **(B and D)** scatter plot graphs showing the distribution of average cell number produced from 720 hPK siRNAs in PCC inducer screen **(B)** and PCC modifier screen **(D)**.

Table 5.1. Identification of hPK-synthetic lethal (SL) siRNA hits based on % cell viability.

The columns highlighted in pink show the difference between % cell viability for PCC modifier siRNA (**CVI**)[a] screens and % cell viability for PCC siRNA inducer (**CVM**)[b] screens. The first five siRNAs were validated, namely PLK1, CDK1/CDC2, STK39, VRK1 and TTK/MPS1.

Screen Name	Well Name	% Cell viability (PCC modifier screen)	Cell death rate (PCC modifier screen)	Average %PCC (modifier screen)	% Cell viability (PCC inducer screen)	Cell death (PCC inducer screen)	Average %PCC (inducer screen)	%CVI[a] -%CVM[b]	Gene symbol
(hPK1)	C6	4.28	95.72	40.08	58.12	41.88	35.2	53.83	PLK1
(hPK1)	D2	38.52	61.48	54.45	63.25	36.75	15.1	24.73	CDC2
(hPK4)	H4	46.18	53.82	18.84	90.35	9.65	1.30	44.18	STK39
(hPK8)	D5	48.18	51.82	22.62	93.23	6.77	1.19	45.06	VRK1
(hPK1)	A2	48.31	51.69	18.96	77.07	22.93	9.6	28.76	TTK
(hPK6)	F7	52.27	47.73	19.03	92.77	7.23	2.33	40.50	BRD4
(hPK9)	D3	53.11	46.89	19.76	78.06	21.94	2.01	24.95	EFNB3
(hPK1)	D8	53.19	46.81	19.34	88.12	11.88	2.59	34.92	PIK4CA
(hPK4)	E3	53.48	46.52	12.86	89.62	10.38	1.35	36.14	CKMT2
(hPK1)	G3	54.78	45.22	18.37	99.89	0.11	2.73	45.10	PHKA2
(hPK4)	C9	55.65	44.35	10.51	86.18	13.82	0.65	30.54	FLT4
(hPK4)	F5	55.97	44.03	12.07	94.90	5.10	0.55	38.93	DKFZP761P0423
(hPK2)	B8	57.41	42.59	10.52	91.16	8.84	1.01	33.75	PRKCE
(hPK7)	C2	59.33	40.67	28.62	103.79	-3.79	2.40	44.47	KCNH2
(hPK5)	H8	59.50	40.50	20.67	89.04	10.96	0.65	29.54	OSR1
(hPK1)	B6	60.90	39.10	24.47	102.18	-2.18	5.60	41.27	MASTL
(hPK6)	A4	61.54	38.46	24.20	100.17	-0.17	0.50	38.63	TLK2
(hPK5)	F6	61.72	38.28	16.23	111.43	-11.43	1.05	49.71	ROR1

5.2.2.1 Selection of hPK-SL siRNA hits for screen validation

The top five SL siRNA hits were initially selected for validation (PLK1, CDK1/CDC2, STK39, VRK1 and TTK/MPS1), which were highlighted in yellow in (Table 5.1).

5.2.3 Validation of hPK-SL siRNA hits using on TARGET *plus* four deconvoluted siRNAs

To statistically validate SL siRNA hits using a logical and robust strategy, the validation experiment was performed in duplicate at two different concentrations (25nM and 50nM).

5.2.3.1 Selection of siRNA controls for valdation of SL siRNA hits

In order to validate the SL siRNA, each individual hit was knocked down using four individual duplex siRNAs under three different conditions as follows;

1. Single knockdown reverse transfection of the siRNA hit

2. Double knockdown of the siRNA hit in combination with *MCPH1/BRIT1* siRNA

3. Double knockdown of the siRNA hit in combination with NT-siRNA.

For more details about siRNA controls used in validation SL siRNA hits see (Chapter 2; Section 2.4.1.2.1; Figure 2.4).

The single knockdown usually has no effect on cell number. However, it is anticipated that the double knockdown of a siRNA hit in combination with *MCPH1/BRIT1* siRNA would greatly decrease the cell number compared to its combination with NT-siRNA that would show no significant effect on cell number.

Since identification of the SL siRNA is based on a double knockdown two controls were selected. One of these was similar to the one used in the PCC modifier screen, NT-siRNA/*MCPH1/BRIT1* siRNA, which assessed the reduction in cell number caused by the treatment of the siRNA hit with *MCPH1/BRIT1* siRNA. The other control was NT-siRNA/NT-siRNA which would not significantly decrease the cell number in the experiment compared to the one treated with the forward transfection *MCPH1/BRIT1* siRNA.

In addition, several further controls were included in the same plate in order to confirm all steps of the experiment were working optimally to help reduce the identification of false positives. Thus, single knockdown reverse and forward

transfection of *MCPH1/BRIT1* were performed and the %PCC determined as a functional read out of efficient MCPH1/BRIT1 knockdown. In addition the forward transfection of *MCPH1/BRIT1* siRNA was also used as a reference for measuring the significant increase or decrease in %PCC so that any SL siRNA hits that showed a reduction in cell number and an increase or decrease in %PCC would be nominated as a potential PCC inducing or siRNA modifying hit. These siRNA hits could add substantial knowledge about the importance of MCPH1/BRIT1 function in regulating chromosome condensation. Moreover, single NT–siRNA at 25nM and 50nM was used as a reference to show no effect either on cell number or %PCC. The *PLK1* siRNA was used as a positive control for siRNA transfection efficiency and this was plated at 25nM and 50nM.

5.2.3.2 Assessment of the single and double transfection of siRNA controls

The validation plate of SL siRNA hits included the single or double siRNA knockdown of the controls. The mean values of cell number or %PCC for these controls when treated with single siRNA knockdown at 25nM or 50nM were plotted and presented as separate figures next to each single siRNA knockdown of SL hits and are only explained in Figure 5.4 A1 and B1. The mean values of cell number or %PCC for these controls when treated with double siRNA knockdown at 25nM or 50nM were plotted and presented as separate figures next to each double siRNA knockdown of SL hits and are only explained in Figure 5.4 A2 and B2.

For the single knockdown controls, the mean cell number (SD) for the FT of *MCPH1/BRIT1* siRNA (100nM) was 2794 (778) (n = 10 wells) and 1645 (1234) for the RT (100nM) (n = 8 wells). *MCPH1/BRIT1* siRNA induced a mean %PCC (SD) of 16.38% (2.9%) for forward transfection compared to 12.6% (6.8%) for RT. In addition, the mean cell number (SD) for the NT-siRNA at 25nM was 5479.08 (3015) vs. 4313 (2599) at 50nM (n = 6 wells). Similarly, NT-siRNA did not induce PCC either at 25nM or 50nM giving 1.72% (0.7%) and 0.86% (0.4%), respectively. Lastly, although the mean cell number for *PLK1* siRNA at 25nM was unexpectedly high at 2066 (33), this decreased dramatically at 50nM to 294 (198) (n = 2 wells). This suggests that the 25nM as a concentration of siRNA was not sufficient to knockdown *PLK1* compared to the 50nM or 100nM that was used experimentally during the performance of the PCC modifier screen by the BSTG or during the validation of siRNA hits from the PCC inducer hPK siRNA screen in (Chapter 4;

Section 4.2.1.5; Figure 4.7B) of this thesis to show transfection efficiency by reduction in cell number.

For the controls with double knockdown in both replicates, the mean cell number was 3515 for the NT-siRNA (25nM)/*MCPH1*/*BRIT1* siRNA control and 3874.50 for NT-siRNA (50nM)/*MCPH1*/*BRIT1* siRNA (n = 6 wells). In addition, the mean %PCC was 11.4% for NT-siRNA (25nM)/*MCPH1*/*BRIT1* siRNA which increased slightly to 13.2% for NT-siRNA (50nM)/*MCPH1*/*BRIT1* siRNA. However, the corresponding control with double knockdown of NT-siRNA at 25nM (NT-siRNA (50nM)/NT-siRNA (50nM)) did not affect the cell number 5864 cells compared to NT-siRNA (50nM)/NT-siRNA (50nM) which reduced cell number to 2877 (n = 4 wells). At 25nM or 50nM the corresponding double transfections of the NT-siRNA control both showed no effect on PCC level (≤ 1%).

5.2.3.3 Validation of SL siRNA hits

As previously mentioned in (Section 6.2.3.1) that each SL siRNA hit was validated using four individual/deconvoluted siRNAs. The individual siRNA underwent three different conditions, which were single knockdown (the siRNA hit was without any treatment) and, double knockdown (siRNA was treated individually either with *MCPH1*/*BRIT1* siRNA or treated with NT-siRNA). The final concentration for siRNA single or double knockdown was 25nM and 50nM.

5.2.3.3.1 *STK39* siRNA

The validation results for single knockdown of *STK39* using the four individual siRNAs revealed no effect on cell viability at 25nM or 50nM. The mean cell number for the deconvoluted *STK39 siRNA* 1, 2, 3 and 4 at 25nM was 6161, 6235, 7890 and 6967, respectively while at 50nM it was 6750, 6616, 7175 and 3552, respectively (Figure 5.4 A1 and B1).

Furthermore, the analysis method, that was used initially with the two original screens (PCC inducer and PCC modifier hPK siRNA screens (Section 6.2.2, 6.2.2.1 and Table 5.1) to identify the SL siRNA hits was employed to calculate the percentage difference in cell viability or/and cell death rate between each individual siRNA duplex treated with or without *MCPH1*/*BRIT1* siRNA in relative to the controls NT-*MCPH1*/*BRIT1* siRNA or NT-siRNA, respectively. Here, the difference in % cell viability caused by the four deconvoluted *STK39* siRNA duplexes at 25nM and 50nM in cells treated with and without *MCPH1*/*BRIT1* siRNA was calculated (Table 5.2 A and B). *STK39* siRNA 1 at 25nM in combination with *MCPH1*/*BRIT1*

siRNA showed no difference in % cell viability (104%) opposite to (112%) for the single knockdown of *STK39* siRNA 1 (Table 5.2A).

Table 5.2. Showing % cell viability and cell death rate for the four deconvoluted *STK39* siRNA in cells treated with/or without *MCPH1*/*BRIT1* siRNA.
The validation experiment of the SL siRNA hit (**STK39**) was performed in two concentrations 25nM **(A)** and 50nM **(B).** (**CVI**)˙ % cell viability for PCC inducer siRNA screen and (**CVM**): % cell viability for PCC modifier siRNA screen.

A. SL siRNA hits	**Double knockdown (in the absence of MCPH1/BRIT1)**			**Single knockdown (in the presence of MCPH1/BRIT1)**			**Difference in %CV**
Deconvoluted siRNA (25nM)	Average cell number	%Cell viability (CV)	Cell death rate	Average cell number	%Cell viability	Cell death rate	**%CVI-%CVM**
STK39 siRNA 1	3657	104	-4	6161	112.4	-12.5	8.4
STK39 siRNA 2	2504	71.2	28.8	6235	113.8	-13.8	42.6
STK39 siRNA 3	1659	47.2	52.8	7890	144	-44	96.8
STK39 siRNA 4	2740	77.9	22.1	6967	127.2	-27.2	49.2
	Control: NT-MCPH1 siRNA			**Control: NT-siRNA**			
	Mean cell number	3516		**Mean cell number**	5479		

B. SL siRNA hits	**Double knockdown (in the absence of MCPH1/BRIT1)**			**Single knockdown (in the presence of MCPH1/BRIT1)**			**Difference in %CV**
Deconvoluted siRNA (50nM)	Average cell number	%Cell viability	Cell death rate	Average cell number	%Cell viability	Cell death rate	**%CVI-%CVM**
STK39 siRNA 1	3150	81.9	18.1	6750	156.5	-56.5	74.6
STK39 siRNA 2	2258	58.7	41.3	6616	153.4	-53.4	94.7
STK39 siRNA 3	1758	45.7	54.3	7175	166.3	-66.3	120.7
STK39 siRNA 4	377.5	9.8	90.2	3552	82.3	17.7	72.5
	Control: NT-MCPH1 siRNA			**Control: NT-siRNA**			
	Mean cell number	3848		**Mean cell number**	4313		

A minimal reduction in % cell viability in cells treated with *STK39* siRNA 2 (25nM) in the absence of MCPH1/BRIT1 71.1% compared to the cells in the presence of MCPH1/BRIT1 (113.8%) (Table 5.2A). Thus, *STK39* siRNA 2 (25nM) may potentially consider as a weak individual siRNA. However, knockdown of *STK39* siRNA 3 or 4 (25nM) demonstrated a noticeable difference in % cell viability between cells treated with and without *MCPH1/BRIT1* siRNA. The cell viability for *STK39* siRNA 3 in the combination of *MCPH1*/*BRIT1* siRNA was 47.2% while in the presence of MCPH1/BRIT1 it was 144% (Table 5.2A). The cell viability for *STK39* siRNA 4 was 77.9% in the absence of MCPH1/BRIT1 and 127.2% in the presence of MCPH1/BRIT1 (Table 5.2A).

On the other hand, a small difference in % cell viability was identified for *STK39* siRNA 1 at (50nM) similarly to those observed at 25nM. The cell viability was 81.9% for *STK39* siRNA 1 in combination with *MCPH1*/*BRIT1* siRNA compared to 156.5% in cells without *MCPH1*/*BRIT1* siRNA treatment (Table 5.2B).

However, *STK39* siRNAs 2, 3 and 4 showed a massive change in % cell viability at 50nM in cells with reduced MCPH1/BRIT1 level compared to cells with functional MCPH1/BRIT1 (Table 5.2B). The % cell viability for *STK39* siRNAs 2, 3 and 4 in cells treated with versus without *MCPH1/BRIT1* siRNA were as follows; siRNA 2 58.7% vs. 153.4%, siRNA 3 45.7% vs.166.3% and siRNA 4 9.8% vs. 82.3%.
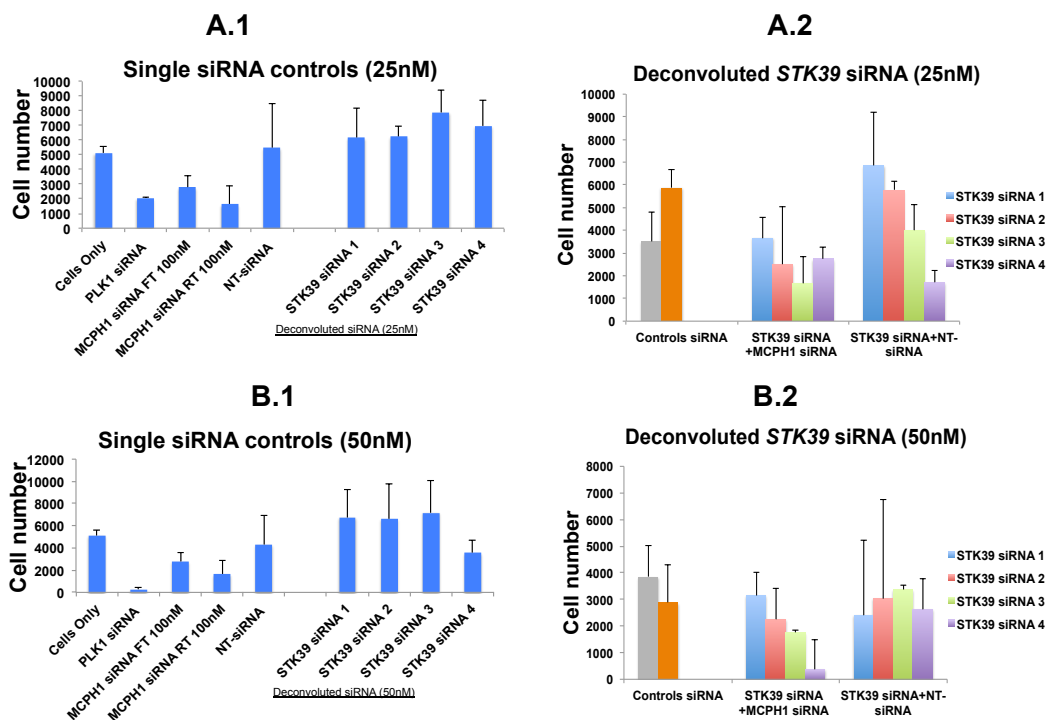
Figure 5.4. *STK39* siRNA was a potential SL hit in MCPH1/BRIT1 deficiency cells.
The validation plate for SL siRNA hits was composed of controls treated with a single siRNA knockdown at 25nM or 50nM in (A1 and B1), these controls are presented as separate figures within each individual description of SL siRNA hits and are only explained in this figure.
(A1 and B1) single siRNA knockdown at 25nM and 50nM, respectively for the following controls; *PLK1* siRNA at 50nM significantly decreased cell number to (294) compared to (2055) at 25nM. The mean cell number for the FT of *MCPH1/BRIT1* siRNA (100nM) was 2794 and 1645.5 for RT. NT-siRNA had little effect on cell number at 25nM (5479) and 50nM (4313). In **(A2 and B2**) (controls siRNA) the first two columns were treated with double siRNA knockdown at 25nM and 50nM representing the cell number in the controls, the grey columns showing NT-siRNA (25nM or/and 50nM) followed by *MCPH1/BRIT1* (100nM) siRNA (control) (3515) and (3874), respectively. The orange columns represent the cell number in NT-siRNA/NT-siRNA at 25nM or 50nM (5864) and (2877), respectively. **(A1 and B1)** showing the single knockdown for STK39 using the four deconvoluted siRNAs at 25nM and 50nM did not effect on cell number compared to NT-siRNA. **(B2)** significant reduction in cell viability observed that with *STK39* siRNA 3 (1758; *p* = 0.0519) and *STK39* siRNA 4 (377; *p* = 0.0072) at 50nM in absence of MCPH1/BRIT1 versus the controls (NT-siRNA/*MCPH1/BRIT1* siRNA represented in grey coloured column) (3874).

Additionally, we compared the cell number output of the double knockdown of siRNA hit with *MCPH1/BRIT1* siRNA in relative to the double knockdown of the

siRNA hit with NT-siRNA. This was to confirm that the transfection efficiency of *MCPH1*/*BRIT1* siRNA specifically in reducing cell number compared to NT-siRNA which has no effect on cell number.

The double knockdown for *STK39* siRNA 1, 2 and 3 at 25nM showed about a 50% reduction in cell number in the absence of MCPH1/BRIT1 compared to transfection for those three individual siRNAs in combination with NT-siRNA (25nM) (Figure 5.4 A2). The unexpected low cell number which resulted from *STK39* siRNA 4 transfection in combination with NT-siRNA could be due to the significant variation in cell number between the two replicates. In addition, at 50nM in the absence of MCPH1/BRIT1, *STK39* siRNAs 2, 3 and 4 but not STK39 siRNA 1 showed a reduction in cell number compared to cells treated with *STK39* siRNA followed by NT-siRNA (Figure 5.4B2). There was a significant variation in the cell number between the two replicates of *STK39* siRNA 1 in combination with NT-siRNA at 50nM (Figure 5.4B2).

Afterwards, the statistical analysis was performed using Unpaired t-test to identify those individual *STK39* siRNAs that significantly affected the cell number compared to the control (NT-siRNA (at 25nM or 50nM)/ *MCPH1*/*BRIT1* siRNA). This showed that the reduction in cell number caused by *STK39* siRNAs 1, 2 and 3 at 25nM in the absence of MCPH1/BRIT1 was not statistically significant compared to the control. In addition, as expected, *STK39* siRNA 4 at 25nM in combination with *MCPH1*/*BRIT1* siRNA, due to cell number variability within the replicates, did not show significant results (Figure 5.4A2). Nevertheless, *STK39* siRNA 1 and *STK39* siRNA 2 at 50nM in combination with *MCPH1*/*BRIT1* siRNA did not reflect statistical significant results vs. the control due to cell number variability that was observed between the replicates. Thus, only *STK39* siRNAs 3 and 4 at 50nM were considered to significantly reduce cell viability in the absence of *MCPH1*/*BRIT1* vs. the control. The mean cell number for *STK39* siRNA 3/MCPH1/BRIT1 siRNA was 1758 (p = 0.0519) and for *STK39* siRNA 4/ *MCPH1*/*BRIT1* siRNA was 377 (p = 0.0072) vs. 3848 for the control (Figure 5.4B2).

Some variability in the results were identified at the different siRNA concentrations. Comparison to *PLK1* siRNA control and other validated hits suggested better knockdown occurred at 50nM rather than 25nM. Further validation confirming the efficiency of the *STK39* siRNA knockdown by RT-PCR and/or WB would identify at least 2 out of 4 individual siRNAs to validate the significance of STK39 as SL in the absence of MCPH1/BRIT1 expression.

During the analysis of the validation plates, it was noticed that some of the SL hits induced an elevated level of PCC, particularly when followed by *MCPH1*/*BRIT1* knockdown. Thus, it was decided to determine if potential SL siRNA hit (*STK39*) also modified the percentage of MCPH1/BRIT1 induced PCC (Figure 5.5).
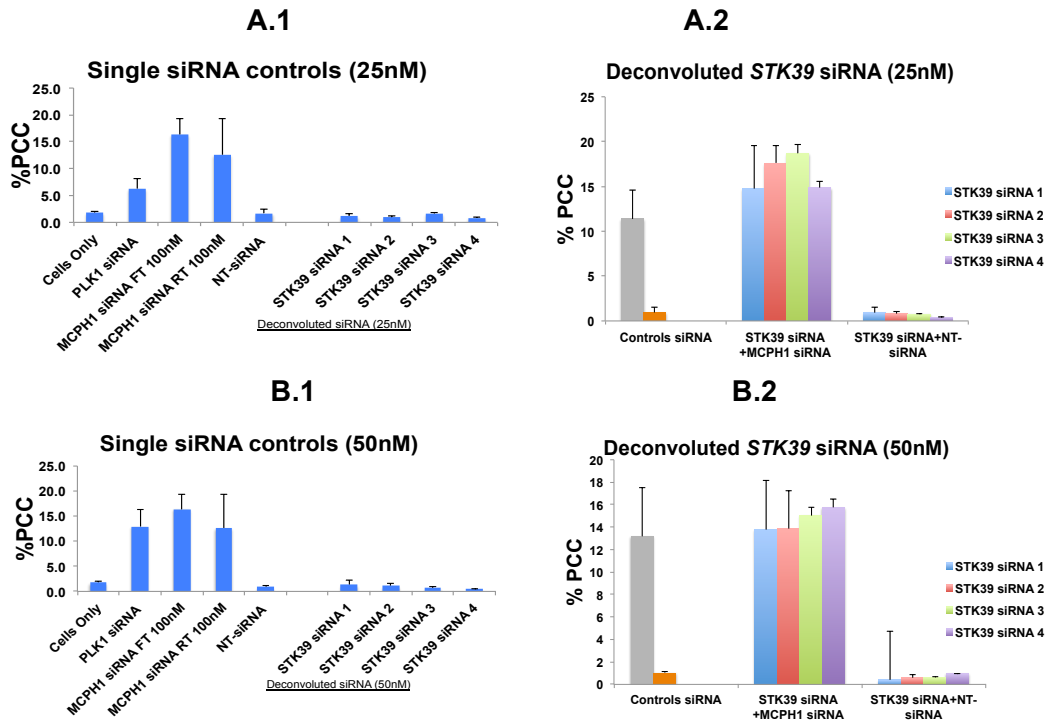
Figure 5.5. *STK39* siRNA may not be involved in inducing PCC.
The %PCC output from the controls treated with single siRNA knockdown at 25nM or 50nM in (A1 and B1) are presented as figures within each individual description of the SL siRNA hits and they will be only explained in this figure. The graphs in **(A1 and B1)** showing the %PCC induced by single knockdown siRNA for the controls at 25nM and 50nM, respectively for the following controls; the %PCC was seen with *PLK1* siRNA was due to cell death not to the sufficient knockdown of PLK1. The mean %PCC for the FT of *MCPH1*/*BRIT1* siRNA (100nM) was 16.38% (n = 10 wells) and 12.6% for the RT (n = 8 wells). NT-siRNA has no effect on %PCC at 25nM and 50nM 1.27% and 0.86%, respectively (n = 6 wells). In **(A2 and B2**) controls siRNA's columns represent the %PCC in the controls treated with double knockdown siRNA at 25nM and 50nM, the grey columns showing the %PCC in the positive control NT-siRNA (25nM or/and 50nM) (11.4%) and (13.9%), respectively in the case of *MCPH1*/*BRIT1* (100nM) siRNA. The orange columns represent the %PCC in NT-siRNA at 25nM or 50nM (≤ 1%) in the case of FT with NT-siRNA **(25nM or 50nM). (A1 and B1)** showing the single knockdown of the four deconvoluted *STK39* siRNAs at 25nM and 50nM did not induce PCC. **(A2)** double knockdown of the four individual *STK39* siRNAs at 25nM with *MCPH1*/*BRIT1* siRNA increased %PCC significantly in particular with *STK39* siRNA 2 (17.6%; *p* = 0.0473) and 3 (18.7%; *p* = 0.0255) compared to the positive control (NT-siRNA/*MCPH1*/*BRIT1* siRNA; presented in grey coloured column) (11.4%,). **(B2)** However, this double knockdown of these two siRNAs at 50nM reduced %PCC, and subsequently reduced the statistical significance *p* value, to 13.9% for *STK39* siRNA 2 and 15% for *STK39* siRNA 3.

MCPH1/BRIT1 knockdown increased %PCC, in particular with the individual *STK39* siRNAs 2 (17.6%) and 3 (18.7%) at 25nM compared to the PCC induced by the positive control (11.4%), demonstrating significant *p* values of 0.0473 and 0.0255, respectively (Figure 5.5 A2). However, this statistical difference was reduced after using 50nM with *STK39* siRNAs 2 and 3 and interestingly resulted in a reduction in %PCC to 13.9% for *STK39* siRNA 2 and 15% for *STK39* siRNA 3 (Figure 5.5 B2). This reduction in %PCC at 50nM may explain that *STK39* siRNA did not consider to be a PCC inducer since the control NT-siRNA/ *MCPH1*/*BRIT1* siRNA (double knockdown), the FT and RT *MCPH1*/*BRIT1* siRNA (single knockdown), usually shows a %PCC of 12 to 20% and the %PCC caused by this double knockdown of the four deconvoluted *STK39* siRNAs at 25nM and 50nM may simply be the consequence of the FT of MCPH1/BRIT1 knockdown. However, this reduction in %PCC after using *STK39* siRNA at 50nM may instead reflect its potential SL activity, killing the MCPH1/BRIT1 deficient cells that would otherwise display a PCC phenotype.

5.2.3.3.2 *VRK1* siRNA

The single knockdown for the four deconvoluted duplex siRNAs targeting *VRK1* clearly showed no effect on cell viability at 25nM and 50nM compared to either NT-siRNA (25nM or 50nM) or to untransfected cells. The mean cell number for *VRK1* siRNAs 1, 2, 3 and 4 at 25nM was 4938, 5766, 5489 and 5150 respectively compared to 5479 for the NT-siRNA. At 50nM, it was 2756, 4960, 5365 and 3912 respectively compared to 4313 for the NT-siRNA (Figure 5.6 A1 and B1).

Additionally, the effect of the four deconvoluted siRNAs targeting *VRK1* (25nM or 50nM) in % cell viability in cells treated with/or without *MCPH1*/*BRIT1* siRNA was analysed (Table 5.3 A and B). At 25nM, only *VRK1* siRNA 1 presented a reasonable reduction in % cell viability in the absence of MCPH1/BRIT1 with 68.9% compared to 90.1% in cells with a single siRNA knockdown of *VRK1* (Table 5.3A). *VRK1* siRNA 2, 3 and 4 at 25nM and in the absence of MCPH1/BRIT1 did not show a noticeable difference in % cell viability compared to those seen in the presence of MCPH1/BRIT1 (Table 5.3A). In contrast, *VRK1* siRNA 1 at 50nM showed no difference in % cell viability in cells treated with and without *MCPH1*/*BRIT1* siRNA (72. 3% and 63.9%, respectively) (Table 5.3B). However, *VRK1* siRNA 2 and 3 at 50nM demonstrated a reasonable reduction in % cell viability in cells in the absence of MCPH1/BRIT1 versus in the presence of MCPH1/BRIT1. The % cell viability was 67.4% vs. 115% for *VRK1* siRNA 2,

whereas it was 89.1% vs.124.4% for *VRK1* siRNA 3 (Table 5.3B). However, the double knockdown of *VRK1* siRNA 4 at 50nM with *MCPH1/BRIT1* siRNA did not greatly affect % cell viability (76.1%) compared to (90.7%) in cells treated with a single knockdown of *VRK1* siRNA 4 (Table 5.3B).

Table 5.3. Showing % cell viability and cell death rate for the four deconvoluted *VRK1* siRNA in cells treated with/or without *MCPH1/BRIT1* siRNA.
The validation experiment of the SL siRNA hit (***VRK1***) was performed in two concentrations 25nM **(A)** and 50nM **(B)**.

A. SL siRNA hits	Double knockdown (in the absence of MCPH1/BRIT1)			Single knockdown (in the presence of MCPH1/BRIT1)			Difference in %CV
Deconvoluted siRNA (25nM)	Average cell number	%Cell viability	Cell death rate	Average cell number	%Cell viability	Cell death rate	**%CVI-%CVM**
VRK1 siRNA 1	2423	68.9	31.1	4938	90.1	9.88	21.2
VRK1 siRNA 2	3707	105.4	-5.4	5766	105.2	-5.23	-0.2
VRK1 siRNA 3	3704	105.3	-5.3	5489	100.2	-0.18	-5.2
VRK1 siRNA 4	4212	119.8	-19.8	5150	94	6.02	-25.8
	Control: NT-MCPH1 siRNA			**Control: NT-siRNA**			
	Mean cell number	**3516**		**Mean cell number**	**5479**		

B. SL siRNA hits	Double knockdown (in the absence			Single knockdown (in the			Difference in %CV
Deconvoluted siRNA (50nM)	Average cell number	%Cell viability	Cell death rate	Average cell number	%Cell viability	Cell death rate	**%CVI-%CVM**
VRK1 siRNA 1	2783	72.3	27.7	2756	63.9	36.1	-8.4
VRK1 siRNA 2	2594	67.4	32.6	4960	115	-15	47.6
VRK1 siRNA 3	3430	89.1	10.9	5365	124.4	-24.4	35.2
VRK1 siRNA 4	2928	76.1	23.9	3912	90.7	9.3	14.6
	Control: NT-MCPH1 siRNA			**Control: NT-siRNA**			
	Mean cell number	**3848**		**Mean cell number**	**4313**		

In addition, all of the double knockdowns of the four deconvoluted *VRK1* siRNAs, at 25n and 50nM, decreased cell number in the absence of MCPH1/BRIT1 compared to those four deconvoluted siRNAs treated with NT-siRNA (25nM or 50nM) (Figure 5.6 A2 and B2).

To identify the deconvoluted *VRK1* siRNAs, at 25nM or 50nM, that were the most effective in significantly reducing the cell number compared to the control (NT-siRNA (25nM or 50nM) /*MCPH1/BRIT1* siRNA), the Unpaired t-test statistical analysis was performed. Consequently, only *VRK1* siRNA 1 at 25nM showed a low cell number (2423) in the absence of MCPH1/BRIT1 compared to the control (3515); however, this difference in the cell number was not significant ($p = 0.3011$) (Figure 5.6A2). The four deconvoluted *VRK1* siRNAs 1, 2, 3 and 4 at 50nM presented low cell number values of 2783, 2594, 3430 and 2928 respectively

compared to 3848 for the control (Figure 5.6B2). However, at 50nM in the absence of MCPH1/BRIT1, no individual *VRK1* siRNA reflected a statistically significant difference in cell number vs. the control (Figure 5.6B2). This is potentially due to the variation in the cell number observed between the two replicates, specifically at 50nM.

Although *VRK1* siRNA 2 and 3 at 50nM showed a reasonable reduction in % cell viability in cells in the absence of MCPH1/BRIT1 versus in the presence of MCPH1/BRIT1 (Table 5.3B), this reduction was not significant in comparison to the cell number of the control, the variation in the cell number between the two replicates may have influenced the results.
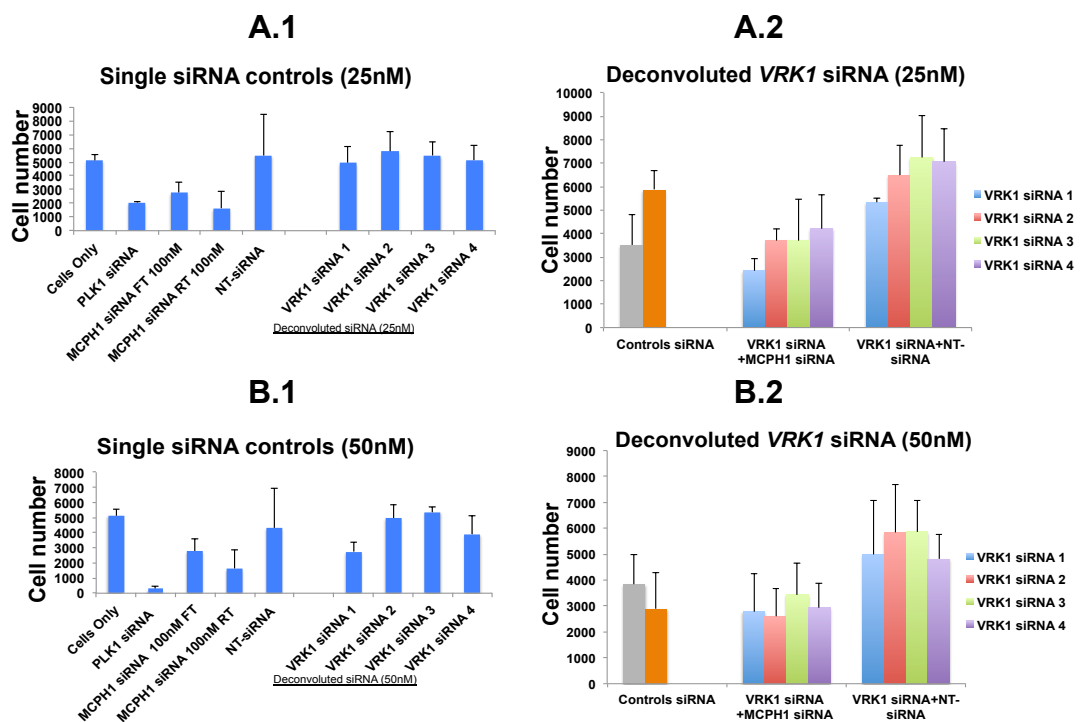
Figure 5.6. *VRK1* siRNA may induce SL in the absence of MCPH1/BRIT1.
(A1 and B1) single knockdown of the four deconvoluted *VRK1* siRNAs, at 25nM and 50nM, presented no significant effect on cell viability compared to the NT-siRNA. **(A2 and B2)** the double knockdown of these deconvoluted *VRK1* siRNAs, at 25nM **(A2)** and 50nM **(B2),** in combination with *MCPH1/BRIT1* siRNA clearly decreased cell viability compared to those deconvoluted *VRK1* siRNAs which were followed by FT with NT-siRNA (25nM or 50nM). **(A2)** in comparison to the cell number in the control (NT-siRNA (25nM)/MCPH1/BRIT1 siRNA presented in the grey coloured column) (3515.9), only *VRK1* siRNA 1 at 25nM showed low cell number (2423) but this was not significant. **(B2)** None of the deconvoluted *VRK1* siRNA 1, 2, 3 and 4 at 50nM followed by FT *MCPH1/BRIT1* siRNA showed a statistically significant difference in cell number (2783, 2594, 3430 and 2928, respectively) compared to 3848 in the control (grey column).

Thus, VRK1 siRNA may be considered as a weak SL siRNA hit and a further repeat of the validation for the *VRK1* siRNA may be warranted to confirm its potential synthetic lethality role in MCPH1/BRIT1 deficient cells.

VRK1 siRNA was not considered to be a PCC inducer since the level of PCC induced by the four deconvoluted *VRK1* siRNAs 1, 2, 3, and 4, at 25nM (14%, 17%, 18% and 14%, respectively) or 50nM (13%, 13%, 15% and 15%) in the absence of MCPH1/BRIT1 (Figures 6.7 A2 and B2) did not differ significantly from the standard level of PCC induced by a single RT or FT MCPH1/BRIT1 siRNA (between 12%-20%) (Figures 6.7 A1 and B1) or even from the %PCC shown in the control (NT-siRNA (25nM)/ MCPH1/BRIT1 siRNA) 11.4% or (NT-siRNA (50nM)/MCPH1/BRIT1 siRNA) 13.2% (Figures 6.7 A2 and B2).

A.1

A.2

B.1

B.2
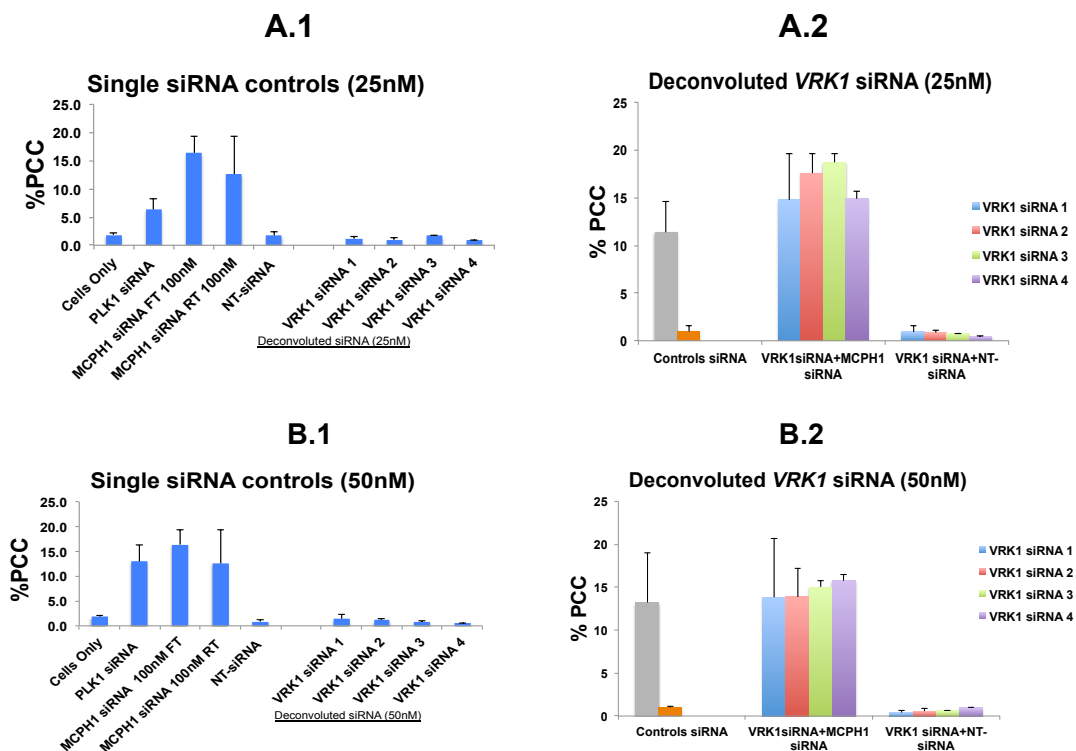
Figure 5.7. VRK1 siRNA is not an inducer for PCC phenotype.
(A1 and B1) Single knockdown with a FT of MCPH1/BRIT1 induced %PCC of 16% and with RT 12.6%. **(A2 and B2)** The %PCC for control (NT-siRNA (25nM)/ *MCPH1/BRIT1* siRNA) was 11.4% (**A2**, grey column) or in (NT-siRNA (50nM)/ *MCPH1/BRIT1* siRNA) was 13.2% (**B2**, grey column). **(A2 and B2)** In the absence of MCPH1/BRIT1 the level of PCC induced by the four deconvoluted *VRK1* siRNAs 1, 2, 3, and 4, at 25nM (14%, 17%, 18% and 14%, respectively) or at 50nM (13%, 13%, 15% and1 5%, respectively) did not differ significantly from the standard level of PCC induced by a single RT or FT *MCPH1/BRIT1* siRNA (between 12%-20%).

5.2.3.3.3 *TTK/MPS1* siRNA

The single knockdown for *TTK/MPS1* using the four deconvoluted siRNAs at 25nM or 50nM showed no significant effect on cell number compared to NT-siRNA (25nM or 50nM) or untransfected cells. The mean cell number for *TTK/MPS1* siRNA 1, 2, 3 and 4 at 25nM was 4143, 4707, 6403 and 5563 respectively

compared to 5479 for the NT-siRNA. Whereas, at 50nM it was 5078, 5063, 5491 and 3589 respectively compared to 4313 for the NT-siRNA (Figure 5.8 A1 and B1).

Furthermore, the impact of the four deconvoluted siRNAs targeting *TTK*/*MPS1* (25nM or 50nM) in % cell viability in cells treated with/or without *MCPH1*/*BRIT1* siRNA was examined (Table 5.4 A and B). At 25nM, *TTK*/*MPS1* siRNA 1 and 2 showed a reasonable difference in % cell viability compared to *TTK*/*MPS1* siRNA 3 and 4 in the absence of MCPH1/BRIT1 (Table 5.4A).

Table 5.4. Showing % cell viability and cell death rate for the four deconvoluted *TTK*/*MPS1* siRNA in cells treated with/or without *MCPH1*/*BRIT1* siRNA.
The validation experiment of the SL siRNA hit (***TTK*/*MPS1***) was performed in two concentrations 25nM **(A)** and 50nM **(B)**.

A. SL siRNA hits	Double knockdown (in the absence of MCPH1/BRIT1)			Single knockdown (in the presence of MCPH1/BRIT1)			Difference in %CV
Deconvoluted siRNA (25nM)	Average cell number	%Cell viability	Cell death rate	Average cell number	%Cell viability	Cell death rate	%CVI-%CVM
TTK siRNA 1	1891	53.8	46.2	4143	75.6	24.39	21.8
TTK siRNA 2	2455	69.8	30.2	4707	85.9	14.1	16.1
TTK siRNA 3	2929	83.3	16.7	6403	116.9	-16.86	33.6
TTK siRNA 4	3081	87.6	12.4	5563	101.5	-1.52	13.9
	Control: NT-MCPH1 siRNA			**Control: NT-siRNA**			
	Mean cell number	3516		**Mean cell number**	5479		

B. SL siRNA hits	Double knockdown (in the absence of MCPH1/BRIT1)			Single knockdown (in the presence of MCPH1/BRIT1)			Difference in %CV
Deconvoluted siRNA (50nM)	Average cell number	%Cell viability	Cell death rate	Average cell number	%Cell viability	Cell death rate	%CVI-%CVM
TTK siRNA 1	2032.5	52.8	47.2	5078.5	117.7	-17.7	64.9
TTK siRNA 2	2088	54.3	45.7	5063.5	117.4	-17.4	63.1
TTK siRNA 3	2927.5	76.1	23.9	5491	127.3	-27.3	51.2
TTK siRNA 4	1977	51.4	48.6	3589.5	83.2	16.8	31.8
	Control: NT-MCPH1 siRNA			**Control: NT-siRNA**			
	Mean cell number	3848		**Mean cell number**	4313		

The cell viability for *TTK*/*MPS1* siRNA 1 and 2 in the absence versus in the presence of MCPH1/BRIT1 was as follows; 53.8% vs. 75.6% and 69.8% vs. 85.9%, respectively (Table 5.4A). The % cell viability for *TTK*/*MPS1* siRNA 3 and 4 in the absence versus the presence of MCPH1/BRIT1 was as follows; 83.3% vs. 116.9% and 87.6% vs. 101.5%, respectively (Table 5.4A). In contrast, at 50nM *TTK*/*MPS1* siRNA 1, 2 and 4 showed a noticeable reduction in cell viability (≤ 54%) compared to *TTK*/*MPS1* siRNA 3 (76%) in the absence of MCPH1/BRIT1 (Table 5.4B). The % cell viability for *TTK*/*MPS1* siRNA 1, 2 and 3 and 4 in the absence versus the presence of MCPH1/BRIT1 was as follows; 52% vs.117%, 54 vs. 117%, 76.1% vs. 127% and 51 vs. 83% respectively.

Additionally, the double knockdown of *TTK*/*MPS1* using the four deconvoluted siRNAs, at 25nM or 50nM, in combination with *MCPH1*/*BRIT1* siRNA resulted in a noticeable reduction in cell number compared to cells with a co-depletion of TTK/MPS1 and NT-siRNA (25nM or 50nM) (Figures 6.8 A2 and B2).
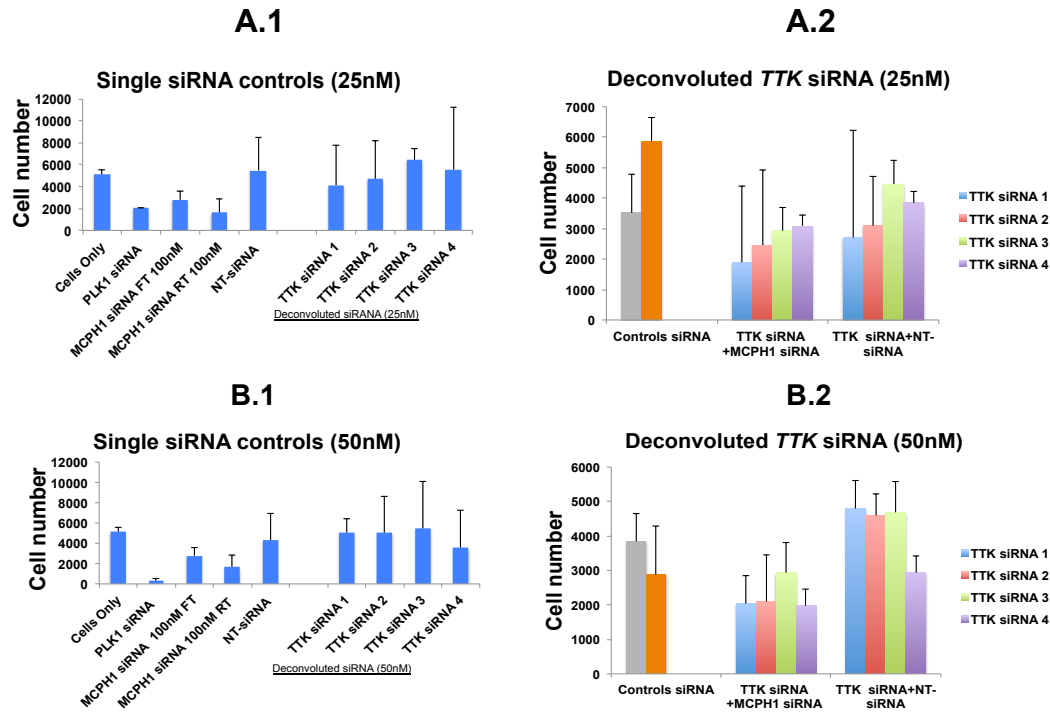
Figure 5.8. *TTK*/*MPS1* siRNA is a potential SL hit in the absence of MCPH1/BRIT1.
(A1 and B1) the single knockdown for *TTK*/*MPS1* using the four deconvoluted siRNA at 25nM or 50nM showed no effect on cell number. **(A2 and B2)** the double knockdown of *TTK*/*MPS1* using the four deconvoluted siRNAs, at 25nM or 50nM, in combination with *MCPH1*/*BRIT1* siRNA obviously decreased cell viability versus the *TTK*/*MPS1* depleted cells that followed with FT NT-siRNA (25nM or 50nM). **(A2)** the mean cell number for the four individual *TTK*/*MPS1* siRNAs (25nM) *MCPH1*/*BRIT1* versus when those deconvoluted siRNAs were followed by NT-siRNA (25nM) was as follows; 1891 vs 2714 for *TTK*/*MPS1* siRNA1, 2455 vs 3095 for *TTK*/*MPS1* siRNA 2, 2929 vs 4463 for *TTK*/*MPS1* siRNA 3 and 3081 vs 3844 for *TTK*/*MPS1* siRNA 4. While at 50nM **(B2)** the mean cell numbers were as follows; 2032 vs 4790 for *TTK*/*MPS1* siRNA1, 2088 vs 4598 for *TTK*/*MPS1* siRNA 2, 2927 vs 4690 for *TTK*/*MPS1* siRNA 3 and 1977 vs 2930 for *TTK*/*MPS1* siRNA 4. **(A2 and B2)** there was no significant statistical difference in the cell number between any of the four deconvoluted *TTK*/*MPS1* siRNAs in the absence of MCPH1/BRIT1, either at 25nM **(A2)** or 50nM **(B2)**, and the control ((NT-siRNA (at 25nM or 50nM)/MCPH1/BRIT1 siRNA; represented in grey column.

Furthermore, the cell number output from these four deconvoluted *TTK*/*MPS1* siRNAs, at 25nM or 50nM, in the absence of MCPH1/BRIT1, was lower than the output from the control (NT-siRNA (25nM)/*MCPH1*/*BRIT1* siRNA; (3516 cells); Figure 5.8A2; control column is grey) or (NT-siRNA (50nM) /*MCPH1*/*BRIT1* siRNA; (3848 cells); Figure 5.8B2; control column is grey). However, there was no significant statistical difference in the cell number between the *TTK*/*MPS1* siRNA in the absence of MCPH1/BRIT1 and the control. This again may potentially be due to

the variation in the cell number of the four deconvoluted siRNAs between the two replicates, which led to a reduction in the statistical significance of the results.

However, TTK/MPS1 may be considered as a SL hit based on the clear reduction in cell viability caused by these four individual siRNAs in the absence of MCPH1/BRIT1 compared to either the double knockdown of these four individual siRNAs with NT-siRNA (Figure 5.8 A2 and B2) or to the single knockdown using these four siRNAs (Table 5.4 A and B).

The four individual *TTK/MPS1* siRNAs at 25nM induced PCC level in the absence of MCPH1/BRIT1 (Figure 5.9).

A.1

A.2

B.1

B.2
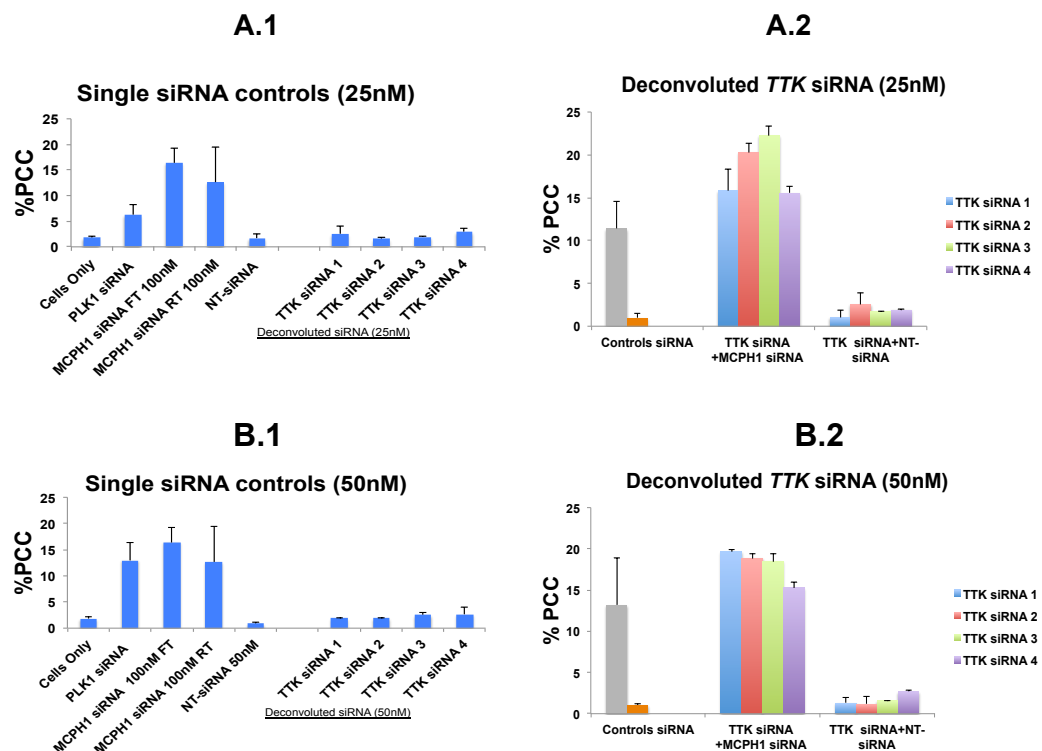
Figure 5.9. *TTK/MPS1* siRNA may have a potential effect on increasing PCC.
(A1 and B1) single knockdown of *TTK/MPS1* siRNA using four individual *TTK/MPS1* siRNAs at 25nM and 50nM did not induce PCC. **(A2)** the double knockdown of the four deconvoluted siRNAs at 25nM increased %PCC level in the absence of MCPH1/BRIT1. The mean %PCC for *TTK/MPS1* siRNAs 1, 2, 3 and 4 when followed by FT *MCPH1/BRIT* siRNA was 15%, 20%, 22%, and 15%, respectively and *TTK/MPS1* siRNA 2 (20.3%; p = 0.0105) and *TTK/MPS1* siRNA 3 (22%; p = 0.0064) showed a significant difference in %PCC in the positive control (grey column) (11.4%). **(B2)** the mean %PCC for the four deconvoluted *TTK/MPS1* siRNAs at 50nM in the absence of MCPH1/BRIT1 remained high, which was 19%, 18%, 18% and 15% for *TTK/MPS1* siRNAs 1, 2, 3, and 4, respectively, but they were not statistically significant compared to the control ((NT-siRNA (50nM)/*MCPH1/BRIT1* siRNA (13.2%), grey column.

The mean %PCC for *TTK/MPS1* siRNAs 1, 2, 3 and 4 when followed by FT *MCPH1/BRIT* siRNA was 15%, 20%, 22%, and 15% respectively. However, only *TTK/MPS1* siRNA 2 (20.3%) and *TTK/MPS1* siRNA 3 (22%) showed a significant

difference in %PCC induced by the siRNA and the control (NT-siRNA (at 25nM)/MCPH1/BRIT1 siRNA) (11.4%), showing a p value of 0.0105 and 0.0064 respectively (Figure 5.9A2). This statistical significance was reduced after using the four deconvoluted siRNAs at 50nM in the absence of MCPH1/BRIT1. The mean %PCC for the four deconvoluted *TTK/MPS1* siRNAs at 50nM in the absence of MCPH1/BRIT1 slightly decreased to 19%, 18%, 18% and 15% for *TTK/MPS1* siRNAs 1, 2, 3, and 4, respectively compared to the control (NT-siRNA (at 50nM)/MCPH1/BRIT1 siRNA) (13.2%) (Figure 5.9B2).

A further repeat for validation *TTK/MPS1* siRNA may be needed to confirm its potential role in induction of PCC alongside its synthetic lethality effect in killing these PCC cells observed in MCPH1/BRIT1 deficient cells.

5.2.3.3.4 *CDK1/CDC2* siRNA

In order to validate whether CDK1/CDC2 is a potential SL siRNA hit, a reverse transfection of four individual siRNAs targeting CDK1/CDC2 at 25nM and 50nM was followed individually by a FT of *MCPH1/BRIT1* siRNA (100nM). In addition, a RT of the four individual *CDK1/CDC2* siRNAs followed by a FT of NT-siRNA individually at 25nM and 50nM was performed to monitor the effect on cell number that might be caused by the double knockdown of the SL siRNA hit in the absence of MCPH1/BRIT1.

Single knockdown of these four individual *CDK1/CDC2* siRNAs did not show any noticeable effect on cell number at 25nM and 50nM compared to the cell number treated with single knockdown NT-siRNA (Figures 6.10 A1 and B1).

Additionally, the percentage difference in cell viability between the double knockdown of the four individual *CDK1/CDC2* with *MCPH1/BRIT1* siRNA and the single knockdown of these individual siRNAs was calculated relative to the controls NT-MCPH1/BRIT1 siRNA and NT-siRNA respectively (Table 5.5 A and B). Unexpectedly the %cell viability for *CDK1/CDC2* siRNA 1 at 25nM was similar in the absence and presence of MCPH1/BRIT1 at 83.6% and 78.1% respectively (Table 5.5A). Double knockdown of *CDK1/CDC2* siRNA 2 (25nM) with *MCPH1/BRIT1* siRNA showed a small difference in % cell viability with the single knockdown of *CDK1/CDC2* siRNA 2 (71.6% compared to 79.5%; Table 5.5A).

However, a reasonable reduction in % cell viability was caused by knockdown of *CDK1/CDC2* siRNA 3 (25nM) in combination with *MCPH1/BRIT1* siRNA (77.1%) compared to the % cell viability in the single siRNA knockdown (112.7%; Table 5.5A).

Table 5.5. Showing % cell viability and cell death rate for the four deconvoluted *CDK1/CDC2* siRNA in cells treated with/or without *MCPH1/BRIT1* siRNA.
The validation experiment of the SL siRNA hit (***CDK1/CDC2***) was performed in two concentrations 25nM **(A)** and 50nM **(B)**.

A. SL siRNA hits	Double knockdown (in the absence of MCPH1/BRIT1)			Single knockdown (in the presence of MCPH1/BRIT1)			Difference in %CV
Deconvoluted siRNA (25nM)	Average cell number	%Cell viability	Cell death rate	Average cell number	%Cell viability	Cell death rate	**%CVI-%CVM**
CDK1 siRNA 1	2941	83.6	16.4	4279	78.1	21.91	-5.6
CDK1 siRNA 2	2519	71.6	28.4	4358	79.5	20.47	7.9
CDK1 siRNA 3	2711	77.1	22.9	6175	112.7	-12.69	35.6
CDK1 siRNA 4	3491	99.3	0.7	6689	122.1	-22.08	22.8
	Control: NT-MCPH1 siRNA			**Control: NT-siRNA**			
	Mean cell number	**3515**		**Mean cell number**	**5479**		

B. SL siRNA hits	Double knockdown (in the absence of MCPH1/BRIT1)			Single knockdown (in the presence of MCPH1/BRIT1)			Difference in %CV
Deconvoluted siRNA (50nM)	Average cell number	%Cell viability	Cell death rate	Average cell number	%Cell viability	Cell death rate	**%CVI-%CVM**
CDK1 siRNA 1	2212	57.5	42.5	4346	100.7	-0.7	43.3
CDK1 siRNA 2	2655	69	31	3704	85.9	14.1	16.9
CDK1 siRNA 3	1251	32.5	67.5	3420	79.3	20.7	46.8
CDK1 siRNA 4	2643	68.7	31.3	4858	112.6	-12.6	44
	Control: NT-MCPH1 siRNA			**Control: NT-siRNA**			
	Mean cell number	**3847.5**		**Mean cell number**	**4313**		

No difference in % cell viability was observed in cells treated with *CDK1/CDC2* siRNA 4 (25nM) either in the absence or presence of MCPH1/BRIT1 (99.3% and 122.1% respectively; Table 5.5A). However, the %cell viability in cells treated with *CDK1/CDC2* siRNA at 50nM was higher than those observed at 25nM (Table 5.5B), suggesting that the 50nM siRNA concentration may be more effective at inhibiting the gene of interest. In addition, this confirmed our initial finding with the transfection efficiency read out control (pooled *PLK1* siRNA) that showed a massive reduction in cell number at 50nM but not at 25nM. The % cell viability in *CDK1/CDC2* siRNA 1 (50nM) was 57% in the absence of MCPH1/BRIT1 compared to 100% in its presence (Table 5.5B). *CDK1/CDC2 siRNA* 2 at 50nM*,* however, showed results similar to those seen at 25nM, causing a small reduction in % cell viability between cells treated with *MCPH1/BRIT1* siRNA and those that were not (69% vs. 85.9%; Table 5.5B). *CDK1/CDC2 siRNA* 3 and 4 at 50nM demonstrated a large difference in % cell viability in the absence of MCPH1/BRIT1 vs. in its presence (32.5% vs. 79.3%) and (68.7% vs. 112.6), respectively (Table 5.5B).

Next, a comparison of cell number was performed between cells treated with *CDK1*/*MCPH1* siRNAs and cells treated with *CDK1*/NT siRNAs at both concentrations. Notably, all four deconvoluted siRNAs targeting *CDK1*/*CDC2* in combination with *MCPH*/*BRIT1* siRNA showed a clear reduction in cell number at 25nM and 50nM compared to the double transfection of CDK1/CDC2 siRNA with NT- siRNA (Figure 5.10 A2 and B2).
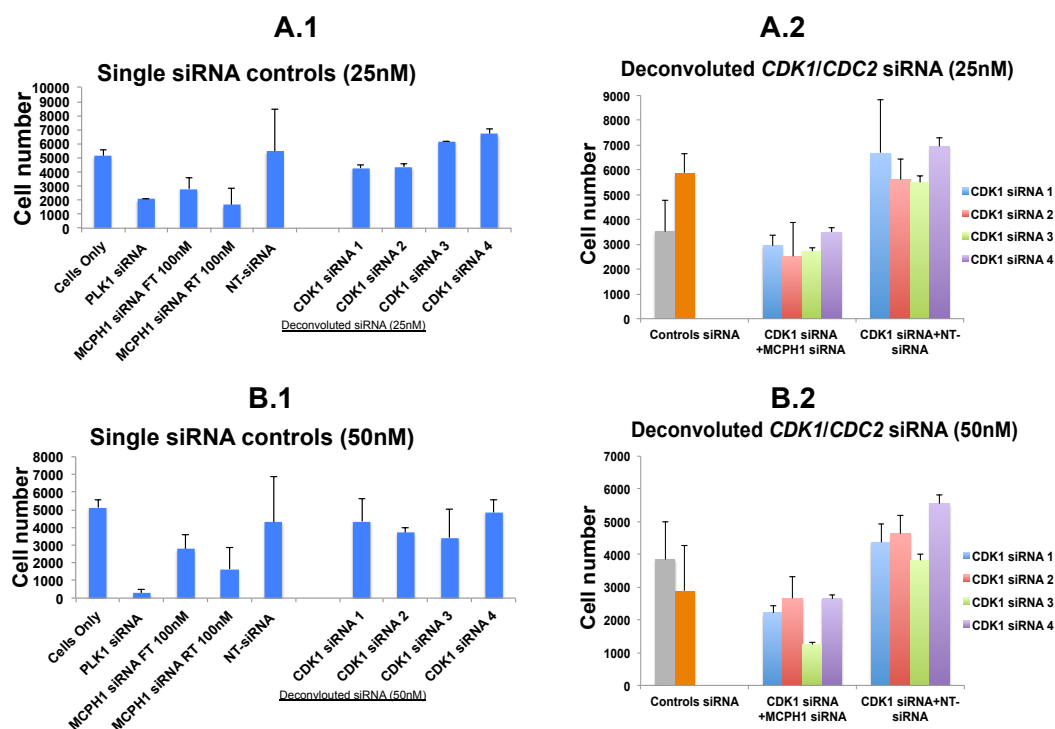
Figure 5.10. CDK1/CDC2 was a potential synthetic lethal siRNA in the absence of MCPH1/BRIT1 function.
Description for the single knockdown siRNA controls **(A1 and B1)** at 25 and 50nM was detailed in (**Figure 5.4**). Validation for *CDK1*/*CDC2* using the four deconvoluted siRNAs alone at 25nM and 50nM showed no effect on cell number compared to NT-siRNA **(A1 and B1)**. These four deconvoluted siRNAs, at 25nM (**A2**) and 50nM (**B2**), clearly reduced the cell number with *MCPH1*/*BRIT1* siRNA compared to those followed by NT-siRNA. Only CDK/CDC siRNA 1 and 3 at 50nM (**B2**) showed a significant reduction in cell number (2212) and (1251) compared to the control (NT-siRNA/*MCPH1*/*BRIT1* siRNA; presented in grey coloured column) (3874.50) with a *p* value of 0.017 and 0.0294, respectively.

Afterwards, statistical analysis was performed using an Unpaired t-test to identify the statistical significance of the individual duplex siRNA that showed a dramatic reduction in cell viability compared to the control with double knockdown (NT-siRNA at 25nM or 50nM/ MCPH1/BRIT1 siRNA 100nM). The control at 25nM showed a cell number of 3516, which was 3848 at 50nM (Figures 6.10 A2 and B2; the control is the grey column). Consequently, at a concentration of 25nM, the four deconvoluted *CDK1*/*CDC2* siRNAs, in the absence of MCPH1/BRIT1, showed cell number values relatively lower than the control (NT-siRNA (25nM)/ *MCPH1/BRIT1* siRNA). However, none of these four siRNAs at a concentration of 25nM showed a

statistically significant reduction in cell number versus the control (Figure 5.10 A2). On the other hand, in comparison to the control, the mean cell number for the four deconvoluted CDK1/CDC2 siRNAs at 50nM and in combination with *MCPH1/BRIT1* siRNA, was reduced, showing a statistically significant result for siRNA 1 (2212) and 3, (1251) with *p* values of 0.017 and 0.0294, respectively (Figure 5.10 B2).

Interestingly, attempts had previously been made to validate CDK1/CDC2 using single knockdown as a potential hPK siRNA that would induce PCC, but without great success (Chapter 4; Section 4.2.1.5; Figure 4.7). Here, similar results were obtained since single knockdown of *CDK1/CDC2* using the four deconvoluted siRNAs at 25nM and 50nM showed no effect on PCC level (Figure 5.11 A1 and B1). However, the double knockdown of the four deconvoluted CDK1/CDC2 siRNAs, at 25nM and 50nM, followed by the FT *MCPH1/BRIT1* siRNA efficiently increased the level of PCC compared to those four deconvoluted *CDK1/CDC2* siRNAs that were followed by FT of NT-siRNA at 25nM or 50nM (Figure 5.11 A2 and B2).

Then, an unpaired t-test was performed to ascertain the extent to which the four individual duplex siRNAs targeting the *CDK1/CDC2* at 25nM and 50nM in the absence of MCPH1/BRIT1 affected the level of PCC relative to the control (NT-siRNA (25 or 50nM)/ *MCPH1/BRIT1* siRNA (100nM)). Consequently, it was found that *CDK1/CDC2* siRNA 1 and 3 at both 25nM and 50nM in the absence of MCPH1/BRIT1 increased the %PCC significantly compared to the control. The mean %PCC for the double knockdown of the control was 11.39% at 25nM and 13.20% at 50nM (n = 6 wells). The mean %PCC for *CDK1/CDC2* siRNA 1 at 25nM in the absence of MCPH1/BRIT1 was 29.11% (*p* = 0.0003; n = 2 wells), which increased to 40% (*p* = 0.0059; n = 2 wells) at 50nM. The mean %PCC for *CDK1/CDC2* siRNA 3 at 25nM in the absence of MCPH1/BRIT1 was 31.6% (*p* = 0.0210; n = 2 wells) and at 50nM it was 23.87% (*p* = 0.0489; n = 2 wells) (Figure 5.11 A2 and B2). In addition, in the absence of MCPH1/BRIT1, at 25nM and 50nM, the *CDK1/CDC2* siRNA 2, showed an increase in %PCC at 31% and 22% respectively. However, in comparison to the %PCC induced by the control at 25nM (11.39%), *CDK1/CDC2* siRNA 2 presented a significant *p* value of 0.0455 at only 25nM (Figure 5.11 A2). Moreover, in the absence of MCPH1/BRIT1, *CDK1/CDC2* siRNA 4 at 25nM showed a mean %PCC of 27.7%, which increased slightly to 32.58% at 50nM, only showing a significant *p* value of 0.0175 at 50nM (Figure 5.11 B2). Depletion of CDK1/CDC2 triggered significant synthetic lethality and may have the potential effect in inducing PCC in MCPH1/BRIT1 deficient cells.
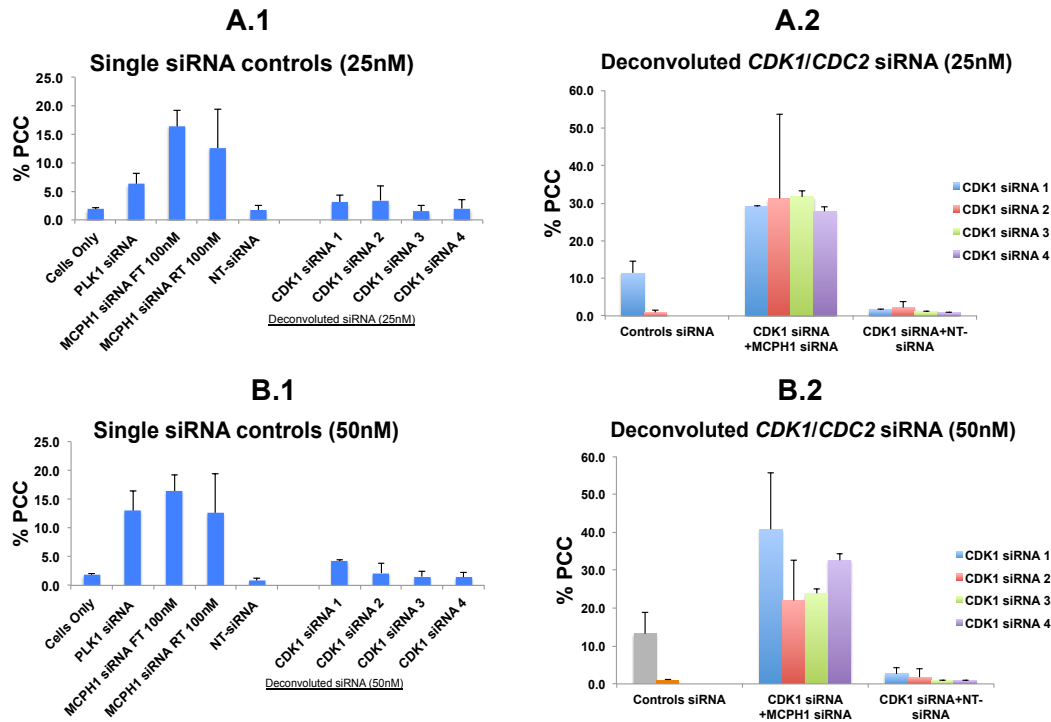
Figure 5.11. CDK1/CDC2 siRNA elevated the level of PCC in the absence of MCPH1/BRIT1 function.

Description for %PCC induced by the single knockdown siRNA controls **(A1 and B1),** at 25 and 50nM was detailed in **(Figure 5.5)**. Single knockdown of *CDK1/CDC2* using the four deconvoluted siRNAs alone at 25nM and 50nM did not induce PCC in the presence of intact MCPH1/BRIT1 in U2OS cells **(A1 and B1)**. These four deconvoluted siRNAs, at 25nM **(A2)** and 50nM **(B2)**, induced a high level of PCC with *MCPH1/BRIT1* siRNA compared to those followed by NT-siRNA. **(A2 and B2)** The forward double transfection of control NT-siRNA (25nM and 50nM)/*MCPH1/BRIT1* siRNA (100nM), represented in grey coloured column, showed a % PCC value of (11.4%) at 25nM **(A2)** and (13.2%) at 50nM **(B2)**. Only *CDK1/CDC2* siRNA 1 and 3 significantly showed a high %PCC at 25 **(A2)** and 50nM **(A2)**; For siRNA 1 this was 29.11% (p = 0.0003) and 40% (p = 0.0059), respectively and for siRNA 3 %PCC this was 31.6% (p = 0.0210) and 23.87% (p = 0.0489), respectively. In the case of *MCPH1/BRIT1* siRNA, *CDK1/CDC2* siRNA 2 at 25nM **(A2)** and *CDK1/CDC2* siRNA 4 at only 50nM **(B2)** showed an increase in %PCC of 31% (p = 0.0455) and 32.58% (p = 0.0175), respectively.

5.2.3.3.5 *PLK1* siRNA

Single knockdown with *PLK1* siRNA at 25nM using the four individual siRNAs revealed similar cell number results to those observed with double knockdown. The mean cell number for *PLK1* knockdown alone at 25nM for siRNA 1, 2 and 3 was 2969, 390 and 1841 which reduced significantly to 119, 97 and 139 at a concentration of 50nM (Figure 5.12 A1 and B1). However, single *PLK1* siRNA 4 or its double knockdown with *MCPH1/BRIT1* siRNA did not decrease cell number either at a 25nM or a 50nM concentration. The mean cell number for *PLK1* siRNA 4 (single knockdown) was 6611 at 25nM and 4705 at 50nM (Figure 5.12 A1 or B1)

The double knockdown of *PLK1* siRNA 4 with *MCPH1/BRIT1* siRNA showed a mean cell number of 5184 at 25nM and 3775 at 50nM (Figures 6.12 A2 and B2).

Additionally, we employed the statistical method to demonstrate the percentage difference in cell viability of each individual siRNA targeting *PLK1* in the presence or absence of MCPH1/BRIT1 to define the most effective individual siRNA out of the four that greatly reduces cell viability in the absence of MCPH1/BRIT1 compared to its presence (Table 5.6 A and B). The deconvoluted *PLK1* siRNA 1 at 25nM combined with *MCPH1/BRIT1* siRNA (100nM) showed a reduction in % cell viability to 26.8% compared to 54% in cells with a knockdown using *PLK1* siRNA 1 alone. Unexpectedly, the % cell viability in cells treated with a double knockdown including *PLK1* siRNA 2 (25nM) and *MCPH1/BRIT1* siRNA was higher 29.7% than the single siRNA knockdown 7.1%. But, no difference in % cell viability for *PLK1* siRNA 3 was observed either in the absence or presence of MCPH1/BRIT1*,* demonstrating similar reduction in % cell viability (36.4% vs. 33.6% respectively). The reduction in cell viability was not seen in cells treated with *PLK1* siRNA 4 (25nM) either in the absence or presence of MCPH1/BRIT1 (147.4% vs. 120.7% respectively (Table 5.6A).

Similar analysis was performed in cells treated with the four individual *PLK1* siRNAs at a concentration of 50nM in both conditions (with or without 100nM *MCPH1/BRIT1* siRNA) (Table 5.6B). A similar reduction in % cell viability was observed in cells treated with *PLK1* siRNA 1, 2 and 3 in the absence or presence of MCPH1/BRIT1, demonstrating a decrease in %cell viability at 1.1%, 1.3% and 3% or 2.8%, 2.2% and 3.2%, respectively. The *PLK1* siRNA 4 at (50nM) showed a similar finding to that observed at 25nM, indicating no reduction in % cell viability in cells treated with *MCPH1/BRIT1* siRNA (98.1%) compared to those without treatment (109.1%) (Table 5.6B). This confirms that the transfection procedures used during the implementation of the SL siRNA experiment were effective and robust.

Table 5.6. Showing % cell viability and cell death rate for the four deconvoluted *PLK1* siRNA in cells with/or without *MCPH1*/*BRIT1* siRNA.

The validation experiment of the SL siRNA hit (*PLK 1*) was performed in two concentrations 25nM **(A)** and 50nM **(B)**.

A. SL siRNA hits	Double knockdown (in the absence of MCPH1/BRIT1)			Single knockdown (in the presence of MCPH1/BRIT1)			Difference in %CV
Deconvoluted siRNA (25nM)	Average cell number	%Cell viability	Cell death rate	Average cell number	%Cell viability	Cell death rate	%CVI-%CVM
PLK1 siRNA 1	942	26.8	73.2	2969	54.2	45.8	27.4
PLK1 siRNA 2	1044	29.7	70.3	390	7.1	92.9	-22.6
PLK1 siRNA 3	1280	36.4	63.6	1841	33.6	66.4	-2.8
PLK1 siRNA 4	5184	147.4	-47.4	6611	120.7	-20.7	-26.8
	Control: NT-MCPH1 siRNA			**Control: NT-siRNA**			
	Mean cell number	**3515**		**Mean cell number**	**5479**		

B. SL siRNA hits	Double knockdown (in the absence of MCPH1/BRIT1)			Single knockdown (in the presence of MCPH1/BRIT1)			Difference in %CV
Deconvoluted siRNA (50nM)	Average cell number	%Cell viability	Cell death rate	Average cell number	%Cell viability	Cell death rate	%CVI-%CVM
PLK1 siRNA 1	41	1.1	98.9	119	2.8	97.2	1.7
PLK1 siRNA 2	51	1.3	98.7	97	2.2	97.8	0.9
PLK1 siRNA 3	115	3	97	139	3.2	96.8	0.2
PLK1 siRNA 4	3775	98.1	1.9	4705	109.1	-9.1	11
	Control: NT-MCPH1 siRNA			**Control: NT-siRNA**			
	Mean cell number	**3848**		**Mean cell number**	**4313**		

Furthermore, since the validation experiment included a double siRNA knockdown using the four individual siRNAs with either *MCPH1*/*BRIT1* siRNA or with NT-siRNA, a comparison of cell number was performed between these conditions. There was no large difference identified in cell number between cultures treated with *PLK1*/*MCPH1*/*BRIT1* siRNAs and *PLK1*/NT siRNAs. However, both types of double knockdown showed a massive loss of cell number, in particular with the individual *PLK1* siRNA1, 2 and 3 whereas *PLK1* siRNA4 showed no noticeable change on cell number when either combined with *MCPH1*/*BRIT1* siRNA or NT-siRNA (Figures 5.12 A2 and B2).

Collectively, all the aforementioned analyses or observations demonstrated that *PLK1* siRNA was not considered to be a valid SL siRNA hit since there was no significant difference in reduction of cell viability between single knockdown of *PLK1* siRNA 1, 2 and 3 or their double knockdown at 50nM with *MCPH1*/*BRIT1* siRNA (Figure 5.12 B1 and B2). Also, as shown in (Figure 5.12) A1 and A2 or B1 and B2, the *PLK1* siRNA 4 as a single knockdown (A1 and B1) or double knockdown (A2 and B2) was not effective in suppressing expression of its target.

A.1

Single siRNA controls (25nM)

A.2

Deconvoluted *PLK1* siRNA (25nM)

B.1

Single siRNA controls (50nM)

B.2

Deconvoluted *PLK1* siRNA (50nM)
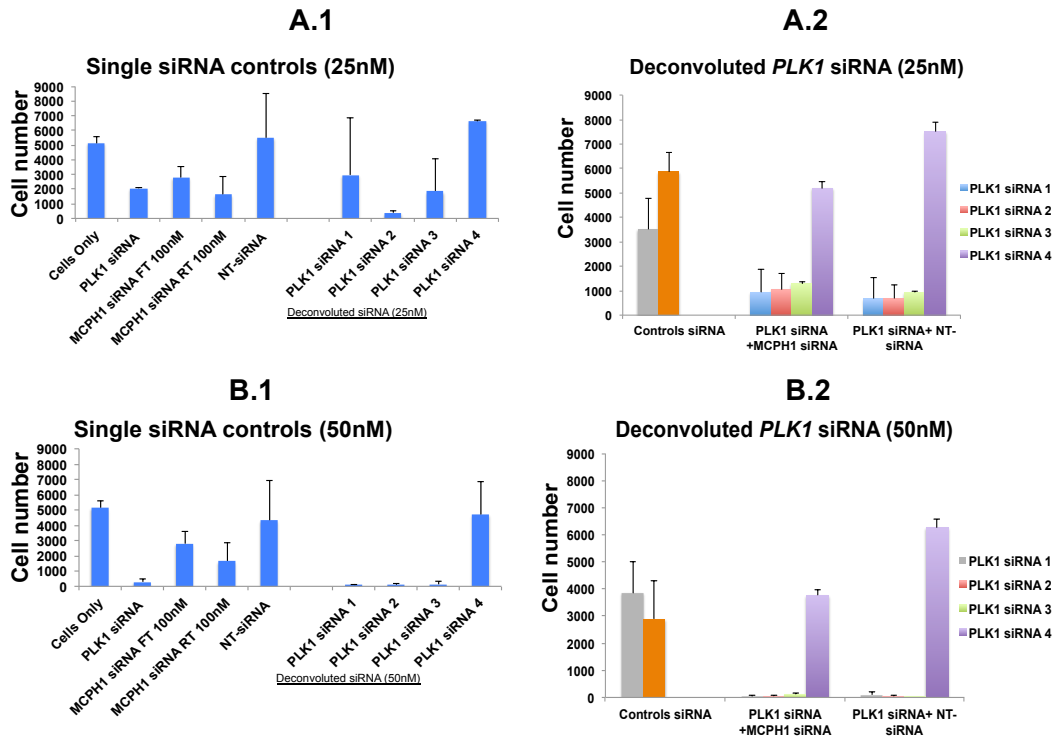
Figure 5.12. *PLK1* siRNA was not considered to be a valid SL siRNA.
Graphs showing the validation results for *PLK1* siRNA using four deconvoluted siRNA at 25nM and 50nM. Description of the single knockdown siRNA controls **(A1 and B1)** at 25nM and 50nM was detailed in **(Figure 5.4)**. In (**A1 and B1**) showing the cell number for single knockdown of four deconvoluted *PLK1* siRNAs at 25nM and 50nM respectively. Graphs in **(A2 and B2)** show that the first three deconvoluted *PLK1* siRNAs unexpectedly reduced the cell number by similar amounts when combined with *MCPH1/BRIT1* siRNA or the NT-siRNA. However the individual *PLK1* siRNA 4 at 25nM and 50nM showed no effect in cell number at either 25nM or 50nM indicating failure to knockdown *PLK1* expression.

Interestingly, single knockdown of *PLK1* siRNA at either 25nM or 50nM showed PCC from 9% to 13% (Figure 5.13 A1 and B1) and this increased to ≥ 20% after knockdown of MCPH1/BRIT1 (Figures 5.13 A2 and B2). However, visual inspection of the wells showed that the PCC detected by the Columbus analysis software was due to a significant loss in cell viability; thus PLK1 was considered to be a false positive hit for inducing PCC in U2OS cells.

Collectively, four SL siRNA hits out of five were successfully validated, namely STK39, VRK1 and TTK/MPS1, which all induced significant synthetic lethality in MCPH1/BRIT1 deficient cells. In addition, CDK1/CDC2 induced significant synthetic lethality and may also be involved in increasing the occurrence of PCC in MCPH1/BRIT1 deficient cells.

A.1

Single siRNA controls (25nM)

A.2

Deconvoluted *PLK1* siRNA (25nM)

B.1

Single siRNA controls (50nM)

B.2

Deconvoluted *PLK1* siRNA (50nM)
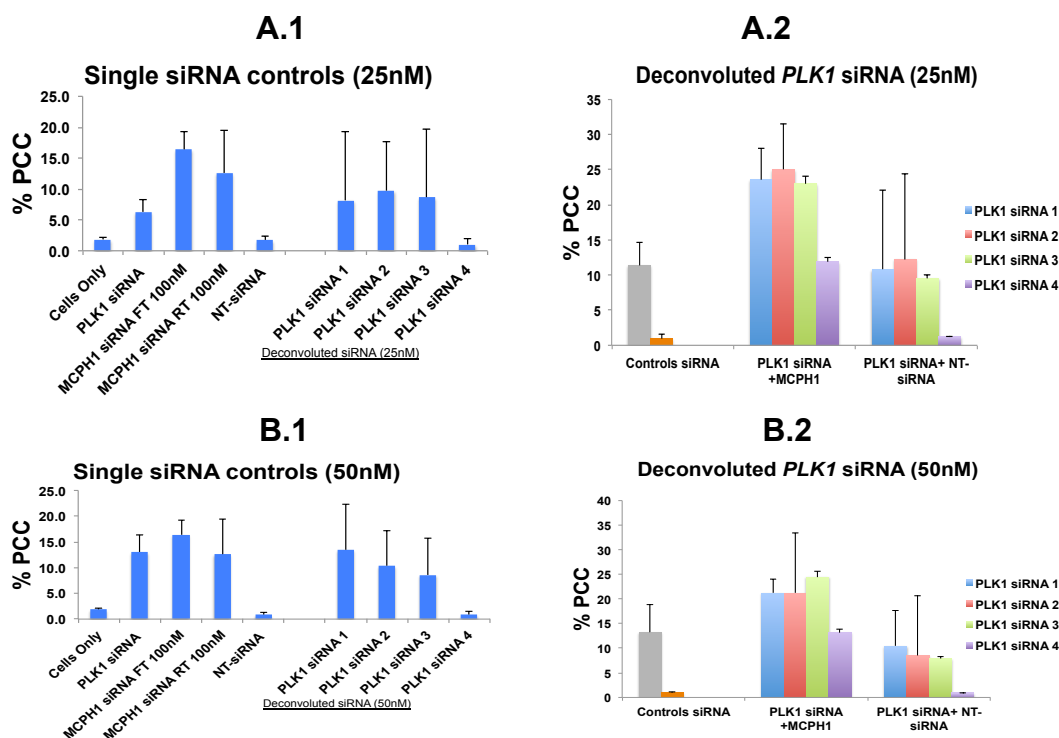
Figure 5.13. *PLK1* siRNA was not considered to be PCC inducer hit.
Description of the single knockdown siRNA controls **(A1 and B1)** at 25nM and 50nM was detailed in **(Figure 5.5)**. Graphs show the %PCC results from *PLK1* siRNA using four deconvoluted siRNA at 25nM and 50nM. The single knockdown **(A1 and B1)** or double knockdown **(A2 and B2)** for *PLK1* using the deconvoluted siRNAs at 25nM and 50nM showed false high %PCC which was due to cell death not the efficient siRNA transfection.

5.2.3.4 Evaluating the knockdown of SL siRNA hits

Due to the time limits imposed on this doctoral research, it was not possible to carry out further confirmation experiments of the knockdown efficiency of the four validated SL siRNAs by qRT-PCR or WB.

5.3 Discussion

5.3.1 Advantages of combining the cell viability data from PCC modifier and PCC inducer hPK siRNA screens to identify SL siRNA hits

The Operetta high throughput imaging system and Columbus analysis software were used to perform two complementary hPK siRNA screens, which were originally performed to identify genes which either induced PCC in the presence of functional MCPH1/BRIT1 (a PCC-inducer screen with a single

knockdown) or increased/decreased PCC caused by MCPH1/BRIT1 knockdown (a PCC-modifier screen with double knockdown). These screens could lead to the identification of potential MCPH1/BRIT1 interaction partner genes that may be involved in the regulation of chromosome condensation and other cellular pathways. In addition, these complementary hPK siRNA screens also provided cell viability data with and without MCPH1/BRIT1 knockdown, which were used in this study to identify SL siRNA hits. These hits would identify genes whose loss of function specifically reduced cell viability in the absence of functional MCPH1/BRIT1.

Each hPK siRNA screen (PCC inducer and PCC modifier) was performed in duplicate. Cell number was compared between the replicate 1 and 2 of each individual screen. Both screens presented a strong, positive and significant Spearman correlation, indicating the robustness of the assay procedures used to perform the hPK siRNA screens. Additionally, the SSMD was calculated for the functional readout siRNA controls (*PLK1* and *INCENP*) that were initially used to assess siRNA transfection efficacy based on a reduction in cell number in both replicates of the PCC modifier screen (Adams *et al.*, 2014). The SSMD for *PLK1* was 9.27 in the first batch and 12.12 in the second whilst for *INCENP*, for the first batch SSMD was 6.38 and for the second 7.41 (Adams *et al.*, 2014). These values confirm a strong reduction in cell number caused by these siRNA controls compared to the NT-siRNA controls, indicating their suitability as markers for monitoring transfection efficiency and the effect on cell number during screening and analysis procedures.

The integration of cell viability data from the PCC inducer and modifier screens does not only identify potential SL siRNA hits, it can also characterise other cellular changes resulting from the single or double siRNA knockdown of the kinase hits as long as these cellular parameters could be derived from the experimental data collected. For example, %PCC was used as an additional readout caused by the depletion of SL siRNA hit in MCPH1/BRIT1 deficient cells. This additional data could potentially lead to the identification of links between MCPH1/BRIT1 and the SL gene product in different cellular pathways, such as cell cycle checkpoints, DNA condensation mechanisms and apoptosis. Defining the role of SL hPK genes in cancer cells deficient in MCPH1/BRIT1 could lead to the identification of potential small molecule therapeutics for those patients with BC (93/319, 29%) and ovarian cancer (89/294, 30%) with reduced MCPH1/BRIT1 protein level who are resistant to current chemotherapies (Richardson *et al.*, 2011; Alsiary *et al.*, 2014). This approach revealed four potential SL hits, three of which exhibited a similar lethality

phenotype in the absence of MCPH1/BRIT1; these were STK39, VRK1 and TTK/MPS1. CDK1/CDC2 was a SL hit that also potentially increased PCC.

PLK1 was excluded as a SL gene in MCPH1/BRIT1 deficient cells and the reason for its identification as a false positive was confirmed. In this study, *PLK1* siRNA induced a similar loss in cell viability alone and in cells treated with double knockdown of *PLK1* and *MCPH1/BRIT1*. Interestingly, PLK1 induces cell death with/without p53 in HeLa, DU145 (prostate carcinoma) and T98G (glioblastoma multiforme) cell lines (Liu and Erikson, 2003). The single or co-depletion of PLK1 with p53 in HeLa cells triggers the DDR, inducing γH2AX foci formation, indicating that the DDR in PLK1 depleted cells is independent of p53. Addtionally, it was previously reported that inhibition of PLK1 alone in normal cell lines, such as MCF10A or hTERT-RPE1, had no effect on cell cycle arrest or cell proliferation (Liu *et al.*, 2006; Yim and Erikson, 2009). However, co-depletion PLK1 with p53 affected mitotic progression and induced cell death in non-cancerous breast MCF10A cells. These displayed multipolar spindles at prophase, misaligned chromosomes during M phase and chromosome lagging during anaphase (Liu *et al.*, 2006; Yim and Erikson, 2009). Thus, in p53-deficient cells, short-term depletion of PLK1 potentially kills tumour cells, allowing normal cells with functional WT-p53 to survive (Guan *et al.*, 2005). We might be speculated that similar bio-reaction potentially occurred in PLK1-MCPH1/BRIT1 co-depleted U2OS cells since both p53 and MCPH1/BRIT1 are essential regulators in DNA damage checkpoint and apoptosis. Consequently, co-depletion PLK1 siRNA with MCPH1/BRIT1 may cause a crucial lethality and affect normal cells instead of targeting only MCPH1/BRIT1 deficient cancer cells.

Further explanation for the SL genes will be detailed below.

An analytical search was conducted using STRING 10 for identifying the regulatory pathways and networks that SL hits and MCPH1/BRIT1 may be involved in. The relationship of each potential SL siRNA hit with MCPH1/BRIT1 was individually identified and is represented in Figures 5.14, 5.15, 5.16 and 5.17.

5.3.2 *STK39* siRNA is a potential SL gene in MCPH1/BRIT1 deficient cells

STK39 is a serine /threonine kinase also known as PASK (proline–alanine-rich Ste20-related kinase) or SPAK (Ste20-related proline-alanine-rich kinase). The full length STK39 is expressed in the cytoplasm in transfected cells, while a mutation of the *C*-terminal region of STK39 at the putative caspase cleavage site

changes protein localisation to the nucleus, indicating that STK39 may function as a stress activated signal in mammals (Johnston *et al.*, 2000). Indeed, STK39 is an upstream activator of p38 MAPK pathway and JNK cascades in HEK293 cells (Polek *et al.*, 2006a). Furthermore, the tumour necrosis factor (TNF)-related apoptosis-inducing ligand (TRAIL) is an important activator of caspase and apoptotic factors, and inhibition of STK39 activity facilitates apoptotic induction of TRAIL in HeLa cells (Polek *et al.*, 2006e; Polek *et al.*, 2006a).

TRAIL enhances cells to apoptosis in two different mechanisms. TRAIL stimulates caspase 3-like proteases to cleave STK39 at two distinct sites, which removed its substrate-binding domain and by caspase independent downregulation of STK39 activity (Polek *et al.*, 2006e; Polek *et al.*, 2006a). A combination of RNAi loss of function and cDNA overexpression screens have been utilised to identify how kinases impact on the bioactivity of TRAIL-induced apoptosis in colon adenocarcinoma cells (So *et al.*, 2015). This identified STK39 as a resistor, a target that increased apoptosis when depleted.

Interestingly, an elevated mRNA level of STK39 has been detected in BC lines such as ZR-75-1, T-47D, SK-BR-3, MAD-MB-468, MAD-MB-231, MAD-MB-361, MAD-MB-175, MCF7, CAMA-1, BT-474, BT-20 and HBL-100 and prostate cancer cell lines such as DU14, PC-3 and LNCaP (Qi *et al.*, 2001). STK39 has been also found to promote K-Cl co-transporter 3 (KCC3)-mediated cervical cancer aggressiveness (Chiu *et al.*, 2014).

Additionally, STK39 was one of the siRNA hits detected in a kinome-wide siRNA screen that identified molecular targets that sensitise pancreatic cancer cells to Aurora kinase inhibitor (AKI) (Xie *et al.*, 2012). Another shRNA library screen targeting kinases, phosphatases and oncogenes was performed to detect SL partners of oncogenic KRAS. The screen identified 250 shRNA whose depletion impaired the proliferation/viability of KRAS mutant cells and STK39 was also on this list (Barbie *et al.*, 2009).

Paclitaxel/Taxol has an effective dual function to destroy cancer cells by inducing mitotic arrest and apoptosis (Amos and Löwe, 1999; Fang *et al.*, 1998a; Rodi *et al.*, 1999). Paclitaxel/Taxol requires an intact mitotic spindle checkpoint function for the induction of apoptosis in tumour cells. MCPH1/BRIT1 regulates DNA repair and spindle checkpoint activity (Chaplet *et al.*, 2006; Lin *et al.*, 2010; Venkatesh and Suresh, 2014). Thus, its expression could effectively influence the response of cancer cells to chemotherapy. Time-lapse imaging data from our laboratory has revealed that MCPH1/BRIT1 deficient cells display reduced mitotic

arrest in response to Paclitaxel/Taxol or Nocodazole, chromosomal aberrations and aneuploidy development (Bell *et al.*, 2008).
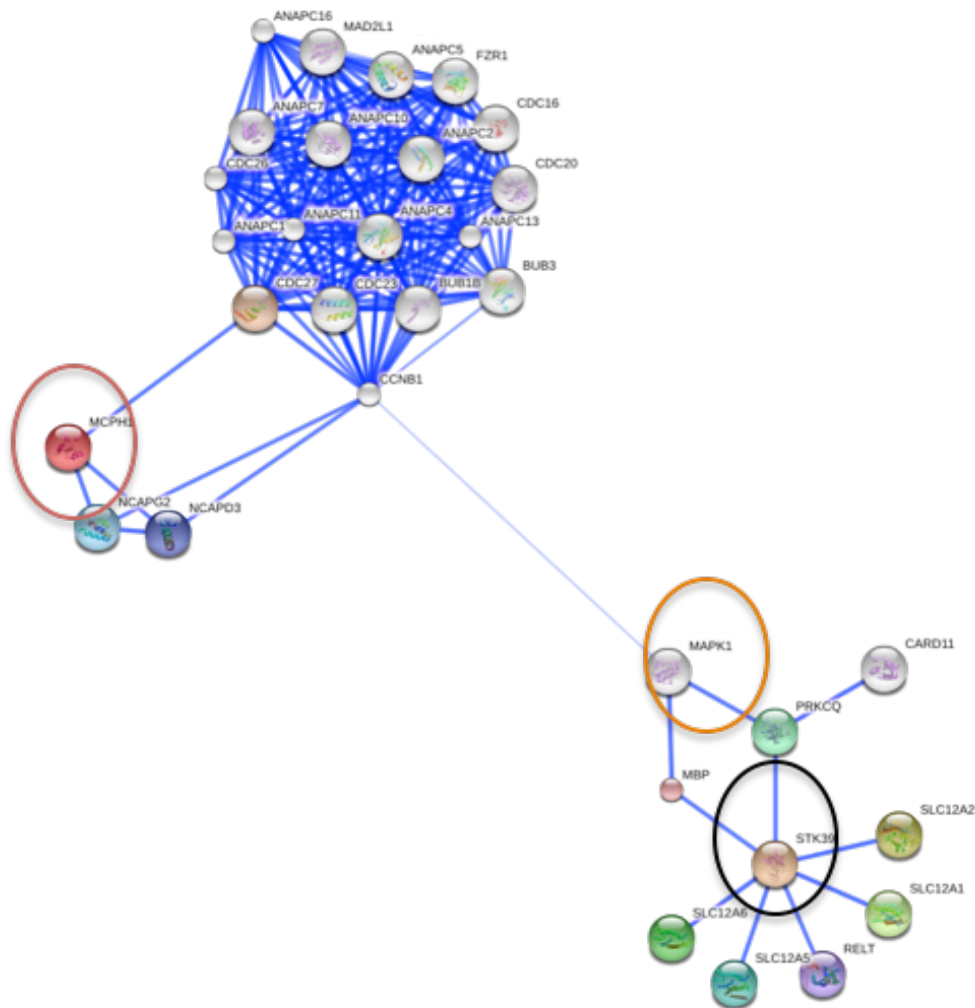
Figure 5.14. Representative image of potential regulatory networks of interaction for SL siRNA hit STK39 with MCPH1/BRIT1.
STK39 is circled in black; MCPH1/BRIT1 is circled in red. MAPK1 (circled in orange) may act as a potential connector for the interaction of STK39 with MCPH1/BRIT1.

Moreover, drug assay data showed that depletion of MCPH1/BRIT1 by siRNA in breast cell lines MCF10A, MCF7 and HCC193 with different MCPH1/BRIT1 backgrounds increased resistance to Paclitaxel/Taxol (Richardson *et al.*, 2010), indicating that loss of MCPH1/BRIT1 function may contribute to the development of resistance to BC chemotherapy. This could suggest that since many mammary and prostate cancer cell lines show elevated expression of STK39, this may substantially prevent the cytotoxic response of MCPH1/BRIT1-deficient cancer cells to Paclitaxel/Taxol. Interestingly, previous investigators Ahmed *et al*. (2011) have suggested that knockdown of kinases that functionally stabilize microtubules, such

as STK39, could greatly enhance anti-tumour responses to Paclitaxel/Taxol treatment with a subsequent induction of apoptosis (Ahmed *et al.*, 2011).

5.3.3 *VRK1* siRNA showed a weak SL effect in MCPH1/BRIT1 deficient cells

Vaccinia-related kinase 1 (VRK1), a serine-threonine kinase and early response protein for entry into G1 phase (Lazo *et al.*, 2005), is correlated with proliferation phenotype and its loss affects cell cycle progression (Vega *et al.*, 2004; Valbuena *et al.*, 2008).
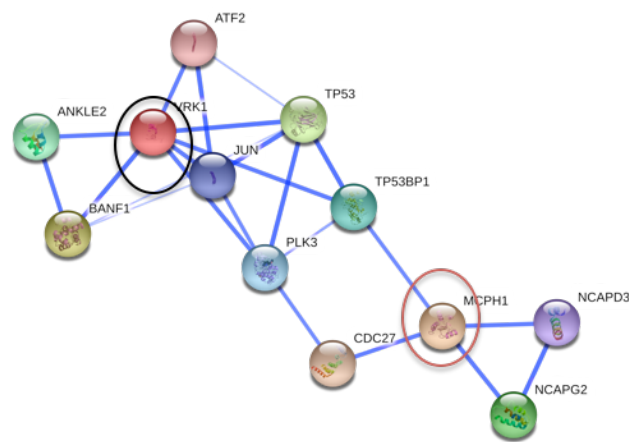
Figure 5.15. Representative image of potential regulatory networks of interaction for SL siRNA hit VRK1 with MCPH1/BRIT1.
VRK1 is circled in black; MCPH1/BRIT1 is circled in red.

It phosphorylates proteins such as p53 (Lopez-Borges and Lazo, 2000), c-Jun (Jun Proto-Oncogene) (Sevilla *et al.*, 2004a), ATF (Activating transcription factor) and BAF (Barrier to autointegration factor) (Sevilla *et al.*, 2004b; Nichols *et al.*, 2006; Gorjánácz *et al.*, 2007). VRK1 specifically phosphorylates Thr18 of p53, which regulates its stabilization and transcriptional activation (Lopez-Borges and Lazo, 2000; Vega *et al.*, 2004). Thus, accumulation of p53 leads to down-regulation of the protein levels of VRK1, forming a novel auto-regulatory loop (Valbuena *et al.*, 2006; López-Sánchez *et al.*, 2014) that is impaired in lung squamous cell carcinomas harbouring p53 mutations (Valbuena *et al.*, 2006; Valbuena *et al.*, 2007).

The overexpression of VRK1 has been considered to be part of a gene expression signature in BC that is associated with poor clinical outcome (Fournier *et al.,* 2006; Martin *et al.*, 2008; Molitor and Traktman, 2013). The stable

overexpression of VRK1 increases the survival ability of highly malignant BC cells MDA-MB-231 under low serum conditions while suppression of *VRK1* expression using shRNA impairs their proliferation. In the murine orthotopic xenograft model of BC, VRK1-depleted cells displayed a reduction in tumour size and incidence of lung and brain metastases (Molitor and Traktman, 2013).

Thus, down-regulation of VRK1 by p53 may be necessary to activate the DNA damage response. Indeed, induction of DNA damage by IR or UV stabilizes p53 and activates DRAM (DNA damage regulated autophagy modulator) expression. This promotes VRK1 protein degradation followed by the de-phosphorylation of Thr18 of p53 (Valbuena *et al.*, 2006; Valbuena *et al.*, 2008; Valbuena *et al.*, 2011). The stability of p53 is required for DDR and MCPH1/BRIT1 is implicated in the regulation of p53 stability, preventing its ubiquitination and proteasomal degradation by MDM2 (proto-oncogene, E3 ubiquitin protein ligase) (Zhang *et al.*, 2013a). Accordingly, MCPH1/BRIT1 expression may contribute to down-regulation of VRK1 activity, supporting the essential activity of p53 in response to DNA damage in cancer cells. Degradation of VRK1 may be associated with activating apoptotic mechanisms in a p53-dependent manner or through an autophagy pathway (Tang *et al.*, 2015). Thus, it is would be useful to investigate the effect of MCPH1/BRIT1 depletion on the expression level of VRK1 in cancer cells and to identify the contribution of VRK1 to cell death in MCPH1/BRIT1-deficient cells through autophagic pathways.

5.3.4 *TTK/MPS1* siRNA is a potential SL gene in MCPH1/BRIT1 deficient cells

Monopolar spindle-1 (MPS1) (also known as TTK) is a cell cycle regulator protein kinase that has multiple functions in mitosis, specifically at the kinetochore which is required for proper chromosomal attachment, and in addition may function at centrosomes (Liu and Winey, 2012). After mitosis, TTK/MPS1 is involved in cytokinesis (Liu and Winey, 2012).

Since the mRNA and protein level of TTK/MPS1 increased in human melanoma cell line with B-Raf^{V600E} mutant, its overexpression in cancer may be associated with this oncogenic signalling pathway (Cui and Guadagno, 2008; Borysova *et al.*, 2008). TTK/MPS1 has a mitotic function and, perhaps for this reason, its deregulated mRNA transcription level is detected in a range of human cancers.
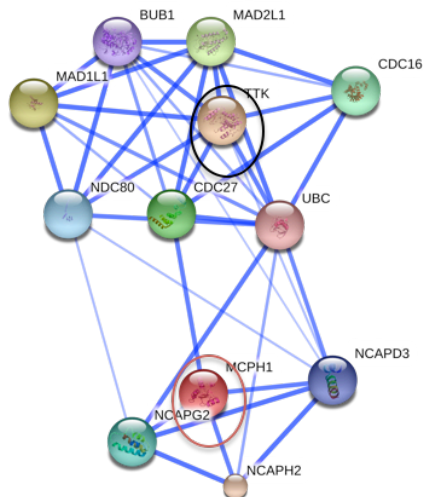
Figure 5.16. Representative image of potential regulatory networks of interaction for SL siRNA hit TTK/MPS1 with MCPH1/BRIT1.
TTK/MPS1 is circled in black; MCPH1/BRIT1 is circled in red.

Elevated TTK/MPS1 mRNA levels are found in several human tumours, including BC, thyroid papillary carcinoma, gastric cancer and lung cancer (Salvatore *et al.*, 2007; Landi *et al.*, 2008; Mills *et al.*, 1992). An increased level of TTK/MPS1 expression serving as a checkpoint protein in human cancers may explain the potential role of checkpoint proteins either in cancer initiation or aneuploidy development (Daniel *et al.*, 2011; Sotillo *et al.*, 2007). Overexpression of TTK/MPS1 in colon cancer cells compromises the spindle assembly checkpoint (SAC) and increases aneuploidy (Ling *et al.*, 2014). Thus, depletion of TTK/MPS1 (Fisk *et al.*, 2003; Daniel *et al.*, 2011), or other checkpoint proteins such as BubRI and Mad2 (Fisk *et al.*, 2003; Kops *et al.*, 2004; Michel *et al.*, 2004), has been found to influence tumour cell viability.

Previously TTK/MPS1 depletion in Hs578T BC cells caused decreased tumour growth in xenograft models (Daniel *et al.*, 2011). Potentially suppression of the checkpoint protein TTK/MPS1 induces chromosome mis-segregation that would result in induction of apoptosis causing a reduction in aneuploidy. Consequently lower level of checkpoint proteins may effectively sensitises tumour cells to low doses of spindle poisons compared to normal human fibroblasts (Daniel *et al.*, 2011; Janssen *et al.*, 2009). This has promoted the identification and development of small molecule inhibitors targeting TTK1/MPS, for example, MPS-IN-1 and MPS-IN-2 (Kwiatkowski *et al.*, 2010), Reversine (Santaguida *et al.*, 2010), or NMS-P715 (Colombo *et al.*, 2010), which may function as sensitisers to anticancer drugs.

Depletion of MCPH1/BRIT1 caused defective mitotic spindles and cytokinesis (Rai *et al.*, 2006). A reduced MCPH1/BRIT1 protein expression level in BC samples is associated with an elevated level of PLK1 (Rai *et al.*, 2006). In addition, MCPH1/BRIT1-deficient U2OS cells displayed less compacted chromosomes, spindle misalignment and chromosome congression failure at metaphase, and bi-nucleated cells with cytokinesis bridges. Thus Rai *et al.* (2008) speculated that MCPH1/BRIT1-depleted cells activate the spindle assembly checkpoint proteins BubRI and Mad2, which are essential components in regulating mitotic cell transition from metaphase to anaphase (Kadura and Sazer, 2005; Janssen *et al.*, 2009; Kops *et al.*, 2004; Liu and Winey, 2012). Interestingly, there is a cooperative function between PLK1 and TTK/MPS1 to regulate the spindle assembly checkpoint in human cell (von Schubert *et al.*, 2015). PLK1 enhances the spindle checkpoint activity of TTK/MPS and the recruitment of Mad1, C-Mad2, BubR1 and Bub3 to kinetochores. Both TTK/MPS 1 and MCPH1/BRIT1 are phosphorylated by PLK1 (von Schubert *et al.*, 2015; Martin, 2011) and their depletion in cancer cells causes similar mitotic deficiencies (Rai *et al.*, 2006; Liu and Winey, 2012). Thus, this may suggest two possible explanations.

The first is that both mitotic proteins, MCPH1/BRIT1 and TTK/MPS1, may function simultaneously, with a contribution from PLK1, in regulating a proper SAC during mitosis and in chromosome segregation during anaphase. The second is that MCPH1/BRIT1 functions as a negative regulator of TTK/MPS1, repressing its activity during the DNA damage response. Thus, MCPH1/BRIT1-mitotic deficient cells entered anaphase, despite the activated spindle checkpoint BubRI and Mad2 in U2OS cells (Rai *et al.*, 2006), suggesting the activity of these spindle checkpoint components is dependent on TTK/MPS1. Indeed, TTK/MPS1 contributes in regulating SAC by the recruitment of Mad1, Mad2, Bub1, BubR1 and Bub 3 to kinetochores (Bayliss *et al.*, 2012).

Furthermore, while the IMPDH central domain of MCPH1/BRIT1 has a role in shaping metaphase chromosomes by physically interacting with condensin II, the *N*-terminal domain regulates the proper loading of condensin II onto chromosomes to initiate DNA condensation (Yamashita *et al.*, 2011). Interestingly, TTK/MPS1 has recently been found to phosphorylate condensin II, which is required for its localisation into chromatin during prophase (Kagami *et al.*, 2014). These authors reported that depletion of TTK/MPS1 caused errors in chromosomal condensation and affected chromosome segregation. Although Kagami *et al.* (2014) used siRNA against *TTK/MPS1* in HeLa cells they did not report PCC induction as a consequence of TTK/MPS1 depletion, which is consistent with our observation.

However, the co-depletion of TTK/MPS1 with MCPH1/BRIT1 in our results showed a significant increase in %PCC caused by knockdown of *TTK/MPS1*siRNA 2 and 3 at 25nM. However, PCC was reduced at 50nM. An explanation for this is that more efficient depletion of *TTK/MPS1* with 50nM siRNA may be sufficient to de-activate the spindle checkpoint activity of TTK/MPS1 and thereby induce the death of PCC cells that were originally produced by *MCPH1*/*BRIT1* siRNA.

5.3.5 CDK1/CDC2 depletion potentially reduces cell viability in MCPH1/BRIT1 deficient cells and increases PCC

According to our results, single *CDK1*/*CDC2* siRNA knockdown did not induce PCC or cell death. Enhanced PCC and reduction in % cell viability was seen only when it was accompanied by *MCPH1*/*BRIT1* siRNA. The mechanism by which combined knockdown of MCPH1/BRIT1-CDK1/CDC2 could induce PCC and promote apoptosis is still unknown. However, some studies showed the involvement of CDK1/CDC2 in regulating chromosome condensation and segregation mechanisms whilst others showed the potential utility of CDK1/CDC2 inhibition in cancer therapy. Therefore, the potential induction of PCC by co-depletion of CDK1/CDC2 in MCPH1/BRIT1 deficient cells merits discussion.

First, MCPH1/BRIT1 has been found to regulate the activity of CDK1/CDC2 during the DNA damage response by activating CHK1 at G2, which is in turn, inactivates the CDC25 phosphatase. This leads to maintenance of inhibitory CDK1/CDC2 phosphorylation preventing early entry into mitosis (Alderton *et al.*, 2006; Niida *et al.*, 2005; Tibelius *et al.*, 2009; Gruber *et al.*, 2011; Zhong *et al.*, 2006). Furthermore, MCPH1/BRIT1 is a negative regulator of Condensin II, a subunit of structural maintenance of chromosome (SMC) protein complexes, that is required for initiating chromosome condensation in prophase (Hirota *et al.*, 2004; Ono *et al.*, 2004; Hirano, 2005; Hirano, 2012). Interestingly, CDK1/CDC2 has been found to contribute to the regulation of chromosome condensation during prophase by phosphorylation of Condensin II enabling proper chromosome assembly in cells preparing for entry into mitosis (Abe *et al.*, 2011). Therefore, a defective function of MCPH1/BRIT1 allowed for unscheduled loading of Condensin II onto chromosome leading to premature mitosis and induction of PCC (Yamashita *et al.*, 2011). Presumably, inactivation of CDK1/CDC2 may also cause deregulation of Condensin II leading to a substantial induction in PCC. Therefore, depletion of CDK1/CDC2 may abnormally activate other chromosomal structure proteins that

are indispensable for timely chromosome condensation during mitosis, which needs further investigation.

Second, the kinase WEE1 is also responsible for phosphorylation and inactivation of CDK1/CDC2 at Tyr15 before the onset of mitosis (Poon *et al.*, 1996; McGowan and Russell, 1993). However, results from our lab showed that U2OS cells display low WEE1 mRNA and protein levels. Reduced WEE1 levels may enable residual CDK1/CDC2 to form a complex with Cyclin B that increases the ability of PCC cells to prematurely enter mitosis in CDK1/CDC2- MCPH1/BRIT1 co-depleted cells.

Last, it has been proposed that CDK2/CDC1-Cyclin A controls the activity of cells during G2 and initiates chromosome condensation during prophase, whilst CDK1/CD2-Cyclin B is located in the cytoplasm in an inactive state until the onset of mitosis (Takizawa and Morgan, 2000; Neitzel *et al.*, 2002). Microinjection of exogenous CDK2/CDC1-Cyclin A into G2 HeLa cells rapidly initiates chromosome condensation whereas its inhibition prevents the onset of chromosome condensation in early prophase (Furuno *et al.*, 1999). Therefore, the co-depletion of MCPH1/BRIT1 with CDK1/CDC2 may lead to premature activation of CDK2/CDC1-Cyclin A to induce PCC in early G2 phase, suggesting MCPH1/BRIT1 has a dual function in regulating activities of CDK2/CDC1 during chromosome condensation in prophase and CDK1/CDC2 at mitotic entry.
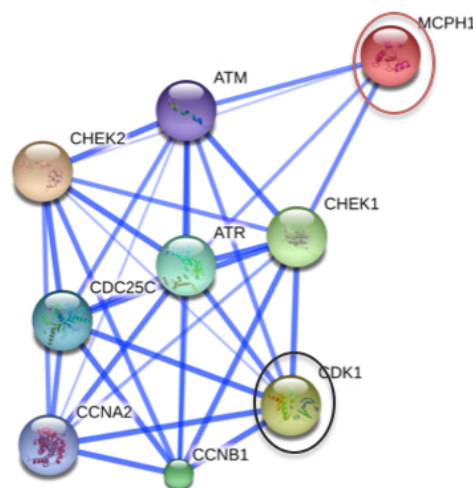
Figure 5.17. Representative image of potential regulatory networks of interaction for SL siRNA hit CDK1/CDC2 with MCPH1/BRIT1.
CDK1/CDC2 is circled in black; MCPH1/BRIT1 is circled in red.

Inhibition of CDK1/CDC2 may be considered as a potential therapeutic target in cancer and therefore it CDK1/CDC2 may consider as a likely SL hit since its

overexpression in HeLa cells disrupts the response to DNA damage and instead stimulates DNA replication and cell division (Chow *et al.*, 2003). Indeed, exposure of HeLa, SW480 and HCT166 cancer cell lines to CDK1/CDC2-Cyclin B inhibitor (RO3066) for up to 24hr showed a mitotic arrest at G2/M phase (Vassilev *et al.*, 2006) whereas removal of the CDK1/CDC2 inhibitor (RO3066) allowed rapid mitotic entry (Vassilev *et al.*, 2006). However, initiation of apoptosis has been observed in the colon cancer cell lines, HCT116 and SW480, after longer exposure (72hr) to the CDK1/CDC2 inhibitor, suggesting Further experiments are required to confirm if depletion of CDK1/CDC2 is a PCC and cell death inducer in the absence of MCPH1/BRIT1. The potential predicted interaction network of the SL hits CDK1/CDC2 with MCPH1/BRIT1, are illustrated in Figure 5.17.

Chapter 6 Evaluation of the role of MCPH1/BRIT1 and p53 expression in response to neoadjuvant chemotherapy and subsequent survival in breast cancer patients

6.1 Introduction

Breast cancer (BC) is a heterogeneous disease; the histological diversity of cancer within and between the individuals demonstrates the urgent need to find specific prognostic and predictive biomarkers to improve patient survival.

A number of evidences indicated that deficiency in MCPH1/BRIT1 expression increases susceptibility to different types of cancer. Loss of heterozygosity on chromosome 8p23.1, where MCPH1/BRIT1 is located, occurs in many types of cancers (Lin *et al.*, 2010; Lu *et al.*, 2007; Zhu *et al.*, 2004; Emi *et al.*, 1992; Wu *et al.*, 1997; Scholnick *et al.*, 1996; Fujiwara *et al.*, 1993; Muscheck *et al.*, 2000; Washburn *et al.*, 2000; Bockmühl *et al.*, 2001; Wright *et al.*, 1998) See Chapter 1: Section 1.1.6.4).

The biological function of MCPH1/BRIT1 in regulating the protein stability of p53 in the absence and presence of DNA damage signalling has been investigated in BC (Zhang *et al.*, 2013a). MCPH1/BRIT1 functions as an early responder to DNA damage in the presence of DNA damage stimulators (Ultraviolet (UV) or γ radiation). Thus, MCPH1/BRIT1 deficiency may subsequently lead to aberration in p53 stabilization and reduce its activity in response to DNA damaged cells.

The mouse model generated by (Liang *et al.*, 2014) clearly demonstrated the association of single knockout Mcph1/Brit1 with tumour initiation at long latency and acceleration of lymphomagenesis, but not carcinoma (epithelial tumours), in the absence of p53. Mcph1/p53 deficiency increased genomic instability, centrosome hyper-amplification and decreased the activity of HR or IR induced foci formation during the DNA DSB repair mechanism. This may confirm the vital role of MCPH1/p53 in maintaining genomic integrity and preventing tumorigenesis. Clinically, the functional status of WT p53 was found to be more sensitive to chemotherapy or radiotherapy than tumours with mutant p53 (Vogelstein and Kinzler, 2004; Brosh and Rotter, 2009). Therefore, MCPH1/BRIT1 deficiency may not respond well to chemotherapy or radiotherapy in the absence of functional p53 expression.

For BC treatment, the preoperative therapy known as neoadjuvant chemotherapy (NACT) has been mainly used before surgery to downstage the locally advanced tumours or lymph node metastasis thus avoiding mastectomy, and to increase the survival outcome (Mieog *et al.*, 2007). Analysis of resection tissue after surgery is usually one of the methods to measure any residual invasive carcinoma and evaluate tumour response to NACT treatment (Kaufmann *et al.*, 2012). However, there is still variation in the response rate to NACT treatment due to the differences in patient cohorts, type of NACT treatment and measurement or reporting methods (Marinovich *et al.*, 2012).

NACT treatment triggers DNA DSB (Capranico *et al.*, 1989; Capranico *et al.*, 1990) and initiates apoptosis particularly when HR associated protein is perturbed (Sancar *et al.*, 2004). There is still a pressing need to identify surrogate markers, which can be used to better assess response of BC to NACT treatment.

The influence of the DNA repair protein MCPH1/BRIT1, in response to NACT treatment in BC remains unknown. Thus, this study aimed to examine the expression of MCPH1/BRIT1 and p53 expression in BC tissue samples pre- and post-NACT treatment to determine the predictive value of MCPH1/BRIT1 or p53 in response to NACT treatment or survival rates. Also, we investigated the association of MCPH1/BRIT and p53 expression with molecular biomarkers such as ER, PR, HER2, triple negative BC, CK5 and Ki67. Change in expression of MCPH1/BRIT1 or p53 after NACT treatment and its association with pathological response or survival rates have been studied herein. In addition, the potential correlation between MCPH1/BRIT1 and p53 expression was also investigated using these BC samples.

6.2 Patients' characteristics

This BC study consisted of a cohort of patients treated with NACT. Samples of both core biopsy (pre-NACT) and matched resection tissue of invasive residual tumour post-NACT were identified for each patient. The post-NACT tissue samples were assembled into a tissue microarray (TMA). The post-NACT sample for 26 cases was unavailable since their tumours had been diagnosed with a pathological complete response (pCR) after NACT, however other clinical data was available for the patients. The expression of MCPH1/BRIT1 and p53 were assessed in both the pre-NACT (core biopsy) and post-NACT (residual invasive TMA core) tissue

samples. After excluding unmatched pairs, core loss and un-scoreable cores, the MCPH1/BRIT1 cohort included 96 cases (96 pre-NACT samples and 70 post-NACT samples), and the p53 study included 92 cases (92 pre-NACT samples and 66 post-NACT samples). The patients' characteristics for both MCPH1/BRIT1 and p53 pre and post-NACT chemotherapy are summarised in (Table 6.1). In this cohort a high frequency of patients were diagnosed with inflammatory breast cancer (IBC) in both studies, for MCPH1/BRIT1 23/96 cases (24%) were diagnosed, while for p53 the number was 23/92 cases (25%).

The median follow up overall survival was 45 and 44 months for MCPH1/BRIT1 and p53 respectively with a range of (8-96 months) for both studies. A similar death rate (22%) was observed in both studies (in MCPH1/BRIT1 this was 22/96 patients while in p53 it was 21/92 patients. Those patients who died had a median survival period of 3 years (range 1-7 years), from date of diagnosis to death. Metastatic BC occurred in a similar proportion of patients (26%) in both studies: 25/96 cases for MCPH1/BRIT1 and for p53, 23/92 cases.

Table 6.1. Patients' characteristics for MCPH1/BRIT1 and p53 studies pre and post NACT treatment.

Variables	MCPH1/BRIT1 n = 96 (%)		p53 n = 92 (%)	
	Pre	Post	Pre	Post
Tumour grade				
G1	4 (4.5)	7 (12.7)	4 (4.8)	6 (11.7)
G2	36 (41.3)	28 (50.9)	32 (38.5)	27 (52.9)
G3	47 (54)	20 (36.3)	47 (56.6)	18 (35.2)
Unknown	9 (Not available (NA))	15 (NA)	9 (NA)	15 (NA)
Histological tumour type				
Invasive ductal carcinoma (IDC)	86 (91.4)	43 (76.7)	82 (91.1)	39 (91.1)
Other special types	8 (8.5)	13 (23.2)	8 (8.8)	12 (8.8)
Unknown	2 (NA)	14 (NA)	2 (NA)	15 (NA)
Age				
Mean	48	NA	49.2	NA
Range	23-77		23-77	
Age distribution				
< 50	60 (63.1)	NA	56 (61.5)	NA
> 50	35 (36.8)		35 (38.5)	
Unknown	1 (NA)		1 (NA)	
Inflammatory				
No	71 (75.5)	NA	67 (74.5)	NA
Yes	23 (24.4)		23 (25.5)	
Unknown	2 (NA)		2 (NA)	
Whole tumour size (mm)				
Mean	NA	30.7	NA	31.16
Range		1-120		1-120
Size distribution (mm)				
< 30	NA	44 (56.4)	NA	43 (59.7)
≥ 30		34 (43.5)		29 (40.2)
Unknown		18 (NA)		20 (NA)
Ductal carcinoma in situ (DCIS)				
No	NA	32 (41)	NA	29 (40.2)
Yes		46 (58.9)		43 (59.7)
Unknown		18 (NA)		20 (NA)
Sterilized axilla				
Negative	NA	29 (51.7)	NA	26 (50)
Positive		27 (48.2)		26 (50)
Unknown		40 (NA)		40 (NA)

Continued Table 6.1.

Variables	MCPH1/BRIT1 n = 96 (%)		p53 n = 92 (%)	
	Pre	Post	Pre	Post
Nottingham prognostic index (NPI)				
Good	NA	8 (15.6)	NA	9 (18.7)
Moderate		25 (49)		22 (45.8)
Poor		18 (35.2)		17 (35.4)
Unknown		19 (NA)		18 (NA)
Lymph node status (LNS)				
N0	NA	39 (51.3)	NA	40 (55.5)
N1		21(27.6)		17 (23.6)
N2		8 (10.52)		8 (11.1)
N3		6 (7.8)		5 (6.9)
Micrometastases		2 (2.6)		2 (2.7)
Unknown		20 (NA)		20 (NA)
Lymphovascular invasion (LVI)				
No	NA	27 (51.9)	NA	26 (54.1)
Yes or extensive		23 (44.2)		20 (41.7)
Probable		2 (3.8)		2 (4.2)
Complete response (CR) cases		26 (NA)		26 (NA)
Unknown		18 (NA)		18 (NA)
Metastases				
No	NA	71 (73.9)	NA	69 (75)
Yes		25 (26)		23 (25)
Neoadjuvant chemotherapy (NACT) [a]				
ECF or FEC and EC	NA	33 (44)	NA	32 (43.2)
EC+Taxotere or Neo-TAnGo EC+TG or Neo-TAnGo Taxotere+EC		41 (54.6)		41 (55.4)
Taxotere/Carboplatin		1 (1.3)		1 (1.4)
Unknown		21 (NA)		21 (NA)
Herceptin (Trastuzumab)				
Not given	NA	57 (75)	NA	55 (76.3)
Given		7 (9.2)		6 (8.3)
Not applicable		12 (15.7)		11 (15.2)
Unknown		20 (NA)		20 (NA)
Endocrine therapy				
Not given	NA	32 (42.6)	NA	31 (43.6)
Given		43 (57.3)		40 (56.3)
Unknown		21 (NA)		21 (NA)
Tumour response (Sarah Pinder)				
No response	NA	9 (9.9)	NA	9 (10.3)
Minimal		1 (1.1)		1 (1.1)
Partial		55 (60.4)		51 (58.6)
CR		26 (28.6)		26 (29.8)
Unknown		5 (NA)		5 (NA)
Deceased				
No	NA	73 (76.8)	NA	70 (76.9)
Yes		22 (23.1)		21 (23)
Unknown		1 (NA)		1 (NA)
Follow up overall survival (FUOS)/ months				
Mean	NA	44	NA	44
Median		45		44
Range		8-96		8-96
Survival duration (from diagnosis to death/ years)				
Median	NA	3	NA	3
Range		1-7		1-7

a. **ECF**: Epirubicin+Cisplatin+Fluorouracil (5-FU). **FEC**: Fluorouracil (5FU5-FU)+Epirubicin+Cyclophosphamide. **EC**: Epirubicin+Cyclophosphamide **NA:** not available. The complete data for 96 or 92 patients pre- and post-NACT in MCPH1/BRIT1 or p53 studies are not available for all variables and thus they were classified as Unknown. All variables post-NACT included data for the 96 or 92 patients including 26 cases who achieved pCR. However, the data relating to the tumour grade, histological tumour type, NPI and LVI were not available for the pCR (26) cases post-NACT in both MCPH1/BRIT1 and p53 studies.

6.3 Study of MCPH1/BRIT1 expression pre- and post-NACT treatment

In this study, the expression of MCPH1/BRIT1 was investigated in 96 BC patients treated with NACT.

6.3.1 Immuno-histochemical assessment and localisation of MCPH1/BRIT1 in BC samples pre- and post-NACT treatment

Optimisation of MCPH1/BRIT1 staining in BC tissues was performed according to the previous ovarian cancer study performed in our lab using the anti-MCPH1/BRIT1 (ab2612, Abcam, Cambridge, UK) antibody at a concentration of 1: 100 (Data not shown) (Alsiary *et al.*, 2014). In the MCPH1/BRIT1 study, the majority of core tumour biopsies (pre-NACT) and TMA core residual invasive samples (post-NACT) revealed MCPH1/BRIT1 expression in both nucleus and cytoplasm, which was similar to the previous observation of MCPH1/BRIT1 in BC (Richardson *et al.*, 2011; Jo *et al.*, 2013; Bhattacharya *et al.*, 2013; Partipilo *et al.*, 2016). The percentage of tumour cells with positive nuclear MCPH1/BRIT1 staining was scored in relation to the total number of tumour cells. Figure 6.1 shows examples of staining intensities of MCPH1/BRIT1 in pre-NACT tumour samples ranging from negative, weak, moderate to strong. Although cytoplasmic expression of MCPH1/BRIT1 was detected in tumour samples pre- and post-NACT treatment it was not considered in this study due to high levels of background staining caused by the anti-MCPH1/BRIT1 antibody, which prevented the accurate scoring of cytoplasmic MCPH1/BRIT1 staining.

In this study, similar statistical analysis strategies to those used previously in BC samples was performed (Richardson *et al.*, 2011). The percentage of tumour cells with positive nuclear MCPH1/BRIT1 staining was considered as a continuous variable. In addition, the percentage of MCPH1/BRIT1 staining was dichotomised into high and low expression using 35% as a cut-off point. This cut-off was selected by sequentially testing different cut-off values of percentage of nuclear MCPH1/BRIT1 staining (e.g 15%, 30% and 35%) versus FUOS using the Kaplan – Meier curves. The cut-off value of 35% that presented a significant survival result between patient groups was selected for subsequent analyses (Richardson *et al.*, 2011).

Since 26 pCR cases did not show any residual invasive tumour, the expression of MCPH1/BRIT1 pre- and post-NACT could only be evaluated in 70 cases using the diagnostic biopsy core pre-NACT and the matched residual invasive tumour resection sample post-NACT. The percentage scores for MCPH1/BRIT1 expression across the cases pre- and post-NACT treatment are illustrated in Figure 6.2.

There were wide variations in MCPH1/BRIT1 expression in pre-NACT samples ranging from negative to 90%. However, in the majority of cases post-NACT, there was a high level of MCPH1/BRIT1 expression with a low or undetected level of expression in only a few cases (Figure 6.3 A and B or C and D). Some cases, which had expressed low or high MCPH1/BRIT1 pre-NACT treatment, did not show any noticeable alteration in the levels of MCPH1/BRIT1 post-NACT (Figure 6.3 G and H or E and F).

Initially the % staining of MCPH1/BRIT1 expression pre- and post-NACT treatment was determined using only the 70 available matched cases. This was mainly to evaluate the overall status of MCPH1/BRIT1 expression specifically in this cohort. Continuous analysis of matched pair for 70 cases using percentage staining of MCPH1/BRIT1 expression showed an overall mean of 36.30% in pre-NACT treatment cases, which increased post-NACT treatment to an overall mean of 64.90%, indicating a significant increase in MCPH1/BRIT1 expression in response to the NACT treatment ($p < 0.0001$; Paired t-test).

Dichotomous data analysis also identified a similar significant difference between MCPH1/BRIT1 expression (high –low) in the matched pairs 70 cases pre and post NACT treatment ($p = 0.0002$; Wilcoxon matched-pairs signed- rank test). The proportion of patients with high MCPH1/BRIT1 expression was 51.4% (36/70 cases) pre-NACT, which increased to 81.4% (57/70 cases) post-NACT.

The differences in the rate of pCR patients (26 cases) with MCPH1/BRIT1 expression (high or low) pre-NACT treatment were investigated. A similar proportion of cases which expressed MCPH1/BRIT1 at high level (12 /26, 46.2%) and low level (14/26, 53.8%) was observed.
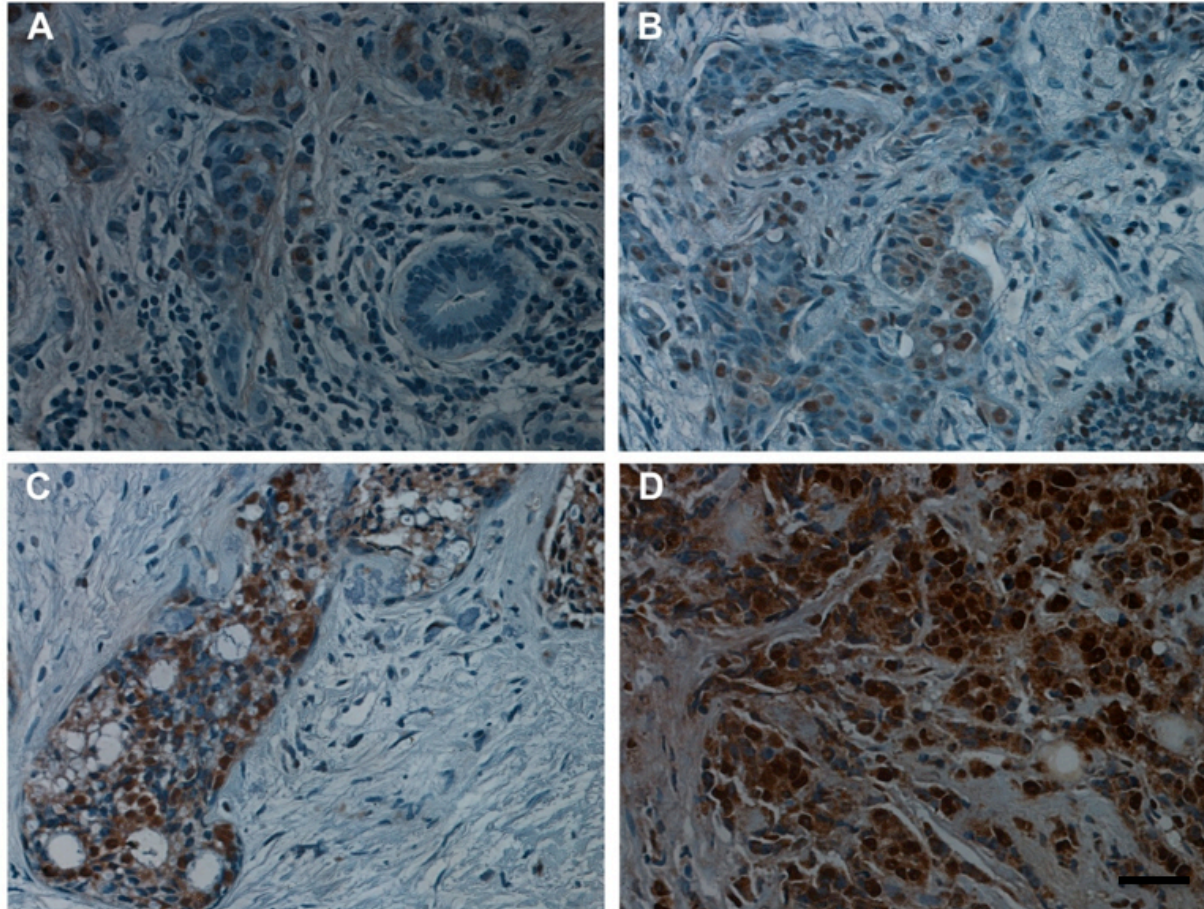
Figure 6.1. MCPH1/BRIT1 immunohistochemistry.
Representative images of breast cancer (BC) core biopsy pre-neoadjuvant (NACT) treatment to evaluate the staining intensity of MCPH1/BRIT1: **(A)** negative, **(B)** weak, **(C)** moderate, and **(D)** strong. 40x Magnification.
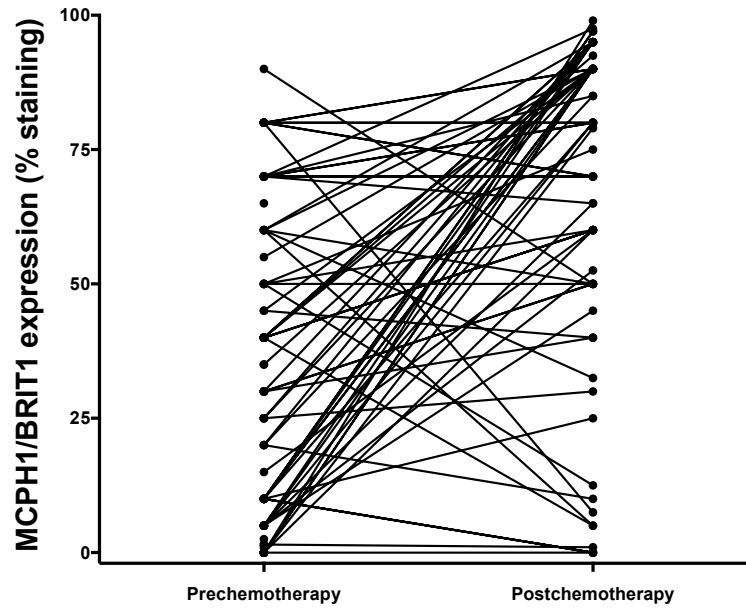
Figure 6.2. Expression levels of nuclear MCPH1/BRIT1 in matched pairs of tumour samples pre- and post-NACT treatment.
The level (% nuclear staining) in each individual is symbolised in lines linking the matched samples. The graph includes also the 26 samples whose tumours are attained the pathological complete response thus they are symbolised as dots without lines linking them with their matched pairs.

6.3.2 Correlation of MCPH1/BRIT1 with clinicopathological parameters

The correlation between the level of MCPH1/BRIT1 expression and clinicopathological tumour characteristics was tested (Tables 6.2 and 6.3). There was an increase in the cases with low grade tumours (grades 1 and 2) from (45%) pre-NACT to (63%) post-NACT, indicating the expected reduction in cases with high grade tumours from 54% pre-NACT to 36% post-NACT treatment (Table 6.1).

The continuous analysis of MCPH1/BRIT1 expression showed no significant correlation with tumour grade either pre- or post-NACT treatment, however, the dichotomous analysis of MCPH1/BRIT1 expression pre-NACT treatment identified a significant correlation between high MCPH1/BRIT1 expression with high tumour grade (grade 3) and low expression of MCPH1/BRIT1 with low tumour grade (grade 2) (p = 0.012; Spearman correlation test). This significant correlation might reflect the fact that the greatest proportion of patients' tumours in this cohort were characterised pre-NACT treatment as grade 3 (47/87 cases (54%)) compared with (36/87 cases (41%)) with grade 2 tumours (Table 6.1).
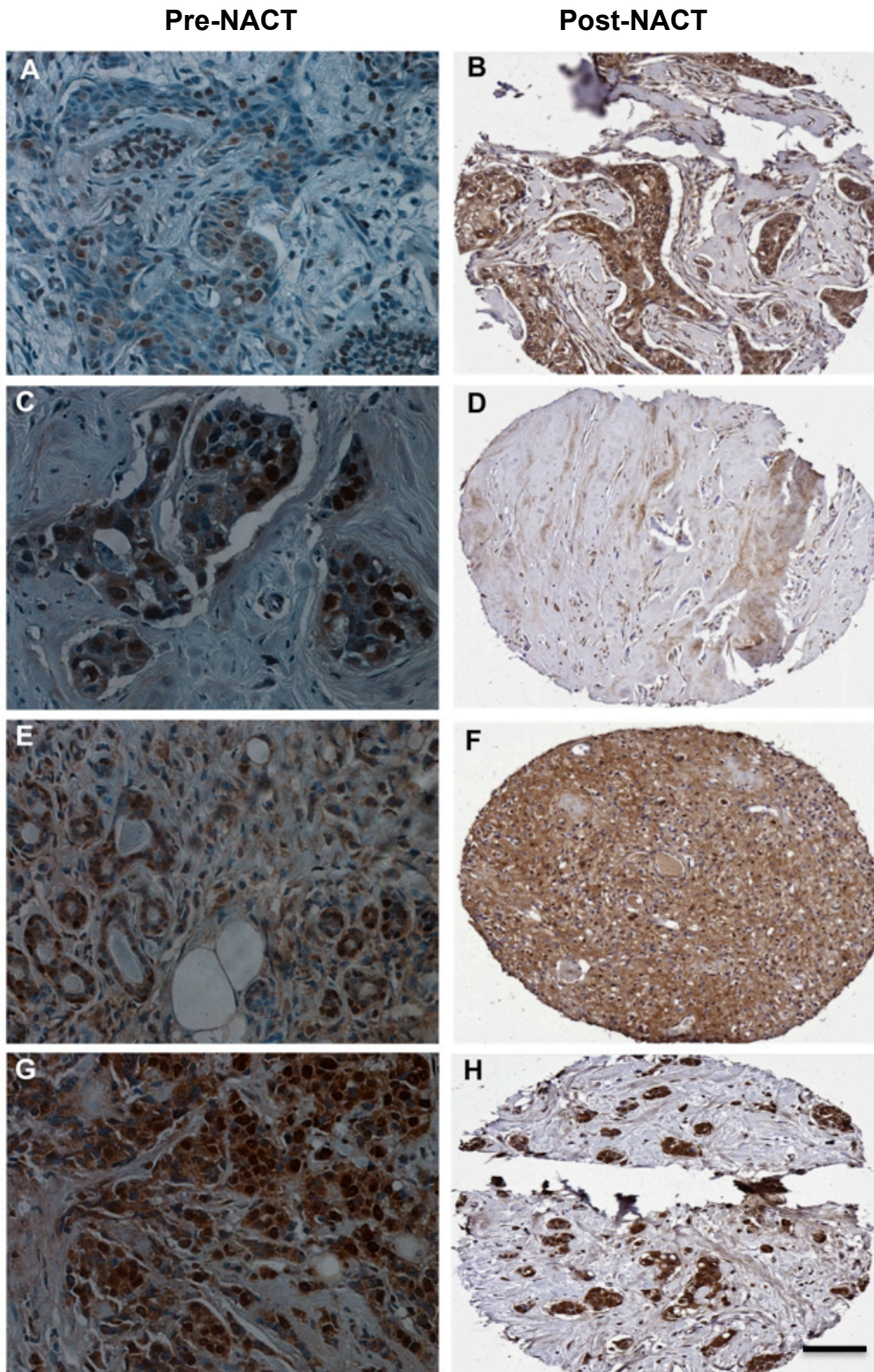
Pre-NACT **Post-NACT**

Figure 6.3. Representative staining of MCPH1/ BRIT1 in matched tumour samples pre-NACT treatment (core biopsy) and post-NACT treatment (surgical resection).
The expression scores for each matched sample were evaluated pre- and post-NACT using the nuclear percentage staining system and the results were as follows: **(A** and **B)** were 10% pre and 80% post. (**C** and **D)** were 40% pre and 5% post. (**E** and **F)** were 25% pre and 30% post. **(G** and **H)** were 60% pre and 95% post. Magnification was x 40 in pre-NACT tissues and x 10 in TMA core post-NACT.

Table 6.2. Correlation of MCPH1/BRIT1 nuclear expression with clinico-pathological features pre- and post-NACT treatment.

Parameters	MCPH1/BRIT1 expression									
	Continuous				Dichotomised					
	Mean (%)	P value	Mean (%)	P value	High n (%)	Low n (%)	P value	High n (%)	Low n (%)	P value
	Pre		Post		Pre			Post		
Tumour grade										
G1	41.25	G1 vs. G2 0.444	63.57	G1 vs. G2 0.801	2 (4.3)	2 (4.8)	**0.012**	6 (13)	1 (10)	0.8
G2	29.69	G1 vs. G3 0.945	60.23	G1 vs. G3 0.516	13 (28.2)	23 (56)		22 (49)	6 (60)	
G3	40.35	G2 vs. G3 0.080	72.75	G2 vs. G3 0.178	31 (67.3)	16 (39)		17 (38)	3 (30)	
Histological tumour type										
IDC	35.19	0.966	62.07	0.244	45 (93.7)	41 (89.1)	0.428	33 (71.7)	10 (100)	0.056
Other special types [a]	35.62		73.65		3 (6.2)	5 (10.8)		13 (28.2)	0 (0)	
Age										
<50	36.3	0.265	64.7	0.881	29 (61.7)	31 (64.5)	0.774	37 (66)	8 (61.5)	0.761
>50	29.81		65.9		18 (38.2)	17 (35.4)		19 (33.9)	5 (38.4)	
Inflammatory										
No	33.91	0.92	66.24	0.549	33 (71.7)	38 (79.1)	0.408	42 (76.3)	9 (69.2)	0.6
Yes	33.26		60.88		13 (28.2)	10 (20.8)		13 (23.6)	4 (30.7)	

a. Other special types include invasive lobular carcinoma (ILC) and mixed (IDC and ILC).

Table 6.3. Correlation of MCPH1/BRIT1 nuclear expression with other clinico-pathological features post-NACT treatment.

Parameters	MCPH1/BRIT1 expression				
	Continuous		Dichotomised		
	Mean (%)	P value	High n (%)	Low n (%)	P value
	Post		Post		
Tumour size (mm)					
< 30	63.47	0.446	16 (36.4)	3 (37.5)	0.952
≥ 30	69.79		28 (63.6)	5 (62.5)	
Nottingham prognostic index					
Good	64.69	G vs. M 0.920	7 (16.3)	1 (12.5)	0.706
Moderate	66	G vs. P 0.484	20 (46.5)	5 (62.5)	
Poor	72.31	M vs. P 0.522	16 (37.2)	2 (25)	
Lymph node status					
N0	70	N0 vs. N1 0.336	16 (36.4)	1 (12.5)	0.529
N1	59.53	N0 vs. N2 0.338	14 (31.8)	5 (62.5)	
N2	79.88	N0 vs. N3 0.489	7 (15.9)	1 (12.5)	
N3	77.75	N1 vs. N2 0.169	6 (13.6)	0 (0)	
Micrometastases	41.25	N1 vs. N3 0.273	1 (2.3)	1 (12.5)	
		N2 vs. N3 0.854			
Lymphovascular invasion					
No	70.37	N vs. Y 0.557	25 (56.8)	2 (25)	0.071
Yes or extensive	65.5	N vs. P 0,333	18 (40.9)	5 (62.5)	
Probable	51.25	Y vs. P 0.592	1 (2.3)	1 (12.5)	
Metastases					
No	64.89	0.996	41 (71.9)	8 (61.5)	0.468
Positive	64.93		16 (28.1)	5 (38.5)	

In addition, this dichotomous analysis of pre-NACT treatment indicated that for grade 3 tumours, the number of cases with high MCPH1/BRIT1 expression (n = 31/46 cases) was higher than the cases with a low level of MCPH1/BRIT1 expression (n= 16/41 cases). This trend was reversed for grade 2 tumours, with low MCPH1/BRIT1 expression being observed in a larger proportion of cases (n = 23/41 cases) than high MCPH1/BRIT1 expression (n = 13/46 cases) (Table 6.2). However, the significant correlation of MCPH1/BRIT1 expression with tumour grade was reduced post-NACT treatment (*p* = 0.08; Spearman correlation test).

Furthermore, the majority of cases in this cohort were diagnosed with the histological BC type of invasive ductal carcinoma (IDC) on pre-NACT core biopsy (86/94 cases (91%)) while in post-NACT samples residual invasive carcinoma was (43/56 cases (76%)) (Table 6.1). However, no significant correlation was found between MCPH1/BRIT1 expression and IDC type pre- or post-NACT treatment in both continuous and dichotomous analysis (Table 6.2).

Moreover, the continuous and dichotomous analysis revealed no statistically significant correlation between MCPH1/BRIT1 expression and other clinico-pathological parameters as shown in (Tables 6.2 and 6.3).

6.3.3 Correlation of MCPH1/BRIT1 with molecular biomarkers

The continuous and dichotomous analyses did not identify any statistically significant correlation between MCPH1/BRIT1 expression and BC molecular prognostic biomarkers (ER, PR, HER2) or other markers such as Ki67 and CK5 in either pre- or post-NACT treatment (Table 6.4).

Table 6.4. Correlation of MCPH1/BRIT1 nuclear expression with molecular biomarkers pre- and post-NACT chemotherapy.

Parameters	MCPH1/BRIT1 expression										
	Continuous				Dichotomised						
	Mean (%)	P value	Mean (%)	P value	High n (%)	Low n (%)	P value	High n (%)	Low n (%)	P value	
	Pre		Post		Pre			Post			
ER											
Negative	31.36	0.31	68.09	0.991	22 (45.8)	22 (45.8)	1	18 (36.7)	5 (50)	0.442	
Positive	37.144		68.18		26 (54.1)	26 (54.1)		31 (63.2)	5 (50)		
PR											
Negative	31.16	0.173	66.89	0.743	28 (58.3)	27 (56.2)	0.839	24 (48.9)	7 (70)	0.232	
Positive	38.96		69.54		20 (41.6)	21 (43.7)		25 (51)	3 (30)		
Her2											
Negative	36.33	0.269	70.64	0.298	39 (81.2)	34 (72.3)	0.308	40 (81.6)	7 (70)	0.414	
Positive	28.81		60.38		9 (18.7)	13 (27.6)		9 (18.3)	3 (30)		
Triple negative											
Negative	33.39	0.594	68.52	0.554	29 (60.4)	34 (70.8)	0.288	37 (74)	6 (54.5)	0.207	
Positive	36.59		63.28		19 (39.5)	14 (29.1)		13 (26)	5 (45.4)		
Ki67											
Negative	44.28	0.5	66.57	0.132	5 (11.9)	2 (5.5)	0.334	17 (39.5)	4 (66.6)	0.217	
Positive	36.88		77.71		37 (88)	34 (94.4)		26 (60.4)	2 (33.3)		
CK5											
Negative	36.1	0.397	75.3	0.405	29 (72.5)	29 (85.2)	0.188	28 (66.6)	4 (66.6)	1	
Positive	42.81		68.5		11 (27.5)	5 (14.7)		14 (33.3)	2 (33.3)		

6.3.4 Correlation of MCPH1/BRIT1 expression pre- and post-NACT treatment with overall survival (OS)

To determine the significance of MCPH1/BRIT1 expression in BC survival, the correlation of MCPH1/BRIT1 expression at both pre- and post-NACT treatment with

OS was examined. The dichotomous analysis of MCPH1/BRIT1 expression in 95 biopsy core cases revealed a significant association between reduced MCPH1/BRIT1 expression and longer survival pre-NACT treatment (Kaplan-Meier test; p = 0.017). The estimated mean OS for patients with low MCPH1/BRIT1 expression was of 83.6 months (95% confidence interval (CI): 74-92) in comparison to 64.8 months (95% CI: 55-74) for patients with high MCPH1/BRIT1 expression (Figure 6.4A). On the other hand, the mean OS post-NACT treatment for patients with low or high MCPH1/BRIT1 expression (63.3 months/(95% CI: 49-75)) and (75 months/(95% CI: 66-84)) did not suggest any statistically significant correlation between MCPH1/BRIT1 expression and OS (Kaplan-Meier test; p = 0.390) (Figure 6.4B).

The death rate in pCR cases was assessed to identify whether MCPH1/BRIT1 expression pre-NACT correlated with their survival outcome. The mean follow up overall survival (FUOS) in pCR cases was 39.58 months, ranging between 14 and 72 months. Of the 26 cases, 4 (15.3%) had died and 22 (84.6%) were still living. The mean survival rate for pCR cases was 3.2 years (with a range of 2 to 5 years). In pCR cases with high MCPH1/BRIT1 pre-NACT treatment, 3/12 (25%) of patients died. However, of the 14 pCR cases who expressed low MCPH1/BRIT1 pre-NACT only one patient died (7.1%). Overall, in pCR cases, no significant correlation was identified between either MCPH1/BRIT1 expression and OS post-NACT treatment or MCPH1/BRIT expression and death rate pre-NACT treatment, which may be due to the small size of this group. However, low pre-NACT MCPH1/BRIT1 expression may potentially be associated with improved response to NACT treatment and increased survival rate.
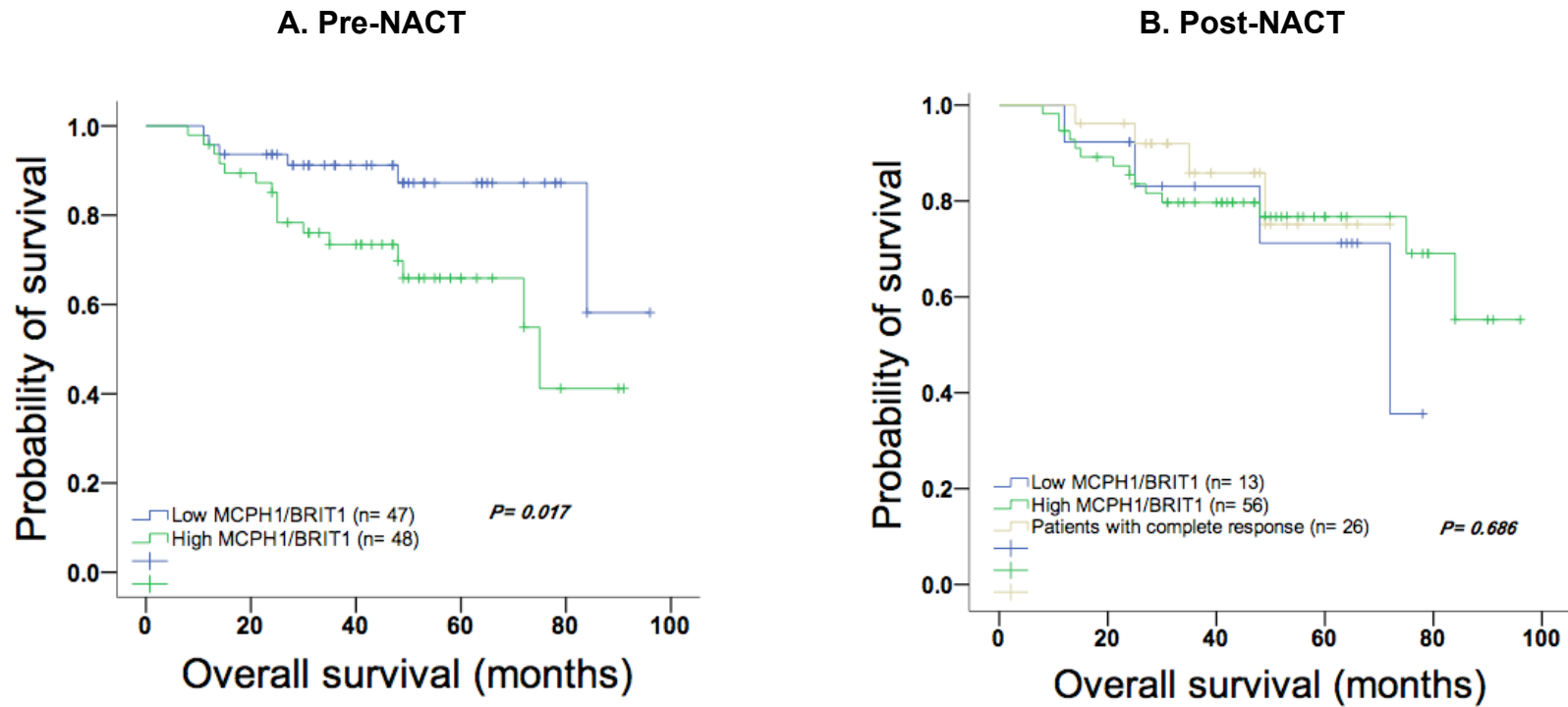
Figure 6.4. Low MCPH1/BRIT1 expression pre-NACT predicts longer overall survival (OS) than high MCPH1/BRIT1 expression.
Kaplan Meier curves showing BC OS in patients with low or high expression levels of MCPH1/BRIT1 pre- NACT **(A)** and in patients with low or high expression levels of MCPH1/BRIT1 or pathological complete response (pCR) cases post-NACT **(B).** A cut-off percentage of 35% was used to dichotomise MCPH1/BRIT1 expression into low and high.

6.3.5 Correlation of NACT treatment and pathological tumour response

The influence of NACT treatment on MCPH1/BRIT1 tumour response was also investigated. Pathological response classification data were available for 91 patients in the MCPH1/BRIT1 cohort. Patient response to the NACT treatment was variable and identified as non responders (NR) 9/91 (9.9%), minimal responders (MR) 1/91 (1.1%), partial responders (PR) 55/91 (60%) and complete responders (CR) 26/91 (28%) (Table 6.1).

NACT regimens were administered to 75 patients in this cohort. According to NACT treatments, patients were split into three groups and categorised according to the type of combination drug used for NACT treatment (Table 7.5). Group 1 treatment was Epirubicin + Cyclophosphamide (EC); 5 Fluorouracil + Epirubicin+Cyclophosphamide (FEC) and finally, Epirubicin + Cisplatin+5-Fluorouracil (ECF). Group 2 treatments was EC + Taxotere or FEC +Taxotere and Neo-tAnGo (phase III trial) +EC + Taxotere whilst Group 3 treatment consisted of Taxotere + Carboplatin.

Table 6.5. Categorisation of breast cancer patients based on the type of combination therapy used for NACT treatment in the MCPH1/BRIT cohort.

NACT group	NACT regimens	Patient No. in MCPH1/BRIT1 study n = 75 (%)
Group 1	Epirubicin + Cyclophosphamide **(EC)**	33 (44%)
	5-Fluorouracil + Epirubicin + Cyclophosphamide **(FEC)**	
	Epirubicin + Cisplatin + 5-Fluorouracil **(ECF)**	
Group 2	EC + Taxotere	41 (54.6%)
	FEC + Taxotere	
	Neo-tAnGo (phase III trial) + EC + Taxotere	
Group 3	Taxotere + Carboplatin	1 (1.3%)

No significant correlation was observed (p = 0.401; Spearman correlation test) when cross-tabulation was used to identify the correlation between the three different NACT treatment groups with pathological tumour response classification. For Group 1, the distribution of cases was NR 2/33 cases (6%), MR 19/33 (57.5%)

and CR 12/33 (36.3%). In Group 2, the proportion of cases was NR 5/41 (12.1%), MR 1 (2.4%), PR 24 (58.5%) and CR 11 (26.8%). In addition, in Group 3, only one case was treated with Taxotere + Carboplatin and it achieved CR.

Then, the effect of each NACT regimen on the change in expression of MCPH1/BRIT1 was investigated using the available matched section samples (70 patients with only residual invasive carcinoma). First, the change in MCPH1/BRIT1 expression (percentage) after NACT treatment was divided into four groups as follows: from low to high n = 27 cases (38.5%), from high to low n = 5 (7.1%), no change low n = 7 (10%) and no change high n = 31 (44.2%). Then, cross-tabulation was employed to identify the association between the NACT regimen and change in expression of MCPH1/BRIT1. There was no significant effect of the first or second NACT regimens on change MCPH1/BRIT1 expression (p = 0.548, Spearman correlation test) (Table 6.6A). For instance, change in expression of MCPH1/BRIT1 from low to high was identified in 7/21 cases (33.3%) of those treated with the first NACT regimen compared to 12/30 cases (40%) for the second. Moreover, the first and second group of NACT regimens showed a similar proportion of cases with unchanged status of MCPH1/BRIT1 expression high or low as presented in (Table 6.6A).

Finally, whether the change/or no change in expression of MCPH1/BRIT1 after NACT treatment improved the degree of pathological tumour response to chemotherapy was investigated. Cross-tabulation analysis between change/or no change in expression of MCPH1/BRIT1 and pathological tumour response (NR, MR and PR) revealed that the majority of patients presented a PR (55/65 cases) to NACT treatment particularly in patients whose MCPH1/BRIT expression had changed from low to high 19/55 cases (34.5%) or in patients who had showed no change in expression of MCPH1/BRIT (high) 25/55 (45.4%) (Table 6.6B). However, no significant correlation was observed between change or no change in expression of MCPH1/BRIT1 and pathological tumour response (p = 0.540, Spearman correlation test).

Table 6.6. Cross-tabulation (Groups 1 and 2) with change/ or no change in MCPH1/BRIT1 expression post-NACT versus type of NACT regimes (A) and tumour response (B).

A	MCPH1/BRIT1 expression	Low to high	High to low	High	Low	Total
NACT regimes	EC, FEC or ECF	7 (33.3%)	1 (4.7%)	11 (52.3%)	2 (9.5%)	21
	EC + Taxotere or FEC + Taxotere or Neo-tAnGo + EC (phase III trial) + Taxotere	12 (40%)	2 (6.6%)	14 (46.6%)	2 (6.6%)	30
P = 0.548	Total	19	3	25	4	51

		Change in expression		No change in expression		
B	MCPH1/BRIT1 expression	Low to high	High to low	High	Low	Total
Pathological tumour response	No response	5 (55.5%)	0	3 (33.3%)	1 (11.1%)	9
	Minimal response	0	0	1 (100%)	0	1
	Partial response	19 (34.5%)	5 (9%)	25 (45.4%)	6 (10.9%)	55
P = 0.540	Total	24	5	29	7	65

Group 3 of NACT regimens contains only one patient as shown in Table 6.5 thus it was not included in this analysis.

6.3.6 Correlation between change in expression of MCPH1/BRIT1 post-NACT treatment and OS

Thereafter, whether the change in MCPH1/BRIT1 expression in response to NACT regimen was correlated with OS was investigated. The Kaplan-Meier survival analyses were performed individually using two groups of patients: one had showed a change in MCPH1/BRIT1 expression (from low to high and vice versa) whilst for the other the expression remained unchanged (whether high or low) (Figure 6.5). These analyses identified a significant association between change in expression of MCPH1/BRIT1 (from low to high) and longer OS (p = 0.010). The mean OS in patients showing a change in MCPH1/BRIT1 expression (from low to high) was 83.7 months (95% CI: 73-94) compared to 54 months (95% CI: 30-77) for those with a high to low change in MCPH1/BRIT1 expression (Figure 6. 5A).

No statistically significant correlation was observed between the group of patients who had showed no change in MCPH1/BRIT1 expression (high and low) after NACT treatment and OS (p = 0.469). The mean OS of 66 months (95% CI: 53-78) in cases with no change in expression (high) was similar to the mean survival rate of 58 months (95% CI: 44-72) for cases with no change in expression (low) (Figure 6.5B). Overall, Group 1 and Group 2 of NACT regimens presented a similar effect on the change in expression of MCPH1/BRIT1 regardless of the type of change in expression levels of MCPH1/BRIT1 (from low to high or vice versa) or if the expression was unchanged (whether high or low). Although a high proportion of patients responded partially to NACT treatment, patients who had showed a change in MCPH1/BRIT1 expression from low to high in particular were significantly associated with increased OS after NACT treatment.
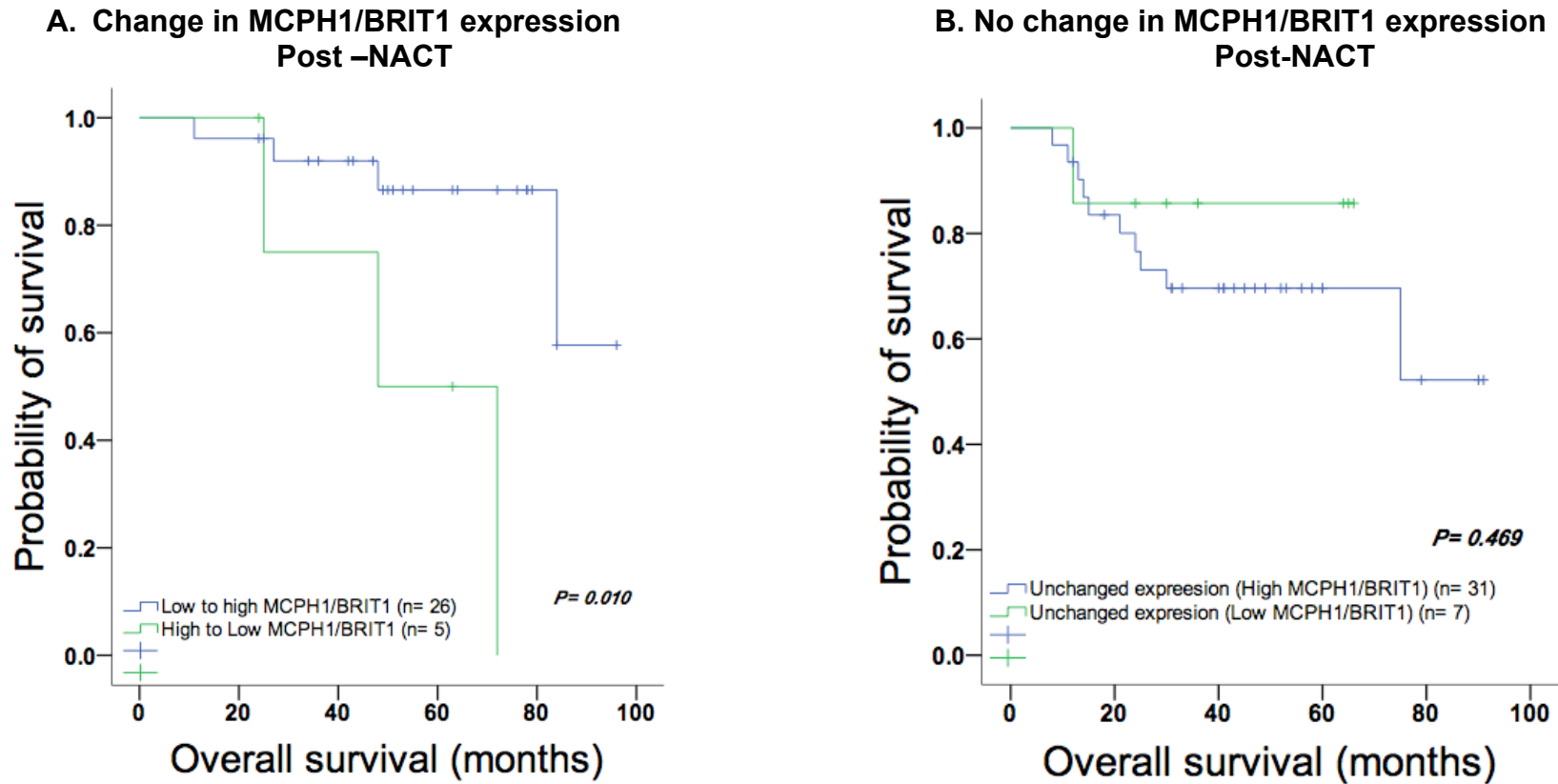
Figure 6.5. Kaplan Meier curves showing correlation between change/no change in MCPH1/BRIT1 expression after NACT treatment and BC OS. (A) Change in MCPH1/BRIT1 expression from low to high shows a significant correlation with OS. (B) No change in MCPH1/BRIT1 expression either (high or low) shows no significant correlation with OS.

6.3.7 Discussion for MCPH1/BRIT1 study

Previously, many studies have been conducted to investigate the involvement of MCPH1/BRIT1 alterations at mRNA or protein levels in various types of cancer including breast, ovarian, leukemia, OSSC and renal cancers (Richardson *et al.*, 2011; Giallongo *et al.*, 2010; Venkatesh *et al.*, 2013; Wang *et al.*, 2014a; Alsiary *et al.*, 2014). However, the influence of its expression in cancer chemosensitivity remains unknown. Thus, the aim of this BC study was to examine the protein expression of MCPH1/BRIT1 in 96 BC cases (96 pre-NACT samples and 70 post-NACT samples). The correlation of MCPH1/BRIT1 expression pre- and post-NACT with clinico-pathological parameters and molecular biomarkers was also investigated. The impact of change in MCPH1/BRIT1 expression on survival rates was clarified. Similar examinations also were employed for the available 92 BC cases (92 pre-NACT samples and 66 post-NACT samples) from the same cohort that were also stained with p53 (Section 6.4). The main aim of investigating p53 expression, simultaneously with MCPH1/BRIT1 expression, was to confirm whether MCPH1/BRIT1 expression is involved in regulation p53 expression using BC tumour samples, compared to a previous study performed on BC cell lines (Zhang *et al.*, 2013a).

IHC staining was performed and the percentage of nuclear MCPH1/BRIT1 staining used as a continuous variable to evaluate its nuclear expression pre- and post-NACT. The specificity of the rabbit MCPH1/BRIT1 antibody ab2612 (Abcam, Cambridge, UK) had been validated previously for western blotting in U2OS, HEK293 and HeLa cell lines (Xu *et al.*, 2004; Wood *et al.*, 2007; Adams *et al.*, 2014) and for IHC in several cancer tissues (Xu *et al.*, 2004; Bruning-Richardson *et al.*, 2011; Venkatesh *et al.*, 2013; Wang *et al.*, 2014a; Alsiary *et al.*, 2014).

In the present study, nuclear and cytoplasmic MCPH1/BRIT1 staining were detected in BC tissues pre- and post-NACT, which was concordant with previous BC studies (Richardson *et al.*, 2011; Bhattacharya *et al.*, 2013; Jo *et al.*, 2013; Partipilo *et al.*, 2016) and a lung cancer study (Zhang *et al.*, 2013i). However, in this study, the cytoplasmic staining was not considered due to potential non-specific background cytoplasmic staining caused by the anti-MCPH1/BRIT1 antibody. Staining a number of BC samples with different batches of anti-MCPH1/BRIT1 antibody (mentioned above) occasionally displayed considerable variation in the level of cytoplasmic staining despite the fact that the lot number for each new batch of antibody was identical. Thus, cytoplasmic staining results were not considered reliable in this study.

Considerable variation in the percentage staining of nuclear MCPH1/BRIT1 expression, pre-NACT treatment was observed among the patients, which may reflect the tumour heterogeneity and aggressiveness of the disease in this BC cohort. The percentage of cases with low MCPH1/BRIT1 expression was 34/70 cases (48.6%) pre-NACT treatment, which decreased to 13/70 cases (18.6%) post-NACT. In other words, high nuclear MCPH1/BRIT1 expression was present in 57/70 cases (81%) post-NACT treatment. Interestingly, patients with tumours demonstrating low MCPH1/BRIT1 expression pre-NACT lived 18.8 months longer compared to patients those tumours demonstrated high MCPH1/BRIT1 expression. Potentially this increased survival suggests that tumours with low levels of MCPH1/BRIT1 expression respond better to NACT treatment.

The tumour grade may greatly influence and improve the response to chemotherapy and survival. Indeed, low nuclear MCPH1/BRIT1 pre-NACT is significantly associated with moderate tumour grade (G2) cases whilst MCPH1/BRIT1 elevation is associated with high tumour grade. After NACT treatment in patients who had expressed high levels of MCPH1/BRIT1 there were a reduction in cases with grade 3 tumours whereas patients with moderate grade tumours (G2) remained high, which may indicate a partial response to NACT treatment for this group of patients compared to the noticeable decrease in the % of cases of low MCPH1/BRIT1 expression post-NACT treatment. This may explain the substantial response to NACT treatment in cases with low MCPH1/BRIT1 expression, which were initially diagnosed with moderate tumour grade pre-NACT treatment.

Additionally, this BC study is clearly different compared to other studies since expression status of MCPH1/BRIT1 pre- and post-NACT treatment can be evaluated and correlated to patients' survival. Based on the previous BC studies that demonstrated low nuclear MCPH1/BRIT1 expression correlates with higher tumour grade and poor survival, chemotherapeutic treatment may influence the response of tumours with defective MCPH1/BRIT1 expression. For instance, an initial BC study that was conducted by Richardson *et al*. (2011) and included 285 IDC patients of which only 59 which had received classical chemotherapy (Cyclophosphamide, Methotrexate and 5-Fluorouracial), demonstrated that reduced MCPH1/BRIT1 expression in 88/285 (30%) BC sample was noticeably but not significantly correlated with poor survival. Indeed, the lower–end survival rate in patients with low MCPH1/BRIT1 expression was 33 months as compared to >100 months in those with high MCPH1/BRIT1 expression (Richardson *et al.*, 2011).

Another BC study of 126 specimens and showed that reduction of MCPH1/BRIT1 protein expression in 17/25 cases (68%) was significantly concordant with their molecular alterations (deletion or methylation) (p = 0.01) (Bhattacharya *et al.*, 2013). Alterations of MCPH1/BRIT1 predicted a significant poor OS (p = 0.01) specifically in patients who underwent chemotherapy with DNA damaging agents and/or radiotherapy treatment.

Potentially the type of tumours in previous studies may not effectively respond to the systemic chemotherapy strategy that has been used to treat these patients in these BC studies. Therefore, the use of NACT treatment as a therapeutic strategy for patients diagnosed with higher tumour grade and expressing lower levels of MCPH1/BRIT1 could be considered as a factor in improving survival compared to other treatment strategies. Thus, therapeutic modalities for BC patients with low or high MCPH1/BRIT1 expression may be considered during treatment decisions.

Furthermore, within this cohort, reduced MCPH1/BRIT1 expression pre-NACT may predict an increase in patient survival. Interestingly, the findings were strengthened by the fact that patients with tumours with low MCPH1/BRIT1 expression which changed to high in response to NACT presented a significantly better OS rate compared to those with tumours which altered their MCPH1/BRIT1 expression from high to low. This suggests that reduced MCPH1/BRIT1 expression pre-NACT may cause the accumulation of DNA damage, which may lead to stimulation of the DNA damage response and a larger increase in MCPH1/BRIT1 expression post-NACT. Also, it is possible that those cases with low MCPH1/BRIT1 expression pre-NACT may still have an undamaged *C*-terminal BRCT domain which plays a key role in activating the DNA damage response and repair mechanism (Wood *et al.*, 2008; Wood *et al.*, 2007). Moreover, Lin *et al*. (2010) reported that cancer did not progress for about 18 months in a mouse model using *Mcph1*/*Brit1* knockout; however, when this mutation was combined with *p53* null knockout the cancer rapidly progressed. Thus, the status of p53 expression may be intact in cases with low MCPH1/BRIT1 expression and may suppress the tumour growth, ensure an effective response to NACT and predict a longer OS rate. Identification of p53 status in tumours with low MCPH1/BTIT1 pre-NACT may enable further understanding of survival statistics.

High MCPH1/BRIT1 expression post-NACT may predict a poor response to chemotherapy, although a change in MCPH1/BRIT1 from low to high expression may contribute to increasing the life expectancy of BC patients post-NACT, meaning that the group of patients which maintained high MCPH1/BRIT1 may be

considered drug-resistant. Although the OS rate was one year higher, although not statistically significant, in patients with high MCPH1/BRIT1 expression tumours post-NACT compared to those who had reduced MCPH1/BRIT1 expression in tumour samples, it is important to specify that in some cases tumours expressing high levels of MCPH1/BRIT1 pre-NACT remained unchanged post-NACT. Additionally, the cohort contained nine cases, which failed to respond to NACT treatment. Among these cases, five of theses cases (55.5%) were identified within the group whose MCPH1/BRIT1 expression levels changed (from low to high), while 3/9 cases (33.3%) were within the group with no change in MCPH/BRIT1 expression (high in both pre and post NACT samples) and 1/9 (11.1%) within the group with no change in MCPH/BRIT1 expression (low in both pre and post NACT samples). Interestingly, two recent studies included BC patients who received NACT treatment showed increased DNA damage repair focus formation of RAD51, BRCA1 and γH2AX or overexpression of RAD9 protein in response to NACT treatment were associated with reduced chemosensitivity (Asakawa *et al.*, 2010; Yun *et al.*, 2014).

The caveat that the BC resection samples after surgery may represent residual tumour and may not necessarily clinically reflect a resistant disease phenotype needs to be considered. Thus, given that low but not high MCPH1/BRIT1 expression pre-NACT was associated with a reduction in BC mortality, it should be considered that increased MCPH1/BRIT1 expression may predict aggressive tumour phenotypes rather than just causing drug resistance. Indeed, although only post-NACT clinico-pathological data was available for patients with high MCPH1/BRIT1 expression, a noticeable number of cases 28/64 cases (63.6%) showed a tumour size of > 30mm, residual tumours with lymphovascular invasion in 18/44 cases (40.9%) and metastases in 16/60 (28.1%), indicating the aggressive nature of tumours which may be but not significantly correlated to the elevated MCPH1/BRIT1 expression in this cohort.

Furthermore, clinicopathological findings within this cohort demonstrated a higher rate of inflammatory BC (IBC) specifically in cases with high MCPH1/BRIT1 expression pre- and post-NACT treatment, 13/46 cases (28.2%) and 13/55 cases (23.6%) respectively, suggesting again the potential influence of IBC on MCPH1/BRIT1 expression and tumour response to NACT. IBC is aggressive form of invasive BC exhibits a poor response and survival rate (Robertson *et al.*, 2010). Thus, further research needs to be carried out using this available BC cohort and Fisher's exact test to investigate the differences in the level of MCPH1/BRIT1 protein expression between two groups of patients including inflammatory and non-

inflammatory BC. This would determine if IBC influences the ability of MCPH1/BRIT1 expression to respond effectively to chemotherapy.

To our knowledge, this is the first study to explore the role of MCPH1/BRIT1 in response to NACT treatment in advanced BC. A significant reduction in cases with low MCPH1/BRIT1 expression was observed post-NACT indicating an increase in MCPH1/BRIT1 expression in response to NACT treatment. Tumours with low MCPH1/BRIT1 expression pre-NACT predicted better OS. However, alteration of MCPH1/BRIT1 expression from low to high was associated with better OS. Whether the association of high MCPH1/BRIT1 expression pre-NACT with reduced chemosensitivity in BC reflects either the nature of tumour aggressiveness or chemotherapy resistance may need further investigation. The results observed in this MCPH1/BRIT1 study are different compared to previous studies due to the variations associated with differences in tumour characteristics in patient cohorts, strategy and type of chemotherapy and methods used for assessment and reporting of tumour response. A larger sample size would be need to consider the clinical predictive or prognostic value of MCPH1/BRIT1 in BC for improving chemosensitivity.

6.4 Study of p53 expression pre- and post-NACT treatment

The p53 expression study contained 92 BC pre-NACT treatment samples. The core biopsy pre-NACT treatment and the matched invasive tumour tissue post-NACT treatment were available for 66 samples. The remaining 26 samples showed no residual invasive tumours post-NACT treatment and achieved pCR thus no resection tissue were available for these patients.

6.4.1 p53 expression status pre- and post-NACT regimen

Optimisation of p53 staining in BC and colorectal carcinoma (control) tissues was performed in collaboration with Dr. Filomena Esteves using the anti-p53 (clone DO-7) antibody at a concentration of 1: 50 (Data not shown). p53 expression was predominantly detected in the nucleus and very few cases were seen with p53 cytoplasmic staining in the core biopsy tumours and the TMA core residual invasive samples.
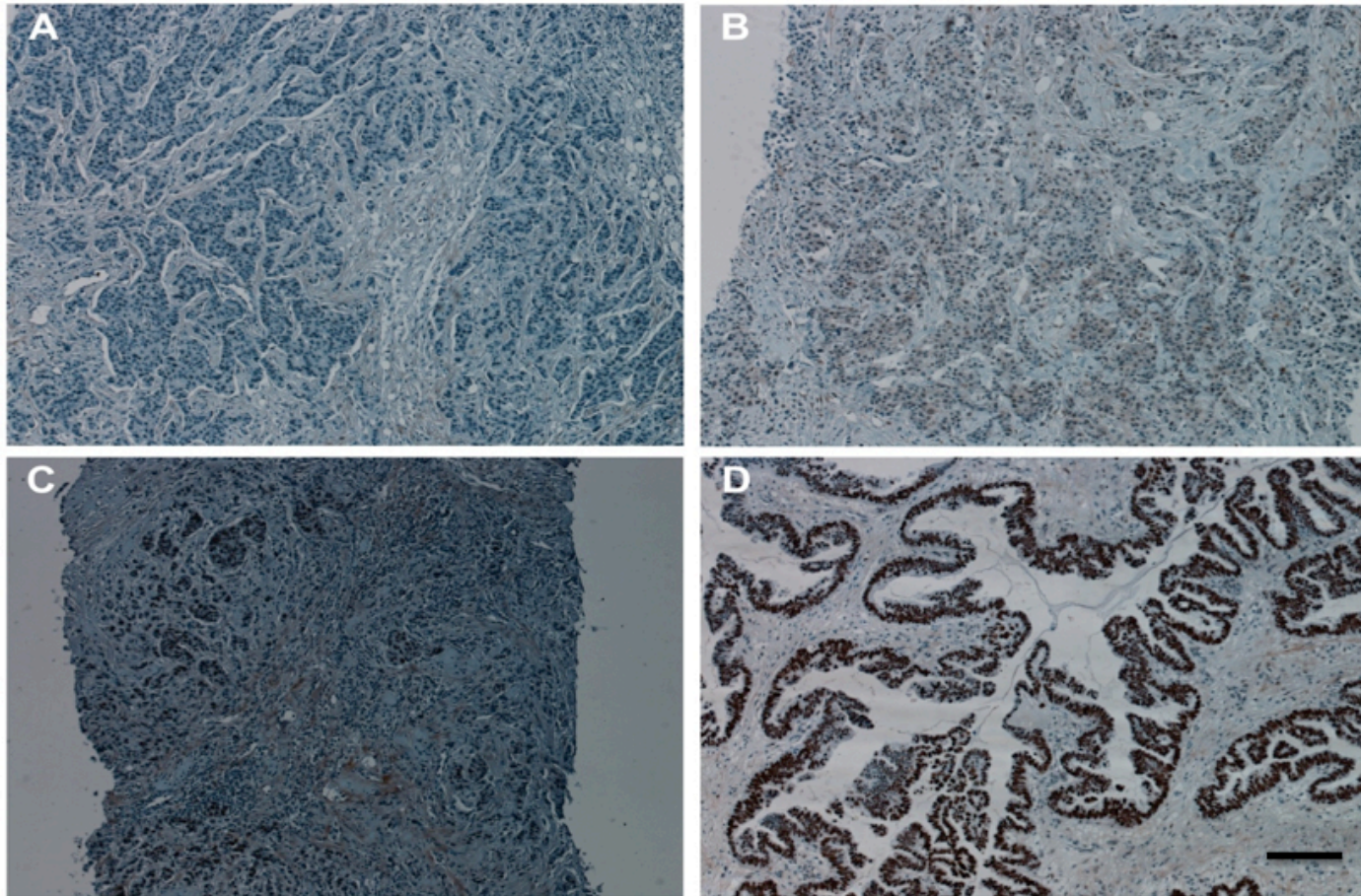
Figure 6.6. p53 immunohistochemistry.
Representative images of pre-NACT core biopsy tissues showing different staining scores of p53 expression, including **(A)** negative, **(B)** 10%, **(C)** 50% and **(D)** and 90%. Magnification was x 10.

The percentage of p53 positive nuclear staining was assessed in relation to the total number of tumour cells. The monoclonal antibody (clone DO-7) detects wild type and mutant type p53; however, as WT p53 has a short half-life and is unstable it is quickly degraded, thus is usually only present in very small amounts often below the detection level of IHC (Cooper and Haffajee, 1997). Thus, the majority of p53 positive nucleus staining in tumour cells represents the mutant type p53 (Varna *et al.*, 2011; Axelrod *et al.*, 2012). The representative images in (Figure 6.6) illustrate the various percentages of p53 nuclear staining ranging from negative, to 10%, 50% and 90% staining levels.

In the p53 study, in order to evaluate the percentage of positive nuclear p53 staining in BC samples, the percentage of tumour cells with positive nuclear p53 staining was considered as a continuous variable. However, for dichotomous analysis, the cut-off of 10% or greater was employed to dichotomise the percentage of positive nuclear p53 staining into negative and positive p53 expression (Vojtěšek *et al.*, 1992; Bartley and Ross, 2002; Rohan *et al.*, 2006; Lara *et al.*, 2011; Yang *et al.*, 2013; Milicevic *et al.*, 2014).
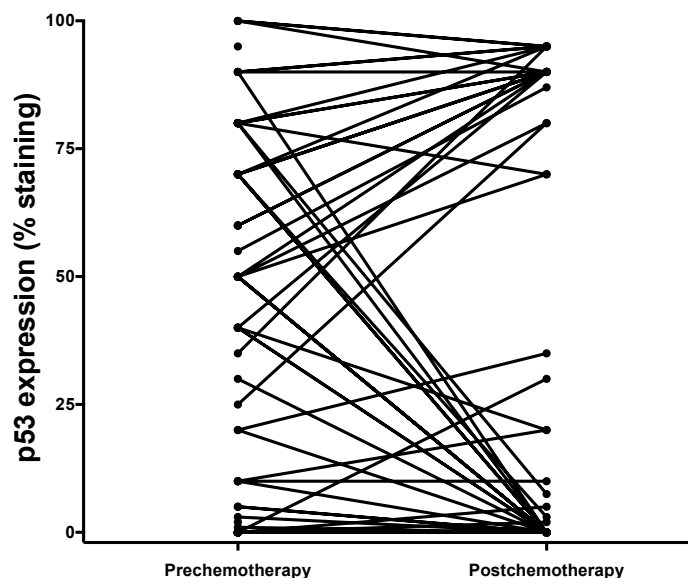
Figure 6.7. Levels of p53 expression in matched tumour samples pre- and post-NACT treatment.
Expression level (% staining) in each patient sample is symbolised by the lines linking the matched samples. There are 26 unmatched samples as their tumours attained pCR.

Thereafter, the expression of p53 was examined using the matched samples (66 cases) of both pre-NACT core biopsy and post-NACT tumour resection. The percentage scores for p53 expression pre- and post-NACT treatment are shown in (Figure 6.7). The vast majority of pre-NACT BC samples expressed positive p53

expression ranging from ≥10% of tumour cells to 100% although in some cases p53 expression was below 10% or barely detectable. Post-NACT the p53 positive scoring for some cases was increased while for others this decreased to below 10%. In addition, in some cases post-NACT p53 expression remained unchanged (positive or negative) (Figure 6.8).

The percentage of nuclear p53 staining pre- and post-NACT was compared using only the available matched sections (66 cases) to evaluate the overall status of p53 expression (Figure 6.7). The continuous analysis of %p53 expression on matched pair samples revealed no statistically significant difference in mean %p53 expression level pre- (39.53%) and post- (32.95%) NACT treatment (p = 0.1136; Paired t-test). Although there was no difference in %p53 pre- and post-NACT, the mean %p53 expression post-NACT treatment clearly displayed a slight reduction, which may indicate a reduction in cases with p53 positive expression in response to NACT treatment.

This difference became significant after applying dichotomous data analysis of p53 expression pre- and post-NACT treatment (p = 0.0001; Wilcoxon matched–pairs signed-rank test). In these matched pair samples (66 cases), the frequency of p53 positive cases was 44 (66.6%) pre-NACT treatment, which was reduced to 28 cases (42.4%) post-NACT treatment.

Of 26 cases who achieved pCR, 12 cases (46.1%) were in p53 negative tumours and 14 (53.8%) in p53 positive tumours.

6.4.2 Correlation of p53 expression with clinicopathological parameters

The vast majority of p53 positive tumours were grade 3 (56.6%) pre-NACT treatment, with grade 2 (38.5%) and grade 1 (4.8%). These proportions shifted dramatically post-NACT treatment to 35.2% for grade 3, 52.9% for grade 2 and 11.7% for grade 1 (Table 6.1). The correlation between p53 expression and grade was examined. Neither continuous or dichotomous analysis data showed a significant correlation for p53 expression with tumour grade pre-NACT treatment (Table 6.7). However, continuous analysis post-NACT treatment showed a highly significant correlation between p53 positive tumour and grade 3 (G2 vs. G3; p < 0.001; t-test and Pearson's correlation test) (Table 6.7).
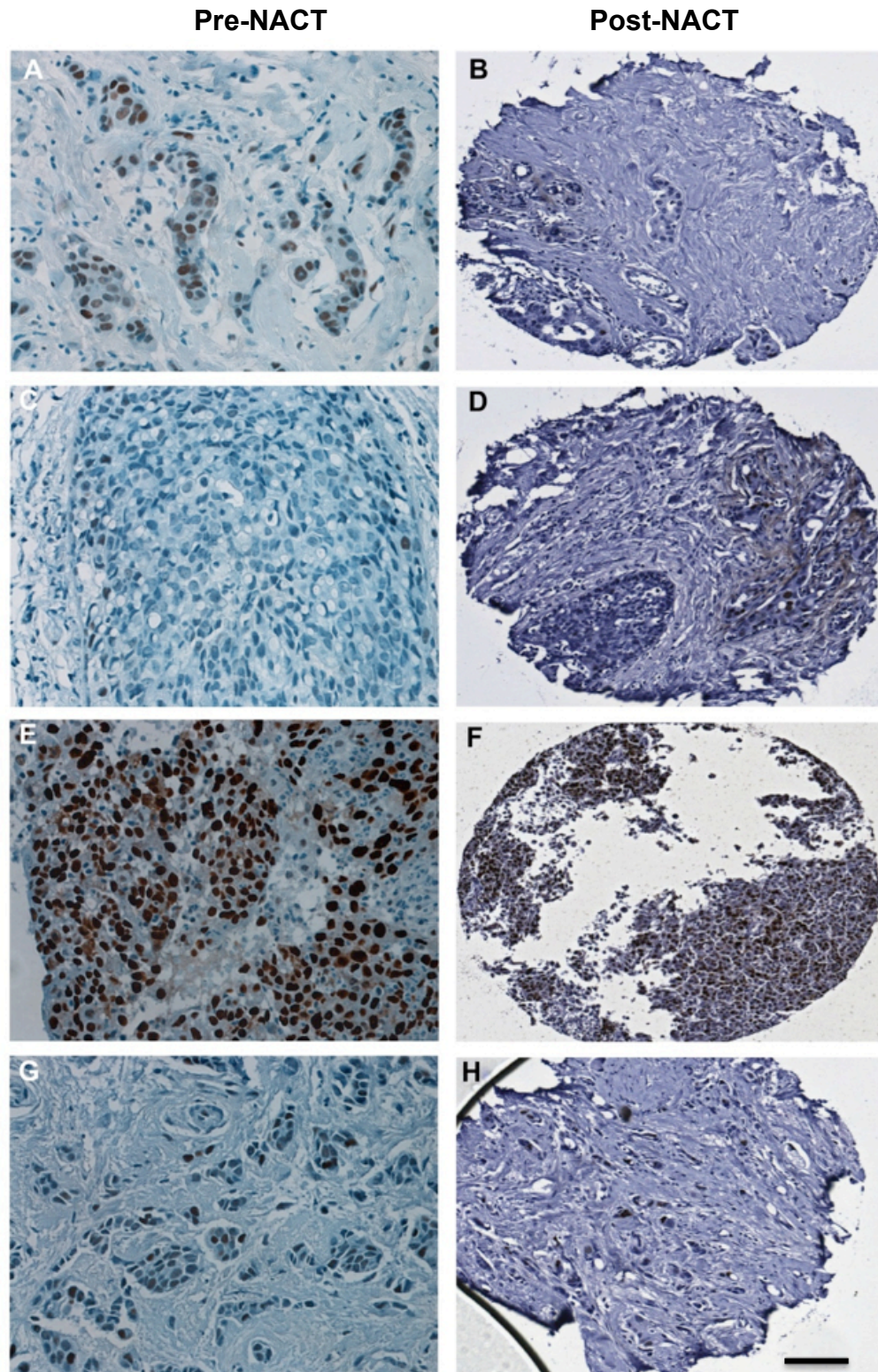
Pre-NACT **Post-NACT**

Figure 6.8. Representative staining of p53 in matched tumour samples pre-NACT treatment (core biopsy) and post-NACT treatment (surgical resection).
Percentage of nuclear p53 staining was evaluated for each individual with matched pair samples. The scoring for (**A** and **B)** was 50% pre and negative post-NACT treatment. **Samples (C** and **D**) showed no change in p53 expression (negative) pre and post-NACT treatment. (**E** and **F)** showed no change in p53 expression (positive) at 80% pre and 70% post-NACT. Panels (**G** and **H)** were negative pre and 30% post-NACT. Magnification in pre-NACT tissues was x 40 and x 10 in post-NACT TMA core.

The mean % p53 positive expression for grade 2 was 14.13% compared to 56% for grade 3. In addition, dichotomous data analysis revealed a significant correlation between p53 expression and tumour grade post-NACT treatment (p = 0.043; Spearman's correlation test). p53 negative tumours were associated with low tumour grade (G2) since the number of cases with negative p53 expression were higher (21/30) than those with positive p53 expression (6/21). Conversely, positive p53 expression was correlated with grade 3. The number of cases who expressed positive p53 expression was higher (12/21) than those with negative p53 expression (6/30) cases (Table 6.7).

As previously explained in the MCPH1/BRIT1 study, the majority of patients were diagnosed with the most common type of breast cancer (IDC) at both pre and post-NACT treatment. The proportion of cases with IDC pre-NACT was 82/90 (91.1%) in comparison to cases with other special types 8/90 (8.8%). Thus, p53 expression pre-NACT was significantly correlated with the histological tumour type IDC as identified by continuous data analysis (p = 0.046; t-test and Pearson's correlation test). The mean % of p53 expression in cases with IDC was 37.45% compared to 11.87% in cases with other special types (Table 6.7). This statistical significance was strongly confirmed by dichotomous analysis data pre-NACT treatment, again showing a significant correlation between p53 positive tumours and IDC (p = 0.042; Spearman's correlation test). The number of p53 positive cases was 51/53 (96.2%) compared to 31/37 cases (83.7%) with p53 negative pre-NACT. The statistical significance correlation was reduced post-NACT treatment in both continuous and dichotomous analyses of p53 expression data (Table 6.7).

Table 6.7. Correlation of p53 expression with clinicopathological features pre- and post-NACT treatment.

Parameters	p53 expression									
	Continuous				Dichotomised					
	Mean (%)	P value	Mean (%)	P value	High n (%)	Low n (%)	P value	High n (%)	Low n (%)	P value
	Pre		Post		Pre			Post		
Tumour grade										
G1	16.25	G1 vs. G2 0.507	21.67	G1 vs. G2 0.581	2 (5.7)	2 (4.2)	0.098	3 (10%)	3 (14.3)	**0.043**
G2	27.93	G1 vs. G3 0.195	14.13	G1 vs. G3 0.092	17 (48.5)	15 (31.3)		21 (70)	6 (28.6)	
G3	40.31	G2 vs. G3 0.124	56	G2 vs. G3 **< 0.001**	16 (45.7)	31 (64.5)		6 (20)	12 (57.1)	
Histological tumour type										
IDC	37.45	**0.046**	34.41	0.147	31(83.7)	51(96.2)	**0.042**	21(70)	18(85.7)	0.2
Other special types[a]	11.87		15.21		6 (16.2)	2(3.7)		9 (30)	3 (14.2)	
Age										
<50	33.94	0.637	32.93	0.896	24 (63)	32 (60.3)	0.791	23 (62.1)	18 (64.2)	0.863
>50	37.57		34.35		14 (37)	21 (39.6)		14 (37.8)	10 (35.7)	
Inflammatory										
No	36.98	0.329	31.22	0.406	26 (68.4)	41 (79)	0.268	27 (72.9)	20 (74)	0.923
Yes	28.6		37.47		12 (31.5)	11 (21)		10 (27)	7 (25.9)	

a. Other special types include invasive lobular carcinoma (ILC) and mixed (IDC and ILC).

Tumour size data was available for 72 patients only post-NACT. Continuous analysis revealed a significant correlation between p53 expression and tumour size

post-NACT treatment (p = 0.003; t-test and Pearson's correlation test). The expression of p53 was 51.5% in tumour size < 3mm and 17% in tumour size ≥ 3mm (Table 6.8). Surprisingly, dichotomous analysis revealed that decreased tumour size was correlated significantly with p53 positive expression while increased tumour size with p53 negative tumours post-NACT treatment (Table 6.8). This observation was surprizing since p53 negative expression is correlated significantly with lower tumour grade while p53 positive was correlated with higher tumour grade post-NACT (Table 6.7). Thus, this correlation may be because the imbalance in the number of number of cases with negative p53 expression, which was higher at 20/27 (74%) in the cohort of large tumours (≥ 3mm) compared to 8/21 cases (38%) with positive p53 expression (Table 6.8).

Table 6.8. Correlation of p53 expression with other clinicopathological features post-NACT treatment.

Parameters	p53 expression				
	Continuous		Dichotomised		
	Mean (%)	*P* value	High n (%)	Low n (%)	*P* value
	Post		Post		
Tumour size (mm)					
< 30	51.5	**0.003**	7 (25.9)	13 (61.9)	**0.011**
≥ 30	17.66		20 (74)	8 (38)	
Nottingham prognostic index					
Good	16.11	G vs. M 0.069	6 (23)	3 (14.2)	0.733
Moderate	46.19	G vs. P 0.610	9 (34.6)	12 (57.1)	
Poor	23.79	M vs. P 0.104	11 (42.3)	6 (28.5)	
Lymph node status					
N0	47.2	**N0 vs. N1 0.021**	7 (25.9)	11 (52.3)	
N1	15.3	N0 vs. N2 0.854	10 (37)	5 (23.8)	0.06
N2	43.8	N0 vs. N3 0.197	4 (14.8)	4 (19)	
N3	18.9	N1 vs. N2 0.086	4 (14.8)	1 (4.7)	
Micrometastases	0	N1 vs. N3 0.831	2 (7.4)	0 (0)	
		N2 vs. N3 0.336			
Lymphovascular invasion					
No	23.8462	N vs. Y 0.295	17 (62.9)	9 (42.8)	0.113
Yes or extensive	36.225	**N vs. P 0.021**	10 (37)	10 (47.6)	
Probable	90	Y vs. P 0.089	0 (0)	2 (9.5)	
Metastases					
No	31.18	0.906	27 (71)	19 (70.3)	0.953
Positive	33.9		11 (28.9)	8 (29.6)	

Lymph node status (LNS) data was available for 72 patients only post-NACT. There were 40/72 cases (55.5%) patients diagnosed with negative LNS (N0) after NACT treatment. Patients with positive LNS were graded into 3 types (N1, N2 and N3) depending on the number of cancer cells deposited in different areas of the lymph nodes. The distribution of patients with positive LNS was as follows; N1 17/72 (23.6%), N2 8/72 (11.1%) and N3 5/72 (6.9%). In addition, 2/72 cases (2.8%) were found with micrometastasis. Continuous analysis of p53 expression revealed a significant correlation with lymph node involvement (N0 vs. N1 p = 0.021; t-test and Pearson's correlation test). The mean % of p53 expression in cases classified

with negative LNS (N0) was 47% compared to 15% in cases with positive LNS (Table 6.8). The significance level of this correlation was reduced after dichotomous analysis of p53 expression into negative and positive (Table 6.8).

The pathological data for lymphovascular invasion (LVI) was available for 48 patients only post-NACT treatment. Another 24 cases were reported as pCR. The absence of LVI was detected in 26/48 cases (54.1%) compared to 20/48 (41.7%) with positive LVI and 2/48 (4.2%) with a probable incidence of LVI. Continuous analysis data of p53 expression identified a significant difference for cases with absence of or probable LVI status (p = 0.021; t-test and Pearson's correlation test). The mean % of p53 expression was 23.8% for cases with no LVI present compared to 90% in cases with probable LVI. No significant correlation was identified after dichotomous p53 expression into negative and positive (Table 6.8). p53 expression did not show any significant correlation with other clinico-pathological features such as the Nottingham Prognostic Index or metastases (Table 7.8).

6.4.3 Correlation of p53 expression with molecular biomarkers

Continuous and dichotomous analyses data of p53 pre-NACT treatment indicated no significant correlation with prognostic biomarkers (ER, PR, HER2) or other markers such as Ki67 and CK5 (Table 6.9). In comparison continuous analysis data post-NACT treatment showed a significant correlation between p53 expression and negative expression of ER or PR (p < 0.001; t-test and Pearson's correlation). Mean % of p53 expression was significantly higher in ER (65.23%) and PR (57.23%) negative tumours compared to ER (18.96%) and PR (13.94%) positive tumours. No significant correlation was identified between p53 expression and HER2 status post-NACT treatment. In addition, mean % of p53 expression was lower in patients with an absence of triple negative BC post-NACT (27.36%) compared to patients who were characterized with triple negative BC (57.94%) (p = 0.011; t-test and Pearson's correlation test) (Table 6.9).

Furthermore, continuous analysis data post-NACT treatment identified a significant association between p53 expression and the Ki67 marker (p = 0.002; t-test and Pearson's correlation test). The mean % of p53 expression was statistically higher in Ki67-positive tumours (57.42%) compared to those with Ki67-negative tumours (15.3%). No significant correlation was observed between p53 expression and CK5 (Table 6.9).

Table 6.9. Correlation of p53 expression pre and post NACT treatment with molecular biomarkers.

Parameters	p53 expression									
	Continuous				Categorised					
	Mean (%)	P value	Mean (%)	P value	Negative n (%)	Positive n (%)	P value	Negative n (%)	Positive n (%)	P value
	Pre		Post		Pre			Post		
ER										
Negative	40.39	0.214	65.23	**0.001**	18 (47.3)	25 (46.2)	0.92	6 (20.6)	16 (59.2)	**0.003**
Positive	31.2		18.96		20 (52.6)	29 (53.7)		23 (79.3)	11 (40.7)	
PR										
Negative	41.07	0.098	57.23	**0.001**	21 (56.7)	32 (59.2)	0.815	11 (37.9)	19 (70.3)	**0.015**
Positive	28.65		13.94		16 (44.2)	22 (40.7)		18 (62)	8 (29.6)	
Her2										
Negative	35.57	0.891	36.58	0.696	29 (78.3)	42 (79.2)	0.922	22 (78.5)	22 (81.4)	0.792
Positive	36.84		42.27		8 (21.6)	11 (20.7)		6 (21.4)	5 (18.5)	
Triple negative										
Negative	33.71	0.426	27.36	**0.011**	24 (64.8)	35 (64.8)	0.966	24 (80)	16 (59.2)	0.09
Positive	39.9		57.94		13 (35.1)	19 (35.1)		6 (20)	11 (40.7)	
Ki67										
Negative	27.85	0.344	15.3	**0.002**	3 (11.5)	4 (8.1)	0.638	11 (52.3)	4 (16)	**0.008**
Positive	41.16		57.42		23 (88.4)	45 (91.8)		10 (47.6)	21 (84)	
CK5										
Negative	38.91	0.956	44.15	0.99	19 (73)	37 (82.2)	0.37	13 (65)	17 (68)	0.837
Positive	38.33		44.33		7 (26.9)	8 (17.7)		7 (35)	8 (32)	

After dichotomising p53 expression into negative and positive, the significant correlation between p53 expression and other biomarkers (ER, PR and Ki67) was found to be similar (p = 0.003; p = 0.015 and p = 0.008, respectively; Spearman correlation test), and this was only reduced in the case of triple negative BC (p = 0.09; Spearman correlation test) (Table 6.9).

6.4.4 Correlation of p53 expression pre- and post-NACT treatment with overall survival (OS)

p53 expression of 90 biopsy core pre-NACT treatment–cases was correlated with OS. The dichotomous analysis of p53 expression showed no statistical significance with OS (p = 0.437; Kaplan-Meier test). No significant differences were observed pre-NACT between the mean OS rate of 73.3 months for patients with negative p53 expression (95% CI: 64-81 months) and that of 73.3 months for patients with positive p53 expression (95% CI: 63-83 months) (Figure 6.9A).

The correlation of p53 expression and OS rates post-NACT treatment using the available 90 resections of residual invasive carcinoma samples was not statistically significant (p = 0.154; Kaplan-Meier test). The mean OS rate for the three subgroups was almost equal, for instance, 67.3 months for negative p53 (95% CI: 68-85), 64 months for positive p53 (95% CI: 49-79) and 63 months for pCR cases (95% CI: 55-70) (Figure 6.9B).

The death rate and mean FUOS duration of pCR cases have been described previously in the MCPH1/BRIT1 study (Section 6.3.4).

Here, in addition, the death occurrence rate for pCR cases was cross-tabulated with p53 expression (negative and positive) to identify the potential association of p53 expression pre-NACT treatment with survival outcome. No significant statistical correlation was identified (p = 0.136; Fisher's Exact test), possibly due to the small size of the sample with pCR (26 cases). However, of the 26 cases, samples from 16 patients expressed negative p53, of which 4/16 had died (25%). However, no deaths had been identified among patients with positive p53 expression.
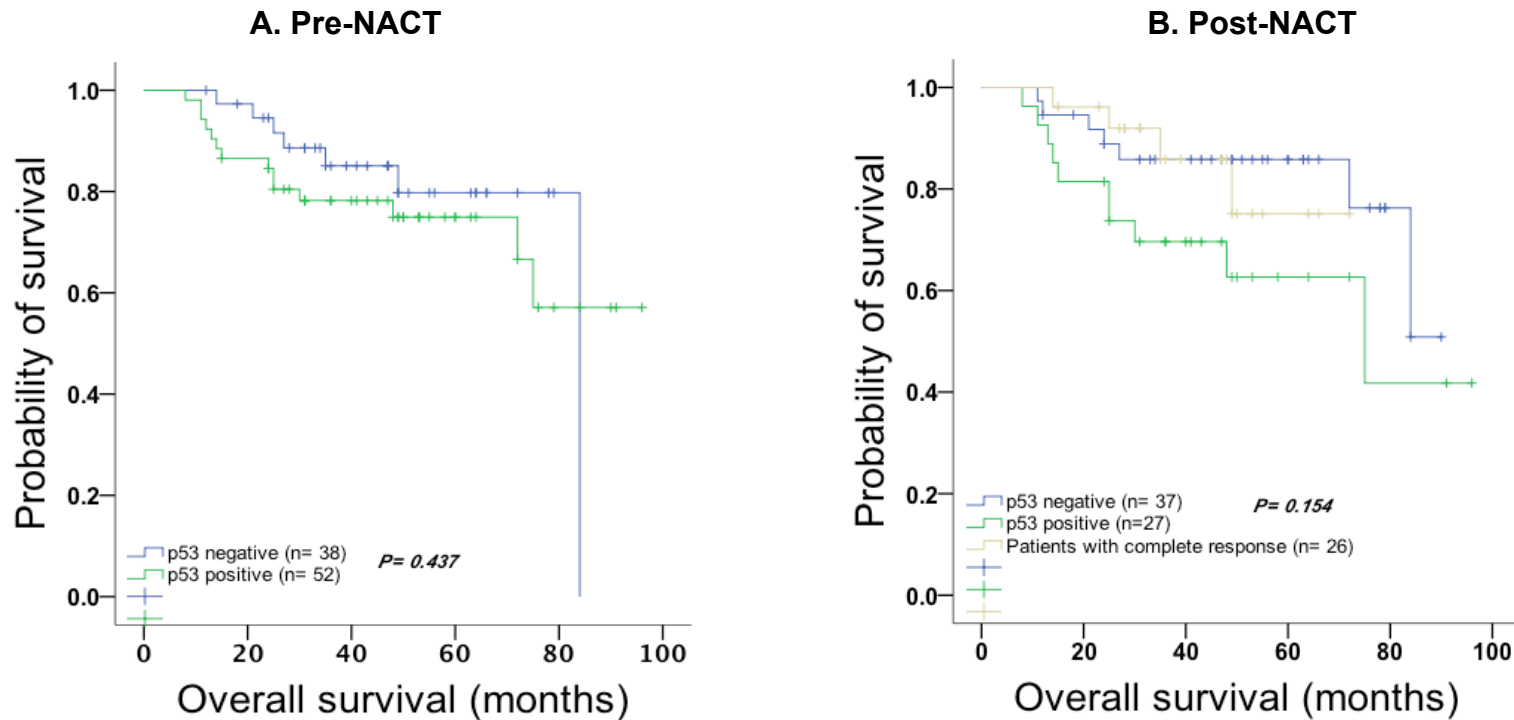
Figure 6.9. Kaplan Meier curves showing BC OS in patients with p53 negative or positive expression pre-NACT treatment (A) and in patients with p53 negative or positive expression or pCR cases post-NACT treatment (B).
The cut-off percentage (≥10%) was used to dichotomise p53 expression into negative and positive.

6.4.5 Correlation of NACT treatment and pathological tumour response

In the p53 expression study, the response to NACT treatment was evaluated using pathological tumour response data available for 87 patients. The response of p53 tumours to NACT treatment was varied. The distribution of pathological tumour response cases within this p53 study was very similar to that previously described in the MCPH1/BRIT1 study. The NR, MR, PR and CR were identified in 9/87 cases (10.3%), 1/87 (1.1%) 51/87 (58.6%) and 26/87 (29.8%), respectively (Table 6.1).

In addition, the administered NACT regimens in p53 expression study were available for 71 patients. Regimen was used again as described in (Table 6.10), for example, as we have previously divided the chemotherapy into three groups, which were as follows: Group 1 includes ((EC), (FEC), and (ECF), Group 2 includes (EC +Taxotere) or (FEC + Taxotere) and (Neo-tAnGo EC +Taxotere) and Group 3 was Taxotere + Carboplatin.

Table 6.10. Categorisation of breast cancer patients based on the type of combination therapy used for NACT treatment in the p53 cohort.

NACT group	NACT regimens	Patient No. in p53 study n = 71 (%)
Group 1	Epirubicin + Cyclophosphamide (**EC**)	32 (45%)
	5-Fluorouracil + Epirubicin + Cyclophosphamide (**FEC**)	
	Epirubicin + Cisplatin + 5-Fluorouracil (**ECF**)	
Group 2	EC + Taxotere	38 (53.5%)
	FEC + Taxotere	
	Neo-tAnGo + EC (phase III trial) + Taxotere	
Group 3	Taxotere + Carboplatin	1 (1.4%)

No significant correlation was observed (p = 0.444; Spearman correlation test) when cross-tabulation analysis was employed to identify the correlation between the three different NACT treatment groups with pathological tumour response classifications. For Group 1 the distribution of cases with NR, PR and CR was 2/32 cases (6.2%), 18/32 (56.2%) and 12/32 (37.5%). In Group 2, the proportion of cases with NR, MR, PR, and CR were 5/38 (13.1%), 1/38 (2.6%), 21/38 (55.2%)

and 11/38 (28.9%), respectively. In addition, only one case was treated with Taxotere + Carboplatin and it achieved the CR.

Next, the available matched section samples (66 patients with residual invasive carcinoma) were used to identify the effect of the individual group of NACT regimens on change in expression of p53. First, the change in percentage of p53 expression after NACT treatment was assessed and, using this, the cases were divided into four groups as follows; The first group showed a change in p53 expression from positive to negative (17/66 cases (25.7%)). The second group included only one case (1/66 (1.5%)) whose p53 expression changed from negative to positive. In the third group p53 expression showed no change and remained negative in 21/66 (31.8%) while the fourth group remained positive in 27/66 (40.9%).

Cross-tabulation analysis was then used to identify the association between NACT regimens and the change in expression of p53. Neither the first nor the second NACT regimens showed any significant change in p53 expression (p = 0.555; Spearman correlation test) (Table 6.11A). For instance, a positive to negative change in expression of p53 was identified in 2/20 cases (10%) treated with the first NACT regimen compared to 6/26 cases (23%) treated with second NACT regimen. In addition, a similar number of cases with unchanged status for p53 expression (negative) were obtained after they were treated with first and second group of NACT regimens, 9/20 cases (45%) and 9/26 (34.6%), respectively (Table 6.11A). Moreover, the prevalence of cases with no change in p53 expression (positive) was similar in the first and second groups of NACT regimens, 9/20 (45%) and 11/26 (42.3%), respectively (Table 6.11A).

Similar to pervious results that were observed in MCPH1/BRIT study in (Section 7.3.5), there was no significant correlation was identified between change/or no change in p53 expression and improved the pathological tumour response (p = 0.784; Spearman correlation test). However, cross-tabulation analysis between change/or no change in expression of p53 and pathological tumour response (NR, MR and PR) revealed that the majority of patients presented a PR in 50/65 cases after NACT treatment which were equally distributed in patients whose p53 expression had showed no change in expression of p53 (negative) 20/50 (40%) or (positive) 20/50 (40%) compared to those patients whose p53 expression changed from positive to negative 10/50 (20%) (Table 6.11B).

Table 6.11. Cross-tabulation groups with change/ or no change in p53 expression post-NACT versus type of neoadjuvant chemotherapy (A) and tumour response (B). Group 3 of NACT regimens contains only one patient as shown in Table 6.10 thus it was not included in table **A**. The second group which showed change in p53 expression from negative to positive in only one patient thus it was not included in tables **A** and **B**.

		Change in p53 expression	No change in p53 expression		
A	p53 expression	Positive to negative	Negative	Positive	Total
Chemotherapy regimes	EC, FEC or ECF	2 (10%)	9 (45%)	9 (45%)	20
	EC + Taxotere or FEC + Taxotere or Neo-tAnGo + EC (phase III trial) + Taxotere	6 (23%)	9 (34.6%)	11 (42.3%)	26
p = 0.555	Total	8	18	20	46

		Change in p53 expression	No change in p53 expression		
B	p53 expression	Positive to negative	Negative	Positive	Total
Pathological tumour response	No response	4 (44.4%)	1 (11.1%)	4 (44.4%)	9
	Minimal response	0	0	1 (100%)	1
	Partial response	10 (20%)	20 (40%)	20 (40%)	50
p = 0.784	Total	14	21	25	65

6.4.6 Correlation between change in expression of p53 post-NACT treatment with OS

The change in p53 expression in response to NACT regimens was correlated with OS rates using the available 63 matched pair samples. The Kaplan-Meier survival analyses were only performed on the three groups of patients, one of which showed a change in p53 expression (from positive-negative) and two which showed no change in p53 expression (negative or positive). Only one individual showed a change in p53 expression from negative to positive; thus this group was excluded from survival analysis.

No significant association was observed between the change in expression of p53 and OS (*p* = 0.184). The mean OS rate for patients with a change in p53 expression (from positive to negative) was 73 months (95% CI: 58-87). For those patients with no change in p53 expression (negative), the mean OS rate was 77 months (95% CI: 67-87) compared to 63 months (95% CI: 48-78) for patients with no change in p53 expression (positive) (Figure 6.10).

6.4.7 Correlation between MCPH1/BRIT1 and p53 expression

The correlation between MCPH1/BRIT1 and p53 expression pre-NACT treatment was examined using 91 core biopsies samples. Continuous analysis data showed no significant association between the expression of MCPH1/BRIT1 and p53 pre-NACT treatment (*p* = 0.301; Pearson's correlation test).
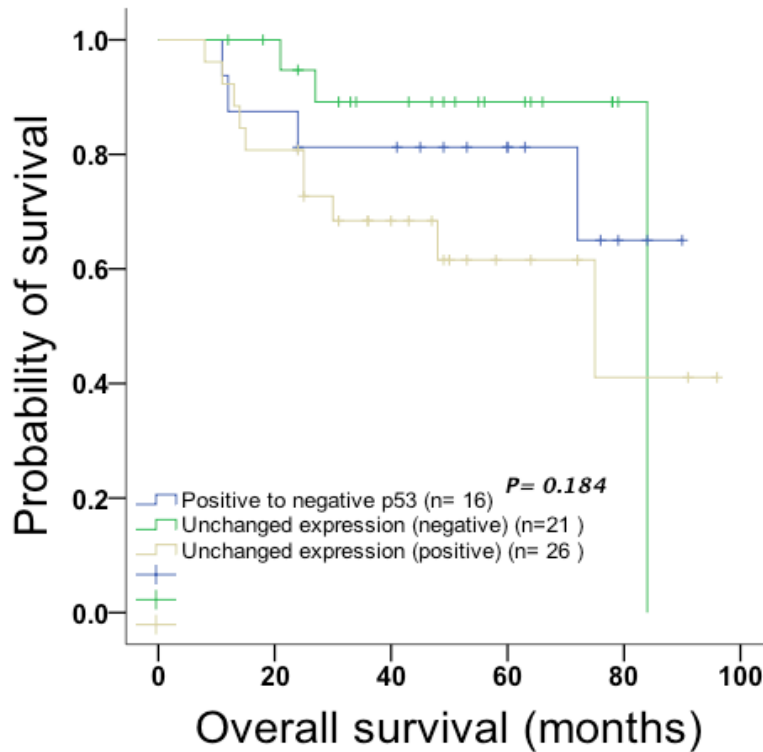
Figure 6.10. Kaplan Meier survival curves showing correlation between change (positive to negative) and no change (negative or positive) in p53 expression post-NACT treatment and BC OS.

The overall mean of % staining of MCPH1/BRIT1 expression was 34.8% compared to 35.6% for % staining of p53 expression. Dichotomous data analyses did not show any significant correlation between MCPH1/BRIT1 and p53 expression pre-NACT (p = 0.353; Spearman's correlation test). The status of p53 expression in patients with low MCPH1/BRIT1 expression pre-NACT treatment was negative in 21/45 cases (46.6%) and positive in 24/45 cases (53.3%). While in samples which expressed high levels of MCPH1/BRIT1, negative p53 expression was identified in 17/46 cases (36.9%) compared to 29/46 cases (63%) with positive p53 expression.

The association between MCPH1/BRIT1 and p53 expression post-NACT treatment using 65 matched resections of invasive tumours samples was examined. A positive weak Pearson's correlation was identified between MCPH1/BRIT1 and p53 expression post-NACT treatment (r = 0.282), resulting in a statistically significant correlation with a p value of 0.023. The overall mean of % staining of MCPH1/BRIT1 expression was 66.9% compared to 33.4% as the mean of % staining of p53 expression. Again, the statistically significant correlation between MCPH1/BRIT1 and p53 was reduced after using the dichotomous analysis

data (p = 0.113; Spearman's correlation test). After NACT treatment, the number of cases with low MCPH1/BRIT1 decreased to 10. There were 8 patients (80%) with negative p53 expression compared to 2 patients (20%) with positive p53 expression. However, patients who expressed high levels of MCPH1/BRIT1 showed similar proportion of cases with p53 expression either negative 29/55 (52.7%) or positive 26/55 (47.2%).

The correlation between MCPH1/BRIT1 with p53 expression in pCR cases (26 cases) pre -NACT chemotherapy was also examined to investigate whether the status of p53 expression in these patients would be an important factor to achieve the pathological complete response. The continuous analysis data using Pearson correlation showed no significant association between MCPH1/BRIT1 and p53 expression (p = 0.886). The mean % of staining of MCPH1/BRIT1 expression was 29.61% compared to the mean % of staining of p53 expression at 25.26%. Dichotomous analysis of MCPH1-p53 expression in CR cases using Spearman test, showed no significant correlation between MCPH1 and p53 expression (p = 0.635). The distribution of cases with negative or positive p53 expression in tumours with high MCPH1/BRIT1 were similar to those with low MCPH1/BRIT1 expression. Negative p53 expression was identified in 8/12 cases (66.6%) compared to 4/12 (33.3%) with positive p53 expression for CR patients with high MCPH1/BRIT1 expression. While, negative p53 expression was identified in 8/14 cases (57.1%) compared to 6/14 (42.8%) with positive p53 expression for CR patients with low MCPH1/BRIT1 expression.

6.4.8 Discussion for p53 study

The aim of investigating the expression status of the p53 protein in BC tissue samples alongside MCPH1/BRIT1 expression was to determine whether a correlation between p53 and MCPH1/BRIT1 expression exists in BC tissues and if this stimulates sensitivity to NACT, increases the survival rate and improves patient outcomes. Since the WT *p53* usually is correlated with chemo- or radio-sensitivity compared to the mutated p53 version (Kandioler-Eckersberger *et al.*, 2000; Vogelstein and Kinzler, 2004; Brosh and Rotter, 2009), the status of p53 expression may be essential to supporting the impact of MCPH1/BRIT1 expression on tumour response to chemotherapy.

In normal tissue, p53 is barely detectable due to its short half-life; however, in tumour cells mutant p53 expression can be detected in the nucleus (Varna *et al.*, 2011), however it has been shown that detection of positive staining for p53 did not always indicate the existence of a p53 mutation (Schmitt *et al.*, 1998). This may be because the detection of p53 positivity by IHC may reflect stabilisation of WT *p53* in response to stress but not mutation (Varna *et al.*, 2011). In addition, the absence of p53 immunostaining has been reported in tumours that contain mutations in the *TP53* gene, specifically nonsense mutations, or deletions/splicing errors (Geisler *et al.*, 2001).

In this study IHC was performed to detect p53 protein expression, but unfortunately it was not possible to determine whether low expression indicated the *TP53* gene was lost or inactivated at the DNA sequence level, due to the lack of the primary fresh tumours for this cohort. However, p53 immunostaining has been considered a useful tool for assessment of p53 expression since the WT-p53 is rapidly degraded and p53 gene mutation often results in a stable form of the p53 protein, which would be easily detected in cancer cells (Petitjean *et al.*, 2007; Yang *et al.*, 2013). Furthermore, the BC tissue samples in this cohort were diagnosed with aggressive, invasive and high grade tumour phenotypes, by the consultant pathologist Dr. Abeer Shaaban; therefore it is expected that detection of positive p53 staining may generally be due to p53 expression of a non functioning form. Sequencing the *p53* gene for more than 90 cases pre- and post-NACT treatment would be expensive and time-consuming, when compared to IHC staining that is more convenient for daily practise.

In this study, the nuclear p53 protein expression data clearly demonstrated the significant effect of NACT treatment on p53 expression. A reduction of p53 positive cases from 44/66 (66%) pre-NACT to 28/66 (42%) post-NACT clearly indicates the frequent reduction in the level of p53 positive expression of tumour cells in response to NACT treatment.

The difference in p53 expression levels pre- and post-NACT detected in this study reached statistical significance in contrast to trends identified in the previous study by Faneyte *et al.* (2003). The latter authors conducted a BC study to evaluate p53 immunostaining in 50 cases that received one type of NACT regimen Cyclophosphamide, Epirubicin and 5-Fluorouracil ($FE_{120}C$). This study demonstrated no change in p53 expression pre-and post-NACT in 39/50 cases (78%) (24 cases remained p53 negative and the other 15 cases p53 positive post-

NACT) compared to 5/50 (10%) cases or 6/50 (12%) cases whose p53 expression changed from positive to negative or from negative to positive, respectively. The p53 results in this current study were slightly similar to the aforementioned study as p53 expression pre- and post-NACT remained the same in 48/66 (72.7%) (21 cases remained p53 negative and other 27 cases p53 positive post-NACT). However, this current study compared to the aforementioned study showed high patient numbers 17/66 (25.7%) whose p53 expression changed from positive to negative and only 1 case (1.5%) form negative to positive. Variations associated with the size of the patient cohorts, NACT treatment strategies, type of tumours and their response to chemotherapy may be considered to be factors may produce different results among these studies.

Furthermore, the analysis in this study demonstrated a reasonable reduction in cases with high-grade (G3) and an increase in cases with low to moderate grade (G1 and G2) post-NACT, representing a significant correlation between p53 positive tumours and high-grade (G3) and between p53 negative tumours and moderate grade (G2). This may indicate the effect of NACT in altering expression of p53 from positive to negative, resulting in tumour regression.

Moreover, in comparison to p53 negative expression post-NACT, p53 positive expression, in this study, bears a direct significant association to the proliferation of marker Ki67 and an inverse relationship to ER, PR receptors and triple negative BC. The expressions of p53 in tumours with negative receptors status and with a high proliferation (Ki67) indicate greater tumour aggressiveness and a potential risk of relapse (Sirvent *et al.*, 1995; De Azambuja *et al.*, 2007).

Many studies have reported that lack of p53 mutations predicts a better OS or disease-free survival after chemotherapy (Linjawi *et al.*, 2004; Overgaard, 2000). p53 immunostaining in BC has not been used as a regular marker in clinical practise, due to the lack of a positive correlation between the accumulation of p53 and survival outcome in early BC (Harris *et al.*, 2007). Similarly, the presented study did not demonstrate the prognostic influence of p53 status as detected by IHC staining on patients' survival pre- and post-NACT treatment. In addition, change in p53 expression analysis failed to show a correlation with survival rate post-NACT. These findings correlated with results of other studies, which demonstrated that p53 expression status is not associated with response specifically to NACT or other anti-BC drugs (Daidone *et al.*, 1995; Faneyte *et al.*,

2003; Yang *et al.*, 2013). However these results may due to the lack of a sufficiently large number of patients included in this study.

Since NACT treatment has been reported to cause a reduction in the expression level of the mitotic index marker Ki67, assessment of Ki67 expression in the re-sectioned samples post-NACT could be used as an indicator for predicting the response of p53 positive tumours to NACT (Faneyte *et al.*, 2003; Lee *et al.*, 2013). Although in this study the dichotomous analysis post-NACT identified a significant association between p53 positive tumours and the high proliferation index (Ki67), the response to NACT within these tumours was partial and life expectancy was low compared to p53 negative tumours. Possibly dysfunctional p53 may contribute to increasing resistance to NACT particularly to Epirubicin therapy due to the abnormal increase in the expression of FOXM1, which is modulated by ATM, that may result in suppression of apoptotic and activating anti-apoptotic proteins such as BCL2 whereas in normal cells, the activity of FOXM1 is suppressed by the intact p53 functions (Millour *et al.*, 2010; Millour *et al.*, 2011; Halasi and Gartel, 2012).

Additionally, these results suggest that the NACT chemotherapy may not work effectively to kill p53 deficient tumours as p53-deficient tumour cells avoid G1 checkpoint arrest and evade induction of apoptosis. Progression of p53-deficient cells in S and G2 phases depends on CHK1, which allows for continual entry into S and M phases leading to genomic instability. Therefore, increased dose and cycles of Paclitaxel/Taxol, which specially acts particularly during the mitotic phase, in combination with CHK1 inhibitor could be highly effective in triggering the cytotoxicity of DNA damaging agents and inducing apoptosis in p53 deficient BC cells (Kandioler-Eckersberger *et al.*, 2000; Anelli *et al.*, 2003; Sánchez-Muñoz *et al.*, 2010; Ma *et al.*, 2012). Moreover, in p53 deficient BC cases, increasing doses of Fluorouracil therapy may alter the expression of G1 regulatory proteins such as p53 and p21 with a subsequent induction of apoptosis (Grem *et al.*, 1999; Li *et al.*, 2004). Also, combining of NACT with radiotherapy would improve patient survival.

Two studies have previously demonstrated the significance of MCPH1/BRIT1 deficiency in tumourigenesis, one of which reported the role of MCPH1/BRIT1 in regulation of p53 stability (Zhang *et al.*, 2013a) and concluded that MCPH1/BRIT1 might repress cell transformation in *vivo* and *vitro* in a manner that was dependent and independent of p53 function. The same group, confirmed their pervious findings with the generation of a mouse model with knockout of Mcph1/Brit1 alone

or in combination with p53 (Mcph1$^{-/-}$ and Mcph1$^{-/-}$/p53$^{-/-}$, respectively) (Liang *et al.*, 2014). Tumours did not develop early in a mouse with Mcph1$^{-/-}$ compared to a Mcph1$^{-/-}$/p53$^{-/-}$ mouse. The MEFs with Mcph1$^{-/-}$/p53$^{-/-}$ displayed an impairment in DSB repair while HR and NHEJ repair mechanisms were significantly reduced in Mcph1$^{-/-}$/p53$^{-/-}$ MEFs compared to Mcph1$^{+/+}$/p53$^{-/-}$ MEFs. The study concluded that MCPH1/BRIT1 deficiency alone could progress tumour initiation and cooperate with p53 deficiency to accelerate lymphomagenesis and impair DNA repair ability.

In contrast, BC tissue has been used in this study to determine if a correlation between MCPH1/BRIT1 and p53 expression exists in human BC samples. The continuous and dichotomous data analyses in this study showed no significant correlation between MCPH1/BRIT1 and p53 expression pre-NACT. However, this current study showed that high MCPH1/BRIT1 and p53 positive status are correlated significantly with high tumour grade, in addition to a converse correlation between p53 positive expression with hormone receptors or triple negative BC and a consistent association with the proliferation marker Ki67. Thus, it may be likely that MCPH1/BRIT1 is mutated in these cases, specifically the cases with no change in MCPH1/BRIT1 expression (high) post-NACT treatment resulting in perturbation and alteration in p53 function and subsequent irregular stabilisation in tumour cells.

Furthermore, in this study, continuous analysis identified a weak positive significant correlation between MCPH1/BRIT1 and p53 expression, post-NACT treatment. An increased percentage of staining of MCPH1/BRIT1 expression (66%) was accompanied with reduced percentage of staining of p53 expression (33%), suggesting that alteration of MCPH1/BRIT1 expression from low to high in response to NACT treatment stimulates regulation of p53 expression. However, the dichotomous analysis failed, post-NACT treatment, to identify the regulation of p53 expression whether by low or high MCPH1/BRIT1 expression in BC, which may be the consequence of the small number of cases included in investigating this correlation. Also, further sophisticated experiments, such as functional analysis of separated alleles in yeast (FASAY) or direct DNA sequencing, are warranted to clarify changes in p53 expression and confirm its correlation with MCPH1/BRIT1 in BC samples. Additionally, a large number of samples are warranted to clarify the potential role of the absence or presence of p53 expression, not only in tumour growth, but also in response to chemotherapy and survival rates, when the MCPH1/BRIT1 function is perturbed.

6.4.9 Limitations of MCPH1/BRIT1 and p53 breast cancer study

This study had some limitations. Firstly, the cohort study lacks a long follow up period (e.g. 5 years), which made it difficult to employ Cox regression analysis to identify the independent prognostic or predicative factors in BC patients with defective MCPH1/BRIT1 or p53 function. Secondly, more than 30 cases from the cohort were excluded due to the absence of the patient code number for the core biopsy or resected TMA sample which reduced the cohort sample size. Thirdly, patients were treated with different NACT regimens therefore creating small sample sizes for each NACT treatment group, which might explain the absence of a significant effect on tumour response or survival, despite the significant change obtained in MCPH1/BRIT1 and p53 expressions after NACT treatment. Fourthly, some of the principal clinicopathological data of patients pre-NACT were unavailable and made it difficult to define differences post-NACT, including the influence of MCPH1/BRIT1 or p53 in enhancing response to NACT.

Finally, although the number of cases included in this cohort was reasonable, clinicians typically recommend inclusion of >150 cases in the study in order to confirm the significance and the value of the tested marker as a prognostic response to chemotherapy and survival predictor in BC. These factors are essential to confirm the use of both MCPH1/BRIT1 and p53 as markers in clinical practise. Unfortunately a cohort of 150 paired pre and post-NACT treatment was not available. An expanded study containing a large cohort, with complete patient data, is warranted to accurately identify differences in MCPH1/BRIT1 and p53 status with clinicopathological or biomarker parameters for patients pre- and post-NACT. However, this study demonstrates for the first time a significant response to NACT by alteration of the protein expression of both MCPH1/BRIT1 (from low to high) and p53 expression (from positive to negative) in matched pairs of BC samples. Moreover, it significantly shows that reduced MCPH1/BRIT1 pre-NACT predicts better OS whereas changes in MCPH1/BRIT1 from low to high predict better OS post NACT. Further validation might be required for patients exhibiting tumours with high MCPH1/BRIT1 or p53 positive expression pre-NACT to make definitive conclusions about their predictive role in improving patient outcomes. These cases may need a combination of NACT, surgery and radiotherapy to supress invasive breast carcinoma growth.

Chapter 7 The impact of MCPH1/BRIT1 expression on drug cytotoxicity

7.1 Introduction

Deficiency of MCPH1/BRIT1 is not only linked to the primary microcephaly but is also associated with cancer (Venkatesh and Suresh, 2014). Numerous studies have been conducted to understand the role of MCPH1/BRIT1 in many types of cancer such as breast, ovarian, endometrial, glioblastoma and oral squamous cell carcinoma (OSCC) (Rai *et al.*, 2006; Hagemann *et al.*, 2008; Bilbao *et al.*, 2010; Richardson *et al.*, 2011; Bruning-Richardson *et al.*, 2011; Venkatesh *et al.*, 2013). Indeed, loss of heterozygosity (LOH) specifically at chromosome 8p23.1, where MCPH1/ BRIT1 is positioned, is also common in breast and ovarian cancer (Rai *et al.*, 2006) (See Chapter 1; Section 1.1.6.4).

MCPH1/BRIT1, a DNA repair protein, may be involved in sensitising the tumour cells to chemotherapy such as Carboplatin and Paclitaxel/Taxol. Carboplatin binds to DNA preventing its replication and leading to DNA breaks, while Paclitaxel/Taxol binds to microtubules to inhibit mitosis and induce apoptosis. Thus, aberration in the function of MCPH1/BRIT1 may compromise the activity of such anti-cancer drugs and lead to cancer growth preventing apoptosis.

Hence, this study aimed to investigate the role of MCPH1/BRIT1 in chemoresistance using different cell viability assays to identify the response of the OVCA cell lines 1847 and SKOV-3 to Carboplatin following *MCPH1*/*BRIT1* siRNA treatment. In addition, a transfected human embryonic kidney 293 (HEK293) cell line with stably overexpression of MCPH1/BRIT1 and inducible system tetracycline was exposed to Carboplatin and paclitaxel/Taxol to elucidate the potential role of MCPH1/BRIT1 overexpression in chemosensitivity.

7.2 Results

7.2.1 DAPI whole cell number assay

The OVCA 1847 cell line, which shows a resistance phenotype to platinum based chemotherapy (Cisplatin) (Godwin *et al.*, 1992) was selected to investigate

whether MCPH1/BRIT1 is implicated in drug resistance. Initially a 96- well plate format was used to treat the cells with siRNA duplex to knockdown *MCPH1/BRIT1* followed 24hr later by treating the cells with a range of concentrations of Carboplatin (µM) for 72hrs. The Operetta imaging system was used to detect the DAPI cell nuclei staining and Columbus software was then used to assess cell viability as previously described in (Chapter 2; Sections 2.2.4 and 2.2.5). This would allow for identifying the effect of depletion of MCPH1/BRIT1 in the response of cancer cells to platinum based chemotherapy.

The experiment was performed in triplicate and the concentration required to kill 50% of cancer cells (IC50) was measured as described previously (Chapter 2; Section 2.6.5). Using Columbus, a visual inspection to detect PCC cells as a consequence of *MCPH1/BRIT1* siRNA was also performed in cells that had not been treated with Carboplatin. PCC was used as an additional surrogate marker to confirm transfection efficiency and *MCPH1/BRIT1* knockdown. Although the triplicate repeats showed the PCC cells, IC50 analysis revealed that the response of the depleted MCPH1/BRIT1 1847 cells to Carboplatin varied compared to controls using either NT-siRNA or untransfected cells (Table 6.1).

The cells treated with *MCPH1/BRIT1* siRNA and Carboplatin needed a higher drug concentration IC50 (SD) = 99.65µM (111.79) than those with the NT-siRNA (IC50 = 40.75µM (6.20)) or untransfected cells (IC50 = 43.61µM (40.46)). However, there was no statistically significant difference in the response to Carboplatin in MCPH1/BRIT1 depleted cells compared to those treated with NT-siRNA (p = 0.413; n = 3 repeats; Student Unpaired t-test) (Figure 7.1). This may potentially indicate the contribution of depletion of MCPH1/BRIT1 in causing resistance to the platinum therapy Carboplatin in 1847 cells, however, the considerable variability in the IC50 results among the triplicate repeats may affect on the final outcome of DAPI whole cell number assay in this study.

Clearly, identifying the potential involvement of MCPH1/BRIT1 in drug resistance was not possible using the DAPI whole cell number assay since considerable variation in the IC50 concentration was observed in the triplicate experiments. This may due to manual pipetting errors thus utilising Fluid-X XRD-384 dispenser could increase the accuracy of DAPI assay outcome. Thus, another cell viability assay such as MTS assay was performed.

Table 7.1. DAPI whole cell number assay represents variability in the IC50 in response to Carboplatin in the triplicate repeats.
The assay utilised the ovarian cancer 1847 cells in a 96-well plate at (5x10^4 cells/well), untransfected or transfected with *MCPH1*/*BRIT1* siRNA or NT-siRNA (control) followed 24hr later by Carboplatin treatment and then incubated for 72hr. The plate was scanned by the Operetta and cell number was analysed by Columbus and the IC50 for each repeat was calculated.

Transfection reagents	IC50 (Repeat 1)	IC50 (Repeat 2)	IC50 (Repeat 3)
Untransfected cells	41.61	4.19	85.03
NT-siRNA (control)	47.22	34.87	40.15
***MCPH1*/*BRIT1* siRNA**	5.18	70.7	223.07
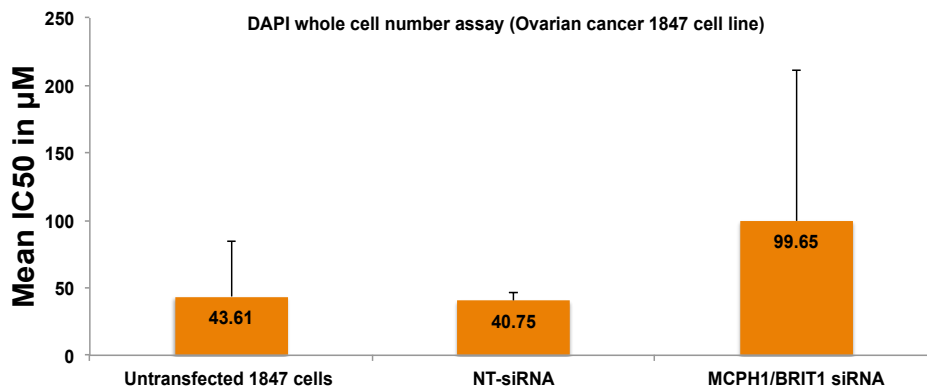
Figure 7.1. The depletion of MCPH1/BRIT1 may confer Carboplatin resistance in 1847 cell line.
The graph shows the mean IC50 of the triplicate (see Table 7.2). No statistically significant difference was identified between the IC50 of cells treated with *MCPH1*/*BRIT1* siRNA (99.65µM) compared to those with NT-siRNA (40.75µM) (p = 0.413728; n = 3 repeats; Student Unpaired t-test). The statistical significance for IC50 is based on a Student test with a p value of ≤ 0.05. The error bar represents the Standard deviation (STDEV) for the three repeats.

7.2.2 MTS cell viability assay using OVCA 1847 and SKOV-3 cell lines

Unlike the DAPI whole cell number assay, the MTS assay depends on cellular metabolism. It is based on the colorimetric change caused by reduction of a tetrazolium compound by the mitochondria in viable cells to produce a formazan that can be quantified by measuring absorbance at 490nm.

Similar experimental procedures were used in regards to knockdown of *MCPH1*/*BRIT1* by siRNA in the 1847 cell line followed by Carboplatin treatment.

After 72hr incubation, the MTS assay was carried out as previously described (Chapter 2; Section 2.6.2; Appendix 8) and the IC50 was calculated for 4 repeats. The subsequent IC50 results for the 4 replicates were noticeably better than those observed using the DAPI whole cell number assay. However, a huge variability in the IC50 results were still observed in response to Carboplatin within the four replicates, specifically in those cells treated with *MCPH1/BRIT1* siRNA in comparison to those treated with NT-siRNA or untransfected cells (Table 7.2).

Table 7.2. MTS cell viability assay representing the IC50 in response to Carboplatin in quadruplicate.
The assay used the 1847 cells plated in a 96-well plate at (5×10^4 cells/well), untransfected or transfected with *MCPH1/BRIT1* siRNA or NT-siRNA (control) followed 24hr later by Carboplatin treatment and then incubated for 72hr. The plate was treated with MTS solution, incubated for 90mins, scanned by using the absorbance reader (Dynex technologies). The IC50 for each repeat was then calculated.

Transfection reagents	IC50 (Repeat 1)	IC50 (Repeat 2)	IC50 (Repeat 3)	IC50 (Repeat 4)
Untransfected cells	310.4	323.5	252.66	265.61
NT-siRNA (control)	159.85	247.5	207.87	163.45
***MCPH1/BRIT1* siRNA**	273.8	540.6	239.02	534.94

To investigate this problem, the cell number of untransfected cells without drug addition was checked to determine if there was any variability in plating densities between the four replicates. This showed a reasonable and expectable difference in cell number (untransfected cells/without drug addition) amongst the four repeats. In addition, during the MTS assay process, another plate was stained with DAPI and processed at the same time to confirm examine the transfection efficiency of the *MCPH1/BRIT1* siRNA knockdown using PCC as a surrogate marker. In this case only those cells treated with siRNA were checked, not those treated with carboplatin. This showed both variability in %PCC and an expected reduction in cell number (Table 7.3). Therefore, the noticeable variability in the IC50 results amongst the 4 replicates particularly in the cells treated with *MCPH1/BRIT1* siRNA and Carboplatin (Table 7.2) may be caused by the level of the transfection efficiency since the siRNA transfection itself affects the cell number and the reduction in cell number became as a major problem when it was combined with use of the cytotoxic drug leading to the variability in cell number for the results of the MTS assay.

Table 7.3. Assessment transfection of *MCPH1/BRIT1* siRNA for the fidelity of MTS assay using PCC cells as a surrogate marker.
The 1847 cell line plated in 96-well and treated individually with *MCPH1/BRIT1* siRNA and NT-siRNA, incubated for 72hr, stained with DAPI and imaged by Operetta. %PCC and cell number output were analysed using Columbus. The samples in the table without Carboplatin treatment to enable examine the sufficiently of siRNA transfection. MCPH1/BRIT1 represented variability in %PCC and remarkable reduction in cell number, which may explain the variability in MTS (IC50 concentrations) results.

Transfection Reagents	Mean %PCC			Mean cell number		
Repeat	Repeat 1	Repeat 2	Repeat 3	Repeat 1	Repeat 2	Repeat 3
MCPH1/BRIT1 siRNA	12.4	5.2	12.35	932	351	432
NT-siRNA	1.4	1.85	4	3167.5	1934.5	2119
Untransfected 1847 cells	2.3	1.85	2.7	5089.5	5481.5	5197.5

However, a similar observation was noted by using MTS assay compared to those observed for the DAPI whole cell number assay. The results showed that treatment with *MCPH1/BRIT1* siRNA and Carboplatin in 1847 cells required twice as much drug to kill 50% of cancer cells compared to the corresponding control NT-siRNA or to untransfected cells that were treated with the drugs. However, this was just reached statistically significant since the mean IC50 in µM (SD) for cells treated with *MCPH1/BRIT1* siRNA was 397.09µM (163.08) as opposed to that for NT-siRNA 194.67µM (41.44) (p = 0.052, n = 4 repeats; Student Unpaired t-test) (Figure 7.2).
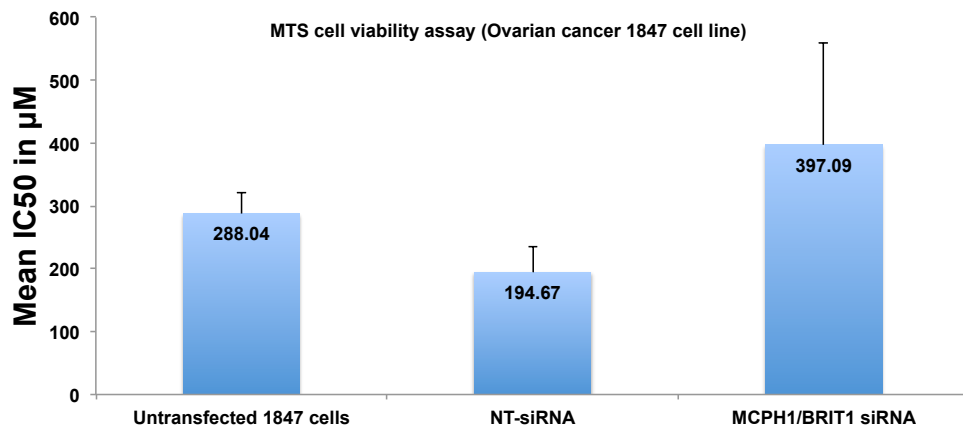
Figure 7.2. MCPH1/BRIT1 siRNA cells may develop a resistant phenotype in response to Carboplatin in 1847 cells.
The graph shows the mean IC50 produced from the MTS assay that was performed in quadruplicate (see Table 7.2). A statistical significant difference was identified between the IC50 of cells treated with *MCPH1/BRIT1* siRNA (397.09µM) compared to that of NT-siRNA (194.67µM) (p = 0.052; n = 4 repeats; Student Unpaired t-test).

The noticeable variations in IC50 values of cells treated with *MCPH1*/*BRIT1* siRNA that was observed among the four repeats may decrease the accuracy of the significant final outcome. Thus, this observation could potentially mean that MCPH1/BRIT1 may not be involved in the chemoresistance of 1847 cell line to platinum-based Carboplatin therapy. However, it may imply the opposite; that its deficiency could reduce the sensitivity of cancer cells to chemotherapy.

Since the OVCA SKOV-3 cell line does not contain endogenous *p53* (Vikhanskaya *et al.*, 1994) and harbours reduced mRNA levels of *MCPH1*/*BRIT1* based on previous RT-PCR results from our lab which may negatively influence the response to chemotherapy, the effect of depletion of MCPH1/BRIT1 in the SKOV-3 cell line was examined. However, the MTS assay unexpectedly showed that the cells treated with Carboplatin were slightly more sensitive to the drug when *MCPH1*/*BRIT1* was depleted by siRNA compared to those treated with NT- siRNA controls throughout the three replicates (Table 7.4).

Table 7.4. MTS cell viability assay represents the IC50 in response to Carboplatin in quadruplicate.
The assay used the SKOV-3 cells plated in a 96-well plate at (5x10^4 cells/well), untransfected or transfected with *MCPH1*/*BRIT1* siRNA or NT-siRNA (control) followed 24hr later by Carboplatin treatment and incubated for 72hr. The plate was treated with MTS solution, incubated for 90mins, scanned by using the absorbance reader. The IC50 for each repeat was then calculated.

Transfection reagents	IC50 (Repeat 1)	IC50 (Repeat 2)	IC50 (Repeat 3)
Untransfected cells	142.12	158.39	102.77
NT-siRNA (control)	44.74	121.49	105.36
MCPH1/*BRIT1* **siRNA**	64.13	50.65	99.46

The three replicates of MTS assay using SKOV-3 cell line displayed reasonable drug response curves when the cells were treated with either *MCPH1*/*BRIT1* siRNA or controls (NT-siRNA, untransfected cells/without drug addition) (Data not shown). However, there was no statistically significant IC50 results identified between cells treated with *MCPH1*/*BRIT1* siRNA 71.41µM (25.21) and NT-siRNA 90.53µM (40.47) (*p* = 0.52; n = 3 repeats; Student Unpaired t-test) (Figure 7.3).
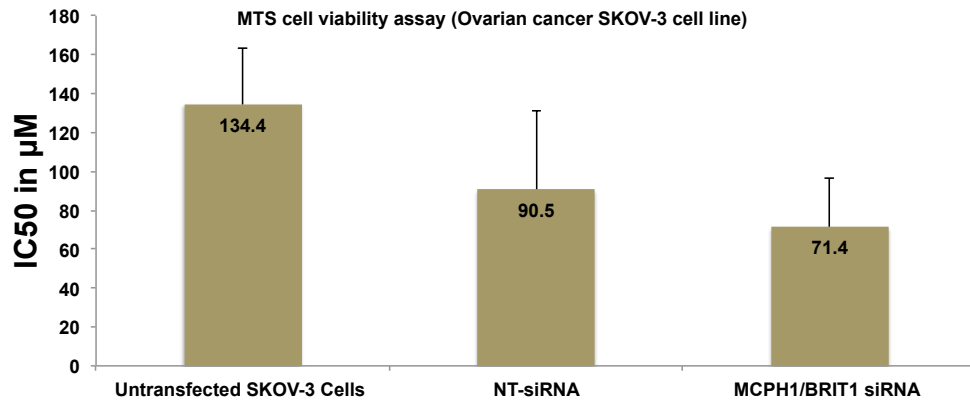
Figure 7.3. *MCPH1/BRIT1* **siRNA cells may enhance sensitivity in response to Carboplatin in SKOV-3 cells.**
The graph shows the mean IC50 generated from MTS assay and was performed in triplicate (see Table 7.4). No statistically significant difference was identified between the IC50 of cells treated with *MCPH1/BRIT1* siRNA (71.4μM) and that of NT-siRNA (90.5μM) (p = 0.52, n = 4 repeats, Student Unpaired t-test).

The dissimilarity in the results observed from MTS assay between the 1847 and SKOV-3 cell lines may represent the different genetic backgrounds of the cells. Consequently it was not possible to identify a specific effect of MCPH1/BRIT1 depletion in response to chemotherapy in these cell lines. Therefore, an inducible (IND) stable cell line HEK293 cells with overexpression of MCPH1/BRIT1 was used to identify its influence in response to anti-cancer agents such as Carboplatin and Paclitaxel/Taxol using the Vi-cell trypan blue dye cell viability assay as detailed below.

7.2.3 Vi-CELL trypan blue dye cell viability assay using the IND stable HEK293 cell line for MCPH1/BRIT1 overexpression

The IND HEK293 cell line for stable MCPH1/BRIT1 overexpression and the control Inducible Flp-In T-REx system HEK293 cell line for stably overexpressing WT-Parkin (Morrison *et al.*, 2011) were used. For both of these cell lines, one sample was treated with the inducible expression system activator tetracycline (Tet) and the other was not. Then, the cell lines were treated with a series of concentrations of Carboplatin or Paclitaxel/Taxol. Cell viability was measured to identify the difference in the IC50 between the two cell lines with and without Tet treatment.

Initially, the efficiency of the Tet inducible system, in HEK293 cells for inducing the expression of the transiently transfected cells of full-length construct of MCPH1/BRIT1 and WT Prakin was confirmed by western blotting by Dr. Victoria Cookson (Figure 7.4A) and by Thomas Ryan (LIBACS, University of Leeds) (Figure 7.4B). It is important to point out that MCPH1/BRIT1 protein expression was unexpectedly highly induced and detectable in transfected stably overexpression MCPH1/BRIT1 HEK293 cells without Tet treatment (Figure 4.8A lanes 1 and 3) compared to the control WT-MCPH1/BRIT1 expression in untransfected HEK293 cells (Figure 4.8A lane 5).

The Vi-CELL cell viability assay to examine the effect of overexpression of MCPH1/BRIT1 in inducible HEK293 cells did not show any difference in response to Carboplatin between cells which had been treated with Tet and those which had not (Table 7.5). From the three replicates, the mean IC50 (SD) for Tet IND HEK293 cells expressing MCPH1/BRIT1 treated with Carboplatin was 18.97µM (3.77) as opposed to those without Tet treatment 19.22µM (9.92) (Figure 7.5A). In addition, the control IND HEK293 cells stably expressing WT Parkin showed similar IC50 under both conditions when treated with Tet system the mean IC50 was 28.26nM (3.04) whilst those without Tet treatment the mean IC50 this was 33.18 (18.01) (Figure 7.5B).
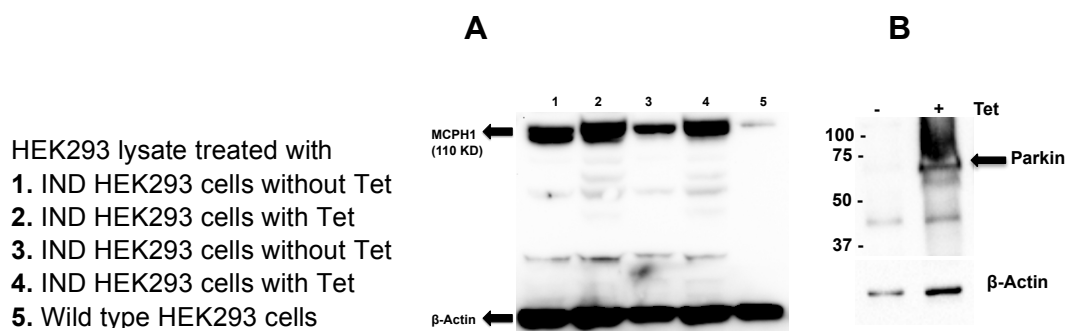
Figure 7.4. Confirmation of the efficiency of the inducible system (IND) in HEK293 cells for stable overexpression MCPH1/BRIT1 using Tetracycline (Tet).
(A) IND or wild type HEK293 cells plated at $5x10^4$ cells/ml using 24-wells plate, and 24hr later Tetracycline was added at 1:2000, mixed with cells and incubated for 72hr. Samples were probed with the rabbit anti-MCPH1/BRIT1 antibody (Abcam, Cambridge, UK; 1:1000 ab2612) or mouse anti– β-Actin antibody (Sigma, St. Louis, MO; 1:5000 100M4789). **(B)** Inducible Flp-In T-REx system HEK293 cells transfected with WT Parkin construct. Cells were treated with tetracycline for 24 hours. Parkin is essentially undetectable in the uninduced WT Parkin line (The transfected cells with WT Parkin and without Tet treatment). Samples were probed with mouse monoclonal anti- Parkin (Prk8) antibody (Cell Signalling Technology; 1; 1000; 4211).

Table 7.5. Vi-CELL cell viability assay shows the IC50 for IND HEK 293 cells with stable overexpression of MCPH1/BRIT1 and WT Parkin (control) in response to Carboplatin.

Cell treated with Carboplatin (µM)	Inducible HEK293 cell (MCPH1/BRIT1)		Control/inducible HEK293 cell (WT Parkin)	
Inducible system	With Tet	Without Tet	With Tet	Without Tet
IC50 (Repeat 1)	15.11	10.97	24.76	53.95
IC50 (Repeat 2)	19.15	30.22	29.76	20.79
IC50 (Repeat 3)	22.64	16.47	30.25	24.79

Vi-CELL trypan blue dye cell viability assay
(A) IND⁺ HEK293 cells for MCPH1/BRIT1 treated wth Carboplatin

Vi-CELL trypan blue dye cell viability assay
(B) IND⁺ HEK293 cells for WT-Parkin treated wth Carboplatin (control)
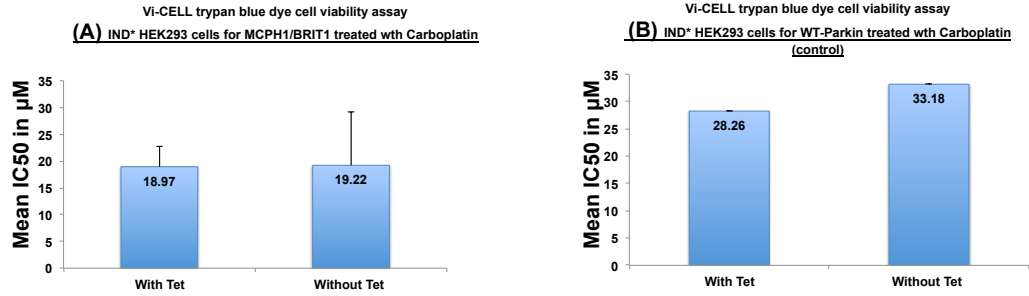
Figure 7.5. Stable overexpression of MCPH1/BRIT1 in Tet inducible HEK293 cells shows no noticeable difference in response to Carboplatin compared to cells without Tet treatment.
The mean IC50 for Tet inducible HEK293 cells for MCPH1/BRIT1 overexpression was not statistically significant 18.97µM in comparison to those without Tet treatment 19.22µM (p = 0.968986; n = 3 repeats; Student Unpaired t-test). Within the control, the Tet IND HEK293 cells for the WT Parkin overexpression did not show significant difference in the IC50 (28.26µM) to those without Tet treatment (33.18µM) (p = 0.666584; n = 3 repeats; Student Unpaired t test).

A similar observation was made when both cell lines were treated with Paclitaxel/Taxol. The response of stable MCPH1/BRIT1 overexpression to Paclitaxel/Taxol in IND HEK293 cells using Tet treatment did not differ to those without Tet treatment among the triplicate repeats. Similarly, the control cell line for WT Parkin overexpression showed no difference in response to Paclitaxel/Taxol treatment with and without Tet treatment (Table 7.6).

Table 7.6. Vi-CELL cell viability assay shows the IC50 for IND HEK 293 cells with stable overexpression of MCPH1/BRIT1 and WT Parkin (control) in response to Paclitaxel/Taxol.

Cell treated with Paclitaxel/Taxol (nM)	HEK293 cell (MCPH1/BRIT1)		Control/ HEK293 cell (WT Parkin)	
Inducible system	With Tet	Without Tet	With Tet	Without Tet
IC50 (Repeat 1)	0.4	0.2	0.4	0.2
IC50 (Repeat 2)	0.4	0.4	0.1	0.3
IC50 (Repeat 3)	0.4	0.3	0.4	0.3

The mean IC50 (SD) for Tet IND HEK293 cells expressing MCPH1/BRIT1 was 0.4nM (0.00) as opposed to those without Tet treatment 0.3nM (0.1) (Figure 7.6A). In comparison, the control IND HEK293 cells expressing WT Parkin showed an IC50 of 0.3nM (0.2) when the cells were induced with the Tet system compared to a mean IC50 of 0.3nM (0.1) without Tet treatment (Figure 7.6B).
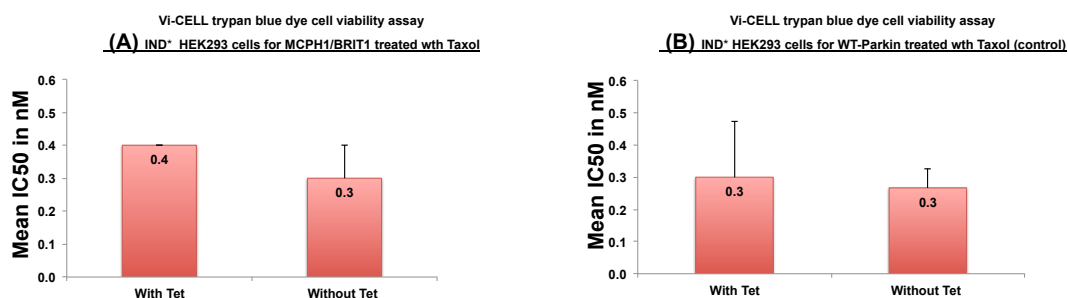
Figure 7.6. Stable overexpression MCPH1/BRIT1 in Tet inducible HEK293 cells shows no significant difference in response to Paclitaxel/Taxol compared to cells without Tet treatment.
The mean IC50 for Tet inducible HEK293 cells for MCPH1/BRIT1 overexpression was not statistically significant 0.4nM compared to those without Tet treatment 0.3nM (p = 0.158302; n = 3 repeats; Student Unpaired t-test). Within the control, using the inducible system (with/without Tet) in HEK293 cells for the WT Parkin overexpression did not show any significant difference in response to Paclitaxel/Taxol, the IC50 for cells with Tet was (0.3nM) to those without Tet treatment (0.3nM) (p = 0.666584, n = 3 repeats, Student Unpaired t-test).

In summary, the cytotoxicity assays DAPI whole number and MTS in MCPH1/BRIT1 depleted 1847 and SKOV-3 cell lines showed conflicting IC50 results in response to Carboplatin. Whereas the Vi-cell trypan blue dye cell viability assay in the inducible Tetracycline HEK293 with stable MCPH1/BRIT1 overexpression cells did not show significant difference in response to Carboplatin or Paclitaxel/Taxol in compared to those without Tet treatment.

7.3 Discussion

MCPH1/BRIT1 is implicated in the activation of DNA damage responses by regulating the expression of cell cycle checkpoint proteins CHK1 and BRCA1, inducing mitotic arrest (Xu *et al.*, 2001; Xu *et al.*, 2004) and allowing accumulation of BRAC2/RAD51 complex at DNA damage sites to proceed with DNA repair (Wu *et al.*, 2009). Deficiency in MCPH1/BRIT1 function is associated with cancer progression. Thus, the sensitivity of cancer cells with defective MCPH1/BRIT1 to

chemotherapy may be compromised leading to accelerated cancer growth and inhibition of apoptosis. Since there is no clear evidence whether MCPH1/BRIT1 is involved in chemosensitivity or chemoresistance to anti-cancer drugs, we investigated the response of the OVCA cell lines 1847 and SKOV-3 with *MCPH1/BRIT1* siRNA knockdown to Carboplatin, using different cell viability assays. Additionally, we utilised a HEK293 cell line with tetracycline inducible overexpression of MCPH1/BRIT1 to further clarify the role of MCPH1/BRIT1 overexpression in chemosensitivity.

There was difference in the cytotoxicity response of 1847 and SKOV3 cell lines with MCPH1/BRIT1 depletion to Carboplatin. A potential explanation could be the genetic heterogeneity of these diverse cell lines. In patients similar considerations usually complicate cancer diagnosis, making the correct choice of appropriate treatment options more difficult.

Furthermore, some studies demonstrated that the 1847 cell line showed a resistant phenotype to platinum-based chemotherapy. Resistance to chemotherapy may increase when the function of MCPH1/BRIT1, a DNA damage response protein, is diminished or lost. Indeed, this cell line has been found to confer low to medium resistance to the platinum-based chemotherapy Cisplatin (1-10 fold) compared to other OVCA Cisplatin-treated cell lines such as A2780/CP8 or A2780/CP70, which increased resistance to the drug 10-50 fold and 50-300 fold, respectively (Godwin *et al.*, 1992). Additionally, Cisplatin-treated 1847 cells showed a reduction in DNA adduct formation and an increase in the repair of platinum DNA adducts and DNA damage tolerance; both of these abnormal characteristics are associated with decreased sensitivity to Cisplatin (Johnson *et al.*, 1997). Moreover, the 1847 cell line has been linked to methylation of BRCA1, which reduced its gene expression (Stordal *et al.*, 2013). Loss of heterozygosity of BRCA1 and BRCA2 (mutation in WT BRCA1/2) has also been reported in the 1847 cell line, which may consider as a potential factor in decreasing the response to platinum based chemotherapy.

In contrast, a potential explanation for the chemosensitivity of SKOV-3 cells with decreased MCPH1/BRIT1 level is that SKOV-3 expresses phosphatase and tensin homolog deleted on chromosome 10 (PTEN) which is involved in tumour suppression, activation of the pro-apoptotic protein BCL-2 and caspases 3, 6, 7, 8, and 9 in response to Cisplatin (Singh *et al.*, 2013). In addition, the SKOV-3 cell line has been found to decrease tumour proliferation in response to combination

therapy using Carboplatin and Alvocidib (an inhibitor of CDK1, 2, 4, 6 and 9) (Baumann *et al.*, 2013).

The Vi-CELL trypan blue dye cell viability assay using the Tet inducible system cell line HEK293 for overexpression of MCPH1/BRIT1 did not reveal any potential role for MCPH1/BRIT1 in chemosensitivity although the protein expression of full length MCPH1/BRIT1 was originally detected by western blot, confirming the efficiency of the Tet inducible system in HEK293 cells. This may have been due to the use of the non-cancerous HEK39 cell line since its genetic background and response to chemotherapy are markedly different to those of cancer cells. More important, and as shown in (Figure 7.4A), the uninduced HEK293 cell line (without tetracycline addition) expresses quite high levels of MCPH1/BRIT1 in the first place, perhaps due to "leaky" expression from the expression cassette. Therefore induction of further overexpression with tetracycline may not cause any difference in response to chemotherapy.

Sensitivity to chemotherapy such as Carboplatin or Taxol may depend on the type of cancer cell and, importantly, the correct choice of cytotoxicity assay being used to quantify the cell viability results. One study used five different methods including MTS and MTT assays which measured the viability of cells with metabolically active mitochondria and dye-based quantifying assays such as adenosine triphosphate (ATP), deoxynucleic acid (DNA) and trypan blue exclusion (Wang *et al.*, 2011). These methods were used for *in vitro* evaluation of cancer cell proliferation and viability in response to the anti-proliferative effect of green tea polyphenols (EGCG) on LNCaP prostate cancer and MCF7 BC cells. The study found that MTS and MTT assays overestimated the number of viable cells compared to ATP, DNA and trypan blue. Consequently the observed IC_{50} concentration of EGCG was 2-fold higher in comparison to the other assays used in the study. The chemical reaction between the MTS or MTT reagents in response to EGCG caused an increase in the activity of mitochondrial dehydrogenase of viable cells, reducing the MTS or MTT of the damaged cells which increased the formation of formazan leading to artificially high results.

Thus, the selection of the correct method for *in vitro* assessment of cell viability, proliferation and apoptotic should be based on the type of cancer cell, nature of the chemotherapy being assessed and experimental design. For example, in our study, the MTS assay reagent was used in cells treated with siRNA, which may both chemically interfere with chemotherapy and influence the metabolic

activity of cells, leading to variations in the results of each MTS experimental repeat performed with the 1847 cell line (Plumb *et al.*, 1989). In addition, the trypan blue cell viability assay using the Tet inducible system requires multiple steps, such as the culture medium to be changed and fresh Tetracycline to be added after Carboplatin or Taxol treatment and multiple PBS washes before cell scraping which may not collect all the available cells in the wells, in addition to the centrifugation steps that are time-consuming when large sets of plates or samples need to be proceeded and transferred to the cell counter instrument (Riss *et al.*, 2003).

Since the MTS assay may overestimate the actual effect of MCPH1/BRIT1 depletion in cytotoxicity by exhibiting an absorbance which is higher than the actual reduction in the tetrazolium produced by dying cells (Jo *et al.*, 2015; Riss *et al.*, 2003), a careful interpretation of the MTS cytotoxic results is required using a more sophisticated method such as flow cytometry to detect apoptosis using annexin V conjugates.

For future investigation, a more robust method would be recommended for the *in vitro* assessment of MCPH1/BRIT1 expression on tumour proliferation in response to anti-cancer drugs, such as the use of stable knockdown or overexpression of MCPH1/BRIT1 in cell lines. Also, generating a cancer cell line with a stable knockout of MCPH1/BRIT1 using the CRISPR/Cas9 gene editing system would be beneficial to circumvent the problems that could occur during the use of inhibitory RNA techniques (Ran *et al.*, 2013; Sánchez-Rivera and Jacks, 2015; Agrotis and Ketteler, 2015). In addition, in order to generate more consistent, reliable and precise measurement of cytotoxic results, it is highly recommended that different cytotoxic assays, such as clonogenic assays (Jo *et al.*, 2015), cell counting Kit-8 (CCK-8) (Sittampalam *et al.*, 2013) or CellTiter-Glo Luminescent cell viability assay for quantifying ATP (Kangas *et al.*, 1983; Petty *et al.*, 1995; Crouch *et al.*, 1993) are also employed.

Chapter 8 Final discussion

Mutations in the *MCPH1/BRIT1* gene are responsible for the PCC cells detected in patients with microcephaly and PCC disorders (Neitzel *et al.*, 2002; Trimborn *et al.*, 2004). PCC occurs when interphase chromatin is abnormally condensed into chromosomes at the early G2 phase, a form of premature entry into mitosis before completion of DNA replication. Intensive investigations have been carried out to study the cellular functions of MCPH1/BRIT1 in multiple pathways including regulation of cell cycle checkpoints, chromosome condensation, DNA damage response and repair, repressed activity of hTERT, regulation of apoptosis and stability of p53 (Chapter 1: Section 1.1.6). PCC phenotype has been seen in multiple types of human cancers (Augustus *et al.*, 1985; Reichmann and Levin, 1981; Kovacs, 1985; Hittelman *et al.*, 1980) and has been induced by *MCPH1/BRIT1* siRNA in HeLa and U2OS cancer cell lines (Trimborn *et al.*, 2004; Trimborn *et al.*, 2006; Adams *et al.*, 2014).

The precise molecular mechanism involved in regulating chromosome condensation in normal and cancer cells by MCPH1/BRIT1 has not yet been determined. Therefore, one of the main aims of this PhD thesis has been to identify the regulatory network that induces PCC in cancer cells in order to understand the cellular mechanisms by which the various defects in MCPH1/BRIT1 induce PCC.

To this end, a high-throughput high-content imaging system (Operetta) and analysis software (Columbus) were utilised to perform both a small molecule and a siRNA screen aimed at identifying compounds or genes that would induce PCC in cancer cells with functional MCPH1/BRIT1. The Dharmacon siGENOME SMARTpool siRNAs targeting the hPK and Ubq siRNA sub-libraries is known as the PCC inducer screen. Another Dharmacon siGENOME SMARTpool siRNAs targeting hPK siRNA sub-library screen was performed using U2OS cells that had also been transfected with *MCPH1/BRIT1* siRNA (forward siRNA transfection). This was principally aimed at identifying genes reducing and/or increasing PCC and it is known as the PCC modifier screen. In this thesis, the cell number data from both the hPK siRNA PCC inducer and modifier screens was also combined to identify synthetically lethal siRNAs in MCPH1/BRIT1 deficient cells.

Furthermore, inactivation of MCPH1/BRIT1 function has been observed in many aggressive types of cancers and may influence tumour response to chemotherapy since MCPH1/BRIT1 is involved in DNA damage response and

repair. Thus, BC samples from a cohort containing patients with advanced BC who had undergone treatment with NACT therapy was utilised to investigate the effect of MCPH1/BRIT1 expression pre- and post-NACT in tumour response and patient survival. The same BC cohort was stained with p53 to study the correlation between MCPH1/BRIT1 and p53 expression in BC tissues pre- and post-NACT.

8.1 General summary and discussion of PhD findings

8.1.1 Identification of four small molecules potentially induced PCC

In this PhD thesis, we have carried out, a small molecule screen (SMS) in cancer cell culture system. 792 CC were selected by Dr. Richard Foster (University of Leeds Chemical Biology and Medicinal Chemistry Group) from an original library of 33,000 compounds after an *in silica* screen based on potential ability of the CC to fit within the *N* -terminal pocket of MCPH1/BRIT1. This SMS is different to other screens that do not specify the target's structure before testing CC (Hoelder *et al.*, 2012). Human *MCPH1*/*BRIT1* gene encodes a protein known as Microcephalin. It contains of three BRCT domains that is common in DNA damage response proteins. One BRCT domain is located on the *N*-terminus while the other two BRCT domains are located on the *C*-terminus (Chapter 1: Section 1.1.3). Richards *et al*., (2009) have determined that the pocket on the surface of *N*-terminal BRCT domain of MCPH1/BRIT1 is necessary to prevent PCC. Thus, identification of small molecule inhibitors that target the *N*-terminal domain of MCPH1/BRIT1 has been mainly aimed to induce PCC. This can be a useful laboratory tool for studying the biological function of MCPH1/BRIT1 in different cellular pathways.

A novel high throughput SMS was developed using the ovarian cancer 1847 cell line. Interestingly, this cell line harbours moderate levels of MCPH1/BRIT1 mRNA and protein, genetic defects in BRCA1/BRCA2 genes (Stordal *et al.*, 2013) and has shown a moderate resistant phenotype to platinum based chemotherapy (Cisplatin) (Godwin *et al.*, 1992; Johnson *et al.*, 1997). Thus, it can be considered an ideal cell line system to be utilised for investigating the biological and potential cytotoxic effect of novel CC on sensitising cancer cells to Cisplatin.

The current SMS was conducted in duplicate after two different incubation periods (24hr and 48hr). The SMS conducted a wider analysis which was not only aimed at identifying CC which induced PCC but also those which affected cell

number or increased numbers of mitotic cell (expressing pHH3 Ser10). This would not have been possible without utilising the Operetta high throughput high content imaging system since this enabled imaging of multiple phenotypes from a large selection of CCs within a short time. The imaging analysis software Columbus was used to numerically describe the cellular phenotypes induced by the CC (PCC, cell number, mitotic index).

Each plate contained the positive control *MCPH1/BRIT1* siRNA to assess PCC while DMSO (0.2%) was used as a negative control. Therefore, in order to eliminate any potential off-target effects, a Z score or Robust Z score analysis for hits identification was performed using the negative control DMSO to assay the alteration of the three phenotypic endpoints (%PCC, cell number and %mitotic cells) caused by CC in this screen. The cut-off used for hits identification with the Z score or Robust Z score was ≥ 2 for CC that increased %PCC or %mitotic cells whereas ≤ -2 for CC hits decreased cell number. The overall performance quality of the SMS was positive; however, the Pearson's correlation between replicates 1 and 2 in inducing %PCC by CCs was weak at 24hr (r = 0.3017; *p* < 0.0001) in comparison to the strong correlation at 48hr (r = 0.7654; *p* < 0.0001). This may due to the variation in %PCC induced by some CCs in the first and second replicate at 24hr leading to a weak linear correlation coefficient between the replicates (Chapter 3; Section 3.2.1.4.2; Figure 3.7).

The initial Z score or Robust Z score analysis for identification of potential CC hits showed 17 hits after 24hr and other 27 hits after 48hr. Further imaging analysis was conducted using Columbus to investigate whether these potential CC hits produce other biological alterations in addition to their potential induction of PCC phenotype. Indeed, changes in chromatin structure that are associated with induction of PCC may be correlated with other cellular phenotypes during mitosis such as expression of pHH3 Ser10 (mitotic marker), or with other cellular mechanisms such as induction of apoptosis although these potential mechanisms need to be confirmed. This suggested that these potential CC hits may induce similar cellular effects to those seen with *MCPH1/BRIT1* siRNA. Initially, noticeable cellular alterations were caused by some CC from 24hr or 48hr hit lists in this SMS. For instance, the CC in MP59-241 (well F5) and MP64-65 (well F7) showed significant Z scores or Robust Z scores (%PCC) at 24hr and 48hr (Chapter 3; Section 3.2.1.5; Table 3.1 A and B). Interestingly, the potential activity of these two

CCs in inducing PCC was also correlated with a decrease in cell number (Chapter 3; Section 3.2.1.5.1; Tables 3.2 A and B).

Furthermore, the CC MP59-241 (well F5) maintained an elevated level of mitotic index/pHH3 Ser10 expression at 24hr and 48hr whereas the CC MP64-65 (well F7) displayed a higher mitotic index at 24hr which dropped noticeably after 48hr (Chapter 3; Section 3.2.1.5.2; Tables 3.3 A and B), suggesting that an increase in mitotic cells at 24hr may be associated with abnormal induction of PCC whereas the reduction in mitotic cells at 48hr may be due to the induction of cell death. The cellular effects (decrease in cell number or increase in mitotic cells) that were induced by the remaining potential CC PCC-inducing hits included on the 24hr and 48hr hit lists were varied, indicating the diversity in the structure of CCs that may be responsible for triggering unique cellular changes in each individual CC at different periods of incubation (Chapter 3; Section 3.2.1.5: Section 3.2.1.5.1; Section 3.2.1.5.2).

Before performing the validation step, a critical visual inspection was carried out of each CC included in the hit lists at 24hr (17 CC) and 48hr (27 CC). This was followed by 2 phases of primary validation that were conducted using the dose-response curve. These were filtration steps that are required to preserve the false negative CC hits and eliminate any false positive CC reducing the off-target effects. Consequently, in the first phase of primary validation, the validation was performed for those CC that had presented significant Z scores or Robust Z scores for %PCC at both 24hr and 48hr, some 7 potential CC hits. Consequently, only 2 of these hits presented an effective dose-response curve for %PCC, namely, MP64-65 (well B2) at 24hr and 48hr and MP59-241 (well F5) at 48hr. The 5 remaining CCs, which were tested, did not present any consistent changes or reactivity in response to different CC concentrations and displayed irregular dose-response curves.

Then, the decision was made to perform the second phase of primary validation for the remaining potential CC hits (n = 20) that were included only in the 48hr hit list. The 7 CC hits that initially were tested in the first phase were re-tested in the second phase at 48hr for further confirmation of their ability to induce PCC. The reason for focusing on validation CC hits at 48hr but not 24hr was due to the increased variability between the replicate CC screens seen after 24hrs. In addition, induction of PCC phenotype by *MCPH1/BRIT1* siRNA in cancer cells requires an incubation time of 48hr. Consequently, from the 27 potential CC hits, 8 validated, namely MP59-241 (wells F5 and F7); MP64-65 (wells F7); MP66-67 (well C1);

MP74-75 (wells B11 and G11); and MP76-77 (wells E3 and G3) (Chapter 3; Section 3.2.1.8). These CC presented a reliable dose-response curve for increased %PCC and, interestingly, this was also correlated by a gradual effect on cell number, suggesting the potential association of these CCs with reducing cell number potentially by inducing cell death, which may warrant further investigation and confirmation.

The secondary validation phase was conducted using fresh stock of these 8 potential CC PCC-inducing hits. At this stage, each CC hit showed an acceptable dose-response curve pattern after optimising the serial dilution for each CC individually; some CC hits responded better (for instance, they triggered PCC) to the use of the higher range of CC concentration, others to the lower range. This indicated that the diversity of the structure of the CC hits might make a noticeable contribution to triggering their distinctive cellular effect in inducing the PCC phenotype. Indeed, the SMS validated 4 promising potential CC hits that induced PCC. Two of them (wells B11 and F5) induced the highest %PCC (20.64% and 12.14% at the lower concentrations of 5µM and 2.5µM, respectively). Thus, they were considered to be strong hits. Another two CC (wells F7 and G11) induced a lower increase in %PCC rate (7.70% and 3.63%, at a slightly higher concentration of 40µM and a moderate concentration of 10µM, respectively) and were thus considered to be weaker hits. Validation of 4 out of 792 CC in this SMS confirmed the overall hit rate 0.5% that was initially estimated by the library supplier.

Although the SMS was mainly conducted for identification of CC inducing PCC, other cellular alterations caused by CC, including reduction in cell number or increase in mitotic index, were also reported (Chapter 3; Sections 3.1.2.6 and 3.1.2.7). Data for CC that displayed reduction in cell number or increase in mitotic index on their images have recently been made available to scientific investigators to perform further essential characterisations of their structure, biological and cellular reactions and subsequently identify the molecular mechanisms that lead to altered cell number or mitotic index. Combining data from our SMS with other available functional genomic and RNAi screening data could be a useful means of identifying lead compounds for biological and molecular research applications and potentially for therapeutic drug discovery.

8.1.2 Analysis of high throughput hPK and hUbc siRNA screens for genes inducing PCC

Although MCPH1/BRIT1 has been shown to regulate multiple cellular pathways, the exact molecular mechanism of MCPH1/BRIT1 in regulating chromosome condensation awaits further clarification. Hence, siRNA screens targeting hPK and Ubq sub-libraries were performed and analysed for genes inducing PCC. The identification of genes inducing PCC in cells with intact MCPH1/BRIT1 function would allow us to determine which defective regulatory networks are potentially responsible for inducing abnormal DNA condensation and causing perturbation to cell cycle progression. Then, the potential interaction of these molecules with MCPH1/BRIT1 can be investigated, our understanding of the biological functions of MCPH1/BRIT1 in cancer can be expanded and, subsequently, therapeutic targets could be identified.

PCC inducer hPK or Ubq siRNA screens displayed significant Pearson correlations for %PCC between the first and the second replicates (r = 0.8391; p < 0.0001; n = 720) or (r = 0.7986; p < 0.0001; n = 720), respectively. The overall false-negative rate was acceptable (5.5%) and extremely low (0.0%) for the hPK and Ubq siRNA screens, respectively; the overall false-positive rate for both siRNA screens was also very low 0% (n = 72), indicating their powerful performance. The initial validation stage only included 4 potential siRNA hits from the hPK sub-library and one from the Ubq sub-library, all of which showed significant Z scores ≥ 2 cut-off. However, none of the 4 hPK siRNAs induced PCC using 4 deconvoluted siRNA's and they were not investigated further. Selection of a small number of potential siRNAs candidates may be considered as a potential factor for unsuccessful validation.

The single selected Ubq siRNA hit *FBXO5*/*EMI1* demonstrated an increase in %PCC cells with condensed chromosomes specifically with the use of the individual siRNA 2 and 4 and these siRNAs were further validated at both mRNA and protein levels. Interestingly, double knockdown of *FBXO5*/*EMI1* siRNA with *MCPH1*/*BRIT1* siRNA noticeably increased %PCC compared to that observed in single knockdown of *FBXO5*/*EMI1* siRNA. Consequently it was speculated that *FBXO5*/*EMI1* siRNA might potentially be implicated in inducing PCC. However, visual inspection of both the single *FBXO5*/*EMI1* siRNA transfection and double *FBXO5*/*EMI1* and *MCPH1*/*BRIT1* knockdown identified large nuclei with condensed chromosomes,

which is slightly different to those observed with *MCPH1*/*BRIT1* siRNA alone. Moreover, a noticeable reduction in cell number was also observed for both conditions. This may suggest that FBXO5/EMI1 functions as an independent pathway of MCPH1/BRIT1 to potentially regulate chromosome condensation during the cell cycle.

However, according to many studies that have demonstrated induction of PCC phenotype in cells with defective function of MCPH1/BRIT1, this occurs during G2/M phase (Neitzel et al., 2002; Trimborn et al., 2004; Trimborn et al., 2006; Trimborn et al., 2010). In contrast, other studies have demonstrated that FBXO5/EMI1 deficient cells terminate in S phase causing abnormal DNA re-replication and this may subsequently lead to the production of cells with larger or elongated nuclear size (Machida and Dutta, 2007; Di Fiore and Pines, 2007; Shimizu *et al.*, 2013). Thus, potentially, the unique phenotype induced by *FBXO5*/*EMI1* siRNA may not correlate with PCC. However, cells with co-depletion of FBXO5/EMI1 and *MCPH1*/*BRIT1* siRNA not only displayed a noticeable reduction in cell number but also a reduction in the well-recognised PCC cells that are usually observed with *MCPH1*/*BRIT1* siRNA. This may suggest that depletion of FBXO5/EMI1 sensitises PCC cells to induce cell death. In this case, *FBXO5*/*EMI1* siRNA can be considered to be a modifier of PCC in MCPH1/BRIT1 deficient cells. This may warrant further investigation using more sophisticated technique such as time-lapse microscopy for live cell imaging and may contribute towards determining the potential involvement of *FBXO5*/*EMI1* siRNA in induction of PCC or driving PCC cells to undergo apoptosis.

Although PCC induction has been detected as a consequence of defects in MCPH1/BRIT1, Condensin II and SET nuclear oncogene protein, the intact MCPH1/BRIT1 is required to reversely regulate the activity of Condensin II and to form a binding partner with SET protein with the ultimate aim of regulating chromosome condensation (Trimborn *et al.*, 2006; Wood *et al.*, 2008; Leung *et al.*, 2011; Yamashita *et al.*, 2011). This means that MCPH1/BRIT1 plays a vital role in controlling cell cycle checkpoints during S and G2/M phases and is thus a unique molecule that is substantially required for timely initiation of chromosome condensation, just after completion of DNA replication, thus preventing transit of prophase cells with incomplete chromatin condensation to mitosis.

An additional potential reason for the unsuccessful identification of genes induced PCC that needs to be mentioned is that the analysis was conducted on

only two siRNA sub-libraries, hPK and Ubq, and these may not directly contribute to the induction of PCC. Nevertheless, an additional benefit arising from PCC inducer hPK siRNA screen is that it allows the identification of synthetic lethal siRNAs, as discussed below.

8.1.3 Combining cell viability data from PCC inducer and modifier hPK siRNA screens identified MCPH1/BRIT1 synthetic lethal siRNAs (SL siRNA)

As mentioned in Chapter 6, 2 complementary hPK siRNA screens were utilised to identify MCPH1/BRIT1 SL siRNA. These were PCC inducer hPK siRNA screen (with a single knockdown) that was originally performed to identify genes induced PCC in the presence of functional MCPH1/BRIT1, and a PCC modifier screen (with double knockdown) that was performed to identify genes with increased/decreased PCC caused by MCPH1/BRIT1 knockdown. Both these screens displayed a strong, positive and significant Spearman correlation, indicating the robustness of the assay procedures used to perform the hPK siRNA screens. Identification of SL siRNA hits was conducted by using the cell viability data from the 2 complementary hPK siRNA screens. Thus, SL siRNA hits can be defined as genes whose loss of function specifically reduced cell viability in the absence of functional MCPH1/BRIT1 but have no lethal effect in the presence of functional MCPH1/BRIT1.

Consequently, the difference in % cell viability analysis revealed a list of the top 20 hPK siRNA hits that displayed the largest reduction in cell viability in the PCC modifier hPK screen compared to the identical siRNA in the PCC inducer screen. Five potential SL hPK siRNA hits were selected for validation. Four of these showed a similar lethality phenotype in the absence of MCPH1/BRIT1, namely, STK39, VRK1, TTK/MPS1 and CDK1/CDC2 (Chapter 5; Sections 5.2.3.3.1-5.2.3.3.3). Interestingly, CDK1/CDC2 was a SL hit that also potentially increased PCC (Chapter 5; Section 5.2.3.3.4). PLK1 was excluded as a SL gene in MCPH1/BRIT1 deficient cells because it presented a noticeable lethality in both the presence and absence of MCPH1/BRIT1 (Chapter 5; Section 5.2.3.3.5).

Identification of SL siRNA hits could greatly enhance our understanding of the cellular and biological interaction of MCPH1/BRIT1 with these SL genes during the cell cycle, DNA damage response and repair, or apoptosis in cancer. A number of

potential explanations needed for the functional and cellular contribution of these hPK SL siRNA hits with MCPH1/BRIT1 were collated from different publications and presented elsewhere in this thesis (Chapter 5; Sections from 5.3.2 to 5.3.6).

Knowing the SL genetic targets in MCPH1/BRIT1 deficient cells could clarify the mechanisms of SL interaction and ultimately lead to the development of small molecule therapies for cancer. However, the lethality of these validated siRNA hits may not only be associated with the known cellular functions of these genes as induction of apoptosis. Other mechanisms, which are unrelated to the known functions of these genes, may be responsible for their synthetic lethality (Chan and Giaccia, 2011). Therefore, it is important to identify the principal molecular pathways implicated in SL interactions with MCPH1/BRIT1 rather than focusing solely on the known functions of these candidate genes. This could reveal additional genetic targets for the development of small molecule inhibitors. SL siRNA hits could lead to the development of novel therapeutic strategies for breast and ovarian tumours with defective MCPH1/BRIT1 function which are resistant to current chemotherapy.

The high throughput RNAi screen will be useful in identification of targeted cancer therapy. Thus, it is important to define which mutated genes are indispensible drivers for progression, proliferation and survival of cancer cells. This would lead to development of small molecular inhibitor targeting theses mutated genes with few side effects compared to chemotherapy drugs (Gao *et al.*, 2014). Interestingly, a number of small molecule inhibitors have been developed to target the protein kinases TTK/MPS1 and CDK1/CDC2.

The spindle mitotic checkpoint TTK/MPS1 is a subunit kinase of the spindle assembly checkpoint (SAC) proteins. It functions at mitosis in centrosome duplication, ensuring a proper attachment of chromosomes to the spindle, and the regulation of chromosomal alignment and segregation (Liu and Winey, 2012). It also contributes in the regulation of cytokinesis (Liu and Winey, 2012) and DNA damage responses (Wei *et al.*, 2005). Although a high frequency of TTK/MPS1 mutations have been observed in microsatellite-unstable colorectal cancer, their selective effect in tumourigenesis was not related to weakening of SAC activity (Niittymäki *et al.*, 2011). However, overexpression of TTK/MPS1 has been observed in various human cancers and its elevated level was associated with poor prognosis (Salvatore *et al.*, 2007; Maire *et al.*, 2013a; Tannous *et al.*, 2013; Slee *et al.*, 2014). Additionally, unregulated activity of TTK/MPS1 has been found to

contribute to aneuploidy, proliferation and survival in BC cells (Daniel *et al.*, 2011). Based on these observations, TTK/MPS1 has been considered as an attractive therapeutic target for anti-cancer therapy and researchers have identified or developed several small molecule inhibitors that target this kinase (Hewitt *et al.*, 2010; Kwiatkowski *et al.*, 2010; Colombo *et al.*, 2010; Tardif *et al.*, 2011; Liu *et al.*, 2015). Two inhibitors are in phase 1 clinical trials, which are BAY 1161909 (Identifier: NCT02138812; https://clinicaltrials.gov/) and BAY 1217389 (Identifier: NCT02366949; https://clinicaltrials.gov/). These inhibitors have been examined *in vitro* and *in vivo* and have found to inactivate the SAC and allow abnormal mitotic progression leading to severe chromosomal mis-segregation, mitotic catastrophe, and apoptosis (Jemaa *et al.*, 2013; Wengner *et al.*, 2015). TTK/MPS1 inhibition causes aberrant mitotic arrest in response to microtubule targeting drugs (such as Paclitaxel/Taxol). Thus, the combination of microtubule posing agents and TTK/MPS1 inhibition has been found to highly prevent proper chromosomal alignment and contribute in inducing chromosomal segregation errors and apoptosis and therefore, this would improve efficiency of anti-mitotic drugs and could help overcome Paclitaxel/Taxol resistance (Jemaa *et al.*, 2013; Wengner *et al.*, 2015).

Furthermore, CDKD1/CDC2 is a key regulator of mitotic progression (Santamaría *et al.*, 2007). Although there is no substantial contribution of direct genetic *CDK1/CDC2* alteration in tumorigenesis (Asghar *et al.*, 2015), abnormal CDK1/CDC2 activity causes unscheduled entry into mitosis, contributes to proliferation that leads to chromosomal and genomic aberrations (Malumbres and Barbacid, 2009) and is associated with an aggressive BC phenotype with poor prognosis (Aaltonen *et al.*, 2009; Niméus Malmström *et al.*, 2010). Thus, CDK1/CDC2 has been considered as a target for cancer therapy and several small molecule inhibitors have been developed against it (de Carcer *et al.*, 2007; Asghar *et al.*, 2015). However, the inhibitors that have gone into clinical trail showed disappointing clinical outcomes which may due to the lack of understanding of the mechanism of action of the kinase, a lack of therapeutic window or selection of an inappropriate group of patients (Stone *et al.*, 2012; Asghar *et al.*, 2015). Additionally, evidence has suggested that tumour cells may rely on specific CDKs (Malumbres and Barbacid, 2009). For example, a study has used siRNA to distinguish between MYC dependent and independent human BC cell lines (Kang *et al.*, 2014). CDK1/CDC2, CDK2/CDC1 or CDK4/6 inhibitors have been used in

theses cell lines. Targeting CDK1/CDC2 but not CDK4/6 or CDK2/CDC1 was found to be selectively lethal to MYC dependent BC cell lines, suggesting that CDK1/CDC2 is a potential therapeutic target in MYC deficient breast cancer cells. Therefore identification of specific genetic backgrounds in which tumour cells are likely to be responsive to CDK inhibitors is necessary to improve selectivity and enhance efficacy of these inhibitors in clinical trials (Malumbres and Barbacid, 2009; Stone *et al.*, 2012; Asghar *et al.*, 2015).

8.1.4 The effect of MCPH1/BRIT1 protein expression on chemosensitivity in BC

MCPH1/BRIT1 is a DNA damage response and repair protein. Consequently its function or deficiency may play a significant role in cancer progression and response to chemotherapy. The association of MCPH1/BRIT1 positive and negative tumours with chemosensitivity or resistance and survival outcome for patients with BC remains unknown. Hence, BC samples from patients who had been treated with NACT were immunostained for MCPH1/BRIT1 and p53. BC patients' samples were collected (for each patient the pre-NACT core biopsy and a matched resection tissue of invasive residual tumour post-NACT). The matched post-NACT resection sample was only available for 70 cases out of 96 since 26 cases achieved pCR after NACT.

Alterations in protein expression for both markers pre- and post-NACT treatment was examined and correlated to overall survival (OS). However the change in protein expression of p53 and its correlation with OS will not be discussed further here (both were previously reviewed (Chapter 6; Section 6.4.8)) since the main aim for investigating p53 expression in this study was to confirm the correlation between MCPH1/BRIT1 and p53 expression in BC tissues compared to the previous study in BC cell lines (Zhang *et al.*, 2013a; Liang *et al.*, 2014).

The frequency of cases with high MCPH1/BRIT1 expression pre-NACT was 36/70 (51.4%), which increased to 57/70 (81.4%) post-NACT, suggesting a significant alteration of MCPH1/BRIT1 expression in response to NACT treatment. However, tumours with low MCPH1/BRIT1 expression pre-NACT predicted a significant higher OS rate compared to those with high MCPH1/BRIT1 expression and only a change in MCPH1/BRIT1 expression from low to high post-NACT was significantly correlated with better OS rate.

It remains to be determined whether increased MCPH1/BRIT1 expression is associated with an impaired NACT treatment response and subsequent reduction in OS rate. Chemotherapy triggers DNA damage that results in activation of DNA damage repair proteins which may increase chemo-resistance in cancer cells (Lord and Ashworth, 2012; Bouwman and Jonkers, 2012). A study revealed that the status of DNA damage proteins could be used as a biomarker for predicting BC chemosensitivity to NACT treatment (Asakawa *et al.*, 2010). The authors reported that the presence of BRCA1, RAD51 or yH2AX foci pre- NACT treatment, or RAD51 foci post-NACT treatment were correlated with poor tumour response, causing resistance to DNA damage-inducing chemotherapy. Indeed, in the current study, during scoring procedures for MCPH1/BRIT1 slides, a few core biopsies stained with MCPH/BRIT1 pre-NACT treatment were seen to present foci formation.

Another study has demonstrated that overexpression of human RAD9, a DNA damage repair protein, is correlated with reduced response to NACT treatment in BC (Yun *et al.*, 2014). Interestingly, this study has found a significant correlation between increased protein levels of RAD9 and CHK1. Inhibiting the activity of RAD9 by siRNA in BC cells MCF-7 and MDA-MB-231 decreased the level of CHK1, enhanced sensitivity to Doxorubicin and increased apoptosis. Similarly, in response to DNA damage MCPH1/BRIT1 has been found to regulate the expression of CHK1 and BRCA1 (Lin *et al.*, 2005), which are key regulators of regulation cell checkpoints at both S and G2/M phases (Sanchez *et al.*, 1997; Xu *et al.*, 2001). Thus, increased MCPH1/BRIT1 expression may abnormally activate CHK1 and stimulate G2 cell cycle arrest that, in turn, may diminish the cytotoxic effects of chemotherapy and allow cancer cells to progress into mitosis without DNA damage repair. Targeting CHK1 as a potential anti-cancer therapy could enhance the cytotoxicity of anti-cancer agents and improve therapeutic outcomes (Archie *et al.*, 2007; Merry *et al.*, 2010; Aarts *et al.*, 2013).

Furthermore, MCPH1/BRIT1 is an essential factor in the regulation of the HR mechanism during DNA repair by binding with BRCA2 to facilitate its recruitment to Rad51, and forming a BRCA2/Rad51 complex that is localised at DNA damage sites (Wu *et al.*, 2009; Liang *et al.*, 2010a; Liang *et al.*, 2010g). Enhanced expression of Rad51, a DNA double stranded break repair protein and HR factor (Baumann and West, 1998), was found in pancreatic cancer (Maacke et al., 2000a), non-small lung cancer (Qiao et al., 2005) and BC (Maacke et al., 2000b).

This increases tumour progression by maintaining DNA damage at a tolerable level, enabling cells to survive with a subsequent increase in genetic instability. Therefore, a similar effect may be seen with high MCPH1/BRIT1 expression in BC that increases the capacity of DNA repair activity in tumour cells instead of destroying them. This predisposes cells to immortalisation contributing to an increase in chromosomal instability and tumour survival and may, consequently, cause drug resistance. Modification of a NACT administered regimen by adding and/or increasing the number of cycles of platinum based chemotherapy (such as Cisplatin a DNA intra-strand and cross linking agent) or using PARP inhibitor may sensitise BC tumours with defective HR repair that express elevated levels of MCPH1/BRIT1 to chemotherapy (Lord and Ashworth, 2012; Bouwman and Jonkers, 2012).

However, the cytotoxicity studies that were performed using ovarian cancer cell lines 1847 and SKOV-3 in this PhD thesis produced contradictory results. Depletion of *MCPH1/BRIT1* using siRNA in ovarian cancer 1847cell line cells was associated with slightly significant chemoresistance effect whereas SKOV-3 cell line showed a potential but not significant chemosensitivity effect, in response to Carboplatin. This may partially account for the noticeable variations among the IC50 observed from the 3 or 4 replicates of the MTS assay used. In addition, the diversity of the cellular and genomic characteristics between both ovarian cancer cell lines may greatly influence the cytotoxicity of chemotherapy (Sun and Yu, 2015) and may need to be considered.

Whether reduced MCPH1/BRIT1 expression diminishes the cytotoxic effect of platinum-based chemotherapy and increases resistance phenotype in ovarian cancer cells remains to be elucidated. To examine the role of MCPH1/BRIT1 in response to chemotherapy effectively, use of an optimal cell line model with stable MCPH1/BRIT1 knockout and a more reproducible cytotoxicity assay (such as the Vi-cell Trypan blue exclusion assay) may give clearer results.

Overall, given the role of MCPH1/BRIT1 in DNA damage repair, it is reasonable to consider that the status of protein expression is an indispensible factor in predicting cell sensitivity to anti-cancer agents. Additionally, since reduced MCPH1/BRIT1 expression in cancer cells elicits S and G2/M cell cycle arrest and induces apoptosis, partial inhibition of elevated MCPH1/BRIT1 function may effectively sensitize tumour cells to chemotherapy. Therefore, it was hypothesised that using potent small molecule inhibitors, of the type validated in this PhD thesis,

to partially inactivate MCPH1/BRIT1 may sensitise cancer cells to chemotherapy and overcoming drug resistance. However, this may have some disadvantages since MCPH1/BRIT1 is an indispensable part of DNA repair and its loss of function may predispose cells to substantial genetic mutation rather than eliminating them. Consequently, it seems more appropriate to consider using the validated SL siRNA hits identified from the hPK siRNA screen to develop small molecule inhibitors as therapeutic targets for cancer cells with a defective MCPH1/BRIT1 function.

8.2 Future research directions

8.2.1 SMS

1- Exposing the ovarian cancer 1847 cell line treated with *MCPH1/BRIT1* siRNA, or for contrast an inducible HEK293 cell line stably overexpressing MCPH1/BRIT1 to the validated CC inhibitors could identify the most effective CC as the one that is expected to either increase the level of PCC (in the case of cells with MCPH1/BRIT1 knockdown) or reduce PCC in the inducible HEK293 cell line when the tetracycline system is on. Weiss *et al*. (2007) suggested using the expression of drug resistant mutants as a method to define the on- and off- target effects involved in validating the specificity of small molecule inhibitors in cells (Girdler et al., 2006).

2- Utilising the surface plasmon resonance technique would be an ideal method of verifying the small molecule-protein interaction and binding affinity and would be a useful means of confirming the binding of these 4 CC hits to the *N*-terminal pocket of MCPH1/BRIT1.

3- Furthermore, immunofluorescence analysis can be performed by the treatment of different cell lines expressing diverse levels of MCPH1/BRIT1 (such as 1847, U2OS, SKOV-3, MCF7, MCF10A and MDA-MB-468 (ATCC[®] HTB-132[™]) with *MCPH1/BRIT1* siRNA or the validated PCC-inducer CC. The cell would be stained with DAPI and pHH3 Ser10. This would allow comparisons to be made between the cellular phenotype alterations induced by siRNA and the CC that would confirm the specificity of validated CC hits in targeting the *N*-terminal domain of MCPH1/BRIT1. The distribution of pHH3 Ser10 on the chromosome could be determined in order to characterise the effect of these CC hits on the activity of chromosome condensation. In normal cells, pHH3 Ser10 usually spreads to the whole chromosome arm. However, chromosomes with an incomplete (or centromeric)

pHH3 Ser10 staining have been detected in cells with a defect on the *N*-terminal domain of MCPH1/BRIT1 (Trimborn *et al.*, 2010).

4- As the gradual increase of %PCC caused by these CC was correlated with a reduction in cell number, the potential implication of these 4 CC in the induction of apoptosis or in inhibiting cell proliferation could be examined. Performing a cell death experiment that show the effect of CC on cell viability would subsequently stress the potential cytoxicity effect of these CC in primary cell culture systems from patients with breast and ovarian cancers expressing low or high levels of MCPH1/BRIT1.

5- Validation of the CC target on the *N*-MCPH1/BRIT1 pocket would provide a useful molecular biology tool for studying the function of MCPH1/BRIT1, not only in DNA condensation but also in investigating whether *N*-MCPH1/BRIT1 function is implicated in cancer. A further area of investigation could involve inducing the PCC phenotype in a cancer cell line using *MCPH1/BRIT1* siRNA followed by screening with the same CC library (792 CC) as a potential means of discovering CC hits that can modify and reduce PCC cells in the absence of MCPH1/BRIT1. This may also pave the way to identifying other CC that increases the rate of PCC in cells. Studying the functional and structural association of these CC hits with their targets could lead to the discovery of personalised medicines designed specifically for women with ovarian or breast cancer patients with defective DNA repair function of MCPH1/BRIT1 and resistance to current chemotherapy.

8.2.2 Improvement of hits identification and validation for high throughput siRNA screening

Recently considerable efforts have been made to improve the quality of siRNA analysis for hit identification and validation. Thus, if new experimental methods, imaging analysis and bioinformatics software were used for future siRNA experiments, then more reliable novel cellular pathways or druggable targets might emerge. It is now important to understand how to improve the analysis of siRNA screens to ensure more efficient hit selection and subsequent successful validation. Some of the sophisticated screening techniques and analysis software that have already been utilised in different studies to improve the screening strategy will be outlined here.

1- shRNA could be used to help search more efficiently for successful transfection and to provide additional verification for assessing siRNA hits (Kulkarni *et al*., 2006).

2- utilising other analysis resources would support analysis of individual siRNA screens, such as an open-source bio-conductor/R package like cellHTS (http://www.dkfz.de/signaling/cellHTS) (Boutros *et al*., 2006).

3- Understanding the function of MCPH1/BRIT1 and its overlap with other cellular regulatory pathways would be possible by incorporating the experimental results of MCPH1/BRIT1 that have been produced by our group with different experimental approaches, such as microarray data (produced from siRNA knockdown of MCPH1/BRIT1 in several ovarian cancer cells), PCC-inducer hPK siRNA screen (based on genes inducing PCC in the presence of MCPH1/BRIT1) and the complementary PCC modifier hPK siRNA screen (based on genes which reduce/induce PCC cells in the absence of MCPH1/BRIT1).

4- The siRNA screening data (from either the PCC inducer or PCC modifier screens) could be incorporated into other available RNAi public database, such as GenomeRNAi (http://genomernai.org/), or PubChem BioAssay (http://pubchem.ncbi.nlm.nih.gov) (Wang *et al.*, 2012) since these databases provide information about phenotypes produced by gene knockdown in different species including human, rat and *Drosophila melanogaster*. This could provide useful functional information that may lead to the development of other hypotheses or models, for example, for identifying phenotypic similarities between gene knockdowns and MCPH1/BRIT1 in regulating chromosome condensation.

5- A genome editing approach such as the CRISPR/CAS9 system for knockout of genes identified in siRNA screens can be used to validate hits. Concordance in the phenotypes of the knockout and knockdown would increase the quality and validation of screening data and could lead to an enhanced understanding of the function of siRNA hits and identification of interaction networks. A genome-wide siRNA screen, using a human glioblastoma cell line, identified FAT as a negative regulator of apoptosis. Thus, the use of the CRISPR/CAS9 system to knockout FAT-enhanced apoptosis confirmed the result from the original siRNA screen (Kranz and Boutros, 2014). Recently, a number of reviews have presented an outline of the latest developments in the CRISPR/CAS9-based functional genomics approach, comparing this with the RNAi-based screening approach (Heintze *et al.*, 2013; Mohr *et al.*, 2014; Shalem *et al.*, 2015; Agrotis and Ketteler, 2015).

6- Browsing other RNAi-related databases would help to improve the design of strategies for siRNA analysis and follow-up studies. For example, a screening guideline website such as Minimum Information About an RNAi Experiment (MIARE) (http://miare.sourceforge.net/) provides guidelines that researchers can utilise to report, produce and interpret results from RNAi experiments.

7- The availability of the RNAi database could be useful for comparing the on-target and OTEs in related RNAi screens, which might help to reduce the false discovery rate (Buehler *et al.*, 2012b; Sigoillot *et al.*, 2012).

8- The siRNA true hits could be evaluated by using an effective control with a siRNA mismatched design. An experimental tool known as C911 control can be designed for any siRNA antisense strand by changing the middle bases 9-11 to their complement bases (Buehler et al., 2012a). The C911 control is based on using the same siRNA seed region (bases 2–8) as the original siRNA reagent; however, it lacks the full complementarity sequence to match with the intended on-target gene. The C911 version of the false positive siRNAs maintains the OTE phenotype when examined whilst the C911 versions of true positive siRNAs reduce or abolish inhibition of the intended mRNA. The C911 controls for siRNA can be designed by using an online C911 calculator (http://rnai.nih.gov/haystack/C911Calc.html).

9- In any siRNA screening experiment, the ability to rescue the observed phenotypic effect by re-expressing the target protein from a construct that cannot be silenced by the siRNA used in the screen is a powerful method of confirming the status of a hit.

8.2.3 Investigation of the connection between SL siRNA hits and MCPH1/BRIT1 in cell biology and apoptosis

1- Confirmation of gene silencing by the 4 individual siRNAs of the SL hits (STK39, VRK1, TTK/MPS1 and CDCK1/CDC2) could be tested at the mRNA and protein expression levels using RT-PCR and western blotting respectively to identify the most potent individual siRNA's.

2- Then, the synthetic lethal effect of the 4 SL siRNA hits could be validated in other breast and ovarian cancer cell lines expressing diverse levels of MCPH1/BRIT1 (such as 1847, SKOV-3, MCF7, MCF10A and MDA-MB-468 (ATCC® HTB-132™).

This could be performed using the most effective siRNA concentration (50nM) that showed reasonable results during the validation stage. The difference in cell viability between cells treated with single knockdown (siRNA hit alone) and double knockdown (siRNA hit in combination with *MCPH1*/*BRIT1* siRNA) would be calculated as previously mentioned (Chapter 2: Section 2.4.1.1; Figure 2.3). The 2 individual siRNAs of each SL hit with the most pronounced effect on cell viability would be selected based on the control (NT-siRNA in single knockdown and NT-*MCPH1*/*BRIT1* siRNA in double knockdown); then they would be considered statistically significant with a *p* value of ≤ 0.05. This could assess the specificity of the most potent individual siRNA targeting each SL siRNA hit in each cell line.

3- Breast and ovarian cancer cells lines without and with *MCPH1*/*BRIT1* siRNA could be used to investigate the biological significance of gene silencing for each SL hits. This could be examined by treating the cells with DNA damaging agents such as Cisplatin or Carboplatin, or anti-microtubule agents such as Docetaxel or Paclitaxel/Taxol. The apoptotic response would be examined using Annexin V/FACS. Moreover, the effect of SL hits on the DNA damage response would be examined by immunofluorescence staining using confocal microscopy to quantify the levels of foci formation induced as a consequence of H2AX phosphorylation, which is a marker of DNA DSB. The involvement of these SL hits in stimulating DNA repair foci by RAD51, a homologous recombination (HR) repair marker, could be examined by pulsing the cell with bromodeoxyuridine (BrdU) to accumulate cells at S phase before exposing them to irradiation. The % of (BrdU) cells with ≥ 5 RAD51 foci would be evaluated in irradiated and non-irradiated cells (Turner *et al.*, 2008). An increase in the basal level of H2AX and RAD51 as a result of SL gene silencing in MCPH1/BRIT1 deficient cells would be viewed as an indicator that SL gene silencing can activate DNA damage response and DNA repair. Reduced HR rate as a consequence of *BRCA1* siRNA has been previously confirmed and thus it can be used as control for this experiment (Turner *et al.*, 2008). Any SL hit showing positive results in activating DNA damage response and repair and with no reverse effect on HR rate would be potentially considered to be a strong hit since its silencing does not reversely effect the DNA repair mechanism. Thus its potential efficacious therapeutic action in human is increased with minimal or no side effects.

4- Live cell imaging could be utilised to demonstrate the effect of known inhibitors against the SL hits on mitosis. For example, HeLa cells stably expressing a H2B-GFP could be grown in 35-mm 4-well, glass-bottomed culture dishes and treated

with small molecule inhibitors of TTK/MPS1 or CDK1/CDC2; cells would then be transfected with or without *MCPH1/BRIT1* siRNA or controls (NT- *MCPH1/BRIT1* siRNA or NT-siRNA). The cells would be observed for 48hr after transfection using time-lapse microscopy. Cells would be imaged every 5min using fluorescent and phase contrast microscopy. This experiment could be supported by Annexin V/FACS analysis for quantification of apoptosis.

5- The synergistic effect of chemotherapy drugs (such as Paclitaxel/Taxol, Docetaxel, Cisplatin and Carboplatin) with small molecule inhibitors of TTK/MPS1 or CDK1/CDC2 could be examined using low dose response relationships, in cells with defective and functional MCPH1/BRIT1. The sensitivity will be measured using Vi-cell Trypan blue exclusion assay and IC_{50} values will be determined experimentally. It is anticipated that the small molecule inhibitors of TTK/MPS1 or CDK1/CDC2 may restore resistance to chemotherapy and increase the sensitivity of cells with defective MCPH1/BRIT1 to anti-cancer agents.

6- MCF7, SKOV-3 cell lines with stable overexpression of each SL hit individually would be generated using FLAG-tagged constructs of each SL gene as previously described in (Zhang *et al.*, 2013a). Each cell line harbouring overexpression of a wild type SL gene would be treated with *MCPH1/BRIT1* siRNA to determine the effect of SL gene hits on cell proliferation using BrdU incorporated assay; any changes in BrdU incorporation would be detected by fluorescence microscopy. Findings from the cell proliferation assay could be complemented by another apoptotic assay such as FITC Annexin V/FACS to compare the effect of stable MCF7 or SKOV-3 knockdown of each individual SL gene (using lentiviral vector based Mission shRNA) in cells with/without *MCPH1/BRIT1* siRNA on early induction of apoptosis as previously described in (Zhang *et al.*, 2013a).

8.2.4 Investigation of the influence of MCPH1/BRIT1 expression in response to chemotherapy in breast and ovarian cancer

1- It would be interesting to investigate the role of MCPH1/BRIT1 as a predictive marker in BC sensitivity to NACT or other platinum-based drug agents, by detecting MCPH1/BRIT1 foci formation in BC tissues and correlating this with response and survival rates pre- and post-chemotherapy.

2- Investigation of the correlation between MCPH1/BRIT protein levels and proteins including CHK1, PARP and the validated SL genes on advanced BC tissue using

IHC. This method would be complemented by *in vitro* assays such as Vi-cell Trypan blue assay and FITC/PI Annexin V/ FACS analysis that will measure the effect of stable MCPH1/BRIT1 knockout or overexpression on chemosensitivity and apoptosis respectively on breast and ovarian cancer cell lines. The mRNA expression and protein levels of CHK1, PARP and SL hits would be measured pre- and post-chemotherapy treatment. This would reveal the effector elements that enhance or prevent susceptibility of MCPH1/BRIT1 deficient cancer cells to chemotherapy and thus this could further confirm the significance of SL hits as therapeutic targets.

3- Another study could be performed to investigate the effect of the nuclear and cytoplasmic localisations of MCPH1/BRIT1 in response to chemotherapy and survival using BC tumour samples and to examine whether different MCPH1/BRIT1 isoforms and microRNA contribute to the failure in response to chemotherapy (Gavvovidis *et al.*, 2012; Venkatesh *et al.*, 2013; Wang *et al.*, 2014a).

References

AALTONEN, K., AMINI, R.-M., HEIKKILÄ, P., AITTOMÄKI, K., TAMMINEN, A., NEVANLINNA, H. & BLOMQVIST, C. 2009. High cyclin B1 expression is associated with poor survival in breast cancer. *British journal of cancer,* 100**,** 1055-1060.

AARTS, M., LINARDOPOULOS, S. & TURNER, N. C. 2013. Tumour selective targeting of cell cycle kinases for cancer treatment. *Curr Opin Pharmacol,* 13**,** 529-35.

ABE, S., NAGASAKA, K., HIRAYAMA, Y., KOZUKA-HATA, H., OYAMA, M., AOYAGI, Y., OBUSE, C. & HIROTA, T. 2011. The initial phase of chromosome condensation requires Cdk1-mediated phosphorylation of the CAP-D3 subunit of condensin II. *Genes Dev,* 25**,** 863-74.

ABRAHAM, R. T. 2001. Cell cycle checkpoint signaling through the ATM and ATR kinases. *Genes & development,* 15**,** 2177-2196.

ADAMS, M., COOKSON, V. J., HIGGINS, J., MARTIN, H. L., TOMLINSON, D. C., BOND, J., MORRISON, E. E. & BELL, S. M. 2014. A high-throughput assay to identify modifiers of premature chromosome condensation. *Journal of biomolecular screening,* 19**,** 176-183.

ADAMSON, B., SMOGORZEWSKA, A., SIGOILLOT, F. D., KING, R. W. & ELLEDGE, S. J. 2012. A genome-wide homologous recombination screen identifies the RNA-binding protein RBMX as a component of the DNA-damage response. *Nature cell biology,* 14**,** 318-328.

AGROTIS, A. & KETTELER, R. 2015. A new age in functional genomics using CRISPR/Cas9 in arrayed library screening. *Frontiers in genetics,* 6.

AHMED, A. A., WANG, X., LU, Z., GOLDSMITH, J., LE, X.-F., GRANDJEAN, G., BARTHOLOMEUSZ, G., BROOM, B. & BAST, R. C. 2011. Modulating microtubule stability enhances the cytotoxic response of cancer cells to Paclitaxel. *Cancer research,* 71**,** 5806-5817.

ALDERTON, G. K., GALBIATI, L., GRIFFITH, E., SURINYA, K. H., NEITZEL, H., JACKSON, A. P., JEGGO, P. A. & O'DRISCOLL, M. 2006. Regulation of mitotic entry by microcephalin and its overlap with ATR signalling. *Nat Cell Biol,* 8**,** 725-33.

ALLISON, K. H. 2012. Molecular pathology of breast cancer: what a pathologist needs to know. *Am J Clin Pathol,* 138**,** 770-80.

ALSBEIH, G. & RAAPHORST, G. 1998. Differential induction of premature chromosome condensation by calyculin A in human fibroblast and tumor cell lines. *Anticancer research,* 19**,** 903-908.

ALSIARY, R., BRUNING-RICHARDSON, A., BOND, J., MORRISON, E. E., WILKINSON, N. & BELL, S. M. 2014. Deregulation of microcephalin and ASPM expression are correlated with epithelial ovarian cancer progression. *PLoS One,* 9**,** e97059.

AMOS, L. A. & LÖWE, J. 1999. How Taxol® stabilises microtubule structure. *Chemistry & biology,* 6**,** R65-R69.

ANDRE, F. & PUSZTAI, L. 2006. Molecular classification of breast cancer: implications for selection of adjuvant chemotherapy. *Nat Clin Pract Oncol,* 3**,** 621-32.

ANELLI, A., BRENTANI, R., GADELHA, A., DE ALBUQUERQUE, A. A. & SOARES, F. 2003. Correlation of p53 status with outcome of neoadjuvant chemotherapy using paclitaxel and doxorubicin in stage IIIB breast cancer. *Annals of oncology,* 14**,** 428-432.

ANNUNZIATA, C. M. & BATES, S. E. 2010. PARP inhibitors in BRCA1/BRCA2 germline mutation carriers with ovarian and breast cancer. *F1000 biology reports,* 2.

ANTONIOU, A., PHAROAH, P., NAROD, S., RISCH, H. A., EYFJORD, J. E., HOPPER, J., LOMAN, N., OLSSON, H., JOHANNSSON, O. & BORG, Å. 2003. Average risks of breast and ovarian cancer associated with BRCA1 or BRCA2 mutations detected in case series unselected for family history: a combined analysis of 22 studies. *The American Journal of Human Genetics,* 72**,** 1117-1130.

APOSTOLOU, P. & FOSTIRA, F. 2013. Hereditary breast cancer: the era of new susceptibility genes. *BioMed research international,* 2013.

ARCHIE, N. T., RENDAHL, K. G., SHEIKH, T., CHEEMA, H., AARDALEN, K., EMBRY, M., MA, S., MOLER, E. J., NI, Z. J. & DE MENEZES, D. E. L. 2007. CHIR-124, a novel potent inhibitor of Chk1, potentiates the cytotoxicity of topoisomerase I poisons in vitro and in vivo. *Clinical Cancer Research,* 13**,** 591-602.

ARMSTRONG, J. W. 1999. A review of high-throughput screening approaches for drug discovery. *American biotechnology laboratory,* 17**,** 26-28.

ARORA, S., BISANZ, K. M., PERALTA, L. A., BASU, G. D., CHOUDHARY, A., TIBES, R. & AZORSA, D. O. 2010. RNAi screening of the kinome identifies modulators of cisplatin response in ovarian cancer cells. *Gynecologic oncology,* 118**,** 220-227.

ASAKAWA, H., KOIZUMI, H., KOIKE, A., TAKAHASHI, M., WU, W., IWASE, H., FUKUDA, M. & OHTA, T. 2010. Prediction of breast cancer sensitivity to neoadjuvant chemotherapy based on status of DNA damage repair proteins. *Breast Cancer Res,* 12**,** R17.

ASGHAR, U., WITKIEWICZ, A. K., TURNER, N. C. & KNUDSEN, E. S. 2015. The history and future of targeting cyclin-dependent kinases in cancer therapy. *Nature reviews Drug discovery,* 14**,** 130-146.

ATKIN, N. 1979. Premature chromosome condensation in carcinoma of the bladder: presumptive evidence for fusion of normal and malignant cells. *Cytogenetic and Genome Research,* 23**,** 217-219.

AUGUSTUS, M., BRÜDERLEIN, S. & GEBHART, E. 1985. Cytogenetic and cell cycle studies in metastatic cells from ovarian carcinomas. *Anticancer research,* 6**,** 283-289.

AWAD, S., AL-DOSARI, M. S., ALYACOUB, N., COLAK, D., SALIH, M. A., ALKURAYA, F. S. & POIZAT, C. 2013. Mutation in PHC1 implicates chromatin remodeling in primary microcephaly pathogenesis. *Human molecular genetics,* ddt072.

AXELROD, D. E., SHAH, K., YANG, Q. & HAFFTY, B. G. 2012. Prognosis for Survival of Young Women with Breast Cancer by Quantitative p53 Immunohistochemistry. *Cancer and Clinical Oncology,* 1.

BAILEY, S. N., ALI, S. M., CARPENTER, A. E., HIGGINS, C. O. & SABATINI, D. M. 2006. Microarrays of lentiviruses for gene function screens in immortalized and primary cells. *Nature methods,* 3**,** 117-122.

BAKER, S. J., FEARON, E. R., NIGRO, J. M., PREISINGER, A., JESSUP, J., LEDBETTER, D., BARKER, D., NAKAMURA, Y., WHITE, R. & VOGELSTEIN, B. 1989. Chromosome 17 deletions and p53 gene mutations in colorectal carcinomas. *Science,* 244**,** 217-221.

BAKER, S. J., PREISINGER, A. C., JESSUP, J. M., PARASKEVA, C., MARKOWITZ, S., WILLSON, J., HAMILTON, S. & VOGELSTEIN, B. 1990. p53 gene mutations occur in combination with 17p allelic deletions as late events in colorectal tumorigenesis. *Cancer research,* 50**,** 7717-7722.

BANIN HIRATA, B. K., ODA, J. M., LOSI GUEMBAROVSKI, R., ARIZA, C. B., DE OLIVEIRA, C. E. & WATANABE, M. A. 2014. Molecular markers for breast cancer: prediction on tumor behavior. *Dis Markers,* 2014**,** 513158.

BARAK, Y., JUVEN, T., HAFFNER, R. & OREN, M. 1993. mdm2 expression is induced by wild type p53 activity. *The EMBO journal,* 12**,** 461.

BARBELANNE, M. & TSANG, W. Y. 2014. Molecular and cellular basis of autosomal recessive primary microcephaly. *BioMed research international*.

BARBIE, D. A., TAMAYO, P., BOEHM, J. S., KIM, S. Y., MOODY, S. E., DUNN, I. F., SCHINZEL, A. C., SANDY, P., MEYLAN, E. & SCHOLL, C. 2009. Systematic RNA interference reveals that oncogenic KRAS-driven cancers require TBK1. *Nature,* 462**,** 108-112.

BARTLEY, A. N. & ROSS, D. W. 2002. Validation of p53 immunohistochemistry as a prognostic factor in breast cancer in clinical practice. *Archives of pathology & laboratory medicine,* 126**,** 456.

BARTZ, S. R., ZHANG, Z., BURCHARD, J., IMAKURA, M., MARTIN, M., PALMIERI, A., NEEDHAM, R., GUO, J., GORDON, M. & CHUNG, N. 2006. Small interfering RNA screens reveal enhanced cisplatin cytotoxicity in tumor cells having both BRCA network and TP53 disruptions. *Molecular and cellular biology,* 26**,** 9377-9386.

BASSING, C. H. & ALT, F. W. 2004. The cellular response to general and programmed DNA double strand breaks. *DNA repair,* 3**,** 781-796.

BAUER, J. A., YE, F., MARSHALL, C. B., LEHMANN, B. D., PENDLETON, C. S., SHYR, Y., ARTEAGA, C. L. & PIETENPOL, J. A. 2010. Research article RNA interference (RNAi) screening approach identifies agents that enhance paclitaxel activity in breast cancer cells. *Breast Cancer Res,* 12**,** R41.

BAUMANN, K., KIM, H., RINKE, J., PLAUM, T., WAGNER, U. & REINARTZ, S. 2013. Effects of alvocidib and carboplatin on ovarian cancer cells in vitro. *Experimental oncology***,** 168-173.

BAUMANN, P. & WEST, S. C. 1998. Role of the human RAD51 protein in homologous recombination and double-stranded-break repair. *Trends in biochemical sciences,* 23, 247-251.

BAYLISS, R., FRY, A., HAQ, T. & YEOH, S. 2012. On the molecular mechanisms of mitotic kinase activation. *Open biology,* 2**,** 120136.

BELL, S., SPEIRS, V. & MORRISON, E. 2008. MCPH1, a potential predictor for response to cancer chemotherapy. *Breast Cancer Research,* 10**,** P58.

BELL, S. P. & DUTTA, A. 2002. DNA replication in eukaryotic cells. *Annual review of biochemistry,* 71**,** 333-374.

BERNS, K., HORLINGS, H. M., HENNESSY, B. T., MADIREDJO, M., HIJMANS, E. M., BEELEN, K., LINN, S. C., GONZALEZ-ANGULO, A. M., STEMKE-HALE, K. & HAUPTMANN, M. 2007. A functional genetic approach identifies the PI3K pathway as a major determinant of trastuzumab resistance in breast cancer. *Cancer cell,* 12**,** 395-402.

BERTWISTLE, D. & ASHWORTH, A. 1998. Functions of the BRCA1 and BRCA2 genes. *Current opinion in genetics & development,* 8**,** 14-20.

BHATTACHARYA, N., MUKHERJEE, N., SINGH, R. K., SINHA, S., ALAM, N., ROY, A., ROYCHOUDHURY, S. & PANDA, C. K. 2013. Frequent alterations of MCPH1 and ATM are associated with primary breast carcinoma: clinical and prognostic implications. *Ann Surg Oncol,* 20 Suppl 3**,** S424-32.

BIEGING, K. T. & ATTARDI, L. D. 2012. Deconstructing p53 transcriptional networks in tumor suppression. *Trends in cell biology,* 22**,** 97-106.

BILBAO, C., RAMIREZ, R., RODRIGUEZ, G., FALCON, O., LEON, L., DIAZ-CHICO, N., PERUCHO, M. & DIAZ-CHICO, J. C. 2010. Double strand break repair components are frequent targets of microsatellite instability in endometrial cancer. *Eur J Cancer,* 46**,** 2821-7.

BIRMINGHAM, A., ANDERSON, E. M., REYNOLDS, A., ILSLEY-TYREE, D., LEAKE, D., FEDOROV, Y., BASKERVILLE, S., MAKSIMOVA, E., ROBINSON, K. & KARPILOW, J. 2006. 3′ UTR seed matches, but not overall identity, are associated with RNAi off-targets. *Nature methods,* 3**,** 199-204.

BIRMINGHAM, A., SELFORS, L. M., FORSTER, T., WROBEL, D., KENNEDY, C. J., SHANKS, E., SANTOYO-LOPEZ, J., DUNICAN, D. J., LONG, A., KELLEHER, D., SMITH, Q., BEIJERSBERGEN, R. L., GHAZAL, P. & SHAMU, C. E. 2009. Statistical methods for analysis of high-throughput RNA interference screens. *Nat Methods,* 6**,** 569-75.

BLATTNER, C., TOBIASCH, E., LITFIN, M., RAHMSDORF, H. J. & HERRLICH, P. 1999. DNA damage induced p53 stabilization: no indication for an involvement of p53 phosphorylation. *Oncogene,* 18**,** 1723-1732.

BOCKMÜHL, U., ISHWAD, C. S., FERRELL, R. E. & GOLLIN, S. M. 2001. Association of 8p23 deletions with poor survival in head and neck cancer. *Otolaryngology--Head and Neck Surgery,* 124**,** 451-455.

BOETTCHER, M. & HOHEISEL, J. 2010. Pooled RNAi screens-technical and biological aspects. *Current genomics,* 11**,** 162-167.

BOND, J., ROBERTS, E., SPRINGELL, K., LIZARRAGA, S., SCOTT, S., HIGGINS, J., HAMPSHIRE, D. J., MORRISON, E. E., LEAL, G. F. & SILVA, E. O. 2005. A centrosomal mechanism involving CDK5RAP2 and CENPJ controls brain size. *Nature genetics,* 37**,** 353-355.

BORK, P., HOFMANN, K., BUCHER, P., NEUWALD, A., ALTSCHUL, S. & KOONIN, E. 1997. A superfamily of conserved domains in DNA damage-responsive cell cycle checkpoint proteins. *The FASEB Journal,* 11**,** 68-76.

BORYSOVA, M., CUI, Y., SNYDER, M. & GUADAGNO, T. 2008. Knockdown of B-Raf impairs spindle formation and the mitotic checkpoint in human somatic cells. *Cell Cycle,* 7**,** 2894-2901.

BOUTROS, M., BRÁS, L. P. & HUBER, W. 2006. Analysis of cell-based RNAi screens. *Genome biology,* 7**,** R66.

BOUTROS, M., KIGER, A. A., ARMKNECHT, S., KERR, K., HILD, M., KOCH, B., HAAS, S. A., PARO, R., PERRIMON, N. & CONSORTIUM, H. F. A. 2004. Genome-wide RNAi analysis of growth and viability in Drosophila cells. *Science,* 303**,** 832-835.

BOUWMAN, P. & JONKERS, J. 2012. The effects of deregulated DNA damage signalling on cancer chemotherapy response and resistance. *Nature Reviews Cancer,* 12**,** 587-598.

BOYLE, P. 2012. Triple-negative breast cancer: epidemiological considerations and recommendations. *Annals of oncology,* 23**,** vi7-vi12.

BRAY, F., REN, J. S., MASUYER, E. & FERLAY, J. 2013. Global estimates of cancer prevalence for 27 sites in the adult population in 2008. *International Journal of Cancer,* 132**,** 1133-1145.

BROSH, R. & ROTTER, V. 2009. When mutants gain new powers: news from the mutant p53 field. *Nature Reviews Cancer,* 9**,** 701-713.

BRÜDERLEIN, S., GEBHART, E., SIEBERT, E. & AUGUSTUS, M. 1986. Premature chromosome condensation—studies on human metastatic carcinoma cells. *Human genetics,* 73**,** 44-52.

BRUNING-RICHARDSON, A., BOND, J., ALSIARY, R., RICHARDSON, J., CAIRNS, D. A., MCCORMACK, L., HUTSON, R., BURNS, P., WILKINSON, N., HALL, G. D., MORRISON, E. E. & BELL, S. M. 2011. ASPM and microcephalin expression in epithelial ovarian cancer correlates with tumour grade and survival. *Br J Cancer,* 104**,** 1602-10.

BUEHLER, E., CHEN, Y.-C. & MARTIN, S. 2012a. C911: A bench-level control for sequence specific siRNA off-target effects.

BUEHLER, E., KHAN, A. A., MARINE, S., RAJARAM, M., BAHL, A., BURCHARD, J. & FERRER, M. 2012b. siRNA off-target effects in genome-wide screens identify signaling pathway members. *Scientific reports,* 2.

BURSTEIN, H. J. 2005. The distinctive nature of HER2-positive breast cancers. *New England Journal of Medicine,* 353**,** 1652-1654.

CAMPEAU, E. & GOBEIL, S. 2011. RNA interference in mammals: behind the screen. *Briefings in functional genomics,* 10**,** 215-226.

CAMPEAU, P. M., FOULKES, W. D. & TISCHKOWITZ, M. D. 2008. Hereditary breast cancer: new genetic developments, new therapeutic avenues. *Human genetics,* 124**,** 31-42.

CAPRANICO, G., DE ISABELLA, P., PENCO, S., TINELLI, S. & ZUNINO, F. 1989. Role of DNA breakage in cytotoxicity of doxorubicin, 9-deoxydoxorubicin, and 4-demethyl-6-deoxydoxorubicin in murine leukemia P388 cells. *Cancer research,* 49**,** 2022-2027.

CAPRANICO, G., ZUNINO, F., KOHN, K. W. & POMMIER, Y. 1990. Sequence-selective topoisomerase II inhibition by anthracycline derivatives in SV40 DNA: relationship with DNA binding affinity and cytotoxicity. *Biochemistry,* 29**,** 562-569.

CATTEAU, A., HARRIS, W. H., XU, C.-F. & SOLOMON, E. 1999. Methylation of the BRCA1 promoter region in sporadic breast and ovarian cancer: correlation with disease characteristics. *Oncogene,* 18**,** 1957-1965.

CHAN, D. A. & GIACCIA, A. J. 2011. Harnessing synthetic lethal interactions in anticancer drug discovery. *Nature reviews drug discovery,* 10**,** 351-364.

CHAPLET, M., RAI, R., JACKSON-BERNITSAS, D., LI, K. & LIN, S.-Y. 2006

. BRIT1/MCPH1: A Guardian of Genome and an Enemy of Tumors. *Cell Cycle,* 5**,** 2579-2583.

CHEANG, M. C., VODUC, D., BAJDIK, C., LEUNG, S., MCKINNEY, S., CHIA, S. K., PEROU, C. M. & NIELSEN, T. O. 2008. Basal-like breast cancer defined by five biomarkers has superior prognostic value than triple-negative phenotype. *Clinical Cancer Research,* 14**,** 1368-1376.

CHEN, S. & PARMIGIANI, G. 2007. Meta-analysis of BRCA1 and BRCA2 penetrance. *Journal of Clinical Oncology,* 25**,** 1329-1333.

CHEN, W. 2013. Factors that Modify Breast Cancer Risk in Women. Uptodate.

CHIU, M. H., LIU, H. S., WU, Y. H., SHEN, M. R. & CHOU, C. Y. 2014. SPAK mediates KCC3 enhanced cervical cancer tumorigenesis. *FEBS Journal,* 281**,** 2353-2365.

CHOW, J. P., SIU, W. Y., HO, H. T., MA, K. H., HO, C. C. & POON, R. Y. 2003. Differential contribution of inhibitory phosphorylation of CDC2 and CDK2 for unperturbed cell cycle control and DNA integrity checkpoints. *J Biol Chem,* 278**,** 40815-28.

CHUMAKOV, P., IOTSOVA, V. & GEORGIEV, G. 1981. [Isolation of a plasmid clone containing the mRNA sequence for mouse nonviral T-antigen]. *Doklady Akademii nauk SSSR,* 267**,** 1272-1275.

COLEMAN, M. P., BABB, P., DAMIECKI, P., GROSCLAUDE, P., HONJO, S., JONES, J., KNERER, G., PITARD, A., QUINN, M. & SLOGGETT, A. 1999. *Cancer survival trends in England and Wales, 1971-1995: deprivation and NHS region*, Stationery Office London.

COLLINS, C. S., HONG, J., SAPINOSO, L., ZHOU, Y., LIU, Z., MICKLASH, K., SCHULTZ, P. G. & HAMPTON, G. M. 2006. A small interfering RNA screen for modulators of tumor cell motility identifies MAP4K4 as a promigratory kinase. *Proceedings of the National Academy of Sciences of the United States of America,* 103**,** 3775-3780.

COLOMBO, R., CALDARELLI, M., MENNECOZZI, M., GIORGINI, M. L., SOLA, F., CAPPELLA, P., PERRERA, C., DEPAOLINI, S. R., RUSCONI, L. & CUCCHI, U. 2010. Targeting the mitotic checkpoint for cancer therapy with NMS-P715, an inhibitor of MPS1 kinase. *Cancer research,* 70**,** 10255-10264.

COOPER, K. & HAFFAJEE, Z. 1997. bcl 2 and p53 protein expression in follicular lymphoma. *The Journal of pathology,* 182**,** 307-310.

CORNEJO, K. M., KANDIL, D. & COSAR, E. F. 2014. Theranostic and molecular classification of breast cancer. *Archives of pathology & laboratory medicine,* 138**,** 44.

CORREA, P. & JOHNSON, W. D. 1978. International variation in the histology of breast carcinoma. *UICC Techn Rep Series,* 35**,** 36-65.

CORTEZ, D., WANG, Y., QIN, J. & ELLEDGE, S. J. 1999. Requirement of ATM-dependent phosphorylation of brca1 in the DNA damage response to double-strand breaks. *Science,* 286**,** 1162-1166.

COSTANZO, V., ROBERTSON, K., YING, C. Y., KIM, E., AVVEDIMENTO, E., GOTTESMAN, M., GRIECO, D. & GAUTIER, J. 2000. Reconstitution of an ATM-dependent checkpoint that inhibits chromosomal DNA replication following DNA damage. *Molecular cell,* 6**,** 649-659.

COWLEY, G. S., WEIR, B. A., VAZQUEZ, F., TAMAYO, P., SCOTT, J. A., RUSIN, S., EAST-SELETSKY, A., ALI, L. D., GERATH, W. F. & PANTEL, S. E. 2014. Parallel genome-scale loss of function screens in 216 cancer cell lines for the identification of context-specific genetic dependencies. *Scientific data,* 1.

CROUCH, S., KOZLOWSKI, R., SLATER, K. & FLETCHER, J. 1993. The use of ATP bioluminescence as a measure of cell proliferation and cytotoxicity. *Journal of immunological methods,* 160**,** 81-88.

CUI, Y. & GUADAGNO, T. 2008. B-RafV600E signaling deregulates the mitotic spindle checkpoint through stabilizing Mps1 levels in melanoma cells. *Oncogene,* 27**,** 3122-3133.

D'ASSORO, A. B., BARRETT, S. L., FOLK, C., NEGRON, V. C., BOENEMAN, K., BUSBY, R., WHITEHEAD, C., STIVALA, F., LINGLE, W. L. & SALISBURY, J. L. 2002. Amplified centrosomes in breast cancer: a potential indicator of tumor aggressiveness. *Breast cancer research and treatment,* 75**,** 25-34.

DAIDONE, M. G., SILVESTRINI, R., LUISI, A., MASTORE, M., BENINI, E., VENERONI, S., BRAMBILLA, C., FERRARI, L., GRECO, M. & ANDREOLA, S. 1995. Changes in biological markers after primary chemotherapy for breast cancers. *International journal of cancer,* 61**,** 301-305.

DANIEL, J., COULTER, J., WOO, J.-H., WILSBACH, K. & GABRIELSON, E. 2011. High levels of the Mps1 checkpoint protein are protective of aneuploidy in breast cancer cells. *Proceedings of the National Academy of Sciences,* 108**,** 5384-5389.

DE AZAMBUJA, E., CARDOSO, F., DE CASTRO, G., COLOZZA, M., MANO, M. S., DURBECQ, V., SOTIRIOU, C., LARSIMONT, D., PICCART-GEBHART, M. & PAESMANS, M. 2007. Ki-67 as prognostic marker in early breast cancer: a meta-analysis of published studies involving 12 155 patients. *British journal of cancer,* 96**,** 1504-1513.

DE CARCER, G., PEREZ DE CASTRO, I. & MALUMBRES, M. 2007. Targeting cell cycle kinases for cancer therapy. *Current medicinal chemistry,* 14**,** 969-985.

DELEO, A. B., JAY, G., APPELLA, E., DUBOIS, G. C., LAW, L. W. & OLD, L. J. 1979. Detection of a transformation-related antigen in chemically induced sarcomas and other transformed cells of the mouse. *Proceedings of the National Academy of Sciences,* 76**,** 2420-2424.

DENT, R., TRUDEAU, M., PRITCHARD, K. I., HANNA, W. M., KAHN, H. K., SAWKA, C. A., LICKLEY, L. A., RAWLINSON, E., SUN, P. & NAROD, S. A. 2007. Triple-negative breast cancer: clinical features and patterns of recurrence. *Clinical Cancer Research,* 13**,** 4429-4434.

DI FIORE, B. & PINES, J. 2007. Emi1 is needed to couple DNA replication with mitosis but does not regulate activation of the mitotic APC/C. *J Cell Biol,* 177**,** 425-37.

DI MASI, A., GULLOTTA, F., CAPPADONNA, V., LEBOFFE, L. & ASCENZI, P. 2011. Cancer predisposing mutations in BRCT domains. *IUBMB Life,* 63**,** 503-12.

DI PASQUA, A. J., GOODISMAN, J. & DABROWIAK, J. C. 2012. Understanding how the platinum anticancer drug carboplatin works: From the bottle to the cell. *Inorganica Chimica Acta,* 389**,** 29-35.

DITCHFIELD, C., JOHNSON, V. L., TIGHE, A., ELLSTON, R., HAWORTH, C., JOHNSON, T., MORTLOCK, A., KEEN, N. & TAYLOR, S. S. 2003. Aurora B couples chromosome alignment with anaphase by targeting BubR1, Mad2, and Cenp-E to kinetochores. *The Journal of cell biology,* 161**,** 267-280.

DO, K., DOROSHOW, J. H. & KUMMAR, S. 2013. Wee1 kinase as a target for cancer therapy. *Cell cycle,* 12**,** 3348-3353.

DONEHOWER, L. A., HARVEY, M., SLAGLE, B. L., MCARTHUR, M. J., MONTGOMERY JR, C. A., BUTEL, J. S. & BRADLEY, A. 1992. Mice deficient for p53 are developmentally normal but susceptible to spontaneous tumours. *Nature,* 356**,** 215-221.

DONZELLI, M. & DRAETTA, G. F. 2003. Regulating mammalian checkpoints through Cdc25 inactivation. *EMBO reports,* 4**,** 671-677.

DOUGLAS ZHANG, X., YANG, X. C., CHUNG, N., GATES, A., STEC, E., KUNAPULI, P., J HOLDER, D., FERRER, M. & S ESPESETH, A. 2006. Robust statistical methods for hit selection in RNA interference high-throughput screening experiments.

EASTON, D. F. 1999. How many more breast cancer predisposition genes are there. *Breast Cancer Res,* 1**,** 14-17.

ECHEVERRI, C. J. & PERRIMON, N. 2006. High-throughput RNAi screening in cultured cells: a user's guide. *Nature Reviews Genetics,* 7**,** 373-384.

EGGERT, U. S. 2013. The why and how of phenotypic small-molecule screens. *Nature chemical biology,* 9**,** 206-209.

EGGERT, U.S., KIGER, A.A., RICHTER, C., PERLMAN, Z.E., PERRIMON, N., MITCHISON, T.J. and FIELD, C.M., 2004. Parallel chemical genetic and genome-wide RNAi screens identify cytokinesis inhibitors and targets. *PLoS Biol*, *2*(12), p.e379.

ELBASHIR, S. M., HARBORTH, J., LENDECKEL, W., YALCIN, A., WEBER, K. & TUSCHL, T. 2001. Duplexes of 21-nucleotide RNAs mediate RNA interference in cultured mammalian cells. *nature,* 411**,** 494-498.

ELIYAHU, D., MICHALOVITZ, D., ELIYAHU, S., PINHASI-KIMHI, O. & OREN, M. 1989. Wild-type p53 can inhibit oncogene-mediated focus formation. *Proceedings of the National Academy of Sciences,* 86**,** 8763-8767.

ELLEDGE, R. M., CLARK, G. M., FUQUA, S. A., YU, Y.-Y. & ALLRED, D. C. 1994. p53 protein accumulation detected by five different antibodies: relationship to prognosis and heat shock protein 70 in breast cancer. *Cancer research,* 54**,** 3752-3757.

ELMEHDAWI, F., WHEWAY, G., SZYMANSKA, K., ADAMS, M., HIGH, A. S., JOHNSON, C. A. & ROBINSON, P. A. 2013. Human Homolog of Drosophila Ariadne (HHARI) is a marker of cellular proliferation associated with nuclear bodies. *Experimental cell research,* 319**,** 161-172.

ESTELLER, M., SILVA, J. M., DOMINGUEZ, G., BONILLA, F., MATIAS-GUIU, X., LERMA, E., BUSSAGLIA, E., PRAT, J., HARKES, I. C. & REPASKY, E. A. 2000. Promoter hypermethylation and BRCA1 inactivation in sporadic breast and ovarian tumors. *Journal of the National Cancer Institute,* 92**,** 564-569.

FAHEEM, M., NASEER, M. I., RASOOL, M., CHAUDHARY, A. G., KUMOSANI, T. A., ILYAS, A. M., PUSHPARAJ, P. N., AHMED, F., ALGAHTANI, H. A. &

AL-QAHTANI, M. H. 2015. Molecular genetics of human primary microcephaly: an overview. *BMC medical genomics,* 8**,** S4.

FALBO, K. B. & SHEN, X. 2006. Chromatin remodeling in DNA replication. *Journal of cellular biochemistry,* 97**,** 684-689.

FAN, S., SMITH, M. L., RIVERT, D. J., DUBA, D., ZHAN, Q., KOHN, K. W., FORNACE, A. J. & O'CONNOR, P. M. 1995. Disruption of p53 function sensitizes breast cancer MCF-7 cells to cisplatin and pentoxifylline. *Cancer research,* 55**,** 1649-1654.

FANEYTE, I. F., SCHRAMA, J. G., PETERSE, J. L., REMIJNSE, P. L., RODENHUIS, S. & VAN DE VIJVER, M. 2003. Breast cancer response to neoadjuvant chemotherapy: predictive markers and relation with outcome. *British journal of Cancer,* 88**,** 406-412.

FANG, G., CHANG, B. S., KIM, C. N., PERKINS, C., THOMPSON, C. B. & BHALLA, K. N. 1998a. "Loop" domain is necessary for taxol-induced mobility shift and phosphorylation of Bcl-2 as well as for inhibiting taxol-induced cytosolic accumulation of cytochrome c and apoptosis. *Cancer research,* 58**,** 3202-3208.

FARMER, H., MCCABE, N., LORD, C. J., TUTT, A. N., JOHNSON, D. A., RICHARDSON, T. B., SANTAROSA, M., DILLON, K. J., HICKSON, I. & KNIGHTS, C. 2005. Targeting the DNA repair defect in BRCA mutant cells as a therapeutic strategy. *Nature,* 434**,** 917-921.

FAVIANA, P., BOLDRINI, L., SPISNI, R., BERTI, P., GALLERI, D., BIONDI, R., CAMACCI, T., MATERAZZI, G., PINGITORE, R. & MICCOLI, P. 2002. Neoangiogenesis in colon cancer: correlation between vascular density, vascular endothelial growth factor (VEGF) and p53 protein expression. *Oncology reports,* 9**,** 617-620.

FINLAY, C. A., HINDS, P. W. & LEVINE, A. J. 1989. The p53 proto-oncogene can act as a suppressor of transformation. *Cell,* 57**,** 1083-1093.

FISK, H. A., MATTISON, C. P. & WINEY, M. 2003. Human Mps1 protein kinase is required for centrosome duplication and normal mitotic progression. *Proceedings of the National Academy of Sciences,* 100**,** 14875-14880.

FLAMAN, J., FREBOURG, T., MOREAU, V., CHARBONNIER, F., MARTIN, C., CHAPPUIS, P., SAPPINO, A., LIMACHER, I., BRON, L. & BENHATTAR, J. 1995. A simple p53 functional assay for screening cell lines, blood, and tumors. *Proceedings of the National Academy of Sciences,* 92**,** 3963-3967.

FOURNIER, M. V., MARTIN, K. J., KENNY, P. A., XHAJA, K., BOSCH, I., YASWEN, P. & BISSELL, M. J. 2006. Gene expression signature in organized and growth-arrested mammary acini predicts good outcome in breast cancer. *Cancer research,* 66**,** 7095-7102.

FRANKUM, J., MOUDRY, P., BROUGH, R., HODNY, Z., ASHWORTH, A., BARTEK, J. & LORD, C. 2015. Complementary genetic screens identify the E3 ubiquitin ligase CBLC, as a modifier of PARP inhibitor sensitivity. *Oncotarget*.

FUJIWARA, Y., EMI, M., OHATA, H., KATO, Y., NAKAJIMA, T., MORI, T. & NAKAMURA, Y. 1993. Evidence for the presence of two tumor suppressor genes on chromosome 8p for colorectal carcinoma. *Cancer research,* 53**,** 1172-1174.

FUKASAWA, K. 2005. Centrosome amplification, chromosome instability and cancer development. *Cancer letters,* 230**,** 6-19.

FURUNO, N., DEN ELZEN, N. & PINES, J. 1999. Human cyclin A is required for mitosis until mid prophase. *The Journal of cell biology,* 147**,** 295-306.

GABRIEL, A. & LONG, J. 2011. Breast Anatomy. *Online]* http://emedicine. medscape. com/article/1273133-overview# aw2aab6b4.

GAO, S., YANG, C., JIANG, S., XU, X.-N., LU, X., HE, Y.-W., CHEUNG, A. & WANG, H. 2014. Applications of RNA interference high-throughput

screening technology in cancer biology and virology. *Protein & cell,* 5**,** 805-815.

GATHANI, T., ALI, R., BALKWILL, A., GREEN, J., REEVES, G., BERAL, V. & MOSER, K. 2014. Ethnic differences in breast cancer incidence in England are due to differences in known risk factors for the disease: prospective study. *British journal of cancer,* 110**,** 224-229.

GAVVOVIDIS, I., PÖHLMANN, C., MARCHAL, J. A., STUMM, M., YAMASHITA, D., HIRANO, T., SCHINDLER, D., NEITZEL, H. & TRIMBORN, M. 2010. MCPH1 patient cells exhibit delayed release from DNA damage-induced G2/M checkpoint arrest *Cell Cycle,* 9**,** 4893-4899.

GAVVOVIDIS, I., ROST, I., TRIMBORN, M., KAISER, F. J., PURPS, J., WIEK, C., HANENBERG, H., NEITZEL, H. & SCHINDLER, D. 2012. A novel MCPH1 isoform complements the defective chromosome condensation of human MCPH1-deficient cells. *PLoS One,* 7**,** e40387.

GE, C., CHE, L., REN, J., PANDITA, R. K., LU, J., LI, K., PANDITA, T. K. & DU, C. 2015. BRUCE regulates DNA double-strand break response by promoting USP8 deubiquitination of BRIT1. *Proc Natl Acad Sci U S A,* 112**,** E1210-9.

GEISLER, S., LØNNING, P. E., AAS, T., JOHNSEN, H., FLUGE, Ø., HAUGEN, D. F., LILLEHAUG, J. R., AKSLEN, L. A. & BØRRESEN-DALE, A.-L. 2001. Influence of TP53 gene alterations and c-erbB-2 expression on the response to treatment with doxorubicin in locally advanced breast cancer. *Cancer Research,* 61**,** 2505-2512.

GERLOFF, D. L., WOODS, N. T., FARAGO, A. A. & MONTEIRO, A. N. 2012. BRCT domains: A little more than kin, and less than kind. *FEBS Lett,* 586**,** 2711-6.

GEYER, F. C., LOPEZ GARCIA, M. A., LAMBROS, M. B. & REIS FILHO, J. S. 2009. Genetic characterization of breast cancer and implications for clinical management. *Journal of cellular and molecular medicine,* 13**,** 4090-4103.

GHOSH, R. N., DEBIASIO, R., HUDSON, C. C., RAMER, E. R., COWAN, C. L. & OAKLEY, R. H. 2005. Quantitative cell-based high-content screening for vasopressin receptor agonists using Transfluor® technology. *Journal of biomolecular screening,* 10**,** 476-484.

GIALLONGO, C., TIBULLO, D., LA CAVA, P., BRANCA, A., PARRINELLO, N., SPINA, P., STAGNO, F., CONTICELLO, C., CHIARENZA, A. & VIGNERI, P. 2010. BRIT1/MCPH1 expression in chronic myeloid leukemia and its regulation of the G2/M checkpoint. *Acta haematologica,* 126**,** 205-210.

GIRDLER, F., GASCOIGNE, K. E., EYERS, P. A., HARTMUTH, S., CRAFTER, C., FOOTE, K. M., KEEN, N. J. & TAYLOR, S. S. 2006. Validating Aurora B as an anti-cancer drug target. *Journal of cell science,* 119**,** 3664-3675.

GODWIN, A. K., MEISTER, A., O'DWYER, P. J., HUANG, C. S., HAMILTON, T. C. & ANDERSON, M. E. 1992. High resistance to cisplatin in human ovarian cancer cell lines is associated with marked increase of glutathione synthesis. *Proceedings of the National Academy of Sciences,* 89**,** 3070-3074.

GOKTUG, A. N., CHAI, S. C. & CHEN, T. 2013. *Data analysis approaches in high throughput screening,* INTECH Open Access Publisher.

GORJÁNÁCZ, M., KLERKX, E. P., GALY, V., SANTARELLA, R., LÓPEZ IGLESIAS, C., ASKJAER, P. & MATTAJ, I. W. 2007. Caenorhabditis elegans BAF 1 and its kinase VRK 1 participate directly in post mitotic nuclear envelope assembly. *The EMBO journal,* 26**,** 132-143.

GOTOH, E., ASAKAWA, Y. & KOSAKA, H. 1995. Inhibition of protein serine/threonine phosphatases directly induces premature chromosome condensation in mammalian somatic cells. *BIOMEDICAL RESEARCH-TOKYO-,* 16**,** 63-63.

GREEN, J., CAIRNS, B. J., CASABONNE, D., WRIGHT, F. L., REEVES, G., BERAL, V. & COLLABORATORS, M. W. S. 2011. Height and cancer incidence in the Million Women Study: prospective cohort, and meta-analysis of prospective studies of height and total cancer risk. *The lancet oncology,* 12**,** 785-794.

GREEN, L. J. & LIN, S.-Y. 2012. *DNA damage response and breast cancer: an overview*, INTECH Open Access Publisher.

GREM, J. L., NGUYEN, D., MONAHAN, B. P., KAO, V. & GEOFFROY, F. J. 1999. Sequence-dependent antagonism between fluorouracil and paclitaxel in human breast cancer cells. *Biochemical pharmacology,* 58**,** 477-486.

GRUBER, R., ZHOU, Z., SUKCHEV, M., JOERSS, T., FRAPPART, P. O. & WANG, Z. Q. 2011. MCPH1 regulates the neuroprogenitor division mode by coupling the centrosomal cycle with mitotic entry through the Chk1-Cdc25 pathway. *Nat Cell Biol,* 13**,** 1325-34.

GUAN, R., TAPANG, P., LEVERSON, J. D., ALBERT, D., GIRANDA, V. L. & LUO, Y. 2005. Small interfering RNA–mediated Polo-like kinase 1 depletion preferentially reduces the survival of p53-defective, oncogenic transformed cells and inhibits tumor growth in animals. *Cancer research,* 65**,** 2698-2704.

GUERNSEY, D. L., JIANG, H., HUSSIN, J., ARNOLD, M., BOUYAKDAN, K., PERRY, S., BABINEAU-STURK, T., BEIS, J., DUMAS, N. & EVANS, S. C. 2010. Mutations in centrosomal protein CEP152 in primary microcephaly families linked to MCPH4. *The American Journal of Human Genetics,* 87**,** 40-51.

GUSTERSON, B. A., ROSS, D. T., HEATH, V. J. & STEIN, T. 2005. Basal cytokeratins and their relationship to the cellular origin and functional classification of breast cancer. *Breast Cancer Res,* 7**,** 143-148.

GÜTGEMANN, I., LEHMAN, N. L., JACKSON, P. K. & LONGACRE, T. A. 2008. Emi1 protein accumulation implicates misregulation of the anaphase promoting complex/cyclosome pathway in ovarian clear cell carcinoma. *Modern Pathology,* 21**,** 445-454.

HAGEMANN, C., ANACKER, J., GERNGRAS, S., KÜHNEL, S., SAID, H. M., PATEL, R., KÄMMERER, U., VORDERMARK, D., ROOSEN, K. & VINCE, G. H. 2008. Expression analysis of the autosomal recessive primary microcephaly genes MCPH1 (microcephalin) and MCPH5 (ASPM, abnormal spindle-like, microcephaly associated) in human malignant gliomas. *Oncology reports,* 20**,** 301-308.

HALASI, M. & GARTEL, A. L. 2012. Suppression of FOXM1 sensitizes human cancer cells to cell death induced by DNA-damage. *PloS one,* 7**,** e31761.

HALL, J. M., LEE, M. K., NEWMAN, B., MORROW, J. E., ANDERSON, L. A., HUEY, B. & KING, M.-C. 1990. Linkage of early-onset familial breast cancer to chromosome 17q21. *Science,* 250**,** 1684-1689.

HANKS, S. K., RODRIGUEZ, L. V. & RAO, P. N. 1983. Relationship between histone phosphorylation and premature chromosome condensation. *Experimental cell research,* 148**,** 293-302.

HARLOW, E., WILLIAMSON, N., RALSTON, R., HELFMAN, D. & ADAMS, T. 1985. Molecular cloning and in vitro expression of a cDNA clone for human cellular tumor antigen p53. *Molecular and cellular biology,* 5**,** 1601-1610.

HARRIS, L., FRITSCHE, H., MENNEL, R., NORTON, L., RAVDIN, P., TAUBE, S., SOMERFIELD, M. R., HAYES, D. F. & BAST, R. C. 2007. American Society of Clinical Oncology 2007 update of recommendations for the use of tumor markers in breast cancer. *Journal of clinical oncology,* 25**,** 5287-5312.

HARVEY, S. L., CHARLET, A., HAAS, W., GYGI, S. P. & KELLOGG, D. R. 2005. Cdk1-dependent regulation of the mitotic inhibitor Wee1. *Cell,* 122**,** 407-420.

HEINTZE, J., LUFT, C. & KETTELER, R. 2013. A CRISPR CASe for high-throughput silencing. *Frontiers in genetics,* 4.

HENDERSON, M. C., GONZALES, I. M., ARORA, S., CHOUDHARY, A., TRENT, J. M., VON HOFF, D. D., MOUSSES, S. & AZORSA, D. O. 2011. High-throughput RNAi screening identifies a role for TNK1 in growth and survival of pancreatic cancer cells. *Molecular Cancer Research,* 9**,** 724-732.

HENDZEL, M. J., WEI, Y., MANCINI, M. A., VAN HOOSER, A., RANALLI, T., BRINKLEY, B., BAZETT-JONES, D. P. & ALLIS, C. D. 1997. Mitosis-specific phosphorylation of histone H3 initiates primarily within pericentromeric heterochromatin during G2 and spreads in an ordered fashion coincident with mitotic chromosome condensation. *Chromosoma,* 106**,** 348-360.

HETTS, S. W. 1998. To die or not to die: an overview of apoptosis and its role in disease. *Jama,* 279**,** 300-307.

HEWITT, L., TIGHE, A., SANTAGUIDA, S., WHITE, A. M., JONES, C. D., MUSACCHIO, A., GREEN, S. & TAYLOR, S. S. 2010. Sustained Mps1 activity is required in mitosis to recruit O-Mad2 to the Mad1–C-Mad2 core complex. *The Journal of cell biology,* 190**,** 25-34.

HIRANO, T. 2000. Chromosome cohesion, condensation, and separation. *Annual review of biochemistry,* 69**,** 115-144.

HIRANO, T. 2005. Condensins: organizing and segregating the genome. *Current Biology,* 15**,** R265-R275.

HIRANO, T. 2012. Condensins: universal organizers of chromosomes with diverse functions. *Genes & development,* 26**,** 1659-1678.

HIROTA, T., GERLICH, D., KOCH, B., ELLENBERG, J. & PETERS, J.-M. 2004. Distinct functions of condensin I and II in mitotic chromosome assembly. *Journal of cell science,* 117**,** 6435-6445.

HITTELMAN, W. N., BROUSSARD, L. C., DOSIK, G. & MCCREDIE, K. B. 1980. Predicting relapse of human leukemia by means of premature chromosome condensation. *New England Journal of Medicine,* 303**,** 479-484.

HITTELMAN, W. N. & RAO, P. N. 1978. Mapping G1 phase by the structural morphology of the prematurely condensed chromosomes. *Journal of cellular physiology,* 95**,** 333-341.

HOELDER, S., CLARKE, P. A. & WORKMAN, P. 2012. Discovery of small molecule cancer drugs: Successes, challenges and opportunities. *Molecular Oncology,* 6**,** 155-176.

HSU, L. C., KAPALI, M., DELOIA, J. A. & GALLION, H. H. 2005. Centrosome abnormalities in ovarian cancer. *International journal of cancer,* 113**,** 746-751.

HU, G. & LUO, J. 2012. A primer on using pooled shRNA libraries for functional genomic screens. *Acta biochimica et biophysica Sinica,* 44**,** 103-112.

HUANG, X., KUROSE, A., TANAKA, T., TRAGANOS, F., DAI, W. & DARZYNKIEWICZ, Z. 2006. Sequential phosphorylation of Ser 10 on histone H3 and ser 139 on histone H2AX and ATM activation during premature chromosome condensation: Relationship to cell cycle phase and apoptosis. *Cytometry Part A,* 69**,** 222-229.

HUGHES-DAVIES, L., HUNTSMAN, D., RUAS, M., FUKS, F., BYE, J., CHIN, S.-F., MILNER, J., BROWN, L. A., HSU, F. & GILKS, B. 2003. EMSY links the BRCA2 pathway to sporadic breast and ovarian cancer. *Cell,* 115**,** 523-535.

HUSSAIN, M. S., BAIG, S. M., NEUMANN, S., NÜRNBERG, G., FAROOQ, M., AHMAD, I., ALEF, T., HENNIES, H. C., TECHNAU, M. & ALTMÜLLER, J. 2012. A truncating mutation of CEP135 causes primary microcephaly and disturbed centrosomal function. *The American Journal of Human Genetics,* 90**,** 871-878.

HUSSAIN, M. S., BAIG, S. M., NEUMANN, S., PECHE, V. S., SZCZEPANSKI, S., NÜRNBERG, G., TARIQ, M., JAMEEL, M., KHAN, T. N. & FATIMA, A. 2013. CDK6 associates with the centrosome during mitosis and is mutated

in a large Pakistani family with primary microcephaly. *Human molecular genetics,* ddt374.

HUTCHINS, J. R., TOYODA, Y., HEGEMANN, B., POSER, I., HÉRICHÉ, J.-K., SYKORA, M. M., AUGSBURG, M., HUDECZ, O., BUSCHHORN, B. A. & BULKESCHER, J. 2010. Systematic analysis of human protein complexes identifies chromosome segregation proteins. *Science,* 328**,** 593-599.

HUYTON, T., BATES, P. A., ZHANG, X., STERNBERG, M. J. & FREEMONT, P. S. 2000. The BRCA1 C-terminal domain: structure and function. *Mutation Research/DNA Repair,* 460**,** 319-332.

IORNS, E., LORD, C. J., TURNER, N. & ASHWORTH, A. 2007. Utilizing RNA interference to enhance cancer drug discovery. *Nature reviews Drug discovery,* 6**,** 556-568.

IORNS, E., TURNER, N. C., ELLIOTT, R., SYED, N., GARRONE, O., GASCO, M., TUTT, A. N., CROOK, T., LORD, C. J. & ASHWORTH, A. 2008. Identification of CDK10 as an important determinant of resistance to endocrine therapy for breast cancer. *Cancer cell,* 13**,** 91-104.

ISHIDA, Y., FURUKAWA, Y., DECAPRIO, J. A., SAITO, M. & GRIFFIN, J. D. 1992. Treatment of myeloid leukemic cells with the phosphatase inhibitor okadaic acid induces cell cycle arrest at either G1/S or G2/M depending on dose. *Journal of cellular physiology,* 150**,** 484-492.

JACKSON, A. P., EASTWOOD, H., BELL, S. M., ADU, J., TOOMES, C., CARR, I. M., ROBERTS, E., HAMPSHIRE, D. J., CROW, Y. J., MIGHELL, A. J., KARBANI, G., JAFRI, H., RASHID, Y., MUELLER, R. F., MARKHAM, A. F. & WOODS, C. G. 2002. Identification of microcephalin, a protein implicated in determining the size of the human brain. *Am J Hum Genet,* 71**,** 136-42.

JACKSON, A. P., MCHALE, D. P., CAMPBELL, D. A., JAFRI, H., RASHID, Y., MANNAN, J., KARBANI, G., CORRY, P., LEVENE, M. I. & MUELLER, R. F. 1998. Primary autosomal recessive microcephaly (MCPH1) maps to chromosome 8p22-pter. *The American Journal of Human Genetics,* 63**,** 541-546.

JAMIESON, C. R., GOVAERTS, C. & ABRAMOWICZ, M. J. 1999. Primary autosomal recessive microcephaly: homozygosity mapping of MCPH4 to chromosome 15. *American journal of human genetics,* 65**,** 1465.

JANSSEN, A., KOPS, G. J. & MEDEMA, R. H. 2009. Elevating the frequency of chromosome mis-segregation as a strategy to kill tumor cells. *Proceedings of the National Academy of Sciences,* 106**,** 19108-19113.

JATOI, I. & KAUFMANN, M. 2010. *Management of breast diseases*, Springer.

JEFFERS, L. J., COULL, B. J., STACK, S. J. & MORRISON, C. G. 2008. Distinct BRCT domains in Mcph1/Brit1 mediate ionizing radiation-induced focus formation and centrosomal localization. *Oncogene,* 27**,** 139-44.

JEMAA, M., GALLUZZI, L., KEPP, O., SENOVILLA, L., BRANDS, M., BOEMER, U., KOPPITZ, M., LIENAU, P., PRECHTL, S. & SCHULZE, V. 2013. Characterization of novel MPS1 inhibitors with preclinical anticancer activity. *Cell Death & Differentiation,* 20**,** 1532-1545.

JEMAL, A., BRAY, F., CENTER, M. M., FERLAY, J., WARD, E. & FORMAN, D. 2011. Global cancer statistics. *CA: a cancer journal for clinicians,* 61**,** 69-90.

JO, H. Y., KIM, Y., PARK, H. W., MOON, H. E., BAE, S., KIM, J., KIM, D. G. & PAEK, S. H. 2015. The Unreliability of MTT Assay in the Cytotoxic Test of Primary Cultured Glioblastoma Cells. *Experimental neurobiology,* 24**,** 235-245.

JO, Y. H., KIM, H. O., LEE, J., LEE, S. S., CHO, C. H., KANG, I. S., CHOE, W. J., BAIK, H. H. & YOON, K.-S. 2013. MCPH1 protein expression and polymorphisms are associated with risk of breast cancer. *Gene,* 517**,** 184-190.

JOHNSON, R. & RAO, P. 1970. Mammalian cell fusion: induction of premature chromosome condensation in interphase nuclei.

JOHNSON, S. W., LAUB, P. B., BEESLEY, J. S., OZOLS, R. F. & HAMILTON, T. C. 1997. Increased platinum-DNA damage tolerance is associated with cisplatin resistance and cross-resistance to various chemotherapeutic agents in unrelated human ovarian cancer cell lines. *Cancer Research,* 57**,** 850-856.

JOHNSTON, A. M., NASELLI, G., GONEZ, L. J., MARTIN, R. M., HARRISON, L. C. & DEAIZPURUA, H. J. 2000. SPAK, a STE20/SPS1-related kinase that activates the p38 pathway. *Oncogene,* 19**,** 4290-4297.

JONES, R. G., PLAS, D. R., KUBEK, S., BUZZAI, M., MU, J., XU, Y., BIRNBAUM, M. J. & THOMPSON, C. B. 2005. AMP-activated protein kinase induces a p53-dependent metabolic checkpoint. *Molecular cell,* 18**,** 283-293.

KADURA, S. & SAZER, S. 2005. SAC ing mitotic errors: How the spindle assembly checkpoint (SAC) plays defense against chromosome mis segregation. *Cell motility and the cytoskeleton,* 61**,** 145-160.

KAELIN JR, W. G. 2009. Synthetic lethality: a framework for the development of wiser cancer therapeutics. *Genome Med,* 1**,** 99.

KAELIN, W. G. 2005. The concept of synthetic lethality in the context of anticancer therapy. *Nature reviews cancer,* 5**,** 689-698.

KAGAMI, Y., NIHIRA, K., WADA, S., ONO, M., HONDA, M. & YOSHIDA, K. 2014. Mps1 phosphorylation of condensin II controls chromosome condensation at the onset of mitosis. *The Journal of cell biology,* 205**,** 781-790.

KAINDL, A. M. 2014. Autosomal recessive primary microcephalies (MCPH). *Eur J Paediatr Neurol,* 18**,** 547-8.

KAINDL, A. M., PASSEMARD, S., KUMAR, P., KRAEMER, N., ISSA, L., ZWIRNER, A., GERARD, B., VERLOES, A., MANI, S. & GRESSENS, P. 2010. Many roads lead to primary autosomal recessive microcephaly. *Progress in neurobiology,* 90**,** 363-383.

KANDA, R., EGUCHI-KASAI, K. & HAYATA, I. 1999. Phosphatase inhibitors and premature chromosome condensation in human peripheral lymphocytes at different cell-cycle phases. *Somatic cell and molecular genetics,* 25**,** 1-8.

KANDIOLER-ECKERSBERGER, D., LUDWIG, C., RUDAS, M., KAPPEL, S., JANSCHEK, E., WENZEL, C., SCHLAGBAUER-WADL, H., MITTLBÖCK, M., GNANT, M. & STEGER, G. 2000. TP53 mutation and p53 overexpression for prediction of response to neoadjuvant treatment in breast cancer patients. *Clinical Cancer Research,* 6**,** 50-56.

KANG, J., SERGIO, C. M., SUTHERLAND, R. L. & MUSGROVE, E. A. 2014. Targeting cyclin-dependent kinase 1 (CDK1) but not CDK4/6 or CDK2 is selectively lethal to MYC-dependent human breast cancer cells. *BMC cancer,* 14**,** 1.

KANGAS, L., GRÖNROOS, M. & NIEMINEN, A. 1983. Bioluminescence of cellular ATP: a new method for evaluating cytotoxic agents in vitro. *Medical biology,* 62**,** 338-343.

KATO, H. & SANDBERG, A. A. 1967. Chromosome pulverization in human binucleate cells following colcemid treatment. *The Journal of cell biology,* 34**,** 35-45.

KEEN, N. & TAYLOR, S. 2004. Aurora-kinase inhibitors as anticancer agents. *Nature Reviews Cancer,* 4**,** 927-936.

KENEMANS, P., VERSTRAETEN, R. & VERHEIJEN, R. 2004. Oncogenic pathways in hereditary and sporadic breast cancer. *Maturitas,* 49**,** 34-43.

KIGER, A. A., BAUM, B., JONES, S., JONES, M. R., COULSON, A., ECHEVERRI, C. & PERRIMON, N. 2003. A functional genomic analysis of cell morphology using RNA interference. *Journal of Biology,* 2**,** 27-27.

KITTLER, R., PELLETIER, L., HENINGER, A.-K., SLABICKI, M., THEIS, M., MIROSLAW, L., POSER, I., LAWO, S., GRABNER, H. & KOZAK, K. 2007a. Genome-scale RNAi profiling of cell division in human tissue culture cells. *Nature cell biology,* 9**,** 1401-1412.

KITTLER, R., SURENDRANATH, V., HENINGER, A.-K., SLABICKI, M., THEIS, M., PUTZ, G., FRANKE, K., CALDARELLI, A., GRABNER, H. & KOZAK, K. 2007b. Genome-wide resources of endoribonuclease-prepared short interfering RNAs for specific loss-of-function studies. *Nature Methods,* 4**,** 337-344.

KLINGBEIL, P., NATRAJAN, R., EVERITT, G., VATCHEVA, R., MARCHIO, C., PALACIOS, J., BUERGER, H., REIS-FILHO, J. S. & ISACKE, C. M. 2010. CD44 is overexpressed in basal-like breast cancers but is not a driver of 11p13 amplification. *Breast cancer research and treatment,* 120**,** 95-109.

KNIGHT, Z. A. & SHOKAT, K. M. 2005. Features of selective kinase inhibitors. *Chemistry & biology,* 12**,** 621-637.

KOPS, G. J., FOLTZ, D. R. & CLEVELAND, D. W. 2004. Lethality to human cancer cells through massive chromosome loss by inhibition of the mitotic checkpoint. *Proceedings of the National Academy of Sciences of the United States of America,* 101**,** 8699-8704.

KOVACS, G. 1985. Premature chromosome condensation: evidence for in vivo cell fusion in human malignant tumours. *International journal of cancer,* 36**,** 637-641.

KRANZ, D. & BOUTROS, M. 2014. A synthetic lethal screen identifies FAT1 as an antagonist of caspase 8 in extrinsic apoptosis. *The EMBO journal,* e201385686.

KRESS, M., MAY, E., CASSINGENA, R. & MAY, P. 1979. Simian virus 40-transformed cells express new species of proteins precipitable by anti-simian virus 40 tumor serum. *Journal of virology,* 31**,** 472-483.

KUIKEN, H. J. & BEIJERSBERGEN, R. L. 2010. Exploration of synthetic lethal interactions as cancer drug targets. *Future Oncology,* 6**,** 1789-1802.

KULKARNI, M. M., BOOKER, M., SILVER, S. J., FRIEDMAN, A., HONG, P., PERRIMON, N. & MATHEY-PREVOT, B. 2006. Evidence of off-target effects associated with long dsRNAs in Drosophila melanogaster cell-based assays. *Nature methods,* 3**,** 833-838.

KUMAR, A., GIRIMAJI, S. C., DUVVARI, M. R. & BLANTON, S. H. 2009. Mutations in STIL, encoding a pericentriolar and centrosomal protein, cause primary microcephaly. *The American Journal of Human Genetics,* 84**,** 286-290.

KWIATKOWSKI, N., JELLUMA, N., FILIPPAKOPOULOS, P., SOUNDARARAJAN, M., MANAK, M. S., KWON, M., CHOI, H. G., SIM, T., DEVERAUX, Q. L. & ROTTMANN, S. 2010. Small-molecule kinase inhibitors provide insight into Mps1 cell cycle function. *Nature chemical biology,* 6**,** 359-368.

LAMB, J., CRAWFORD, E. D., PECK, D., MODELL, J. W., BLAT, I. C., WROBEL, M. J., LERNER, J., BRUNET, J.-P., SUBRAMANIAN, A. & ROSS, K. N. 2006. The Connectivity Map: using gene-expression signatures to connect small molecules, genes, and disease. *science,* 313**,** 1929-1935.

LANDI, M. T., DRACHEVA, T., ROTUNNO, M., FIGUEROA, J. D., LIU, H., DASGUPTA, A., MANN, F. E., FUKUOKA, J., HAMES, M. & BERGEN, A. W. 2008. Gene expression signature of cigarette smoking and its role in lung adenocarcinoma development and survival. *PloS one,* 3**,** e1651.

LANE, D. & CRAWFORD, L. 1979. T antigen is bound to a host protein in SY40-transformed cells.

LARA, J. F., THOR, A. D., DRESSLER, L. G., BROADWATER, G., BLEIWEISS, I. J., EDGERTON, S., COWAN, D., GOLDSTEIN, L. J., MARTINO, S. & INGLE, J. N. 2011. p53 Expression in node-positive breast cancer patients:

results from the Cancer and Leukemia Group B 9344 Trial (159905). *Clinical Cancer Research,* 17**,** 5170-5178.

LAZO, P., VEGA, F. & SEVILLA, A. 2005. Vaccinia-related kinase-1. *Afcs Nature Molecule Page doi,* 10.

LEE, H., LEE, D. J., OH, S. P., PARK, H. D., NAM, H. H., KIM, J. M. & LIM, D.-S. 2006. Mouse emi1 has an essential function in mitotic progression during early embryogenesis. *Molecular and cellular biology,* 26**,** 5373-5381.

LEE, H.-C., KO, H., SEOL, H., NOH, D.-Y., HAN, W., KIM, T.-Y., IM, S.-A. & PARK, I. 2013. Expression of immunohistochemical markers before and after neoadjuvant chemotherapy in breast carcinoma, and their use as predictors of response. *Journal of breast cancer,* 16**,** 395-403.

LEHMAN, N. L., TIBSHIRANI, R., HSU, J. Y., NATKUNAM, Y., HARRIS, B. T., WEST, R. B., MASEK, M. A., MONTGOMERY, K., VAN DE RIJN, M. & JACKSON, P. K. 2007. Oncogenic regulators and substrates of the anaphase promoting complex/cyclosome are frequently overexpressed in malignant tumors. *Am J Pathol,* 170**,** 1793-805.

LEUNG, J. W., LEITCH, A., WOOD, J. L., SHAW-SMITH, C., METCALFE, K., BICKNELL, L. S., JACKSON, A. P. & CHEN, J. 2011. SET nuclear oncogene associates with microcephalin/MCPH1 and regulates chromosome condensation. *J Biol Chem,* 286**,** 21393-400.

LEVINE, A. J. & OREN, M. 2009. The first 30 years of p53: growing ever more complex. *Nat Rev Cancer,* 9**,** 749-58.

LI, C., URIBE, D. & DALING, J. 2005. Clinical characteristics of different histologic types of breast cancer. *British journal of cancer,* 93**,** 1046-1052.

LI, M.-H., ITO, D., SANADA, M., ODANI, T., HATORI, M., IWASE, M. & NAGUMO, M. 2004. Effect of 5-fluorouracil on G1 phase cell cycle regulation in oral cancer cell lines. *Oral oncology,* 40**,** 63-70.

LIANG, Y., GAO, H., LIN, S.-Y., GOSS, J. A., DU, C. & LI, K. 2014. Mcph1/Brit1 deficiency promotes genomic instability and tumor formation in a mouse model. *Oncogene.*

LIANG, Y., GAO, H., LIN, S.-Y., PENG, G., HUANG, X., ZHANG, P., GOSS, J. A., BRUNICARDI, F. C., MULTANI, A. S. & CHANG, S. 2010a. BRIT1/MCPH1 is essential for mitotic and meiotic recombination DNA repair and maintaining genomic stability in mice. *PLoS Genet,* 6**,** e1000826.

LIANG, Y., LIN, S.-Y. & LI, K. 2010g. MCPH1 (microcephalin 1).

LIN, S.-Y. & ELLEDGE, S. J. 2003. Multiple tumor suppressor pathways negatively regulate telomerase. *Cell,* 113**,** 881-889.

LIN, S.-Y., RAI, R., LI, K., XU, Z.-X. & ELLEDGE, S. J. 2005. BRIT1/MCPH1 is a DNA damage responsive protein that regulates the Brca1–Chk1 pathway, implicating checkpoint dysfunction in microcephaly. *Proceedings of the National Academy of Sciences of the United States of America,* 102**,** 15105-15109.

LIN, S. Y., LIANG, Y. & LI, K. 2010. Multiple roles of BRIT1/MCPH1 in DNA damage response, DNA repair, and cancer suppression. *Yonsei Med J,* 51**,** 295-301.

LING, Y., ZHANG, X., BAI, Y., LI, P., WEI, C., SONG, T., ZHENG, Z., GUAN, K., ZHANG, Y., ZHANG, B., LIU, X., MA, R. Z., CAO, C., ZHONG, H. & XU, Q. 2014. Overexpression of Mps1 in colon cancer cells attenuates the spindle assembly checkpoint and increases aneuploidy. *Biochemical and Biophysical Research Communications,* 450**,** 1690-1695.

LINGLE, W. L., BARRETT, S. L., NEGRON, V. C., D'ASSORO, A. B., BOENEMAN, K., LIU, W., WHITEHEAD, C. M., REYNOLDS, C. & SALISBURY, J. L. 2002. Centrosome amplification drives chromosomal instability in breast tumor development. *Proceedings of the National Academy of Sciences,* 99**,** 1978-1983.

LINJAWI, A., KONTOGIANNEA, M., HALWANI, F., EDWARDES, M. & METERISSIAN, S. 2004. Prognostic significance of p53, bcl-2, and Bax expression in early breast cancer. *Journal of the American College of Surgeons,* 198**,** 83-90.

LINZER, D. I. & LEVINE, A. J. 1979. Characterization of a 54K dalton cellular SV40 tumor antigen present in SV40-transformed cells and uninfected embryonal carcinoma cells. *Cell,* 17**,** 43-52.

LIU, X. & ERIKSON, R. L. 2003. Polo-like kinase (Plk) 1 depletion induces apoptosis in cancer cells. *Proceedings of the National Academy of Sciences,* 100**,** 5789-5794.

LIU, X., LEI, M. & ERIKSON, R. L. 2006. Normal cells, but not cancer cells, survive severe Plk1 depletion. *Molecular and cellular biology,* 26**,** 2093-2108.

LIU, X. & WINEY, M. 2012. The MPS1 family of protein kinases. *Annual review of biochemistry,* 81**,** 561.

LIU, Y., LANG, Y., PATEL, N. K., NG, G., LAUFER, R., LI, S.-W., EDWARDS, L., FORREST, B., SAMPSON, P. B. & FEHER, M. 2015. The Discovery of Orally Bioavailable Tyrosine Threonine Kinase (TTK) Inhibitors: 3-(4-(heterocyclyl) phenyl)-1 H-indazole-5-carboxamides as Anticancer Agents. *Journal of Medicinal Chemistry,* 58**,** 3366-3392.

LÖFFLER, H., REBACZ, B., HO, A. D., LUKAS, J., BARTEK, J. & KRÄMER, A. 2006. Chk1-dependent regulation of Cdc25B functions to coordinate mitotic events. *Cell cycle,* 5**,** 2543-2547.

LOHRUM, M. A., WOODS, D. B., LUDWIG, R. L., BÁLINT, É. & VOUSDEN, K. H. 2001. C-terminal ubiquitination of p53 contributes to nuclear export. *Molecular and cellular biology,* 21**,** 8521-8532.

LOPEZ-BORGES, S. & LAZO, P. A. 2000. The human vaccinia-related kinase 1 (VRK1) phosphorylates threonine-18 within the mdm-2 binding site of the p53 tumour suppressor protein. *Oncogene,* 19**,** 3656-3664.

LÓPEZ-SÁNCHEZ, I., VALBUENA, A., VÁZQUEZ-CEDEIRA, M., KHADAKE, J., SANZ-GARCÍA, M., CARRILLO-JIMÉNEZ, A. & LAZO, P. A. 2014. VRK1 interacts with p53 forming a basal complex that is activated by UV-induced DNA damage. *FEBS Letters,* 588**,** 692-700.

LORD, C. J. & ASHWORTH, A. 2012. The DNA damage response and cancer therapy. *Nature,* 481**,** 287-294.

LOSADA, A., HIRANO, M. & HIRANO, T. 2002. Cohesin release is required for sister chromatid resolution, but not for condensin-mediated compaction, at the onset of mitosis. *Genes & development,* 16**,** 3004-3016.

LU, T., HANO, H., MENG, C., NAGATSUMA, K., CHIBA, S. & IKEGAMI, M. 2007. Frequent loss of heterozygosity in two distinct regions, 8p23. 1 and 8p22, in hepatocellular carcinoma. *World journal of gastroenterology: WJG,* 13**,** 1090-1097.

MA, C. X., CAI, S., LI, S., RYAN, C. E., GUO, Z., SCHAIFF, W. T., LIN, L., HOOG, J., GOIFFON, R. J. & PRAT, A. 2012. Targeting Chk1 in p53-deficient triple-negative breast cancer is therapeutically beneficial in human-in-mouse tumor models. *The Journal of clinical investigation,* 122**,** 1541-1552.

MAACKE, H., JOST, K., OPITZ, S., MISKA, S., YUAN, Y., HASSELBACH, L., LÜTTGES, J., KALTHOFF, H. & STÜRZBECHER, H. 2000a. DNA repair and recombination factor Rad51 is over-expressed in human pancreatic adenocarcinoma. *Oncogene,* 19**,** 2791-2795.

MAACKE, H., OPITZ, S., JOST, K., HAMDORF, W., HENNING, W., KRÜGER, S., FELLER, A. C., LOPENS, A., DIEDRICH, K. & SCHWINGER, E. 2000b. Over expression of wild type Rad51 correlates with histological grading of invasive ductal breast cancer. *International journal of cancer,* 88**,** 907-913.

MACHIDA, Y. J. & DUTTA, A. 2007. The APC/C inhibitor, Emi1, is essential for prevention of rereplication. *Genes & development,* 21**,** 184-194.

MACKEIGAN, J. P., MURPHY, L. O. & BLENIS, J. 2005. Sensitized RNAi screen of human kinases and phosphatases identifies new regulators of apoptosis and chemoresistance. *Nature cell biology,* 7**,** 591-600.

MAI, L., YI, F., GOU, X., ZHANG, J., WANG, C., LIU, G., BU, Y., YUAN, C., DENG, L. & SONG, F. 2014. The overexpression of MCPH1 inhibits cell growth through regulating cell cycle-related proteins and activating cytochrome c-caspase 3 signaling in cervical cancer. *Mol Cell Biochem,* 392**,** 95-107.

MAIRE, V., BALDEYRON, C., RICHARDSON, M., TESSON, B., VINCENT-SALOMON, A., GRAVIER, E., MARTY-PROUVOST, B., DE KONING, L., RIGAILL, G. & DUMONT, A. 2013a. TTK/hMPS1 is an attractive therapeutic target for triple-negative breast cancer. *PloS one,* 8**,** e63712.

MALHOTRA, G. K., ZHAO, X., BAND, H. & BAND, V. 2014. Histological, molecular and functional subtypes of breast cancers. *Cancer Biology & Therapy,* 10**,** 955-960.

MALUMBRES, M. & BARBACID, M. 2009. Cell cycle, CDKs and cancer: a changing paradigm. *Nature Reviews Cancer,* 9**,** 153-166.

MANTERE, T., WINQVIST, R., KAUPPILA, S., GRIP, M., JUKKOLA-VUORINEN, A., TERVASMÄKI, A., RAPAKKO, K. & PYLKÄS, K. 2016. Targeted Next-Generation Sequencing Identifies a Recurrent Mutation in MCPH1 Associating with Hereditary Breast Cancer Susceptibility. *PLoS Genet,* 12**,** e1005816.

MARCOTTE, R., BROWN, K. R., SUAREZ, F., SAYAD, A., KARAMBOULAS, K., KRZYZANOWSKI, P. M., SIRCOULOMB, F., MEDRANO, M., FEDYSHYN, Y. & KOH, J. L. 2012. Essential gene profiles in breast, pancreatic, and ovarian cancer cells. *Cancer discovery,* 2**,** 172-189.

MARGOLIS, S. S. & KORNBLUTH, S. 2004. When the checkpoints have gone: insights into Cdc25 functional activation. *Cell Cycle,* 3**,** 423-426.

MARINE, S., BAHL, A., FERRER, M. & BUEHLER, E. 2012. Common seed analysis to identify off-target effects in siRNA screens. *J Biomol Screen,* 17**,** 370-8.

MARINOVICH, M., SARDANELLI, F., CIATTO, S., MAMOUNAS, E., BRENNAN, M., MACASKILL, P., IRWIG, L., VON MINCKWITZ, G. & HOUSSAMI, N. 2012. Early prediction of pathologic response to neoadjuvant therapy in breast cancer: systematic review of the accuracy of MRI. *The Breast,* 21**,** 669-677.

MARTIN, C.-A. 2011. Role of microcephalin at mitosis.

MARTIN, H. L., ADAMS, M., HIGGINS, J., BOND, J., MORRISON, E. E., BELL, S. M., WARRINER, S., NELSON, A. & TOMLINSON, D. C. 2014. High-content, high-throughput screening for the identification of cytotoxic compounds based on cell morphology and cell proliferation markers. *PLoS One,* 9**,** e88338.

MARTIN, K. J., PATRICK, D. R., BISSELL, M. J. & FOURNIER, M. V. 2008. Prognostic breast cancer signature identified from 3D culture model accurately predicts clinical outcome across independent datasets. *PLoS One,* 3**,** e2994.

MATLASHEWSKI, G., LAMB, P., PIM, D., PEACOCK, J., CRAWFORD, L. & BENCHIMOL, S. 1984. Isolation and characterization of a human p53 cDNA clone: expression of the human p53 gene. *The EMBO journal,* 3**,** 3257.

MAUGHAN, K. L., LUTTERBIE, M. A. & HAM, P. S. 2010. Treatment of breast cancer. *Am Fam Physician,* 81**,** 1339-46.

MCGOWAN, C. H. & RUSSELL, P. 1993. Human Wee1 kinase inhibits cell division by phosphorylating p34cdc2 exclusively on Tyr15. *The EMBO journal,* 12**,** 75.

MEISTER, G. & TUSCHL, T. 2004. Mechanisms of gene silencing by double-stranded RNA. *Nature,* 431**,** 343-349.

MERRY, C., FU, K., WANG, J., YEH, I.-J. & ZHANG, Y. 2010. Targeting the checkpoint kinase Chk1 in cancer therapy. *Cell Cycle,* 9**,** 279-283.

MICHEL, L., DIAZ-RODRIGUEZ, E., NARAYAN, G., HERNANDO, E., MURTY, V. V. & BENEZRA, R. 2004. Complete loss of the tumor suppressor MAD2 causes premature cyclin B degradation and mitotic failure in human somatic cells. *Proceedings of the National Academy of Sciences of the United States of America,* 101**,** 4459-4464.

MIEOG, J., VAN DER HAGE, J. & VAN DE VELDE, C. 2007. Neoadjuvant chemotherapy for operable breast cancer. *British Journal of Surgery,* 94**,** 1189-1200.

MIHARA, M., ERSTER, S., ZAIKA, A., PETRENKO, O., CHITTENDEN, T., PANCOSKA, P. & MOLL, U. M. 2003. p53 has a direct apoptogenic role at the mitochondria. *Molecular cell,* 11**,** 577-590.

MIKI, Y., SWENSEN, J., SHATTUCK-EIDENS, D., FUTREAL, P., HARSHMAN, K., TAVTIGIAN, S., LIU, Q., COCHRAN, C., BENNETT, L. & DING, W. 1994. Isolation of BRCA1, the 17q-linked breast and ovarian cancer susceptibility gene. *Science,* 266**,** 1.

MILES, C. P. & WOLINSKA, W. 1973. A comparative analysis of chromosomes and diagnostic cytology in effusions from 58 cancer patients. *Cancer,* 32**,** 1458-1469.

MILICEVIC, Z., BAJIC, V., ZIVKOVIC, L., KASAPOVIC, J., ANDJELKOVIC, U. & SPREMO-POTPAREVIC, B. 2014. Identification of p53 and its isoforms in human breast carcinoma cells. *ScientificWorldJournal,* 2014**,** 618698.

MILLOUR, J., CONSTANTINIDOU, D., STAVROPOULOU, A. V., MYATT, S., KWOK, J. M., SIVANANDAN, K., COOMBES, R., MEDEMA, R., HARTMAN, J. & LYKKESFELDT, A. E. 2010. FOXM1 is a transcriptional target of ERα and has a critical role in breast cancer endocrine sensitivity and resistance. *Oncogene,* 29**,** 2983-2995.

MILLOUR, J., DE OLANO, N., HORIMOTO, Y., MONTEIRO, L. J., LANGER, J. K., ALIGUE, R., HAJJI, N. & LAM, E. W.-F. 2011. ATM and p53 regulate FOXM1 expression via E2F in breast cancer epirubicin treatment and resistance. *Molecular cancer therapeutics,* 10**,** 1046-1058.

MILLS, G. B., SCHMANDT, R., MCGILL, M., AMENDOLA, A., HILL, M., JACOBS, K., MAY, C., RODRICKS, A.-M., CAMPBELL, S. & HOGG, D. 1992. Expression of TTK, a novel human protein kinase, is associated with cell proliferation. *Journal of Biological Chemistry,* 267**,** 16000-16006.

MOHR, S., BAKAL, C. & PERRIMON, N. 2010. Genomic screening with RNAi: results and challenges. *Annual review of biochemistry,* 79**,** 37.

MOHR, S. E., SMITH, J. A., SHAMU, C. E., NEUMÜLLER, R. A. & PERRIMON, N. 2014. RNAi screening comes of age: improved techniques and complementary approaches. *Nature Reviews Molecular Cell Biology,* 15**,** 591-600.

MOLITOR, T. & TRAKTMAN, P. 2013. Molecular genetic analysis of VRK1 in mammary epithelial cells: depletion slows proliferation in vitro and tumor growth and metastasis in vivo. *Oncogenesis,* 2**,** e48.

MOMAND, J., ZAMBETTI, G. P., OLSON, D. C., GEORGE, D. & LEVINE, A. J. 1992. The mdm-2 oncogene product forms a complex with the p53 protein and inhibits p53-mediated transactivation. *Cell,* 69**,** 1237-1245.

MOOK, S., SCHMIDT, M. K., RUTGERS, E. J., VAN DE VELDE, A. O., VISSER, O., RUTGERS, S. M., ARMSTRONG, N., VAN'T VEER, L. J. & RAVDIN, P. M. 2009. Calibration and discriminatory accuracy of prognosis calculation for breast cancer with the online Adjuvant! program: a hospital-based retrospective cohort study. *The lancet oncology,* 10**,** 1070-1076.

MORRISON, A. J., HIGHLAND, J., KROGAN, N. J., ARBEL-EDEN, A., GREENBLATT, J. F., HABER, J. E. & SHEN, X. 2004. INO80 and γ-H2AX

interaction links ATP-dependent chromatin remodeling to DNA damage repair. *Cell,* 119**,** 767-775.

MORRISON, E., THOMPSON, J., WILLIAMSON, S. J., CHEETHAM, M. E. & ROBINSON, P. A. 2011. A simple cell based assay to measure Parkin activity. *Journal of neurochemistry,* 116**,** 342-349.

MOYNIHAN, L., JACKSON, A. P., ROBERTS, E., KARBANI, G., LEWIS, I., CORRY, P., TURNER, G., MUELLER, R. F., LENCH, N. J. & WOODS, C. G. 2000. A third novel locus for primary autosomal recessive microcephaly maps to chromosome 9q34. *The American Journal of Human Genetics,* 66**,** 724-727.

MUKAMAL, K. 2010. Overview of the risks and benefits of alcohol consumption. *UpToDate, Basow, DS (Ed), UpToDate, Waltham, MA*.

MULLENDERS, J. & BERNARDS, R. 2009. Loss-of-function genetic screens as a tool to improve the diagnosis and treatment of cancer. *Oncogene,* 28**,** 4409-4420.

MUSCHECK, M., SÜKÖSD, F., PESTI, T. & KOVACS, G. 2000. High density deletion mapping of bladder cancer localizes the putative tumor suppressor gene between loci D8S504 and D8S264 at chromosome 8p23. 3. *Laboratory investigation,* 80**,** 1089-1093.

NASMYTH, K. 2002. Segregating sister genomes: the molecular biology of chromosome separation. *Science,* 297**,** 559-565.

NEITZEL, H., NEUMANN, L. M., SCHINDLER, D., WIRGES, A., TÖNNIES, H., TRIMBORN, M., KREBSOVA, A., RICHTER, R. & SPERLING, K. 2002. Premature chromosome condensation in humans associated with microcephaly and mental retardation: a novel autosomal recessive condition. *The American Journal of Human Genetics,* 70**,** 1015-1022.

NEUMANN, B., HELD, M., LIEBEL, U., ERFLE, H., ROGERS, P., PEPPERKOK, R. & ELLENBERG, J. 2006. High-throughput RNAi screening by time-lapse imaging of live human cells. *Nature methods,* 3**,** 385-390.

NEUMANN, B., WALTER, T., HERICHE, J.-K., BULKESCHER, J., ERFLE, H., CONRAD, C., ROGERS, P., POSER, I., HELD, M. & LIEBEL, U. 2010. Phenotypic profiling of the human genome by time-lapse microscopy reveals cell division genes. *Nature,* 464**,** 721-727.

NEVE, R. M., CHIN, K., FRIDLYAND, J., YEH, J., BAEHNER, F. L., FEVR, T., CLARK, L., BAYANI, N., COPPE, J.-P. & TONG, F. 2006. A collection of breast cancer cell lines for the study of functionally distinct cancer subtypes. *Cancer cell,* 10**,** 515-527.

NGHIEM, P., PARK, P. K., KIM, Y., VAZIRI, C. & SCHREIBER, S. L. 2001. ATR inhibition selectively sensitizes G1 checkpoint-deficient cells to lethal premature chromatin condensation. *Proc Natl Acad Sci U S A,* 98**,** 9092-7.

NICHOLS, R. J., WIEBE, M. S. & TRAKTMAN, P. 2006. The vaccinia-related kinases phosphorylate the N′ terminus of BAF, regulating its interaction with DNA and its retention in the nucleus. *Molecular biology of the cell,* 17**,** 2451-2464.

NICKE, B., BASTIEN, J., KHANNA, S. J., WARNE, P. H., COWLING, V., COOK, S. J., PETERS, G., DELPUECH, O., SCHULZE, A., BERNS, K., MULLENDERS, J., BEIJERSBERGEN, R. L., BERNARDS, R., GANESAN, T. S., DOWNWARD, J. & HANCOCK, D. C. 2005. Involvement of MINK, a Ste20 Family Kinase, in Ras Oncogene-Induced Growth Arrest in Human Ovarian Surface Epithelial Cells. *Molecular Cell,* 20**,** 673-685.

NIELSEN, T. O., HSU, F. D., JENSEN, K., CHEANG, M., KARACA, G., HU, Z., HERNANDEZ-BOUSSARD, T., LIVASY, C., COWAN, D. & DRESSLER, L. 2004. Immunohistochemical and clinical characterization of the basal-like subtype of invasive breast carcinoma. *Clinical Cancer Research,* 10**,** 5367-5374.

NIGG, E. A. 2001. Mitotic kinases as regulators of cell division and its checkpoints. *Nature reviews Molecular cell biology,* 2**,** 21-32.

NIGG, E. A. 2002. Centrosome aberrations: cause or consequence of cancer progression? *Nature Reviews Cancer,* 2**,** 815-825.

NIIDA, H., TSUGE, S., KATSUNO, Y., KONISHI, A., TAKEDA, N. & NAKANISHI, M. 2005. Depletion of Chk1 leads to premature activation of Cdc2-cyclin B and mitotic catastrophe. *Journal of Biological Chemistry,* 280**,** 39246-39252.

NIITTYMÄKI, I., GYLFE, A., LAINE, L., LAAKSO, M., LEHTONEN, H. J., KONDELIN, J., TOLVANEN, J., NOUSIAINEN, K., POUWELS, J. & JÄRVINEN, H. 2011. High frequency of TTK mutations in microsatellite-unstable colorectal cancer and evaluation of their effect on spindle assembly checkpoint. *Carcinogenesis,* 32**,** 305-311.

NIMÉUS MALMSTRÖM, E., KOLIADI, A., AHLIN, C., HOLMQVIST, M., HOLMBERG, L., AMINI, R. M., JIRSTRÖM, K., WÄRNBERG, F., BLOMQVIST, C. & FERNÖ, M. 2010. Cyclin B1 is a prognostic proliferation marker with a high reproducibility in a population based lymph node negative breast cancer cohort. *International Journal of Cancer,* 127**,** 961-967.

OLIVIER, M., LANGER, A., CARRIERI, P., BERGH, J., KLAAR, S., EYFJORD, J., THEILLET, C., RODRIGUEZ, C., LIDEREAU, R. & BI, I. 2006. The clinical value of somatic TP53 gene mutations in 1,794 patients with breast cancer. *Clinical cancer research,* 12**,** 1157-1167.

ONO, T., FANG, Y., SPECTOR, D. L. & HIRANO, T. 2004. Spatial and temporal regulation of Condensins I and II in mitotic chromosome assembly in human cells. *Molecular biology of the cell,* 15**,** 3296-3308.

OSBORNE, M. P. 1996. Breast development and anatomy. *Diseases of the breast. Lippincott-Raven, Philadelphia***,** 1-14.

OVERGAARD, J. 2000. TP53 mutation is an independent prognostic marker for poor outcome in both node-negative and node-positive breast cancer. *Acta Oncologica,* 39**,** 327-333.

PARKER, J. S., MULLINS, M., CHEANG, M. C., LEUNG, S., VODUC, D., VICKERY, T., DAVIES, S., FAURON, C., HE, X. & HU, Z. 2009. Supervised risk predictor of breast cancer based on intrinsic subtypes. *Journal of clinical oncology,* 27**,** 1160-1167.

PARTIPILO, G., SIMONE, G., SCATTONE, A., SCARPI, E., AZZARITI, A. & MANGIA, A. 2016. Expression of proteins involved in DNA damage response in familial and sporadic breast cancer patients. *International Journal of Cancer,* 138**,** 110-120.

PATTISON, L., CROW, Y. J., DEEBLE, V. J., JACKSON, A. P., JAFRI, H., RASHID, Y., ROBERTS, E. & WOODS, C. G. 2000. A fifth locus for primary autosomal recessive microcephaly maps to chromosome 1q31. *The American Journal of Human Genetics,* 67**,** 1578-1580.

PELZ, O., GILSDORF, M. & BOUTROS, M. 2010. web cellHTS2: a web-application for the analysis of high-throughput screening data. *BMC bioinformatics,* 11**,** 185.

PENG, G. & LIN, S.-Y. 2009a. BRIT1/MCPH1 is a multifunctional DNA damage responsive protein mediating DNA repair-associated chromatin remodeling. *Cell Cycle,* 8**,** 3071-3072.

PENG, G. & LIN, S.-Y. 2009c. The linkage of chromatin remodeling to genome maintenance: contribution from a human disease gene BRIT1/MCPH1. *Epigenetics,* 4**,** 457-461.

PENG, G., YIM, E.-K., DAI, H., JACKSON, A. P., VAN DER BURGT, I., PAN, M.-R., HU, R., LI, K. & LIN, S.-Y. 2009. BRIT1/MCPH1 links chromatin remodelling to DNA damage response. *Nature cell biology,* 11**,** 865-872.

PEPPERCORN, J., PEROU, C. & CAREY, L. 2008. Molecular subtypes in breast cancer evaluation and management: divide and conquer. *Cancer investigation,* 26**,** 1-10.

PEROU, C. M., SØRLIE, T., EISEN, M. B., VAN DE RIJN, M., JEFFREY, S. S., REES, C. A., POLLACK, J. R., ROSS, D. T., JOHNSEN, H. & AKSLEN, L. A. 2000. Molecular portraits of human breast tumours. *Nature,* 406**,** 747-752.

PETERS, J.-M. 2003. Emi1 Proteolysis: How SCFβ-Trcp1 Helps to Activate the Anaphase-Promoting Complex. *Molecular cell,* 11**,** 1420-1421.

PETITJEAN, A., ACHATZ, M., BORRESEN-DALE, A., HAINAUT, P. & OLIVIER, M. 2007. TP53 mutations in human cancers: functional selection and impact on cancer prognosis and outcomes. *Oncogene,* 26**,** 2157-2165.

PETTY, R. D., SUTHERLAND, L. A., HUNTER, E. M. & CREE, I. A. 1995. Comparison of MTT and ATP based assays for the measurement of viable cell number. *Journal of bioluminescence and chemiluminescence,* 10**,** 29-34.

PICKART, C. M. & FUSHMAN, D. 2004. Polyubiquitin chains: polymeric protein signals. *Current opinion in chemical biology,* 8**,** 610-616.

PLUMB, J. A., MILROY, R. & KAYE, S. 1989. Effects of the pH dependence of 3-(4, 5-dimethylthiazol-2-yl)-2, 5-diphenyltetrazolium bromide-formazan absorption on chemosensitivity determined by a novel tetrazolium-based assay. *Cancer Research,* 49**,** 4435-4440.

POLEK, T. C., TALPAZ, M. & SPIVAK-KROIZMAN, T. 2006a. The TNF receptor, RELT, binds SPAK and uses it to mediate p38 and JNK activation. *Biochemical and biophysical research communications,* 343**,** 125-134.

POLEK, T. C., TALPAZ, M. & SPIVAK-KROIZMAN, T. R. 2006e. TRAIL-induced cleavage and inactivation of SPAK sensitizes cells to apoptosis. *Biochemical and biophysical research communications,* 349**,** 1016-1024.

POON, R. Y., JIANG, W., TOYOSHIMA, H. & HUNTER, T. 1996. Cyclin-dependent kinases are inactivated by a combination of p21 and Thr-14/Tyr-15 phosphorylation after UV-induced DNA damage. *Journal of Biological Chemistry,* 271**,** 13283-13291.

POYUROVSKY, M. V., KATZ, C., LAPTENKO, O., BECKERMAN, R., LOKSHIN, M., AHN, J., BYEON, I.-J. L., GABIZON, R., MATTIA, M. & ZUPNICK, A. 2010. The C terminus of p53 binds the N-terminal domain of MDM2. *Nature structural & molecular biology,* 17**,** 982-989.

PRIGENT, C. & DIMITROV, S. 2003. Phosphorylation of serine 10 in histone H3, what for? *Journal of cell science,* 116**,** 3677-3685.

PULVERS, J. N., JOURNIAC, N., ARAI, Y. & NARDELLI, J. 2015. MCPH1: a window into brain development and evolution. *Front Cell Neurosci,* 9**,** 92.

QI, H., LABRIE, Y., GRENIER, J., FOURNIER, A., FILLION, C. & LABRIE, C. 2001. Androgens induce expression of SPAK, a STE20/SPS1-related kinase, in LNCaP human prostate cancer cells. *Molecular and cellular endocrinology,* 182**,** 181-192.

QIAO, G. B., WU, Y. L., YANG, X. N., ZHONG, W. Z., XIE, D., GUAN, X. Y., FISCHER, D., KOLBERG, H. C., KRUGER, S. & STUERZBECHER, H. W. 2005. High-level expression of Rad51 is an independent prognostic marker of survival in non-small-cell lung cancer patients. *Br J Cancer,* 93**,** 137-43.

RAI, R., DAI, H., MULTANI, A. S., LI, K., CHIN, K., GRAY, J., LAHAD, J. P., LIANG, J., MILLS, G. B. & MERIC-BERNSTAM, F. 2006. BRIT1 regulates early DNA damage response, chromosomal integrity, and cancer. *Cancer cell,* 10**,** 145-157.

RAI, R., PHADNIS, A., HARALKAR, S., BADWE, R. A., DAI, H., LI, K. & LIN, S.-Y. 2008. Differential regulation of centrosome integrity by DNA damage response proteins. *Cell cycle,* 7**,** 2225-2233.

RAKHA, E. A., REIS-FILHO, J. S. & ELLIS, I. O. 2008. Basal-like breast cancer: a critical review. *Journal of Clinical Oncology,* 26**,** 2568-2581.

RAKHA, E. A., REIS-FILHO, J. S. & ELLIS, I. O. 2010. Combinatorial biomarker expression in breast cancer. *Breast cancer research and treatment,* 120**,** 293-308.

RAN, F. A., HSU, P. D., WRIGHT, J., AGARWALA, V., SCOTT, D. A. & ZHANG, F. 2013. Genome engineering using the CRISPR-Cas9 system. *Nature protocols,* 8**,** 2281-2308.

RANTALA, J. K., KWON, S., KORKOLA, J. & GRAY, J. W. 2013. Expanding the diversity of imaging-based rnai screen applications using cell spot microarrays. *Microarrays,* 2**,** 97-114.

REEVES, G. K., PIRIE, K., BERAL, V., GREEN, J., SPENCER, E. & BULL, D. 2007. Cancer incidence and mortality in relation to body mass index in the Million Women Study: cohort study. *Bmj,* 335**,** 1134.

REICHMANN, A. & LEVIN, B. 1981. Premature chromosome condensation in human large bowel cancer. *Cancer genetics and cytogenetics,* 3**,** 221-225.

REICHMANN, A., MARTIN, P. & LEVIN, B. 1981. Chromosomal banding patterns in human large bowel cancer. *International Journal of Cancer,* 28**,** 431-440.

REIMANN, J. D., FREED, E., HSU, J. Y., KRAMER, E. R., PETERS, J.-M. & JACKSON, P. K. 2001a. Emi1 is a mitotic regulator that interacts with Cdc20 and inhibits the anaphase promoting complex. *Cell,* 105**,** 645-655.

REIMANN, J. D., GARDNER, B. E., MARGOTTIN-GOGUET, F. & JACKSON, P. K. 2001c. Emi1 regulates the anaphase-promoting complex by a different mechanism than Mad2 proteins. *Genes & development,* 15**,** 3278-3285.

REIS-FILHO, J., WESTBURY, C. & PIERGA, J. 2006. The impact of expression profiling on prognostic and predictive testing in breast cancer. *Journal of clinical pathology,* 59**,** 225-231.

REIS-FILHO, J. & TUTT, A. 2008. Triple negative tumours: a critical review. *Histopathology,* 52**,** 108-118.

RICHARDS, M. W., LEUNG, J. W., ROE, S. M., LI, K., CHEN, J. & BAYLISS, R. 2010. A pocket on the surface of the N-terminal BRCT domain of Mcph1 is required to prevent abnormal chromosome condensation. *Journal of molecular biology,* 395**,** 908-915.

RICHARDSON, J., SHAABAN, A., KAMAL, M., ELLIS, I., SPEIRS, V., GREEN, A. & BELL, S. 2010. Reduced MCPH1 expression in breast cancer and response to chemotherapy. *Breast Cancer Research,* 12**,** 1-1.

RICHARDSON, J., SHAABAN, A. M., KAMAL, M., ALISARY, R., WALKER, C., ELLIS, I. O., SPEIRS, V., GREEN, A. R. & BELL, S. M. 2011. Microcephalin is a new novel prognostic indicator in breast cancer associated with BRCA1 inactivation. *Breast Cancer Res Treat,* 127**,** 639-48.

RISS, T., O'BRIEN, M. & MORAVEC, R. 2003. Choosing the right cell-based assay for your research. *Cell notes,* 6**,** 6.

ROBERTS, E., JACKSON, A. P., CARRADICE, A. C., DEEBLE, V. J., MANNAN, J., RASHID, Y., JAFRI, H., MCHALE, D. P., MARKHAM, A. F. & LENCH, N. J. 1999. The second locus for autosomal recessive primary microcephaly (MCPH2) maps to chromosome 19q13. 1-13.2. *European Journal of Human Genetics,* 7**,** 815-820.

ROBERTSON, F. M., BONDY, M., YANG, W., YAMAUCHI, H., WIGGINS, S., KAMRUDIN, S., KRISHNAMURTHY, S., LE PETROSS, H., BIDAUT, L. & PLAYER, A. N. 2010. Inflammatory breast cancer: the disease, the biology, the treatment. *CA: a cancer journal for clinicians,* 60**,** 351-375.

RODI, D. J., JANES, R. W., SANGANEE, H. J., HOLTON, R. A., WALLACE, B. & MAKOWSKI, L. 1999. Screening of a library of phage-displayed peptides identifies human bcl-2 as a taxol-binding protein. *Journal of molecular biology,* 285**,** 197-203.

RODIER, F., CAMPISI, J. & BHAUMIK, D. 2007. Two faces of p53: aging and tumor suppression. *Nucleic acids research,* 35**,** 7475-7484.

ROHAN, T. E., LI, S.-Q., HARTWICK, R. & KANDEL, R. A. 2006. p53 Alterations and protein accumulation in benign breast tissue and breast cancer risk: a cohort study. *Cancer Epidemiology Biomarkers & Prevention,* 15**,** 1316-1323.

ROOT, D. E., HACOHEN, N., HAHN, W. C., LANDER, E. S. & SABATINI, D. M. 2006. Genome-scale loss-of-function screening with a lentiviral RNAi library. *Nature methods,* 3**,** 715-719.

ROUZIER, R., PEROU, C. M., SYMMANS, W. F., IBRAHIM, N., CRISTOFANILLI, M., ANDERSON, K., HESS, K. R., STEC, J., AYERS, M. & WAGNER, P. 2005. Breast cancer molecular subtypes respond differently to preoperative chemotherapy. *Clinical Cancer Research,* 11**,** 5678-5685.

RUCHAUD, S., CARMENA, M. & EARNSHAW, W. C. 2007. Chromosomal passengers: conducting cell division. *Nature reviews Molecular cell biology,* 8**,** 798-812.

RUSSO, J., CHAGPAR, A. B. & DIZON, D. S. 2013. Breast Development and Morphology.

RYBACZEK, D. & KOWALEWICZ-KULBAT, M. 2013. Relation of the Types of DNA Damage to Replication Stress and the Induction of Premature Chromosome Condensation.

SALISBURY, J. L., D'ASSORO, A. B. & LINGLE, W. L. 2004. Centrosome amplification and the origin of chromosomal instability in breast cancer. *Journal of mammary gland biology and neoplasia,* 9**,** 275-283.

SALVATORE, G., NAPPI, T. C., SALERNO, P., JIANG, Y., GARBI, C., UGOLINI, C., MICCOLI, P., BASOLO, F., CASTELLONE, M. D. & CIRAFICI, A. M. 2007. A cell proliferation and chromosomal instability signature in anaplastic thyroid carcinoma. *Cancer research,* 67**,** 10148-10158.

SANCAR, A., LINDSEY-BOLTZ, L. A., ÜNSAL-KAÇMAZ, K. & LINN, S. 2004. Molecular mechanisms of mammalian DNA repair and the DNA damage checkpoints. *Annual review of biochemistry,* 73**,** 39-85.

SANCHEZ, Y., WONG, C., THOMA, R. S., RICHMAN, R., WU, Z., PIWNICA-WORMS, H. & ELLEDGE, S. J. 1997. Conservation of the Chk1 checkpoint pathway in mammals: linkage of DNA damage to Cdk regulation through Cdc25. *Science,* 277**,** 1497-1501.

SÁNCHEZ-MUÑOZ, A., DUENAS-GARCIA, R., JAEN-MORAGO, A., CARRASCO, E., CHACON, I., GARCIA-TAPIADOR, A., ORTEGA-GRANADOS, A., MARTINEZ-ORTEGA, E., RIBELLES, N. & FERNANDEZ-NAVARRO, M. 2010. Is it possible to increase pCR in the neoadjuvant treatment with a dose-dense/sequential combination?: results from a phase II Trial combining epirubicin and cyclophosphamide followed by paclitaxel and gemcitabine±trastuzumab in stage II and III breast cancer patients. *American journal of clinical oncology,* 33**,** 432-437.

SÁNCHEZ-RIVERA, F. J. & JACKS, T. 2015. Applications of the CRISPR-Cas9 system in cancer biology. *Nature Reviews Cancer*.

SANTAGUIDA, S., TIGHE, A., D'ALISE, A. M., TAYLOR, S. S. & MUSACCHIO, A. 2010. Dissecting the role of MPS1 in chromosome biorientation and the spindle checkpoint through the small molecule inhibitor reversine. *The Journal of cell biology,* 190**,** 73-87.

SANTAMARÍA, D., BARRIÈRE, C., CERQUEIRA, A., HUNT, S., TARDY, C., NEWTON, K., CÁCERES, J. F., DUBUS, P., MALUMBRES, M. & BARBACID, M. 2007. Cdk1 is sufficient to drive the mammalian cell cycle. *Nature,* 448**,** 811-815.

SAUVÉ, D. M., ANDERSON, H. J., RAY, J. M., JAMES, W. M. & ROBERGE, M. 1999. Phosphorylation-induced rearrangement of the histone H3 NH2-

terminal domain during mitotic chromosome condensation. *The Journal of cell biology,* 145**,** 225-235.

SCHMIDT, E. E., PELZ, O., BUHLMANN, S., KERR, G., HORN, T. & BOUTROS, M. 2013. GenomeRNAi: a database for cell-based and in vivo RNAi phenotypes, 2013 update. *Nucleic acids research,* 41**,** D1021-D1026.

SCHMITT, E., BOUTROS, R., FROMENT, C., MONSARRAT, B., DUCOMMUN, B. & DOZIER, C. 2006. CHK1 phosphorylates CDC25B during the cell cycle in the absence of DNA damage. *Journal of cell science,* 119**,** 4269-4275.

SCHMITT, F. C., SOARES, R., CIRNES, L. & SERUCA, R. 1998. P53 in breast carcinomas: association between presence of mutation and immunohistochemical expression using a semiquantitative approach. *Pathology-Research and Practice,* 194**,** 815-819.

SCHOLNICK, S. B., HAUGHEY, B. H., SUNWOO, J. B., EL-MOFTY, S. K., BATY, J. D., PICCIRILLO, J. F. & ZEQUEIRA, M. R. 1996. Chromosome 8 allelic loss and the outcome of patients with squamous cell carcinoma of the supraglottic larynx. *Journal of the National Cancer Institute,* 88**,** 1676-1682.

SCHOR, S., JOHNSON, R. & WALDREN, C. 1975. Changes in the organization of chromosomes during the cell cycle: response to ultraviolet light. *Journal of cell science,* 17**,** 539-565.

SCULLY, R. & LIVINGSTON, D. M. 2000. In search of the tumour-suppressor functions of BRCA1 and BRCA2. *Nature,* 408**,** 429-432.

SERRANO, M., LIN, A. W., MCCURRACH, M. E., BEACH, D. & LOWE, S. W. 1997. Oncogenic ras provokes premature cell senescence associated with accumulation of p53 and p16 INK4a. *Cell,* 88**,** 593-602.

SEVILLA, A., SANTOS, C. R., BARCIA, R., VEGA, F. M. & LAZO, P. A. 2004a. c-Jun phosphorylation by the human vaccinia-related kinase 1 (VRK1) and its cooperation with the N-terminal kinase of c-Jun (JNK). *Oncogene,* 23**,** 8950-8958.

SEVILLA, A., SANTOS, C. R., VEGA, F. M. & LAZO, P. A. 2004b. Human vaccinia-related kinase 1 (VRK1) activates the ATF2 transcriptional activity by novel phosphorylation on Thr-73 and Ser-62 and cooperates with JNK. *Journal of Biological Chemistry,* 279**,** 27458-27465.

SEVIOUR, E. G. & LIN, S.-Y. 2010. The DNA damage response: Balancing the scale between cancer and ageing. *Aging (Albany NY),* 2**,** 900.

SHALEM, O., SANJANA, N. E. & ZHANG, F. 2015. High-throughput functional genomics using CRISPR-Cas9. *Nature Reviews Genetics.*

SHAO, Z., LI, F., SY, S. M., YAN, W., ZHANG, Z., GONG, D., WEN, B., HUEN, M. S., GONG, Q., WU, J. & SHI, Y. 2012. Specific recognition of phosphorylated tail of H2AX by the tandem BRCT domains of MCPH1 revealed by complex structure. *J Struct Biol,* 177**,** 459-68.

SHI, L., LI, M. & SU, B. 2012. MCPH1/BRIT1 represses transcription of the human telomerase reverse transcriptase gene. *Gene,* 495**,** 1-9.

SHIMIZU, N., NAKAJIMA, N. I., TSUNEMATSU, T., OGAWA, I., KAWAI, H., HIRAYAMA, R., FUJIMORI, A., YAMADA, A., OKAYASU, R., ISHIMARU, N., TAKATA, T. & KUDO, Y. 2013. Selective enhancing effect of early mitotic inhibitor 1 (Emi1) depletion on the sensitivity of doxorubicin or X-ray treatment in human cancer cells. *J Biol Chem,* 288**,** 17238-52.

SHINTOMI, K. & HIRANO, T. 2010. Sister chromatid resolution: a cohesin releasing network and beyond. *Chromosoma,* 119**,** 459-467.

SIGOILLOT, F. D., LYMAN, S., HUCKINS, J. F., ADAMSON, B., CHUNG, E., QUATTROCHI, B. & KING, R. W. 2012. A bioinformatics method identifies prominent off-targeted transcripts in RNAi screens. *Nat Methods,* 9**,** 363-6.

SILVA, J. M., MIZUNO, H., BRADY, A., LUCITO, R. & HANNON, G. J. 2004. RNA interference microarrays: high-throughput loss-of-function genetics in

mammalian cells. *Proceedings of the National Academy of Sciences of the United States of America,* 101**,** 6548-6552.

SINGH, M., CHAUDHRY, P., FABI, F. & ASSELIN, E. 2013. Cisplatin-induced caspase activation mediates PTEN cleavage in ovarian cancer cells: a potential mechanism of chemoresistance. *BMC cancer,* 13**,** 233.

SINGH, N., BASNET, H., WILTSHIRE, T. D., MOHAMMAD, D. H., THOMPSON, J. R., HEROUX, A., BOTUYAN, M. V., YAFFE, M. B., COUCH, F. J., ROSENFELD, M. G. & MER, G. 2012a. Dual recognition of phosphoserine and phosphotyrosine in histone variant H2A.X by DNA damage response protein MCPH1. *Proc Natl Acad Sci U S A,* 109**,** 14381-6.

SINGH, N., WILTSHIRE, T. D., THOMPSON, J. R., MER, G. & COUCH, F. J. 2012e. Molecular basis for the association of microcephalin (MCPH1) protein with the cell division cycle protein 27 (Cdc27) subunit of the anaphase-promoting complex. *J Biol Chem,* 287**,** 2854-62.

SIRVENT, J., SALVADO, M., SANTAFE, M., MARTINEZ, S., BRUNET, J., ALVARO, T. & PALACIOS, J. 1995. p53 in breast cancer. Its relation to histological grade, lymph-node status, hormone receptors, cell-proliferation fraction (ki-67) and c-erbB-2. Immunohistochemical study of 153 cases.

SITTAMPALAM, G. S., GAL-EDD, N., ARKIN, M., AULD, D., AUSTIN, C., BEJCEK, B., GLICKSMAN, M., INGLESE, J., LEMMON, V. & LI, Z. 2013. Cell Viability Assays.

SLEDZ, C. A., HOLKO, M., DE VEER, M. J., SILVERMAN, R. H. & WILLIAMS, B. R. 2003. Activation of the interferon system by short-interfering RNAs. *Nature cell biology,* 5**,** 834-839.

SLEE, R. B., GRIMES, B. R., BANSAL, R., GORE, J., BLACKBURN, C., BROWN, L., GASAWAY, R., JEONG, J., VICTORINO, J. & MARCH, K. L. 2014. Selective inhibition of pancreatic ductal adenocarcinoma cell growth by the mitotic MPS1 kinase inhibitor NMS-P715. *Molecular cancer therapeutics,* 13**,** 307-315.

SMITH, A. E., SMITH, R. & PAUCHA, E. 1979. Characterization of different tumor antigens present in cells transformed by simian virus 40. *Cell,* 18**,** 335-346.

SO, J., PASCULESCU, A., DAI, A. Y., WILLITON, K., JAMES, A., NGUYEN, V., CREIXELL, P., SCHOOF, E. M., SINCLAIR, J. & BARRIOS-RODILES, M. 2015. Integrative analysis of kinase networks in TRAIL-induced apoptosis provides a source of potential targets for combination therapy. *Science signaling,* 8.

SØRLIE, T., PEROU, C. M., TIBSHIRANI, R., AAS, T., GEISLER, S., JOHNSEN, H., HASTIE, T., EISEN, M. B., VAN DE RIJN, M. & JEFFREY, S. S. 2001. Gene expression patterns of breast carcinomas distinguish tumor subclasses with clinical implications. *Proceedings of the National Academy of Sciences,* 98**,** 10869-10874.

SØRLIE, T., TIBSHIRANI, R., PARKER, J., HASTIE, T., MARRON, J., NOBEL, A., DENG, S., JOHNSEN, H., PESICH, R. & GEISLER, S. 2003. Repeated observation of breast tumor subtypes in independent gene expression data sets. *Proceedings of the National Academy of Sciences,* 100**,** 8418-8423.

SOTILLO, R., HERNANDO, E., DÍAZ-RODRÍGUEZ, E., TERUYA-FELDSTEIN, J., CORDÓN-CARDO, C., LOWE, S. W. & BENEZRA, R. 2007. Mad2 overexpression promotes aneuploidy and tumorigenesis in mice. *Cancer cell,* 11**,** 9-23.

SOTIRIOU, C. & PUSZTAI, L. 2009. Gene-expression signatures in breast cancer. *New England Journal of Medicine,* 360**,** 790-800.

SOTIRIOU, C., WIRAPATI, P., LOI, S., HARRIS, A., FOX, S., SMEDS, J., NORDGREN, H., FARMER, P., PRAZ, V. & HAIBE-KAINS, B. 2006. Gene expression profiling in breast cancer: understanding the molecular basis of

histologic grade to improve prognosis. *Journal of the National Cancer Institute,* 98**,** 262-272.

SOUSSI, T. 2000. The p53 tumor suppressor gene: from molecular biology to clinical investigation. *Annals of the New York Academy of Sciences,* 910**,** 121-139.

SOUSSI, T., ASSELAIN, B., HAMROUN, D., KATO, S., ISHIOKA, C., CLAUSTRES, M. & BÉROUD, C. 2006. Meta-analysis of the p53 mutation database for mutant p53 biological activity reveals a methodologic bias in mutation detection. *Clinical Cancer Research,* 12**,** 62-69.

SOUSSI, T. & WIMAN, K. G. 2007. Shaping genetic alterations in human cancer: the p53 mutation paradigm. *Cancer cell,* 12**,** 303-312.

SREEKANTAIAH, C., BHARGAVA, M. K. & SHETTY, N. J. 1987. Premature chromosome condensation in human cervical carcinoma. *Cancer genetics and cytogenetics,* 24**,** 263-269.

STEC, E., LOCCO, L., SZYMANSKI, S., BARTZ, S. R., TONIATTI, C., NEEDHAM, R. H., PALMIERI, A., CARLETON, M., CLEARY, M. A. & JACKSON, A. L. 2012. A Multiplexed siRNA Screening Strategy to Identify Genes in the PARP Pathway. *Journal of biomolecular screening,* 17**,** 1316-1328.

STONE, A., SUTHERLAND, R. L. & MUSGROVE, E. A. 2012. Inhibitors of cell cycle kinases: recent advances and future prospects as cancer therapeutics. *Critical Reviews™ in Oncogenesis,* 17.

STORDAL, B., TIMMS, K., FARRELLY, A., GALLAGHER, D., BUSSCHOTS, S., RENAUD, M., THERY, J., WILLIAMS, D., POTTER, J., TRAN, T., KORPANTY, G., CREMONA, M., CAREY, M., LI, J., LI, Y., ASLAN, O., O'LEARY, J. J., MILLS, G. B. & HENNESSY, B. T. 2013. BRCA1/2 mutation analysis in 41 ovarian cell lines reveals only one functionally deleterious BRCA1 mutation. *Molecular Oncology,* 7**,** 567-579.

SUN, X.-X. & YU, Q. 2015. Intra-tumor heterogeneity of cancer cells and its implications for cancer treatment. *Acta Pharmacologica Sinica,* 36**,** 1219-1227.

SWANTON, C., MARANI, M., PARDO, O., WARNE, P. H., KELLY, G., SAHAI, E., ELUSTONDO, F., CHANG, J., TEMPLE, J. & AHMED, A. A. 2007. Regulators of mitotic arrest and ceramide metabolism are determinants of sensitivity to paclitaxel and other chemotherapeutic drugs. *Cancer cell,* 11**,** 498-512.

SWEDLOW, J. R. & HIRANO, T. 2003. The making of the mitotic chromosome: modern insights into classical questions. *Molecular cell,* 11**,** 557-569.

TAKIZAWA, C. G. & MORGAN, D. O. 2000. Control of mitosis by changes in the subcellular location of cyclin-B1–Cdk1 and Cdc25C. *Current opinion in cell biology,* 12**,** 658-665.

TANG, J., DI, J., CAO, H., BAI, J. & ZHENG, J. 2015. p53-mediated autophagic regulation: A prospective strategy for cancer therapy. *Cancer Letters,* 363**,** 101-107.

TANNOUS, B. A., KERAMI, M., VAN DER STOOP, P. M., KWIATKOWSKI, N., WANG, J., ZHOU, W., KESSLER, A. F., LEWANDROWSKI, G., HIDDINGH, L. & SOL, N. 2013. Effects of the selective MPS1 inhibitor MPS1-IN-3 on glioblastoma sensitivity to antimitotic drugs. *Journal of the National Cancer Institute***,** djt168.

TAO, W. & LEVINE, A. J. 1999. P19ARF stabilizes p53 by blocking nucleo-cytoplasmic shuttling of Mdm2. *Proceedings of the National Academy of Sciences,* 96**,** 6937-6941.

TARDIF, K. D., ROGERS, A., CASSIANO, J., ROTH, B. L., CIMBORA, D. M., MCKINNON, R., PETERSON, A., DOUCE, T. B., ROBINSON, R. & DORWEILER, I. 2011. Characterization of the cellular and antitumor effects

of MPI-0479605, a small-molecule inhibitor of the mitotic kinase Mps1. *Molecular cancer therapeutics,* 10**,** 2267-2275.

TERCERO, J. A., LABIB, K. & DIFFLEY, J. F. 2000. DNA synthesis at individual replication forks requires the essential initiation factor Cdc45p. *The EMBO Journal,* 19**,** 2082-2093.

THOMPSON, A. & MOULDER-THOMPSON, S. 2012. Neoadjuvant treatment of breast cancer. *Annals of Oncology,* 23**,** x231-x236.

TIBELIUS, A., MARHOLD, J., ZENTGRAF, H., HEILIG, C. E., NEITZEL, H., DUCOMMUN, B., RAUCH, A., HO, A. D., BARTEK, J. & KRAMER, A. 2009. Microcephalin and pericentrin regulate mitotic entry via centrosome-associated Chk1. *J Cell Biol,* 185**,** 1149-57.

TISCHKOWITZ, M., BRUNET, J.-S., BÉGIN, L. R., HUNTSMAN, D. G., CHEANG, M. C., AKSLEN, L. A., NIELSEN, T. O. & FOULKES, W. D. 2007. Use of immunohistochemical markers can refine prognosis in triple negative breast cancer. *BMC cancer,* 7**,** 134.

TOLEDO, F. & WAHL, G. M. 2006. Regulating the p53 pathway: in vitro hypotheses, in vivo veritas. *Nature Reviews Cancer,* 6**,** 909-923.

TORRE, L. A., BRAY, F., SIEGEL, R. L., FERLAY, J., LORTET TIEULENT, J. & JEMAL, A. 2015. Global cancer statistics, 2012. *CA: a cancer journal for clinicians,* 65**,** 87-108.

TRIMBORN, M., BELL, S. M., FELIX, C., RASHID, Y., JAFRI, H., GRIFFITHS, P. D., NEUMANN, L. M., KREBS, A., REIS, A. & SPERLING, K. 2004. Mutations in microcephalin cause aberrant regulation of chromosome condensation. *The American Journal of Human Genetics,* 75**,** 261-266.

TRIMBORN, M., GHANI, M., WALTHER, D. J., DOPATKA, M., DUTRANNOY, V., BUSCHE, A., MEYER, F., NOWAK, S., NOWAK, J., ZABEL, C., KLOSE, J., ESQUITINO, V., GARSHASBI, M., KUSS, A. W., ROPERS, H. H., MUELLER, S., POEHLMANN, C., GAVVOVIDIS, I., SCHINDLER, D., SPERLING, K. & NEITZEL, H. 2010. Establishment of a mouse model with misregulated chromosome condensation due to defective Mcph1 function. *PLoS One,* 5**,** e9242.

TRIMBORN, M., SCHINDLER, D., NEITZEL, H. & HIRANO, T. 2006. Misregulated chromosome condensation in MCPH1 primary microcephaly is mediated by condensin II Cell Cycle 2006 5. *N,* 3**,** 322-326.

TURNBULL, C. & RAHMAN, N. 2008. Genetic predisposition to breast cancer: past, present, and future. *Annu. Rev. Genomics Hum. Genet.,* 9**,** 321-345.

TURNER, N., REIS-FILHO, J., RUSSELL, A., SPRINGALL, R., RYDER, K., STEELE, D., SAVAGE, K., GILLETT, C., SCHMITT, F. & ASHWORTH, A. 2007. BRCA1 dysfunction in sporadic basal-like breast cancer. *Oncogene,* 26**,** 2126-2132.

TURNER, N., TUTT, A. & ASHWORTH, A. 2004. Hallmarks of'BRCAness' in sporadic cancers. *Nature Reviews Cancer,* 4**,** 814-819.

TURNER, N. C., LORD, C. J., IORNS, E., BROUGH, R., SWIFT, S., ELLIOTT, R., RAYTER, S., TUTT, A. N. & ASHWORTH, A. 2008. A synthetic lethal siRNA screen identifying genes mediating sensitivity to a PARP inhibitor. *The EMBO journal,* 27**,** 1368-1377.

TUSCHL, T., ZAMORE, P. D., LEHMANN, R., BARTEL, D. P. & SHARP, P. A. 1999. Targeted mRNA degradation by double-stranded RNA in vitro. *Genes & development,* 13**,** 3191-3197.

VAKIFAHMETOGLU, H., OLSSON, M. & ZHIVOTOVSKY, B. 2008. Death through a tragedy: mitotic catastrophe. *Cell Death & Differentiation,* 15**,** 1153-1162.

VALBUENA, A., CASTRO-OBREGON, S. & LAZO, P. A. 2011. Downregulation of VRK1 by p53 in response to DNA damage is mediated by the autophagic pathway. *PLoS One,* 6**,** e17320.

VALBUENA, A., LÓPEZ-SÁNCHEZ, I. & LAZO, P. A. 2008. Human VRK1 is an early response gene and its loss causes a block in cell cycle progression. *PLoS One,* 3**,** e1642-e1642.

VALBUENA, A., SUÁREZ-GAUTHIER, A., LÓPEZ-RIOS, F., LÓPEZ-ENCUENTRA, A., BLANCO, S., FERNÁNDEZ, P. L., SÁNCHEZ-CÉSPEDES, M. & LAZO, P. A. 2007. Alteration of the VRK1-p53 autoregulatory loop in human lung carcinomas. *Lung Cancer,* 58**,** 303-309.

VALBUENA, A., VEGA, F. M., BLANCO, S. & LAZO, P. A. 2006. p53 downregulates its activating vaccinia-related kinase 1, forming a new autoregulatory loop. *Molecular and cellular biology,* 26**,** 4782-4793.

VAN HOOSER, A., GOODRICH, D. W., ALLIS, C. D., BRINKLEY, B. & MANCINI, M. A. 1998. Histone H3 phosphorylation is required for the initiation, but not maintenance, of mammalian chromosome condensation. *Journal of Cell Science,* 111**,** 3497-3506.

VARNA, M., BOUSQUET, G., PLASSA, L.-F., BERTHEAU, P. & JANIN, A. 2011. TP53 status and response to treatment in breast cancers. *BioMed Research International,* 2011.

VASSILEV, L. T., TOVAR, C., CHEN, S., KNEZEVIC, D., ZHAO, X., SUN, H., HEIMBROOK, D. C. & CHEN, L. 2006. Selective small-molecule inhibitor reveals critical mitotic functions of human CDK1. *Proceedings of the National Academy of Sciences,* 103**,** 10660-10665.

VEGA, F. M., SEVILLA, A. & LAZO, P. A. 2004. p53 Stabilization and accumulation induced by human vaccinia-related kinase 1. *Molecular and cellular biology,* 24**,** 10366-10380.

VENKATESH, T., NAGASHRI, M. N., SWAMY, S. S., MOHIYUDDIN, S. M., GOPINATH, K. S. & KUMAR, A. 2013. Primary microcephaly gene MCPH1 shows signatures of tumor suppressors and is regulated by miR-27a in oral squamous cell carcinoma. *PLoS One,* 8**,** e54643.

VENKATESH, T. & SURESH, P. S. 2014. Emerging roles of MCPH1: expedition from primary microcephaly to cancer. *Eur J Cell Biol,* 93**,** 98-105.

VENKITARAMAN, A. R. 2002. Cancer susceptibility and the functions of BRCA1 and BRCA2. *Cell,* 108**,** 171-182.

VERSCHUREN, E. W., BAN, K. H., MASEK, M. A., LEHMAN, N. L. & JACKSON, P. K. 2007. Loss of Emi1-dependent anaphase-promoting complex/cyclosome inhibition deregulates E2F target expression and elicits DNA damage-induced senescence. *Molecular and cellular biology,* 27**,** 7955-7965.

VIALE, G. 2012. The current state of breast cancer classification. *Ann Oncol,* 23 Suppl 10**,** x207-10.

VIKHANSKAYA, F., ERBA, E., D'LNCALCI, M. & BROGGINI, M. 1994. Introduction of wild-type p53 in a human ovarian cancer cell line not expressing endogenous p53. *Nucleic acids research,* 22**,** 1012-1017.

VOGELSTEIN, B. & KINZLER, K. W. 2004. Cancer genes and the pathways they control. *Nature medicine,* 10**,** 789-799.

VOGELSTEIN, B., LANE, D. & LEVINE, A. J. 2000. Surfing the p53 network. *Nature,* 408**,** 307-310.

VOJTĚŠEK, B., BARTEK, J., MIDGLEY, C. & LANE, D. 1992. An immunochemical analysis of the human nuclear phosphoprotein p53: new monoclonal antibodies and epitope mapping using recombinant p53. *Journal of immunological methods,* 151**,** 237-244.

VON SCHUBERT, C., CUBIZOLLES, F., BRACHER, JASMINE M., SLIEDRECHT, T., KOPS, GEERT J. P. L. & NIGG, ERICH A. 2015. Plk1 and Mps1 Cooperatively Regulate the Spindle Assembly Checkpoint in Human Cells. *Cell Reports,* 12**,** 66-78.

WAHL, G. M. & CARR, A. M. 2001. The evolution of diverse biological responses to DNA damage: insights from yeast and p53. *Nature cell biology,* 3**,** E277-E286.

WANG, N., LU, H., CHEN, W., GAN, M., CAO, X., ZHANG, J. & CHEN, L. 2014a. Primary microcephaly gene MCPH1 shows a novel molecular biomarker of human renal carcinoma and is regulated by miR-27a. *International journal of clinical and experimental pathology,* 7**,** 4895.

WANG, S., YU, H. & WICKLIFFE, J. K. 2011. Limitation of the MTT and XTT assays for measuring cell viability due to superoxide formation induced by nano-scale TiO2. *Toxicol In Vitro,* 25**,** 2147-51.

WANG, Y., XIAO, J., SUZEK, T. O., ZHANG, J., WANG, J., ZHOU, Z., HAN, L., KARAPETYAN, K., DRACHEVA, S. & SHOEMAKER, B. A. 2012. PubChem's BioAssay database. *Nucleic acids research,* 40**,** D400-D412.

WANG, Z., LIU, P., INUZUKA, H. & WEI, W. 2014e. Roles of F-box proteins in cancer. *Nat Rev Cancer,* 14**,** 233-47.

WASHBURN, J. G., WOJNO, K. J., DEY, J., POWELL, I. J. & MACOSKA, J. A. 2000. 8pter–p23 deletion is associated with racial differences in prostate cancer outcome. *Clinical cancer research,* 6**,** 4647-4652.

WEAVER, B. A. 2014. How Taxol/paclitaxel kills cancer cells. *Molecular biology of the cell,* 25**,** 2677-2681.

WEI, J.-H., CHOU, Y.-F., OU, Y.-H., YEH, Y.-H., TYAN, S.-W., SUN, T.-P., SHEN, C.-Y. & SHIEH, S.-Y. 2005. TTK/hMps1 participates in the regulation of DNA damage checkpoint response by phosphorylating CHK2 on threonine 68. *Journal of Biological Chemistry,* 280**,** 7748-7757.

WEI, Y., YU, L., BOWEN, J., GOROVSKY, M. A. & ALLIS, C. D. 1999. Phosphorylation of histone H3 is required for proper chromosome condensation and segregation. *Cell,* 97**,** 99-109.

WEIDERPASS, E., MEO, M. & VAINIO, H. 2011. Risk factors for breast cancer, including occupational exposures. *Safety and health at work,* 2**,** 1-8.

WEIGELT, B., BAEHNER, F. L. & REIS-FILHO, J. S. 2010. The contribution of gene expression profiling to breast cancer classification, prognostication and prediction: a retrospective of the last decade. *The Journal of pathology,* 220**,** 263-280.

WEIGELT, B. & REIS-FILHO, J. S. 2009. Histological and molecular types of breast cancer: is there a unifying taxonomy? *Nat Rev Clin Oncol,* 6**,** 718-30.

WEISS, W. A., TAYLOR, S. S. & SHOKAT, K. M. 2007. Recognizing and exploiting differences between RNAi and small-molecule inhibitors. *Nature chemical biology,* 3**,** 739-744.

WELCSH, P. L., OWENS, K. N. & KING, M.-C. 2000. Insights into the functions of BRCA1 and BRCA2. *Trends in Genetics,* 16**,** 69-74.

WENGNER, A. M., SIEMEISTER, G., KOPPITZ, M., SCHULZE, V., KOSEMUND, D., KLAR, U., STOECKIGT, D., NEUHAUS, R., LIENAU, P. & BADER, B. 2015. Novel Mps1 kinase inhibitors with potent anti-tumor activity. *Cancer Research,* 75**,** 3090-3090.

WILLIAMS, D. M., SCOTT, C. D. & BECK, T. M. 1976. Premature chromosome condensation in human leukemia. *Blood,* 47**,** 687-693.

WOOD, J. L., LIANG, Y., LI, K. & CHEN, J. 2008. Microcephalin/MCPH1 associates with the Condensin II complex to function in homologous recombination repair. *J Biol Chem,* 283**,** 29586-92.

WOOD, J. L., SINGH, N., MER, G. & CHEN, J. 2007. MCPH1 functions in an H2AX-dependent but MDC1-independent pathway in response to DNA damage. *Journal of Biological Chemistry,* 282**,** 35416-35423.

WOOSTER, R., BIGNELL, G., LANCASTER, J., SWIFT, S., SEAL, S., MANGION, J., COLLINS, N., GREGORY, S., GUMBS, C. & MICKLEM, G. 1995.

Identification of the breast cancer susceptibility gene BRCA2. *Nature,* 378**,** 789-792.

WOOSTER, R., NEUHAUSEN, S. L., MANGION, J., QUIRK, Y., FORD, D., COLLINS, N., NGUYEN, K., SEAL, S., TRAN, T. & AVERILL, D. 1994. Localization of a breast cancer susceptibility gene, BRCA2, to chromosome 13q12-13. *Science,* 265**,** 2088-2090.

WRIGHT, K., WILSON, P., KERR, J., DO, K., HURST, T., KHOO, S., WARD, B. & CHENEVIX-TRENCH, G. 1998. Frequent loss of heterozygosity and three critical regions on the short arm of chromosome 8 in ovarian adenocarcinomas. *Oncogene,* 17**,** 1185-1188.

WU, C. L., ROZ, L., SLOAN, P., READ, A. P., HOLLAND, S., PORTER, S., SCULLY, C., SPEIGHT, P. M. & THAKKER, N. 1997. Deletion mapping defines three discrete areas of allelic imbalance on chromosome arm 8p in oral and oropharyngeal squamous cell carcinomas. *Genes, Chromosomes and Cancer,* 20**,** 347-353.

WU, X., BAYLE, J. H., OLSON, D. & LEVINE, A. J. 1993. The p53-mdm-2 autoregulatory feedback loop. *Genes & development,* 7**,** 1126-1132.

WU, X., MONDAL, G., WANG, X., WU, J., YANG, L., PANKRATZ, V. S., ROWLEY, M. & COUCH, F. J. 2009. Microcephalin regulates BRCA2 and Rad51-associated DNA double-strand break repair. *Cancer Res,* 69**,** 5531-6.

XIE, L., KASSNER, M., MUNOZ, R. M., QUE, Q. Q., KIEFER, J., ZHAO, Y., MOUSSES, S., YIN, H. H., VON HOFF, D. D. & HAN, H. 2012. Kinome-wide siRNA screening identifies molecular targets mediating the sensitivity of pancreatic cancer cells to Aurora kinase inhibitors. *Biochemical pharmacology,* 83**,** 452-461.

XU, B., KIM, S.-T. & KASTAN, M. B. 2001. Involvement of Brca1 in S-phase and G2-phase checkpoints after ionizing irradiation. *Molecular and cellular biology,* 21**,** 3445-3450.

XU, X., LEE, J. & STERN, D. F. 2004. Microcephalin is a DNA damage response protein involved in regulation of CHK1 and BRCA1. *J Biol Chem,* 279**,** 34091-4.

YAMASHITA, D., SHINTOMI, K., ONO, T., GAVVOVIDIS, I., SCHINDLER, D., NEITZEL, H., TRIMBORN, M. & HIRANO, T. 2011. MCPH1 regulates chromosome condensation and shaping as a composite modulator of condensin II. *J Cell Biol,* 194**,** 841-54.

YANG, P., DU, C., KWAN, M., LIANG, S. & ZHANG, G. 2013. The impact of p53 in predicting clinical outcome of breast cancer patients with visceral metastasis. *Scientific reports,* 3.

YANG, S. Z., LIN, F. T. & LIN, W. C. 2008. MCPH1/BRIT1 cooperates with E2F1 in the activation of checkpoint, DNA repair and apoptosis. *EMBO Rep,* 9**,** 907-15.

YANG, Y. J., BALTUS, A. E., MATHEW, R. S., MURPHY, E. A., EVRONY, G. D., GONZALEZ, D. M., WANG, E. P., MARSHALL-WALKER, C. A., BARRY, B. J. & MURN, J. 2012. Microcephaly gene links trithorax and REST/NRSF to control neural stem cell proliferation and differentiation. *Cell,* 151**,** 1097-1112.

YILMAZEL, B., HU, Y., SIGOILLOT, F., SMITH, J. A., SHAMU, C. E., PERRIMON, N. & MOHR, S. E. 2014. Online GESS: prediction of miRNA-like off-target effects in large-scale RNAi screen data by seed region analysis. *BMC bioinformatics,* 15**,** 192.

YIM, H. & ERIKSON, R. L. 2009. Polo-like kinase 1 depletion induces DNA damage in early S prior to caspase activation. *Mol Cell Biol,* 29**,** 2609-21.

YUN, H., SHI, R., YANG, Q., ZHANG, X., WANG, Y., ZHOU, X. & MU, K. 2014. Over expression of hRad9 protein correlates with reduced chemosensitivity

in breast cancer with administration of neoadjuvant chemotherapy. *Scientific reports,* 4.

ZHANG, B., WANG, E., DAI, H., HU, R., LIANG, Y., LI, K., WANG, G., PENG, G. & LIN, S. Y. 2013a. BRIT1 regulates p53 stability and functions as a tumor suppressor in breast cancer. *Carcinogenesis,* 34**,** 2271-80.

ZHANG, B., WANG, E., DAI, H., SHEN, J., HSIEH, H.-J., LU, X. & PENG, G. 2014. Phosphorylation of the BRCA1 C terminus (BRCT) repeat inhibitor of hTERT (BRIT1) protein coordinates TopBP1 protein recruitment and amplifies ataxia telangiectasia-mutated and Rad3-related (ATR) Signaling. *Journal of Biological Chemistry,* 289**,** 34284-34295.

ZHANG, J., WU, X.-B., FAN, J.-J., MAI, L., CAI, W., LI, D., YUAN, C.-F., BU, Y.-Q. & SONG, F.-Z. 2013i. MCPH1 Protein Expression in Normal and Neoplastic Lung Tissues. *Asian Pacific Journal of Cancer Prevention,* 14**,** 7295-7300.

ZHANG, J. H. 1999. A Simple Statistical Parameter for Use in Evaluation and Validation of High Throughput Screening Assays. *Journal of Biomolecular Screening,* 4**,** 67-73.

ZHANG, W., PENG, G., LIN, S.-Y. & ZHANG, P. 2011. DNA damage response is suppressed by the high cyclin-dependent kinase 1 activity in mitotic mammalian cells. *Journal of Biological Chemistry,* 286**,** 35899-35905.

ZHANG, X. D. 2007. A pair of new statistical parameters for quality control in RNA interference high-throughput screening assays. *Genomics,* 89**,** 552-561.

ZHANG, X. D. 2011. Illustration of SSMD, z score, SSMD*, z* score, and t statistic for hit selection in RNAi high-throughput screens. *Journal of biomolecular screening,* 16**,** 775-785.

ZHAO, Y., TANG, Q., NI, R., HUANG, X., WANG, Y., LU, C., SHEN, A., WANG, Y., LI, C. & YUAN, Q. 2013. Early mitotic inhibitor-1, an anaphase-promoting complex/cyclosome inhibitor, can control tumor cell proliferation in hepatocellular carcinoma: correlation with Skp2 stability and degradation of p27 Kip1. *Human pathology,* 44**,** 365-373.

ZHONG, X., PFEIFER, G. P. & XU, X. 2006. Microcephalin encodes a centrosomal protein. *Cell Cycle,* 5**,** 457-458.

ZHOU, B.-B. S. & ELLEDGE, S. J. 2000. The DNA damage response: putting checkpoints in perspective. *Nature,* 408**,** 433-439.

mouse model. *DNA Repair (Amst),* 12**,** 645-55.

ZHU, G.-N., ZUO, L., ZHOU, Q., ZHANG, S.-M., ZHU, H.-Q., GUI, S.-Y. & WANG, Y. 2004. Loss of heterozygosity on chromosome 10q22-10q23 and 22q11. 2-22q12. 1 and p53 gene in primary hepatocellular carcinoma. *World Journal of Gastroenterology,* 10**,** 1975-1978.

Appendix

1. List of reagents' suppliers (email and addresses)

Supplier	Address
Abcam	330 Cambridge Science Park, Cambridge, CB4 0FL. www.abcam.com
Alfa Aesar	Shore Road, Port Of Heysham Industrial Park, LA3 2XY Heysham. www.alfa.com
ATCC	Supplied by LGC Promochem. www.atcc.org
Applied Biosystem by life Technologies	Supplied by Invitrogen Life Technologies
Beckman Coulter	Oakley Court, Kingsmead Business Park, London Road, High Wycombe, Buckinghamshire, HP11 1JU. www.beckmancoulter.co.uk
Bio-Rad Laboratories	Bio-Rad House, Maylands Avenue, Hemel Hempstead, Herts HP2 7TD. www.bio-rad.com
BIORON GmbH	Rheinhorststraße 18, D-67071 Ludwigshafe, German. www.bioron.net
Biotium	3159 Corporate Place, Hayward, CA 94545 U.S.A. www.biotium.com
DAKO	Produktionsvej 42, 2600 Glostrup, Denmark. www.dako.com
Dharmacon	Supplied by GE Healthcare Life Sciences. dharmacon.gelifesciences.com
Dualsystems Biotech AG	Grabenstrasse 11A, 8952 Schlieren, Switzerland. www.dualsystems.com
G-Bioscience	92 Weldon Parkway, Maryland Heights, MO 63043-3202, U.S.A. www.gbiosciences.com
GE Healthcare Life Sciences	Amersham Place, Little Chalfont, Buckinghamshire, HP7 9NA. www.gelifesciences.com
Invitrogen	Supplied by Life Technologies Ltd, 3 Fountain Drive, Inchinnan Business Park, Paisley, PA4 9RF. www.lifetech.com
Leica	Leica Microsystems (UK) Ltd, Davy Avenue, Knowlhill, Milton Keynes, Buckinghamshire, MK5 8LB. www.leica-microsystems.com
Mayne Pharma	1538 Main N Rd, Salisbury South SA 5106, Australia. www.maynepharma.com
New England Biolabs	75-77 Knowl Piece, Wilbury Way, Hitchin, Hertfordshire, SG4 0TY. www.neb.com
Novocastra	Supplied by Leica Biosystems
Novex	Supplied by Life Technologies
Novus Biologicals	19 Barton Lane, Abingdon Science Park, Abingdon, OX14 3NB. www.novusbio.com
PerkinElmer	940 Winter St, Waltham, MA 02451, USA. www.perkinelmer.co.uk
Qiagen	27220 Turnberry Lane. Suite 200. Valencia, CA 91355. www.perkinelmer.co.uk
Roche Applied Biosystem	Supplied by Life Technologies
Roche Diagnostics GmbH	Sandhofer Strasse, 116 68305 Mannheim Germany. www.roche.com
Sigma-Aldrich	Fancy Road, Poole, Dorset BH17 7NH. www.sigma-aldrich.com
Thermo Fisher Scientific	Bishop Meadow Road, Loughborough, Leicestershire, LE11 5RG. www.fisher.co.uk
Vector Laboratories	Bakewell Rd, Peterborough PE2 6XS. www.vectorlabs.co.uk

2. Preparation of drug stock solutions used in SMS as controls

All chemotherapy drugs controls were added at the same time the CC were dispensed on to the cells and incubated for 24hr and 48hr.

2.1 Doxorubicin 0.4µg/ml

Doxorubicin stock solution at 0.4mg/ml was first prepared by mixing 4µl of Doxorubicin (stock 10mg/ml / Sigma) with 96µl RPMI1640 medium without P/S. This solution was diluted to final concentration of 0.4µg/ml (1:1000) by mixing 5ml RPMI1640 medium (no P/S) with 5µl of 0.4mg/ml Doxorubicin mixture. Thus, the suspension media was removed from the desired wells of the 96 well plates and 100µl of 0.4µg/ml Doxorubicin was added.

2.2 Nocodozole 1µM

A 20µM Nocodozole solution was first prepared by mixing 3.01µl of Nocodozole (stock 6.64mM), 6.99µl of 100% DMSO with 990µl RPMI1640 medium. Then, this mixture was diluted to a final concentration of 1µM with a final amount of 1% DMSO by mixing 20µL of 20µM dilution of Nocodozole with 380µl of medium contains 1% DMSO then 20µl of 1µM Nocodozole was added to the desired wells.

3. siRNA

3.1 siRNA controls

Oligo Name	Sense strand sequence
MCPH1/BRIT1 (Dharmacon)	CUCUCUGUGUGAAGCACCA
Stealth™ RNAi negative control Duplex (Invitrogen)	Control for transfection efficiency of MCPH1/BRIT1 siRNA in SMS experiments; Cat. No. 12935-300
ON-TARGET plus single NT-siRNA (Dharmacon)	UGGUUUACAUGUCGACUAA
PLK1 pool (Dharmacon)	GCACAUACCGCCUGAGUCU, CCACCAAGGUUUUCGAUUG, GCUCUUCAAUGACUCAACA, UCUCAAGGCCUCCUAAUAG

3.2 ON-TARGT plus four individual siRNAs (Dharmacon)

Oligo Name	Sense strand sequence
CDK1/CDC2 siRNA 1	GGUUAUAUCUCAUCUUUGA
CDK1/CDC2 siRNA 2	UCGGGAAAUUUCUCUAUUA
CDK1/CDC2 siRNA 3	GUAUAAGGGUAGACACAAA
CDK1/CDC2 siRNA 4	CAAACGAAUUUCUGGCAAA
TTK/MPS1 siRNA 1	GAUAAGAUCAUCCGACUUU
TTK/MPS1 siRNA 2	GCAAUACCUUGGAUGAUUA
TTK/MPS1 siRNA 3	CCAGUUAACCUUCUAAAUA
TTK/MPS1 siRNA 4	GAUAGUUGAUGGAAUGCUA
CAMK2N1 siRNA 1	GCAAGCGGGUUGUUAUUGA
CAMK2N1 siRNA 2	GAUUGAUGACGUGCUGAAA
CAMK2N1 siRNA 3	CGACAAGGCACCUCCUGGU
CAMK2N1 siRNA 4	CAAAGACAAUGAGUUAAGG
WEE1 siRNA 1	AAUAGAACAUCUCGACUUA
WEE1 siRNA 2	AAUAUGAAGUCCCGGUAUA
WEE1 siRNA 3	GAUCAUAUGCUUAUACAGA
WEE1 siRNA 4	CGACAGACUCCUCAAGUGA
STK39 siRNA 1	GGUGGAUGGUCACGAUGUA
STK39 siRNA 2	GAGCAGCGCCUUAUCACAA
STK39 siRNA 3	GGGUGAGGAUGGUUCAGUA
STK39 siRNA 4	AAACAGGGGUAGAGGAUAA
VRK1 siRNA 1	GCAGUUGGAGAGAUAAUAA
VRK1 siRNA 2	AUACUUGGUUAUUGCAUGA
VRK1 siRNA 3	GGCUUUGGCUGUAUAUAUC
VRK1 siRNA 4	AGGUGUACUUGGUAGAUUA
PLK1 siRNA 1	GCACAUACCGCCUGAGUCU
PLK1 siRNA 2	CCACCAAGGUUUUCGAUUG
PLK1 siRNA 3	GCUCUUCAAUGACUCAACA
PLK1 siRNA 4	UCUCAAGGCCUCCUAAUAG
FBXO5/EMI1 siRNA 1	CAACAGACACUUAAUAGUA
FBXO5/EMI1 siRNA 2	CGAAGUGUCUCUGUAAUUA
FBXO5/EMI1 siRNA 3	UGUAUUGGGUCACCGAUUG
FBXO5/EMI1 siRNA 4	GAAUUUCGGUGACAGUCUA

4. An example of the 96 well plate layout (View Plates; PerkinElmer) used for preparing PCC inducer hPK or Ubq siRNA screens

	1	2	3	4	5	6	7	8	9	10	11	12
A	RNAiMAX	siRNA	siRNA	siRNA	siRNA	siRNA	siRNA	siRNA	siRNA	siRNA	siRNA	RNAiMAX
B	NT-siRNA	siRNA	siRNA	siRNA	siRNA	siRNA	siRNA	siRNA	siRNA	siRNA	siRNA	NT-siRNA
C	NT-siRNA	siRNA	siRNA	siRNA	siRNA	siRNA	siRNA	siRNA	siRNA	siRNA	siRNA	NT-siRNA
D	*EB1*	siRNA	siRNA	siRNA	siRNA	siRNA	siRNA	siRNA	siRNA	siRNA	siRNA	*EB1*
E	*MCPH1*	siRNA	siRNA	siRNA	siRNA	siRNA	siRNA	siRNA	siRNA	siRNA	siRNA	*MCPH1*
F	*PLK1*	siRNA	siRNA	siRNA	siRNA	siRNA	siRNA	siRNA	siRNA	siRNA	siRNA	*PLK1*
G	1x siRNA buffer +Nocodazole	siRNA	siRNA	siRNA	siRNA	siRNA	siRNA	siRNA	siRNA	siRNA	siRNA	1x siRNA buffer +Nocodazole
H	1x siRNA buffer +Taxol	siRNA	siRNA	siRNA	siRNA	siRNA	siRNA	siRNA	siRNA	siRNA	siRNA	1x siRNA buffer +Taxol

Controls for PCC inducer screen

Columns 1 and 12

Row	siRNA	Details
A	**1x buffer**	5x siRNA buffer Dharmacon Cat.No. B-002000-UB-100 RNase free water Dharmacon Cat.No. B-003000-WB-100
B	**NT-siRNA**	siGENOME control pool Non-Targeting 1 Dharmacon - Cat.No. D-001206-13-05
C	**NT-siRNA**	
D	*EB1*	siGENOME SMARTpool Human MAPRE1 Dharmacon - Cat.No. M-006824-00
E	*MCPH1*	'Custom siRNA' – see above
F	*PLK1*	siGENOME SMARTpool Human PLK1 Dharmacon - Cat.No. M-003290-01
G	**1x buffer**	As stated in row A
H	**1x buffer**	

All the wells on the plate are treated with RNAiMAX.

Wells G1 and G12 were treated with Nocodazole and wells H1 and H12 were treated with Paclitaxel/Taxol. Drugs were added to the cells and incubated at 37°C for 1hr only before cell fixation and IF staining.

5. An example of the 96 well plate layout (View Plates; PerkinElmer) used for preparing PCC modifier hPK siRNA screens

	1	2	3	4	5	6	7	8	9	10	11	12
A	NT-siRNA	siRNA	siRNA	siRNA	siRNA	siRNA	siRNA	siRNA	siRNA	siRNA	siRNA	NT-siRNA
B	NT-siRNA	siRNA	siRNA	siRNA	siRNA	siRNA	siRNA	siRNA	siRNA	siRNA	siRNA	NT-siRNA
C	*CAPG2*	siRNA	siRNA	siRNA	siRNA	siRNA	siRNA	siRNA	siRNA	siRNA	siRNA	*CAPG2*
D	*CAPG2*	siRNA	siRNA	siRNA	siRNA	siRNA	siRNA	siRNA	siRNA	siRNA	siRNA	*CAPG2*
E	*CAPH2*	siRNA	siRNA	siRNA	siRNA	siRNA	siRNA	siRNA	siRNA	siRNA	siRNA	*CAPH2*
F	*CAPH2*	siRNA	siRNA	siRNA	siRNA	siRNA	siRNA	siRNA	siRNA	siRNA	siRNA	*CAPH2*
G	*Incenp*	siRNA	siRNA	siRNA	siRNA	siRNA	siRNA	siRNA	siRNA	siRNA	siRNA	*Incenp*
H	*PLK1*	siRNA	siRNA	siRNA	siRNA	siRNA	siRNA	siRNA	siRNA	siRNA	siRNA	*PLK1*

Controls for PCC modifier screen

Columns 1 and 12

Row	siRNA	Details
A	**NT-siRNA**	siGENOME control pool Non-Targeting #1
B	**NT-siRNA**	Dharmacon - Cat.No. D-001206-13-05
C	*CAPG2*	siGENOME SMARTpool Human NGAP G2 Dharmacon - Cat.No. M-018283-01
D	*CAPH2*	siGENOME SMARTpool Human NGAP H2 Dharmacon - Cat.No. M-016186-01
E	*Incenp*	siGENOME SMARTpool Human INCENP Dharmacon - Cat.No. M-006823-01
F	*KIF11*	siGENOME SMARTpool Human KIF11 Dharmacon - Cat.No. M-003317 -01
G	*PLK1*	siGENOME SMARTpool Human PLK1 Dharmacon - Cat.No. M-003290-01
H	**1x buffer**	Dharmacon 5x siRNA buffer Cat.No. B-002000-UB-100 RNase free water Cat.No. B-003000-WB-100

After 24hr incubation, all the wells on the plates are treated with RNAiMax and *MCPH1*/*BRIT1* siRNA.

6. Preparation of chemical solutions used in this PhD thesis

All chemical solutions were made using dH$_2$O.

6.1 Preparation of RIPA buffer

Buffer	Volume
1% Nonidet-P-40	1 ml
0.5% Sodium Deoxycholate	500mg
0.1% SDS	1ml of 10%
1x PBS	Up to 100ml

6.2 Preparation of bovine serum albumin (BSA) standard dilution series

The serial dilution were prepared from 2mg/ml BSA and 10% RIPA buffer solutions that were mentioned in Chapter 2; Section 1.

Dilution series	BSA (2mg/ml)	10% RIPA buffer
0.1µg/µl	5µl	95µl
0.25µg/µl	12.5µl	87.5µl
0.5µg/µl	25µl	75µl
0.8µg/µl	40µl	60µl
1µg/µl	50µl	50µl
1.5µg/µl	75µl	25µl
2µg/µl	100µl	-

6.3 Preparation of Antigen retrieval 10mM citric acid buffer (pH 6.0)

About 5 big sizes of sodium hydroxide pellets were mixed with 800ml dH$_2$O in a 1L media bottle (containing magnetic stir bar) and placed on magnetic stirrer plate allowing the pellets to be dissolved. Next, 2.1g citric acid was added to the solution, the mixture solution was allowed to be well dissolved. Then, pH of the solution was first checked using calibrated pH probe and 10% w/v sodium hydroxide (NaOH) was used to adjust the pH of the solution to 6. The final volume of the solution was made up to 1L with dH$_2$O.

7. Ethical approval for IHC staining of breast cancer tissues provided by Dr. Abeer Shaaban

Tissue Transfer Agreement
Between the SUPPLIER, RECIPIENT and SPONSOR (if applicable) as described below.
Agreement for the transfer of human tissues / organs for non-commercial, non-therapeutic research, when the Human Tissue Act, 2004 does not apply (eg NRES project specific approval has been obtained).

RECIPIENT:
University of Leeds

RECIPIENT'S LOCAL INVESTIGATOR:
Dr Sandra Bell

SUPPLIER:
Department of Histopathology, SJUH, Leeds

SUPPLIERS LOCAL INVESTIGATOR:
Dr Abeer Shaaban

SPONSOR (if applicable):

PROTOCOL [ref]:

ETHICAL OPINION ref:
06/Q1206/180 and amendment 4

STUDY:
MCPH1 expression in breast carcinoma treated with neoadjuvant chemotherapy

MATERIALS:
MCPH1 expression in breast carcinoma treated with neoadjuvant chemotherapy

FORM OF MATERIALS SUPPLY:
Sections on slides

PURPOSES:
Immunohistochemical staining

RECIPIENT'S PREMISES:
Microcephaly and Cancer Group, Leeds Institute of Molecular Medicine, Wellcome Trust Brenner Building, St James's University Hospital, Leeds, LS9 7TF
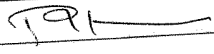
1. The relevant PROTOCOL and ETHICAL OPINION is attached to this Agreement. If there is any proposed change to the PROTOCOL or ETHICAL OPINION that would have an impact upon the use, storage or otherwise of the MATERIALS, the RECIPIENT'S LOCAL INVESTIGATOR must obtain the written consent of the SUPPLIER'S LOCAL INVESTIGATOR and the SPONSOR. A change in the type of NRES approval from project specific to research tissue bank status will require a new Tissue Transfer Agreement. All agreed changes to the PROTOCOL or ETHICAL OPINION are to be attached by both parties to their copies of this Agreement.

2. The RECIPIENT agrees to only use the MATERIALS for the PURPOSES and in accordance with the PROTOCOL and ETHICAL OPINION. The MATERIALS are only to be used and stored on the RECIPIENT'S PREMISES.

3. The SUPPLIER confirms the necessary informed consents of donors/donor's representatives have been given or ETHICAL OPINION has provided an exemption to the requirement to obtain consent.

Continued Appendix 7.

4. The SUPPLIER will deliver the MATERIALS to the RECIPIENT on the agreed delivery date(s) in the FORM OF MATERIALS SUPPLY prescribed above. A copy of the "Tissue Sample Form" to be supplied by the SUPPLIER will be forwarded with the MATERIALS.

5. The RECIPIENT agrees to ensure that all persons involved in access or use of the MATERIALS shall be made aware of, and bound by, the terms of this Agreement.

6. The RECIPIENT agrees not to transfer or distribute any part of the MATERIALS or any extracts, replications, summaries or derivatives thereof to any third party without the prior approval of the SUPPLIER, the SPONSOR and any relevant ethics committee. The RECIPIENT will provide assurance that any such transfer or distribution is within the scope of the relevant consents. Any such transfer or distribution will be subject to a separate material transfer agreement.

7. MATERIALS cannot be used for any purpose that is commercial or therapeutic. Sponsored academic or clinical research is not for these purposes deemed to be commercial.

8. The MATERIALS are supplied without warranty as to its properties, merchantable quality or fitness for any particular purposes and without any other warranty whatsoever, expressed or implied.

9. The RECIPIENT confirms that the LOCAL INVESTIGATOR is suitably qualified and will be responsible for the proper and safe handling, storage, use and disposal of the MATERIALS.

10. As soon as the STUDY has been completed by the RECIPIENT, the RECIPIENT's LOCAL INVESTIGATOR shall inform the SUPPLIER. Used MATERIALS may be retained under the terms of this Agreement only for audit and verification purposes relating to the STUDY. Unused MATERIALS will be returned to the SUPPLIER.

11. On or before expiry of NRES project specific approval (if applicable), unused MATERIALS taken from a diagnostic archive will be returned to the archive. Any other unused MATERIALS and products of the STUDY that contain human cells will be returned to the SUPPLIER and stored in premises licenced by the Human Tissue Authority. The SUPPLIER's LOCAL INVESTIGATOR agrees to inform the DESIGNATED INDIVIDUAL for research should this situation arise, and to follow all relevant policies and standard operating procedures on the instruction of the Designated Individual.

12. Subject to the SUPPLIER meeting its commitments under this Agreement, the RECIPIENT agrees to hold harmless the SUPPLIER from any and all claims, suits and liabilities arising from any use by the RECIPIENT of the MATERIALS.

13. This Agreement may be terminated by a party upon written notice if the other party shall be in material breach of its commitments and not remedied such commitments following thirty days' written notice of the breach upon termination. Upon request the RECIPIENT shall on termination securely and confidentially either dispose of or return the MATERIALS as directed by the SUPPLIER .

14. MATERIALS shall be returned to the SUPPLIER or securely and confidentially destroyed where required for ethical reasons by the relevant ethics committee or if the donor withdraws consent.

15. This Agreement represents the entire understanding of the parties relating to the use of the MATERIALS and supersedes and overrides all other understandings. Variations require the written consent of both parties nominated representatives.

Continued Appendix 7.

16. All communications between the parties relating to the substance of this Agreement shall take place through the RECIPIENTS LOCAL INVESTIGATOR and the SUPPLIER'S LOCAL INVESTIGATOR.

17. This Agreement shall be interpreted in accordance with English Law and be subject to the jurisdiction of the English Courts.

18. No third party may rely upon the provisions of this Agreement.

Authorised by the HEAD OF DEPARTMENT holding the tissues (essential for tissues from LTHT diagnostic archives)	Authorised by the RECIPIENT'S LOCAL INVESTIGATOR
	Designation: Dr
Department: Histopathology	
Signature:	Signature: *SMB00Q*
Name: Dr Patricia Harnden	Name: Sandra Bell
Date: 18 /7/12	Date: 18 / 7 / 2012
Signed for and on behalf of the SUPPLIER	Signed for and on behalf of the RECIPIENT
	Signature:
Signature: A Shaaban	
Name: Abeer Shaaban	Name:
	Designation:
Designation: Consultant Pathologist	
Date: 18 / 7 / 2012	Date:

Signed for and on behalf of the SPONSOR (only if applicable and the SPONSOR is not the SUPPLIER)
Signature:
Name:
Date:

8. Calculation of IC$_{50}$ concentration designed by Sally Jackson (University of Leeds)

Calculating 50% inhibition concentrations (IC50)

For ease of manipulation, input cell data into Excel sheet in this format. Use 'IC50 Template' saved on P drive as a guide.

CELL	DRUG	CONC	REP	VALUE	CONTROL
1	1	0	3	2.34	2.54
1	1	0	1	2.45	2.54
1	1	0	2	2.83	2.54
1	1	0.0001	3	1.56	2.54
1	1	0.0001	2	1.61	2.54
1	1	0.0001	1	1.77	2.54
1	1	0.0005	1	1.66	2.54
1	1	0.0005	2	1.88	2.54
1	1	0.0005	3	1.98	2.54
1	1	0.001	1	1.75	2.54
1	1	0.001	3	1.8	2.54
1	1	0.001	2	1.81	2.54
1	1	0.005	2	1.46	2.54
1	1	0.005	3	1.46	2.54
1	1	0.005	1	1.81	2.54
1	1	0.01	2	0.98	2.54
1	1	0.01	3	1.2	2.54
1	1	0.01	1	1.32	2.54
1	1	0.05	1	0.33	2.54
1	1	0.05	3	0.36	2.54
1	1	0.05	2	0.4	2.54
1	1	0.1	2	0.3	2.54
1	1	0.1	3	0.33	2.54
1	1	0.1	1	0.36	2.54
1	1	0.5	1		2.54
1	1	0.5	2		2.54
1	1	0.5	3		2.54
1	1	1	1		2.54
1	1	1	2		2.54
1	1	1	3		2.54

Cell. Assign numbers for different cell lines.

Drug. Assign numbers for different drugs.

Conc. Drug concentration.

Rep. Number of replicate.

Value. Viable cell number x10^6

Control. Average of control cell number.

Transforming the data.

Cell numbers are likely to be skewed with the drug concentration range. Log transformation of the data will give a straight line graph which can be better used to calculate an IC50.

EFFECT (dead cells)*	LOGDOSE	LOGODDSEFFECT**
0.385826772	-9.210340372	-0.46489
0.366141732	-9.210340372	-0.5488
0.303149606	-9.210340372	-0.83234
0.346456693	-7.60090246	-0.63465
0.25984252	-7.60090246	-1.04679
0.220472441	-7.60090246	-1.26292
0.311023622	-6.907755279	-0.79534
0.291338583	-6.907755279	-0.88889
0.287401575	-6.907755279	-0.90804
0.42519685	-5.298317367	-0.30148
0.42519685	-5.298317367	-0.30148
0.287401575	-5.298317367	-0.90804
0.614173228	-4.605170186	0.464889
0.527559055	-4.605170186	0.110348
0.480314961	-4.605170186	-0.07878
0.87007874	-2.995732274	1.901655
0.858267717	-2.995732274	1.800976
0.842519685	-2.995732274	1.677097
0.881889764	-2.302585093	2.010449
0.87007874	-2.302585093	1.901655
0.858267717	-2.302585093	1.800976

EFFECT. 1-(value/control)
This gives you number of dead cells so any values of 0 or less (minus) need removing from the data set.
LOGDOSE. Ln drug conc.
LOGODS EFFECT. ln⌈effect-(1-effect)⌉

Continued Appendix 8.

Graphing the data.

Select **Tools** and then **Data Analysis** from the drop down menu.

Select **Regression** from the options box and click **OK**.

The Regression analysis tool performs linear regression analysis by using the "least squares" method to fit a line through a set of observations. You can analyze how a single dependent variable is affected by the values of one or more independent variables.

For example, you can analyze how an athlete's performance is affected by such factors as age, height, and weight. You can apportion shares in the performance measure to each of these three factors, based on a set of performance data, and then use the results to predict the performance of a new, untested athlete.

To add Data Analysis option if not already on menu.

From the main menu select **Tools**, then **Add-ins** from the drop down menu.

Check the box next to **Analysis ToolPak** and click **OK**.

X input is the logdose values.

Continued Appendix 8.
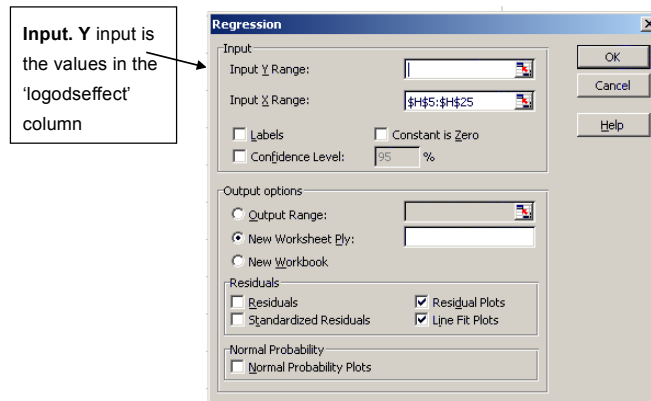
For each drug and cell line combination; make sure that any blanks are taken out from any negative results in the effects column. (Copy and paste the results into new columns alongside and cut the blanks so there are no gaps and you can easily select the column for the input ranges).

Select residual plot. This will produce a graph that should be random and would show up inconsistency in the data.

Select line fit plots.

Graphs and statistical output will be displayed in separate sheet.

There will be a number of tables showing regression statistics, ANOVA and confidence levels. However, just key values are needed to calculate the IC50; Multiple R, Intercept and X variable.

Graphing the data.

Select **Tools** and then **Data Analysis** from the drop down menu.

Select **Regression** from the options box and click **OK**.

The Regression analysis tool performs linear regression analysis by using the "least squares" method to fit a line through a set of observations. You can analyze how a single dependent variable is affected by the values of one or more independent variables.

For example, you can analyze how an athlete's performance is affected by such factors as age, height, and weight. You can apportion shares in the performance measure to each of these three factors, based on a set of performance data, and then use the results to predict the performance of a new, untested athlete.

To add Data Analysis option if not already on menu.

From the main menu select **Tools**, then **Add-ins** from the drop down menu.

Continued Appendix 8.

Multiple R

Intercept
and X
variable
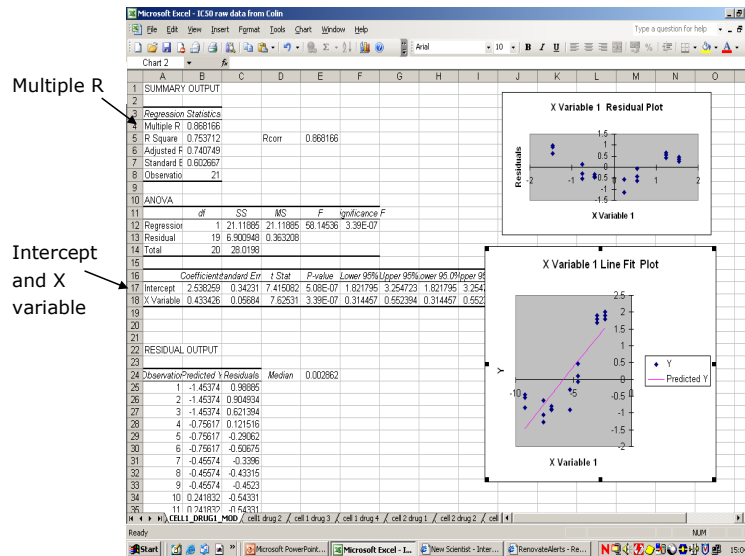
To calculate the IC50.

Graphs can be manipulated in the usual way. Here, the predicted Y line has been formatted to show automatic line and no markers.

Right click on one of the predicted markers and select **Format Data Series.**
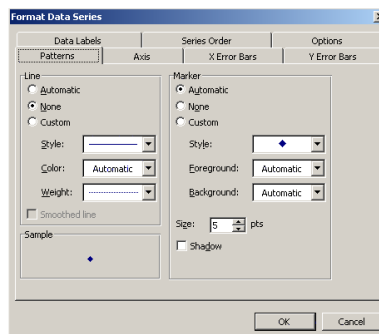
From the values produced the relevant numbers have to be transformed back to drug concentration. This can be done using the following equation. **=Exp(-intercept/X variable)**

Select an empty cell. Type in '=' to indicate a formula. Type 'Exp' which is the function. *[Alternatively it can be selected from the option box opened with the formulas button (fx in the toolbar) in the 'Math and Trig' function category].* Next, open brackets.

Type a minus sign. With the mouse, select the cell with the intercept coefficient value from the table. Type in a forward slash /

Click on the cell with the X-variable co-efficient value from the table. Close brackets. Click enter.

The resulting value is the IC50 value, which will have the same units as the values used for drug concentration.

X variable = the slope of the predicted values. This generates the IC50 value as X variable, or drug concentration.

In the regression statistics box, 'Multiple R' is the correlation co-efficient. This gives an indication of how strong the effect is, with values closer to 1 showing more confident results.

9. Identification of CC hits that reduce cell number

9.1 CC hits that reduce cell number after 24hr

Cytotoxic CC hits		Batch 1			Batch 2			Average		
Master Plate Name	Well Name	Whole Cells Number	Z score	Robust Z score	Whole Cells Number	Z score	Robust Z score	Whole Cells Number	Z score	Robust Z score
MP72-MP73	D11	42	-10.2	-30.08	56	-14.69	-17.48	49	-12.44	-23.78
MP72-MP73	D4	89	-10	-29.51	7	-15.03	-17.88	48	-12.52	-23.7
MP74-MP75	B11	220	-17.71	-26.81	243	-6.65	-9.72	232	-12.18	-18.26
MP76-MP77	E8	1136	-1.06	-29.1	1155	-2.15	-3.08	1146	-1.6	-16.09
MP64-MP65	F7	171	-7.02	-13.21	600	-8.72	-14.55	386	-7.87	-13.88
MP64-MP65	B2	473	-5.43	-10.19	471	-9.28	-15.54	472	-7.35	-12.87
MP72-MP73	F6	1322	-4.89	-14.75	1163	-7.03	-8.25	1243	-5.96	-11.5
MP59-MP241	F5	119	-5.65	-9.13	116	-10.95	-13.57	118	-8.3	-11.35
MP74-MP75	G11	1269	-9.86	-14.95	649	-5.01	-7.3	959	-7.44	-11.13
MP62-MP63	D11	514	-8.46	-15.54	828	-5.61	-6.7	671	-7.03	-11.12
MP70-MP71	F6	982	-11.71	-17.73	301	-2.1	-4.21	642	-6.9	-10.97
MP59-MP241	C8	403	-4.64	-7.53	145	-10.73	-13.3	274	-7.68	-10.41
MP74-MP75	C5	1119	-10.99	-16.65	1183	-2.86	-4.13	1151	-6.92	-10.39
MP76-MP77	G7	1913	-0.21	-12.21	4	-5.22	-7.46	959	-2.71	-9.83
MP72-MP73	G8	1664	-3.47	-10.65	1105	-7.43	-8.73	1385	-5.45	-9.69
MP72-MP73	D8	1768	-3.04	-9.41	967	-8.39	-9.88	1368	-5.71	-9.65
MP72-MP73	G6	1717	-3.25	-10.02	1071	-7.67	-9.02	1394	-5.46	-9.52
MP72-MP73	D6	1825	-2.8	-8.72	954	-8.48	-9.99	1390	-5.64	-9.36
MP72-MP73	B7	1709	-3.29	-10.11	1128	-7.27	-8.54	1419	-5.28	-9.33
MP59-MP241	F7	296	-5.02	-8.13	435	-8.51	-10.52	366	-6.76	-9.33
MP72-MP73	F8	1720	-3.24	-9.98	1127	-7.28	-8.55	1424	-5.26	-9.27
MP72-MP73	F7	1643	-3.56	-10.9	1248	-6.44	-7.54	1446	-5	-9.22
MP74-MP75	D5	1376	-9.06	-13.75	1138	-3.04	-4.39	1257	-6.05	-9.07
MP76-MP77	F6	1765	-0.37	-15.42	1378	-1.55	-2.23	1572	-0.96	-8.83
MP72-MP73	C6	1840	-2.74	-8.54	1090	-7.54	-8.86	1465	-5.14	-8.7
MP76-MP77	G5	1883	-0.24	-12.86	796	-3.1	-4.45	1340	-1.67	-8.65
MP72-MP73	E7	1877	-2.59	-8.1	1060	-7.75	-9.11	1469	-5.17	-8.61
MP72-MP73	G7	1924	-2.39	-7.54	998	-8.17	-9.63	1461	-5.28	-8.58
MP72-MP73	D7	1924	-2.39	-7.54	1008	-8.11	-9.54	1466	-5.25	-8.54
MP72-MP73	E8	1915	-2.43	-7.65	1106	-7.43	-8.73	1511	-4.93	-8.19
MP74-MP75	G7	1678	-6.8	-10.33	883	-4.07	-5.91	1281	-5.44	-8.12
MP76-MP77	E3	1831	-0.3	-13.99	1388	-1.53	-2.19	1610	-0.91	-8.09
MP74-MP75	D8	1688	-6.73	-10.22	948	-3.81	-5.52	1318	-5.27	-7.87
MP74-MP75	C7	1668	-6.88	-10.45	988	-3.65	-5.29	1328	-5.26	-7.87
MP70-MP71	E7	1410	-8.36	-12.69	910	-1.23	-2.73	1160	-4.8	-7.71
MP74-MP75	B7	1717	-6.51	-9.89	1009	-3.56	-5.16	1363	-5.04	-7.53
MP72-MP73	D5	1947	-2.3	-7.26	1227	-6.59	-7.72	1587	-4.44	-7.49
MP72-MP73	C7	1951	-2.28	-7.22	1223	-6.62	-7.75	1587	-4.45	-7.48
MP74-MP75	D6	1671	-6.85	-10.41	1126	-3.09	-4.46	1399	-4.97	-7.44
MP74-MP75	G8	1728	-6.43	-9.77	1027	-3.49	-5.05	1378	-4.96	-7.41
MP74-MP75	E6	1649	-7.02	-10.66	1196	-2.81	-4.05	1423	-4.91	-7.35
MP78-MP79	C10	907.5	-5.6	-8.71	761	-4.34	-5.94	834	-4.97	-7.32
MP74-MP75	B5	1685	-6.75	-10.25	1143	-3.02	-4.36	1414	-4.88	-7.31
MP72-MP73	B6	1967	-2.22	-7.02	1302	-6.07	-7.09	1635	-4.14	-7.06
MP60-MP61	F7	502	-9.49	-9.89	1150	-1.67	-4.22	826	-5.58	-7.05
MP70-MP71	G6	1678	-6.26	-9.54	254	-2.17	-4.33	966	-4.22	-6.93
MP74-MP75	F5	1735	-6.38	-9.69	1182	-2.86	-4.13	1459	-4.62	-6.91
MP74-MP75	E8	1808	-5.83	-8.86	1090	-3.23	-4.68	1449	-4.53	-6.77
MP70-MP71	B6	1708	-6.03	-9.19	367	-2.01	-4.05	1038	-4.02	-6.62
MP74-MP75	G6	1930	-4.92	-7.49	993	-3.62	-5.26	1462	-4.27	-6.37
MP74-MP75	F6	1842	-5.58	-8.48	1189	-2.83	-4.09	1516	-4.2	-6.28
MP62-MP63	D6	1019	-4.22	-7.89	1052	-3.88	-4.66	1036	-4.05	-6.27
MP74-MP75	F8	1955	-4.73	-7.2	996	-3.61	-5.24	1476	-4.17	-6.22
MP64-MP65	E5	841	-3.48	-6.51	1772	-3.57	-5.53	1307	-3.53	-6.02
MP70-MP71	C5	1678	-6.26	-9.54	1092	-0.97	-2.29	1385	-3.62	-5.92
MP59-MP241	F8	1008	-2.48	-4.12	737	-6.19	-7.63	873	-4.34	-5.87
MP59-MP241	F6	788	-3.26	-5.36	871	-5.17	-6.35	830	-4.22	-5.85
MP70-MP71	C6	1867	-4.79	-7.32	296	-2.11	-4.23	1082	-3.45	-5.77
MP70-MP71	B7	1824	-5.12	-7.82	533	-1.77	-3.65	1179	-3.45	-5.74
MP59-MP241	G5	1234	-1.67	-2.85	661	-6.78	-8.36	948	-4.22	-5.6
MP74-MP75	C8	2088	-3.73	-5.7	958	-3.77	-5.46	1523	-3.75	-5.58
MP70-MP71	F5	1728	-5.87	-8.95	1148	-0.89	-2.15	1438	-3.38	-5.55
MP70-MP71	G5	1748	-5.72	-8.72	1068	-1.01	-2.35	1408	-3.36	-5.53
MP62-MP63	F8	1044	-4.01	-7.51	1175	-2.93	-3.54	1110	-3.47	-5.52
MP74-MP75	B6	1927	-4.94	-7.52	1284	-2.45	-3.52	1606	-3.69	-5.52
MP70-MP71	F7	1790	-5.39	-8.22	878	-1.28	-2.81	1334	-3.33	-5.52
MP59-MP241	E8	1232	-1.67	-2.86	684	-6.6	-8.14	958	-4.14	-5.5
MP74-MP75	D7	2066	-3.9	-5.95	1046	-3.41	-4.94	1556	-3.66	-5.44
MP60-MP61	E1	886	-6.58	-6.86	1170	-1.58	-4.01	1028	-4.08	-5.43
MP78-MP79	G10	1589	-2.52	-3.9	613	-4.99	-6.85	1101	-3.75	-5.37
MP64-MP65	F5	833	-3.53	-6.59	1955	-2.77	-4.13	1394	-3.15	-5.36
MP74-MP75	F7	2017	-4.27	-6.5	1169	-2.91	-4.21	1593	-3.59	-5.36
MP59-MP241	B5	1175	-1.88	-3.18	762	-6	-7.39	969	-3.94	-5.28
MP60-MP61	F6	1015	-5.6	-5.85	1104	-1.87	-4.71	1060	-3.74	-5.28
MP62-MP63	F6	1041	-4.04	-7.55	1235	-2.47	-3	1138	-3.25	-5.27

Continued 9.1 CC hits that reduce cell number after 24hr

Master Plate Name	Well Name	Whole Cells Number	Z score	Robust Z score	Whole Cells Number	Z score	Robust Z score	Whole Cells Number	Z score	Robust Z score
MP59-MP241	E5	1036	-2.38	-3.96	850	-5.33	-6.55	943	-3.85	-5.26
MP74-MP75	C6	2058	-3.96	-6.04	1126	-3.09	-4.46	1592	-3.52	-5.25
MP74-MP75	G5	2014	-4.29	-6.54	1215	-2.73	-3.93	1615	-3.51	-5.24
MP70-MP71	D6	1998	-3.76	-5.78	105	-2.38	-4.69	1052	-3.07	-5.23
MP60-MP61	B7	1326	-3.25	-3.4	888	-2.82	-7.01	1107	-3.04	-5.2
MP62-MP63	C7	1312	-1.77	-3.45	807	-5.77	-6.89	1060	-3.77	-5.17
MP70-MP71	C7	1896	-4.56	-6.98	701	-1.53	-3.24	1299	-3.05	-5.11
MP59-MP241	G8	1247	-1.62	-2.77	760	-6.02	-7.41	1004	-3.82	-5.09
MP70-MP71	G7	1900	-4.53	-6.93	712	-1.51	-3.21	1306	-3.02	-5.07
MP59-MP241	E6	1096	-2.16	-3.62	855	-5.29	-6.5	976	-3.73	-5.06
MP62-MP63	F5	1096	-3.58	-6.72	1190	-2.81	-3.4	1143	-3.2	-5.06
MP60-MP61	F8	983	-5.85	-6.1	1172	-1.57	-3.98	1078	-3.71	-5.04
MP59-MP241	D6	1268	-1.55	-2.65	759	-6.03	-7.42	1014	-3.79	-5.04
MP70-MP71	G8	1841	-4.99	-7.62	1040	-1.05	-2.42	1441	-3.02	-5.02
MP74-MP75	F11	2125	-3.46	-5.28	1090	-3.23	-4.68	1608	-3.35	-4.98
MP59-MP241	G6	1123	-2.06	-3.47	861	-5.24	-6.44	992	-3.65	-4.96
MP59-MP241	C5	1068	-2.26	-3.78	895	-4.98	-6.12	982	-3.62	-4.95
MP62-MP63	F7	1034	-4.1	-7.66	1322	-1.79	-2.2	1178	-2.95	-4.93
MP60-MP61	C6	1268	-3.69	-3.85	992	-2.36	-5.9	1130	-3.03	-4.88
MP70-MP71	E5	1852	-4.9	-7.49	1113	-0.94	-2.24	1483	-2.92	-4.87
MP64-MP65	G5	932	-3	-5.6	1956	-2.76	-4.12	1444	-2.88	-4.86
MP59-MP241	G7	1238	-1.65	-2.82	814	-5.6	-6.89	1026	-3.63	-4.86
MP76-MP77	E6	2243	0.16	-5.03	741	-3.25	-4.66	1492	-1.55	-4.84
MP74-MP75	E7	2106	-3.6	-5.5	1177	-2.88	-4.16	1642	-3.24	-4.83
MP59-MP241	D5	1250	-1.61	-2.75	816	-5.59	-6.88	1033	-3.6	-4.82
MP70-MP71	B8	1880	-4.69	-7.16	1020	-1.07	-2.46	1450	-2.88	-4.81
MP59-MP241	C6	1183	-1.85	-3.13	864	-5.22	-6.42	1024	-3.54	-4.77
MP62-MP63	G7	1084	-3.68	-6.9	1276	-2.15	-2.62	1180	-2.91	-4.76
MP59-MP241	E7	1383	-1.13	-2.01	751	-6.09	-7.5	1067	-3.61	-4.75
MP70-MP71	D8	1921	-4.36	-6.68	945	-1.18	-2.65	1433	-2.77	-4.66
MP70-MP71	F8	1876	-4.72	-7.21	1163	-0.87	-2.12	1520	-2.79	-4.66
MP62-MP63	B8	1227	-2.48	-4.73	1064	-3.79	-4.55	1146	-3.13	-4.64
MP74-MP75	B8	2152	-3.26	-4.98	1166	-2.93	-4.23	1659	-3.09	-4.6
MP62-MP63	G5	1252	-2.27	-4.36	1040	-3.97	-4.77	1146	-3.12	-4.56
MP64-MP65	B5	855	-3.41	-6.37	2140	-1.96	-2.7	1498	-2.68	-4.54
MP70-MP71	D5	1943	-4.19	-6.42	986	-1.12	-2.55	1465	-2.66	-4.49
MP59-MP241	B6	1162	-1.92	-3.25	942	-4.62	-5.67	1052	-3.27	-4.46
MP60-MP61	G5	1242	-3.88	-4.06	1092	-1.92	-4.84	1167	-2.9	-4.45
MP60-MP61	G7	1341	-3.13	-3.28	1021	-2.24	-5.59	1181	-2.69	-4.43
MP70-MP71	E8	1934	-4.26	-6.53	1111	-0.94	-2.24	1523	-2.6	-4.39
MP62-MP63	E8	1225	-2.5	-4.77	1133	-3.25	-3.92	1179	-2.87	-4.34
MP60-MP61	G8	1337	-3.16	-3.31	1046	-2.13	-5.32	1192	-2.65	-4.32
MP70-MP71	C8	1961	-4.05	-6.21	1038	-1.05	-2.42	1500	-2.55	-4.32
MP60-MP61	C5	1291	-3.51	-3.67	1082	-1.97	-4.94	1187	-2.74	-4.31
MP64-MP65	F6	944	-2.94	-5.48	2086	-2.19	-3.12	1515	-2.57	-4.3
MP64-MP65	G7	1051	-2.38	-4.41	1959	-2.75	-4.1	1505	-2.56	-4.25
MP62-MP63	B5	1255	-2.24	-4.31	1107	-3.45	-4.16	1181	-2.85	-4.23
MP74-MP75	E5	2187	-2.99	-4.58	1223	-2.7	-3.89	1705	-2.85	-4.23
MP62-MP63	G8	1199	-2.71	-5.16	1209	-2.67	-3.23	1204	-2.69	-4.2
MP60-MP61	B5	1280	-3.6	-3.76	1126	-1.77	-4.47	1203	-2.69	-4.12
MP62-MP63	E6	1251	-2.28	-4.37	1147	-3.15	-3.8	1199	-2.71	-4.08
MP60-MP61	B8	1390	-2.76	-2.89	1054	-2.09	-5.24	1222	-2.43	-4.07
MP66-MP67	E7	1242	0.12	0.23	1402	-3.03	-8.3	1322	-1.45	-4.04
MP60-MP61	E7	1382	-2.82	-2.96	1091	-1.93	-4.85	1237	-2.38	-3.9
MP62-MP63	D7	1291	-1.94	-3.77	1123	-3.33	-4.01	1207	-2.64	-3.89
MP62-MP63	C6	1343	-1.51	-2.98	1039	-3.98	-4.78	1191	-2.74	-3.88
MP60-MP61	F5	1179	-4.36	-4.56	1255	-1.21	-3.1	1217	-2.78	-3.83
MP78-MP79	B11	1709	-1.97	-3.05	1005	-3.26	-4.43	1357	-2.61	-3.74
MP60-MP61	D7	1494	-1.97	-2.07	1042	-2.14	-5.37	1268	-2.06	-3.72
MP64-MP65	E8	1114	-2.04	-3.78	2017	-2.5	-3.65	1566	-2.27	-3.72
MP60-MP61	C8	1387	-2.79	-2.92	1130	-1.76	-4.43	1259	-2.27	-3.67
MP64-MP65	G8	1110	-2.06	-3.82	2035	-2.42	-3.51	1573	-2.24	-3.67
MP62-MP63	B7	1342	-1.51	-2.99	1092	-3.57	-4.3	1217	-2.54	-3.64
MP68-MP69	D6	1682	-8.83	-9.53	1720	0.97	2.26	1701	-3.93	-3.63
MP60-MP61	E8	1455	-2.27	-2.38	1120	-1.8	-4.54	1288	-2.04	-3.46
MP60-MP61	G6	1430	-2.46	-2.58	1146	-1.69	-4.26	1288	-2.07	-3.42
MP60-MP61	C7	1326	-3.25	-3.4	1235	-1.29	-3.31	1281	-2.27	-3.36
MP62-MP63	B6	1388	-1.13	-2.3	1092	-3.57	-4.3	1240	-2.35	-3.3
MP59-MP241	G3	1109	-2.11	-3.55	1243	-2.32	-2.79	1176	-2.22	-3.17
MP62-MP63	G6	1350	-1.45	-2.87	1186	-2.84	-3.44	1268	-2.15	-3.16
MP64-MP65	B8	1111	-2.06	-3.81	2174	-1.81	-2.44	1643	-1.93	-3.13
MP60-MP61	B6	1462	-2.22	-2.33	1186	-1.51	-3.84	1324	-1.86	-3.08
MP70-MP71	E6	2213	-2.08	-3.25	854	-1.31	-2.87	1534	-1.7	-3.06
MP60-MP61	E5	1470	-2.16	-2.26	1198	-1.46	-3.71	1334	-1.81	-2.99
MP62-MP63	E7	1407	-0.97	-2.01	1160	-3.05	-3.68	1284	-2.01	-2.84

9.2 CC hits that reduce cell number after 48hr

Cytotoxic CC hits		Batch 1			Batch 2			Average		
Master Plate Name	Well Name	Whole Cells Number	Z score	Robust Z score	Whole Cells Number	Z score	Robust Z score	Whole Cells Number	Z score	Robust Z score
MP64-MP65	F7	60	-22.75	-58.86	216	-28.99	-33.85	138	-25.87	-46.35
MP64-MP65	B2	78	-22.62	-58.54	290	-28.49	-33.26	184	-25.56	-45.9
MP66-MP67	F6	7	-34.19	-62.95	6	-17.21	-25.79	7	-25.7	-44.37
MP74-MP75	G11	305	-13	-14.4	148	-39.01	-57.28	227	-26.01	-35.84
MP74-MP75	B11	121	-13.61	-15.08	260	-37.75	-55.42	191	-25.68	-35.25
MP59-MP241	F5	186	-26.44	-34.76	96	-19.51	-33	141	-22.98	-33.88
MP59-MP241	F7	226	-26.17	-34.39	501	-16.92	-28.57	364	-21.54	-31.48
MP59-MP241	C8	563	-23.87	-31.34	280	-18.33	-30.99	422	-21.1	-31.17
MP66-MP67	C1	1091	-23.01	-42.11	1848	-10.01	-15.02	1470	-16.51	-28.56
MP64-MP65	B6	1949	-9.58	-25.13	458	-27.35	-31.92	1204	-18.46	-28.52
MP74-MP75	F11	432	-12.58	-13.94	1407	-24.75	-36.3	920	-18.66	-25.12
MP66-MP67	E8	961	-24.35	-44.61	3590	-3.19	-4.83	2276	-13.77	-24.72
MP64-MP65	D8	1565	-12.25	-31.98	2658	-12.37	-14.39	2112	-12.31	-23.19
MP64-MP65	G5	1140	-15.22	-39.57	4194	-1.92	-2.16	2667	-8.57	-20.86
MP72-MP73	D4	31	-6.39	-35.92	1	-3.79	-5.04	16	-5.09	-20.48
MP72-MP73	D11	56	-6.35	-35.72	843	-2.72	-3.66	450	-4.54	-19.69
MP64-MP65	E5	1871	-10.12	-26.52	3008	-9.99	-11.61	2440	-10.06	-19.06
MP64-MP65	F6	1729	-11.11	-29.05	3961	-3.5	-4.01	2845	-7.31	-16.53
MP59-MP241	C6	2437	-11.12	-14.38	1464	-10.75	-18.05	1951	-10.93	-16.22
MP60-MP61	E1	1236	-2.11	-9.5	955	-9.29	-21.71	1096	-5.7	-15.61
MP66-MP67	D8	2306	-10.49	-18.74	2571	-7.18	-10.79	2439	-8.83	-14.76
MP59-MP241	G8	3415	-4.46	-5.53	979	-13.86	-23.35	2197	-9.16	-14.44
MP64-MP65	E6	2137	-8.27	-21.77	3639	-5.69	-6.58	2888	-6.98	-14.17
MP74-MP75	G7	3327	-2.93	-3.29	2124	-16.62	-24.35	2726	-9.78	-13.82
MP59-MP241	F8	2849	-8.31	-10.66	1682	-9.35	-15.67	2266	-8.83	-13.16
MP64-MP65	G8	2245	-7.51	-19.84	3654	-5.59	-6.46	2950	-6.55	-13.15
MP64-MP65	G7	2377	-6.59	-17.48	3361	-7.59	-8.79	2869	-7.09	-13.14
MP64-MP65	D6	2183	-7.95	-20.95	3835	-4.36	-5.02	3009	-6.15	-12.98
MP66-MP67	C6	2181	-11.78	-21.14	3612	-3.11	-4.7	2897	-7.44	-12.92
MP66-MP67	C7	2265	-10.91	-19.53	3385	-4	-6.03	2825	-7.45	-12.78
MP74-MP75	C7	3169	-3.46	-3.87	2304	-14.58	-21.35	2737	-9.02	-12.61
MP59-MP241	B8	2788	-8.73	-11.21	1889	-8.03	-13.4	2339	-8.38	-12.31
MP64-MP65	C8	2234	-7.59	-20.04	3895	-3.95	-4.54	3065	-5.77	-12.29
MP66-MP67	B7	2286	-10.69	-19.13	3542	-3.38	-5.11	2914	-7.04	-12.12
MP66-MP67	F5	2272	-10.84	-19.39	3617	-3.09	-4.67	2945	-6.96	-12.03
MP64-MP65	B5	2277	-7.29	-19.27	3883	-4.03	-4.63	3080	-5.66	-11.95
MP66-MP67	B5	2365	-9.88	-17.61	3386	-3.99	-6.02	2876	-6.94	-11.81
MP64-MP65	F5	2294	-7.17	-18.96	3918	-3.79	-4.35	3106	-5.48	-11.66
MP59-MP241	E8	3042	-7	-8.91	1858	-8.23	-13.74	2450	-7.61	-11.33
MP66-MP67	E6	2356	-9.97	-17.78	3662	-2.91	-4.41	3009	-6.44	-11.09
MP68-MP69	G7	1486	-6.7	-8.63	1605	-5.35	-13.55	1546	-6.02	-11.09
MP74-MP75	D8	3567	-2.13	-2.41	2413	-13.35	-19.53	2990	-7.74	-10.97
MP66-MP67	C5	2427	-9.24	-16.41	3475	-3.64	-5.5	2951	-6.44	-10.96
MP74-MP75	C8	3415	-2.64	-2.97	2457	-12.85	-18.8	2936	-7.74	-10.88
MP66-MP67	D6	2470	-8.8	-15.59	3359	-4.1	-6.18	2915	-6.45	-10.88
MP64-MP65	C5	2332	-6.91	-18.29	4112	-2.47	-2.81	3222	-4.69	-10.55
MP64-MP65	B8	2454	-6.06	-16.11	3874	-4.09	-4.71	3164	-5.08	-10.41
MP59-MP241	F6	3275	-5.41	-7.55	1917	-7.85	-13.1	2596	-6.63	-10.32
MP64-MP65	F8	2515	-5.63	-15.02	3768	-4.82	-5.55	3142	-5.22	-10.28
MP66-MP67	B6	2454	-8.96	-15.89	3629	-3.04	-4.6	3042	-6	-10.25
MP66-MP67	G7	2460	-8.9	-15.78	3627	-3.05	-4.61	3044	-5.97	-10.2
MP64-MP65	E8	2461	-6.01	-15.98	3927	-3.73	-4.28	3194	-4.87	-10.13
MP64-MP65	C6	2460	-6.02	-16	3948	-3.59	-4.12	3204	-4.8	-10.06
MP74-MP75	F6	3559	-2.16	-2.44	2535	-11.97	-17.5	3047	-7.06	-9.97
MP66-MP67	D7	2553	-7.94	-13.99	3434	-3.8	-5.74	2994	-5.87	-9.87
MP64-MP65	D7	2502	-5.72	-15.25	3904	-3.89	-4.47	3203	-4.81	-9.86
MP59-MP241	G7	3440	-4.29	-5.31	1812	-8.52	-14.25	2626	-6.41	-9.78
MP66-MP67	E7	2491	-8.58	-15.18	3701	-2.76	-4.18	3096	-5.67	-9.68

Continued 9.2 CC hits that reduce cell number after 48hr

Cytotoxic CC hits		Batch 1			Batch 2			Average		
Master Plate Name	Well Name	Whole Cells Number	Z score	Robust Z score	Whole Cells Number	Z score	Robust Z score	Whole Cells Number	Z score	Robust Z score
MP66-MP67	F7	2586	-7.6	-13.36	3446	-3.76	-5.67	3016	-5.68	-9.51
MP70-MP71	B7	2446	-1.94	-6.2	1122	-7.1	-12.81	1784	-4.52	-9.51
MP74-MP75	E6	3250	-3.19	-3.58	2663	-10.52	-15.37	2957	-6.85	-9.47
MP66-MP67	G6	2533	-8.15	-14.38	3644	-2.98	-4.51	3089	-5.57	-9.44
MP66-MP67	D5	2478	-8.72	-15.43	3859	-2.14	-3.26	3169	-5.43	-9.35
MP60-MP61	D7	2972	-0.22	-2.53	1433	-6.92	-16.15	2203	-3.57	-9.34
MP64-MP65	B7	2550	-5.39	-14.39	3931	-3.71	-4.25	3241	-4.55	-9.32
MP64-MP65	D5	2501	-5.73	-15.27	4046	-2.92	-3.33	3274	-4.33	-9.3
MP66-MP67	E5	2501	-8.48	-14.99	3802	-2.36	-3.59	3152	-5.42	-9.29
MP66-MP67	B8	2585	-7.61	-13.38	3567	-3.28	-4.96	3076	-5.45	-9.17
MP59-MP241	E6	3524	-3.72	-4.55	1856	-8.24	-13.77	2690	-5.98	-9.16
MP64-MP65	C7	2509	-5.67	-15.13	4091	-2.62	-2.98	3300	-4.15	-9.05
MP74-MP75	B5	3471	-2.45	-2.76	2665	-10.49	-15.33	3068	-6.47	-9.05
MP59-MP241	G5	3486	-3.97	-4.89	1908	-7.91	-13.2	2697	-5.94	-9.04
MP60-MP61	F5	2764	-0.44	-3.37	1562	-6.28	-14.65	2163	-3.36	-9.01
MP64-MP65	E7	2549	-5.39	-14.41	4025	-3.07	-3.5	3287	-4.23	-8.96
MP60-MP61	F6	1902	-1.38	-6.83	1869	-4.75	-11.08	1886	-3.07	-8.95
MP60-MP61	F7	989	-2.38	-10.49	2188	-3.17	-7.37	1589	-2.77	-8.93
MP59-MP241	B5	3388	-4.64	-5.78	2035	-7.09	-11.81	2712	-5.87	-8.79
MP59-MP241	G6	3450	-4.22	-5.22	2026	-7.15	-11.91	2738	-5.69	-8.56
MP74-MP75	G5	3294	-3.04	-3.41	2769	-9.32	-13.6	3032	-6.18	-8.51
MP59-MP241	C5	3550	-3.54	-4.31	1963	-7.56	-12.6	2757	-5.55	-8.45
MP74-MP75	E8	3309	-2.99	-3.36	2774	-9.26	-13.52	3042	-6.12	-8.44
MP59-MP241	B7	3332	-5.02	-6.29	2156	-6.32	-10.49	2744	-5.67	-8.39
MP74-MP75	E5	3485	-2.4	-2.71	2745	-9.59	-14	3115	-6	-8.36
MP60-MP61	F8	2132	-1.13	-5.9	1905	-4.57	-10.66	2019	-2.85	-8.28
MP74-MP75	G1	3219	-3.29	-3.69	2839	-8.52	-12.43	3029	-5.91	-8.06
MP66-MP67	C8	2749	-5.92	-10.22	3411	-3.89	-5.88	3080	-4.91	-8.05
MP59-MP241	C7	3719	-2.39	-2.78	1899	-7.97	-13.3	2809	-5.18	-8.04
MP59-MP241	B6	3572	-3.39	-4.11	2022	-7.18	-11.95	2797	-5.28	-8.03
MP59-MP241	D5	3692	-2.57	-3.03	1987	-7.4	-12.33	2840	-4.99	-7.68
MP62-MP63	D11	1000	-9.47	-11.01	1305	-3.72	-4.34	1153	-6.59	-7.67
MP64-MP65	B12	2720	-4.2	-11.36	3977	-3.39	-3.88	3349	-3.8	-7.62
MP59-MP241	E5	3676	-2.68	-3.17	2022	-7.18	-11.95	2849	-4.93	-7.56
MP60-MP61	B7	2541	-0.69	-4.26	1913	-4.53	-10.57	2227	-2.61	-7.42
MP66-MP67	F8	2813	-5.26	-8.99	3440	-3.78	-5.71	3127	-4.52	-7.35
MP59-MP241	E7	3717	-2.4	-2.8	2041	-7.06	-11.74	2879	-4.73	-7.27
MP66-MP67	G5	2691	-6.52	-11.34	3882	-2.05	-3.12	3287	-4.29	-7.23
MP60-MP61	C5	2792	-0.41	-3.25	1876	-4.72	-11	2334	-2.57	-7.13
MP64-MP65	G6	2850	-3.3	-9.04	3817	-4.48	-5.16	3334	-3.89	-7.1
MP70-MP71	F7	2539	-1.81	-5.85	1960	-4.31	-7.91	2250	-3.06	-6.88
MP70-MP71	G5	1520	-3.25	-9.7	2625	-2.09	-4.02	2073	-2.67	-6.86
MP74-MP75	C5	3598	-2.03	-2.3	2900	-7.83	-11.42	3249	-4.93	-6.86
MP70-MP71	E12	2236	-2.23	-7	2184	-3.56	-6.6	2210	-2.9	-6.8
MP60-MP61	B6	3058	-0.12	-2.18	1841	-4.89	-11.41	2450	-2.51	-6.8
MP60-MP61	G5	2496	-0.73	-4.44	2071	-3.75	-8.73	2284	-2.24	-6.59
MP60-MP61	C8	3018	-0.17	-2.35	1981	-4.2	-9.78	2500	-2.18	-6.06
MP60-MP61	B5	2891	-0.3	-2.86	2056	-3.82	-8.91	2474	-2.06	-5.88
MP64-MP65	B11	2878	-3.1	-8.54	4098	-2.57	-2.92	3488	-2.84	-5.73
MP64-MP65	G3	2878	-3.1	-8.54	4129	-2.36	-2.67	3504	-2.73	-5.6
MP60-MP61	C7	2745	-0.46	-3.44	2179	-3.21	-7.48	2462	-1.84	-5.46
MP60-MP61	G7	2914	-0.28	-2.76	2125	-3.48	-8.1	2520	-1.88	-5.43
MP60-MP61	B8	2942	-0.25	-2.65	2118	-3.52	-8.19	2530	-1.88	-5.42
MP60-MP61	G8	2828	-0.37	-3.11	2175	-3.23	-7.52	2502	-1.8	-5.32
MP59-MP241	G3	3192	-5.98	-7.55	2838	-1.95	-3.03	3015	-3.96	-5.29
MP70-MP71	C6	2951	-1.22	-4.3	2360	-2.97	-5.57	2656	-2.1	-4.93
MP70-MP71	F5	3073	-1.05	-3.84	2388	-2.88	-5.41	2731	-1.97	-4.62
MP70-MP71	C5	2831	-1.39	-4.75	2550	-2.34	-4.46	2691	-1.87	-4.61
MP60-MP61	G9	2831	-0.37	-3.1	2297	-2.63	-6.1	2564	-1.5	-4.6
MP76-MP77	G3	2339	-5.66	-7.54	644	-1.4	-1.65	1492	-3.53	-4.6
MP70-MP71	B5	2744	-1.52	-5.08	2616	-2.12	-4.07	2680	-1.82	-4.58

10. Identification of CC hits inducing increased numbers of mitotic cells

10.1 CC hits inducing increased numbers of mitotic cells after 24hr

CC hits increase %mitotic cells (24hr)		Batch 1				Batch 2				Average			
Master Plate Name	Well Name	Whole Cells Number	%mitotic cells	Z score	Robust Z score	Whole Cells Number	%mitotic cells	Z score	Robust Z score	Whole Cells Number	%mitotic cells	Z score	Robust Z score
MP74-MP75	B11	220	38.84	9.78	27.98	243	32.5	22.6	43.46	232	35.67	16.19	35.72
MP64-MP65	B2	473	42.18	6.23	10.78	471	42.18	6.23	10.78	472	42.18	6.23	10.78
MP76-MP77	C3	2536	2.38	1.24	3.03	961	37.52	8.18	15.48	1749	19.95	4.71	9.26
MP64-MP65	F7	171	37.22	4.87	8.35	600	37.22	4.87	8.35	386	37.22	4.87	8.35
MP72-MP73	D8	1768	28.04	4.62	8.61	967	23.43	1.84	2.33	1368	25.74	3.23	5.47
MP74-MP75	G2	2667	15.02	0.79	2.77	1597	10.19	3.8	7.68	2132	12.6	2.29	5.23
MP74-MP75	B6	1927	15.58	1	3.37	1284	9.54	3.26	6.65	1606	12.56	2.13	5.01
MP76-MP77	C4	2364	3.2	2.55	6.46	1551	22.65	1.22	2.48	1958	12.92	1.88	4.47
MP76-MP77	C2	2182	2.97	2.18	5.5	2140	22.96	1.36	2.75	2161	12.96	1.77	4.13
MP72-MP73	D2	2562	25.63	2.94	5.28	2191	23.5	1.88	2.37	2377	24.56	2.41	3.82
MP76-MP77	G2	2508	2.32	1.15	2.81	2443	24.87	2.26	4.43	2476	13.6	1.71	3.62
MP76-MP77	C12	2422	2.52	1.47	3.65	1928	22.74	1.26	2.56	2175	12.63	1.36	3.1
MP64-MP67	E7	1319	25.81	1.74	2.78	2337	25.81	1.74	2.78	1828	25.81	1.74	2.78
MP76-MP77	D2	2670	2.22	0.99	2.4	2290	23.28	1.51	3.03	2480	12.75	1.25	2.72
MP64-MP68	E8	1114	25.33	1.61	2.54	2017	25.33	1.61	2.54	1566	25.33	1.61	2.54
MP59-MP241	F5	119	6.57	0.7	2.14	116	24.12	1.79	2.7	118	15.34	1.24	2.42

10.2 CC hits inducing increased numbers of mitotic cells after 48hr

CC hits increase %mitotic cells (48hr)		Batch 1				Batch 2				Average			
Master Plate Name	Well Name	Whole Cells Number	%mitotic cells	Z score	Robust Z score	Whole Cells Number	%mitotic cells	Z score	Robust Z score	Whole Cells Number	%mitotic cells	Z score	Robust Z score
MP59-MP241	F5	186	15.38	1.71	2.68	96	20	35.57	42.81	141	17.69	18.64	22.75
MP74-MP75	B11	121	6.17	7.34	11.55	260	10.14	13.5	19.19	191	8.15	10.42	15.37
MP64-MP65	F7	60	4.2	1.81	4.03	216	10.53	7.42	11.65	138	7.36	4.61	7.84
MP62-MP63	G12	3665	16.58	2.75	7.06	3372	6.58	1.7	2.96	3519	11.58	2.23	5.01